UNIVERSIDAD COMPLUTENSE DE MADRID

FACULTAD DE FARMACIA

DEPARTAMENTO DE MICROBIOLOGÍA II

PAPEL FUNCIONAL DE LAS PROTEÍNAS CRH EN LA BIOGÉNESIS DE LA PARED CELULAR Y LA MORFOGÉNESIS DE *SACCHAROMYCES CEREVISIAE*

TESIS DOCTORAL DE:

NOELIA BLANCO TALAVÁN

DIRIGIDA POR:

FRANCISCO JAVIER ARROYO NOMBELA

Madrid, 2013

UNIVERSIDAD COMPLUTENSE DE MADRID

FACULTAD DE FARMACIA

DEPARTAMENTO DE MICROBIOLOGÍA II

Papel funcional de las proteínas Crh en la biogénesis de la pared celular y la morfogénesis de *Saccharomyces cerevisiae*

Memoria presentada para optar al grado de Doctor por:

Noelia Blanco Talaván

Director:

Francisco Javier Arroyo Nombela

Dª. CONCEPCIÓN GIL GARCIA, Directora del Departamento de Microbiología II de la Facultad de Farmacia de la Universidad Complutense de Madrid,

CERTIFICA: Que Dª **NOELIA BLANCO TALAVÁN** ha realizado en el Departamento de Microbiología II de la Facultad de Farmacia de la Universidad Complutense de Madrid, bajo la dirección del doctor **FRANCISCO JAVIER ARROYO NOMBELA**, el trabajo que presenta para optar al Grado de Doctor con el título:

"Papel funcional de las proteínas Crh en la biogénesis de la pared celular y la morfogénesis de *Saccharomyces cerevisiae*"

Y para que así conste, firmo la presente certificación en Madrid, 2013

Fdo. Dra. Concepción Gil García

El desarrollo de esta Tesis Doctoral ha sido posible gracias a la concesión de las siguientes ayudas:

- Contrato por obra y servicios para personal de apoyo a la investigación asociado al proyecto de investigación **BIO2004-06376** del **Consejo Interinstitucional de Ciencia y Tecnología** (CICYT) durante el periodo Enero 2006 hasta Diciembre 2007.

- Ayuda predoctoral para realizar trabajos de investigación asociada al proyecto **"Cátedra Extraordinaria de Genómica y Proteómica"** suscrito entre **D. Cesar Nombela Cano** y **Merck Sharp and Dohme** durante el periodo Diciembre 2007 hasta Agosto 2008.

- Ayuda predoctoral de Formación de Personal Investigador (FPI) asociada al proyecto de investigación **BIO2007-67821** del **Ministerio de Ciencia e Innovación** durante el período Septiembre de 2008 hasta Marzo de 2013.

El trabajo que se muestra en esta Tesis Doctoral forma parte de los siguientes proyectos:

- **Genómica Funcional de la integridad celular fúngica: análisis molecular de la construcción y estabilidad de la pared celular e identificación de dianas de antifúngicos.**

  Proyecto BIO2004-06376.
  Entidad Financiadora: CICYT. 2005-2007.
  IP: Javier Arroyo

- **Biogénesis de la pared celular fúngica como base del mantenimiento de la integridad celular: una aproximación genómica global en el organismo modelo *S. cerevisiae.***

  Proyecto BIO2007-67821.
  Entidad Financiadora: CICYT. 2008-2010.
  IP: Javier Arroyo

- **Reguladores, efectores y conexión entre rutas de señalización implicadas en la integridad celular de la levadura: aproximación a la identificación de nuevas dianas antifúngicas.**

  Proyecto BIO2010-22146.
  Entidad Financiadora: CICYT. 2008-2010.
  IP: Javier Arroyo

A mis padres y mi hermana

A mis amigas

A Juanjo

Si no conozco una cosa, la investigaré

Louis Pasteur, 1822 - 1895

AGRADECIMIENTOS

En primer lugar quiero dar las gracias a mi director Javier Arroyo por haberme seleccionado en aquella, mi primera entrevista, allá por noviembre del 2005, de modo que yo no lo sabía entonces, pero me brindaste una oportunidad de oro al permitirme formar parte de tu equipo de investigación. Quiero agradecerte la generosidad en cuanto al tiempo dedicado para enseñarme a nivel experimental y transmitirme tus conocimientos. Me has enseñado a hacer ciencia y a pensar en ciencia. Has conseguido que me encantara lo que hacía y por ello me siento afortunada de haber contado con tu dirección, atención y dedicación. A la hora de la escritura, como no podía ser de otra manera, me has contagiado tu elegancia y perfección. Te agradezco el esfuerzo final para que todo quedara terminado. También quiero agradecerte que te hayas preocupado por mí y siempre hayas estado dispuesto a ayudarme, muy acorde con la gran humanidad y bondad de tu persona ¡¡¡MUCHAS GRACIAS JAVIER!!!

A continuación quisiera agradecer de corazón a Enrico Cabib, al que considero un auténtico genio, todo lo aprendido en estos años. Usted me ha enseñado la paciencia, el tesón, la generosidad y mantener viva la curiosidad científica. Para mí ha sido un placer haber trabajado con usted, formado parte de esta bonita colaboración científica con la que he aprendido, disfrutado y finalmente hemos podido encontrar "la piedra filosofal" de la pared. Para lo que usted quiera, en mí tiene una amiga. Le deseo una plácida jubilación.

A Ramón Hurtado por su amabilidad y acogida durante mi estancia en Dundee. Admiro tu persistencia y tus ganas de hacer ciencia, invencibles ante cualquier tempestad. Gracias también a tu mujer, María tan simpática y agradable conmigo. Os deseo mucha suerte!

I would like to thank Dr. Vladimir Farkas and Dr. Mariam Mazan to give me the opportunity to learn technical advices in vitro assays. A special thank for Dr. Farkas for the technical support and reactives provided without which some results could not have obtained during my thesis. Thank for your generosity Dr. farkas.

A Jose Manuel Rodríguez-Peña, te agradezco tu esfuerzo en inicial este proyecto, así como tu inestimable ayuda en el laboratorio tanto a la hora del diseño de experimentos y discusión de resultados, como de los muchos momentos de humor. Esta tesis también es parte tuya, así que espero que te guste.

Agradezco al Dr. Cesar Nombela por su inestimable apoyo durante el desarrollo de esta tesis y por contagiarnos a todos con su espíritu científico. A continuación, quiero dar las gracias a las directoras del departamento, en su momento María Molina y actualmente Concha Gil, por su dedicación y esfuerzo en mantener al departamento como un ejemplo tanto a nivel de investigación de excelencia como de familia unida.

Quiero agradecer a Víctor Cid por toda su ayuda y paciencia con el manejo del microscopio, sus consejos en la preparación de los manuscritos y por prestarme el plásmido pLA10. También quiero agradecer al resto de los profesores que siempre se han mostrado dispuestos a solucionar mis dudas y ayudarme en todo lo que les pedía. A Mar, Inma y Almudena, siempre me habéis solucionado todos mis problemas tan "urgentes", con una sonrisa y una gran efectividad. Charlar con vosotras siempre ha sido un placer. Vuestro trabajo es insustituible e imprescindible para el funcionamiento del departamento.

¡Benito y José Alberto, nadie como vosotros para alegrarme el día! Bajar y subir las escaleras era más divertido escuchándoos tararear: Noeeelia, Noeeelia, Noeeelia…! Os agradezco tooodaa vuestra ayuda durante estos años, siempre dispuestos, siempre alegres, siempre encontrabais la solución que necesitaba. ¡Sin vosotros sería muy difícil hacer experimentos! os echaré mucho de menos!

A los miembros de la Unidad de Genómica y Proteómica del Parque Científico de Madrid-UCM, en especial a Maribel García y Rosana Torremocha por toda su ayuda y paciencia en secuenciación. A Felipe Clemente, Lola Gutiérrez y Mª Luisa Hernáez por su ayuda con las huellas e identificación de mis proteínas. A los miembros del Centro de Citometría y Microscopía de Florescencia (UCM) en especial a Amalia Vázquez por su inestimable ayuda en el citómetro y a Agustín Fernández por la paciencia en la adquisición de las imágenes de M. electrónica.

Al entrar en la U4 me encontré con personas increíbles que formaban un grupo de trabajo unido, con ilusión por aprender e investigar, enamorados de su trabajo y encantados con la entrada de los "piolines". Quiero agradecerles su apoyo incondicional, su ayuda, sus ánimos y todos los buenos momentos que hemos compartido. Empezando por aquellos que se fueron: Cecilia, fuiste mi maestra, me enseñaste todo lo que el tiempo dejó y me diste muy buenos consejos. Fue difícil cubrir tu hueco porque eres una persona fabulosa. A pesar del poco tiempo compartido tienes un hueco en mi corazón. Clarichi!!, mi compi de poyata, mi amiga, mi guía, mi apoyo. Cuanto tengo que agradecerte!, cuanto he aprendido de ti!, que buenos momentos tengo en mi memoria. Tu marcha fue dura pero ver que a pesar de la distancia nuestra amistad y cariño prevalece me hace muy feliz. Conocerte en el labo ha sido una de las mejores cosas que me han pasado en la vida. Patricia, iniciamos juntas nuestras tesis y hemos compartido grandes momentos que atesoro en mi memoria. Raúl, eres el genio de la unidad, inteligente, bondadoso, siempre dispuesto a ayudar y a enseñar a todos!. Te agradezco tooodaa tu ayuda (que ha sido mucha) experimental, con las figuras, resolviendo mis dudas, enseñándome con el Adobe… y siempre con amabilidad. Mucho de este trabajo no hubiera sido posible sin ti. Sonia, me has ayudado mucho y he aprendido tantas cosas contigo que no sabes que afortunada me siento de haberte tenido tan cerquita porque gracias a ti siempre encontraba una respuesta a ¿Alguien sabe...? ¿Alguien me deja..?. Además siempre me han encantado tus Buenos Días Noe!, suena tan tierno. Belén, Belenchí la alegría de la unidad, siempre es agradable charlar contigo y echarse unas risas. Además tu espíritu trabajador nos contagia a todos. Eres un ejemplo de lucha y superación. Muchas gracias porque siempre me estás animando. Quique, mi actual compi de poyata!, muchas gracias porque me has hecho reír mucho y me has alegrado con tus piropos. Te deseo mucha suerte, que eres el siguiente, príncipe☺. Y aunque no era compi de unidad pero a efectos como si lo fuera, también quiero dar las gracias especialmente a Pablo, compi de doctorado, siempre me has ayudado en todo lo que te he pedido. Te deseo que te vaya súper bien, que te lo mereces por lo buena persona que eres.

Euge y Elvis, ¡¡¡ Amigaaas !!! Cuantos momentos buenos hemos compartido, llenos de risas y alegrías. Gracias por acompañarme en el día a día en esta fase de mi vida. Vuestra ayuda y compañía ha sido fundamental para el desarrollo de la tesis. Gracias por vuestro continuo y afectuoso apoyo, sois las mejores compañeras que he podido tener. Gracias por la motivación y el optimismo que llenaban nuestras comidas. Habéis sido mis aliadas y un ejemplo de lucha y amor por la tesis y la ciencia. Euge, mucho ánimo que estás en la recta final, ya no te queda nada, que vas a ser la siguiente!

A todos los compis de las demás unidades: Claudia, José Antonio, Vital, Carolina, Ana y Aída de la U1; Elvira, Dani, Carmen, Inés y Blanca de la U2; Isa, Teresa, Almu, María, María Olivier, Esmeralda y Ahmad de la U3; Andrea y Victoria de la U5 y Clarisa, Nacho y Leti de la U7, muchas gracias a todos por los buenos momentos pasados durante las cenas de navidad, celebraciones y desayunos; gracias por hacer que la estancia a lo largo de este tiempo haya sido muy agradable. ¡Os echaré de menos a todos!, aunque gracias al Facebook estaremos actualizados!

Quiero mostrar un agradecimiento especial a mis amigas más queridas: Lucia, Pilar, Teresa, Galardi, María, Elvira y Eugenia, que siempre habéis confiado en mi capacidad para finalizar este trabajo, animándome a seguir hasta el final. Gracias por vuestra compresión, paciencia y ánimo constantes. Gracias por estar pendiente de mí, por escucharme y darme tan buenos consejos. Con vosotras he aprendido, he crecido, he reído y he disfrutado de la vida. Siempre me levantáis el ánimo y conseguís que sea mejor persona. Os agradezco vuestra amistad incondicional y el "*lazo emocional*" tan bonito y fuerte que existe entre nosotras.

A Juanjo, quiero agradecerte toda tu ayuda en lograr esta meta profesional y el poder contar contigo en todo momento incondicional e desinteresadamente. Gracias por tu apoyo y cuidados. Gracias por compartir conmigo las cosas importantes de mi vida. Gracias por amarme como tú puedes hacer, trayendo más felicidad a mi vida. Me llenas por dentro y me permites dar el máximo de mí.

A mi hermana, Mª José por haber fomentado en mí el deseo de superación y el anhelo de triunfo en la vida. Mil palabras no bastarían para agradecerte tu apoyo, tu comprensión y tus consejos. Por estar conmigo, apoyarme, cuidarme y quererme siempre. Me siento muy orgullosa de ti y de la bella persona que eres, Te quiero.

Pero mi mayor agradecimiento se lo debo a mis padres porque son una indudable referencia y guía en mi camino. Vosotros me habéis infundado ética y rigor, habéis velado por mi bienestar y educación a lo largo de toda mi vida. Por ello, ahora os quiero dar las gracias por vuestra eterna entrega y capacidad para mantener mi ilusión, por enseñarme a luchar por lo que quiero y a terminar lo que he empezado. Gracias por el apoyo incondicional que me disteis a lo largo de la carrera, sin dudar ni un solo momento de mi inteligencia y capacidad. Gracias por apoyarme en todas las decisiones y darme la fortaleza para continuar. Porque el orgullo que sentís por mí, es la fuerza que me impulsa en todos los momentos de mi vida. Sin vosotros nunca habría terminado esta tesis doctoral. Es por vosotros que soy lo que soy ahora. Os quiero.

ÍNDICE

ÍNDICE.....15

ENGLISH SUMMARY 23

1. INTRODUCTION.....25

2. AIM 26

3. RESULTS.....26

4. CONCLUSIONS 30

ABREVIATURAS.....35

INTRODUCCIÓN.....41

1. LA PARED CELULAR DE *Saccharomyces cerevisiae*.....43

2. ESTRUCTURA, COMPOSICIÓN Y ORGANIZACIÓN DE LA PARED CELULAR.....44

2.1. ESTRUCTURA.....44

2.2. COMPOSICIÓN.....45

2.2.1. β-1,3 Glucano 46
2.2.2. β-1,6 Glucano 47
2.2.3. Quitina 48
2.2.4. Proteínas de pared.....50
2.2.4.1. Proteínas no unidas covalentemente a la pared celular 52
2.2.4.2. Proteínas unidas covalentemente a la pared celular 52
2.2.4.2.1. Proteínas GPI.....52
2.2.4.2.2. Proteínas PIR 53

2.3. ORGANIZACIÓN 53

3. BIOGÉNESIS DE LA PARED CELULAR.....54

3.1. DEGRADACIÓN DE LOS COMPONENTES 57

3.1.1. Glucanasas.....57
3.1.2. Quitinasas 59

3.2. SÍNTESIS DE LOS COMPONENTES.....60

3.2.1. Síntesis del β-1,3 glucano ... 60
3.2.1.1. Subunidad catalítica ... 60
3.2.1.2. Subunidad reguladora ... 61
3.2.2. Síntesis del β-1,6 glucano ... 62
3.2.2.1. Proteínas del Retículo Endoplasmático (RE) ... 63
3.2.2.2. Proteínas del Aparato de Golgi ... 64
3.2.2.3. Proteínas del citoplasma ... 64
3.2.2.4. Proteínas de la superficie celular ... 65
3.2.3. Síntesis de la quitina ... 65
3.2.3.1. Quitín-sintasa I ... 67
3.2.3.2. Quitín-sintasa II ... 67
3.2.3.3. Quitín-sintasa III ... 69

3.3. ENSAMBLAJE DE LOS COMPONENTES ... 72

3.3.1. Familia Gas ... 72
3.3.2. Familia Crh ... 73

4. MORFOGÉNESIS ... 76

4.1. CRECIMIENTO POLARIZADO ... 76

4.1.1. Selección del sitio de gemación ... 78
4.1.2. Polarización de Cdc42 ... 78
4.1.2.1. Proteín quinasas activadas por p21 (PAKs) ... 81
4.1.2.1.1. Ste20 ... 81
4.1.2.1.2. Cla4 ... 82
4.1.2.1.3. Skm1 ... 85
4.1.3. Polarización del citoesqueleto ... 85
4.1.3.1. Actina ... 85
4.1.3.2. Septinas ... 87
4.1.3.3. Anillo de quitina ... 90

4.2. CAMBIO DE CRECIMIENTO APICAL A ISOTRÓPICO ... 90

4.3. CITOQUINESIS ... 91

4.3.1. Reorganización del citoesqueleto ... 92
4.3.2. Formación del anillo citoquinético/actomiosina (AMR) ... 92
4.3.3. Formación del septo primario y secundario ... 93
4.3.4. Coordinación entre la constricción del AMR y la formación del septo ... 95
4.3.5. Separación celular ... 97

ANTECEDENTES ... 101

OBJETIVOS ... 107

RESULTADOS **111**

CAPÍTULO 1: Crh1 Y Crh2 SON RESPONSABLES DEL ENLACE ENTRE LA QUITINA Y EL GLUCANO EN LA PARED CELULAR DE Saccharomyces cerervisiae .. 113

RESUMEN DE LOS RESULTADOS DEL CAPÍTULO 1 115

ARTÍCULO 1: *Crh1p and Crh2p are required for the cross-linking of chitin to β(1-6)glucan in the Saccharomyces cerevisiae* 117

CAPÍTULO 2: Crh1 Y Crh2 ACTÚAN COMO TRANSGLICOSILASAS IN VIVO E IN VITRO 135

RESUMEN DE LOS RESULTADOS DEL CAPÍTULO 2 137

ARTÍCULO 2: *Assembly of the yeast cell wall. Crh1p and Crh2p act as transglycosylases in vivo and in vitro* 139

CAPÍTULO 3: PROPIEDADES CATALÍTICAS DE LAS TRANSGLICOSILASAS Crh1 Y Crh2 IN VIVO E IN VITRO 159

RESUMEN DE LOS RESULTADOS DEL CAPÍTULO 3 161

ARTÍCULO 3: *Catalytic properties and substrate specificity of Crh1 and Crh2 yeast cell wall transglycosylases in vivo and in vitro* 165

CAPÍTULO 4: ESTUDIO ESTRUCTURA-FUNCIÓN DE LA ACTIVIDAD TRANSGLICOSILASA DE Crh1 Y Crh2 195

RESUMEN DE LOS RESULTADOS DEL CAPÍTULO 4 197

ARTÍCULO 4: *Structural and functional analysis of yeast Crh1 and Crh2 transglycosilases* 201

CAPÍTULO 5: PARTICIPACIÓN DEL COMPLEJO QUITINA-β-1,3 GLUCANO EN LA MORFOGÉNESIS DE Saccharomyces cerevisiae 235

RESUMEN DE LOS RESULTADOS DEL CAPÍTULO 5 237

ARTÍCULO 5: *Presence of a large beta(1-3)glucan linked to chitin at the Saccharomyces cerevisiae mother-bud neck suggests involvement in localized growth control* 239

CAPÍTULO 6: IMPLICACIÓN DEL ENLACE ENTRE LA QUITINA Y EL GLUCANO EN EL CONTROL DE LA MORFOGÉNESIS DEL CUELLO DURANTE LA DIVISIÓN DE Saccharomyces cerevisiae 255

RESUMEN DE LOS RESULTADOS DEL CAPÍTULO 6 257

ARTÍCULO 6: *Cross-links in the cell wall of budding yeast control morphogenesis at the mother-bud neck* 259

DISCUSIÓN GENERAL 279

1. Crh1 y Crh2 SON LAS RESPONSABLES DEL ENSAMBLAJE DEL GLUCANO Y LA QUITINA EN LA PARED CELULAR DE LA LEVADURA 282

2. PROPIEDADES BIOQUÍMICAS DE LA REACCIÓN ENZIMÁTICA CATALIZADA POR Crh1 Y Crh2 288

2.1. DESARROLLO DE UN SISTEMA DE TRANSGLICOSIDACIÓN *IN VIVO* 288

2.2. DETERMINACIÓN DE LAS PROPIEDADES BIOQUÍMICAS DE LA REACCIÓN DE TRANSGLICOSILACIÓN *IN VITRO* 291

2.3 ESTUDIOS ESTRUCTURA-FUNCIÓN DE LAS PROTEÍNAS Crh 293

3. IMPLICACIÓN DEL ENLACE QUITINA-GLUCANO EN LA REGULACIÓN DE LA MORFOGÉNESIS 297

CONCLUSIONES 307

BIBLIOGRAFÍA 313

ENGLISH SUMMARY

1. INTRODUCTION

The cell wall is an essential structure that preserves the osmotic integrity of fungal cells, protects the cell from mechanical injury, regulates the uptake of substances and determines cellular morphology during cell division. The fungal cell walls is a potential targets not only for natural defences but also for antifungal agents of medical importance, considering that the cell walls contains substances that are often not found in the host cell such as polysaccharides, it may be possible to find drugs that are able to block their biosynthesis without interfering with the host metabolism.

The *Saccharomyces cerevisiae* cell wall is basically composed of mannosylated proteins, β-1,3 glucan, β-1,6 glucan and chitin. Glucans make up about half of the dry weight of the cell wall, while chitin accounts for only 1 to 5 %. Although chitin is the minor component, is essential for the formation of a proper primary septum during cytokinesis and for the characteristic ring-like structures at the mother-bud neck that leave a scar on the mother cell wall after cell division. The cell wall components are covalently linked to form macromolecular complexes, which are assembled to form the intact cell wall. The structure of the modules shows that there must be enzymes that link each pair of components and others that interlink the modules. The extracellular locations of the products of β-glucan and chitin suggest that these processes occur exterior to the plasma membrane. Because of their role in imparting form and their relatively simple composition, fungal cell walls have been widely used as a model for morphogenesis. Although this is an apparently rigid structure is very dynamic and it needs to be remodelled during morphogenetic processes involving changes in cell morphology. During this situation growth occurs at defined positions on cell surfaces and involves asymmetric growth from one region of the cell to form particular cell structures or shapes.

In contrast to the knowledge about the synthesis of the components, little is known about the mechanisms by which cross-links between the different components are created. In our laboratory, we have described a novel family of cell wall related proteins: Crh1, Crh2 (Congo Red Hypersensitive) and Crr1 (CRH-related). A defect in Crh1 and Crh2 causes hypersensitivity to certain drugs as Congo Red and Calcofluor White, indicating some abnormality in the cell wall. These proteins, which are differently expressed during

the life cycle, are involved in cell wall assembly. Crh1 and Crh2, which are both GPI-anchored cell wall proteins, localize to polarized growth sites. This localization is reminiscent of the distribution of chitin at the cell wall. Chemical fractionation of isolated cell walls from wild type WT and *crh1*Δ, *crh2*Δ and *crh1*Δ *crh2*Δ mutants was carried out to detect possible modifications in the distribution of cell wall polymers. The alkali-soluble fraction was almost doubled in the *crh1*Δ *crh2*Δ strain compared to that in the WT, in detriment to the alkali insoluble fraction. Collectively, all data suggest a probable role for these proteins in the cross-linking quitin to other components.

2. AIM

The overall objective of this thesis has been the characterization of the proteins Crh in relation to processes of the cell wall biogenesis and the morphogenesis of *Saccharomyces cerevisiae*.

3. RESULTS

We analyzed the complexes present in the cell wall of WT, *crh1*Δ, *crh2*Δ and *crh1*Δ *crh2*Δ mutants by using a recently developed strategy. This strategy is based on the carboximethylation, before or after digestion with β-1,3- or β-1,6-glucanase, followed by size chromatography, for the solubilization of the cell wall complexes. The obtained results were the following: chitin linked to β-1,6 glucan is diminished in mutants of the *CRH1* or *CRH2* gene and completely absent in the double mutant. This indicates that Crh1 and Crh2 ferry chitin chains to β-1,6 glucan. The chitin- β-1,3 glucan complexes were slightly diminished in *crh1*Δ when compared to *crh2*Δ where the decrease is more evident. In the *crh1*Δ *crh2*Δ double mutant the chitin- β-1,3 glucan complexes is totally absent, indicating that all chitin appeared to be free. Therefore, Crh1 and Crh2 transfer chitin to β-1,3- and β-1,6 glucan and the biosynthetic mechanism for all chitin cross-links in the cell wall has been established.

To explore the linking reaction *in vivo* we used fluorescent sulforhodamine-linked laminarin-oligosaccharides (β-1,3 glucan) and pustulan-oligosaccharides (β-1,6 glucan) as artificial acceptors. *In vivo*, fluorescence was detected mainly in bud scars and at a lower

level in the cell contour, both being dependent on the Crh proteins since deletions in both *CRH1* and *CRH2* genes were similar in aspect to the *chs3*Δ mutant. There are three possible sources of chitin for cross-linking's to oligosaccharide: the portion of the ring chitin that is still free, the chitin in the primary septum and the newly formed chitin near the plasma membrane. The binding of the fluorescent material to chitin was verified by chitinase digestion. The intensity of the fluorescence clearly increases with the length of the oligosaccharide chain. Since we had observed that N-acetyl chitooligosaccharides (ChitoOS) were acting as effective inhibitors of β-1,3-linked oligosaccharide incorporation into the cell walls, we explored their ability to serve as acceptors as well. In fact, ChitoOS were found to incorporate with the same pattern of fluorescence localization and with the same high efficiency as the β-1,3- and β-1,6-linked oligosaccharides in WT strain. We characterized the involvement of Crh proteins in the crosslinking of different acceptors to chitin in the cell wall with the three types of oligosaccharides. The fact that there was not fluorescence incorporation in the double mutant indicates that there is no transglicosylation in the absence of both proteins. The comparison of the fluorescence incorporated into the single mutants with respect to the WT revealed that the crosslinking is mainly dependent on Crh2 for β-1,6-linked oligosaccharides and ChitoOS. However, the fluorescence incorporation for β-1,3-linked oligosaccharide depends in this case on both enzymes.

For *in vitro* assays, the proteins encoded by *CRH1* and *CRH2* were heterologously expressed in *Pichia pastoris* and a sensitive fluorescent *in vitro* soluble assay were devised for determination of their transglycosylation activities. Both proteins act as chitin transglycosylases, since they use soluble chitin derivatives such as carboximethyl-chitin, glycol-chitin and N-acetyl chitooligosaccharides as donors and chitin, β-1,3- and β-1,6-linked oligosaccharides as acceptors. We identified the minimal number of hexopyranose units required by Crh proteins in the acceptor oligosaccharide as two and the efficacy of the acceptor increases with increasing the length of the chain. The optimum pH of both enzymes was 3.5 and the temperature is 37ºC. Divalent cations as well as 1mM EDTA did not significantly influence the reaction. Both Crh1 and Crh2 proteins lost about 50% activity upon heating at 95ºC for 15 min. The product obtained by the reaction with CM-chitin as the donor and laminarin-oligosaccharides as the acceptor is a high-Mr polysaccharide containing incorporated fluorescent label. The IR (Infrared) spectra of the principal fluorescent fragments after chitinase treatment exhibited similar features as those reported for the spectrum of CM-chitin. In agreement with their incorporation into the cell

wall of living yeast, Crh proteins are responsible for the crosslinking's between CM-chitin as donor and Chito-OS, β-1,3- and β-1,6-linked oligosaccharides as acceptors. According to *in vivo* results, the Michaelis-Menten constants obtained with ChitoOS and β-1,3-linked oligosaccharides as acceptors showed the ChitoOS binds to the enzymes more ready than the β-1,3-linked oligosaccharides. The result of Dixon graph indicates that the ChitoOS inhibited the transglycosylation between CM-chitin and Laminarin-oligosaccharides, as previously observed in vivo, and the inhibition was of competitive nature in relation to the acceptor. Both proteins exhibited a weak chitinolytic activity measured in different assays. The rate of CM-chitin degradation by Crh1 was markedly stimulated by ChitoOS. In order to distinguish between exochitinase and endochitinase activities, specific substrates were used. The results show that both enzymes act as endochitinases although the prevailing modes of action may be different.

Morphogenesis is a fundamental process in all organisms that must be rigorously controlled to ensure the correct growth. A specialized portion of the cell wall of *Saccharomyces cerevisiae*, the septum, has been studied for many years as a model for morphogenesis. During the cell cycle, the bud and the cell wall are continuously growing. However, there is an area between mother and daughter cell termed the neck which does not change after budding initiation. Previous data suggest that chitin ring and septins ring collaborate to preserve the widening of the neck. How does the chitin ring control morphogenesis at the neck? We reasoned that chitin might be mostly linked to at β-1,3 glucan in view to the high concentration of chitin at the neck. Thus it would compete with the attachment to the same sites of β-1,6 glucan, which is linked to the cell wall after β-1,3 glucan is synthesized. As consequence, mannoproteins also could not become part of the cell wall. Thus, synthesis of the cell wall at the neck would eventually be stopped. In order to check this hypothesis, firstly, we explored whether the linkage of chitin to β-1,3 glucan may prevent the remodelling of this polysaccharides that would be necessary for cell wall growth. The study of isolated β-1,3 glucan from cell wall, by a novel mild procedures, gave rise to a very high-molecular-weight peak and to highly polydisperse material. The first material corresponds to the final cross-linked structural product whereas the latter corresponds to glucan that is being remodelled. By alkali treatment and chromatography on wheat germ agglutinin-agars, it was shown that the β-1, 3 glucan attached to chitin consists mostly of a high-molecular-weight peak. Therefore, it appears that the linkage to chitin

results in a polysaccharide that cannot be further remodelled and does not contribute to growth at the neck.

Then, we analyzed whether the mere presence of chitin would not block growth at the neck, unless the chitin is glucan-bound. We showed that Crh1 and Crh2 act as transglycosylases to transfer chitin to β-1,3 glucan and β-1,6 glucan. Armed with this knowledge, we could demonstrate that the binding of chitin to glucan controls growth at the neck, by deleting *CRH1* and *CRH2* in a *cla4*Δ mutant, thus eliminating chitin-glucan linkages without presumably affecting chitin content. The mutant *crh1*Δ *crh2*Δ *cla4*Δ grew very slowly and showed wide and growing necks, elongated bud and swollen cells with large vacuoles. This aberrant morphology matched that of *chs3*Δ *cla4*Δ. A similar behaviour was observed by inhibition of the Crh proteins with ChitoOS. Single deletions of *CRH1* or *CRH2* in a *cla4*Δ strain led to cells with an intermediate morphology. Crh2 function seemed to be more important than that of Crh1, because *crh2*Δ *cla4*Δ cells were considerably more abnormal than *crh1*Δ *cla4*Δ. The morphological defects of the triple mutant were completely corrected by transformation with a plasmid carrying, *CLA4* and partially by plasmids carrying *CRH1* and *CRH2*. By contrast, plasmids harbouring mutations of *CRH1* and *CRH2* in the putative glutamyl proton donor did not complement the defect. Despite the anomalous morphology, nuclear division seemed to take place efficiently in the triple mutant. The same cannot be said for septin organization and localization. Often septa were abnormal, as visualized by electron microscopy. We were also able to obtain a quadruple mutant, *chs3*Δ *crh1*Δ *crh2*Δ *cla4*Δ. The phenotype of this strain is the same as that of *crh1*Δ *crh2*Δ *cla4*Δ or *chs3*Δ *cla4*Δ, confirming that Crh1 and Crh2 are not operative en the absence of Chs3. The bud elongation observed in the triple mutant probably results from the neck widening, which leads to disorganization of the septin ring and subsequent activation of the morphogenesis checkpoint. We then deleted *SWE1*, protein kinase responsible of apical growth, in the triple mutant. As expected, the length of the buds decreases dramatically, but no completely, however the necks remained wide. Because of the crucial importance of events at the neck, we measured neck diameter in the different strains. We detected a small increase in diameter going from WT to a *cla4*Δ strain. The necks of the triple mutant were much wider, in fact even wider than those of the *chs3*Δ *cla4*Δ strain, whereas those of the triple mutant deleted for *SWE1* showed only a small decrease relative to *crh1*Δ *crh2*Δ *cla4*Δ. In summary, lack of linkages between the chitin ring and β-1,3 glucan at the mother-bud neck leads to neck growth and consequent

widening. Thus, this is a clear case in which a specific chemical bond between two substances is essential for the control of morphogenesis.

4. CONCLUSIONS

1) Crh1 and Crh2 proteins are responsible for the formation of links chitin-glucan of the cell wall of *Saccharomyces cerevisiae*. Thus, in the absence of these proteins, chitin no cell wall glucan is covalently attached. The two proteins are functionally redundant, although Crh2 activity has a more important role in the formation of these links in normal yeast growth.

2) Under stress, by increasing temperature, an increase in the fraction bound to chitin β-1, 6 glucan, dependent Crh1, Crh2 and the MAP kinase cell integrity Slt2. Under these conditions, induces the expression of *CRH1* and also Crh1 and Crh2 both are redistributed in the side wall.

3) The simultaneous deletion of *CRH1* and *CRH2* not affect yeast growth under normal conditions, but significantly aggravates the phenotype of the mutants and *gas1*Δ *fks1*Δ, indicating an essential role of chitin-glucan binding to cell survival in situations which the cell wall integrity is compromised.

4) Using fluorescent oligosaccharides derived from β-1, 3 glucan as acceptors, various systems have been developed transglycosylation in living cells, and permeabilized cells isolated cell walls. In all cases the formation occurs chitin-glucan linkages by transglycosylation of the donor molecule (nascent chitin or pre-existing) to acceptor (β-1, 3 glucan or β-1, 6 glucan) dependently Crh1 and Crh2 proteins. We have developed an in vitro system transglycosylation soluble chitin-glucan, proteins using recombinant Crh1 and Crh2 expressed in *Pichia pastoris*. Tranglicosilation reaction is enzymatic nature.

5) Using this system, soluble in vitro have been studied the catalytic properties of Crh1 and d Crh2. Both proteins developed using carboxymethylchitin transglycosylation reactions, glycol chitin or chito-oligosaccharides as donors and β-1, 3 gluco-oligosaccharides, β-1 ,6-gluco-oligosaccharides and quito-oligosaccharides as acceptors, the latter being more

efficient acceptors followed by β-1, 3 gluco-oligosaccharides. This reaction, which requires at least 2 hexopyranose units at the non reducing end of acceptor, is competitively inhibited in the presence of N-acetyl-chitotriose. Furthermore, both as Crh1 and Crh2 chitinolytic have some activity, which in the case of Crh1 is stimulated in the presence of chito-oligosaccharides and laminarin-oligosaccharides.

6) The data of the transglycosylase activity in vitro correlate well with the incorporation of the labeled oligosaccharides with sulforhodamine various in vivo. These in vivo experiments have confirmed the functional redundancy and Crh1 and Crh2. Crh2 greater relevance regarding the incorporation of various acceptors to the yeast cell wall.

7) Was generated and validated by mutagenesis and transglycosylase activity assays in vivo structural model Crh1, based on known three-dimensional structure of a β-1,3-1, 4 glucanase (lichenasa) from *Paenibacillus macerans*, belonging to the family GH16 of glycosyl hydrolases. Residues Glu134 (acid / base), Asp136 and Glu138 (nucleophile) of the active center Crh1 theoretical and Crh2 counterparts, are essential for catalysis. Other residues probably involved in binding of sugars, such as W219, F152 and Y160 are also important for the transglycosylase activity of Crh1.

8) Crh2 shows a family 18 carbohydrate binding domain (CBM). Mutations in residues P38, S41, Y43, G44, G47, Y51 and F62 of this domain dramatically decrease of Crh2 transglycosylase activity, whereas the G49 residue is essential for this activity. Furthermore residues C33, C39 and C40 of this domain are essential for the stability of the protein.

9) Based on the results of this work, we propose a model for Crh1 and Crh2 mediated catalysis that include double displacement mechanism similar to other glycosyl hydrolase family 16 (GH16) with bond breaking β-1, 4 of the chitin molecule and the subsequent transfer of the fragment through the new reducing end generated by non-reducing end of the acceptor, β-1, 3 glucan or β-1, 6 glucan.

10) Morphology mutant *crh1*Δ *cla4*Δ *crh2*Δ, together with the location of the links chitin-β-1, 3 glucan and chitin, β-1, 6 glucan in the cell wall and the characterization data of the size of β-1.3 free glucan (polydispersed) and attached to chitin (large size), supporting the

idea that in the neck, the binding of chitin to glucan blocks the metabolism of this latter and thus the growth of the cell wall at this location.

11) Morphological defects loss of growth control in the neck of the yeasts during its division are observed in both mutant *cla4*Δ *chs3*Δ, chitin ring lacking, as in *crh2*Δ *crh1*Δ *cla4*Δ mutant, possessing chitin ring but bonds have lost chitin-glucan. Therefore, chitin-glucan binding is essential to control morphogenesis in the neck.

ABREVIATURAS

Δ Deleción

µm Micra

β-1,3-OS-SR Oligosacárido de glucosas unidas β-1,3 fusionado a sulforodamina

β-1,6-OS-SR Oligosacárido de glucosas unidas β-1,6 fusionado a sulforodamina

AMR Anillo de actomiosina (*Actomyosin Ring*)

AQ Anillo de quitina

ATP Adenosín trifosfosfato

ºC Grados centígrados

CBM Módulo de unión a carbohidratos (*Carbohydrate-Binding Module*)

CDK Quinasa dependiente de ciclina *(Cyclin-Dependent Kinase*)

CFW Blanco de Calcoflúor (*Calcofluor White*)

CM-quitina Carboximetil quitina

CM-quitina-RBV Carboximetil quitina Violeta brillante de remazol (*Carboxymethyl-chitin-Remazol Brillant Violet*)

CS Quitín sintasa *(Chitin Syntase)*

CSI Actividad quitín sintasa I

CSII Actividad quitín sintasa II

CSIII Actividad quitín sintasa III

CWPS Proteínas de pared celular (*Cell Wall Proteins*)

DAPI 4',6-diamindino-2-fenilindol

Dp Grado de polimerización

DTT Ditiotreitol

EDTA Ácido etilendiamino tetra acético

GAP Proteína activadora de GTPasa (*GTPase Activating Protein*)

GDP Guanosín difosfato

GEF Factor intercambiador de GTP (*Guanine nucleotide exchange factor*)

GFP Proteína fluorescente verde (*Green Fluorescent Protein*)

GH Familia glicosilhidrolasa

GPI Glicosil fosfatidil inositol

GS Glucán sintasa

GTP Guanosín trifosfato

GTPasa Guanosín trifosfatasa

HA Hemaglutinina

kDa Kilodalton

KRE Familia de proteínas de pared (*killer toxin resistant*)

MAPK Proteín quinasa activada por mitógeno (*Mitogen Activated Protein Kinase*)

MU Metilumbeliferona

NAG N-acetil-glucosamina

nm Nanómetros

PAK Quinasa activada por P21 (*p21-Activated Kinase*)

pH Potencial de Hidrógeno

PH Dominio tipo plectrina (*Plekstrin Homology domain*)

PIR Proteínas de repeticiones internas unidas mediante enlaces covalentes (*Proteins with Internal Repeats*)

Quito-OS Oligosacáridos de quitina

Quito-OS-SR Oligosacáridos de quitina fusionados a sulforodamina

RC Rojo Congo

RE Retículo endoplasmático

RNA Ácido ribonucleico

RNAm Ácido ribonucleico mensajero

SDS Dodecil sulfato sódico

SH3 Dominios con homología a Src (*Src Homology 3*)

SR Sulforodamina

SR-oligosacárido Oligosacáridos fusionado a sulforodamina

T^{a} temperatura

UDP Uridil difosfato

UV Ultravioleta

ZL Zimoliasa

WGA *Wheat germ agglutinin*

WT cepa silvestre *(Wild type)*

INTRODUCCIÓN

1. LA PARED CELULAR DE *Saccharomyces cerevisiae*

La levadura *Saccharomyces cerevisiae* presenta unas características que han hecho de ella un formidable organismo modelo de células eucariotas superiores. *S. cerevisiae* es un hongo unicelular que posee una envoltura nuclear que separa al núcleo del citoplasma. Fue el primer organismo eucariota en ser secuenciado y actualmente es el genoma eucariota mejor conocido. La comodidad de su manejo y su corto tiempo de generación, han permitido que esta levadura haya ganado protagonismo en el laboratorio. Su uso frecuente en investigación básica ha proporcionado un enriquecimiento en el estudio de los mecanismos moleculares que gobiernan la expresión génica y la reprogramación genética, en procesos generales de biología y fisiología celular, en sistemas de señalización celular, etc.

La pared celular fúngica es una estructura que rodea la célula y es de vital importancia para la protección de misma, ya que permite soportar el estrés osmótico al que se haya sometida en el medio natural. A su vez, es responsable de la forma de la célula convirtiéndola en un modelo idóneo para el estudio de la morfogénesis (Duran and Nombela, 2004; Klis et al., 2006; Latge, 2010; Lesage and Bussey, 2006; Levin, 2011; Orlean, 2012). Adicionalmente, la pared celular desempeña importantes funciones en la vida de las células:

- Funciona como una barrera física o filtro evitando tanto la entrada como la salida de grandes moléculas.
- Contiene proteínas que juegan un papel en el apareamiento, el dimorfismo, la aglutinación celular, la interacción con otros organismos y con el medio ambiente, etc.
- Engloba una alta variedad de antígenos reconocidos por el sistema inmunitario del hospedador.
- En ella se localizan diferentes enzimas implicadas en el propio metabolismo de la pared celular (sintasas, transglicosilasas) y enzimas necesarias para la ruptura y asimilación de nutrientes (lipasas, proteasas, fosfatasas).
- Sirve como lugar de anclaje transitorio de enzimas que son secretadas por la célula y posteriormente liberadas al medio externo.

- Algunos de sus componentes, en determinadas circunstancias, pueden servir como reserva de nutrientes.

La pared celular fúngica es una estructura esencial no solo para el mantenimiento de la morfología celular sino también para la protección de la célula frente a las diversas condiciones adversas del medio externo (Levin, 2005; Lipke and Ovalle, 1998). Además, la mayoría de sus componentes están ausentes en la matriz extracelular de células de mamífero, lo que convierte en crucial la caracterización de todos los procesos relacionados con la biogénesis y el mantenimiento de esta estructura para la posible identificación de nuevas dianas terapéuticas. El logro de este objetivo se ve facilitado por la similitud existente entre los procesos de construcción de la pared celular de la levadura *S. cerevisiae* con otros hongos patógenos como los pertenecientes a los géneros *Cándida* o *Aspergillus* (Arroyo et al., 2007; Beauvais et al., 1997; Klis et al., 2002; Nierman et al., 2005). De hecho, en los últimos años se han introducido en la clínica varios antifúngicos inhibidores de la glucan sintasa (GS) de la familia de las equinocandinas (Caspofungina, Anidulafungina, Micafungina) que tienen como diana la síntesis de β-1-3 glucano (Hector and Bierer, 2011; Sucher et al., 2009).

2. ESTRUCTURA, COMPOSICIÓN Y ORGANIZACIÓN DE LA PARED CELULAR

2.1. ESTRUCTURA

La visualización al microscopio electrónico de la pared celular pone de manifiesto una organización laminar (figura 1A). Así, se distingue una capa interna de aspecto amorfo y transparente al paso de los electrones y orientada paralelamente a la membrana citoplasmática, y otra capa externa de apariencia fibrosa y densa al paso de los electrones (Osumi, 1998), constituida principalmente por manoproteínas (figura 1A) (Cappellaro et al., 1994; Lipke and Ovalle, 1998). La capa interna, de unos 70-100 nm de grosor, es la que proporciona la fuerza mecánica de la pared celular y está compuesta por glucano y quitina que en conjunto suponen entre el 60-70% del peso seco de la pared celular. Dentro de esta capa nos encontrarnos con una parte externa rica en β-1,6 glucano y una parte

interna más cercana a la membrana plasmática rica en β-1,3 glucano y quitina (Horisberger and Vonlanthen, 1977; Kopecka et al., 1974; Shaw et al., 1991).

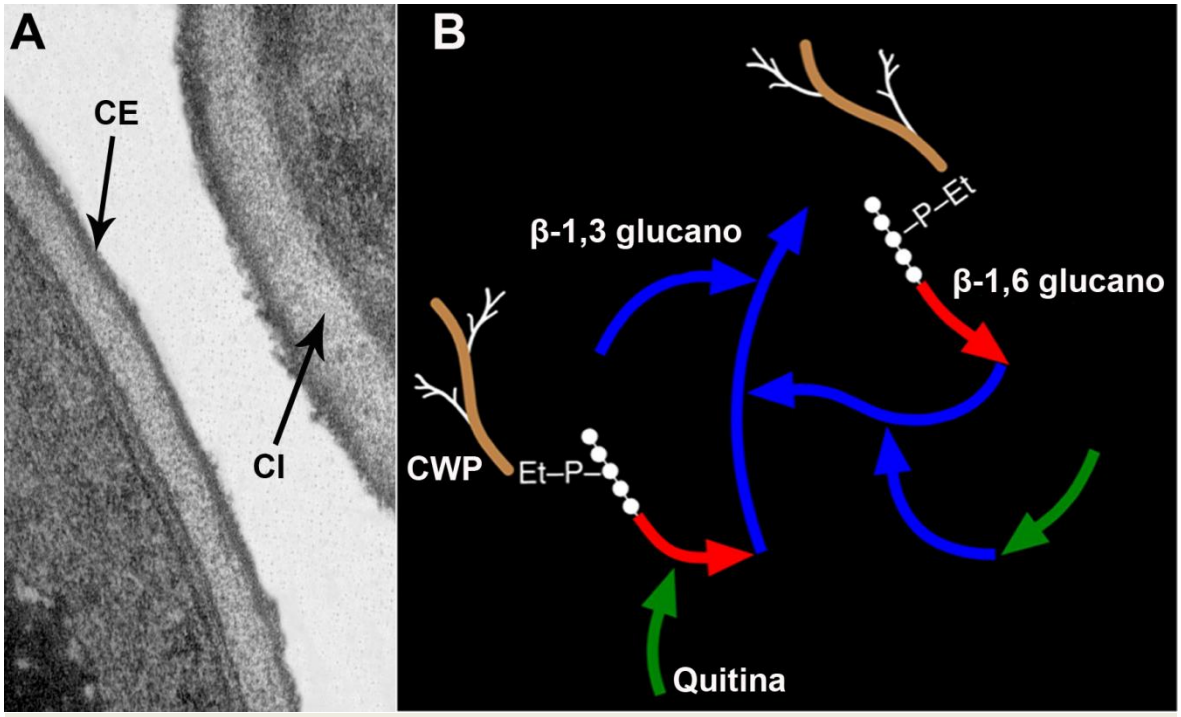

Figura 1. Estructura de la pared celular. A, fotografía de microscopía electrónica de la pared celular. En ella se distingue la estructura en bicapa de la misma: capa externa (CE) y capa interna (CI). B, imagen modificada de Cabib, Blanco et al. (2012). En ella se muestra un modelo molecular de los enlaces que establecen los componentes entre sí. El β-1,3 glucano está representado en azul, el β-1,6 glucano en rojo, la quitina en verde, las manoproteínas en marrón (CWP) y el anclaje GPI mediante residuos de etanolamina-fosfato (Et-P). El β-1-6 glucano se une por su extremo reducido al β-1-3 glucano y por su extremo no reducido a las manoproteínas tipo GPI. La quitina se une por su extremo reducido al extremo no reducido del β-1-3 glucano o del β-1-6 glucano.

2.2. COMPOSICIÓN

La pared celular fúngica con un grosor entre el 0.1-0.2 μm representa el 20%-25% del peso seco de la célula (Fleet, 1985; Klis, 1994). Su principal componente son los carbohidratos en forma de polisacáridos o glicoproteínas, que constituyen cerca del 85-90% del peso seco. El resto de componentes son proteínas, lípidos y sales inorgánicas (Bartnicki-Garcia, 1968; Nguyen et al., 1998).

Existen tres tipos de polisacáridos en la pared celular (figura 1B). En primer lugar polímeros de glucosas unidos mediante enlaces β-1-3 o β-1,6, formando el β-1,3 glucano y el β-1,6 glucano respectivamente (Cabib et al., 1988; Ruiz-Herrera, 1991). El segundo

polímero mayoritario está constituido por manosas unidas covalentemente a las proteínas formando las manoproteínas (Cappellaro et al., 1994; Lipke and Ovalle, 1998). Existe un tercer polímero formado por residuos de N-acetil-glucosamina (NAG) unidos mediante enlaces β-1,4 que forman la quitina (figura 1B) (Minke and Blackwell, 1978; Muzzarelli et al., 1979). La quitina está presente en la pared celular como componente minoritario. Los enlaces que se establecen entre los diferentes polímeros, proporcionan a la pared celular su fuerza mecánica. Estos enlaces pueden ser tanto covalentes, como los existentes entre el glucano y la quitina, el glucano y las manosas y las proteínas y las manosas; o no covalentes como puentes de hidrógeno o fuerzas Van der Waals que contribuyen a la interacción individual de cada componente (Farkas, 1990; Farkas, 2003).

Una primera aproximación para la caracterización de los componentes de la pared celular es su solubilización y/o extracción mediante tratamientos con álcali. Así, se identifica una fracción álcali soluble y una fracción álcali insoluble. La fracción álcali insoluble está compuesta por glucano y quitina (Elorza et al., 1987; Hartland et al., 1994; Roncero et al., 1988b). La extracción de los glucanos de la pared celular depende de su longitud y de su asociación con otros componentes. Generalmente, la solubilización de glucanos con álcali es baja, obteniéndose mayoritariamente cadenas de corta longitud y pocas ramificaciones. Para la extracción de polímeros de glucanos unidos mediante enlaces β-1,3 y β-1,6 altamente ramificados, la pared celular debe someterse a un tratamiento con ácido acético y calor tras el tratamiento con álcali (Manners et al., 1973a). Tras este tratamiento el material liberado está formado predominantemente por cadenas lineales de β-1,3 glucano (Fleet, 1985). La insolubilidad del glucano se aumenta con su unión a la quitina, que es insoluble en agua (Mol, 1987). Las manoproteínas son extraídas fácilmente de la pared celular a través de un tratamiento con tampón citrato a pH neutro o con álcali a bajas Tª. Los productos obtenidos son heterogéneos en cuanto al tamaño y el contenido en azúcar.

2.2.1. β-1,3 Glucano

Este glucano es el componente estructural más abundante de la pared celular, constituyendo entre el 50-60 % de su peso seco (Klis et al., 2006; Klis et al., 2002). Es un polímero lineal de glucosas unidas con enlaces β-1,3 con un grado de polimerización de

aproximadamente 1500 unidades por cadena y 600 nm de longitud (Manners et al., 1973a). La asociación lateral de tres o más cadenas entre sí, mediante puentes de hidrógeno, forman fibras (Kopecka et al., 1974). La visualización intacta de una fibra al microscopio electrónico determinó que el grosor de la fibra variaba entre 10 ó 30 nm de diámetro, dato que concuerda con la asociación de tres o más cadenas, ya que cada cadena posee un diámetro variable entre 0.5 a 1 nm (Kopecka and Kreger, 1986). Las cadenas y las fibras adquieren una conformación helicoidal que puede existir con varios grados de extensión permitiendo una alta flexibilidad y elasticidad (Krainer et al., 1994).

Las cadenas de β-1,3 glucano están ramificadas con glucosas enlazadas a través de uniones β-1,3 y β-1,6. Cada 40-50 glucosas, el carbono en la posición 6 es susceptible de ser ramificado (Fleet, 1991). El grado de polimerización de las cadenas varía dependiendo de la fase de crecimiento y la fuente de carbono (Cabib et al., 1998). Las cadenas de β-1,3 glucano se encuentran unidas al β-1,6 glucano y a la quitina a través de su extremo no reducido, mientras que por su extremo reducido se encuentra unido a las manoproteínas (figura 1B) (Kollar et al., 1995; Kollar et al., 1997; Mrsa et al., 1999). La alta ramificación del glucano, junto con su asociación con los demás componentes proporcionan a la pared celular una elevada fuerza mecánica (Cid et al., 1995).

2.2.2. β-1,6 Glucano

Es un polímero de aproximadamente 350 residuos de glucosa unidas entre sí a través de enlaces β-1,6, que en su forma madura presenta un alto grado de ramificación (aproximadamente en un 15% de sus residuos) con cadenas de β-1,6 glucano (Kollar et al., 1997; Magnelli et al., 2002). Representa el 10% del total de la pared celular (Manners et al., 1973b). La mayor parte del β-1,6 glucano queda expuesto hacia el exterior, sirviendo como puente de unión de las glicoproteínas con la capa interna de la pared celular (Kollar et al., 1997). Entre otras funciones, también actúa como receptor de la quitina que aumenta en condiciones de estrés (Kapteyn et al., 1997).

2.2.3. Quitina

Es un polímero lineal de residuos NAG unidos mediante enlaces β-1,4 (Ruiz-Herrera and Martinez-Espinoza, 1999). Las diferentes cadenas de quitina se asocian entre sí mediante puentes de hidrogeno establecidos entre el grupo amino de una cadena y el grupo carboxilo de la cadena adyacente formando fibras (Carlstrom, 1957; Minke and Blackwell, 1978). El alto número de puentes de hidrógeno establecidos entre las cadenas, así como su estructura en fibra, hacen de la quitina un polímero insoluble en agua (Muzzarelli et al., 1979). Las fibras de quitina son polimorfas, existiendo tres isoformas en las que podemos encontrar a la quitina en función de la orientación de las cadenas: α, β, γ.

Una de las razones del amplio estudio de la quitina presente en los hongos es por su papel esencial en la morfogénesis celular, tanto por su contribución a la formación del septo como de la pared celular (Cabib, 2004; Cabib et al., 1982; Cabib et al., 2001). Gracias a estos estudios se sabe que la quitina presente en la pared celular de la levadura *S. cerevisiae* representa un 1-3% del total del peso seco de la misma (Fleet, 1985; Molano et al., 1980). El tamaño de las cadenas en *S. cerevisiae* puede variar entre 100-200 unidades en función del momento del ciclo celular en el que se encuentre la célula, así como su estado: libre o unida al glucano (Cabib, 1987; Kollar et al., 1995). La cuantificación de las diferentes fracciones, quitina libre y unida a los diferentes glucanos, fue posible gracias a la metodología desarrollada por los doctores E. Cabib y A. Durán, mediante carboximetilación de la misma y cromatografía de exclusión (Cabib and Duran, 2005). Así, un 43% de la quitina total se encuentra en estado libre, un 41% se encuentra unida al β-1,3 glucano y por último el 16% es quitina unida al β-1,6 glucano (Cabib, 2009; Cabib and Duran, 2005).

La quitina en la pared celular se encuentra fundamentalmente en cuatro localizaciones diferentes (figura 2A): en la base de la yema en forma de anillo; en el septo primario (SP) entre la célula madre y la célula hija; en las cicatrices que presenta la célula madre después de la división celular y uniformemente repartida por la pared lateral (Cabib et al., 2001; Horisberger and Vonlanthen, 1977; Molano et al., 1980). El depósito de quitina en *S. cerevisiae* es un proceso asociado a ciclo celular (Roberts et al., 1983) y está controlado tanto espacial (Cabib and Bowers, 1975; Molano et al., 1980) como

temporalmente (figura 2A) (Bulawa, 1993; Cabib, 1987). Durante el inicio de la gemación, se forma el anillo de quitina (AQ) en la base de la yema que permanece intacto durante el crecimiento de la misma y que quedará en el lado de la madre tras la separación celular (figura 2b y 2e). Este anillo de quitina contiene el mayor porcentaje de quitina presente en la pared celular y es sintetizado por la CSIII. Al final de la mitosis se produce la formación del septo primario llevado a cabo por la enzima CSII. El septo primario se deposita en el cuello de manera centrípeta entre la madre y la hija y constituye aproximadamente el 10% de la quitina total (figura 2c). Adicionalmente a estas dos estructuras ricas en quitina y que posteriormente formarán parte de la cicatriz de la célula madre tras la división celular (Cabib and Bowers, 1971), la célula hija presenta una pequeña cantidad de quitina en la pared lateral sintetizada por la enzima CS III que se deposita tras la citoquinesis (figura 2d) (Shaw et al., 1991). De este modo, se cierra el ciclo de división generando dos células listas para volver a dividirse (figura 2e).

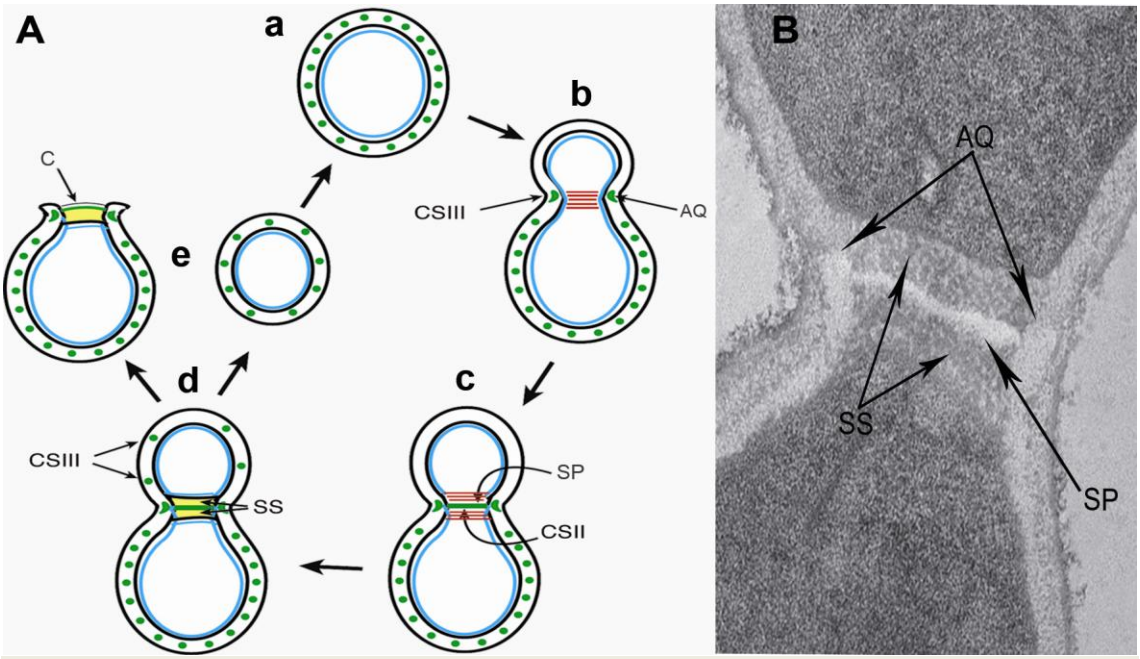

Figura 2. Depósito de la quitina en la pared de la levadura durante el ciclo celular. La imagen 2A ha sido modificada de Cabib and Duran (2005). En ella se muestra una célula adulta preparada para gemar. La quitina se encuentra dispersa por la pared lateral, señalizada como puntos verdes (a). En la imagen b, se observa la célula con el anillo de quitina formado (AQ) en la base de la yema por la quitín-sintasa III (CSIII) al inicio de la gemación. Al final de la mitosis, se lleva a cabo la formación del septo primario (SP) gracias a la acción de la quitín-sintasa II (CSII) (c). Al comienzo de la citoquinesis se deposita el septo secundario (SS) a ambos lados del septo primario y comienza la síntesis de la quitina en la pared lateral de la célula hija por la acción de la CSIII (d). El depósito de quitina en la pared lateral de la célula continúa hasta alcanzar su maduración. Tras la separación celular (e), la célula madre conserva los restos de quitina procedentes del AQ y del SP formando parte de la cicatriz (C). La imagen 2B es una fotografía de microscopia electrónica del septo. En ella se puede distinguir el anillo de quitina (AQ) que rodea al septo primario (SP) y al septo secundario (SS). El SP se encuentra flanqueado a ambos lados por el SS.

2.2.4. Proteínas de pared

Las manoproteínas o proteínas de la pared (CWP) están formadas por una o varias cadenas de polisacáridos, generalmente manosas, de tamaño variable unidas covalentemente a una proteína (Ballou, 1976). Las CWP son el componente mayoritario de la capa externa de la pared celular y constituyen entre el 30-50% del peso seco de la misma (Orlean, 1997). Son fácilmente liberadas tras un tratamiento con álcali a bajas Tª o con β-1,6 glucanasa, dejando al descubierto la capa interna de la pared celular (Kopecka et al., 1974). Las manoproteínas están participando en múltiples funciones:

- Limitan la porosidad celular gracias al enlace N-glicosil entre la proteína y el glúcido (de Nobel et al., 1990; Zlotnik et al., 1984). La limitada porosidad evita la pérdida de pequeños precursores de proteínas de pared y ofrece una protección extra frente a enzimas degradativas producidas por los hospedadores.
- La alta glicosilación de las proteínas de pared evita la desecación celular, ya que los puentes fosfodiéster de las cadenas de carbohidratos aportan numerosas cargas negativas que permiten la retención de agua.
- Están participando en la construcción de la pared celular, ya que entre ellas se encuentran proteínas con actividad sintetasas, hidrolasas, quitinasas, glucanasas o transglicosilasas.
- La localización de las proteínas en la parte más exterior de la pared celular facilita la comunicación y adhesión celular, favoreciendo la aglutinación y el contacto con feromonas (Klis et al., 2010; Lipke and Ovalle, 1998). Adicionalmente, las proteínas de adhesión juegan un papel relevante en virulencia y por tanto un papel importante en la respuesta inmunitaria.
- La presencia de proteínas implicadas en el procesamiento de carbohidratos facilita la creación de biofilms (De Groot et al., 2005).
- Contribuyen a mantener la integridad celular, ya que en situaciones de estrés sobre la pared celular, las manoproteínas con función de mecanosensor trasladan el daño al interior celular. Como respuesta al daño, se produce un aumento de la transcripción de genes que codifican para proteínas implicadas en la biogénesis de la pared celular a través de la ruta de MAP quinasas de integridad celular CWI

(Boorsma et al., 2004; de Nobel et al., 2000; Garcia et al., 2004; Jung and Levin, 1999; Lagorce et al., 2003; Levin, 2011).

Las proteínas una vez sintetizadas son translocadas al Retículo endoplasmático (RE) y glicosiladas mediante mecanismos de N-glicosilación u O-glicosilación (Gemmill and Trimble, 1999). Una vez glicosiladas, son enviadas al Golgi para su procesamiento y finalmente internalizadas en vesículas para su transporte a la membrana donde son secretadas al periplasma. La N-glicosilación, comienza con un lípido precursor anclado en la membrana del RE. Este precursor está compuesto por dos residuos de N-acetil-glucosamina unidos a nueve manosas y tres glucosas ($Glc_3Man_9Nac_2Glc$). Este precursor se transfiere en bloque a la proteína (mediante un enlace N-glicosídico sobre una asparagina) y se procesa dando lugar a un glúcido que es el núcleo de la N-glicosilación (Man_8Nac_2Glc). A continuación, este glúcido sufre una elongación en el Golgi con cadenas de manosa o galactosa (Burda and Aebi, 1999). En *S. cerevisiae*, el núcleo N-glicosil se elonga con cadenas de manosa unidas con enlaces α-1,2, α-1,3 o α-1,6, de tamaño variable, por la familia de proteínas Kre, Ktr, Och y Mnn (Ballou, 1976; Lussier et al., 1999; Nakanishi-Shindo et al., 1993; Nakayama et al., 1992). La O-glicosilación se caracteriza por la adición directa del glúcido mediante enlace α-1,2 a la proteína en el RE (Strahl-Bolsinger et al., 1999). La O-glicosilación inicial de los residuos de serina o treonina de la proteína es llevada a cabo por la familia de proteínas Pmt. Posteriormente, en el Golgi se produce la elongación del glúcido con más residuos de manosa por las familias Kre, Ktr y Mnn1 (Ballou, 1990; Romero et al., 1997b; Romero et al., 1999). Finalmente, se establecen puentes fosfodiéster entre ambas cadenas N- y O- manosiladas, proporcionando a la superficie celular múltiples cargas negativas (Orlean, 1997).

La unión de las CWP a los demás componentes de la pared celular se produce mediante distintos tipos de enlaces: uniones de tipo no covalente, como por ejemplo puentes disulfuro (Cappellaro et al., 1998; Mrsa et al., 1999; Mrsa et al., 1997) y uniones covalentes. Dentro de este segundo grupo se distingue dos subgrupos en base a su estructura: un primer grupo denominado CWP modificadas con anclaje tipo GPI (glicosilfosfatidilinositol) y un segundo grupo denominado proteínas de pared tipo PIR (Proteínas con Repeticiones Internas) sensible a álcali (Kapteyn et al., 1999a; Kapteyn et al., 1999b).

2.2.4.1. Proteínas no unidas covalentemente a la pared celular

Esta fracción de proteínas es extraíble por ditiotreitol (DTT) (Cappellaro et al., 1998). Entre ellas se encuentran la quitinasa Cts1, la exoglucanasa Exg1, la endoglucanasa Bgl2 y otras proteínas de pared como Scw3, Scw4, Scw10 y Scw11.

2.2.4.2. Proteínas unidas covalentemente a la pared celular

2.2.4.2.1. Proteínas GPI

Las proteínas tipo GPI están covalentemente unidas al β-1,6 glucano mediante un remanente de GPI. El núcleo de este remanente está compuesto por etanolamina, unida a un grupo fosfato y a una cadena de oligosacáridos, que generalmente son cuatro o cinco residuos de manosa, en los cuales al menos tres de ellas contienen etanolamina (Imhof et al., 2004). La unión al β-1,6 glucano incluye enlaces fosfodiéster entre el grupo etanolamina y la tercera manosa del núcleo glúcido de la N-glicosilación (de Groot et al., 2004). Las proteínas GPI se caracterizan por tener una secuencia hidrofóbica en su extremo amino terminal que codifica para un péptido señal que le permite ser translocada a la membrana del RE y un domino hidrofóbico en su extremo carboxilo terminal que codifica para el anclaje GPI. Tras su entrada en el RE, se elimina el péptido señal y se modifica el anclaje GPI mediante una serie de procesos que conllevan la ruptura proteolítica, uniones de residuos aminoacídicos y transamidación con el grupo etanolamina fosfato (Pittet and Conzelmann, 2007). Posteriormente, estas proteínas son empaquetadas en vesículas COPII especializadas para su salida del RE y su viaje desde el Golgi hacia la membrana plasmática (Lesage and Bussey, 2006). El motivo GPI es muy importante para que la proteína se encuentre retenida en la pared celular de la levadura, así proteínas truncadas en el extremo C-terminal, carentes del anclaje GPI, son secretadas al medio (Ram et al., 1998). Su liberación de la pared celular se puede hacer a través de un tratamiento con β-1,6 glucanasa (Cabib et al., 1982). El desarrollo de un modelo de predicción *in sílico* (Caro et al., 1997) de proteínas tipo GPI basado en la secuencia consenso para este anclaje (Nuoffer et al., 1993) y su refinamiento posterior (De Groot et al., 2003), permitió identificar 66 proteínas tipo GPI en *S. cerevisiae* (Hamada et al., 1998). Entre ellas se encuentran

lisofosfolipasas, aglutininas, floculinas, proteasas y las proteínas que participan en el ensamblaje y entrecruzamiento de carbohidratos como las proteínas de la familia Gas, Crh o Ecm33.

2.2.4.2.2. Proteínas PIR

Las proteínas PIR se unen directamente al β-1,3 glucano mediante un enlace sensible a álcali (Kapteyn et al., 2001; Klis et al., 2002; Toh-e et al., 1993). Se ha propuesto la existencia de una unión tipo éster entre el grupo carboxilo de un residuo de ácido glutámico de la proteína y un grupo hidroxilo de una molécula de glucosa del β-1,3-glucano (Ecker et al., 2006). Adicionalmente a las proteínas PIR, se han encontrado proteínas unidas mediante enlaces covalentes sensibles a álcali que no presentan repeticiones internas (Yin et al., 2005). Las proteínas PIR se caracterizan por presentar un sitio de reconocimiento para la proteasa Kex2, una zona interna con repeticiones, un extremo carboxilo terminal altamente conservado y ausencia de anclaje GPI. Las proteínas PIR suelen presentar modificaciones postransduccionales tipo O-glicosilación, que se creen que ayudan a su retención en la pared celular y parecen estar implicadas en protección osmótica (Kapteyn et al., 1999b; Mrsa et al., 1997).

2.3. ORGANIZACIÓN

La organización molecular de la pared celular ha sido dilucidada gracias al trabajo de muchos años de investigación. Como ya se comentó anteriormente el β-1,3 glucano es el componente principal y es el más cercano a la membrana plasmática. Los polisacáridos ramificados de este glucano se unen lateralmente mediante puentes de hidrógeno formando una malla a la que se unen covalentemente la quitina y las manoproteínas. Las uniones entre el β-1,3 glucano, el β-1,6 glucano y la quitina ocurren mediante el extremo no reducido del mismo, mientras que por su extremo reducido se encuentra unido a las manoproteínas de pared tipo PIR (Kapteyn et al., 2001; Kollar et al., 1995; Kollar et al., 1997). Las manoproteínas tipo GPI se unen indirectamente, a la red β-1,3 glucano-quitina a través de la unión al β-1,6 glucano, constituyendo de esta forma un complejo

macromolecular denominado *flexible building block*, es decir, estructura flexible en bloques (figura 1B) (Kapteyn et al., 1996; Kapteyn et al., 1997; Klis et al., 1997).

El complejo glucano-quitina-proteínas tipo GPI es muy abundante en células crecidas en medios ricos y se encuentra presente en la zona más externa de la pared celular (Kapteyn et al., 1999a; Klis et al., 2006; Klis et al., 2002), mientras que el complejo glucano-quitina-proteína tipo PIR, se localiza mayoritariamente en la parte más interna de la pared celular (Kapteyn et al., 1999b; Mrsa et al., 1997; Mrsa and Tanner, 1999). Otras proteínas, como por ejemplo Cwp1p (proteína GPI), pueden unirse directamente al β-1,3 glucano a través de un enlace sensible a álcali como lo hacen las proteínas PIR (uniones simples) y de manera simultánea unirse al β-1,6 glucano pudiendo presentar uniones dobles, siendo este último caso más frecuente en situaciones de estrés sobre la pared celular (Kapteyn et al., 2001). Por último, otro complejo existente en la pared celular, aunque menos frecuente en células crecidas en medio rico, es el formado por proteínas GPI unidas a quitina a través de la unión al β-1,6 glucano. La abundancia de estos complejos puede variar en determinadas condiciones, como por ejemplo, en situaciones de daño sobre la pared celular. Así, situaciones que provocan una pérdida de β-1,3 glucano dan lugar a un aumento en la proporción de quitina, que puede pasar de un 1-3% a un 20% del peso seco de la pared celular, aumentando también las uniones entre el β-1,6 glucano y la quitina (Garcia-Rodriguez et al., 2000; Kapteyn et al., 1997; Popolo et al., 1993b; Ram et al., 1998). Finalmente, la quitina puede aparecer o bien unida directamente al extremo no reductor de las cadenas de β-1,6 glucano en las paredes laterales de la célula (Kollar et al., 1995) y por lo tanto estaría presente en los complejos anteriormente citados, o bien unida a β-1,3 glucano en la zona del septo, o como quitina libre (Cabib and Duran, 2005).

3. BIOGÉNESIS DE LA PARED CELULAR

El crecimiento de la pared celular requiere de la acción conjunta de proteínas degradadoras, sintéticas y ensambladoras. De este modo, la degradación parcial previa de esta estructura acompañada por la síntesis e inserción de los nuevos componentes favorece un modelo idóneo para el crecimiento (figura 3A). Las principales actividades líticas son las desarrolladas por glucanasas, quitinasas y mananasas. La síntesis de los componentes tiene lugar a nivel de la membrana plasmática mediante la acción de enzimas especificas

(glucan- y quitín-sintasas) localizadas en la membrana plasmática (figura 3A) (Lussier et al., 1997; Molina et al., 2000; Ram et al., 1994). A continuación, enzimas ensambladoras (transglicosilasas o glucanosiltransferasas) unen los nuevos componentes a los ya existentes en la pared celular, mediante una reacción de transglicosilación, que consiste en la ruptura de los enlaces glicosídicos de la molécula donadora y la creación de un nuevo enlace entre el extremo reducido del fragmento generado y la molécula aceptora (figura 3B) (Goldman et al., 1995; Mrsa et al., 1993; Popolo and Vai, 1999; Rodriguez-Pena et al., 2000).

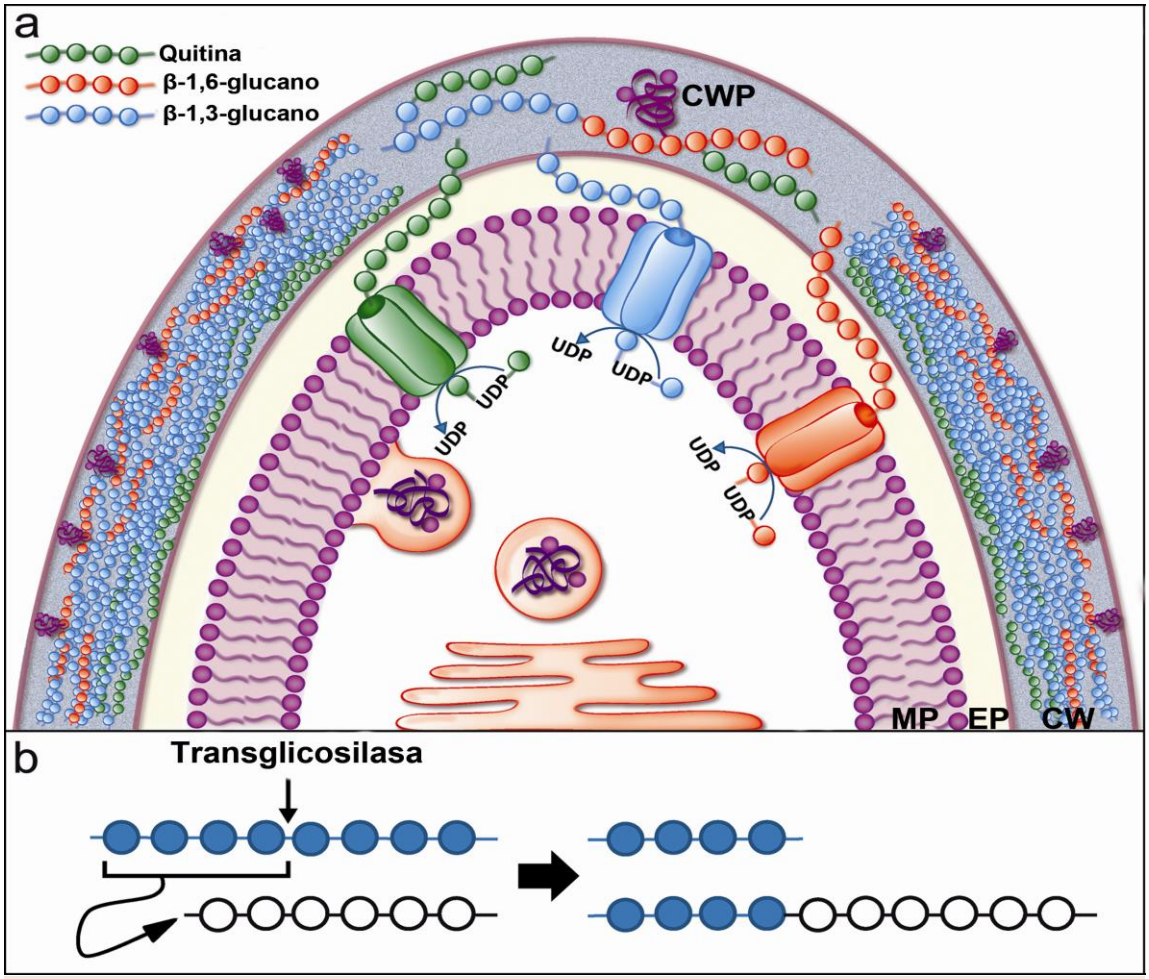

Figura 3. Representación esquemática de la biogénesis de la pared celular. A, Modelo de la pared celular. Imagen modificada de Cabib and Arroyo (2005). En él se muestra la membrana plasmática (MP) donde se encuentran las subunidades catalíticas sintetizando los nuevos polímeros que serán extruidos al espacio periplásmico (EP) para su posterior incorporación a otros de los componentes de la pared celular (CW) por la acción de las transglicosilasas. En el modelo de la pared celular se distinguen comenzando por la zona más externa: en lila a las manoproteínas (CWP), seguidas del β-1,6-glucano en naranja, el β-1,3-glucano en azul y la quitina en verde como último polisacárido más cercano al interior celular. En la figura B se representa una reacción de transglicosilación. En azul el polisacárido donador y en blanco el polisacárido aceptor. Tras la reacción de transglicosilación se obtiene un nuevo polisacárido y el fragmento del donador restante.

El orden de incorporación de los componentes en la pared celular se dilucidó mediante experimentos de regeneración de la pared celular de esferoplastos en mutantes delecionados en genes implicados en la síntesis de los diferentes componentes de la pared celular (figura 4). El primer componente que se incorpora es el β-1,3-glucano, que se sintetiza en la membrana plasmática y constituye la red a la que se unen el resto de los componentes (figura 4A) (Roh et al., 2002a). Esta premisa está avalada por la capacidad de los esferoplastos de sintetizar β-1,3-glucano en ausencia de β-1,6-glucano y manoproteínas y porque mutantes en genes implicados en la síntesis del β-1,6-glucano presentan un nivel de β-1,3-glucano similar a una cepa WT (Shahinian and Bussey, 2000). A continuación, se incorpora el β-1,6-glucano seguido de las manoproteínas (figura 4B y 4C). Este orden está apoyado por la presencia de β-1,3-glucano unido a β-1,6-glucano cuando la síntesis del anclaje GPI se encuentra inhibida (Roh et al., 2002a) y por la disminución en la incorporación de las proteínas de pared tipo GPI en ausencia de β-1,6-glucano (Kapteyn et al., 1997; Lu et al., 1995). Por último, debido a que la presencia de quitina en la pared celular no se detecta hasta la citoquinesis (Shaw et al., 1991), se concluyó que la quitina es el último componente en ser incorporado a la pared celular (figura 4D). Cada componente se une al extremo no reducido del siguiente (Kollar et al., 1995; Kollar et al., 1997)

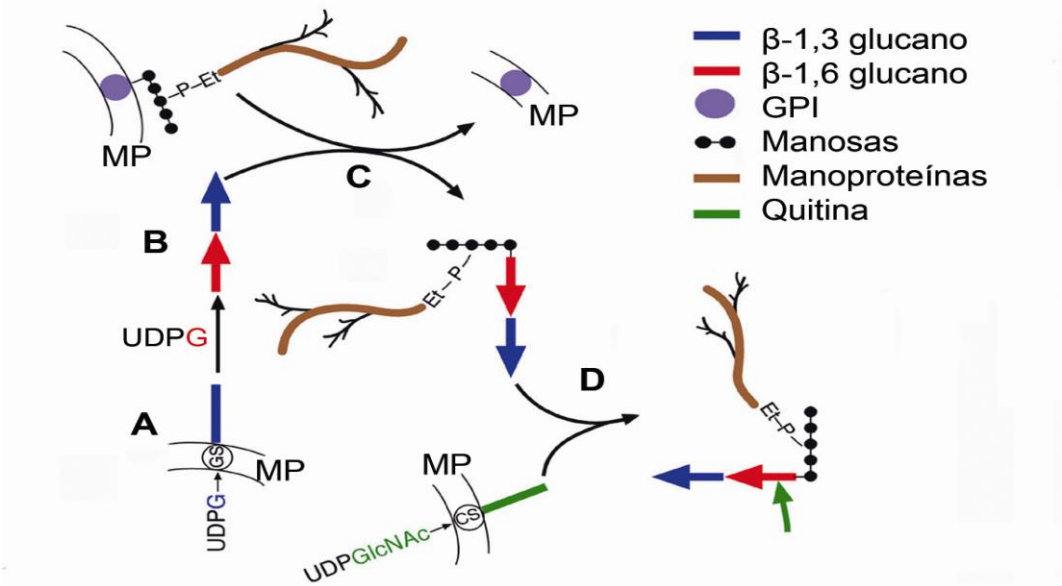

Figura 4. Orden propuesto para la incorporación de los componentes en la pared celular. Imagen modificada de Roh, Bowers et al. (2002). MP: membrana plasmática, GS: glucan.-sintasa, CS: quitín-sintasa, Et-P: etanolamina fosfato, UDPG: UDP-glucosa, UDPGlcNAc: UDP-N-acetil-glucosamina. En azul el β-1,3-glucano, en rojo el β-1,6-glucano, en marrón las manoproteínas, en verde la quitina, en lila el anclaje GPI y en negro las manosas. La secuencia de unión sería: β-1,3-glucano → β-1,6-glucano → manoproteínas → quitina.

El mantenimiento de una pared celular organizada a lo largo del ciclo celular requiere un estricto control, de modo que si algunos de los procesos de biogénesis se vieran modificados, interrumpidos o bloqueados, se producirían cambios en la organización espacial de la pared celular para lograr la supervivencia celular. El control de la integridad de la pared celular está mediado por la ruta de MAP quinasa denominada CWI (Levin, 2005; Levin, 2011). Esta ruta se activa en respuesta a distintos estímulos como la presencia de feromonas (Buehrer and Errede, 1997), el estrés oxidativo (Vilella et al., 2005), la despolimerización del citoesqueleto de actina (Harrison et al., 2001), mutaciones en componentes de la pared celular (de Nobel et al., 2000), compuestos que dañan la pared celular de forma directa o indirecta (Garcia et al., 2004; Garcia et al., 2009; Rodriguez-Pena et al., 2010), la radiación UV (Bryan et al., 2004), el estrés térmico o situaciones de hipoosmolaridad (Davenport et al., 1995), que dan lugar a una respuesta transcripcional específica frente al daño que le permite adaptarse y sobrevivir al mismo.

3.1. DEGRADACIÓN DE LOS COMPONENTES

La hidrólisis de manera controlada y dirigida de polímeros preexistentes en la pared celular por la acción de glucanasas y quitinasas permiten el crecimiento de la pared celular acoplado al proceso de biosíntesis (Elango et al., 1982).

3.1.1. Glucanasas

S.cerevisiae presenta una alta variedad de endo- y exo-β-glucanasas que cortan sobre β-1,3 y β-1,6 glucano (Baladron et al., 2002). Las exo-glucanasas hidrolizan los enlaces β-O-glicosídicos en los extremos no reductores de la cadena para liberar residuos de glucosa (Nombela et al., 1988). Las β-1,3 endoglucanasas actúan sobre diferentes puntos intermedios de las cadenas liberando una mezcla de oligosacáridos, siendo la glucosa el producto de menor tamaño (Cid et al., 1995). Se han caracterizado varias familias de genes que codifican para proteínas con actividad β-1,3 endoglucanasas como la familia ENG: Eng1 y Eng2, y la proteína Bgl2; y con actividad β-1,3 exoglucanasas como la familia *EXG*: Exg1, Exg2 y Ssg1 y la familia SCW: Scw3, Scw4 y Scw10 (Larriba et al., 1995).

La familia de los genes *ENG* está compuesta por dos miembros: Eng1 y Eng2. Presentan un alto grado de homología con la familia *EXG*. A su vez, Eng1 muestra una alta homología con la proteína Acf2 implicada en el ensamblaje de actina *in vitro* y con proteínas de unión a glucanos de plantas. Ambas proteínas poseen actividad β-1,3 endoglucanasa. Eng1 es una proteína extracelular altamente glicosilada, mientras que Eng2 no se glicosila y presenta una localización intracelular (Martin-Cuadrado et al., 2008). *ENG1* presenta un máximo de transcripción durante M/G1 dependiente del factor de transcripción Ace2 (Ufano et al., 2004). Se localiza de manera asimétrica, únicamente en el lado de la célula hija y su deleción provoca defectos en separación celular. Estos resultados sugieren su implicación, junto a la quitinasa 1, en la degradación del septo. Su papel sería la degradación del β-1,3 glucano del septo secundario (Baladron et al., 2002; Martin-Cuadrado et al., 2003).

El gen *BGL2* codifica para una proteína de 29 kDa con homología a β-1,3 glucanasa de plantas (Klebl and Tanner, 1989). Se ha caracterizado su actividad β-1,3 endoglucanasa *in vitro* (Mrsa et al., 1993). Adicionalmente, los resultados del estudio *in vivo* llevado a cabo por Goldman y colaboradores (Goldman et al., 1995) sugieren que Bgl2 podría estar participando como transferasa o endotransglicosilasa, formando enlaces β-1,6 entre cadenas de β-1,3 glucano. Las células *bgl2*Δ no muestran ningún fenotipo notable al menos en las condiciones de crecimiento estándar de laboratorio, salvo un incremento en el nivel de quitina (Kalebina et al., 1998). A su vez, la sobreexpresión de *BGL2* produce una disminución del tiempo de crecimiento de algunos mutantes como por ejemplo *scw4*Δ (Kalebina et al., 2003; Kalebina et al., 2008; Kalebina et al., 2006). En hongos patógenos como *C.albicans*, se ha identificado a Bgl2 como marcador de candidiasis sistémicas (Pitarch et al., 2006) y está relacionada con su virulencia mediante su actividad β-1,3 glucosiltransferasa (Sarthy et al., 1997).

EXG1, codifica para un polipéptido que se glicosila y se procesa de manera diferente en cada uno de sus dos sitios de N-glicosilación (Nebreda et al., 1986), generando dos polipéptidos diferentes: Exg1a y Exg1b (Nebreda et al., 1987; Vazquez de Aldana et al., 1991). Estas dos proteínas representan un alto porcentaje de la actividad β-1,3 exoglucanasa de la célula. *EXG2*, codifica para una proteína de pared tipo GPI con una menor actividad catalítica que Exg1 (Correa et al., 1992). El gen *SSG1* codifica para una proteína con actividad β-1,3 exoglucanasa específica en esporulación. Su transcripción,

regulada por feromonas y la accesibilidad a los nutrientes, coincide con el comienzo de la meiosis y presenta un pico de máxima transcripción durante la formación de la espora (Muthukumar et al., 1993; San Segundo et al., 1993). Las tres proteínas comparten un alto porcentaje de homología en su secuencia y un su sitio catalítico altamente conservado.

La familia de los genes *SCW* está compuesta por tres miembros Scw3, Scw4 y Scw10. Son proteínas de pared tipo PIR, fácilmente extraíbles de la pared celular mediante tratamiento con SDS (Dodecil sulfato sódico). Scw4 y Scw10 muestran un 56 % y 49% de homología con Bgl2, mientras que Scw3 presenta homología con la actividad β-glucanasa de *C. wickerhamii*. En la cepa *scw10*Δ *scw4*Δ la cantidad de proteínas extraíbles por laminarasa es menor que en la cepa WT, sugiriendo un posible papel directo o indirecto en la unión de las proteínas al β-1,6 glucano (Cappellaro et al., 1998).

3.1.2. Quitinasas

Las quitinasas son responsables de la degradación de enlaces β-1,4 entre residuos de NAG. Existe una familia de quitinasas en *S. cerevisiae*, compuesta por dos miembros, Cts1 y Cts2. Cts1 es una endoquitinasa implicada en la degradación de la quitina del septo, de modo que las células *cts1*Δ no pueden completar su división celular y forman agregados celulares (Kuranda and Robbins, 1991). El efecto degradativo de Cts1 se ve contrarrestado por la acción sintética de Chs1 (Cabib et al., 1992). Sin embargo, ambas proteínas no presentan una regulación recíproca (Selvaggini et al., 2004). En su secuencia podemos identificar una región rica en serinas y treoninas que son O-manosiladas, un dominio de unión a carbohidratos en su extremo carboxilo terminal, posiblemente implicado en su localización temporal en septo por el lado de la célula hija y un centro catalítico con similitud a las quitinasas de plantas (Cappellaro et al., 1998). Adicionalmente a su localización temporal en pared celular, Cts1 presenta un acúmulo en el espacio periplasmático procedente de la secreción de vesículas desde el citoplasma (Elango et al., 1982). *CTS1*, presenta un pico de expresión en fase G1 bajo el control del factor de transcripción Ace2. La acción quitinolítica *in vitro* fue reconstituida a través de extractos celulares en tampón ácido (Correa et al., 1982). Cts2 posee actividad endoquitinasa y está codificada por el gen *CTSII*. Su función es específica de esporulación, ya que células

delecionadas en dicho gen presentan la pared de la espora anormal y fallos en la formación de la espora madura (Giaever et al., 2002).

3.2. SÍNTESIS DE LOS COMPONENTES

3.2.1. Síntesis del β-1,3 glucano

Los polímeros de β-1,3 glucano son generados por la actividad β-1,3 glucan-sintasa (GS) localizada en la membrana plasmática (figura 3A). Tras su síntesis vectorial son secretados al espacio extracelular para facilitar la asociación de la cadena naciente de glucano al resto de los componentes de la pared celular (Douglas, 2001). La GS cataliza la transferencia de un residuo glicosil procedente del precursor citoplasmático UDP-glucosa a la cadena de β-1,3 glucano en crecimiento (figura 3A) (Cabib and Kang, 1987). Este proceso ocurre inicialmente donde se haya activado la actividad GS, que normalmente son las zonas de crecimiento polarizado (Qadota et al., 1996). El complejo β-1,3 GS de *S. cereviseae* está compuesto por una fracción que contiene la actividad catalítica y otra fracción que engloba a la subunidad reguladora (Kang and Cabib, 1986; Mol et al., 1994). La investigación en profundidad de ambas fracciones permitió dilucidar que existen dos subunidades catalíticas codificadas por dos genes con alta homología entre sí, denominados *FKS1*, que es la subunidad principal y *FKS2/GSC2*, que es la subunidad alternativa, y una subunidad reguladora codificada por el gen *RHO1* (Dijkgraaf et al., 2002).

3.2.1.1. Subunidad catalítica

El gen *FKS1* codifica para una proteína con 16 dominios transmembrana (Douglas et al., 1994; Inoue et al., 1995), que se localiza en los sitios de crecimiento polarizado mediante los parches de actina (Utsugi et al., 2002). En su estructura se pueden diferenciar: un dominio catalítico, una región de seis y otra de diez dominios transmembrana implicadas en su correcta localización en membrana y en los sitios de crecimiento polarizado respectivamente, y por último cerca del extremo amino terminal una secuencia

de 400 aminoácidos orientados hacia el citosol, que participa en la activación del dominio catalítico (Okada et al., 2010). El gen *FKS2* codifica para una proteína con un 88% de homología con Fks1 y una estructura en dominios similar. Fks2, al igual que Fks1, se localiza en sitios de crecimiento polarizado (Dijkgraaf et al., 2002). Las células *fks1*Δ presentan un descenso en los niveles de β-1,3 glucano (75%) y un aumento de los niveles de quitina y manano (Dallies et al., 1998; Garcia-Rodriguez et al., 2000; Lesage et al., 2004), así como fenotipos de sensibilidad a los compuestos como el Blanco de Calcoflúor (CFW) y las equinocandinas. Sin embargo, los mutantes *fks2*Δ no presentan defectos en crecimiento vegetativo pero sí en esporulación. El doble mutante *fks1*Δ *fks2*Δ es inviable, lo que sugiere un papel parcialmente redundante de ambas proteínas (Inoue et al., 1995).

FKS1 y *FKS2* presentan patrones de expresión diferentes. Mientras que *FKS1* se expresa durante el ciclo vegetativo y su expresión depende de los factores de transcripción Swi4 y Rlm1 (Igual et al., 1996; Jung and Levin, 1999; Mazur et al., 1995; Ram et al., 1995), la expresión de *FKS2* se ve favorecida en condiciones de baja concentración de glucosa en el medio o presencia de galactosa, glicerol o acetato. La regulación de *FKS2* bajo restricción de glucosa está regulada por la proteín-quinasa Snf1 (Zhao et al., 1998). Adicionalmente, existe una activación de *FKS2* regulada por la ruta CWI y la ruta de Calcineurina ante una gran variedad de estímulos ambientales como son: la presencia de calcio en el medio, el tratamiento con factor α, un aumento de la Tª (39ºC) (Zhao et al., 1998) o el tratamiento con agentes que causan daños en la pared celular como la Caspofunfina, el Rojo Congo (RC) o la Zimoliasa (Garcia et al., 2004; Lagorce et al., 2003).

3.2.1.2. Subunidad reguladora

La subunidad reguladora es la proteína Rho1. Su descubrimiento fue complejo debido a la dificultad para su obtención homogénea del extracto de membranas. Para su identificación se testaron mutantes defectivos en la unión a GTP que presentaran defectos en la pared celular y que fueran capaces de restablecer la actividad GS estimulados por la presencia de GTP a niveles de una cepa WT. Así, se aisló el mutante *rho1*Δ (Drgonova et al., 1996; Qadota et al., 1996). Rho1 es una GTPasa que cicla entre sus dos estados: activo (unida a GTP) e inactivo (unida a GDP), gracias a la actividad de las proteínas GEFs

(Factores intercambiadores de GTP) y GAPs (Proteínas activadoras de GTPasas), respectivamente. Las GEFs de Rho1 son Rom1, Rom2 y Tus1, mientras que las proteínas que actúan como GAPs de Rho1 son Lrg1, Bag7, Bem2, Sac7 (Levin, 2005; Sekiya-Kawasaki et al., 2002; Watanabe et al., 2001). Rho1 participa en la organización de la pared celular a través de la regulación sobre la subunidad catalítica Fks1 (Cabib et al., 1997; Imamura et al., 1997; Roh et al., 2002a; Roumanie et al., 2005), en la morfogénesis a través de la polarización del citoesqueleto de actina mediante la activación de las forminas (Imamura, Tanaka et al. 1997) y durante la citoquinesis a través de la activación de proteínas implicadas en las rutas de secreción (Roumanie, Wu et al. 2005). Además, Rho1 forma parte de la ruta CWI, transmitiendo las señales externas desde los sensores hacia la proteína quinasa C1 (PKC1). Rho1 se localiza en los sitios de crecimiento polarizado y se co-purifica junto a Fks1 (Inoue et al., 1999). Ambas proteínas se relocalizan al cuello durante la formación del septo (Mazur and Baginsky, 1996).

Se ha propuesto un modelo de interacción de los componentes del complejo β-1,3 GS (Cabib et al., 1998). En él, Fks1 se encuentra en estado inactivo unida a la membrana. Cuando se recluta a los sitios de crecimiento polarizado se encuentra con Rho1, que por la acción de sus GEFs sufre un cambio conformacional que la capacita para unirse a la subunidad catalítica. La unión de Rho1 a Fks1 genera un cambio conformacional en la misma que facilita la entrada del precursor, UDP-glucosa, al sitio activo de la enzima. La síntesis de la cadena de glucano queda garantizada con la extrusión simultánea del polisacárido al espacio extracelular (figura 3A).

3.2.2. Síntesis del β-1,6 glucano

Aunque no se conoce exactamente donde ocurre la síntesis de este polímero, varios trabajos sugieren que ocurriría a nivel de membrana plasmática pero requeriría de eventos intracelulares previos (Aimanianda et al., 2009; Montijn et al., 1999; Vink et al., 2004). Así, una correcta maduración del β-1,6 glucano requiere tanto de la participación de proteínas de la vía secretora del aparato de Golgi y del RE, como proteínas presentes en la membrana plasmática (Shahinian and Bussey, 2000). La identificación de estas proteínas ha sido posible mediante escrutinios de resistencia a la toxina *killer* K1 (Hutchins and Bussey, 1983; Page et al., 2003), que permitieron la identificación de una familia de genes

llamados KRE (*Killer toxin resistant*) (Boone et al., 1990). Esta familia está compuesta por 14 genes y sus homólogos *SKN1* y *HKN1* (Lussier et al., 1997; Nagahashi et al., 1998). Adicionalmente, se han identificado genes denominados *CWH (Calcofluor White Hypersensitive*) relacionados con la síntesis del β-1,6 glucano mediante el escrutinio de mutantes sensibles al compuesto CFW que debilita la pared celular debido a que se une a la quitina e impide su unión con los demás componentes (Cabib and Bowers, 1975; Elorza et al., 1983; Ram and Klis, 2006; Ram et al., 1994).

3.2.2.1. Proteínas del Retículo Endoplasmático (RE)

Existen 5 proteínas localizadas en el RE y que participan en la síntesis del β-1,6 glucano en *S. cerevisiae*:

KRE5, codifica para una proteína con similitud a una glucosiltransferasa (UGGT) identificada en *Drosophila* y en *S. pombe* (Herrero et al., 2004; Levinson et al., 2002). Las UGGT catalizan la unión de un residuo de glucosa a la proteína mediante un enlace N-glicosídico en el RE. Por lo tanto se cree que podría actuar como una posible glucosiltransferasa, glicosilando el motivo GPI de las proteínas de pared celular en el RE y ayudando en la secreción de las mismas (Shahinian et al., 1998). Su deleción genera una disminución en los niveles de β-1,6 glucano, un defecto en el crecimiento, una mayor cantidad de β-1,3 glucano y un aumento de proteínas unidas al β-1,3 glucano con respecto a la cepa WT (Meaden et al., 1990).

CNE1 codifica para una proteína con homología a la calnexina de mamíferos. Su deleción intensifica los fenotipos individuales de las cepas *kre6*Δ y *cwh41*Δ (Shahinian and Bussey, 2000).

CWH41/GSL1 y *ROT2/GLS2* codifican para la glucosidasa I y glucosidasa II del RE respectivamente (Romero et al., 1997a). La deleción de estos genes no presenta un fenotipo característico de defecto en la síntesis del β-1,6 glucano. Sin embargo, su deleción junto a otros genes *KRE* acrecienta los fenotipos individuales de los mismos e incluso llega a ser letal en el caso del gen *KRE6* (Roemer and Bussey, 1991). Estos datos apuntan a que

podrían participar como aceptores para la iniciación de la cadena y/o en el mantenimiento de la maquinaria de síntesis de β-1,6 glucano (Jiang et al., 1996).

3.2.2.2. Proteínas del Aparato de Golgi

Localizadas en la membrana del aparato del Golgi, se encuentran la proteína Kre6 y su homólogo Skn1 (Boone et al., 1990; Roemer et al., 1993). Las células *kre6*Δ poseen una morfología aberrante con tendencia a agruparse, en las cuales los niveles de β-1,3 glucano y β-1,6 glucano se encuentran aumentados y disminuidos respectivamente con respecto a una cepa WT (Roemer and Bussey, 1991). Adicionalmente, *KRE6* interactúa genéticamente con miembros de la ruta de MAP quinasas CWI sugiriendo una posible regulación por parte de dicha ruta en la biosíntesis del β-1,6 glucano (Roemer et al., 1994). Ambos genes presentan una expresión dependiente de ciclo celular, con un pico de máxima transcripción durante las etapas G1/S y M (Igual et al., 1996; Spellman et al., 1998). Kre6 presenta homología a las glucosilhidrolasas o transglicosilasas (Montijn et al., 1999), sugiriendo una posible participación en la síntesis o procesamiento del β-1,6 glucano.

SKN1 es un homólogo de *KRE6*, que codifica para una proteína de membrana tipo II (Roemer et al., 1994). Skn1 es capaz de complementar los defectos en crecimiento y los niveles de β-1,6 glucano presentes en el mutante *kre6*Δ de manera dosis dependiente. Un mutante *skn1*Δ no presenta ningún defecto en el crecimiento, en la cantidad de β-1,6 glucano o en la sensibilidad a la toxina *killer* K1. Sin embargo, la deleción de *skn1*Δ sobre un fondo *kre6*Δ provoca una tasa de crecimiento y un nivel de β-1,6 glucano mucho menor que las mutaciones individuales (Roemer et al., 1993), sugiriendo un papel para Skn1 junto a Kre6 en el acoplamiento entre los componentes secretores y plasmáticos.

3.2.2.3. Proteínas del citoplasma

Kre11 es una proteína de citoplasma, cuya ausencia no provoca defectos en los niveles de β-1,6 glucano. Sin embargo, presenta epistasis con el mutante *kre1*Δ y es sintética letal con el mutante *kre6*Δ (Brown et al., 1993). Se ha sugerido que Kre11 está

participando en el movimiento del β-1,6 glucano a través de la ruta secretora desde el RE hacia el Golgi (Sacher et al., 2000)

3.2.2.4. Proteínas de la superficie celular

Kre1, es una proteína O-glicosilada localizada en la membrana plasmática que participa en las etapas tardías de la síntesis del glucano (Roemer and Bussey, 1995). Las células *kre1*Δ presentan defectos en los niveles del β-1,6 glucano (Boone et al., 1990).

KRE9 y su homólogo *KNH1* codifican para dos proteínas homólogas entre sí y presentes en la superficie celular. Su deleción está asociada a un descenso elevado en los niveles de β-1,6 glucano en la pared celular (Dijkgraaf et al., 1996). Adicionalmente, las células *kre9*Δ presentan una interacción sintética letal con *kre1*Δ, *kre6*Δ y *kre11*Δ y epistasis con el mutante *kre5*Δ (Brown and Bussey, 1993). Se ha sugerido su participación en el anclaje o entrecruzamiento de las nuevas cadenas de β-1,6 glucano en la pared celular o como subunidad catalítica de la β-1,6 GS (Aimanianda et al., 2009). Como ocurría para las células *skn1*Δ, la deleción de *KNH1* no presenta ningún defecto en el crecimiento y en la cantidad de β-1,6 glucano. Por lo que es muy probable que los homólogos funcionales de Kre6 (Skn1) (Roemer et al., 1993) y Kre9 (Knh1) (Dijkgraaf et al., 1996) actúen en una ruta alternativa minoritaria o en determinadas condiciones de crecimiento.

Entre todas las proteínas que participan en la ruta, Kre5, Kre6 y Kre9 parecen estar implicadas en la síntesis del β-1,6 glucano, ya que su deleción implica una disminución en los niveles del polímero de la pared celular. Sin embargo, actualmente no hay evidencia bioquímica de cuál de estas proteínas es la subunidad catalítica β-1,6 GS, siendo Kre9 y Kre5 los candidatos con mayor probabilidad (Aimanianda et al., 2009).

3.2.3. Síntesis de la quitina

Los primeras evidencias de la existencia de una actividad quitín-sintasa (CS) en hongos data de 1971 (Cabib and Bowers, 1971). Estos primeros trabajos proporcionaron información esencial para el descubrimiento de las enzimas, ya que permitieron identificar

a los cofactores (Cabib and Keller, 1971), finalmente caracterizados como proteasas (Cabib and Ulane, 1973), que eran necesarios para la activación de la enzima que se encontraba en un estado inactivo denominado zimógeno (Cabib et al., 1973; Duran and Cabib, 1978). La primera actividad CS caracterizada en el género *Saccharomyces* fue en la levadura *S. carlsbergensis*, que marcó el protocolo para el estudio de las actividades sintetasas posteriores (Keller and Cabib, 1971). La reacción enzimática consiste en la adición de un residuo de UDP-N-acetil-glucosamina formado en el citosol (UDP-NAG) a la cadena de quitina en formación (figura 3A) (Cabib et al., 1987). La reacción de síntesis de la quitina se caracteriza por ser un proceso vectorial, de modo que la enzima cataliza la incorporación de las unidades del sustrato secuencialmente al producto (Cabib et al., 1983; Orlean, 1987; Roberts et al., 1983). Los aminoácidos importantes para la catálisis (QXXEY, EDRXL y QXRRW) se encuentran formando parte del dominio catalítico de las CS y sirven para la clasificación de las CS dentro de la familia 2 de las glicosiltransferasas, a la que también pertenecen las hialuronico-sintasas y celulosa-sintasas (Cos et al., 1998; Nagahashi et al., 1995). Este dominio abarca unos 250 aminoácidos y presenta una estructura terciaria conservada en la mayoría de los hongos (Ruiz-Herrera et al., 2002). Adicionalmente, en el extremo carboxilo terminal o en la zona central de la proteína se encuentra una secuencia que codifica para varios dominios transmembrana, que además de permitir la correcta localización de la proteína, están implicados en la activación de la proteína y en la extrusión de la quitina a través de la membrana (Ford et al., 1996; Jimenez et al., 2010). En función de la posición y el tamaño de este domino, las CS se clasifican dentro de ocho clases evolutivamente diferentes, que a su vez se engloban en dos subgrupos. El grupo 1 engloba las clases I-III y el grupo 2 incluye las clases IV-VIII (Bowen et al., 1992).

S.cerevisiae tiene tres actividades CS (CSI, CSII y CSIII), que requieren la participación de las proteínas catalíticas Chs1, Chs2 y Chs3 respectivamente (Cabib, 2004; Cabib et al., 2001). Las proteínas Chs se localizan en la membrana plasmática de forma activa. Sin embargo, al sintetizarse en el RE requieren de una ruta de secreción para su correcta localización y activación en la membrana plasmática (Cabib, 2000). La quitina sintetizada *in vivo* en situaciones basales tiene un tamaño polidisperso (Cabib and Duran, 2005). Sin embargo, el tamaño de las cadenas de quitina se incrementa en situaciones de estrés constitutivo como ocurre en las células *fks1*Δ y *gas1*Δ o durante un estrés transitorio generado por el tratamiento con CFW; mientras que la deleción de Chs4, implicada en el

funcionamiento del complejo CSIII, genera cadenas de quitina más cortas (Grabinska et al., 2007).

3.2.3.1. Quitín-sintasa I

Inicialmente, Chs1 se encontró en un extracto de paredes en estado inactivo o zimógeno (Duran et al., 1975), que se activaba tras un tratamiento proteolítico parcial (Duran and Cabib, 1978) y llevaba a cabo la reacción de síntesis de quitina *in vitro* (Cabib and Farkas, 1971). Esta síntesis se ve estimulada con la adicción de magnesio e inhibida por cobalto (Kang et al., 1984). La sobrexpresión de *CHS1* en células *chs2Δ* no es capaz de rescatar el fenotipo de defectos en la formación del septo y crecimiento celular que presenta este mutante (Silverman et al., 1988). Por otro lado, la deleción de *CHS1* no influye en la cantidad de quitina sintetizada *in vivo* (Bulawa et al., 1986), pero bajo condiciones ácidas el mutante *chs1*Δ presenta una pérdida de la permeabilidad y lisis celular debido a la presencia de un orificio en el centro de la cicatriz (Cabib et al., 1989). De acuerdo a estos resultados, se ha sugerido que Chs1 está implicada en la reparación de la pared celular (Cabib et al., 1989; Cabib et al., 1992) tras la acción hidrolítica de la endoquitinasa Cts1 (Correa et al., 1982), lo que facilita la separación celular por la digestión de la quitina del septo primario (Kuranda and Robbins, 1991). Los niveles de la proteína Chs1 permanecen constantes durante todo el ciclo celular, a pesar que la expresión del gen *CHS1* presenta un máximo de transcripción en la fase G1 del ciclo celular (Ziman et al., 1996). Los niveles de mRNA se ven inducidos por la adición extracelular de calcio y feromonas (Appeltauer and Achstetter, 1989; Choi et al., 1994a). Chs1 se localiza mayoritariamente en quitosomas aunque también se encuentra en la membrana plasmática (Pammer et al., 1992).

3.2.3.2. Quitín-sintasa II

CHS2 codifica para la subunidad catalítica del complejo CSII responsable de la síntesis de quitina que forma el septo (Shaw et al., 1991). Chs2 fue descubierta en forma de zimógeno en células *chs1*Δ (Sburlati and Cabib, 1986). A pesar de coincidir con Chs1 en su estado de zimógeno y su localización en membrana, presenta diferencias en cuanto a los

estimuladores de su actividad, siendo el cobalto el mejor estimulador seguido del magnesio (Silverman, 1989). El gen *CHS2* es esencial para el crecimiento de la levadura ya que su ausencia genera un septo primario anormal y la división celular queda interrumpida (Silverman et al., 1988). Sin embargo, las esporas con deleción en el gen *CHS2* inicialmente germinan y durante un breve periodo de tiempo crecen con normalidad. Es más tarde cuando forman grupos aberrantes de pequeñas células que dependiendo del fondo genético terminan muriendo (Bulawa and Osmond, 1990).

La expresión de *CHS2* fluctúa a lo largo del ciclo celular, presentando un pico de expresión durante la fase M (metafase) y un segundo pico al final de la mitosis (Choi and Cabib, 1994; Chuang and Schekman, 1996; Pammer et al., 1992). La transcripción del gen concuerda con la síntesis de la proteína (Pammer et al., 1992). Chs2 es retenida en el RE a través de la fosforilación de los residuos de serina localizados en su extremo N-terminal por la quinasa dependiente de ciclinas (CDK) Cdc28, proteína central en la regulación del ciclo de división. La fosforilación directa de Chs2 por Cdc28 evita su salida en vesículas CPOII del RE al Golgi, de modo que la fosforilación es importante para su estabilidad antes del transporte (Martinez-Rucobo et al., 2009; Teh et al., 2009; Zhang et al., 2006). Su correcta localización en el cuello durante un breve periodo de tiempo depende del correcto ensamblaje de las septinas y concuerda con la salida de la mitosis y la reorganización del collar de septinas en dos anillos. Su transporte requiere la coordinación entre la ruta secretora y su degradación en la vacuola. Así, Chs2 tras su paso por el RE y su salida del Golgi en las vesículas COPII (Zhang et al., 2006) continúa su viaje hacia el cuello donde se localiza de manera temporal desde anafase hasta telofase. Este transporte está regulado por proteínas del complejo exocítico como son Exo84, End4, Sec1 y proteínas de la familia SNARE (Chuang and Schekman, 1996; VerPlank and Li, 2005). Una vez terminada la telofase, rápidamente ocurre su endocitosis dependiente de End4, para ser degradada en la vacuola previo marcaje con la proteína Pep4 (Chuang and Schekman 1996; Roh, Bowers et al. 2002; Zhang, Kashimshetty et al. 2006; Teh, Chai et al. 2009). Por lo tanto, la expresión, localización y degradación de Chs2 es dependiente de ciclo celular, ya que se expresa principalmente durante mitosis y es transportada desde RE hacia el cuello a la salida de mitosis para sintetizar el septo primario. Tras la citoquinesis se procesa por proteólisis en la vacuola (Martinez-Rucobo et al., 2009).

3.2.3.3. Quitín-sintasa III

A pesar de la importancia de Chs1 y Chs2 *in vivo*, juntas apenas sintetizan un pequeño porcentaje del total de la quitina existente en la pared celular. El aislamiento de mutantes resistentes a CFW (Roncero and Duran, 1985; Roncero et al., 1988a; Roncero et al., 1988b) permitió la identificación del gen *CAL1*, que posteriormente se identificó como la subunidad catalítica de la actividad CSIII (Bulawa, 1992; Orlean, 1987; Pammer et al., 1992; Valdivieso et al., 1991). Chs3 es la responsable de la mayoría de la síntesis de la quitina presente en la célula. Chs3 sintetiza la quitina durante la emergencia de la yema, el crecimiento celular, el apareamiento y la formación de la espora (Bulawa, 1993).

La quitina que se sintetiza en la base de la yema en forma de anillo, ocurre durante la gemación al inicio de la fase G1, mientras que la quitina presente en la pared lateral ocurre en las etapas tardías del ciclo celular (figura 2A). Sin embargo, los niveles de Chs3 permanecen constantes a lo largo del todo el ciclo celular, a pesar de presentar un pico de transcripción en la fase G1 del ciclo celular (Chuang and Schekman, 1996; Ziman et al., 1996), lo que indica que la síntesis de quitina por parte de Chs3 está regulada postranscripcionalmente (Osmond et al., 1999). De este modo, Chs3 presenta una regulación durante su reclutamiento al sitio de gemación al inicio de la fase G1, seguida por una endocitosis al final del ciclo celular y de nuevo una redistribución en el cuello de la madre durante la citoquinesis y su depósito en la membrana (Chuang and Schekman, 1996). Los niveles de quitina están relacionados con la cantidad de Chs3 en la membrana plasmática. Así, en mutantes con una pared celular anormal por ejemplo *fks1*Δ o *gas1*Δ la síntesis de quitina está aumentada. Ese incremento se correlaciona con un aumento de Chs3 en la membrana y la activación de la ruta CWI (Carotti et al., 2002; Carotti et al., 2004; Garcia-Rodriguez et al., 2000; Gomez et al., 2009; Valdivia and Schekman, 2003).

Justo antes de la gemación, en la base de la yema se forma el anillo de quitina, que permanece allí durante el crecimiento de la misma y formará parte de la cicatriz de la célula madre. Es la estructura con mayor porcentaje de quitina de la célula. Su síntesis depende de la activación y del correcto anclaje en membrana plasmática del complejo CS III. Las septinas, junto a otras proteínas, participan en la localización de Chs2 y Chs3 en el cuello (Roh et al., 2002b). El anillo de quitina no se forma con normalidad cuando el anillo

de septinas presenta alguna alteración. A su vez, los defectos en el anillo de septinas en una cepa *chs3*Δ generan un engrosamiento del cuello (Schmidt et al., 2003). Estos datos sugieren que el anillo de septinas y el anillo de quitina colaboran para que ocurra una correcta división celular (Cabib and Schmidt, 2003; Schmidt et al., 2003). Adicionalmente, el anillo de quitina colabora para un correcto ensamblaje del anillo actino-miosina (AMR) y de ahí que esté implicado en una correcta formación de septo primario. A su vez, mutantes *chs2*Δ carentes de septo primario, contienen un septo engrosado y amorfo de quitina formado por Chs3 (Shaw et al., 1991). De este modo, cuando el ensamblaje del anillo de septinas o el depósito del septo primario se encuentran comprometidos, el anillo de quitina que inicialmente no es imprescindible para que ocurra la citoquinesis, se vuelve esencial.

Al igual que Chs1, Chs3 se acumula en compartimentos intracelulares denominados quitosomas. El transporte de Chs3 al sitio de gemación está mediado por el tráfico vesicular de la ruta secretora desde los endosomas hasta la membrana plasmática. Varias proteínas codificadas por un grupo de genes denominados *CHS* son requeridas para su correcta localización en la pared celular. A modo de resumen, la salida de Chs3 del RE depende de la proteína Chs7 (Trilla et al., 1999), que media la incorporación de Chs3 a las vesículas de transporte tipo COPII y su viaje hacia el Golgi (Kota and Ljungdahl, 2005). A continuación, tiene lugar la salida de Chs3 del aparato de Golgi y su transporte hacia a la membrana plasmática mediante su empaquetamiento en vesículas especializadas de la red trans-Golgi (TGN) que son liberadas en la membrana plasmática de manera polarizada. Las proteínas Chs5 y Chs6 son las responsables de la formación de dichas vesículas (Santos et al., 1997; Santos and Snyder, 1997; Ziman et al., 1998). Chs6 pertenece a una familia de proteínas llamadas ChAPs, que median el cargo de Chs3 en las vesículas TGN; mientras que Chs5 juega un papel más general en la formación de estas vesículas (Trautwein et al., 2006). Durante el tránsito desde el Golgi hasta la membrana plasmática, Chs3 sufre modificaciones postransducionales (Bulik et al., 2003). Finalmente, el anclaje de Chs3 en la membrana plasmática (DeMarini et al., 1997) está mediado por la acción de Chs4 que permite su unión con el anillo de septinas mediante su interacción con Bin4 (Kozubowski et al., 2003; Ono et al., 2000). Adicionalmente, Chs4 participa como subunidad reguladora esencial para la actividad sintetasa de Chs3 (Choi et al., 1994b; Trilla et al., 1997). La degradación de la enzima se hace por endocitosis y su anclaje en la membrana plasmática la previene de la misma. Chs3 es endocitada a vesículas de

transporte retrógrado de baja densidad. Sin embargo, la mayoría de estas vesículas no son liberadas a la vacuola para su degradación, sino que se reciclan en vesículas de transporte anterógrado (TGN), quedándose en un estado latente para su posterior liberación de nuevo a la membrana plasmática (Valdivia and Schekman, 2003). Estas vesículas procedentes del reciclaje, junto con las vesículas derivadas de la síntesis *de novo*, sirven como reservorio total de Chs3 listo para su depósito en la membrana. De modo que el desequilibro entre la síntesis/degradación de Chs3 hacia un transporte anterógrado o de reciclaje, genera la acumulación polarizada de Chs3 facilitando la síntesis del anillo de quitina en el cuello (Sacristan et al., 2012).

La correcta localización del anillo de quitina en el cuello no solo depende del correcto transporte por parte de las proteínas Chs y de la localización de las septinas, sino también de Bni4 (Sanz et al., 2004). Bni4 se acumula en el sitio de emergencia antes de la formación de la yema. Según se avanza en el ciclo celular, se inmoviliza a ambos lados del cuello. Su acumulación en el cuello depende de las septinas, a las que se une directamente. Bni4 se encuentra asociada a Glc7, que es una proteína fosfatasa tipo I (Ppt1) que está implicada en un amplio rango de procesos biológicos (Bloecher and Tatchell, 2000). La llegada al cuello de Glc7 es independiente de Bni4, pero su interacción con las septinas es Bni4 dependiente. El complejo Bni4-Glc7 es necesario para el depósito de la quitina en las etapas tempranas del ciclo celular (Kozubowski et al., 2003).

Chs4 se moviliza al sito de gemación justo antes de la formación de la yema y tras la emergencia de la yema desaparece. Al final del ciclo celular, vuelve a visualizarse en el cuello en concentraciones tanto o más grandes que las existentes en el inicio de la gemación. Chs4 requiere a Bni4 para acumularse en el cuello en fases tempranas del ciclo celular, no así en su localización en cuello durante la citoquinesis. La localización de Chs4 condiciona la localización de Chs3, por lo que la reaparición de Chs4 en el cuello durante las fases finales del ciclo celular apoya la hipótesis de que Chs3 participa como enzima auxiliar en la formación de septo en ausencia de Chs2.

A pesar de que Chs1, Chs2 y Chs3 tienen importantes papeles en septación y citoquinesis, mutaciones sencillas de estos tres genes, así como la combinación de mutaciones del gen *CHS1* con los genes *CHS2* y *CHS3* no son letales. Sin embargo, el doble mutante *chs2*Δ *chs3*Δ y el triple mutante *chs1*Δ *chs2*Δ *chs3*Δ son letales. Por tanto, a

pesar de que la quitina es el menor de los componentes de la pared celular, parece ser esencial para la supervivencia y viabilidad celular, siendo por tanto una potencial diana antifúngica.

3.3.ENSAMBLAJE DE LOS COMPONENTES

Tras la síntesis vectorial y la extrusión al espacio periplasmático de los polímeros tiene lugar la integración de la nueva cadena sintetizada con los diversos componentes de la pared celular (figura 3A). Este ensamblaje, que ocurre en determinadas zonas de la pared en crecimiento, se lleva a cabo por proteínas con actividad catalítica implicadas en la elongación o remodelación de los polisacáridos de la pared celular. Debido a que en el espacio periplasmático la disponibilidad de energía libre en forma de ATP es baja, se ha propuesto que la ruptura de los enlaces previos proporcionaría la energía necesaria para la formación de los nuevos enlaces, en una reacción denominada transglicosilación (figura 3B) (Cabib et al., 1988). Actualmente, las proteínas de la familia Gas y la familia Crh son las mejor caracterizas con respecto a su posible implicación en la remodelación de los carbohidratos de la pared celular.

3.3.1. Familia Gas

En *S. cerevisiae* la familia de los genes *GAS* consta de 5 miembros, que codifican para cinco proteínas diferentes: Gas1, Gas2, Gas3, Gas4 y Gas5. Son consideradas como glicosidasas o transglicosilasas que participan en la elongación y ramificación de cadenas β-1,3 glucano (Ragni et al., 2007b; Rolli et al., 2011; Rolli et al., 2010). Están incluidas en la familia 72 de la clasificación Henrrisat que le asigna un papel como glicosiltransferasa (GH72) (Henrissat et al., 1995). Estas proteínas realizan la unión entre el extremo reductor de una cadena de β-1,3 glucano donadora y el extremo no reductor de una molécula de β-1,3 glucano aceptora (Carotti et al., 2004; Mazan et al., 2012; Mouyna et al., 2000). El alineamiento de las cinco proteínas revela que existe una organización en tres dominios diferentes: un dominio catalítico dividido en seis cajas cerca del extremo amino terminal; una región rica en cisteínas que participa en las interacciones entre proteínas y por último en el extremo carboxilo terminal una zona rica en serinas y treoninas (dianas para la O-

glicosilación) que desempeñan un papel estructural y son dispensable para su actividad (Popolo et al., 2008). Actualmente, existen datos *in vitro* de la actividad β-1,3 glucanosiltransferasa llevada a cabo por Gas1 y Gas5 presentes durante la fase vegetativa y Gas2 y Gas4 específicas de esporulación (Mazan et al., 2012; Ragni et al., 2007a). También se dispone de la estructura tridimensional de Gas2 que ha ayudado a esclarecer el mecanismo de acción de estas proteínas (Hurtado-Guerrero et al., 2009). El dominio catalítico se encuentra separado físicamente del sitio de unión al carbohidrato, el cual presenta una conformación mayoritariamente de hélices α unidas por láminas β, en forma de ranura, que facilitaría la entrada del glucano. Se ha propuesto un modelo de oclusión para su funcionamiento, de manera que la enzima protegería el producto intermedio formado entre las dos cadenas de β-1,3 glucano en el sitio aceptor del ataque nucleófilo de una molécula de agua. El producto sería desplazado por la entrada de una nueva cadena de β-1,3 glucano de tamaño mayor que induciría un cambio conformacional en la enzima y la salida del producto (Hurtado-Guerrero et al., 2009).

Gas1 es una proteína altamente O-glicosilada y N-glicosilada localizada en la capa exterior de la pared celular mediante su dominio GPI (Popolo et al., 1993a; Popolo and Vai, 1999). Juega un papel importante en la biogénesis de la pared celular, por lo que presenta interacciones sintético letales con otras proteínas que participan en la formación de la pared celular (Tomishige et al., 2003). La pérdida de Gas1 genera defectos morfológicos severos, una disminución en el entrecruzamiento de los glucanos y una alta sensibilidad a compuestos como el CFW o la Caspofungina (Ram et al., 1995; Ram and Klis, 2006). Estos defectos disparan el mecanismo compensatorio de la célula mediado por la ruta CWI que garantiza su supervivencia. La ausencia de Gas1 en la pared celular produce un debilitamiento de la misma, el cual es compensado por un aumento en el nivel de quitina, de manoproteínas y del entrecruzamiento de los polímeros (Kapteyn et al., 1997; Popolo et al., 1997; Ram et al., 1995).

3.3.2. Familia Crh

La familia de proteínas Crh está compuesta por tres miembros: Crh1, Crh2 (*Congo Red Hypersensitive*) y Crr1 (*CRH-related*) (Rodriguez-Pena et al., 2000). Su estructura es común en cuanto a que presentan un péptido señal en su extremo N-terminal que le permite

su incorporación a la ruta de secreción, un dominio catalítico conservado, DE(I/L)DXE homólogo al endo β-1,3 y endo β-1,4 glucanasa de procariotas (Tabernero et al., 1994) y al de varias Xiloglucan-endotransglicosilasas de plantas (figura 5) (Campbell and Braam, 1998). Por ello ha sido incluida en la familia 16 de las enzimas glicosilhidrolasas según la clasificación de Henrissat (Henrissat et al., 1995). Ambas proteínas Crh1 y Crh2 son CWP-GPI que poseen una región rica en serinas y treoninas y un anclaje GPI en su extremo carboxilo susceptible a la fosfolipasa C (Hamada et al., 1998). Este anclaje GPI no se encuentra en Crr1. A su vez, Crh2 presenta un dominio de unión a quitina que no tiene Crh1 (figura 5). La presencia del dominio DE(I/L)DXE es fundamental para que estas proteínas complementen los fenotipos de sensibilidad al RC y al CFW, lo que indica que su actividad enzimática es esencial para su funcionalidad (Rodriguez-Pena et al., 2000). El patrón de expresión transcripcional de los tres genes es diferente. Mientras que *CRH1* se expresa en ciclo vegetativo y en condiciones de esporulación, *CRH2* se expresa exclusivamente durante el ciclo vegetativo y *CRR1* en condiciones de esporulación. *CRH1* tiene un máximo de expresión en fase G1 y en la transición G1/M, mientras que la expresión de *CRH2* no varía a lo largo de todo el ciclo celular (Rodriguez-Pena et al., 2000).

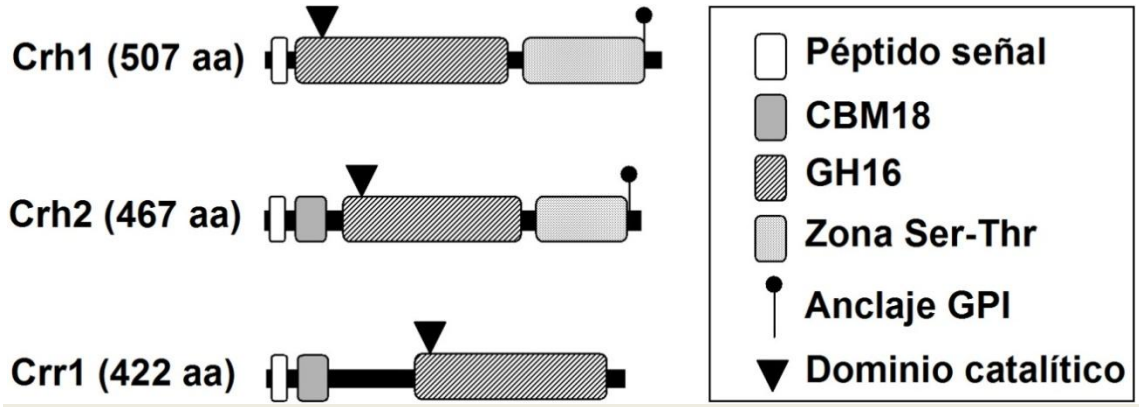

Figura 5. Esquema de la estructura de las proteínas Crh de *S. cerevisiae*. Imagen modificada de Cabib, Farkas et al. (2008). En la imagen se muestra el tamaño de cada proteína expresados en aminoácidos (aa) y los dominios funcionales presentes en su estructura.

Con respecto a la localización celular de las proteínas, se construyeron fusiones de estas proteínas a la proteína verde fluorescente (GFP) y se observó que están localizadas en sitios de crecimiento polarizado (Rodriguez-Pena et al., 2002), mostrando un patrón de distribución que coincide en gran medida con el depósito de quitina. La localización de Crh2 requiere la presencia de las proteínas Chs5 y Bni4, que están implicadas en la

localización de Chs3 en el cuello durante la gemación. Sin embargo, la localización de Crh1 y Crh2 no depende del depósito de quitina, ya que la localización de ambas proteínas no varía en mutantes *chs2*Δ y *chs3*Δ (Rodriguez-Pena et al., 2000; Rodriguez-Pena et al., 2002). Crr1, se localiza en la pared de la espora, de acuerdo con su papel en la biogénesis de esta estructura (Gomez-Esquer et al., 2004). Estudios fenotípicos de los mutantes *crh2*Δ y *crh1*Δ muestran sensibilidad al tratamiento con sustancias que interfieren con el correcto ensamblaje de los polímeros de la pared celular, como el RC y el CFW. Esta sensibilidad se agrava en el doble mutante *crh1*Δ *crh2*Δ, indicando una función solapante de ambos genes en la biogénesis de la pared celular. Ninguno de estos mutantes presentan variaciones en los componentes de la pared celular respecto a una cepa WT, sin embargo sí presentan alteraciones en las fracciones de glucano insoluble en álcali. Teniendo en cuenta que la solubilidad del glucano depende de su unión a la quitina, se propuso que estas proteínas tendrían un papel en la unión del β-glucano a la quitina (Rodriguez-Pena et al., 2000). El mutante *crr1*Δ muestra defectos en el depósito de las capas de glucano, quitosán y ditirosina que forman la pared de las ascosporas durante la esporulación, indicando una posible función durante la biogénesis de la pared de la ascosporas en la unión del quitosán al glucano (Gomez-Esquer et al., 2004).

Esta familia de proteínas está altamente conservada en otros hongos, Así, las proteínas YlCrh1 y YLCrh2 de *Yarrowia lipolytica*, presentan homología con las proteínas Crh1 y Crh2 de *S. cerevisiae.* Mutantes en estas proteínas, también muestran al igual que sus homólogos en *S. cerevisiae*, sensibilidad a compuestos que interfieren con la construcción de la pared celular. *In vitro* las formas solubles de dichas proteínas presentan actividad glicosidasa (Hwang et al., 2006).

La familia de los genes *CRH* en *Cándida albicans* está formada por tres genes: *UTR2, CRH11 y CRH12* con homología a los genes *CRH1* y *CRH2* de *S. cerevisiae.* Al igual que en *S. cerevisiae* mutantes en dichos genes presentan un fenotipo de sensibilidad a diferentes compuestos como el RC, CFW, SDS y altas concentraciones de calcio. Una cepa mutante en los tres genes presenta defectos en la pared celular, un incremento en la sensibilidad a las enzimas degradativas de la pared celular, una disminución de la capacidad de los protoplastos para la regeneración de la pared celular, así como una activación constitutiva de la proteína Mkc1, que es MAP quinasa de la ruta de integridad de *C. albicans*. Adicionalmente, este mutante también presenta una disminución en la

cantidad de la fracción insoluble del β-1,3 glucano. Interesantemente, la deleción por separado de estos genes da lugar a cepas avirulentas en un modelo murino (Pardini et al., 2006).

4. MORFOGÉNESIS

S. cerevisiae presenta un proceso de división asimétrico que genera la aparición de estructuras polarizadas durante la reproducción y la citoquinesis. Ambos procesos requieren la polimerización de actina y la participación de la maquinaría exocítica. Adicionalmente, la citoquinesis requiere la adquisición de un sistema adicional de actino-miosina que inicie la invaginación de la membrana necesaria para la separación celular. El crecimiento polarizado ocurre tanto en la reproducción asexual o ciclo vegetativo mediante gemación, como en el ciclo sexual con la formación del *shmoo*. Durante la gemación la maquinaria de crecimiento se encuentra dirigida hacia el córtex celular promoviendo el crecimiento de la yema. Más tarde en el ciclo celular, la misma maquinaria es redirigida hacia el cuello para impulsar la citoquinesis. Todos estos pasos están acoplados a mitosis y a su vez están regulados por las ciclinas y las quinasas dependientes de ciclinas (CDK) que controlan la división celular (Bi and Park, 2012; Howell and Lew, 2012; Park and Bi, 2007; Pruyne and Bretscher, 2000a; Pruyne and Bretscher, 2000b).

4.1. CRECIMIENTO POLARIZADO

El crecimiento de la yema durante la gemación requiere la participación del citoesqueleto de actina, las septinas, los microtúbulos y una ruta secretora específica para la liberación de los componentes. La polarización del citoesqueleto de actina y el anillo de septinas son clave para mantener el crecimiento polarizado en la yema. Este proceso se desarrolla en varias etapas secuencialmente coordinadas y reguladas por un módulo de proteínas de la familia GTPasas (Pringle et al., 1995; Pruyne and Bretscher, 2000b; Pruyne et al., 2004b). En la figura 6 se muestra un esquema de todo el proceso:

- Al comienzo de un nuevo ciclo celular se selecciona el sitio de gemación, que será el punto donde se concentrarán los parches de actina, convergerán los cables de

actina y se ensambla el anillo de septinas procedentes de la célula madre (Kim et al., 1991; Moseley and Goode, 2006). La proteína Rsr1/Bud1 perteneciente a la familia Ras GTPasa es la encargada de regular este proceso.

- Una vez seleccionado el punto de gemación, coincidiendo con la fase S del ciclo celular y hasta finales de la fase G2, se produce el ensamblaje de los componentes que dará lugar al crecimiento polarizado de la yema. Para ello existe una ruta exocítica específica, regulada por la familia de proteínas Rab GTPasa, que dirige el tráfico vesicular hacia esta zona por los cables y los parches de actina (Bretscher et al., 1994; Finger and Novick, 1998). A su vez, las septinas adquieren una conformación más compleja denominada collar. A nivel general, todos estos procesos están controlados por la proteína Rho GTPasa Cdc42 y sus efectores.
- Al final de la fase G2 y hasta finales de la fase M ocurre el cambio de crecimiento polarizado a crecimiento isotrópico en la yema (Farkas et al., 1974).
- Durante un breve periodo de tiempo y justo antes de que ocurra la citoquinesis, se rompe el crecimiento asimétrico de manera que los parches y los cables de actina se distribuyen aleatoriamente dentro de la célula madre y de la hija, pudiéndose originar un crecimiento en ambas células.
- Al inicio de la telofase, tiene lugar una repolarización de los parches y los cables de actina hacia el cuello que coincide con la división del collar de septinas en dos anillos y el comienzo de la citoquinesis (Finger et al., 1998; Finger and Novick, 1998; VerPlank and Li, 2005).

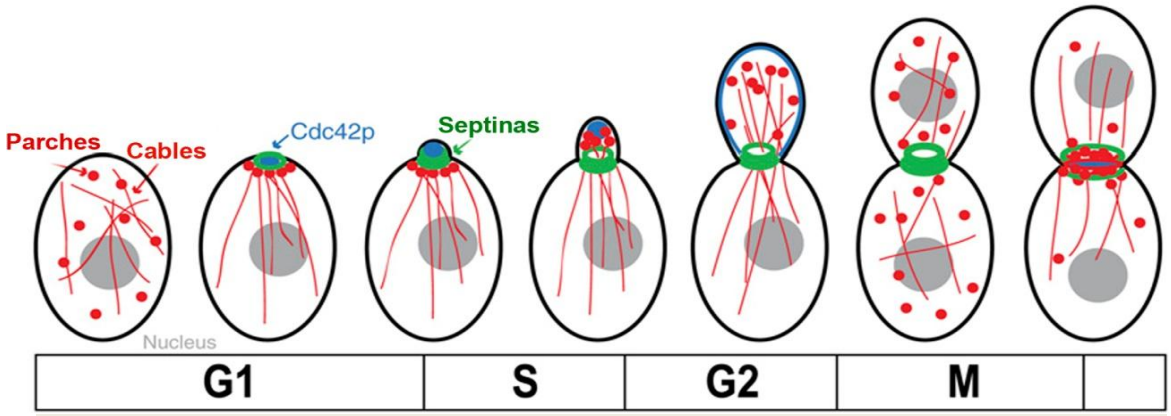

Figura 6. Eventos morfogenéticos durante el ciclo celular. Imagen adaptada de Howell and Lew (2012). La actina está señalizada en rojo, las septinas en verde y Cdc42 en azul. Al inicio del ciclo tiene lugar la selección del sitio de gemación, la polarización de los parches y los cables de actina, el ensamblaje del anillo de septinas y el acúmulo de Cdc42 en la yema. Al final de la fase G2 ocurre el cambio de crecimiento polarizado a isotrópico de la yema. A lo largo de la fase M tiene lugar la ruptura del crecimiento asimétrico. Finalmente, se produce la relocalización al cuello de la maquinaria polarizada para el comienzo de la citoquinesis.

4.1.1. Selección del sitio de gemación

Al comienzo de un nuevo ciclo de división, en la fase G1 se selecciona el sitio de gemación (Chant, 1996; Chant, 1999). El sitio de gemación viene determinado por la carga genética de la célula. Las células haploides (a o α) muestran un patrón de gemación axial. En este caso ambas células, madre e hija, seleccionan el nuevo sitio de gemación inmediatamente adyacente al previo, de modo que la gemación queda restringida a un único polo. Las células diploides presentan un patrón de gemación bipolar, en el que la célula madre puede elegir un sitio adyacente u opuesto al previo, mientras que la célula hija elige el inmediatamente adyacente al polo que eligió la célula madre, de modo que usan ambos polos para gemar. Estos patrones de gemación ocurren en respuesta a proteínas específicas para cada tipo de gemación codificadas por la familia de genes *BUD* (figura 7A). En la gemación axial estas proteínas se localizan en el córtex de manera transitoria, mientras que en la gemación bipolar se localizan de manera permanente (Chant and Pringle, 1991; Chant and Pringle, 1995). *BUD8*, *BUD9*, *RAX2* y *RAX1* codifican para los marcadores específicos del patrón bipolar (Harkins et al., 2001). En el caso de patrón axial, son las proteínas Bud3, Bud4, Axl1 y Axl2/Bud10 las encargadas de marcar el sitio de gemación (figura 7A). Por último, existe un módulo central de GTPasa para ambos patrones formado por Rsr1/Bud1 (Ras-GTPasa), Bud5 (GEF) y Bud2 (GAP) que se encargan de reclutar al sitio de gemación a la quinasa reguladora de la polaridad Cdc42 (figura 7A) (Chant et al., 1991; Chant and Herskowitz, 1991; Park et al., 1993; Park et al., 1999; Roemer et al., 1996a). Así, en levaduras haploides Axl1 se une directamente con Bud5 y activan a Bud1/Rsr1 en el sitio de gemación. Bud1 activada es capaz de reclutar a este punto de la membrana a la quinasa Cdc42 conectando los marcadores del sitio de gemación con el siguiente paso del ciclo celular (figura 7A) (Chant, 1999; Chant et al., 1995; Kozminski et al., 2003; Park et al., 1993; Pringle et al., 1995).

4.1.2. Polarización de Cdc42

La regulación del crecimiento polarizado en levaduras está mediada por la proteína Cdc42 que pertenece a la familia de las Rho GTPasas (Adams et al., 1990). La activación de Cdc42 depende de su única GEF que es Cdc24 (Hartwell et al., 1974; Sloat et al., 1981)

y sus GAPs que son Bem2, Bem3, Rga1 y Rga2 (figura 7B) (Holt et al., 2009; Stevenson et al., 1995; Ziman et al., 1991). Ambos factores presentan efectos antagónicos, regulando así la activación o inhibición de la proteína. A diferencia de las GAPs, Cdc24 es esencial para la viabilidad celular y juega un papel fundamental en establecer y mantener el crecimiento polarizado. Cdc42 presenta en su extremo amino terminal un motivo efector tipo RAS, a través del cual se une a proteínas que tienen un dominio CRIB (dominio de interacción con Cdc42/Ras), que también es conocido como dominio p-21. Cdc42 sufre diferentes modificaciones postraducionales, entre las que se encuentra la prenilación de su extremo carboxilo terminal que facilita su anclaje en la membrana y permite el desarrollo de sus funciones (Gladfelter et al., 2001; Ziman et al., 1991). Cdc42 se localiza en la membrana plasmática y en los sitios de crecimiento polarizado, donde recluta a una gran variedad de efectores promoviendo la remodelación del citoesqueleto de actina y el comienzo de la gemación (figura 7B).

Entre las múltiples funciones de Cdc42 están: la orientación de los cables y el agrupamiento de los parches de actina hacia el sitio de gemación, el ensamblaje del anillo de septinas y la exocitosis o el transporte dirigido de las vesículas (figura 7B) (Adamo et al., 2001; Adams et al., 1990; Adams and Pringle, 1984). Para realizar sus funciones Cdc42 presenta una amplia variedad de sustratos efectores como son (figura 7B):

- Las proteínas quinasas activadas por p21 (PAKs): Ste20 y Cla4 (Davis et al., 1998; Eby et al., 1998). Cdc42-GTP se une al extremo N-terminal de las PAKs (Vojtek and Cooper, 1995) y las activa, consiguiendo así la acción efectora sobre el citoesqueleto de actina (Eby et al., 1998).
- Las proteínas Gic1 y Gic2 que participan en la organización de las actinas y las septinas.
- La formina Bni1, implicada en el ensamblaje de filamentos de actina no ramificados.
- Las proteínas Boi1 y Boi2 implicadas en la ruta de secreción (McCusker et al., 2007).
- Por último Sec3, un componente del complejo Exocisto que interviene en la exocitosis de las vesículas secretoras a la membrana (Finger et al., 1998; Pruyne et al., 2004a).

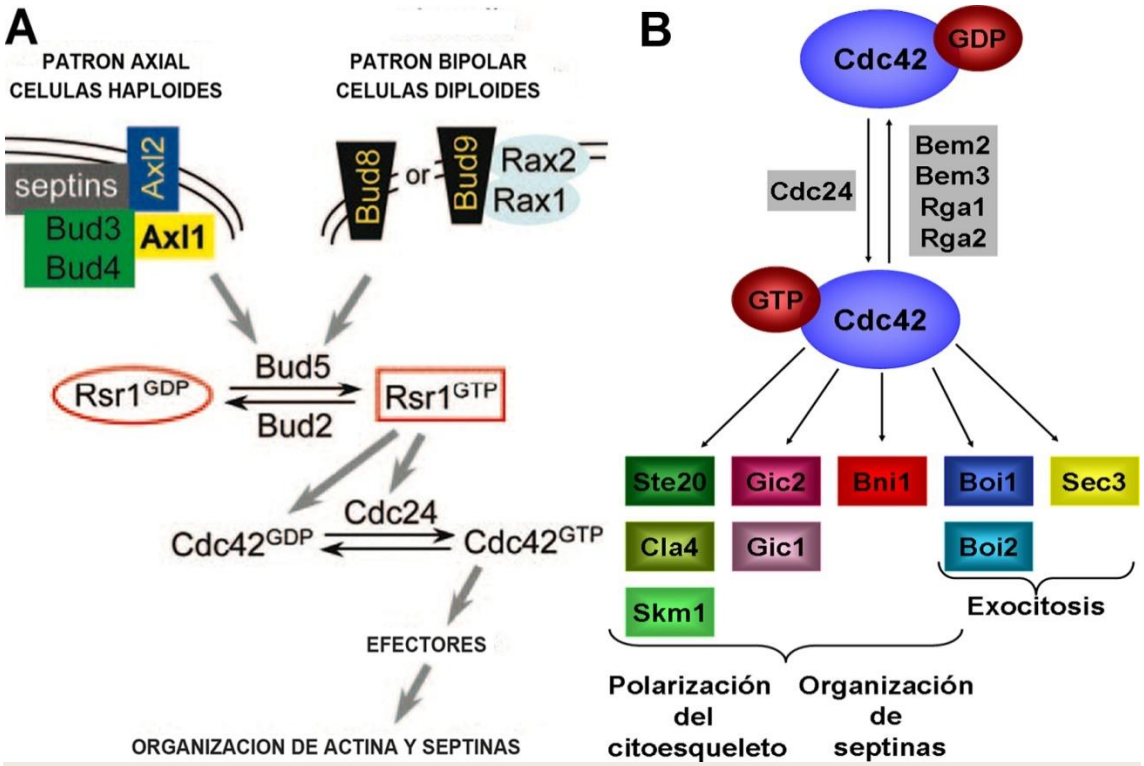

Figura 7. Patrón de gemación y efectores de Cdc42. A, Imagen adaptada de Park and Bi (2007). El patrón de gemación viene determinado por las proteínas Bud. Existen diferentes marcadores de gemación en función de la carga genética de la célula: haploide y diploide. La GTPasa Rsr1/Bud1, común a ambos patrones, es la encargada de reclutar al sitio de gemación a la GTPasa Cdc42 que regula el crecimiento polarizado. En la imagen B, se muestran los reguladores y efectores de Cdc42. Cdc42-GTP regula el crecimiento polarizado, el ensamblaje de las septinas y la exocitosis, mediante la acción de sus efectores.

El reclutamiento y la activación de Cdc42 en el sitio de gemación son un paso fundamental para el inicio y la progresión del crecimiento polarizado de la yema. Respecto al reclutamiento a la membrana de Cdc42 se han propuesto varios modelos. El modelo principal implica la participación de la maquinaria del sitio de selección. Como anteriormente se ha descrito, las proteínas Bud junto a la quinasa Rsr1/Bud1 permiten un acúmulo y activación en membrana de Cdc42 (figura 7A) (Benton et al., 1993; Zheng et al., 1995). Adicionalmente, se han descrito dos mecanismos que ayudarían a mantener un enriquecimiento de Cdc42 en los sitios de crecimiento polarizado. El primero está mediado por la proteína Rdi que es capaz de extraer de la membrana al complejo inactivo Cdc42-GDP (Koch et al., 1997). Como consecuencia de esta extracción, se facilitaría una mayor difusión de Cdc42 hacia las zonas enriquecidas con Cdc24, donde se produciría su activación (Tiedje et al., 2008). Un segundo mecanismo alternativo implicaría la participación de la ruta vesicular, mediada por los cables de actina polarizados hacia la yema, de modo que la dinámica entre el aporte de Cdc42 procedente de las vesículas y su

reciclaje en endosomas permitiría mantener a Cdc42 polarizada en la yema (Marco et al., 2007; Slaughter et al., 2009). Adicionalmente, en células *rsr1*Δ se ha observado un mecanismo de retroalimentación positiva que permitiría mantener el patrón de gemación polarizado a pesar de la ausencia de la señal de gemación. Este mecanismo se lleva a cabo por el complejo formado por las proteínas Bem1, Cdc24 y Cla4. La presencia de Cla4 en el complejo facilitaría la unión de Cdc42-GTP al mismo. La unión de Cdc42 al complejo, promovería la formación de más Cdc42-GTP por parte de Cdc24, lo que fomentaría la retroalimentación positiva y la polarización de Cdc42 (Fujimura-Kamada et al., 2012; Kozubowski et al., 2008; Li and Wedlich-Soldner, 2009). Este mecanismo estaría de acuerdo con la premisa de que la carga de Cdc42 por su GEF es necesaria para su concentración en el sitio de polarización. A su vez, el estado en el que podemos encontrar el complejo Cdc42-Cdc24 varía desde un alto grado de conglomeración durante la emergencia de la yema, pasando por un grado medio de agrupación durante el crecimiento apical, a una distribución difusa durante el crecimiento isotrópico (figura 6) (Nern and Arkowitz, 1999; Peter et al., 1996).

4.1.2.1. Proteín quinasas activadas por p21 (PAKs)

La familia de proteínas serín-treonín quinasas activadas por p21 (PAK) se caracteriza por presentar un dominio quinasa en su extremo carboxilo terminal altamente conservado en eucariotas. En *S. cerevisiae* existen tres PAKs: Ste20, Cla4 y Skm1. El reclutamiento a los sitios de crecimiento polarizado de las PAKs por Cdc42 ocurre mediante interacciones proteína-proteína a través del domino CRIB (Hofmann et al., 2004) o mediante interacciones proteína-lípido. Estas últimas pueden ocurrir gracias a un dominio de unión al fosfoinositol presente en ambas quinasas; un dominio de unión con homología a plectrina (PH) presente en Cla4 y Skm1 o una región rica en aminoácidos básicos presentes en Ste20 que promueve su asociación con los lípidos de la membrana (Boyce and Andrianopoulos, 2011; Holly and Blumer, 1999; Leberer et al., 1992; Peter et al., 1996).

4.1.2.1.1. Ste20

Ste20 fue la primera proteína quinasa tipo PAK descubierta en *S. cerevisiae* (Leberer, Wu et al. 1997;Herskowitz 1988). Está relacionada con múltiples procesos en la levadura,

desde la señalización a través de diferentes vías de proteínas quinasas activadas por mitógenos (MAPK) implicadas en el apareamiento (Herskowitz 1995;Liu, Styles et al. 1993), el crecimiento filamentoso y la respuesta a estrés osmótico; hasta el ciclo celular (Hofken and Schiebel 2002; Hofken and Schiebel 2004;Herskowitz, Park et al. 1995), la inducción de apoptosis, la biosíntesis de esterol (Lin, Grillitsch et al. 2009; Lin, Unden et al. 2009) o la herencia vacuolar (Bartholomew and Hardy 2009).

Ste20 se une a Cdc42-GTP *in vivo* e *in vitro* mediante su dominio CRIB. Esta unión libera a Ste20 de la propia autoinhibición de su dominio quinasa, permitiéndole su autofosforilación y su activación. Durante el ciclo vegetativo, la asociación de Ste20 a Cdc42-GTP permite su participación en la polaridad celular gracias a su implicación en la reorganización del citoesqueleto de actina, vía fosforilación de la formina Bni1 y de las miosinas Myo3 y Myo5 (Eby et al., 1998; Evangelista et al., 2002; Heinrich et al., 2007; Wu et al., 1997).

4.1.2.1.2. Cla4

CLA4 fue aislado en una búsqueda de genes sintéticos letales con las ciclinas mitóticas Clb1 y Clb2. Codifica para una proteína de 842 aminoácidos con actividad serina treonina quinasa. Esto, junto con el hecho de que fuera efector de Cdc42 sugería su implicación en morfogénesis y ciclo celular (Benton et al., 1997; Benton et al., 1993; Cvrckova et al., 1995; Cvrckova and Nasmyth, 1993). Cla4 colocaliza con Cdc42 en los sitios de crecimiento polarizado. Así, en células con yemas pequeñas, Cla4 está concentrada en la punta y los lados de la yema, mientras que en células con tamaño de yema mediano está localizada en forma de puntos o parches distribuidos por todo el córtex de la célula. La unión de Cla4 a Cdc42-GTP es esencial para promover la actividad quinasa de esta proteína (figura 8). Al inicio de un nuevo ciclo, Cla4 no se encuentra unida a Cdc42-GTP, de modo que el dominio quinasa de Cla4 inhibe su propia actividad catalítica. Tras la gemación, Cdc42-GTP se une a Cla4 a través de su dominio CRIB, revirtiendo la autoinhibición sobre su dominio quinasa. Tras la citoquinesis, GTP-Cdc42 se disocia de Cla4 provocando una bajada en la actividad catalítica de la misma (Benton et al., 1997). *CLA4* presenta una expresión dependiente de ciclo celular y participa en varios eventos a lo largo del ciclo celular (figura 8):

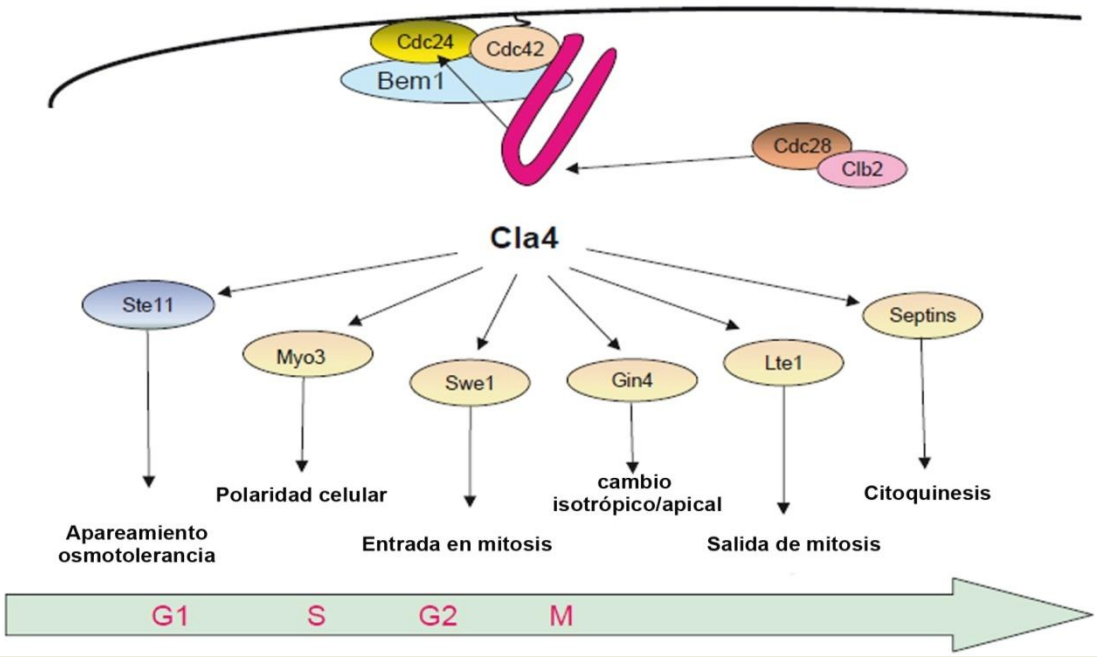

Figura 8. Esquema de las funciones de Cla4. Imagen adaptada de Hofmann, Shepelev et al. (2004). Cla4 está formando parte de un multicomplejo proteico junto a Cdc42, Cdc24 y Bem1 localizado en los sitios de crecimiento polarizado. La actividad de Cla4 está sujeta a su propia autorregulación y la acción del complejo Cdc28-Ciclina2. Cla4 presenta múltiples efectores a través de los cuales participa en los diferentes eventos celulares. Así, participa en la entrada y salida de mitosis a través de la fosforilación de Swe1 y Lte1.También está implicada la organización de las septinas, polaridad celular y cambió de crecimiento apical a isotrópico.

(I) como un posible regulador negativo en la ruta de apareamiento posiblemente mediante la fosforilación de Ste11 (Heinrich et al., 2007; Hofmann et al., 2004); (II) en el establecimiento de la polaridad durante la división celular a varios niveles: a través de la fosforilación de la miosina Myo3 durante el ensamblaje de los filamentos de actina para la formación y posterior contracción del anillo actomiosina (AMR) (Wu et al., 1996) y a través de la fosforilación de la quinasa Gin4 implicada tanto en el cambio de crecimiento de polarizado a isotrópico mediado por el complejo Clb2/Cdc28 (Tjandra et al., 1998) como en el ensamblaje de las septinas en el cuello al inicio de la gemación (Kozubowski et al., 2005; Longtine et al., 1998). También participa de manera indirecta en la nucleación de los cables de actina necesarios para el reclutamiento de las septinas al cuello (Caviston et al., 2003; Kadota et al., 2004); (III) en la regulación de los procesos de entrada y salida de la mitosis, mediante la fosforilación de las proteínas: Lte1 (GEF de la GTPasa Tem1) esencial en la ruta reguladora MEN (Hofken and Schiebel, 2002; Hofken and Schiebel, 2004; Seshan and Amon, 2005) y la quinasa reguladora del *checkpoint* morfogenético Swe1 (Sakchaisri et al., 2004); (IV) en la localización y el ensamblaje del anillo de septinas durante la citoquinesis, mediante la fosforilación de las septinas Cdc10 y Cdc3

promoviendo la remodelación de los filamentos de septinas a collar de septinas (Kadota et al., 2004; Schmidt et al., 2003; Versele and Thorner, 2004; Versele and Thorner, 2005; Weiss et al., 2000); (V) también colabora junto a las septinas y el anillo de quitina en conservar la integridad celular, manteniendo el grosor del cuello constante durante la división (Schmidt et al., 2003; Weiss et al., 2000).

El éxito en el proceso de división celular requiere la progresión en orden de los eventos celulares. Esta progresión está controlada por los niveles de ciclinas y la quinasa dependiente de ciclina Cdc28. De esta manera se establecen puntos de control o *checkpoint* capaces de detectar problemas y solucionarlos, mediante el retraso en el avance del ciclo celular (Howell and Lew, 2012). El punto de chequeo o *checkpoint* morfogenético es llevado a cabo por la tirosina quinasa Swe1 que se mantiene activa y fosforila a la quinasa Cdc28 provocando su inhibición y como resultado final un arresto en la fase G2/M del ciclo celular, proporcionando el tiempo necesario para la reparación del daño y el correcto avance del ciclo celular. Swe1 presenta una regulación dependiente de ciclo, de manera que al inicio del ciclo se encuentra restos procedentes del ciclo anterior. Durante la fase G1, se produce una leve degradación de Swe1 por ubiquitinación. Sin embargo en la fase G2/M, se aumenta la velocidad de degradación de forma dependiente del complejo Clb2-Cdc28. La activación de Swe1 está asociada a un fenotipo característico de células con yemas alargadas y retraso en la división nuclear. Swe1 se activa por problemas con la polaridad celular, disrupción en la estructura de las septinas, problemas con la organización de los filamentos de actina y frente a variedad de estreses medioambientales (Lew and Reed, 1995a; Lew and Reed, 1995b; McMillan et al., 1999a; McMillan et al., 1999b). Swe1 se inactiva por la acción conjunta de la mentiltransferasa Hsl7 y la quinasa Hsl1 localizadas en el anillo de septinas (Cid et al., 2001b; Shulewitz et al., 1999).

La inhibición de la actividad quinasa Cla4 provoca un arresto celular dependiente de Swe1. Las células *cla4*Δ presentan un aumento del grosor del cuello, yemas alargadas en las cuales la actina y las septinas se encuentran altamente polarizadas (Weiss et al., 2000). La deleción del gen *SWE1* sobre un fondo *cla4*Δ provoca un recorte en la longitud de las yemas pero el defecto en la organización de las septinas permanece, indicando que existe otro mecanismo que está colaborando en la conservación del diámetro del cuello. *CLA4* y *CDC11* son sintéticos letales con *CHS3*. Las células *cla4*Δ *chs3*Δ presentan un mayor porcentaje de septinas desorganizadas y deslocalizadas, un diámetro de cuello superior y

un aumento de septos aberrantes con respecto a la cepa WT. Estos datos sugieren que el anillo de quitina y el anillo de septinas colaboran en el mantenimiento del tamaño del cuello constante entre la célula madre e hija necesario para preservar la integridad celular (Schmidt et al., 2003).

4.1.2.1.3. Skm1

Skm1 es el tercer miembro de la familia de quinasas PAK (Martin et al., 1997). A pesar de la alta homología de secuencia con Cla4, no se ha encontrado una relación funcional entre ellas, ni tampoco con Ste20. La deleción de *SKM1* aparentemente no afecta a la morfogénesis, mientras que sobreexpresión de *SKM1* produce células multigemadas que presentan defectos en separación. Más recientemente se ha asignado un papel a Skm1, junto a sus homólogos Ste20 y Cla4, en la biosíntesis de esteroles (Lin et al., 2009a; Lin et al., 2009b).

4.1.3. Polarización del citoesqueleto

El citoesqueleto de actina es responsable, entre otras funciones, del crecimiento polarizado (Adams and Pringle, 1984), del tráfico de vesículas (Bretscher et al., 1994; Finger and Novick, 1998), la herencia de las mitocondrias y las vacuolas (Catlett and Weisman, 1998; Hill et al., 1996; Simon et al., 1997) y la orientación del huso mitótico (Theesfeld et al., 1999).

4.1.3.1. Actina

Los cables y los parches de actina son dos de las estructuras morfológicas en las que se pueden organizar los filamentos actina en levadura y son los responsables, junto a otras proteínas, de que exista un crecimiento polarizado (Moseley and Goode, 2006). Los parches de actina están formados por moléculas de actina-F agrupadas en discretos conjuntos situados en el córtex de la célula. Los cables de actina están compuestos por largos filamentos de actina (Act1p), fibrina (Sac6p) y tropomiosina (Tpm1 y Tpm2), creando una estructura altamente dinámica ideal para el trasporte dirigido de las vesículas

hacia la célula hija (Adams and Pringle, 1984; Amberg, 1998). La polarización de los cables de actina está íntimamente ligada a la estructura conocida como *caps proteins* que se localiza en el extremo terminal de la yema a lo largo del todo el ciclo celular, controlando la polaridad y el transporte de las vesículas (Lew and Reed, 1995a; Sloat et al., 1981).

Los cables polarizados de actina actúan como guías para la exocitosis o ruta secretora, implicada en la liberación dirigida de vesículas que portan las proteínas necesarias para el crecimiento de la célula hija. Esta ruta se encarga principalmente del movimiento intracelular de las proteínas desde el aparato de Golgi y/o RE hasta la membrana plasmática. En este transporte participan: los cables de actina, que actúan como carriles, la miosina tipo V Myo2 que ejerce como proteína motora y el complejo proteico denominado Exocisto que entre otras proteínas contiene a la proteína Rab GTPasa Sec4 y a su GEF Sec2 que viajan junto a la vesícula (Munchow et al., 1999; Pashkova et al., 2005; Schott et al., 1999). Una vez las vesículas llegan a la membrana, se produce la fusión mediada por las proteínas SNARE. Existen diferentes etiquetas ubicadas en discretos puntos a lo largo de la membrana que dirigen la fusión de las vesículas a la misma. Dependiendo de la localización de estas etiquetas en la célula será necesaria la participación de diferentes proteínas estructurales (Takizawa et al., 1997). Un ejemplo es el transporte de las proteínas Chs3, Bud3 y Bud4 al cuello, que requieren la participación del anillo de septinas (DeMarini et al., 1997; Kamei et al., 1998).

El polarisoma es una estructura implicada en la regulación del ensamblaje y unión de los filamentos de actina (Amberg et al., 1997; Evangelista et al., 1997; Kohno et al., 1996; Sheu et al., 2000). Está compuesto por las proteínas: Spa2, que actúa como andamio (Sheu et al., 1998; van Drogen and Peter, 2002), Pea2, que regula la localización de Spa2, Bud6 que es un activador de Bni1 (nucleadora de filamentos de actina) (Kohno et al., 1996), Msb3 y Msb4, GAPs de la GTPasa Sec4, Bem1 y las septinas (Bender and Pringle, 1991). Bem1 promueve el acoplamiento entre las proteínas del polarisoma y el complejo Cdc42-Cdc24 a través de su unión directa (Chenevert et al., 1992). Cdc42 regula la polimerización de los cables de actina y la exocitosis, modulando la actividad de la formina Bni1 y su unión física con Sec4 y el polarisoma (Roemer et al., 1998; Sheu et al., 1998). El grado de asociación entre el complejo Cdc42-Cdc24 y el polarisoma varía a lo largo de las diferentes etapas de crecimiento.

4.1.3.2. Septinas

Las septinas son una familia de proteínas altamente conservadas en eucariotas que contienen un módulo de unión a GTP. Son capaces de asociarse entre sí formando estructuras con diferente grado de complejidad: fibras (octámero), filamentos, anillo, collar y malla (Cid et al., 1995; Field and Kellogg, 1999; Gladfelter, 2010; Oh and Bi, 2011). Estas estructuras se encuentran interaccionando con el citoesqueleto o asociadas a la membrana plasmática del cuello durante el ciclo celular excepto en el ensamblaje y desensamblaje que sufren durante la fase G1. En su estructura podemos diferenciar un extremo amino terminal de tamaño variable, un dominio central de unión a GTP y un extremo carboxilo terminal con estructura de hélice súper enrollada. El papel funcional del domino de unión a GTP aún está por establecer. Inicialmente se relacionó a este dominio con la formación de los filamentos de septinas gracias a la hidrólisis del GTP (Frazier, Wong et al. 1998). Trabajos posteriores demostraron que la formación de los filamentos de septinas no requiere de la unión ni la hidrólisis de GTP (Mitchison and Field, 2002), aunque la formación del collar de septinas es claramente dependiente de la unión a GTP y de la reorganización de los parches de septinas preexistentes, generados de manera GTP independiente. El dominio de unión a GTP se ha visto que es importante para mantener la propia arquitectura de las septinas *in vivo* (Rodriguez-Escudero et al., 2005). Adicionalmente, también se conoce que la fosforilación por parte de Cla4 de las septinas Cdc10, Cdc3 y Cdc11 (Kadota et al., 2004; Schmidt et al., 2003; Weiss et al., 2000) y la actividad de la quinasa Gin4 sobre Shs1 (Longtine et al., 1998) juegan un papel importante en la iniciación y estabilización del anillo durante la emergencia de la yema. Ambas proteínas son reclutadas tempranamente en el ciclo celular y se asocian a las septinas (Kadota et al., 2004; McMurray and Jeremy, 2008; Nagaraj et al., 2008; Schmidt et al., 2003; Versele and Thorner, 2004; Weiss et al., 2000). Otros autores proponen que la hidrólisis de GTP permitiría a las septinas unirse a otras proteínas o a fosfolípidos en la membrana (Casamayor and Snyder, 2003; Weirich et al., 2008).

En *S. cerevisiae* los genes que codifican para las septinas fueron identificados hace más de 30 años, como genes cuya ausencia evitaban la citoquinesis a Tª restrictiva, generando células en cadenas multinucleadas y multigemadas. El genoma de *S. cerevisiae* codifica para siete septinas. Cinco de ellas participan durante la mitosis (Cdc3, Cdc10,

Cdc11, Cdc12 y Sec7/Shs1) y las dos restantes son específicas de esporulación (Spr3 y Spr28). Cdc42 regula el ensamblaje de las septinas reclutándolas desde el citoplasma al sitio de gemación y ensamblándolas al citoesqueleto. La regulación se ejerce de manera directa mediante la fosforilación de las septinas por las proteínas quinasas Gin4 y Cla4 y de manera indirecta acoplando el proceso morfogenético al avance del ciclo de división celular (DeMay et al., 2009; Gladfelter et al., 2002; Gladfelter et al., 2005; Gladfelter et al., 2001; Gladfelter et al., 2004; Versele and Thorner, 2004; Versele and Thorner, 2005). Las septinas participan en múltiples procesos a lo largo del ciclo celular, como la selección del sito de gemación, el anclaje de proteínas en las zonas de crecimiento polarizado, la orientación del huso mitótico, la secreción vesicular, la citoquinesis, el depósito de quitina, el control en la progresión en el ciclo celular, la estabilización y mantenimiento del crecimiento polarizado, el cambio de crecimiento apical a isotrópico, la separación celular o la repolarización de la actina entre otros (Barral et al., 1999; Cid et al., 1998a; Chant and Stowers, 1995; Douglas et al., 2005; Gladfelter, 2010; Sanders and Field, 1994; Spiliotis and Gladfelter, 2012).

Las septinas se ensamblan y desensamblan adquiriendo diferentes estructuras a lo largo del ciclo celular (figura 6). El grado de organización de las septinas en sus diferentes estructuras es ciclo dependiente. De modo que al comienzo de un nuevo ciclo celular durante la fase G1, las septinas son reclutadas al el sitio de gemación a través de su unión con las proteínas Bud1/Shs1, Bud2 y Cdc42, aglomerándose en parches en la región yuxtapuesta al sitio de emergencia (Cid et al., 2001a). En esta fase las subunidades tienen gran movilidad y son invisibles al microscopio electrónico (Caviston et al., 2003; Park et al., 1999; Roemer et al., 1996a; Roemer et al., 1996b). Tras la selección del sitio de gemación las septinas se organizan en una estructura más compleja conocida como el anillo de septinas (figura 6). El anillo de septinas colabora en el mantenimiento de la integridad celular controlando el grosor que alcanza el cuello a lo largo del ciclo celular y garantizando un crecimiento polarizado. El desarrollo de estas funciones ocurre gracias a una acción conjunta entre las septinas, los cables de actina y las vesículas secretoras. Las septinas participan en el reclutamiento y activación de la formina Bnr1, así como en las proteínas de la ruta secretora. Inicialmente los cables de actina y las septinas están unidos y dirigidos hacia el sitio de gemación. Una vez producida la gemación, se encargan del crecimiento de la yema para lo cual las septinas y la actina se separan espacialmente. Los cables de actina quedan orientados hacia la punta de la yema de manera que el crecimiento

sea polarizado quedando el anillo de septinas en la base de la yema (figura 6) (Pruyne et al., 2004a; Pruyne et al., 2004b). Durante el crecimiento polarizado de la yema, las septinas se expanden por el cuello en forma de collar promovido por una fosforilación directa de las septinas del anillo por la quinasa Cla4 (Cvrckova et al., 1995; Versele and Thorner, 2004). Durante esta etapa las subunidades son básicamente inmóviles y se pueden visualizar los filamentos de un diámetro de 10 nm en el cuello (Frazier et al., 1998). El collar de septinas está implicado en la localización y reclutamiento en el cuello de más de ciento treinta proteínas. Entre las proteínas reclutadas están aquellas con actividades catalíticas necesarias durante la citoquinesis, la separación celular y la remodelación de la pared celular como: Chs3 (DeMarini et al., 1997), componentes de la maquinaria de la selección del sitio de gemación (Cid et al., 2001a; Cid et al., 2002; Versele and Thorner, 2004) y factores implicados directamente en la citoquinesis: Sec3, Spa2 y Chs2. Al final de la telofase el collar de septinas que inicialmente está orientado paralelamente al eje de división, sufre un giro de 90ºC y se divide en dos anillos diferentes, dando comienzo la citoquinesis (McMurray and Thorner, 2009a; McMurray and Thorner, 2009b). Tras la separación celular se produce un desensamblaje y reciclaje del viejo anillo de septinas y la formación de un nuevo anillo de septinas adyacente al viejo (Jimenez et al., 1998; McMurray and Thorner, 2008).

Se han propuesto dos modelos funcionalmente no excluyentes para explicar cómo la organización de las septinas en estructuras supramoleculares más complejas sería necesaria para la progresión del ciclo celular y el desarrollo de sus funciones. En primer modelo las septinas estarían actuando como andamio para el anclaje de otras proteínas, que explicaría el papel de las septinas en la selección del sitio de gemación, crecimiento polarizado de la yema y citoquinesis (Field and Kellogg, 1999; Gladfelter, 2010; Longtine et al., 1996; Longtine et al., 2000). En otro modelo, conocido como “barrera para la difusión”, el diferente grado de asociación entre las septinas y la membrana plasmática evitaría una libre difusión del citoplasma, del RE, de la envoltura nuclear y proteínas desde la célula madre a la célula hija, permitiendo mantener la asimetría celular durante el ciclo celular (Barral et al., 2000). Este modelo se apoya en la organización de las septinas en la estructura denominada collar, estructura altamente organizada en filamentos circulares continuos por todo el cuello cuando la difusión cortical de los componentes celulares entre la madre y la yema está restringida. A su vez, las septinas al estar asociadas a la membrana servirían como una barrera eficaz para impedir físicamente la difusión de proteínas integrales de

membrana, ya sea directamente o indirectamente, mediante la unión a lípidos y su participación en la estructuración de la membrana plasmática (Bertin et al., 2012; Bertin et al., 2010). Recientemente, se ha propuesto un tercer modelo en el que la escisión del collar en dos anillos actuaría como un "corral" para secuestrar las vesículas secretoras, enzimas sintetizadoras de quitina y otros componentes de la pared celular necesarios para la terminación de la citoquinesis y la septación, pero a los que las septinas no se unirían directamente (Dobbelaere and Barral, 2004; Oh and Bi, 2011).

4.1.3.3. Anillo de quitina

Al inicio del ciclo celular, se produce un depósito de quitina en forma de anillo en el cuello dependiente de Chs3 (Shaw et al., 1991). Este anillo se localiza en la base de la yema y representa el mayor porcentaje de quitina que contiene la célula (Molano et al., 1980). Al final de la citoquinesis, el anillo de quitina queda rodeando la estructura trilaminar formada por el septo primario y el septo secundario (figura 2B). Finalmente, tras la separación celular, parte del anillo de quitina quedará reminiscente en la célula madre formando parte de la cicatriz. Su papel durante la citoquinesis era ambiguo, hasta que el grupo del Dr. E. Cabib demostró que colabora, junto a las septinas, en conservar la integridad celular, limitando el grosor del cuello durante el crecimiento (Cabib and Schmidt, 2003). La función del anillo de quitina, se dedujo de manera inesperada durante la búsqueda de genes sintéticos letales con *CHS3*. En este rastreo genómico aparecieron dos genes: *CLA4* y *CDC11*. Un análisis en profundidad de la interacción de estos genes con *CHS3*, mostró que las septinas y el anillo de quitina cooperan en el mantenimiento del tamaño del cuello, de manera que la deleción simultánea de *CHS3* y *CLA4* o *CDC11* da lugar a un aumento del grosor del cuello, lo que conlleva un aumento de la muerte celular (Schmidt et al., 2003).

4.2. CAMBIO DE CRECIMIENTO APICAL A ISOTRÓPICO

Tras la emergencia de la yema, la mayoría del crecimiento ocurre en la punta de la yema, proceso conocido como crecimiento apical. En un determinado momento a lo largo de la fase G2 cambia de un crecimiento polarizado a un crecimiento generalizado de toda

la yema, conocido como crecimiento isotrópico (Farkas et al., 1974). Este cambio depende de la ciclina mitótica 2 y de la quinasa dependiente de ciclina Cdc28 (Lew, 2003) y ocurre gracias a que las proteínas que se mantenían altamente polarizadas en la punta de la yema durante la fase G1, pasan a estar distribuidas alrededor del córtex celular y a que los parches y los cables de actina que antes permanecían polarizados en la punta de la yema, ahora se distribuyen aleatoriamente dentro de la célula hija. Tras el cambio a crecimiento isotrópico, la mayoría del crecimiento ocurre únicamente en la célula hija, manteniéndose así la asimetría en el crecimiento. Esta asimetría requiere la polimerización de la actina en parches, la participación de las miosinas y el mantenimiento intacto del collar de septinas. Durante un breve periodo de tiempo y justo antes de que ocurra la citoquinesis, los parches y los cables de actina se distribuyen aleatoriamente dentro de la célula madre y de la hija, pudiéndose originar un crecimiento en ambas células, rompiéndose así el crecimiento asimétrico.

4.3.CITOQUINESIS

La citoquinesis es el paso final del ciclo celular, en el cual se produce la separación física de las dos células (figura 9). En *S. cerevisiae* la citoquinesis ocurre a través del estrechamiento del cuello e implica una acción concertada entre los parches de actina, la contracción del AMR, la división del collar de septinas y la síntesis del septo primario.

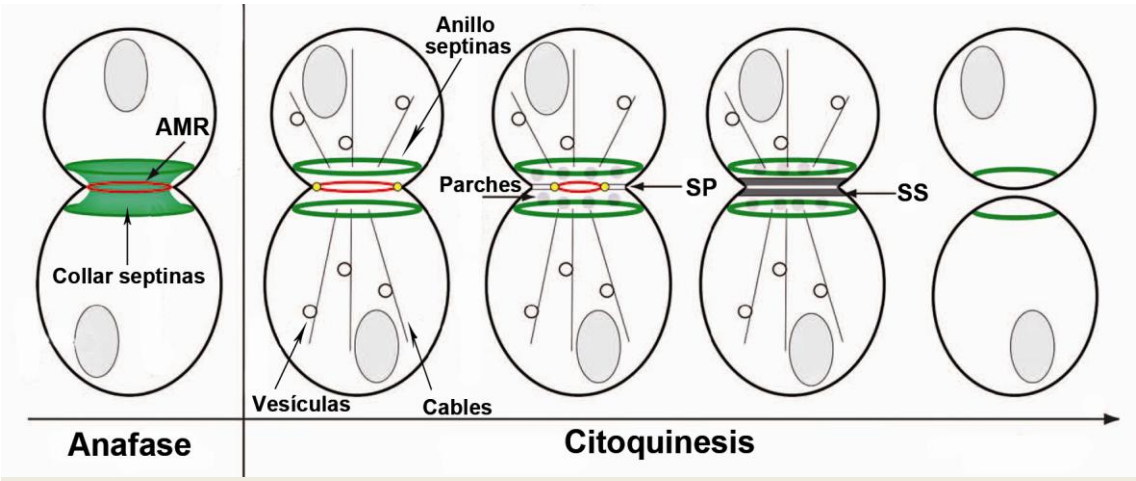

Figura 9. Esquema de la citoquinesis y la separación celular. Imagen adaptada de Meitinger, Palani et al. (2012). AMR, anillo de actomiosina. SP, septo primario. SS, septo secundario. El comienzo de la citoquinesis requiere la división del collar de septinas en dos anillos, la reorientación hacia el cuello de los cables y los parches de actina y la constricción del AMR. Una vez se ha sintetizado el septo primario (SP), se deposita el septo secundario (SS) a ambos lados del SP. Finalmente, ocurre la separación celular.

De este modo, los parches corticales, que inicialmente están concentrados en la superficie de la yema, pasan a acumularse alrededor del cuello dirigiendo las vesículas secretoras a esta zona. A continuación ocurre la contracción del anillo compuesto por la actina y la miosina tipo II que provoca la invaginación de la membrana hacia el centro del cuello. Posteriormente, ocurre la síntesis centrípeta en el cuello del septo primario compuesto principalmente por quitina, seguido por el depósito del septo secundario formado principalmente por glucanos y mananos. Finalmente, ocurre la separación de ambas células a través de la degradación del septo primario y secundario mediado por la acción de las quitinasas y las glucanasas. Estos pasos ocurren de manera coordinada en el tiempo y espacio (figura 9).

4.3.1. Reorganización del citoesqueleto

Tras completarse el crecimiento de la yema, el citoesqueleto sufre una reorientación hacia la zona de unión entre la madre y la hija promoviendo la entrada en la citoquinesis y la formación del septo primario (Finger et al., 1998; Finger and Novick, 1998; VerPlank and Li, 2005). A continuación, el citoesqueleto participa en el sellado de la membrana entre las dos células regulando el tráfico de las vesículas secretoras, que transportan a proteínas como Chs2 que son requeridas para la citoquinesis, hacia el cuello (Finger et al., 1998; Finger and Novick, 1998; Pashkova et al., 2005; Pruyne and Bretscher, 2000a; Pruyne and Bretscher, 2000b; Pruyne et al., 2004a; Pruyne et al., 2004b). Una vez las vesículas descargan las proteínas, éstas son capturadas por Myo2 asegurándose un acoplamiento entre el cierre de la membrana y la constricción del AMR (Fang et al., 2010).

4.3.2. Formación del anillo citoquinético/actomiosina (AMR)

En la levadura *S. cerevisiae*, la formación del AMR es un proceso secuencial que requiere la participación de diferentes proteínas: las septinas, la miosina tipo II, la F-actina, las forminas y las proteínas reguladoras (Lillie and Brown, 1994). La formación del AMR, compuesto por miosina tipo II (Myo1) y actina F, comienza durante la transición de la fase G1 a S, a través la de localización de la miosina tipo II (Myo1) junto a los marcadores del sitio de gemación en la membrana plasmática. La localización de este anillo depende de las

septinas y no de la actina preexistente. Durante el crecimiento de la yema, el anillo formado por Myo1 permanece en la base de la yema conservando un diámetro constante. Una vez la yema se ha formado, Myo1 se mantiene en el cuello hasta que la F-actina es reclutada para formar el AMR contráctil al final de la anafase. Una vez completado, se produce la contracción del mismo que genera la fuerza necesaria para la invaginación de la membrana plasmática en la citoquinesis (Fang et al., 2010). La contracción del AMR se produce de manera coordinada temporal y espacialmente con la formación del septo primario (Bi et al., 1998; Field et al., 1999; Lippincott et al., 2001). El desensamblaje del anillo Myo1 tras la contracción es actina independiente y es guiado por señales del ciclo celular (Imamura et al., 1997; Tolliday et al., 2002).

4.3.3. Formación del septo primario y secundario

La mayoría de la quitina que contiene la célula se encuentra localizada en el cuello y en la cicatriz. Durante la emergencia de la yema, el anillo de quitina se deposita en el cuello, a través de la actividad de Chs3. Sin embargo es durante la citoquinesis cuando se forma el septo primario a través de la actividad quitina sintasa II (Balasubramanian et al., 2004; Bi, 2001; Bi and Park, 2012; Cabib, 2004; Cabib et al., 1993; Cabib et al., 2001; Roncero and Sanchez, 2010; Wloka and Bi, 2012). Chs2 es una proteína integral de membrana que polimeriza la formación de quitina a través del precursor citosólico UDP-NAG. Chs2 se localiza en el cuello de manera temporal al final de la telofase, cuando se han separado las cromátidas hermanas y el collar de septinas se ha dividido en dos anillos (Bi et al., 1998; Chuang and Schekman, 1996; DeMarini et al., 1997; Lippincott et al., 2001). Una vez llega al cuello, Chs2 empieza a depositar una capa de quitina inmediatamente detrás de la línea de constricción de la membrana plasmática generada por la contracción del AMR (Bi, 2001; Cabib, 2004; Cabib et al., 2001; Schmidt et al., 2002; Tolliday et al., 2003). Ambos procesos, la constricción del AMR y la síntesis del septo primario, se producen de manera simultánea. La célula asegura está simultaneidad a través de dos mecanismos que garantizan que ambos procesos quedan acoplados en el tiempo y en el espacio: (I) la unión de Chs2 al anillo AMR a través de su interacción con la proteína Myo1 y (II) la llegada de Chs2 al cuello coincide con la sustitución de los cables por los parches de actina unidos al AMR, comenzándose así la constricción del anillo (Fang et al., 2010). La contracción del AMR produce la fuerza inicial necesaria para la invaginación de

la membrana plasmática hacia el centro del cuello y el simultáneo depósito del septo primario, estructura que aporta resistencia, permite mantener la invaginación de la membrana plasmática y evita que la célula se lise debido a la alta presión osmótica a la que se encuentra sometida. Una vez completada la citoquinesis, Chs2 es fosforilada a través del complejo quinasa Dbf2-Mob1, que causa su disociación del AMR (Oh et al., 2012).

En ausencia de AMR las células pueden terminar la citoquinesis y separarse, sugiriendo que solo la mera formación del septo es suficiente para que ocurra la citoquinesis (Fang et al., 2010; Schmidt et al., 2002). La citoquinesis y el depósito del septo en levaduras no ocurren hasta que se haya completado la segregación de los cromosomas asegurando una herencia genética exitosa. Por lo tanto, la coordinación temporal entre la citoquinesis y el ciclo celular es esencial para mantener la integridad del genoma tras múltiples divisiones. Y una manera de garantizarlo son los varios niveles de regulación transcripcional y postranscripcional que presenta Chs2.

Las células *chs3*Δ presentan un septo normal y son células viables. Sin embargo, células *chs2*Δ forman un anillo de quitina de manera correcta, pero presentan un patrón de septación anormal, donde no se observa la formación de un septo primario o la constricción del AMR durante la citoquinesis (Shaw et al., 1991). En su lugar ocurre una invaginación de la membrana hacia el centro del cuello, seguida de un depósito anormal de quitina que genera un septo aberrante, ancho y abultado denominado septo remediador. El septo remediador es rico en quitina, y al igual que el anillo de quitina, está formado por Chs3 (Osmond et al., 1999).

Inmediatamente tras la formación del septo primario, se produce la síntesis y depósito de una estructura electrodensa, a cada lado del septo primario denominada septo secundario. La composición del septo secundario es similar a la de la pared celular y contiene glucanos y manoproteínas. Su formación depende del transporte de vesículas secretoras dirigidas al cuello que portan el material y las proteínas implicadas en la síntesis de la nueva pared celular. Entre ellas se encuentra la proteína Fks1 y su unidad reguladora Rho1 (Lesage and Bussey, 2006).

4.3.4. Coordinación entre la constricción del AMR y la formación del septo

La coordinación entre el depósito del septo primario y la contracción del AMR (Fang et al., 2010; Lippincott and Li, 1998b; Schmidt et al., 2002) implica la participación de al menos tres tipos de proteínas: (I) las que participan solo en la síntesis de las estructuras como Myo1 y Chs2 (Bi et al., 1998; Lippincott and Li, 1998b; Roh et al., 2002b); (II) proteínas requeridas para la formación de cada estructura como las forminas, las proteínas IQGAP y los reguladores de Miosina II (Evangelista et al., 1997; Imamura et al., 1997; Kohno et al., 1996; Shannon, 2012) y (III) proteínas que conectan ambos procesos como las septinas, Hof1, Inn1 y Cyk3 (Bi, 2001; Wloka and Bi, 2012).

La proteína Cyk1/Iqg1 es una proteína de la familia IQGAP que forma un anillo único alrededor del cuello y participa en el ensamblaje del anillo de actina (Shannon, 2012). Su localización en el cuello depende de las septinas (Tully et al., 2009). Una vez allí, promueve la formación del anillo de actina a través del reclutamiento de la actina-F por el lado de la célula madre de manera específica y ordenada. Se ha sugerido que Iqg1 se uniría a la actina-F mediante su dominio CHD (dominio con homología a calpoína) y usando como molde el anillo formado por Myo1. Cyk1/Igq1 ayudada por las forminas Bni1 y Bnr1 formaría el anillo de actina y completaría el AMR. De hecho, Iqg1 se contrae como Myo1 y es necesaria para la localización de Myo1 en el cuello durante la citoquinesis (Fang et al., 2010).

Las septinas participan en la coordinación de ambos sucesos ya que son requeridas tanto para el ensamblaje del AMR como para la formación del septo primario (Bi et al., 1998; Cid et al., 2001a; Cid et al., 1998b; Lippincott and Li, 1998b; Lippincott et al., 2001; Longtine et al., 1996; Roh et al., 2002b; Tang and Reed, 2002). Las proteínas Hof1, Inn1 y Cyk3 forman un complejo que está implicado tanto en la formación del septo primario, como en el ensamblaje del AMR (Meitinger et al., 2011; Meitinger et al., 2012; Meitinger et al., 2010; Nishihama et al., 2009). Hof1 juega un papel en la formación del septo primario de manera independiente al papel en la formación del AMR. Hof1 se localiza en el cuello entre la célula madre y la célúla hija formando un anillo que se contrae como lo hace el anillo AMR durante la citoquinesis y es Myo1 dependiente. Tras la contracción del

AMR, Hof1 se divide en dos anillos uniformes y posicionados uno en cada lado del cuello. Este comportamiento sugiere que Hof1 podría acoplar la contracción de AMR a la formación del septo primario (Balasubramanian et al., 2004; Kamei et al., 1998; Korinek et al., 2000; Lippincott and Li, 1998b; Lippincott et al., 2001). A su vez, la asociación de Hof1 con el AMR promueve la constricción del mismo y la invaginación de la membrana plasmática (Meitinger et al., 2011). Adicionalmente, Hof1 interactúa directamente con Cyk3 y a través de su dominio SH3 con Inn1, regulando la localización en el cuello de ambas proteínas (Meitinger et al., 2010). Inn1 está implicada en la coordinación de la contracción del AMR y la invaginación de la membrana plasmática (Sanchez-Diaz et al., 2008). A su vez, Inn1 interactúa con Iqg1, Holf1 y Cyk3 asegurando la conexión de ambos procesos (Meitinger et al., 2010; Nishihama et al., 2009; Sanchez-Diaz et al., 2008). Cyk3 se localiza en el cuello momentos previos a la contracción del AMR y participa en el marcaje para la secreción o formación del septo primario. Al igual que Hof1, el papel de Cyk3 en la síntesis del septo primario es independiente de su papel en la constricción del AMR (Korinek et al., 2000).

El modelo propuesto para el ensamblaje y la regulación de ambos procesos contempla la llegada al cuello de estas proteínas de manera secuencial, desde el inicio del ciclo celular (fase G1) hasta el final de la citoquinesis. Las septinas, esenciales para la citoquinesis, son las primeras que se localizan en el sitio de gemación que posteriormente será donde ocurra la citoquinesis. Así, al final de la fase G1 quedan formados el collar de septinas rodeado del anillo de Myo1 junto a su proteína reguladora de la cadena ligera Mlc2 y la formina Bnr1. En fase S del ciclo celular, se produce la llegada al cuello de la proteína reguladora esencial de la cadena ligera de la miosina, Mlc1. En la fase S/G2, se incorpora la proteína reguladora Hof1/Cyk2. Durante la fase G2/M lo hacen las proteínas Iqg1/Cyk1 y Bni1. Por útimo, al final de anafase, se incorporan la actina F y Cyk3, de modo que el anillo AMR solo está completo y funcional al final de la anafase (Balasubramanian et al., 2004; Bi, 2001; Lippincott and Li, 1998a; Lippincott and Li, 1998b; Lippincott and Li, 2000; Wloka and Bi, 2012). La presencia de Chs2 en el cuello unicamente momentos antes de comenzar la constricción del AMR genera un aumento de la estabilidad del anillo, estableciéndose una clara coordinación e interdependencia entre la contracción del AMR y el depósito de quitina (Bi, 2001; Schmidt et al., 2002; VerPlank and Li, 2005; Wloka and Bi, 2012).

4.3.5. Separación celular

Tras el correcto depósito del septo primario y del septo secundario, las células madre e hija quedan unidas por un septo trilaminar compuesto por el anillo de quitina, el septo primario y el septo secundario (figura 2B) (Barr and Gruneberg, 2007; Lesage and Bussey, 2006; Walther and Wendland, 2003; Yeong, 2005). Para una correcta finalización de la citoquinesis debe ocurrir una separación física de ambas células, de manera que se asegure que tras la separación celular ambas células serán viables. Por ello, la separación celular es un complicado y dinámico proceso que debe evitar el inicio en un nuevo ciclo celular antes de que las células se hayan separado. Para ello, la célula hija sintetiza y secreta la quitinasa Cts1 encargada de degradar el septo primario (Kuranda and Robbins, 1991). Cts1 es una proteína O-manosilada que se libera en el cuello mediante la ruta secretora de vesículas procedentes del Golgi. La expresión y localización asimétrica de esta enzima, explica que en la célula madre se observe un "cráter" o cicatriz mientas que en la célula hija solamente se observe una pequeña o débil señal de la acción degradativa de esta enzima (Bacon et al., 1969; Cabib and Bowers, 1971; Cabib and Farkas, 1971; Cabib and Keller, 1971; Pringle et al., 1995). La acción de Cts1 está modulada por Chs1 que repara la pared celular del lado de la célula hija, previniendo que la célula muera debido a un exceso de actividad la de Cts1 (Cabib et al., 1988; Cabib et al., 1987; Cabib et al., 1989).

Adicionalmente, la célula hija también se encarga de sintetizar endoglucanasas como Eng1 y Eng2 que hidrolizan enlaces β 1-3 (Baladron et al., 2002; Martin-Cuadrado et al., 2008) y glucanasas como Scw11 que se encargan de degradar el resto de los componentes del septo secundario que mantienen ambas células unidas (Baladron et al., 2002; Cappellaro et al., 1998; Colman-Lerner et al., 2001; Larriba et al., 1995; Martin-Cuadrado et al., 2008; Nombela et al., 1988). Existe una transcripción asimétrica de los genes *CTS1*, *ENG1*, *EGT2* y *SWC11* en la célula hija durante la fase G1, que se debe a la localización asimétrica del factor de transcripción Ace2 específicamente en el núcleo de la célula hija (Kurischko et al., 2005; Weiss et al., 2002). La asimétrica localización y activación de este factor de transcripción depende de la ruta RAM, una ruta de señalización conservada en eucariotas (Colman-Lerner et al., 2001; Weiss et al., 2002). Dos de los elementos de la ruta RAM implicados en la separación celular son la quinasa Cbk1 y su subunidad reguladora Mob2 (Nelson et al., 2003). La asociación de Cbk1 con Mob2 provoca la activación de la

quinasa. Cbk1 activada fosforila a Ace2, permitiendo su activación y manteniéndolo en el núcleo de la célula hija, donde promueve la transcripción de los genes necesarios para la separación celular. Tras la separación celular, una fracción de Ace2 se degrada y otra fracción permanece en el citoplasma hasta final de G1 (Mazanka and Weiss, 2010).

ANTECEDENTES

La secuenciación del genoma de levadura (Arroyo et al., 1997; Nierman et al., 2005) permitió la identificación del gen *YGR189c*/*CRH1* que codifica para una proteína cuya secuencia muestra homología con β-1,3 β-1,4 glucanasas de procariotas, lo que sugería su implicación en la biogénesis de la pared celular (Rodriguez-Pena et al., 1998). Un estudio más exhaustivo de este gen llevó a la identificación de una nueva familia de genes de pared celular llamada Crh (*Congo Red Hypersensitive*) que presenta en su secuencia el dominio DE(I/L)DXE presente en endotransglicosilasas de procariotas y plantas (Rodriguez-Pena et al., 2000). Esta familia está compuesta por tres miembros: Crh1, Crh2 y Crr1. Las dos primeras se expresan en ciclo vegetativo y el tercero en esporulación. La deleción sintética de ambos genes *CRH1* y *CRH2* afecta parcialmente a la integridad de la célula. La fracción álcali insoluble del doble mutante *crh1*Δ *crh2*Δ se incrementa con respecto a la cepa WT. Sin embargo, ambas cepas presentan niveles similares de quitina. Este hecho, junto con el hecho de que las proteínas Crh co-localizan con los depósitos de quitina en la pared celular sugerían que estas proteínas podrían actuar como transglicosilasas de quitina a glucano (Rodriguez-Pena et al., 2000).

En el año 2005, los doctores E. Cabib y A. Durán (Cabib and Duran, 2005), describieron un nuevo método para cuantificar las diferentes fracciones en las que se encuentra la quitina en la pared celular. Brevemente, este método consiste en el crecimiento de las células en presencia de ^{14}C-glucosamina, de modo que se realiza un marcaje *in vivo* de la quitina localizada en la pared celular. Las paredes celulares, previamente digeridas con β-1,3 glucanasa, β-1,6 glucanasa o sin tratar, se solubilizan mediante carboximetilación. El material solubilizado se separa por tamaño mediante una cromatografía de exclusión, pudiéndose así cuantificar los porcentajes de quitina unida a los diferentes polisacáridos. De esta manera, se pudo determinar que la quitina se encuentra distribuida en la pared celular en tres formas: quitina libre (43%), cadenas de quitina largas unidas al β-1,3 glucano (30%), cadenas cortas de quitina unidas al β-1,3 glucano (11%) y quitina unida al β-1,6 glucano (16%).

La utilización de este método para el análisis de las paredes celulares del doble mutante *crh1*Δ *crh2*Δ permitirá demostrar el papel de las proteínas Crh en la biogénesis de la pared celular y sí estas proteínas pueden actuar como transglicosilasas quitina-glucano como habíamos sugerido anteriormente (Rodriguez-Pena et al., 2000).

Por otro lado, a pesar de conocer la existencia del anillo de quitina desde 1973 (Hayashibe, 1973), su función en ciclo celular era desconocida. Los resultados obtenidos en el trabajo Schmidt M. et al. (2003) sugerían que el anillo de quitina formado por Chs3 cooperaba con el anillo de septinas en mantener constante el tamaño del cuello. ¿Cómo ejerce este control el anillo de quitina? Teniendo en cuenta el orden de incorporación de los diferentes componentes durante el crecimiento de la pared celular y que la incorporación de la quitina en el cuello está asociada al β-1,3 glucano (Cabib and Duran, 2005), el Dr. Cabib y colaboradores (Cabib and Schmidt, 2003; Schmidt et al., 2003) propusieron que la quitina competiría con el β-1,6 glucano por la unión al extremo no reducido del β-1,3 glucano en la zona del cuello, lo que prevendría la remodelación del mismo y por lo tanto el crecimiento de la pared celular en esta zona, al no poderse unir el β-1,3 glucano al β-1,6 glucano y por tanto a las manoproteínas necesarias para la biogénesis de la pared celular en el cuello. Si las proteínas Crh estuvieran implicadas en el entrecruzamiento quitina-glucano, se podría corroborar esta hipótesis.

OBJETIVOS

El objetivo principal de este trabajo ha sido la caracterización de las proteínas Crh de *Saccharomyces cerevisiae* en relación a los procesos de biogénesis de la pared celular y la morfogénesis. Este objetivo se ha realizado mediante dos objetivos parciales:

1. Caracterizar la participación de Crh1 y Crh2 en el entrecruzamiento de los componentes de la pared celular. Este objetivo se ha abordado a través de tres aproximaciones diferentes:

    a. Cuantificar las diferentes fracciones de quitina presentes en la cepa WT y en los mutantes en los genes *CRH*, usando el método de carboximetilación-cromatografía (Cabib and Duran, 2005) tanto en condiciones basales como de estrés sobre la pared celular.

    b. Desarrollo de un sistema de estudio *in vivo* e *in vitro* de la reacción de transglicosilación entre la quitina y el glucano para la determinar las propiedades bioquímicas de la actividad transglicosilasa de Crh1 y Crh2.

    c. Caracterización de residuos de Crh1 y Crh2 importantes para la actividad catalítica de las mismas, efectuando un estudio estructura-función.

2. Participación de la actividad transglicosilasa, llevada a cabo por las proteínas Crh, en el proceso de morfogénesis celular. La ejecución de este objetivo se ha alcanzado utilizando:

    a. Estudios estructurales y de distribución del β-1,3 glucano.

    b. Análisis morfogenéticos de levaduras en ausencia del enlace entre la quitina y el glucano.

RESULTADOS

CAPÍTULO 1

Crh1 Y Crh2 SON RESPONSABLES DEL ENLACE ENTRE LA QUITINA Y EL GLUCANO EN LA PARED CELULAR DE *Saccharomyces cerervisiae*

RESUMEN DE LOS RESULTADOS DEL CAPÍTULO 1

La biogénesis de la pared celular requiere del entrecruzamiento entre los diversos polímeros que la integran, incluidos el glucano y la quitina. Sin embargo, hasta la fecha no se había demostrado la existencia de esta actividad en levaduras. En este trabajo se ha caracterizado la actividad transglicosilasa llevada a cabo por las proteínas Crh mediante la aplicación de una nueva metodología que permite la solubilización de la quitina mediante carboxilametilación de la misma. La utilización de este método (Cabib and Duran, 2005) permite distinguir y cuantificar entre quitina libre, quitina de diferentes longitudes (corta y larga) unida al β-1,3 glucano y quitina unida al β-1,6 glucano. Nuestros resultados muestran que la fracción de quitina unida al β-1,6 glucano presente en los mutantes sencillos *crh1*Δ y *crh2*Δ se ve reducida con respecto a su homóloga en una cepa WT. Esta disminución va asociada con un aumento de la fracción de quitina libre. El análisis de las paredes celulares de la cepa *crh1*Δ *crh2*Δ reveló la ausencia total de quitina unida al β-1,6 glucano en este mutante. Este resultado, junto con el hecho de que la ramificación del β-1,6 glucano no se ve afectada en el doble mutante con respecto a la cepa WT, nos permite concluir que Crh1 y Crh2 actúan como transglicosilasas entre la quitina y el β-1,6 glucano, siendo la primera vez que se demuestra *in vivo* una actividad transglicosilasa implicada en el entrecruzamiento de los polisacáridos de la pared celular en hongos. El complejo formado por la quitina y el β-1,6 glucano ejerce su papel biológico no solo en el reforzamiento de la pared lateral tras la división celular, sino en situaciones de estrés sobre la pared celular, donde se ve aumentado cuantitativamente y modificado por su unión a las manoproteínas. La deleción de *CRH1* y/o *CRH2* sobre un fondo *fks1*Δ o *gas1*Δ, que presentan un daño constitutivo en su pared, como consecuencia de defectos importantes en la síntesis y estructura del β-1,3 glucano, produce un agravamiento de los fenotipos de estos mutantes medido como un aumento del tiempo de generación y lisis celular, así como de la sensibilidad a compuestos que interfieren con la síntesis pared celular como es el RC. Cabe destacar que el mutante *crh1*Δ *crh2*Δ *fks1*Δ presenta una sensibilidad a RC similar a la del mutante delecionado en la MAP quinasa de la ruta de integridad celular *slt2*Δ, demostrando la importancia del complejo quitina-glucano para la supervivencia de la célula en condiciones en las que la estructura del β-1,3 glucano está seriamente afectada. Por otro lado, cuando las células son sometidas a un estrés transitorio mediado por Tª (de 24ºC a 38ºC), se produce un aumento de la quitina unida al β-1,6 glucano, dependiente de

la actividad de ambas proteínas, Crh1 y Crh2. Este aumento del complejo quitina-β-1,6 glucano se localiza mayoritariamente en el perímetro celular. A su vez, el choque térmico genera un aumento transcripcional de *CRH1*, dependiente de Slt2, que se traduce en un aumento de los niveles de proteína. *CRH2* no ve afectado su patrón transcripcional, ni los niveles de proteína que codifica en estas condiciones. Sin embargo, tanto Crh1 como Crh2 sufren una relocalización como consecuencia del estrés térmico, pasando de localizarse en sitios de crecimiento polarizado (cuello y cicatrices) a situarse mayoritariamente en la pared lateral.

.

ARTÍCULO 1

Crh1p and Crh2p are required for the cross-linking of chitin to β(1-6)glucan in the Saccharomyces cerevisiae

Molecular Microbiology (2007) **63**(3), 921–935 doi:10.1111/j.1365-2958.2006.05565.x
First published online 9 January 2007

Crh1p and Crh2p are required for the cross-linking of chitin to β(1-6)glucan in the *Saccharomyces cerevisiae* cell wall

Enrico Cabib,[1]* Noelia Blanco,[2] Cecilia Grau,[2†] José Manuel Rodríguez-Peña[2] and Javier Arroyo[2]
[1]*National Institute of Diabetes and Digestive and Kidney Diseases, Laboratory of Biochemistry and Genetics, Bethesda, MD 20892, USA.*
[2]*Departamento de Microbiología II, Facultad de Farmacia, Universidad Complutense de Madrid, 28040 Madrid, Spain.*

Summary

In budding yeast, chitin is found in three locations: at the primary septum, largely in free form, at the mother-bud neck, partially linked to β(1-3)glucan, and in the lateral wall, attached in part to β(1-6)glucan. By using a recently developed strategy for the study of cell wall cross-links, we have found that chitin linked to β(1-6)glucan is diminished in mutants of the *CRH1* or the *CRH2/UTR2* gene and completely absent in a double mutant. This indicates that Crh1p and Crh2p, homologues of glycosyltransferases, ferry chitin chains from chitin synthase III to β(1-6)glucan. Deletion of *CRH1* and/or *CRH2* aggravated the defects of *fks1Δ* and *gas1Δ* mutants, which are impaired in cell wall synthesis. A temperature shift from 30°C to 38°C increased the proportion of chitin attached to β(1-6)glucan. The expression of *CRH1*, but not that of *CRH2*, was also higher at 38°C in a manner dependent on the cell integrity pathway. Furthermore, the localization of both Crh1p and Crh2p at the cell cortex, the area where the chitin–β(1-6)glucan complex is found, was greatly enhanced at 38°C. Crh1p and Crh2p are the first proteins directly implicated in the formation of cross-links between cell wall components in fungi.

Introduction

The fungal cell wall consists of a tightly woven network of polysaccharides and glycoproteins. Cross-links between the different components stabilize the wall structure and allow it to wrap the cell as a continuous mesh. This fabric is strong enough to withstand the internal turgor pressure and to protect the cells from mechanical injury. In *Saccharomyces cerevisiae*, the chemical structure of the cell wall has been studied in some detail (see Lipke and Ovalle, 1998; Cabib *et al*., 2001; Klis *et al*., 2002; for reviews). The components of the wall are β(1-3)glucan, the major structural polysaccharide, β(1-6)glucan, mannoproteins and chitin. β(1-3)glucan is linked to β(1-6)glucan and the latter to mannoprotein. Other proteins, the Pir proteins, are attached to β(1-3)glucan by an alkali labile linkage (Klis *et al*., 2002; Ecker *et al*., 2006). Part of the chitin is free, part attached to non-reducing ends of β(1-3)glucan and another portion to side branches of β(1-6)glucan (Kollár *et al*., 1995; 1997). Something is also known about the order in which these components are joined to each other. Based on a study with mutants of Rho1p, an activator of β(1-3)glucan synthase, we came to the conclusion that β(1-3)glucan is the first product (Roh *et al*., 2002). β(1-6)glucan is then attached to it and mannoprotein comes in next. As for chitin, the bulk of it is laid down at the neck between mother cell and an emerging bud, but the remainder, which is dispersed throughout the wall, is only deposited in the daughter cell after septation (Shaw *et al*., 1991). Both the chitin at the neck and that dispersed in the cell wall are synthesized by chitin synthase III (CSIII) (Shaw *et al*., 1991). The primary septum formed at cytokinesis also consists of chitin, most of it free (Shaw *et al*., 1991; Cabib and Durán, 2005), but the polysaccharide synthesized here requires chitin synthase II for its formation (Shaw *et al*., 1991).

Our previous work suggested that the chitin ring at the mother-bud neck cooperates with the septin ring located at the intracellular side of the plasma membrane, to prevent growth at the neck (Schmidt *et al*., 2003). We offered as a hypothesis to explain these findings that the large amount of chitin found at the neck would be mostly linked to β(1-3)glucan at its non-reducing ends. In this way, it would compete with β(1-6)glucan for the same sites. Thus, both β(1-6)glucan and mannoprotein could not be incorporated and growth of the wall would be blocked (Schmidt *et al*., 2003). To test this hypothesis, we developed a new strategy for the study of chitin cross-links to other cell wall components (Cabib and Durán, 2005). Basically, the procedure consisted in using

Accepted 7 December, 2006. *For correspondence. E-mail enricoc@bdg10.niddk.nih.gov; Tel. (+1) 301 496 1008; Fax (+1) 301 496 9431.
†Present address: Biogen Idec, Castellana 41, 28046 Madrid, Spain.

carboxymethylation to solubilize in water either intact cell walls or walls previously incubated with β(1-3)glucanase or β(1-6)glucanase or with both. The solubilized material was then fractionated by size-exclusion chromatography. In this way, the chitin linked to other polysaccharides, of higher molecular weight, could be separated from that which originally was free or which was liberated by each enzyme. Thus, we were able to calculate the distribution of chitin in its various forms. The results confirmed our hypothesis: most of the bound chitin at the neck was attached to β(1-3)glucan, whereas that dispersed in the cell wall was linked predominantly to β(1-6)glucan (Cabib and Durán, 2005).

Despite all the information accumulated over many years about cell wall structure, nothing is known about the mechanisms by which cross-links between the different components are created. We decided to use the new approach devised for the analysis of chitin cross-links to look into their formation. One of our laboratories has studied three proteins, encoded by the genes *CRH1*, *CRH2/UTR2* and *CRR1*, which show homology to β-glucanases and transglycosidases (Rodríguez-Peña *et al*., 2000). Whereas Crh1p is expressed during both the vegetative and sporulation phase, Crh2p is only expressed during vegetative growth and Crr1p mostly during sporulation. A defect in Crh1p or Crh2p causes hypersensitivity to Congo Red and Calcofluor White, indicating some abnormality in the cell wall. Later work showed that Crr1p has a role in the formation of spore cell wall (Gómez-Esquer *et al*., 2004). Both Crh1p and Crh2p are glycosylphosphatidylinositol-anchored proteins and have been found to be, at least in part, covalently associated with the cell wall (Hamada *et al*., 1998; Yin *et al*., 2005). Intriguingly, the localization of Crh1p and Crh2p during the cell cycle largely coincided with that of chitin deposition (Rodríguez-Peña *et al*., 2000). Thus, it seemed likely that these proteins might act as transglycosidases, transferring chitin synthesized through CSIII to an acceptor. Our results indeed show that Crh1p and Crh2p are necessary for the formation of the linkage between chitin and β(1-6)glucan.

Results

Crh1p and Crh2p are required for the formation of chitin–β(1-6)glucan linkages

To ascertain whether Crh1p and Crh2p were involved in the formation of chitin cross-links, we analysed the distribution of the various forms of the polysaccharide in the wild type, in single mutants of the two genes, and in a double mutant. It soon became apparent that the mutants were defective in the linkage of chitin to β(1-6)glucan. The amount of chitin bound to β(1-6)glucan can be appreciated by comparing the elution profile of solubilized intact cell walls with that of a β(1-6)glucanase digest (Cabib and Durán, 2005). The difference between the two profiles in the free chitin area (fraction 30–45, Fig. 1) measures the amount of chitin previously linked to the glucan and liberated by glucanase. That difference is somewhat reduced in a *crh1Δ*, much more so in *crh2Δ* cells and totally eliminated in the double mutant (Fig. 1). The relative amount of four fractions can be determined with our procedure: free chitin, large chitin attached to β(1-3)glucan, short chitin oligosaccharides ('small chitin') linked to the same polysaccharide, and chitin bound to β(1-6)glucan (Cabib and Durán, 2005). In going from the wild type to the double mutant, the decrease in chitin linked to β(1-6)glucan is matched by an increase in free chitin (Fig. 2), whereas the percentage of chitin–β(1-3)glucan complex is practically unchanged. Surprisingly, a decrease in the small chitin attached to β(1-3)glucan was shown by all the strains containing the *CRH1* or the *CRH2* deletion. As the amount of chitin attached to β(1-6)glucan in a *crh2* mutant is very small, we overexpressed *CRH1* in a double mutant, to find out whether Crh1p really contributed to that linkage. Overexpression of *CRH1* resulted in a substantial increase in the chitin–β(1-6)glucan complex, compared with the strain in which the gene was expressed at the chromosomal locus (Fig. 3). At the same time, the small chitin linked to β(1-3)glucan also increased, again suggesting that Crh1p somehow contributes to its formation.

We also overexpressed *CRH2* in a wild-type strain and in a strain with a double *crh1 crh2* deletion. In both cases there was little difference in the percentage of chitin linked to β(1-6)glucan, compared, respectively, with the wild-type strain or with the *crh1Δ* mutant without the plasmid (results not shown). This suggests that there is some limiting factor for the cross-linking, such as availability of substrate or acceptor sites, especially if the Crh proteins are tethered to the cell wall (Hamada *et al*., 1998; Yin *et al*., 2005). On the other hand, the percentage of small chitin linked to β(1-3)glucan increased about 50% in both cases.

Crh1p and Crh2p do not modify the branching of β(1-6)glucan

Because of their homology to glucanases and transglycosidases, it seemed probable that Crh1p and Crh2p could act by transferring chitin chains from CSIII to β(1-6)glucan. However, a quite different scenario was possible. We previously found that chitin is attached to β(1-3)-linked glucose residues branching out from the main β(1-6)glucan chain (Kollár *et al*., 1997). Thus, it was possible that the function of the Crh proteins, still acting as transglycosidases, was to give rise to those glucose side branches. In other words, they would be needed to make the acceptor, not the transfer. If this were true, in a mutant

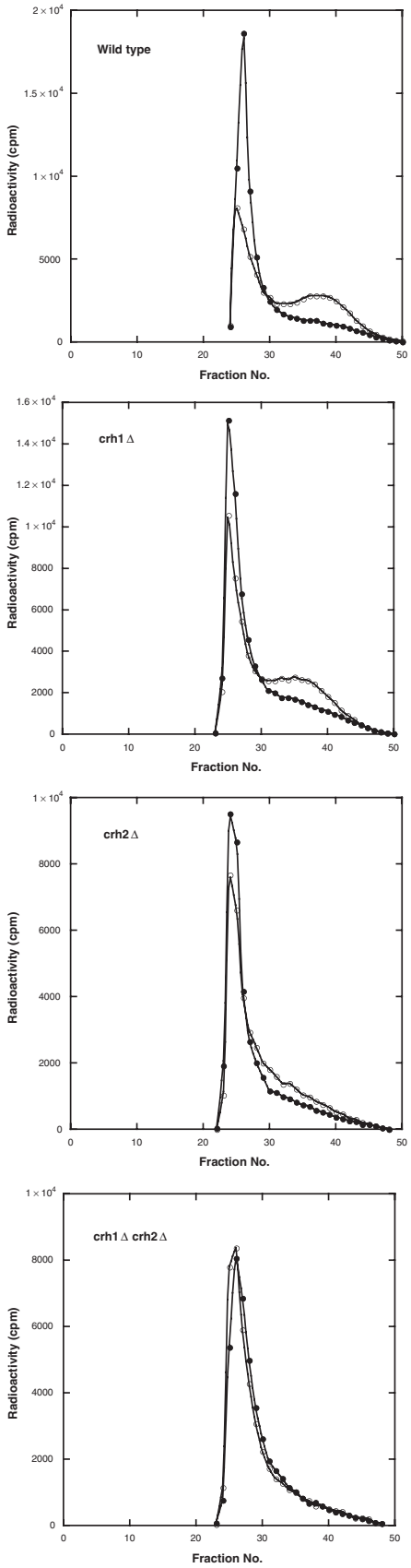

Fig. 1. Chromatography on Sephacryl S-300 of carboxymethylated cell walls (filled circles) or carboxymethylated wall digests with β(1-6)glucanase (open circles) of different strains. All of the radioactivity represents chitin, because the cells were labelled with ^{14}C-glucosamine (see *Experimental procedures*). Wild type, FY001; *crh1Δ*, RCA001; *crh2Δ*, RCA002; *crh1Δ crh2Δ*, RCA003.

defective in both Crh proteins, the β(1-6)glucan would lack the side branches.

To investigate this possibility, we used a procedure based on the finding of Magnelli *et al*. (2002) that the recombinant β(1-6)glucanase from *Trichoderma harzianum* liberates branched oligosaccharides from β(1-6)glucan. In our experiments, the strains used were in a *chs3Δ* background, to eliminate possible interference of bound chitin with β(1-6)glucanase action. Cell walls labelled *in vivo* with ^{14}C-glucose were first digested with β(1-3)glucanase and the liberated oligosaccharides were dialysed out. The dialysate was then treated with β(1-6)glucanase and the products were fractionated on a Bio-Gel P-2 column (Fig. 4). In the oligosaccharide elution zone, three peaks were found (Fig. 4) in positions similar to those previously detected by Magnelli *et al*. (2002). According to their analysis, from right to left they correspond to gentiobiose, a branched trisaccharide and a branched tetrasaccharide. The presence of deletions in *CRH1* and *CRH2* did not alter the pattern (Fig. 4), whereas if Crh1p and/or Crh2p had been responsible for the branching, the two branched oligosaccharides should be missing from the double mutant. We conclude that Crh1p and Crh2p do not contribute to the branched structure of β(1-6)glucan, which strongly supports the hypothesis that the Crh proteins act as chitin transglycosidases.

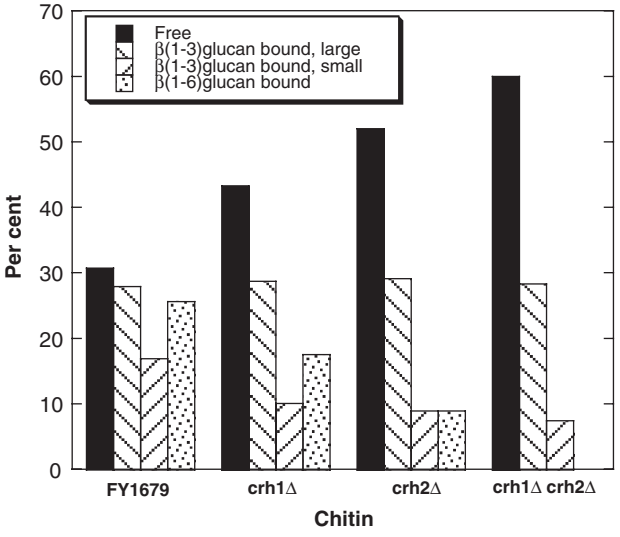

Fig. 2. Distribution of chitin cross-links to different cell wall polysaccharides in the strains of Fig. 1. Note that the β(1-6)glucan-bound chitin is missing in the double *crh1Δ crh2Δ* mutant.

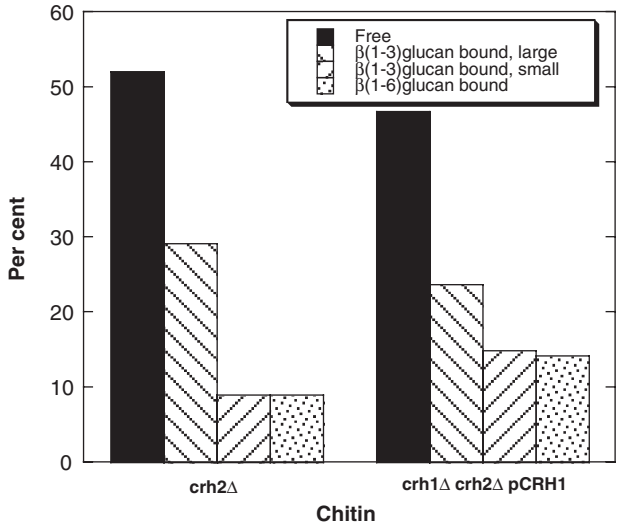

Fig. 3. Overexpression of *CRH1* in a *crh1Δ crh2Δ* mutant results in an increased β(1-6)glucan-bound chitin. A similar increase is observed in the small chitin linked to β(1-3)glucan. The plasmid was pJV89E (YEp352-*CRH1*).

Biological consequences of a defect in chitin linkage to β(1-6)glucan

Although the chitin made by CSII has a clear role in septation (Shaw *et al*., 1991) and that at the mother-bud neck appears to act in the regulation of growth at that site (Schmidt *et al*., 2003; Cabib and Durán, 2005), the function of the chitin dispersed in the cell wall is poorly understood. According to our previous findings, this chitin is partly free and partly linked to β(1-6)glucan (Cabib and Durán, 2005). Hartland *et al*. (1994) concluded that the dispersed chitin contributes to strengthen the wall, because when a *chs3* mutant was cultured in the presence of sorbitol and then subjected to osmotic shock, most of the cells lysed. We were unable to repeat their results in several attempts, either with the same strains they used (a *cdc24* mutant and a *cdc24 chs3* double mutant, both originated in our laboratory) or comparing a wild-type strain with a *chs3Δ* strain. For instance, in one of the experiments the wild type gave rise to 3.3% lysis upon osmotic shock and the *chs3* mutant to 5.8%. Even less of a difference was found by comparing our present wild type (FY1679) with the *crh1Δ crh2Δ* mutant. Therefore, we had to use a different approach to ascertain the physiological significance of the chitin–β(1-6)glucan linkage.

In previous work, it was found that certain wall-defective mutants, such as *fks1* and *gas1*, have an increased chitin content and accumulate mannoproteins linked to chitin through β(1-6)glucan (Kapteyn *et al*., 1997). This was attributed to a cell repair mechanism activated by the cell wall defects. It has also been reported that *CRH1* is upregulated in *fks1* and *gas1* mutants (Terashima *et al*., 2000; Lagorce *et al*., 2003). We reasoned that, if the binding of chitin to β(1-6)glucan was important for the compensatory mechanisms, its decrease or elimination in the *crh* mutants should aggravate the defects of *fks1* and *gas1* mutants. This is certainly the case for *fks1*. Introduction of *CRH1* and *CRH2* deletions in that mutant substantially increased the generation time (Fig. 5A) and the percentage of lysed cells (Fig. 5B) as well as the sensitivity to Congo Red, an

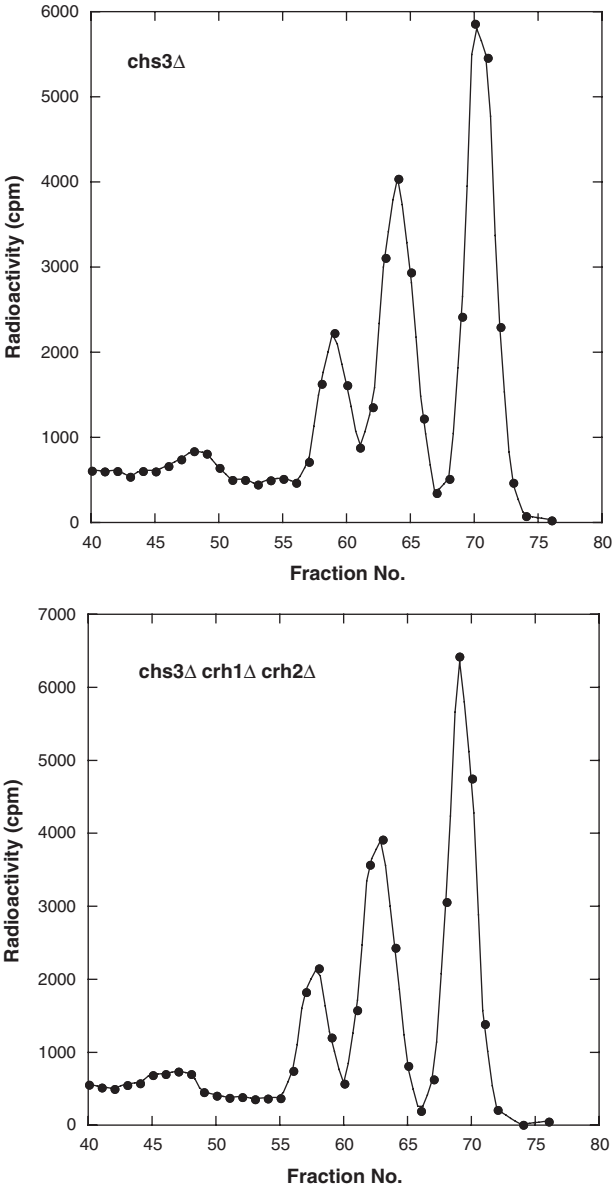

Fig. 4. A double mutation in *CRH1* and *CRH2* does not change the branching pattern of β(1-6)glucan. Chromatography of oligosaccharides resulting from β(1-6)glucanase digestion on Bio-Gel P-2. Only the later part of the elution profile is shown. Both digests exhibited a very large peak at the void volume, due to the mannoproteins present in the preparation. For details, see *Experimental procedures* and the text.

A

Strain	Duplication Time (hours)
BY4741	1.8 ± 0.1
crh1Δ	1.8 ± 0.2
crh2Δ	1.9 ± 0.2
crh1Δ crh2Δ	2.2 ± 0.2
fks1Δ	2.4 ± 0.2
crh2Δ fks1Δ	2.7 ± 0.2
crh1Δ crh2Δ fks1Δ	3.8 ± 0.7
gas1Δ	2.9 ± 0.6
crh2Δ gas1Δ	3.2 ± 0.5
crh1Δ crh2Δ gas1Δ	2.8 ± 0.5

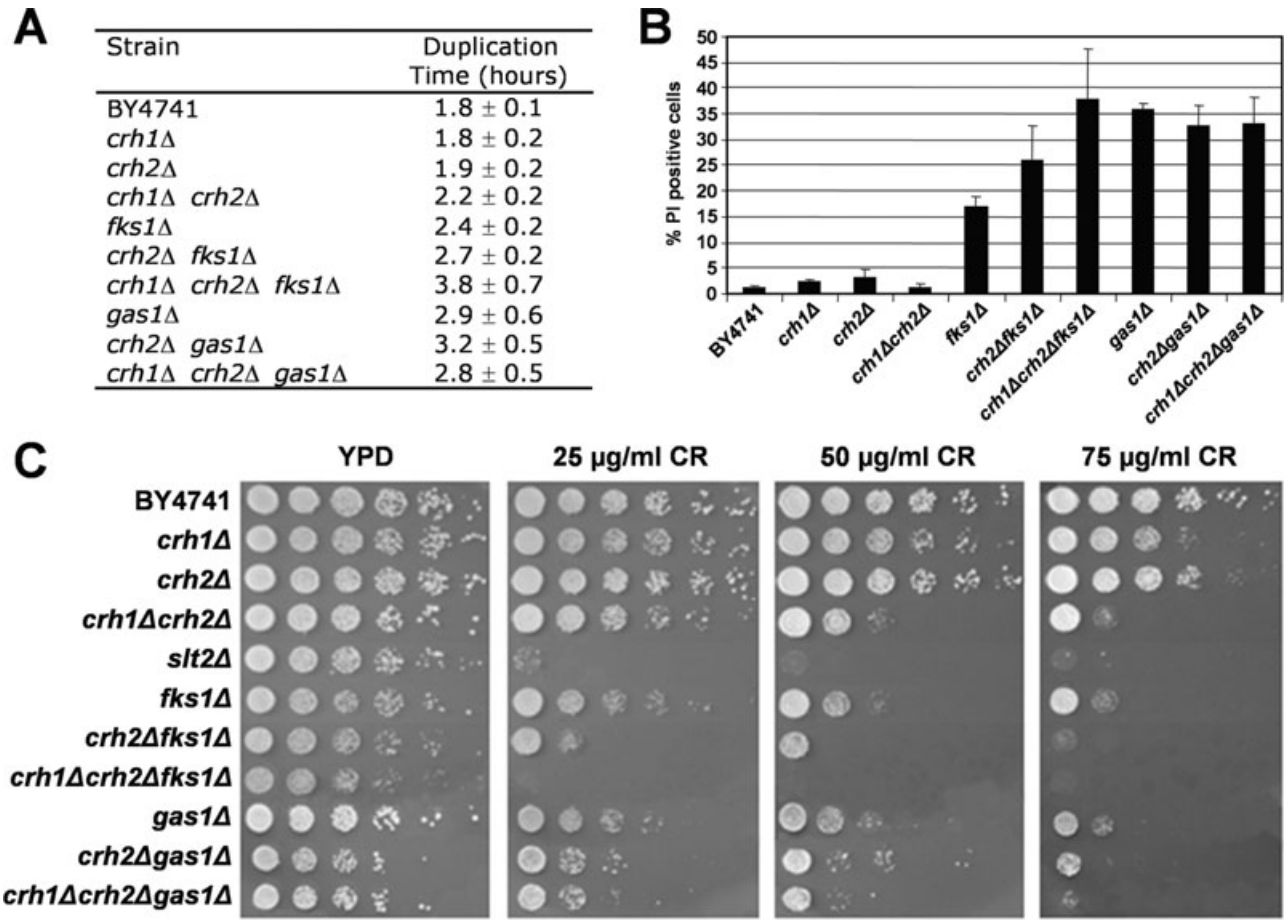

Fig. 5. Phenotypic analysis of strains bearing different combinations of deletions of *CRH1* and *CRH2* with deletions of *FKS1* and *GAS1*. The strains were in the BY background, as listed in Table 1.
A. Duplication times of the different mutant strains during exponential growth in YEPD. The experiments were done in triplicate and the standard deviation is shown.
B. Percentage of propidium iodide-positive (PI) cells in the same cultures analysed by flow cytometry. Statistics as in A.
C. Sensitivity to Congo Red of these strains. Cells were exponentially grown on YEPD and 1/5 dilution series of each strain were spotted onto YEPD plates containing the indicated amounts of Congo Red (CR).

indication of cell wall defects (Fig. 5C). Interestingly, the triple mutant *crh1 crh2 fks1* showed a sensitivity to Congo Red similar to the *slt2* mutant, a strain deleted in the MAPK of the cell integrity pathway, revealing the importance of the chitin–β(1-6)glucan cross-link for *fks1* survival under stress conditions. With the *gas1* mutant, the growth rate and lysis were not affected by *crh* mutations, but the sensitivity to Congo Red was also increased (Fig. 5).

The percentage distribution of chitin in its various forms in the *fks1* mutant was not very different from that in the wild type (results not shown). However, it should be kept in mind that the chitin content increased several-fold in the *fks1* cells compared with wild type (Kapteyn *et al*., 1997). Therefore, even if the percentage of chitin–β(1-6)glucan complex was unchanged, its absolute amount was much greater, which is consistent with the increase of protein bound to chitin through β(1-6)glucan (Kapteyn *et al*., 1997).

The distribution of chitin in *gas1* cells could not be studied, because apparently the chitin in this strain is of very large size. Even after action by β(1-3) or β(1-6)glucanase, most of the radioactivity eluted at the void volume (results not shown).

Regulation of the chitin–β(1-6)glucan bond: the effect of temperature

The previous finding that Crh1p expression is regulated during the cell cycle, the fact that *CRH1* is transcriptionally induced in many cell wall stress conditions (Jung and Levin, 1999; Lagorce *et al*., 2003; García *et al*., 2004) and the general knowledge that cell wall synthesis is strictly regulated by the cell integrity pathway (Levin, 2005)

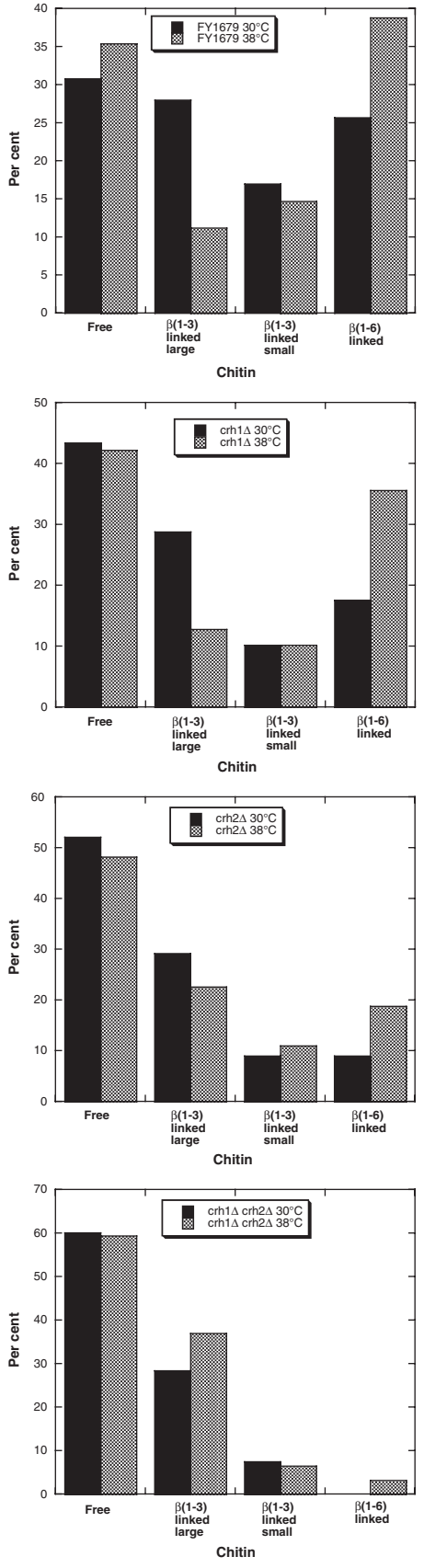

Fig. 6. Distribution of chitin cross-links in different strains after growth at 30°C or 38°C. The strains used are the same of Fig. 1. The small amount of chitin linked to β(1-6)glucan in the double mutant at 38°C is close to the limit of detection, therefore of doubtful significance. For experimental details see *Experimental procedures* and the text.

encouraged us to study the effect of stress on the synthesis of the chitin–β(1-6)glucan linkage. Stress was applied as an increase in temperature, one of the situations that activates the MAP kinase cascade of the cell integrity pathway (Levin, 2005). Wild-type cells were incubated for 24 h either at 30°C or at 38°C, labelled with ^{14}C-glucosamine and the distribution of chitin determined. The proportion of chitin bound to β(1-6)glucan increased substantially in the wild type under heat stress conditions (Fig. 6, top panel), suggesting the importance of this cross-link for cell wall remodelling under stress. Correspondingly, the proportion of chitin–β(1-3)glucan decreased. This decrease was not unexpected, because values are expressed in percentages, and if one goes up others must come down.

To test if this increase was dependent on Crh1p, Crh2p or both, we carried out the same experiments in *crh1Δ*, *crh2Δ* and *crh1Δ crh2Δ* mutants. The proportion of chitin bound to β(1-6)glucan increased both in *crh2* and *crh1* mutants when shifted to 38°C (Fig. 6) but not in the double *crh1 crh2* mutant, suggesting that both proteins are involved in the increase of this chitin fraction in the wild type at this temperature. On the basis of these observations we wanted to know if expression of *CRH1* and/or *CRH2* was induced by heat stress. Transcription of *CRH1* was strongly induced by a shift from 24°C to 38°C, even after 18 h incubation (Fig. 7A). This transcriptional activation was strictly dependent on the Slt2-MAP kinase cascade, because it was abolished by an *slt2* mutation (Fig. 7B). Western blotting showed that the induction could also be observed at the protein level (Fig. 7C). In contrast to *CRH1*, the expression of *CRH2* was not affected by temperature (results not shown).

When the experiments were repeated in an *slt2* background, the increase in the chitin–β(1-6)glucan fraction at 37°C was abolished in the *crh2Δ* strain (Fig. 8), in line with the Slt2p requirement for increase in expression of Crh1p. In the *crh1Δ* mutant there was still an increase at 37°C, although smaller than in the strain with only the *slt2* mutation. The significance of this difference is not understood.

Effect of temperature on the localization of chitin and of the Crh proteins

Because, as already mentioned, the chitin linked to β(1-6)glucan appears to be dispersed in the wall, one

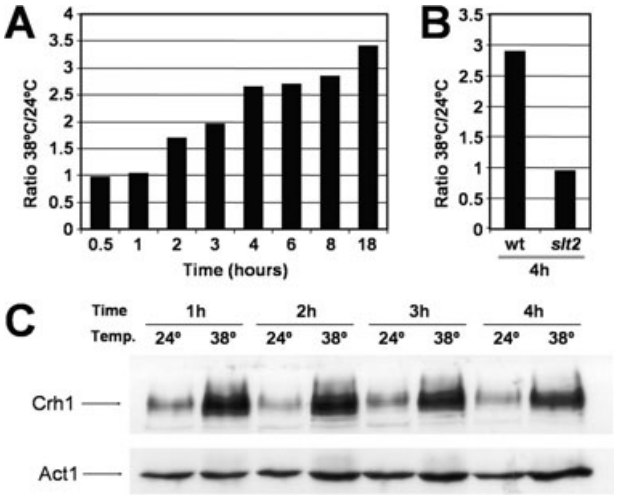

Fig. 7. *CRH1* expression is induced after shifting to 38°C.
A. *CRH1* mRNA levels in wild-type (FY001) cells growing exponentially at 38°C relative to 24°C at different times after temperature shift.
B. *CRH1* mRNA levels in wild-type and *slt2*Δ cells (strain FYDK) 4 h after temperature shift.
C. Crh1–GFP protein levels determined by Western blotting, using an anti-GFP antibody, in wild-type cells transformed with the plasmid pJV89GL, grown at 24°C and 38°C.

would expect an increase in this localization at higher temperature. This appears to be the case, based on staining of chitin with Calcofluor White (Fig. 9). At 38°C there is more fluorescence on the cell periphery than at 24°C. This difference decreases dramatically from wild type to *crh2Δ*, and more gradually going from wild type to *crh1Δ* or from *crh2Δ* to the double mutant (Fig. 9), as expected from the decrease in chitin linked to β(1-6)glucan (Fig. 6).

We then wanted to ask whether in addition to the induction of Crh1 expression at 38°C, the increase in the chitin linked to β(1-6)glucan at 38°C could also be explained by a redistribution of Crh1p and/or Crh2p to the cell surface. Previous published data had shown a partial redistribution of Chs3–GFP from internal compartments to the plasma membrane during heat stress (Valdivia and Schekman, 2003). Because chitin is insoluble in water, it seems likely that it would be linked to other cell wall components near the site where it is synthesized. We previously showed that Crh1p–GFP localizes at the tip of emerging buds and later in the septal area (Rodríguez-Peña *et al*., 2000). A new construction of Crh1–GFP (see *Experimental procedures*) in which a longer fragment of the *CRH1* promoter (1158 bp) was driving its transcription, revealed a similar pattern of polarized localization, but also some localization at the lateral cell wall at 24°C (Fig. 10A). However, when cells were cultured at 38°C, most of them showed Crh1–GFP uniformly distributed over the cell cortex, while some of the protein remained in the neck area

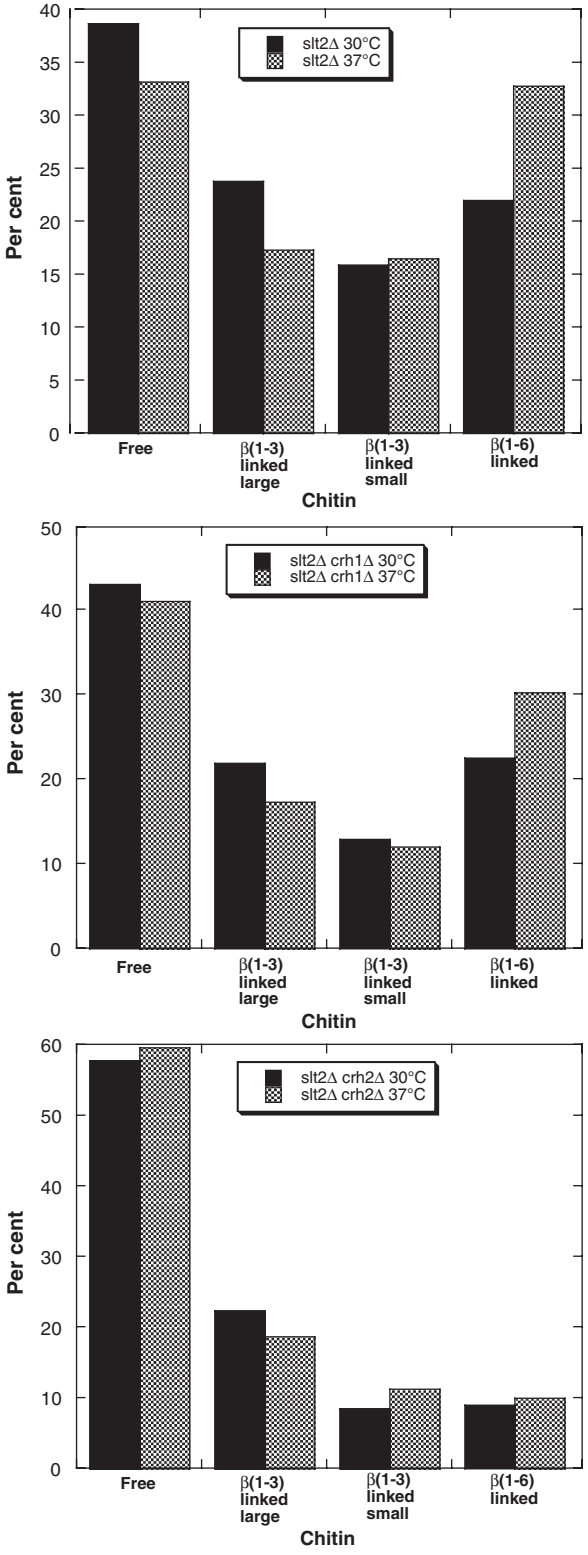

Fig. 8. Distribution of chitin in an *slt2* mutant (strain FYDK) and in *crh* mutants (strains GRA003 and GRA004, see Table 1) in an *slt2* background, after growth at 30°C or 37°C. A temperature of 37°C was used here, instead of 38°C, because strains harbouring the *slt2* mutation did not grow well at 38°C.

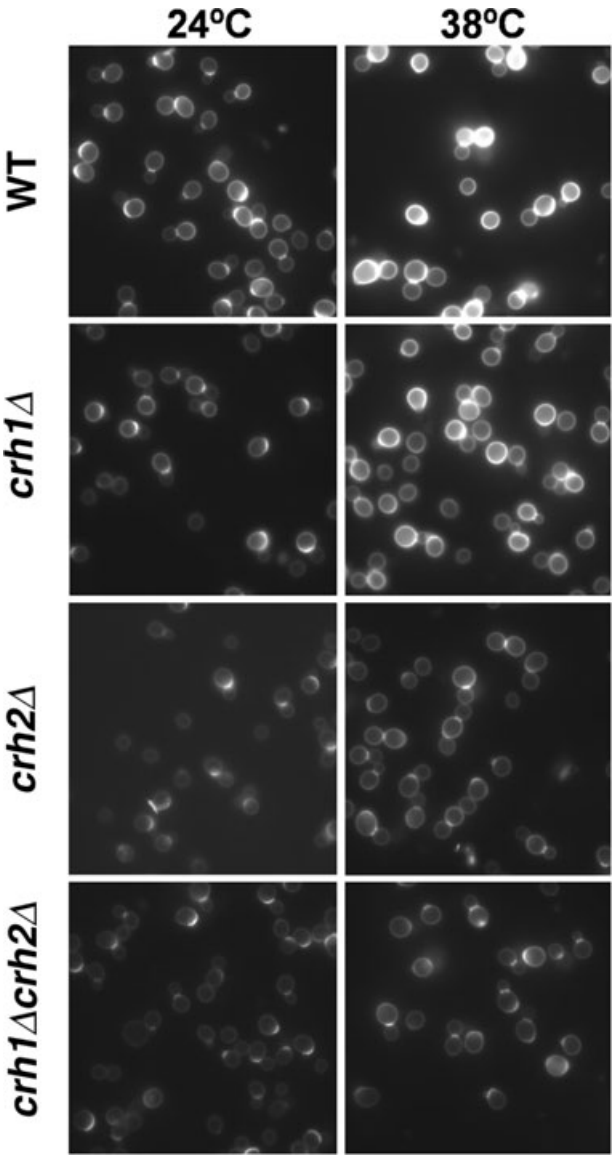

Fig. 9. Calcofluor White staining of wild-type and mutant strains. Fluorescence microscopy of cells either growing at 24°C or after a shift to 38°C for 3 h. Cells were stained with Calcofluor White (see *Experimental procedures*) and imaged with a Nikon Ellipse TE2000-U inverted fluorescence microscope. WT, FY001; *crh1Δ*, RCA001; *crh2Δ*, RCA002; *crh1Δ crh2Δ*, RCA003.

(Fig. 10A and B). Quantification of the results showed a threefold increase in unbudded cells staining in lateral walls and a fourfold increase in budded cells (Fig. 10B). Analysis of the fluorescence in the cell sorter revealed a clear increase at 38°C (Fig. 10C), in agreement with the elevated expression of Crh1p at this temperature. Cells in the higher range of fluorescence, isolated with the cell sorter, showed an enhanced difference in Crh1–GFP distribution between the 24°C and the 38°C sample (Fig. 10D). Because the Crh1p–GFP fusion did not complement the Congo Red sensitivity of a *crh1* mutant, we constructed a strain harbouring a *crh1* deletion and a plasmid carrying a Crh1p–HA fusion. This plasmid effectively suppressed the sensitivity to Congo Red both a 24°C and 38°C and gave rise to a cellular distribution of Crh1p–HA similar to that of Crh1p–GFP at both temperatures (Fig. 10E), thus validating the results obtained with the former construct.

For Crh2p, the experiment could not be carried out with the Crh2p–GFP construct, because at 38°C this protein was degraded, as shown by Western blots, and fluorescence accumulated in the vacuole. However, a Crh2p–HA fusion protein did not present this problem and its localization could be ascertained by immunofluorescence (Fig. 10F and G). At 24°C, most of the protein was found at the mother-bud neck or on bud scars, but at 38°C this localization was sharply reduced, whereas a majority of cells showed fluorescence all around the cortex, often with a punctate appearance (Fig. 10F and G), as observed for Crh1p–HA. Thus, the change in distribution of Crh2p at the higher temperature was similar to that of Crh1p. However, the total fluorescence intensity did not change appreciably with temperature (Fig. 10H), consistent with the lack of increase in *CRH2* expression at 38°C. Subsequent experiments showed that the Crh2p–HA fusion protein fully complements the Congo Red hypersensitivity of *crh1Δ* and *crh2Δ* mutants.

All these results suggest that both Crh1p and Crh2p change their localization during heat stress. While both proteins are mainly localized to polarized growth sites at 24°C, a partial redistribution of both proteins to the cell surface is seen when the cells are shifted to 38°C.

Discussion

Our results on the distribution of chitin in the *crh* mutants clearly establishes the requirement of the Crh proteins for the formation of the chitin–β(1-6)glucan linkage. Quantitatively, it appears that Crh2p is the major contributor to synthesis of the linkage, at least under normal conditions. These proteins function in the transfer of chitin to the glucan rather than in a modification of the acceptor, whose structure is unchanged in their absence.

In principle, there could be a number of steps between the synthesis of chitin and its transfer to another polysaccharide. However, we favour the idea that the nascent chitin is directly transferred to the acceptor through the agency of a Crh protein, because if chitin chains are allowed to associate, they bind tightly to each other by hydrogen bonding and form water-insoluble fibres. Instead, once they are linked to β(1-6)glucan they can no longer associate among themselves, as shown by the water solubility of chitin–β(1-6)glucan complexes (Cabib and Durán, 2005). Apparently, the Crh proteins are capable of transferring chitin chains of many

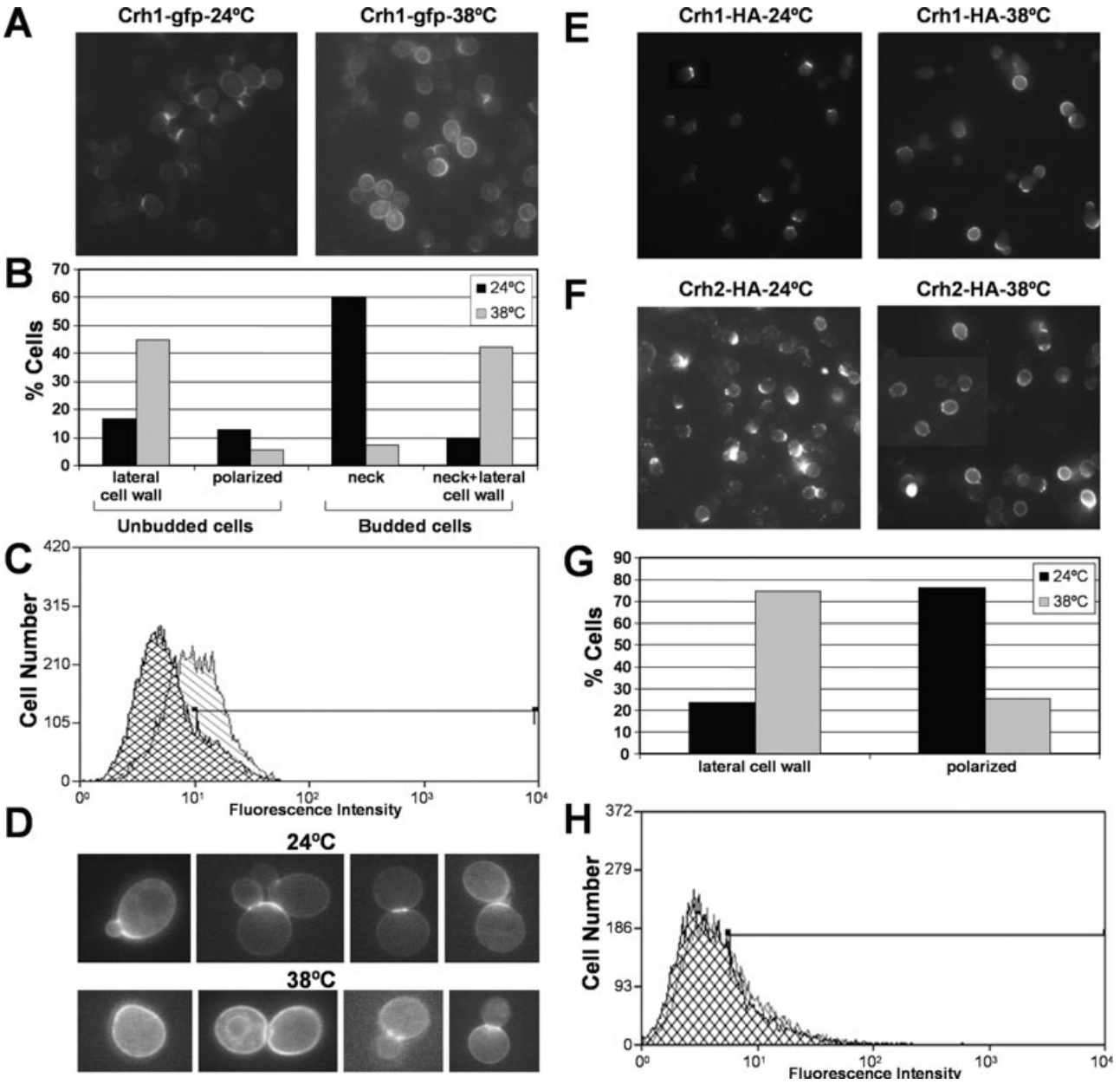

Fig. 10. Temperature upshift affects Crh1p and Crh2p localization.
A. *crh1Δ* cells carrying the plasmid pJV89GL, containing *CRH1*–GFP, were grown at 24°C or shifted to 38°C for 3 h and visualized by fluorescence microscopy.
B. Quantification of the different Crh1p localization patterns. For unbudded cells, cells with Crh1p distribution at the lateral cell wall or at polarized growth sites were evaluated. For budded cells, cells with Crh1p localization at the neck region and cells showing a simultaneous localization at neck and lateral cell wall were scored. In both cases, the quantification is expressed as percentage of the total cell population under study at 24°C or 38°C ($n = 550$).
C. Overlay histogram of cells shown in A analysed by flow cytometry (single-hatched, 38°C, double-hatched, 24°C). Horizontal bar marks the GFP-positive cells.
D. GFP-positive cells were sorted directly using a MoFlo flow cytometer with the sorting criteria shown in C (cells with higher fluorescence than the left end of the horizontal line) onto slides and visualized in a Nikon Eclipse TE2000-U inverted fluorescence microscope.
E. *crh1Δ* cells carrying plasmid pNBC15, which contains *CRH1*–HA, were grown at 24°C or shifted to 38° for 3 h and analysed by immunofluorescence microscopy.
F. *crh2Δ* cells harbouring plasmid pNBC13, which contains *CRH2*–HA, were grown at 24°C or shifted to 38°C for 3 h and analysed by immunofluorescence microscopy. The picture at 38°C is a composite of two photographs.
G. Quantification of the Crh2p–HA localization patterns (lateral cell wall or polarized) at 24°C and 38°C. Values are expressed as percentage of the population at both temperatures ($n = 300$).
H. Overlay histogram of cells shown in E, analysed by flow cytometry. The curve for cells at 38°C is only slightly displaced to the right of that for 24°C cells.

different lengths, because the chitin attached to β(1-6)glucan is about as polydisperse as the free chitin (Fig. 1).

It is curious that the 'small chitin' attached to β(1-3)glucan is partly dependent on Crh1p and Crh2p (Figs 2 and 3). One should keep in mind, however, that chitin is linked to β(1-6)glucan through a side-chain glucose, attached to the main chain by a β(1-3)linkage (Kollár *et al*., 1997). Thus, it would not be too surprising if the Crh proteins were able to transfer some chitin chains to the β(1-3)-linked polysaccharide.

As cells lacking Chs3p grow well, it is clear that the chitin dispersed in the cell wall is not indispensable, at least under laboratory conditions. However, *crh1* and *crh2* mutations aggravated the phenotype of the cell wall-defective *fks1* and *gas1* mutants, suggesting that the chitin–β(1-6)glucan linkage is of some importance for the integrity of the cell wall. Particularly, the phenotype of the triple *crh1 crh2 fks1* is very sick, suggesting that in the absence of the main glucan synthase activity (encoded by *FKS1*) leading to an impaired β(1-3)glucan network, the cross-linking of chitin to the β(1-6)glucan is very important for cell survival. A function of the Crh proteins in wall maintenance is also suggested by the finding that the proportion of chitin attached to β(1-6)glucan increases as a response to stress, here represented by a higher temperature. For Crh1p, but not for Crh2p, the increase in temperature also resulted in an enhanced expression of the corresponding gene as well as of the protein. This induction was totally dependent on the cell integrity pathway, because it was abolished in an *slt2* mutant. We also detected a heightened expression of *CRH1* under conditions that destabilize the cell wall, such as treatment with zymolyase (results not shown). In those cases, however, no increase in chitin–β(1-6)glucan could be shown (results not shown). While we do not fully understand these results, they may be related to the fact that zymolyase interferes with the formation of β(1-3)glucan, the polysaccharide to which the chitin–β(1-6)glucan complex is attached. Anyway, all these results plus the cell cycle-dependent transcription of *CRH1* (Rodríguez-Peña *et al*., 2000) indicate that the expression of Crh1p is highly regulated, whereas a similar regulation for Crh2p was not detected. This situation is reminiscent of the β(1-3)glucan synthase proteins, Fks1p and Fks2p, where the latter, a minor contributor to the synthesis of the polysaccharide, is the only one that appears to be highly regulated (Levin, 2005).

The Crh1p-dependent increase in the chitin–β(1-6)glucan linkage observed at high temperature requires the enhancement in Crh1p expression induced by the cell integrity pathway, because it is nullified by deletion of *SLT2* (Figs 7 and 8). However, the expression of Crh2p, which also participates in the increase in chitin bound to β(1-6)glucan at higher temperature, does not change. Therefore, some other factors must be at work, at least in the case of Crh2p. One such factor may be the localization of the proteins. Our previous results indicated that most of the chitin attached to β(1-6)glucan is dispersed over the cell wall (Cabib and Durán, 2005). Consistent with this finding, an enhanced presence of chitin in the cell cortex was detected at 38°C by Calcofluor White staining (Fig. 9). On the other hand, Crh1p is present mainly at the bud tip and at the mother-bud neck region during the cell cycle at 30°C (Rodríguez-Peña *et al*., 2000). Based on that localization, we (Rodríguez-Peña *et al*., 2000) and Klis *et al*. (2006) suggested that Crh1p would participate in the formation of the chitin–β(1-3)glucan linkage mostly found at the neck, a notion that we have now shown to be incorrect. Moreover, Crh1–GFP, when expressed under the control of a complete *CRH1* promoter was mainly localized to polarized growth sites but also to the lateral cell wall. During the cell cycle, Crh2p was, like Crh1p, localized to the septal region, but it was also found at the cortex of large buds, where the chitin–β(1-6)glucan linkage is formed after septation and during daughter cell maturation (Rodríguez-Peña *et al*., 2000). Thus, it seemed possible that the enhancement in the formation of that linkage observed at the higher temperature might be accompanied by an increased localization of the Crh proteins at the cortex, in a random distribution. This was certainly the case for both Crh1p and Crh2p (Fig. 10).

Why are Crh1p and Crh2p mostly found during the cell cycle at the mother-bud neck, where there is little, if any, chitin attached to β(1-6)glucan (Cabib and Durán, 2005)? It is possible that they are there as an inactive reservoir, to be directed elsewhere at the appropriate point in the cell cycle or when the cell responds to stress. At least part of Crh1p and Crh2p is covalently linked to the cell wall (Hamada *et al*., 1998; Yin *et al*., 2005) and it would be difficult for that fraction to migrate to a different location. However, GPI-anchored proteins can also reside in the plasma membrane or in vesicles (de Sampaio *et al*., 1999), which would facilitate the displacement. It is interesting that the localization at the mother-bud neck of both Chs3p and Crh2p requires the septin ring and Chs5p (DeMarini *et al*., 1997; Santos and Snyder, 1997; Rodríguez-Peña *et al*., 2002). Like Crh1p and Crh2p, Chs3p, the protein responsible for the synthesis of chitin in the lateral cell wall, shifts from a preferential association with the mother-bud neck to a depolarized localization in the cortex during heat stress (Valdivia and Schekman, 2003). This suggests that these proteins, which cooperate in the formation of the chitin–β(1-6)glucan linkage, might travel together. Future studies will be needed to explore this interesting possibility.

Crh1p and Crh2p are the two first proteins to be directly implicated in the formation of cross-links in the yeast cell wall. Application of the approach used here to other link-

Table 1. Strains used in this study.

Strain	Genotype	Source
FY background		
FY001 (FY1679)	*MATα his3Δ200 ura3-52 leu2Δ1 trp1Δ63*	Rodríguez-Peña *et al.* (2000)
RCA001	*MATα his3Δ200 ura3-52 leu2Δ1 crh1::KanMX4*	Rodríguez-Peña *et al.* (2000)
RCA002	*MATα his3Δ200 ura3-52 leu2Δ1 crh2::HIS3*	Rodríguez-Peña *et al.* (2000)
RCA003	*MATα his3Δ200 ura3-52 leu2Δ1 crh1::KanMX4 crh2::HIS3*	Rodríguez-Peña *et al.* (2000)
GRA001	FY1679 haploid derivative *chs3::URA3*	This work
GRA002	*MATα his3Δ200 ura3-52 leu2Δ1 crh1::KanMX4 crh2::HIS3 crh3::URA3*	This work
FYDK	*MAT***a** *his3Δ200 ura3-52 leu2Δ1 trp1Δ63 leu2-1 slt2::URA3*	Ruiz *et al.* (2003)
GRA003	*MATα his3Δ200 ura3-52 leu2Δ1 crh1::KanMX4 slt2::URA3*	This work
GRA004	*MATα his3Δ200 ura3-52 leu2Δ1 crh2::HIS3 slt2::URA3*	This work
BY background		
BY4742	*MATα his3Δ1 leu2Δ0 lys2Δ0 ura3Δ0*	EUROSCARF
BY4741	*MAT***a** *his3Δ1 leu2Δ0 met15Δ0 ura3Δ0*	EUROSCARF
GRA005	*MAT***a** *his3Δ1 leu2Δ0 met15Δ0 ura3Δ0 crh1::hphMX4*	This work
GRA006	*MAT***a** *his3Δ1 leu2Δ0 ura3Δ0 crh2::HIS3*	This work
GRA007	*MAT***a** *his3Δ1 leu2Δ0 ura3Δ0 crh2::HIS3 crh1::hphMX4*	This work
Y00993	*MAT***a** *his3Δ1 leu2Δ0 met15Δ0 ura3Δ0 slt2::KanMX4*	EUROSCARF
Y05251	*MAT***a** *his3Δ1 leu2Δ0 met15Δ0 ura3Δ0 fks1::KanMX4*	EUROSCARF
GRA008	*MAT***a** *his3Δ1 leu2Δ0 ura3Δ0 met15Δ0 lys2Δ0 crh2::HIS3 fks1::KanMX4*	This work
GRA009	*MAT***a** *his3Δ1 leu2Δ0 ura3Δ0 met15Δ0 lys2Δ0 crh2::HIS3 fks1::KanMX4 crh1::hphMX4*	This work
Y00897	*MAT***a** *his3Δ1 leu2Δ0 met15Δ0 ura3Δ0 gas1::KanMX4*	EUROSCARF
GR010	*MAT***a** *his3Δ1 leu2Δ0 met15Δ0 ura3Δ0 gas1::KanMX4 crh2::HIS3*	This work
GR011	*MAT***a** *his3Δ1 leu2Δ0 met15Δ0 ura3Δ0 gas1::KanMX4 crh2::HIS3 crh1::hphMX4*	This work

ages and other fungi may facilitate the exploration of this so far untrodden area and perhaps help to find new targets for antifungal agents.

Experimental procedures

Strains and growth conditions

The strains used in this study are listed in Table 1. The culture medium was YEPGal/Raf (Cabib and Durán, 2005) when the cells were labelled with ^{14}C-glucosamine. In other cases, YEPD (2% peptone, 1% yeast extract, 2% glucose) was used, as described for each experiment. When ^{14}C-glucose was used as label, the cells were cultured in YEPD, then centrifuged and suspended at ~3×10^7 cells ml^{-1} in a medium of similar composition, except that it contained 0.5% glucose. Then, 5 μCi ml^{-1} of [U-^{14}C]glucose (MP Biochemicals, 1 mCi ml^{-1}) was added. In experiments at two different temperatures (usually 30°C and 38°C) cells were cultured at both temperatures during the day, followed by overnight growth with an inoculum calculated, in each case, to yield a logarithmic phase culture the next morning. Cell concentration was adjusted to ~3×10^7 cells ml^{-1} and labelling was carried out as described (Cabib and Durán, 2005) with 0.5 μCi ml^{-1} of [1-^{14}C]glucosamine (55 mCi mmol^{-1}, American Radiolabelled Chemicals, St Louis, MO). In all labelling experiments, after the addition of radioactivity the culture was incubated until the OD_{660} doubled.

Analysis of chitin cross-links

Preparation of [^{14}C]glucosamine-labelled and alkali-treated cell walls, treatment with β(1-3)glucanase or β(1-6)glucanase, carboxymethylation and chromatography on a Sephacryl S-300 column were carried out as previously described (Cabib and Durán, 2005). Calculations were also done as already outlined, except for the following: with previously used strains, the amount of chitin bound to β(1-6)glucan could be calculated in two ways (Cabib and Durán, 2005). One (Method I) was by subtracting the originally free chitin in untreated cell walls from the total free chitin in β(1-6)glucanase digests (comprising both the originally free chitin and that liberated by the glucanase). The other way (Method II) was by taking advantage of the finding that a water-soluble complex of chitin and β(1-6)glucan was liberated by digestion of the β(1-3)glucan attached to this complex by β(1-3)glucanase. A correction to this amount for some complex that was not solubilized was made by a double incubation of cell walls with β(1-3) and β(1-6)glucanase (Cabib and Durán, 2005). With some of the strains used here and different labelling conditions, a substantial portion of the chitin–β(1-6)glucan complex remained insoluble after β(1-3)glucanase digestion and was counted as chitin attached to β(1-3)glucan. To correct for this error, we subtracted the radioactivity calculated from Method II from that obtained from Method I. The result, which corresponds to the radioactivity of chitin bound to β(1-6)glucan remaining in the β(1-3)glucanase insoluble residue, was subtracted from the total chitin–β(1-3)glucan calculated amount to give the corrected value.

All the results presented are the average of two, and in some cases three, independent experiments.

Structure of β(1-6)glucan from different strains

To compare the branching of β(1-6)glucan in different strains, we used a procedure based on the finding by Magnelli *et al.* (2002) that a recombinant β(1-6)glucanase (the same used here) cuts between β(1-6)-linked glucoses, yielding as final products branched oligosaccharides that can be separated by size-exclusion chromatography. ^{14}C-glucose-labelled cell

walls (see above for preparation) from ~1.7×10^9 cells, in a volume of 150 μl, were incubated overnight on a rotator at 37°C with 25 μl of 1 M potassium phosphate, pH 6.3, and 220 μl of phenylmethylsulphonylfluoride-treated (Kollár *et al*., 1997) Zymolyase 100T (corresponds to 0.075 mg of dry enzyme, Seikagaku America, Falmouth, MA), as a source of β(1-3)glucanase. To eliminate liberated oligosaccharides, the solubilized material was dialysed overnight against water in a cassette with a cut-off at molecular weight 3500 (Pierce Biotechnology, Rockford, IL). To the dialysate (~700 μl), 40 μl of 1 M sodium acetate, pH 5, and 30 μl (0.1 unit) of recombinant β(1-6)glucanase (Bom *et al*., 1998) were added, and the mixture was incubated at 37°C overnight. To the digest, 80 μl of 1 M acetic acid was added and the mixture was applied to a Bio-Gel P-2 column (1.63 cm × 92 cm), previously equilibrated with 0.1 M acetic acid. The column was eluted with 0.1 M acetic acid, 2 ml fractions were collected and the radioactivity of fractions was determined.

Strain construction

To obtain the double mutants *crh2Δ fks1Δ* and *crh2Δ gas1Δ* in the BY background, the *CRH2* ORF was initially deleted in the BY4742 strain using the His3MX6 module as previously described (Rodríguez-Peña *et al*., 2000). This *crh2Δ* strain was crossed with single deletants in *fks1Δ* and *gas1Δ* (Y05251 and Y00897 in the BY4741 background) to generate the corresponding heterozygous disruptants. After sporulation and tetrad analyses of these strains with standard yeast genetics techniques, haploid double mutant segregants were selected, in addition to the single *crh2* (*MAT***a**) mutant. To generate the triple mutant strains *crh1Δ crh2Δ fks1Δ* and *crh1Δ crh2Δ gas1Δ*, the *CRH1* ORF was replaced in the double deletant strains described above. To delete *CRH1*, the ORF was replaced by the hygromycin B-resistant marker (*hphMX4* module) using the Long Flanking Homology PCR technique (Wach, 1996). The BsgI insert from plasmid pCG01 (see below) was employed as interruption cassette. Correct ORF replacements were verified by analytical PCR using primers and conditions previously described for *CRH1* (YGR189c) (Rodríguez-Peña *et al*., 1998) and *CRH2* (Rodríguez-Peña *et al*., 2000). For construction of the *chs3Δ* strains, a disruption module including the *URA3* selection marker (Sanz *et al*., 2004) was used. Correct ORF replacement was verified by PCR using the following primer pairs: 5′-ATAGGTGACCCTCTTTGGCT-3′ and 5′-CATCTGCTCCT GCGTTTTCT-3; 5′-AACCCGGTAACAGAGGTAAG-3′ and 5′-GCTTTCTCTTAGGGAAAGTC-3′. Deletion of the *SLT2* gene in *crh1Δ* and *crh2Δ* strains was carried out as described by Torres *et al*. (1991). Verification of the replacement was carried out by phenotypic analysis and Western blotting with an anti-Slt2 antibody.

Plasmids

Plasmids pJV89E (YEp352-*CRH1*) and pJV40E (YEp352-*CRH2*) have been already described (Rodríguez-Peña *et al*., 2000).

Plasmid pJV89CL was constructed by cloning an EcoRI-XhoI fragment from the pEGH059 cosmid subclone E3 (Arroyo *et al*., 1997) into pRS416 to obtain a vector bearing the *CRH1* coding sequence flanked by 1158 bp and 487 bp of the *CRH1* promoter and terminator regions respectively. Then, to construct the pJV89GL plasmid, the *CRH1* internal fragment ClaI-SalI (1.6 kb) of pJV89CL was replaced by a fragment from the pJV89G plasmid (Rodríguez-Peña *et al*., 2000), digested with the same enzymes and including the in-frame *CRH1*–GFP fusion.

The pCG01 plasmid was constructed replacing the KanMX4 module (BamHI/EcoRI-Klenow) from the pYORC-YGR189C plasmid (Rodríguez-Peña *et al*., 1998) with the BamHI/EcoRV fragment from the pAG32 plasmid, including the *hphMX4* module (Goldstein and McCusker, 1999).

To construct plasmid pNBC15, carrying *CRH1*–HA, we used the following strategy. A DNA fragment containing the complete *CRH1* ORF was obtained by digesting the plasmid pJV89CL with EcoRI and XhoI. This fragment was cloned into the pBlueScript-SK plasmid previously cut with the same enzymes to generate the plasmid pBlueScript-CRH1. A DNA fragment containing three HA epitopes in tandem flanked by EcoRV restriction sites was generated by PCR using the following primers: 5′-CCCGATATCACCATACCCATACGA TGTTCCTGACT-3′ and 5′-GGGGATATCTGTGGAGCGTA ATCTGGAACGTCATATG-3′. After digestion of the PCR product with EcoRV, it was cloned into pBlueScript-CRH1 previously cut with EcoRV. A correct construction, named as pNBC14, with the HA cassette in frame and properly orientated, was chosen after analysis of several clones by DNA sequencing. Finally, an EcoRI-XhoI DNA fragment isolated from pNBC14 was cloned into the YEp352 plasmid previously digested with the same enzymes to generate the construction pNBC15.

To obtain plasmid pNBC13, harbouring *CRH2*–HA, a DNA fragment containing three HA epitopes in tandem flanked by SpeI sites was generated by PCR using the following primers: 5′-GCACTAGTCCATACCCATACGATGTTCCTGA CT-3′ and 5′-GGACTAGTTGGAGCGTAATCTGGAACGTC ATATG-3′. The cassette was then cloned into the plasmid pJV40G (Rodríguez-Peña *et al*., 2000) previously digested with SpeI, to generate a construction in which the GFP cassette from plasmid pJV40G was replaced by the HA cassette.

RNA isolation and quantitative RT-PCR assays

Saccharomyces cerevisiae strains were grown overnight in YEPD at 24°C to a concentration of 12–15 × 10^6 cells ml^{-1}. This culture was diluted to ~4×10^6 cells ml^{-1}, incubated at 24°C for 2 h and then divided into two parts. One part was allowed to continue growing under the same conditions while the other one was shifted to 38°C. For the 18 h sample, the culture was diluted just before shifted to 38°C to a cellular concentration that allowed the cells to reach a concentration of 6–7 × 10^6 cells ml^{-1} 18 h after the temperature shift. Total RNA was isolated from cells (5×10^7) collected at different time intervals (30 min to 18 h) by using the 'mechanical disruption protocol' and the RNeasy MINI kit (QIAGEN, Hilden, Germany), following manufacturer's instructions. RNA concentrations were always determined by measuring absorbance at 260 nm. RNA purity and integrity were assessed using RNA Nano Labchips in an Agilent 2100B Bioanalyzer (Agilent Technologies, Palo Alto, CA).

Real-time Q-RT-PCR assays were performed as described by García *et al*. (2004) using an ABI 7700 instrument (Applied Biosystems, Foster City, CA). For quantification, the abundance of each gene at different time intervals was determined relative to the standard transcript of *ACT1* and to the sample $t = 0$ h (1× sample) following the $2^{-\Delta\Delta CT}$ method, as described in Livak and Schmittgen (2001). Eventually, the ratio from treated/non-treated condition for each data point was calculated. The following forward and reverse primers, respectively, were used: *ACT1*, 5′-ATCACCGCTTTGGC TCCAT-3′ and 5′-CCAATCCAGACGGAGTACTTTCTT-3′; *CRH1*, 5′-ACTACCCAGATATCAAGCAAATACACA-3′ and 5′-TCAGCACCGTTAGAAATTTGAACA-3′; *CRH2*, 5′-AGCG CCTCCAGCAGTACAA-3′ and 5′-GCCAGTTTGCCGCTA CGTT-3′.

Preparation of yeast extracts and Western blotting

The procedures employed for immunoblot analyses including cell collection, lysis, fractionation of proteins by SDS-polyacrylamide gel electrophoresis and transfer to nitrocellulose membranes were carried out as previously described (Martín *et al*., 2000). Detection of Crh1–GFP was carried out using the anti-GFP JL-8 monoclonal antibody (Clontech, Mountain View, CA). The levels of actin were quantified to monitor protein load using the mouse anti-actin monoclonal antibody C4 (ICN Biomedicals, Aurora, OH).

Phenotypic analysis

Yeast cells were grown overnight in YEPD at 24°C to mid-log phase. The cultures were then diluted to approximately 3×10^6 cells ml^{-1}, incubated at 24°C and the OD_{600} was measured at different time intervals. Using data from three independent experiments, duplication times for each strain were calculated. Cell viability of these cultures was also quantified by staining cells with propidium iodide (0.05 mg ml^{-1}) (De la Fuente *et al*., 1992) and subsequent analysis in a CyAn MLE flow cytometer (Dako, Glostrup, Denmark) acquiring fluorescence through a 610/40 BP filter.

To determine the sensitivity of the different strains to Congo Red, yeast cells were grown overnight in YEPD liquid media at 24°C to mid-log phase. The cultures were then diluted to 3×10^6 cells ml^{-1}, incubated at 24°C for three additional hours and diluted again to the previous concentration. Of these cultures, 5 µl (approximately 15×10^3 cells) plus five 1:5 serial dilutions were spotted on YEPD solid media containing different concentrations of Congo Red. Growth was monitored on the plates after 2 days at 30°C.

Flow cytometry and microscopic analysis

Yeast strains were grown overnight at 24°C in YEPD or SD-Ura (for cells bearing the pJV89GL plasmid) to mid-log phase. The culture was diluted to 3×10^6 cells ml^{-1}, incubated at 24°C in YEPD for 2 h and then maintained at 24°C or 38°C for three additional hours. After this time, cells were processed as follows. For Calcofluor White staining, 1 ml of cells was collected, washed with PBS and stained with Calcofluor White (Fluorescent brightener 28, Sigma-Aldrich, St Louis, MO, final concentration 50 µg ml^{-1}) for 10 min. Stained yeasts were then analysed by fluorescence microscopy, using a Nikon TE2000 fluorescence inverted microscope equipped with CCD. Digital images were acquired with an Orca C4742-95-12ER camera (Hamamatsu Photonics, Japan) and processed with the Aquacosmos Imaging Systems software.

For Crh1–GFP analysis, 1 ml of cells was collected, washed twice with PBS and visualized at the fluorescence inverted microscope mentioned above or analysed with a MoFlo flow cytometer (Dako, Glostrup, Denmark) by acquiring green fluorescence through 530/30 BP filter (BFP). GFP positive cells were sorted in Eppendorf tubes and then visualized by fluorescence microscopy.

For Crh2p–HA analysis, 3 ml of cells was collected, washed twice with PBS and suspended in 200 µl of 10% formaldehyde for permeabilization. After 60 min at room temperature, cells were washed again twice with PBS and incubated with goat serum diluted 1:1000 (Sigma-Aldrich, St Louis, MO) for 30 min at room temperature. After additional washing with PBS, cells were incubated overnight at 4°C with an anti-HA monoclonal antibody (HA.11, 1:500, BAbCO, Berkeley, CA), washed three times with PBS and incubated with a Cy3-conjugated anti-mouse secondary antibody (1:1000, Sigma-Aldrich, St Louis, MO) for 45 min at room temperature. Finally, cells were analysed by fluorescence microscopy after washing three times with PBS.

For flow cytometry analysis of Crh2p–HA expression, cells were processed identically but using different antibodies. A monoclonal antibody anti-HA (clone 3F10) (Roche, Mannheim, Germany) was used as primary antibody and an anti-rat IgG FITC conjugate (Sigma-Aldrich, St Louis, MO) as a secondary antibody. Cells were analysed in this case by flow cytometry acquiring green fluorescence through a 530/30 BP filter (BFP).

Acknowledgements

We thank Humberto Martín and César Roncero for providing plasmids and strains. Special thanks to Raul García for assistance in the design of the figures, to Sonia Díez for technical help, to Victor Cid and Will Prinz for comments on the manuscript and to César Nombela and Jean-Paul Latgé for fruitful discussion and support. We also thank the people at the Unidad de Genómica (UCM/PCM) for their help in DNA sequencing and Q-PCR experiments. The work was supported in part by the Intramural Research Program of the NIH, National Institute of Diabetes and Digestive and Kidney Diseases, and by Grants CICYT-BIO2004-06376 from the Ministerio de Educación y Ciencia (Spain) and FUNWALL LSHB-CT-2004-511952 from the Commission of the European Union.

References

Arroyo, J., García-González, M., García-Sáez, M.I., Sánchez, M., and Nombela, C. (1997) DNA sequence analysis of a 23,002 bp DNA fragment of the right arm of *Saccharomyces cerevisiae* chromosome VII. *Yeast* **13:** 357–363.

Bom, I.J., Dielbandhoesing, S.K., Harvey, K.N., Oomes, S.J. C.M., Klis, F.M., and Brul, S. (1998) A new tool for studying the molecular architecture of the fungal cell wall: one-step purification of recombinant *Trichoderma* β-(1-6)-glucanase expressed in *Pichia pastoris*. *Biochim Biophys Acta* **1425:** 419–424.

Cabib, E., and Durán, A. (2005) Synthase III-dependent chitin is bound to different acceptors depending on location on the cell wall of budding yeast. *J Biol Chem* **280:** 9170–9179.

Cabib, E., Roh, D.-H., Schmidt, M., Crotti, L.B., and Varma, A. (2001) The yeast cell wall and septum as paradigms of cell growth and morphogenesis. *J Biol Chem* **276:** 19679–19682.

De la Fuente, J.M., Alvarez, A., Nombela, C., and Sánchez, M. (1992) Flow cytometric analysis of *Saccharomyces cerevisiae* autolytic mutants and protoplasts. *Yeast* **8:** 39–45.

DeMarini, D.J., Adams, A.E.M., Fares, H., De Virgilio, C., Valle, G., Chuang, J.S., and Pringle, J.R. (1997) A septin-based hierarchy of proteins required for localized deposition of chitin in the *Saccharomyces cerevisiae* cell wall. *J Cell Biol* **139:** 75–93.

Ecker, M., Deutzmann, R., Lehle, L., Mrsa, V., and Tanner, W. (2006) Pir proteins of *Saccharomyces cerevisiae* are attached to β-1,3-glucan by a new protein-carbohydrate linkage. *J Biol Chem* **281:** 11523–11529.

García, R., Bermejo, C., Pérez, R., Rodríguez-Peña, J.M., François, J., Nombela, C., and Arroyo, J. (2004) The global transcription response to transient cell wall damage in *Saccharomyces cerevisiae*. *J Biol Chem* **279:** 15183–15195.

Goldstein, A.L., and McCusker, J.H. (1999) Three new dominant drug resistance cassettes for gene disruption in *Saccharomyces cerevisiae*. *Yeast* **15:** 1541–1553.

Gómez-Esquer, F., Rodríguez-Peña, J.M., Díaz, G., Rodríguez, E., Briza, P., Nombela, C., and Arroyo, J. (2004) *CRR1*, a gene encoding a putative transglycosidase, is required for proper spore wall assembly in *Saccharomyces cerevisiae*. *Microbiology* **150:** 3269–3280.

Hamada, K., Fukuchi, S., Arisawa, M., Baba, M., and Kitada, K. (1998) Screening for glycosylphosphatidylinositol (GPI)-dependent cell wall proteins in *Saccharomyces cerevisiae*. *Mol Gen Genet* **258:** 53–59.

Hartland, R.P., Vermeulen, C.A., Klis, F.M., Sietsma, J.H., and Wessels, J.G.H. (1994) The linkage of (1-3)-β-glucan to chitin during cell wall assembly in *Saccharomyces cerevisiae*. *Yeast* **10:** 1591–1599.

Jung, U.S., and Levin, D.E. (1999) Genome-wide analysis of gene expression regulated by the yeast cell wall integrity signalling pathway. *Mol Microbiol* **34:** 1049–1057.

Kapteyn, J.C., Ram, A.F.J., Groos, E.M., Kollár, R., Montijn, R.C., Van den Ende, H., *et al.* (1997) Altered extent of cross-linking of β1,6-glucosylated mannoproteins to chitin in *Saccharomyces cerevisiae* mutants with reduced cell wall β1,3-glucan content. *J Bacteriol* **179:** 6279–6284.

Klis, F.M., Mol, P., Hellingwerf, K., and Brul, S. (2002) Dynamics of cell wall structure in *Saccharomyces cerevisiae*. *FEMS Microbiol Rev* **26:** 239–256.

Klis, F.M., Boorsma, A., and De Groot, P.W.J. (2006) Cell wall construction in *Saccharomyces cerevisiae*. *Yeast* **23:** 185–202.

Kollár, R., Petráková, E., Ashwell, G., Robbins, P.W., and Cabib, E. (1995) Architecture of the yeast cell wall. The linkage between chitin and β (1→3) glucan. *J Biol Chem* **270:** 1170–1178.

Kollár, R., Reinhold, B.B., Petráková, E., Yeh, H.J.C., Ashwell, G., Drgonová, J., *et al.* (1997) Architecture of the yeast cell wall. β (1→6) Glucan interconnects mannoprotein, β (1→3) glucan and chitin. *J Biol Chem* **272:** 17762–17775.

Lagorce, A., Hauser, N.C., Labourdette, D., Rodríguez, C., Martin-Yken, H., Arroyo, J., *et al.* (2003) Genome-wide analysis of the response to cell wall mutation in the yeast *Saccharomyces cerevisiae*. *J Biol Chem* **278:** 20345–20357.

Levin, D.E. (2005) Cell wall integrity signaling in *Saccharomyces cerevisiae*. *Microbiol Mol Biol Rev* **69:** 262–291.

Lipke, P.N., and Ovalle, R. (1998) Cell wall architecture in yeast: new structure and new challenges. *J Bacteriol* **180:** 3735–3740.

Livak, K.J., and Schmittgen, T.D. (2001) Analysis of relative gene expression data using real-time quantitative PCR and the $2^{-\Delta\Delta CT}$ method. *Methods* **25:** 402–408.

Magnelli, P., Cipollo, J.F., and Abeijón, C. (2002) A refined method for the determination of *Saccharomyces cerevisiae* cell wall composition and β-1,6-glucan fine structure. *Anal Biochem* **301:** 136–150.

Martín, H., Rodríguez-Pachón, J.M., Ruiz, C., Nombela, C., and Molina, M. (2000) Regulatory mechanisms for modulation of signaling through the cell integrity Slt2-mediated pathway in *Saccharomyces cerevisiae*. *J Biol Chem* **275:** 1511–1519.

Rodríguez-Peña, J.M., Cid, V.J., Sánchez, M., Molina, M., Arroyo, J., and Nombela, C. (1998) The deletion of six ORFs of unknown function from *Saccharomyces cerevisiae* chromosome VII reveals two essential genes: *YGR195w* and *Ygr198w*. *Yeast* **14:** 853–860.

Rodríguez-Peña, J.M., Cid, V.J., Arroyo, J., and Nombela, C. (2000) A novel family of cell wall-related proteins regulated differently during the yeast life cycle. *Mol Cell Biol* **20:** 3245–3255.

Rodríguez-Peña, J.M., Rodríguez, C., Alvarez, A., Nombela, C., and Arroyo, J. (2002) Mechanisms for targeting of the *Saccharomyces cerevisiae* GPI-anchored cell wall protein Crh2p to polarised growth sites. *J Cell Sci* **115:** 2549–2558.

Roh, D.-H., Bowers, B., Riezman, H., and Cabib, E. (2002) Rho1p mutations specific for regulation of β (1→3) glucan synthesis and the order of assembly of the yeast cell wall. *Mol Microbiol* **44:** 1167–1183.

Ruiz, C., Escribano, V., Morgado, E., Molina, M., and Mazón, M.J. (2003) Cell-type-dependent repression of yeast a-specific genes requires Itc1p, a subunit of the Isw2p-Itc1p chromatin remodelling complex. *Microbiology* **149:** 341–351.

de Sampaio, G., Bourdineaud, J.P., and Lauquin, G.J.-M. (1999) A constitutive role for GPI anchors in *Saccharomyces cerevisiae*: cell wall targeting. *Mol Microbiol* **34:** 247–256.

Santos, B., and Snyder, M. (1997) Targeting of chitin synthase 3 to polarized growth sites in yeast requires Chs5p and Myo2p. *J Cell Biol* **136:** 95–110.

Sanz, M., Castrejón, F., Durán, A., and Roncero, C. (2004) *Saccharomyces cerevisiae* Bni4p directs the formation of

the chitin ring and also participates in the correct assembly of the septum structure. *Microbiology* **150:** 3229–3241.

Schmidt, M., Varma, A., Drgon, T., Bowers, B., and Cabib, E. (2003) Septins, under Cla4p regulation, and the chitin ring are required for neck integrity in budding yeast. *Mol Biol Cell* **14:** 2128–2141.

Shaw, J.A., Mol, P.C., Bowers, B., Silverman, S.J., Valdivieso, M.H., Durán, A., and Cabib, E. (1991) The function of chitin synthases 2 and 3 in the *Saccharomyces cerevisiae* cell cycle. *J Cell Biol* **114:** 111–123.

Terashima, H., Yabuki, N., Arisawa, M., Hamada, K., and Kitada, K. (2000) Up-regulation of genes encoding glycosylphosphatidylinositol (GPI)-attached proteins in response to cell wall damage caused by disruption of *FKS1* in *Saccharomyces cerevisiae*. *Mol Gen Genet* **264:** 64–74.

Torres, L., Martín, H., García-Sáez, M.I., Arroyo, J., Molina, M., Sánchez, M., and Nombela, C. (1991) A protein kinase gene complements the lytic phenotype of *Saccharomyces cerevisiae lyt2* mutants. *Mol Microbiol* **5:** 2845–2854.

Valdivia, R.H., and Schekman, R. (2003) The yeast Rho1p and Pkc1p regulate the transport of chitin synthase III (Chs3p) from internal stores to the plasma membrane. *Proc Natl Acad Sci USA* **100:** 10287–10292.

Wach, A. (1996) PCR synthesis of marker cassettes with long flanking homology regions for gene disruptions in *S. cerevisiae*. *Yeast* **12:** 259–265.

Yin, Q.Y., de Groot, P.W.J., Dekker, H.L., de Jong, L., Klis, F.M., and de Koster, C.G. (2005) Comprehensive proteomic analysis of *Saccharomyces cerevisiae* cell walls. Identification of proteins covalently attached via glycosylphosphatidylinositol remnants or mild alkali-sensitive linkages. *J Biol Chem* **280:** 20894–20901.

CAPÍTULO 2

Crh1 Y Crh2 ACTÚAN COMO TRANSGLICOSILASAS *IN VIVO E IN VITRO*

RESUMEN DE LOS RESULTADOS DEL CAPÍTULO 2

En trabajos previos, habíamos demostrado que Crh1 y Crh2 son responsables de la transglicosilación de la quitina al β-1,6 glucano *in vivo* mediante el análisis de las paredes celulares carboximetiladas de la cepa *crh1*Δ *crh2*Δ. Con el objetivo de estudiar la actividad de estas proteínas, de manera que la insolubilidad de la quitina en agua no fuera una limitación, se llevó a cabo una aproximación experimental que permitiese observar la reacción de transglicosilación *in vivo*, mediante el uso de gluco-oligosacáridos conjugados a sulforodamina (SR) como sustratos artificiales en lugar del glucano. El método consiste en el crecimiento de las células en presencia de los gluco-oligosacáridos marcados en el medio de cultivo, el tiempo suficiente para permitir su incorporación en la pared celular y detectar posteriormente su emisión de fluorescencia. Inicialmente, se usaron gluco-oligosacáridos unidos mediante enlaces β-1,3 o β-1,6, en una cepa silvestre. En contra de lo esperado los β-1,3 gluco-oligosacáridos funcionan mejor como aceptores que los unidos mediante enlaces β-1,6, que apenas funcionaron en la reacción de transglicosilación. La fluorescencia de los gluco-oligosacáridos se localiza principalmente en la cicatriz y de manera difusa en el contorno de la pared lateral (la distinción entre cicatriz y septo se hizo mediante una tinción simultánea con CFW de las células crecidas en presencia de los gluco-oligosacáridos). Los gluco-oligosacáridos se incorporan a la pared celular mediante su unión a la quitina, ya que cuando las células crecidas en presencia de los gluco-oligosacáridos se someten a un tratamiento con quitinasa se elimina mayoritariamente la fluorescencia incorporada. No se detectó fluorescencia en las células *crh1*Δ *crh2*Δ crecidas en presencia de los gluco-oligosacáridos, por lo que concluimos que ambas proteínas son requeridas para la incorporación de los β-1,3 gluco-oligosacáridos en la cicatriz, donde probablemente se unan a la quitina libre procedente del anillo de quitina, del septo primario o de la síntesis *de novo* que ocurre cerca de la membrana plasmática. El mutante *gas1*Δ, que posee un incremento considerable de quitina con respecto a la cepa WT, exhibe un marcaje exacerbado con los gluco-oligosacáridos tanto en la pared lateral como en las cicatrices con respecto a una cepa WT. Además, el marcaje del mutante *gas1*Δ *crh1*Δ *crh2*Δ permitió verificar que toda la fluorescencia localizada en la cicatriz y en la pared lateral del mutante *gas1*Δ procedente de la incorporación de los β-1,3 gluco-oligosacáridos es dependiente de Crh1 y Crh2.

Adicionalmente, la reacción de transglicosilación se trasladó a un sistema *in vitro* utilizando células permeabilizadas con digitonina como fuente de quitina y proteínas Crh, UDP-NAG como precursor de la síntesis de quitina y gluco-oligosacáridos marcados como aceptores. En este sistema, se pudo comprobar también la incorporación de los β-1,3 gluco-oligosacáridos a las células permeabilizadas, de manera Crh dependiente y dependiente también de la adición de UDP-NAG, lo que confirma que la reacción de entrecruzamiento entre la quitina y el glucano requiere de una síntesis activa de quitina, mediada en este caso por Chs1 y no por Chs3 que es la enzima activa *in vivo*. Complementario a los dos sistemas anteriores, células vivas y células permeabilizadas con digitonina, se desarrolló una tercera estrategia, en este caso con paredes celulares aisladas en presencia de los gluco-oligosacáridos fluorescentes y en ausencia de UDP-NAG, en el que de nuevo se comprobó que la incorporación de los parches de fluorescencia en las paredes celulares es Crh dependiente. Cuando estos experimentos se llevaron a cabo con paredes celulares procedentes de la cepa *gas1*Δ, se observa que existe una cierta incorporación de los gluco-oligosacáridos en ausencia del precursor UDP-NAG, lo que sugiere la existencia de dos rutas paralelas para la incorporación a la pared celular de los gluco-oligosacáridos. Una que es dependiente de la síntesis activa de quitina y es necesaria para la incorporación en la pared lateral y otra, para la incorporación en las cicatrices, que depende de la quitina preformada. Probablemente, lo más importante de este trabajo es que se ha desarrollado un sistema *in vitro* mediante el cual se generan enlaces quitina-glucano de forma dependiente de las proteínas Crh, en presencia de células permeabilizadas o paredes celulares aisladas. Interesantemente, la incorporación de los gluco-oligosacáridos en estos ensayos es completamente inhibida por la presencia de quito-oligosacáridos solubles de quitina.

ARTÍCULO 2

Assembly of the yeast cell wall. Crh1p and Crh2p act as transglycosylases in vivo and in vitro

THE JOURNAL OF BIOLOGICAL CHEMISTRY VOL. 283, NO. 44, pp. 29859–29872, October 31, 2008
Printed in the U.S.A.

Assembly of the Yeast Cell Wall

*Crh1p AND Crh2p ACT AS TRANSGLYCOSYLASES IN VIVO AND IN VITRO**[S]

Received for publication, June 3, 2008, and in revised form, August 11, 2008 Published, JBC Papers in Press, August 11, 2008, DOI 10.1074/jbc.M804274200

Enrico Cabib[‡1], **Vladimir Farkas**[§], **Ondrej Kosík**[§], **Noelia Blanco**[¶], **Javier Arroyo**[¶], **and Peter McPhie**[‡]

From the [‡]*Laboratory of Biochemistry and Genetics, NIDDK, National Institutes of Health, Department of Health and Human Services, Bethesda, Maryland 20892, the* [§]*Institute of Chemistry, Center of Excellence GLYCOBIOS, Slovak Academy of Sciences, 84538 Bratislava, Slovakia, and the* [¶]*Departamento de Microbiología II, Facultad de Farmacia, Universidad Complutense de Madrid, 28040 Madrid, Spain*

The cross-linking of polysaccharides to assemble new cell wall in fungi requires mechanisms by which a preexisting linkage is broken for each new one made, to allow for the absence of free energy sources outside the plasma membrane. Previous work showed that Crh1p and Crh2p, putative transglycosylases, are required for the linkage of chitin to β(1–3)glucose branches of β(1–6)glucan in the cell wall of budding yeast. To explore the linking reaction *in vivo* and *in vitro*, we used fluorescent sulforhodamine-linked laminari-oligosaccharides as artificial chitin acceptors. *In vivo*, fluorescence was detected in bud scars and at a lower level in the cell contour, both being dependent on the CRH genes. The linking reaction was also shown in digitonin-permeabilized cells, with UDP-*N*-acetylglucosamine as the substrate for nascent chitin production. Both the nucleotide and the Crh proteins were required here. A *gas1* mutant that overexpresses Crh1p showed very high fluorescence both in intact and permeabilized cells. In the latter, fluorescence was still incorporated in patches in the absence of UDP-GlcNAc. Isolated cell walls of this strain, when incubated with sulforhodamine-oligosaccharide, also showed Crhp-dependent fluorescence in patches, which were identified as bud scars. In all three systems, binding of the fluorescent material to chitin was verified by chitinase digestion. Moreover, the cell wall reaction was inhibited by chitooligosaccharides. These results demonstrate that the Crh proteins act by transferring chitin chains to β(1–6)glucan, with a newly observed high activity in the bud scar. The importance of transglycosylation for cell wall assembly is thus firmly established.

Fungal cells are endowed with a cell wall, external to the plasma membrane, which is essential for cell survival. The wall protects the cell against bursting caused by the internal turgor pressure and against mechanical injury. It also acts as a filter for large molecules that could injure the plasma membrane (1). Furthermore, the cell wall is the surface at which pathogenic fungi interact with the host, whether animal or plant, and against which host defenses are often mounted. Because the cell wall imparts shape to the fungal cell, we have used it for many years in *Saccharomyces cerevisiae* as a model for morphogenesis (2). On account of its essentiality and its composition, which includes substances not found in animal cells, the fungal cell wall is an obvious target for antifungal compounds. In fact, inhibitors of the echinocandin type against β(1–3)glucan synthase have recently entered clinical use (3).

The mechanical strength of the cell wall is explained by the linkage of its components to each other, which results in a tightly linked network (4–6). To build this structure, the cell needs to solve several problems as follows: how to synthesize the wall components, how to export them outside the plasma membrane, and how to assemble them in an orderly frame outside the cell.

In *S. cerevisiae*, the components of the cell wall are polysaccharides and mannoproteins. The latter are synthesized at the endoplasmic reticulum and the Golgi, followed by export in vesicles to the plasma membrane, to which they are tethered by glycosylphosphatidylinositol anchors (7). On the other hand, the polysaccharides, such as chitin (8), β(1–3)glucan (9), and probably β(1–6)glucan (10), are formed at the plasma membrane and extruded into the periplasmic space. Thus, no cross-linking of the components is possible intracellularly, because they do not become available to each other until they are outside the plasma membrane. Because in the cell wall the different components are covalently attached to each other, how are the cross-links made extracellularly? This poses a thermodynamic puzzle; inside the cell, ATP, directly or indirectly, provides the free energy for the formation of new chemical bonds. However, outside the plasma membrane there cannot be ATP or other small molecules, because they would be dissipated into the medium; so what is the source of the free energy? This problem is not limited to fungal cells. Bacterial and plant cells also have cell walls, and in many cases animal cells are endowed with an extracellular matrix, which may require some assembly.

Because small molecules are absent, the free energy for the formation of new bonds must come from the large components themselves, which can use up some of their preexisting linkages to make new ones or can enter into a reaction with some substance readily available outside the cell. Examples of both

* This work was supported, in whole or in part, by a National Institutes of Health grant (Intramural Research Program, NIDDK). This work was also supported by Grant MRTN-CT-2004-512265 from the 6FP of the European Commission, by Grant 2/3158/25 from the Scientific Grant Agency VEGA, Slovakia, and by Projects BIO2007–67821 from the MEC (Spanish Government) and S-SAL-0246/2006 from Comunidad de Madrid. The costs of publication of this article were defrayed in part by the payment of page charges. This article must therefore be hereby marked "*advertisement*" in accordance with 18 U.S.C. Section 1734 solely to indicate this fact.

[S] The on-line version of this article (available at http://www.jbc.org) contains supplemental Figs. S1–S3.

[1] To whom correspondence should be addressed: National Institutes of Health, Bldg. 8, Rm. 403, Bethesda, MD 20892. Fax: 301-496-9431; E-mail: enricoc@bdg10.niddk.nih.gov.

mechanisms have been described; thus, in bacteria, cross-linking of peptidoglycan chains occurs by transpeptidation, with the liberation of D-alanine (11). During formation of the fertilization envelope in sea urchin eggs, proteins are cross-linked by peroxidative formation of intermolecular tyrosine bonds (12). About 20 years ago we proposed that linkages between different polysaccharides of the yeast cell wall might be generated by transglycosylation (13). A test for that hypothesis became possible only recently, when we developed a new procedure for the quantitative determination of some cross-links in the yeast cell wall (14). With that approach, it was found that the putative transglycosylases Crh1p and Crh2p are required for the formation of cross-links between chitin and β(1–6)glucan but not between chitin and β(1–3)glucan (15). In these cross-links, chitin becomes attached to β(1–3)glucose branches of the β(1–6)glucan (5) (Fig. 1*A*). Crh1p and Crh2p are members of a group of three highly homologous proteins (16) (Fig. 1*B*), the third being Crr1p, which appears to have a function in the formation of the spore wall (17). These proteins are endowed with motifs similar to the catalytic group of certain bacterial glucanases and plant transglycosidases (16). Introduction of a Crh1p mutated in that motif in a *crh1*Δ *crh2*Δ strain failed to suppress the sensitivity of that strain to Congo Red (16). In addition to this presumptive catalytic site, both Crh2p and Crr1p contain a chitin-binding domain (CBM18), shown for Crh2p in Fig. 1*C*. Curiously, Crh1p is devoid of such a domain. It may have a previously unidentified chitin-binding site, or perhaps an appropriate binding site might be created by folding of the protein (19). All these data supported our hypothesis that the Crh proteins may link chitin and β(1–6)glucan by transglycosylation, but it was desirable to buttress this proposition by better characterizing the activity of the Crh proteins and demonstrating it, if possible, in an *in vitro* system. There is, however, a formidable obstacle to that endeavor, which is that chitin, as available to the researcher, is totally insoluble in water, because of hydrogen bonding between the sugar chains. Thus, it is unlikely that this material would serve for an *in vitro* transglycosylation reaction. The situation may be quite different *in vivo*, where individual chains emerge from the plasma membranes and may be captured by a transglycosylase positioned nearby, before they have an opportunity to interact with other chitin chains and form an insoluble fiber. To circumvent this problem, we used a stepwise approach, which started by offering artificial transglycosylation acceptors to growing cells and led to the use of permeabilized cells and finally of cell walls in an *in vitro* system. Unexpectedly, in the course of these experiments we uncovered a very high activity of the system for chitin-β(1–6)glucan linkage in bud scars.

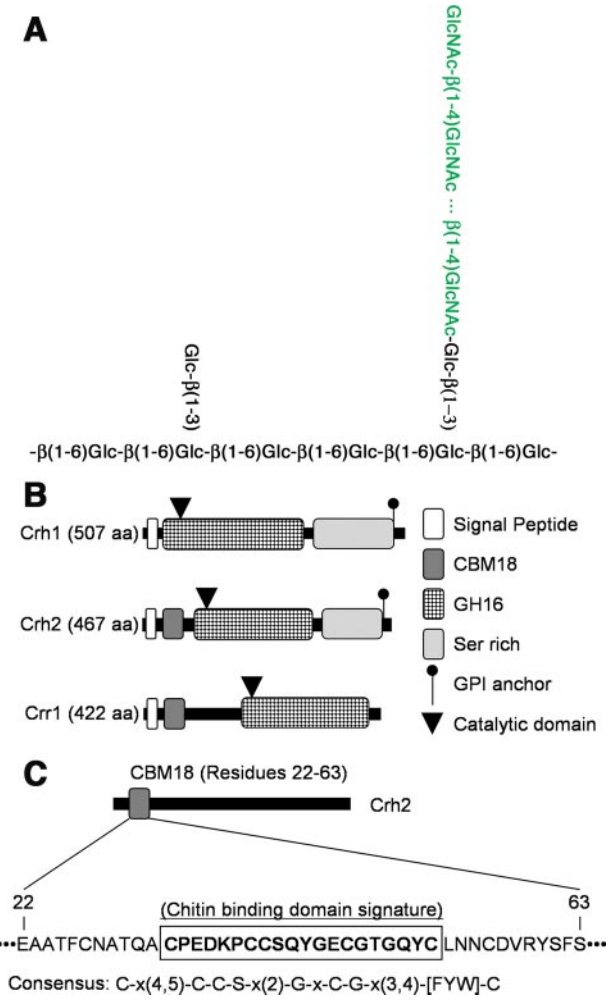

FIGURE 1. **Cross-links between chitin and β(1–6)glucan and domain architecture of cell wall proteins of the Crh family.** *A*, scheme of chitin-β(1–6)glucan cross-linking. The main β(1–6)glucose chain is shown, with two β(1–3)-linked glucose branches. To one of them, a chitin chain (*in green*) is attached. *Glc*, glucose; *GlcNAc*, *N*-acetylglucosamine. *B*, functional domains of Crh1p, Crh2p, and Crr1p are depicted in the schematic. According to the Carbohydrate-Active Enzyme Database (CAZy) (18), the three proteins present a common domain belonging to the glycoside hydrolase family 16 (GH16) that includes a putative catalytic domain. According to the same data base, both Crh2p and Crr1p also possess a carbohydrate-binding module (*CBM*) belonging to family 18 with a chitin-binding function. *aa*, amino acid. *C*, CBM18 overlaps with a chitin-binding domain type 1 described in InterPro and Prosite Databases. The complete sequence of the CBM18 of Crh2p is shown. The sequence of the chitin-binding domain signature (20 amino acids) of Crh2p according to the consensus sequence of the signature is in *boldface type and boxed*.

EXPERIMENTAL PROCEDURES

Strains and Growth Conditions—The strains used are listed in Table 1. Cells were grown in minimal medium (2% glucose, 0.67% yeast nitrogen base) plus requirements, at 30 °C or 38 °C, as indicated in each case.

Strain Construction—To delete *GAS1* in the LC355 background, yielding strain NBT001, the open reading frame was replaced by the *HIS3* marker from plasmid pFA-HIS3MX6, with the long flanking homology PCR technique (22) and primers 5′-CTGATAAAACAAAAACAACAAACACAGCTAAATCTCAACAATGCGTACGCTGCAGGTCGAC-3′ and 5′-GATACCATACCTTATCGAGTTATTATGTATGTGTCGAAGCATCGATGAATTCGAGCTCG-3′. Correct open reading frame replacement was verified by PCR, using the following primer pairs: 5′-CTGACAAAGAAGCTGCCTC-3′; 5′-GCCCAGATGCGAAGTTAAG-3′ and 5′-GCCAGCCCTGGCTATTCTT-3′; 5′-CCGTGCGGCCATCAAAATG-3′.

Plasmids Used—The plasmids used were PJV89E (YEp352-CRH1) (16), and PJV40S (PCM190-CRH2) (16).

Synthesis of Sulforhodamine-labeled Oligosaccharides—Fluorescence-tagged oligosaccharides were obtained as described previously (23), by reacting lissamine rhodamine sulfonyl chlo-

TABLE 1
Strains used in this study

Strain	Genotype	Source
FY1679	*MAT***a**/α *ura3-52/ura3-52 his3Δ200/HIS3 leu2Δ1/LEU2 trp1Δ63/TRP1 GAL2/GAL2*	EUROSCARF
FY001	*MATα ura3-52 his3Δ200 leu2Δ1 trp1Δ63*	15
GRA001	*MATα ura3-52 his3Δ200 leu2Δ1 trp1Δ63 chs3::URA3*	15
RCA001	*MATα ura3-52 his3Δ200 leu2Δ1 crh1::KanMX4*	16
RCA002	*MATα ura3-52 his3Δ200 leu2Δ1 crh2::HIS3*	16
RCA003	*MATα ura3-52 his3Δ200 leu2Δ1 crh1::KanMX4 crh2::HIS3*	16
SECRH2	FY001 transformed with plasmid pJV40S (high copy *CRH2*)	16
EPICRH1	FY001 transformed with plasmid pJV89E (high copy *CRH1*)	16
BY4741	*MAT***a** *ura3Δ0 his3Δ1 leu2Δ0 met15Δ0*	EUROSCARF
Y00897	*MAT***a** *ura3Δ0 his3Δ1 leu2Δ0 met15Δ0 gas1::KanMX4*	EUROSCARF
GRO11	*MAT***a** *ura3Δ0 his3Δ1 leu2Δ0 met15Δ0 gas1::KanMX4 crh1::hphMX4 crh2::HIS3*	15
W303	*MAT***a** *ura3-1 ade2-1 leu2–3,112 his3-11,15 trp1-1*	A. Conzelmann
LC355	*MAT***a** *ura3-1 ade2-1 leu2–3,112 his3-11,15 trp1-1 exg1 exg2::ADE2 eng1::URA3 eng2::KanMX4 bgl2::TRP1*	F. del Rey and C. Vázquez de Aldana
NBT001	*MAT***a** *ura3-1 ade2-1 leu2–3,112 his3-11,15 trp1-1 exg1 esg2::ADE2 eng1::URA3 eng2::KanMX4 bgl2::TRP1 gas1::HIS3*	This work
X2180	*MAT***a**/*MATα SUC2+/SUC2+ mal/mal gal2/gal2 CUP1+/CUP1+*	Laboratory collection
YPH499	*MAT***a** *ura3-52 lys2-801 ade2-101 trp1-Δ63 his3-Δ200 leu2-Δ1*	20
ECY46-1-8D	*MAT***a** *ura3-52 lys2-801 ade2-101 trp1-Δ63 his3-Δ200 leu2-Δ1 chs1::HIS3*	21
YMS11	*MAT***a** *ura3-52 lys2-801 ade2-101 trp1-Δ63 his3-Δ200 leu2-Δ1 chs2::TRP1*	21
ECY46-41B	*MAT***a** *ura3-52 lys2-801 ade2-101 trp1-Δ63 his3-Δ200 leu2-Δ1 chs3::LEU2*	21
GRA001	*MATα ura3-52 his3Δ200 leu2Δ1 trp1Δ63 chs3::URA3*	15
GRA002	*MATα ura3-52 his3Δ200 leu2Δ1 trp1Δ63 crh1::KanMX4 crh2::HIS3 chs3::URA3*	15

ride (AnaSpec, San Jose, CA, or Invitrogen) with a mixture of reductively aminated β(1–3)- or β(1–6)-linked glucose oligosaccharides or with individual reductively aminated oligosaccharides. The oligosaccharide mixtures, containing chains of 2–8 glucoses in length, were obtained by partial hydrolysis, with 4 M trifluoroacetic acid at 100 °C, of laminarin (Sigma) for β(1–3)-linked oligosaccharides, or pustulan (EMD-Calbiochem) for β(1–6)-linked compounds, followed by fractionation on a Bio-Gel P-6 column. The single β(1–3)-linked oligosaccharides were obtained from Associates of Cape Cod, East Falmouth, MA. The concentration of SR[2]-oligosaccharides was determined from the absorbance at 570 nm.

Purification of Z-protease—Four ml of a 10 mg/ml solution of zymolyase 100T (Associates of Cape Cod) in 1 M Tris, pH 7.5, was applied to a Sephacryl S-200 column (1.6 × 90 cm), previously equilibrated with the same Tris buffer. Elution was also carried out with 1 M Tris buffer with the help of a peristaltic pump. Fractions of 5 ml were collected. β(1–3)Glucanase in the fractions was determined with reduced laminarin as substrate, from the liberation of reducing power as described by Park and Johnson (24). Protease activity was measured with Azocoll (EMD-Calbiochem) as substrate. The reaction mixture contained, in a total volume of 300 μl, 6.25 mg of Azocoll and 50 μl of the column eluate. After 1 h of incubation at 37 °C, 0.35 ml of cold water was added, and tubes were centrifuged in the cold for 5 min at 18,500 × *g*. A_{520} was measured in the supernatant. An A_{520} of 1.0, as measured under those conditions, is taken as 1 unit of protease activity. β(1–3)Glucanase emerged from the column before protease, but the two activities partially overlapped. Fractions with protease activity but little glucanase contamination (in one batch, fractions 32–37) were pooled and concentrated to ~4 ml in an Amicon cell equipped with a YM-10 filter. The concentrate was applied to the same Sephacryl S-200 column, and the fractionation was repeated. The pooled fractions were concentrated to a final volume of 0.8 ml by ultrafiltration. The yield of protease activity varied between 20 and 40% in different batches. The purified protein still had some β(1–3)glucanase activity, but the ratio protease/glucanase increased between 60- and 120-fold with the purification.

Uptake of Fluorescent Oligosaccharides by Living Yeast Cells—To 0.5 ml of culture in a vial, 30 μl of either a 200 μM SR-oligosaccharide mixture or a 200 μM individual SR-oligosaccharide was added. Ampicillin was also added to the culture to a final concentration of 75 μg/ml. The cell concentration was such that the culture would be in early stationary phase after overnight incubation at 30 °C. Growth, from the A_{660}, was monitored in a parallel larger culture. After overnight growth, the cultures were transferred to Eppendorf tubes, which were centrifuged for 3 min at 6000 × *g*. Cells were washed three times with 1 ml of 20% ethanol and once with 0.5 ml of water, followed by suspension in 0.3–0.5 ml of water for fluorescence observation in the microscope.

For chitinase treatment, 150 μl of the *gas1*Δ (strain Y00897) fluorescent cells were incubated with 1.4 unit of Z-protease in Tris, pH 7.5, at a final 0.05 M concentration for 1 h at 37 °C. Tubes were centrifuged for 3 min at 16,000 × *g*. The cells were washed with 0.4 ml of 0.05 M MES, pH 6, and suspended in 0.2 ml of the same buffer. Purified *Serratia marcescens* chitinase (25) (20 milliunits) and 2 μl of 2% sodium azide were added, and the tubes were rotated overnight at 37 °C in the dark. Incubated cells were observed in the fluorescence microscope.

Digitonin-permeabilized Cells—Cells were permeabilized with digitonin as described previously (26). All cells were permeabilized, as verified by staining with methylene blue. The cells were suspended in twice as many milliliters of 25 mM MES, pH 6,3, as grams (wet weight) of cells used. A typical incubation mixture with SR-oligosaccharides contained 10 μl of cell suspension, 0.05 M MES, pH 6.3, 4 mM magnesium acetate, 2 mM UDP-GlcNAc, 32 mM *N*-acetylglucosamine, 0.1% digitonin, and 20 μM SR-oligosaccharides, in a total volume of 50 μl. Incubation was on an Eppendorf shaker at 37 °C, usually for 1–3 h. If

[2] The abbreviations used are: SR, sulforhodamine; MES, 2-(*N*-morpholino)-ethanesulfonate.

the incubation time was more than 1 h, a new addition of UDP-GlcNAc was made every hour. After incubation, 1 ml of cold 25 mM MES, pH 6.3, was added to each tube. Tubes were centrifuged 5 min in the cold at 18,500 × *g*. Cells were washed twice with 1 ml of 20% ethanol and once with 0.5 ml of 0.05 M Tris, pH 7.5 (centrifugations for 5 min at 16,000 × *g*). They were suspended in 0.5 ml of the Tris buffer, followed by addition of 1.3 units of Z-protease, and incubated on a rotator at 37 °C for 1 h. After centrifugation for 5 min at 16,000 × *g*, the cells were washed once with 0.5 ml of 25 mM MES, pH 6.3, and suspended in 0.5 ml of 1% SDS. The tubes were rotated overnight in the dark at room temperature, followed by centrifugation as above. The cells were washed once with 0.5 ml of the MES buffer and suspended in 0.3 ml of the same buffer for observation in the fluorescence microscope.

For the time course experiments of Fig. 8, a 10-fold scaled-up mixture was used in 15-ml Corex tubes, with SR-hexasaccharide as substrate. After incubation at 37 °C with shaking for different times, 5 ml of cold 25 mM MES buffer, pH 6.3, were added and the tubes were centrifuged for 5 min at 15,000 × *g* in a swinging bucket rotor. Cells were washed twice with 5 ml of 20% ethanol and once with 2.5 ml of 50 mM Tris, pH 7.5, then suspended in 1 ml of the Tris buffer, and transferred to Eppendorf tubes. To each tube, 2.7 units of Z-protease were added, and tubes were rotated at 37 °C for 1 h, followed by centrifugation for 5 min at 16,000 × *g*. After two washings with 1 ml of 25 mM MES, pH 6.3, and suspension of the cells in 1 ml of 1% SDS, the tubes were incubated overnight in the dark on a rotator at room temperature. After incubation, tubes were centrifuged 5 min at 16,000 × *g*. Cells were washed with 1 ml of 0.05 M MES, pH 6, and suspended in 1 ml of the same buffer. A 10-μl sample was used for inspection and imaging in the fluorescence microscope. Of the suspension, 50 μl were set apart as controls, and to the remainder 50 μl (90 milliunits) of *S. marcescens* chitinase were added. Both the controls and the mixtures with chitinase were incubated overnight in the dark on a rotator at 30 °C. The tubes were centrifuged 5 min at 16,000 × *g*, and fluorescence was measured in the supernatants with a PTI Quantamaster spectrofluorimeter. The excitation wavelength was 566 nm, and the emission spectrum was acquired between 580 and 680 nm.

Cell Walls—For preparation of cell walls, 0.6 g (wet weight) of cells, or permeabilized cells from 0.6 g of intact cells, were suspended in 1.2 ml of 25 mM MES, pH 6.3. Of this suspension, 1.2 ml was transferred to a 15-ml Corex tube, followed by 4 g of glass beads (0.5 mm diameter). The tube was vortexed for 6 periods of 1 min, with 1 min cooling in ice in-between. The extract was withdrawn with a Pasteur pipette, and the beads were washed with six 0.5-ml portions of the MES buffer. The combined fractions were centrifuged 10 min at 3800 × *g* to sediment the cell walls, followed by one washing with 5 ml of the MES buffer and suspension in the same buffer to a final volume of 0.8 ml.

Incubation mixtures included 10 μl of cell wall suspension, 50 mM succinate, pH 5.5, and 20 μM SR-oligosaccharide, in a total volume of 50 μl. Incubation was on an Eppendorf shaker at 37 °C. After incubation, 1 ml of cold 25 mM MES, pH 6.3, was added, and the tubes were centrifuged 10 min in the cold at 18,500 × *g*. Cell walls were washed once with 1 ml of 1% SDS and once with 1 ml of the MES buffer, followed by suspension in 0.3 ml of the same buffer for observation in the fluorescence microscope.

For the time course experiments of Fig. 10, a 10-fold scaled-up mixture was used. The treatment was the same as for the time course of permeabilized cells, except that after the first incubation and centrifugation, the cell walls were washed twice with 5 ml of 50 mM Tris, pH 7.5, rather than with 20% ethanol followed by Tris. Also, in the Z-protease incubation, the amount of Z-protease added to each tube was 6.6 units.

Flow Cytometry—Sulforhodamine fluorescence was detected using a FACSVantage SE (BD Biosciences) with DIVA option. Lasers utilized were a Coherent Innova 90 at 488 nm, and a coherent model 599 dye laser pumped with an Innova 70 argon laser and generating 200 milliwatts at 575 nm. Sulforhodamine fluorescence was detected in the FL5 channel using a 730LP dichroic mirror and 600LP filter. Light scattering was also measured in parallel.

Paper Chromatography of SR-oligosaccharides—SR-oligosaccharides were separated by ascending paper chromatography on silica-impregnated Whatman paper SG81 with butanol-1/ethanol/water (5:3:2) as solvent (27). The paper chromatogram was examined and photographed with a UV illuminator.

Chitooligosaccharide Inhibition—For the determination of the effect of oligosaccharides on incorporation of fluorescence by cell walls, each reaction mixture contained cell walls from 12 to 15 mg of yeast (wet weight), 50 mM succinate buffer, pH 4.5, and various concentrations of chitooligosaccharides in a total volume of 30 μl. Incubation was at 37 °C for various times. The reaction was stopped by addition of 10 μl of 40% formic acid, and 10-μl aliquots were spotted in triplicate onto a Whatman 3MM paper template, corresponding in shape and size to a 96-well microtitration plate. The positions for spotting the samples corresponded exactly to the positions of wells on the plate. The paper was dried at 50 °C and washed for several hours against 3–4 changes of 66% ethanol containing 5% formic acid. The washing removed unreacted label, whereas the cell walls remained entrapped within the paper structure. The paper was dried, placed between two glass plates matching in size the microtiter plate, and the fluorescence at the individual positions was measured in a Synergy HT-1 (BioTek) microplate reader equipped with a fluorescent detector and appropriate filters, with excitation wavelength at 530 ± 25 nm and emission wavelength at 575 ± 15 nm.

Fluorescence Observation and Imaging—Samples were observed in the rhodamine channel of a Zeiss Axioskop microscope equipped for fluorescence. Images were captured with a Qimaging Retiga Exi SVGA digital camera and processed with iVision software (BioVision Technologies). Images to be compared were obtained with the same exposure and normalized with the same parameters.

For Calcofluor staining, cells were suspended in a 0.01% solution of Calcofluor White. After 5 min, they were observed in the UV channel (4′,6-diamidino-2-phenylindole channel) of the fluorescence microscope.

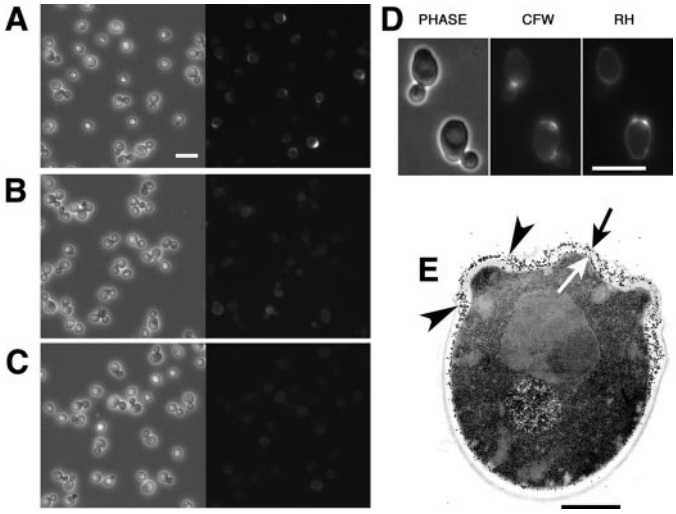

FIGURE 2. **Incorporation of fluorescent oligosaccharides in growing cells.** In this and similar figures, the *left panel* shows an image under phase, whereas the *right panel* shows the same image as seen in the rhodamine fluorescence channel. Images to be compared were obtained with the same exposure and normalization. Overnight incubation of an SR-oligosaccharide mixture with wild type (FY001) (*A*), a *chs3*Δ mutant (GRA001) (*B*), and a *crh1*Δ *crh2*Δ mutant (RCA003) (*C*). *D*, incubation of fluorescent oligosaccharides with a wild type diploid (FY1679), followed by staining with Calcofluor White (*CFW*). The cells were imaged through the UV channel (*CFW*) and the rhodamine channel (*RH*), as indicated. Here, cells were viewed at higher magnification, under oil immersion. *E*, electron micrograph of a wild type cell (×2180) stained with wheat germ agglutinin attached to gold particles (28) to reveal the localization of chitin. The cell shows several adjacent bud scars. *Arrowheads*, chitin from the ring formed at bud emergence. *Black arrow*, chitin from the primary septum. *White arrow*, a layer of chitin next to the plasma membrane. *Scale bars* in *A* and *D* represent 10 μm. *Scale bar* in *E* represents 1 μm.

RNA Isolation and Quantitative Reverse Transcription-PCR Assays—Total RNA was isolated and purified from strains YPH499 (wild type), ECY46-1-8D (*chs1*Δ), YMS11 (*chs2*Δ) and ECY46-41B (*chs3*Δ) as described (15). Quantification of mRNA levels for *CRH1* was carried out by quantitative reverse transcription-PCR as reported previously (15).

RESULTS

Fluorescent Oligosaccharides as in Vivo Transglycosylation Acceptors—As a first step toward an *in vitro* transglycosylation system, we investigated whether sulforhodamine-labeled oligosaccharides would function *in vivo* as artificial substrates for such a reaction. Compounds of this type have been used successfully to study transglycosylation in plant extracts (28). Because the cell wall is permeable to small molecules (29, 30), it was thought that the oligosaccharides (2–8 glucose units in length) would be able to penetrate the periplasmic space and interact with the nascent chitin chains through the agency of appropriate transglycosylases. In addition, the fluorescent label would pinpoint where the reaction took place. Indeed, when wild type cells were grown in the presence of a mixture of β(1–3)-linked glucose oligosaccharides, observation in the fluorescence microscope showed bright patches in many cells and a diffuse fluorescence in the cell perimeter (Fig. 2*A*). On the other hand, there was no labeling with β(1–6)-linked glucose oligosaccharides (results not shown). Cells lacking Chs3p, the chitin synthase required for synthesis of the chitin bound to both β(1–6)glucan and β(1–3)glucan (14), showed only a weak diffuse fluorescence but no bright patches (Fig. 2*B*). Finally, cells with deletions in both the *CRH1* and the *CRH2* genes were similar in aspect to the *chs3*Δ mutant (Fig. 2*C*). On the other hand, strains in which either one of the *CRH* genes was deleted showed a distribution of fluorescence akin to that of wild type (results not shown), whereas overexpression of either Crh1p or Crh2p resulted in some increase in fluorescence (supplemental Fig. S1). In the case of Crh1p, the fluorescence had a punctate appearance (supplemental Fig. S1). Because of the specific requirement of Crh1p and Crh2p for the linkage between chitin and β(1–6)glucan (15), these results suggested that the oligosaccharides were functioning as acceptors in place of the glucan. It may seem surprising that it was the β(1–3)-linked, rather than the β(1–6)oligosaccharides, that were active in the reaction. However, it should be kept in mind that in the cell wall, chitin is not connected directly to the main chain of β(1–6)glucan but to a glucose branch that is attached to the main chain by a β(1–3) linkage (5) (Fig. 1*A*). This is presumably the linkage that is specifically recognized by the transglycosylase.

By comparing phase and fluorescence images, it was observed that the buds were almost totally devoid of fluorescence (Fig. 2*A*), in agreement with the absence of chitin in their cell wall. In budded cells, the bright patches were close to the mother-daughter neck. Because in haploid cells each new budding occurs next to the previous one, bud scars remain close to the mother-daughter neck, which makes difficult to distinguish between the neck chitin ring and an adjacent bud scar. To clarify the precise location of the bright patches, we took advantage of the polar budding in diploids, which often results in bud scars at the opposite pole of the mother-daughter neck. A diploid (FY1679), isogenic with the haploid wild type previously used, was grown in the presence of fluorescent oligosaccharides. The cells were stained with Calcofluor White, which labels the chitin both in the neck ring and in bud scars, and were observed both in the UV (Calcofluor) and in the rhodamine channel (Fig. 2*D*). It could be seen that bud scars situated at the distal pole with respect to the bud showed both Calcofluor and rhodamine fluorescence (*lower cell* in Fig. 2*D*), whereas the mother-bud neck was only stained by Calcofluor (*both cells* in Fig. 2*D*). Statistical results confirmed the observations. Of 81 cells with bud scars but no bud, or with bud scars opposite to bud, 80 stained in both the Calcofluor and rhodamine channels and only one in the Calcofluor channel only. Of 122 cells with bud, but no scar adjacent to the bud, in 115 the mother bud neck was visible in the Calcofluor channel only and in 7 it could be seen in both channels. Thus, the bright patches observed after growth in the presence of SR-labeled oligosaccharides are bud scars. This explains why the patches are not observed in all cells, because only about half of the cells in a culture have bud scars.

The synthesis of chitin-oligosaccharide linkages in bud scars was unexpected. The bud scar contains both the chitin ring made at the mother-bud neck during bud emergence and the chitinous primary septum formed at cytokinesis (31). In a previous study we found that most of the cross-linked chitin in the just synthesized chitin ring is bound to β(1–3)glucan, whereas about one-third of the chitin is free (14). In the primary septum,

made at cytokinesis, almost all of the chitin is free (14). We reexamined the distribution of chitin in bud scars in EM sections stained with wheat germ agglutinin attached to gold particles from a previous study (31) and found that, in addition to the two localizations already mentioned, often a chitin layer could be seen along the plasma membrane at the bud scar (Fig. 2*E*). Thus, there are three possible sources of chitin for cross-linking to β(1–6)glucan during bud scar formation after cytokinesis as follows: the portion of the ring chitin that is still free, the chitin in the primary septum, and the newly formed chitin near the plasma membrane.

Whereas the requirement of the Crh proteins for the appearance of fluorescent patches was clear, the involvement of those proteins in the weaker fluorescence around the cell contour was more doubtful, because such fluorescence was also present to some extent in the *chs3*Δ and *crh1*Δ *crh2*Δ mutants. We hypothesized that part of this fluorescence might be due to the Gas1 protein, which catalyzes transglycosylation between β(1–3)glucan chains (32). Because β(1–3)glucan is dispersed all over the surface of the cell, an exchange between that polysaccharide and the β(1–3)-linked SR-oligosaccharides would result in widespread fluorescence over the cell wall. To test this supposition, we grew a *gas1*Δ mutant (strain Y00897) in the presence of SR-oligosaccharides. Surprisingly, these cells became much brighter than the corresponding wild type, BY4741 (Fig. 3, *A* and *B*). In some cells, the fluorescence was still in patches, and in others it invaded most of the cell. Furthermore, the cell contour was also bright. However, when both *CRH1* and *CRH2* were deleted in the *gas1*Δ mutant (strain GR011), all fluorescence, both in patches and in the cell cortex, disappeared (Fig. 3*C*). Expression of *CRH2* in a high copy plasmid restored the fluorescence of the triple mutant (results not shown). This result shows that both the fluorescence in bud scars and the contour require the Crh proteins. The enhanced fluorescence of the *gas1*Δ mutant may be accounted for by the overexpression of *CRH1* (33) coupled to the high chitin content (34) in that mutant.

The high fluorescence of the *gas1*Δ cells provided an opportunity to confirm that the oligosaccharides were bound to chitin. If this is the case, they should be solubilized when chitin is hydrolyzed by chitinase. Treatment of intact cells with chitinase led to only partial reduction of the fluorescence. In the assumption that the chitinase was not able to penetrate completely the cell wall, we treated the cells with a protease purified from zymolyase (Z-protease), which effectively removes the surface mannoproteins, thereby increasing the cell wall permeability (1). This treatment affected the contrast of the cells under phase but not their fluorescence (Fig. 3, *D* and *E*). However, the fluorescence was then readily removed by chitinase (Fig. 3*F*), as expected if the oligosaccharides were linked to chitin.

In all the experiments described so far, a mixture of SR-linked laminari-oligosaccharides of different lengths was used. To obtain some information about the specificity of the reaction, we synthesized individual oligosaccharides attached to sulforhodamine and tested them on wild type cells (supplemental Fig. S2). The intensity of the fluorescence clearly increased with the length of the oligosaccharide chain. Furthermore, the contribution of the cell cortex to the total fluorescence was higher in the longer oligosaccharides (supplemental Fig. S2). This effect may be partially due to a higher activity of Gas1p in catalyzing an exchange between the cell wall β(1–3)glucan and those oligosaccharides, because in the *gas1*Δ mutant, although the general level of fluorescence was higher, there was little increase in the cell cortex with the hexa- and heptasaccharide (results not shown).

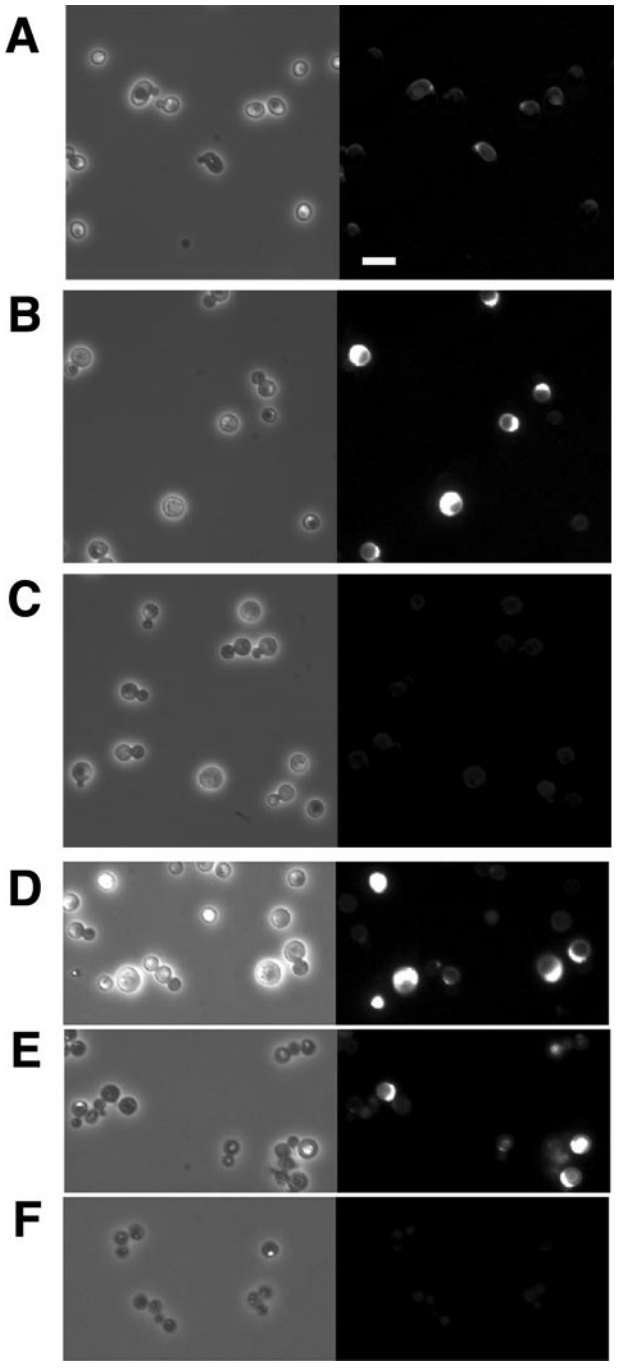

FIGURE 3. **Incorporation of fluorescence in a *gas1*Δ mutant.** *A*, cells of BY4741 (wild type isogenic with the *gas1*Δ mutant) grown in the presence of SR-oligosaccharides. *B*, same with the *gas1*Δ mutant (strain Y00897); *C*, with the *gas1*Δ *crh1*Δ *crh2*Δ triple mutant (strain GR011). *D* and *E*, cells of the *gas1*Δ mutant before and after treatment with Z-protease, respectively. *F*, the same cells, after subsequent incubation with chitinase. *Scale bar*, 10 μm.

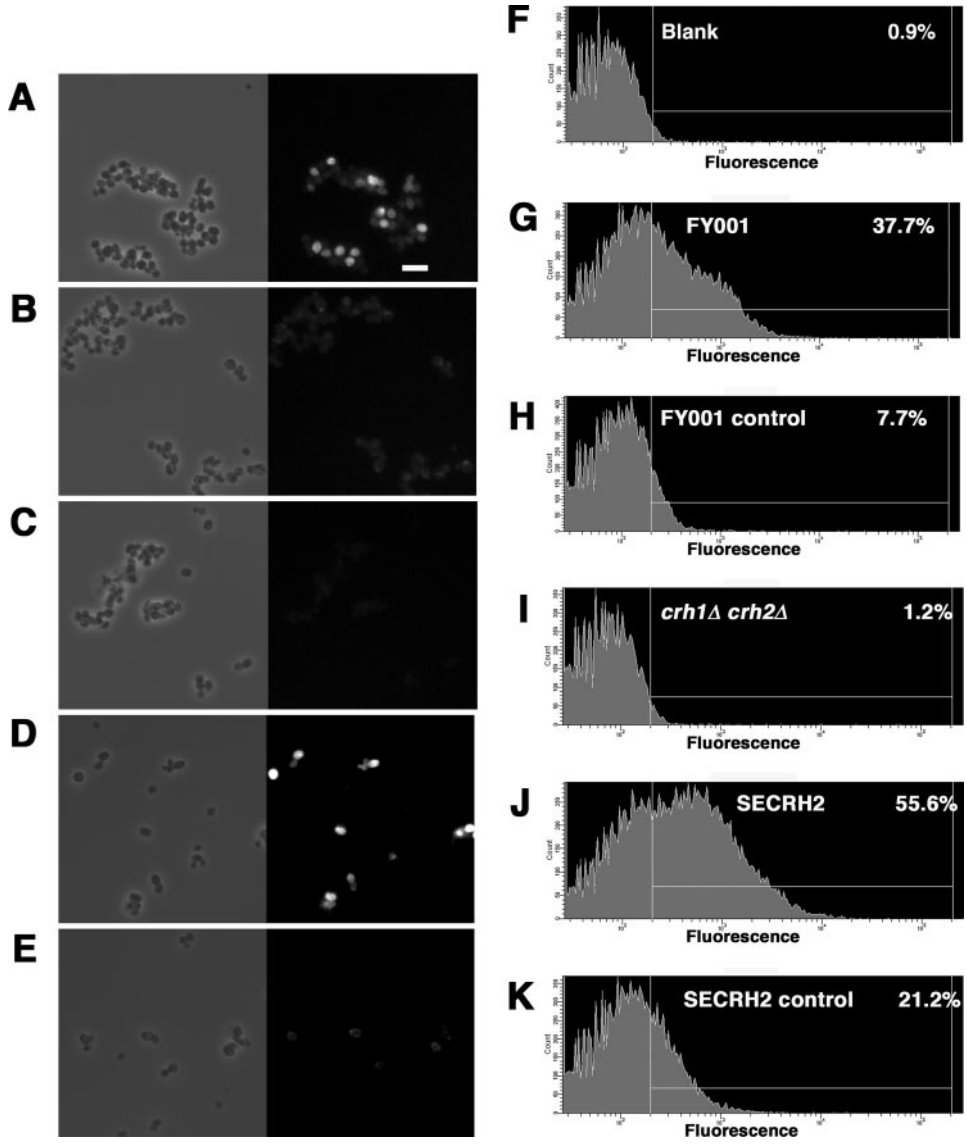

FIGURE 4. **Fluorescence of digitonin-permeabilized cells incubated with SR-oligosaccharides and UDP-GlcNAc.** The incubation time was 3 h at 37 °C. *A*, strain FY001 (wild type). *B*, same as *A* but without UDP-GlcNAc. *C*, strain RCA003 (*crh1*Δ *crh2*Δ). *D*, strain SECRH2 (FY001 transformed with a high copy *CRH2* plasmid). *E*, same as *D* but without UDP-GlcNAc. *F–K*, flow cytometry histograms of the cells shown on the *left column*. In each graph, the *vertical line* on the *left* represents the maximum value for the blank (*F*), which was obtained with cells never exposed to SR-sugars. The number on the *upper right* of each graph is the percentage of cells whose fluorescence exceeds that basal value. *Controls* are cells incubated without UDP-GlcNAc. *Scale bar*, 10 μm.

Permeabilized Cells as Containers for the Transglycosylase Reaction—The experiments with intact cells showed the feasibility of using SR-linked oligosaccharides as acceptors of chitin chains to mimic the *in vivo* transglycosylation. It also revealed the bud scars as sites of high transglycosylase activity. To move now toward an *in vitro* system, we made use of two of our previous observations. One is that when yeast cells are treated with digitonin and incubated briefly at 30 °C, the permeabilized (and inviable) cells acquire a very high chitin synthase activity (26), which can be measured by adding [^{14}C]UDP-GlcNAc to the cells and determining incorporation of radioactivity into insoluble material. Thus, under these conditions, it appears that one or more of the usually zymogenic chitin synthases are activated.

The second observation was that nascent chitin is a much better substrate for chitinases than preformed chitin (35, 36). Our interpretation of this result was that the chitinase could act on nascent chitin before the chains could become cross-linked by hydrogen bonds and thus more impervious to enzymatic attack (35). On the basis of those two previous results, we decided to incubate digitonin-treated cells with both UDP-GlcNAc and SR-linked oligosaccharides. The idea was that the sugar nucleotide in the presence of the activated synthase would give rise to nascent chitin. Because the treated cells would be permeable to the oligosaccharides, they would be present at sites where the chitin was synthesized and, if the transglycosylases were also at the same location, a transfer reaction could occur. In other words, each permeabilized cell would act as an individual test tube for the transglycosylase reaction.

Initial results showed highly fluorescent cells, with little difference between experimental mixtures and controls. It was realized that the SR-linked oligosaccharides that permeated the cells could bind unspecifically to proteins and other substances and that it would be necessary to eliminate as much extraneous material as possible. Of the various procedures attempted to this end, the one that worked best was to first treat the cells with Z-protease (as for intact cells to be treated with chitinase, see above), followed by overnight extraction with 1% SDS. The partially emptied cells lost contrast under phase and showed a tendency to aggregate (Fig. 4*A*). However, cells incubated with UDP-GlcNAc and an oligosaccharide mixture still retained significant fluorescence after that treatment (Fig. 4*A*). When the nucleotide was omitted from the reaction mixture, most of the fluorescence disappeared, showing that chitin formation was necessary for oligosaccharide retention (Fig. 4*B*). Even dimmer were *crh1*Δ *crh2*Δ cells, although incubated with the complete system (Fig. 4*C*). Furthermore, overexpression of Crh2p in a wild type strain led to a clear increase in fluorescence (Fig. 4*D*). Again, most of the fluorescence disappeared when the nucleotide-sugar was omitted (Fig. 4*E*). As with intact cells, those with a *gas1*Δ deletion were very bright (Fig. 5*C*; compare with the corresponding wild type in Fig. 5, *A* and *B*). Here,

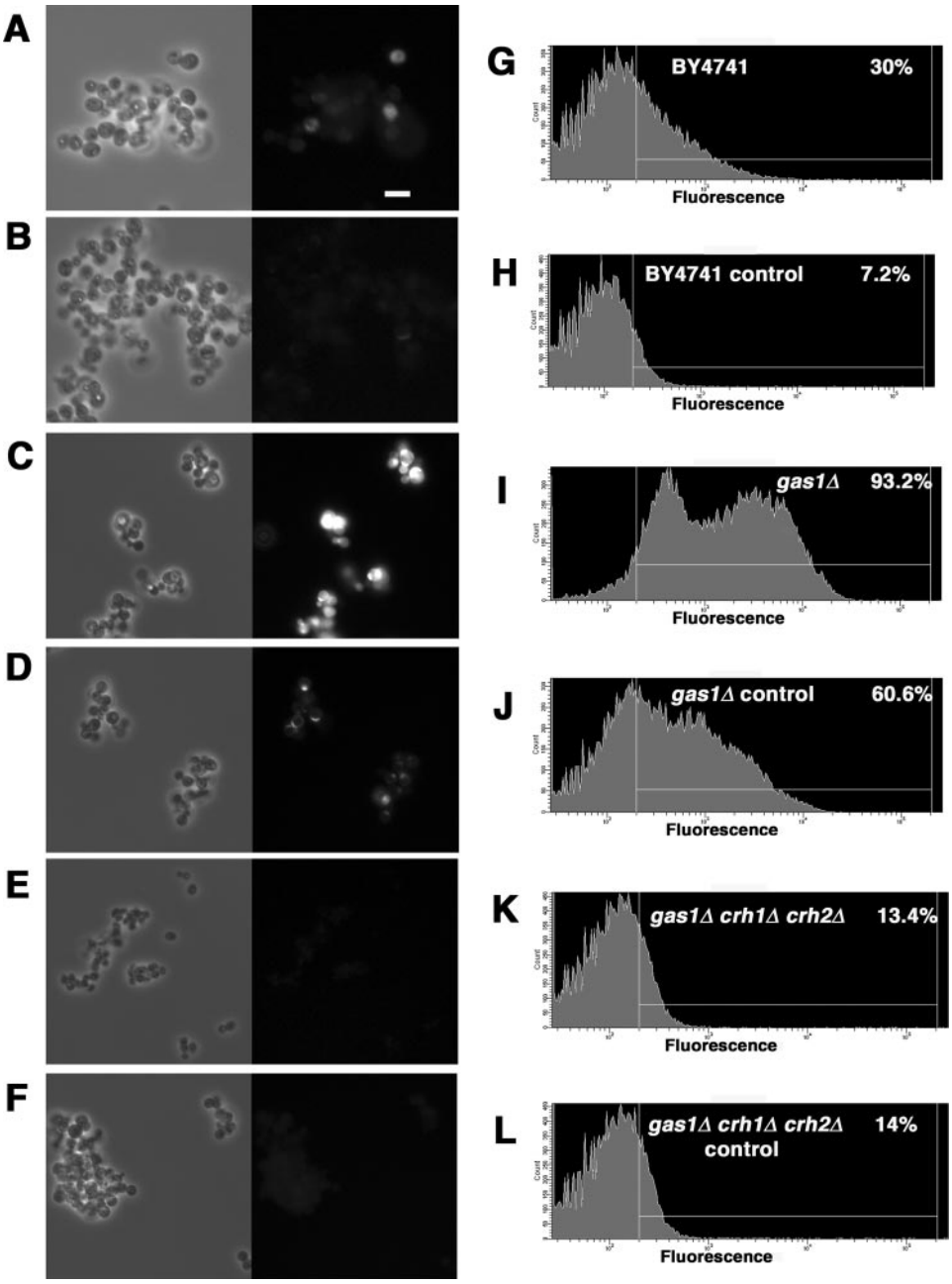

FIGURE 5. **Fluorescence of digitonin-permeabilized cells of *gas1*Δ mutants after incubation with SR-oligosaccharides and UDP-GlcNAc.** Incubation was for 3 h at 37 °C. *A*, strain BY4741 (wild type of *gas1*Δ). *B*, same as *A* but without UDP-GlcNAc. *C*, strain Y00897 (*gas1*Δ). *D*, same as *C* but without UDP-GlcNAc. *E*, strain GR011 (*gas1*Δ *crh1*Δ *crh2*Δ). *F*, same as *E* but without UDP-GlcNAc. *G–L*, similar design as in *G–K* of Fig. 4. *Scale bar*, 10 μm.

however, many bright patches persisted in the absence of UDP-GlcNAc (Fig. 5*D*), suggesting that at some locations (possibly bud scars) a limited reaction could occur with the utilization of preexisting chitin. On the other hand, deletion of *CRH1*and *CRH2* in a *gas1*Δ strain abolished the fluorescence almost completely (Fig. 5, *E* and *F*).

For a better comparison among strains, it was desirable to obtain quantitative results for these experiments. To this end, cells from the reaction mixture were subjected to flow cytometry, and the percentage of cells that exceeded the fluorescence of a blank was measured (Figs. 4 and 5). Thus, the value for one of the wild types used, FY001, was about 37% (Fig. 4*G*), whereas in the corresponding control without UDP-GlcNAc, only 7% of the cells exceeded the blank limit (Fig. 4*H*). The double mutant *crh1*Δ *crh2*Δ behaved as the blank (Fig. 4*I*), whereas the SECRH2 cells, overexpressing Crh2p, were substantially higher than wild type (Fig. 4*J*). Consistent with their bright fluorescence, almost all of the *gas1*Δ cells exceeded the blank range (Fig. 5*I*). In addition, in this case two peaks were observed, suggesting two populations with different levels of fluorescence.

The controls, incubated without sugar nucleotide, gave much lower but still significant values, indicating that some reaction took place in the absence of chitin synthesis (Fig. 4, *H* and *K*). The control value was much higher in the case of the *gas1*Δ control (Fig. 5*J*), in agreement with the presence of residual patches in the fluorescence picture (Fig. 5*D*).

The triple mutant *gas1*Δ *crh1*Δ *crh2*Δ graph shows some residual fluorescence, independent of the presence of nucleotide (Fig. 5, *K* and *L*). The source of this fluorescence is unknown.

When we found that digitonin-permeabilized cells showed high chitin synthase activity (26), it was not known that budding yeast contains three different chitin synthases (2). We used mutants in those chitin synthases, in addition to the corresponding wild type, to find out which enzyme(s) were responsible for the activity. Three of the four strain tested yielded high activity, whereas the *chs1*Δ mutant was totally inactive (Table 2). The conditions used, which were the same as for the incor-

TABLE 2

Chitin synthase activity in digitonin-permeabilized cells of different *chs* mutants

Activity was measured as described previously 23.

Strain	Activity[a]
YPH499 (WT)	2132
ECY46-1-8D (*chs1*Δ)	30
YMS11 (*chs2*Δ)	2311
ECY46-4-1B (*chs3*Δ)	4931
Control (blank)	38

[a] Counts/min incorporated in 30 min with [^{14}C]UDP-GlcNAc as substrate.

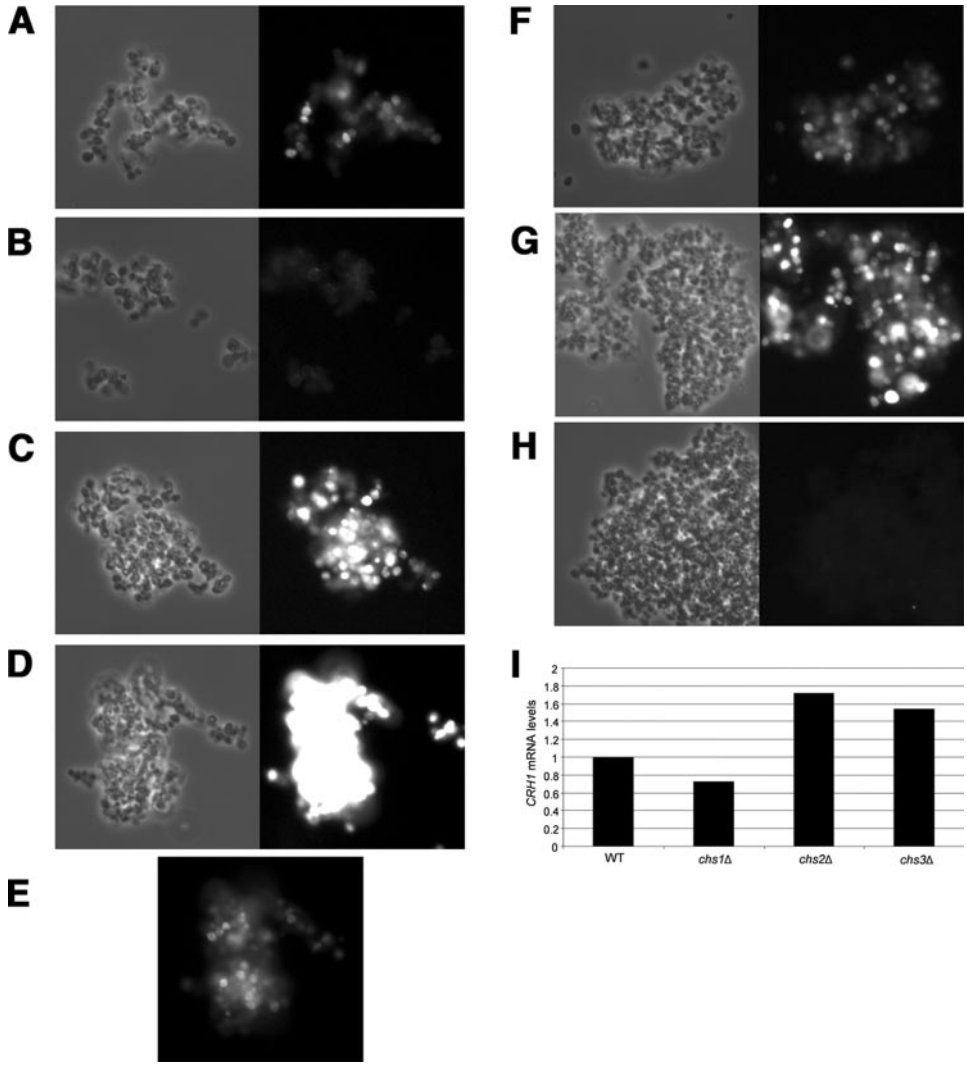

FIGURE 6. **Incorporation of fluorescence in permeabilized cells of chitin synthase mutants.** Incubation was for 3 h at 37 °C in the presence of the SR-oligosaccharide mixture. *A*, wild type (YPH499); *B*, *chs1*Δ strain (ECY-1-8D); *C*, *chs2*Δ strain (YMS11); *D*, *chs3*Δ strain (ECY46-4-1B); *E*, same as *D* but with a shorter exposure; *F*, wild type (FY001); *G*, *chs3*Δ (GRA001); *H*, *chs3*Δ *crh1*Δ *crh2*Δ (GRA002). *I*, *CRH1* mRNA levels in wild type (*WT*) and different *chs* mutants.

poration of SR-oligosaccharides, are optimal for Chs1p (37). When conditions for the measurement of Chs2p and Chs3p were tried, no activity was detected (results not shown). Accordingly, the *chs1*Δ mutant showed no incorporation of fluorescence (Fig. 6*B*). Surprisingly, the fluorescence of the *chs2*Δ strain and, even more, that of the *chs3*Δ strain, were much higher than that of wild type (Fig. 6, *C–E*). The high fluorescence of the *chs3*Δ mutant was totally eliminated by mutation of *CRH1* and *CRH2*, as expected (Fig. 6, *F–H*). For the *chs3*Δ strain, the increased fluorescence may be due in part to a greater Chs1 activity (Table 2) and in part to enhancement of *CRH1* expression (Fig. 6*I*). In the *chs2*Δ strain there was no increase in chitin synthase activity, but again an augmented expression of *CRH1* was detected. There was no increase in *CRH2* expression in any of the mutants (results not shown). These results clearly show that Chs1p and not Chs3p, the physiologically active enzyme *in vivo*, is operating in permeabilized cells.

Enhanced Fluorescence of Glucanase and chs3 Mutants Allows Quantitation of the Transglycosylase Reaction—During this study, it was found, by the use of paper chromatography, that both intact and permeabilized cells degraded the SR-oligosaccharides (see supplemental Fig. S3 for an example in which the hexasaccharide was used as substrate during cell growth). The degradation occurred both in the wild type strains used and in the corresponding mutants. Because this degradation might affect the results by depleting substrate, we looked for strains with mutations in β(1–3)glucanase genes. Among different mutants, kindly provided by F. del Rey and C. Vázquez de Aldana, we chose strain LC355, which is defective in five glucanases (Exg1p, Exg2p, Eng1p, Eng2p, and Bgl2p). Both intact and permeabilized cells of LC355 did not degrade the oligosaccharides, even after prolonged incubation (supplemental Fig. S3 and results not shown). Cells of this strain grew well, although giving rise to small clumps, because in the absence of Eng1p the cells show a separation defect (38). Despite the lack of oligosaccharide degradation, intact or permeabilized cells of LC355 were not more fluorescent than those of FY001 after incubation with SR-oligosaccharides (see Fig. 7, *top*, for permeabilized cells). Based on our previous observation that the percentage of chitin bound to β(1–6)glucan increases at higher temperature, we tested different strains, including LC355, for fluorescence incorporation during growth at 38 °C rather than 30 °C, and we found only marginal increases (results not shown). However, when LC355 cells were grown at 38 °C, followed by permeabilization and incubation with SR-oligosaccharides, a dramatic increase in fluorescence was observed (Fig. 7). Note that omission of UDP-GlcNAc in the reaction mixture leads to almost total disappearance of the fluorescence (Fig. 7), in sharp contrast with the behavior of *gas1*Δ cells (Fig. 5*D*). Part of the increased fluorescence of the LC355 cells grown at 38 °C is because of the genetic background, because cells of the corresponding wild type (W303) also showed a similar, although less marked, effect (results not shown). Another wild type strain (FY001) only presented a small increase with growth temperature (results not shown).

The high fluorescence of the 38 °C-grown LC355 permeabilized cells suggested the possibility of measuring the extent of

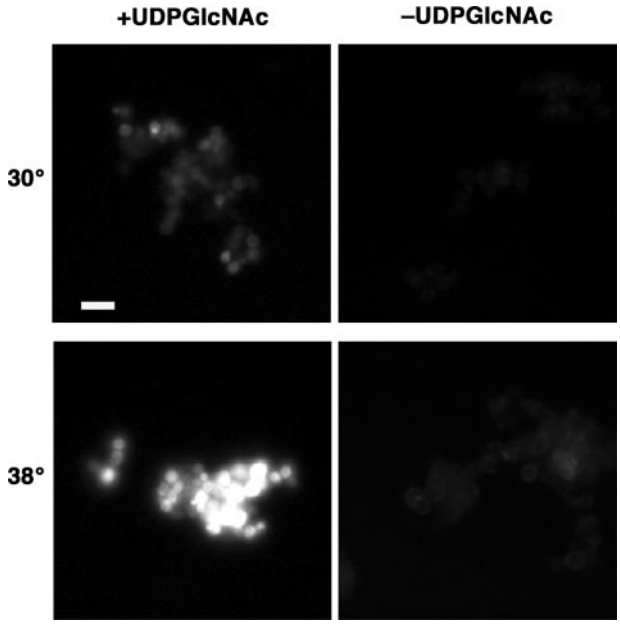

FIGURE 7. **Fluorescence of LC355 cells, permeabilized after growth at 30 or 38 °C and incubated with SR-oligosaccharides and UDP-GlcNAc.** Incubation was for 3 h at 37 °C. *Scale bar*, 10 μm.

the reaction as a function of time by fluorimetry. To this end, 10-fold scaled-up reaction mixtures were incubated for different times, followed by treatment with Z-protease and SDS, as outlined above. To enhance the fluorescence in this experiment, SR-hexasaccharide was used as substrate rather than an oligosaccharide mixture. The cells became brighter as the incubation time increased (Fig. 8, *left*). After chitinase treatment, almost all fluorescence disappeared, showing that in this case, as in intact cells, the oligosaccharides were bound to chitin (Fig. 8, *upper right*). The fluorescence of the chitinase digestion supernatants was measured in a spectrofluorimeter, yielding the curve of Fig. 8. It can be seen that the reaction proceeded linearly for the first 30 min and then became slower. However, the incorporation continued for at least 2 h.

Because of the high fluorescence of the *chs3*Δ mutant, the experiment was repeated with that strain. In this case, however, although the initial rate was similar to that of strain LC355, the time course of the incorporation flattened much earlier (results not shown). Part of this difference may be due to degradation of the substrate by the chitin synthase mutant (results not shown).

By the use of appropriate standards, it was possible to calculate the amount of SR-oligosaccharide incorporated. Surprisingly, this amounted to 19 pmol for the 2-h incubation mixture with LC355 cells, *i.e.* only 0.075% of the total amount of substrate added. The very small incorporation indicates that little substrate is required. This suggests that other factors, in addition to hydrolysis of the substrate, caused the flattening of the *chs3*Δ incorporation curve. In view of the small amount of substrate needed, it is understandable that in growth experiments the presence or absence of glucanases in the cells did not make much of a difference, because at the end of growth the ratio of cells to SR-oligosaccharides added initially was about 10 times lower than with permeabilized cells, and at early times much smaller.

Cell-free System: Incorporation of SR-oligosaccharide into Isolated Cell Walls—The results with the *gas1*Δ mutant permeabilized cells, where in the absence of UDP-GlcNAc fluorescent patches still arose (Fig. 5, *C* and *D*), suggested that in those cells two pathways for the formation of chitin-oligosaccharide complexes were functioning. One, giving rise mostly to peripheral fluorescence, utilized the nascent chitin formed during incubation. The other, possibly in bud scars, would take advantage of preformed chitin. We wondered whether this latter mechanism would still be functional in isolated cell walls. This was indeed the case. Incubation of cell walls, prepared either from intact or permeabilized cells of the *gas1*Δ strain, with SR-hexasaccharide but in absence of UDP-GlcNAc resulted in the appearance of bright patches on the cell walls (Fig. 9). In many cases, the patches could be identified as chains of bud scars (Fig. 9). In contrast, cell walls of the *gas1*Δ *crh1*Δ *crh2*Δ strain were uniformly dim (Fig. 9). On the other hand, incubation of cell wall supernatants, which included particulate material and soluble proteins, in the presence or absence of nucleotide-sugar, gave rise to little or no fluorescence, despite the presence of considerable chitin synthase activity in this fraction (results not shown).

To compare the cell wall results with those obtained with permeabilized cells, the time course of the reaction was determined in an experiment similar to that of Fig. 8. Here too, the fluorescence intensity of the patches increased with time and was totally abolished by chitinase treatment, again indicating that the oligosaccharide became linked to chitin (Fig. 10). The time course of incorporation, as determined by fluorimetry (Fig. 10*A*, *solid circles*), was not very different from that observed in permeabilized cells, except that it flattened out somewhat earlier.

Like intact and permeabilized cells, the *gas1*Δ cell walls degraded the oligosaccharide substrate (results not shown). To verify whether this degradation had an effect on the course of the reaction, we deleted *GAS1* in the multiple glucanase mutant LC355 and repeated the experiments with cell walls of the resulting strain NBT001. Whereas the cell walls of LC355 showed only a few fluorescent spots, those of NBT001 acquired many bright patches (Fig. 9). Cell walls of either strain did not degrade the substrate (results not shown). However, the amount of fluorescent material incorporated and then released by chitinase for strain NBT001 was lower than in the case of strain Y00897 (Fig. 10*A*, *open circles*). This may have resulted from the different genetic background of LC355, which is the same as that of W303. Anyway, these data show that elimination of the glucanase activity does not result in a major change in the course of fluorescence incorporation.

An interesting corollary of the use of strain NBT001 came from the fact that its parent strain, W303, buds more or less randomly, because of a *bud4* defect (39). Correspondingly, in contrast with strain LC355, an even distribution of fluorescent rings can be observed on the cell walls of NBT001, confirming nicely the nature of the patches as bud scars (Fig. 9).

We also tested the effect of chitooligosaccharides on the cell wall reaction. Interestingly, these oligosaccharides were strong inhibitors of fluorescence incorporation, again implicating chitin as one of the substrates (Fig. 10*B*). We explored the pos-

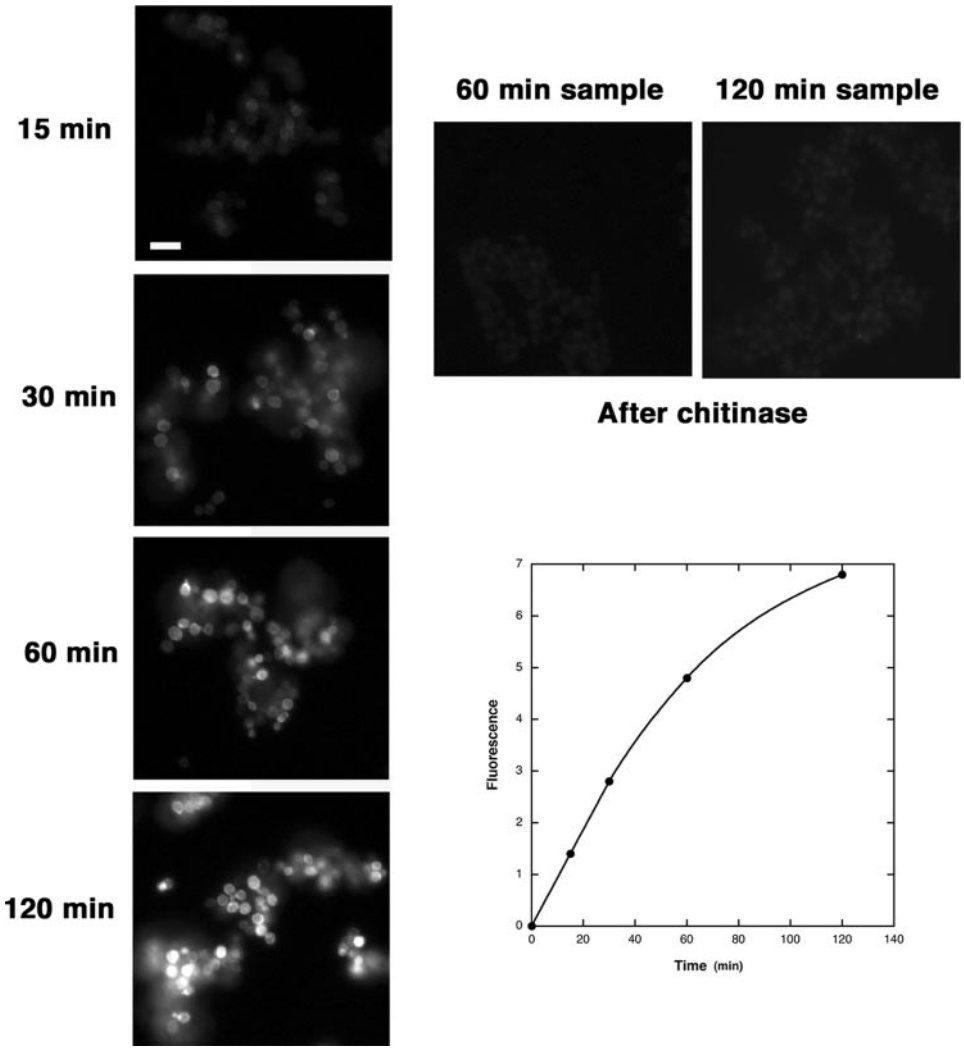

FIGURE 8. **Time course of incorporation of SR-hexasaccharide in LC355-permeabilized cells.** Cells were incubated and processed as outlined under "Experimental Procedures." *Left*, fluorescence of LC355 cells after different incubation times, as indicated. *Upper right*, fluorescence is almost completely eliminated by incubation of the permeabilized cells with chitinase. *Lower right*, quantitative determination of fluorescence in supernatants of chitinase digestion. Fluorescence is expressed in arbitrary units. *Scale bar*, 10 μm.

sibility that the chitooligosaccharides might function as donors in this reaction, by subjecting reaction mixtures with the SR-heptasaccharide to thin layer chromatography and looking for fluorescent products of higher molecular weight. However, no such products were found (results not shown), suggesting that the oligosaccharides are too short to act as donors.

DISCUSSION

Faced with the impossibility of using chitin as a substrate, because of its insolubility, we initially left to the cell the task of providing the polysaccharide and supplied instead a possible artificial acceptor, in the form of SR-linked oligosaccharides. The fluorescence of these compounds was essential, not only to detect the products but also their localization. Thus, cells growing in the presence of the oligosaccharides accumulated fluorescence in the bud scars and, to a lesser extent, at the cell cortex (Figs. 2 and 3). The latter localization was expected (14), but the high fluorescence at the bud scars was a surprise. In a previous study of chitin cross-links at different locations in the cell, we found that chitin at the neck ring was preponderantly linked to β(1–3)glucan, whereas that in lateral walls was mostly bound to β(1–6)glucan, and in the primary septum the chitin was free (14). The setup in those experiments did not include the bud scar, and we do not know of a way to find out what cross-links are made at the time of bud scar maturation. However, there is plenty of chitin in the bud scar, such as the chitin formerly at the neck ring, part of which was free at the time of ring formation, and the chitin we detected along the plasma membrane (Fig. 2*E*). Moreover, both Crh1p and Crh2p were previously detected at the bud scar, in addition to the cell cortex (15, 16). What the function could be of an enhanced cross-linking of chitin to β(1–6)glucan in the bud scar, is an open question. Because mannoproteins are attached to β(1–6)glucan (5), the chitin linkage may help to tether some protein to the bud scar.

We have previously shown that the deletion of *CRH1* and *CRH2* abolishes *in vivo* the binding of chitin to β(1–6)glucan, but it does not affect the chitin-β(1–3)glucan linkage. Thus, the Crh1p-Crh2p requirement for fluorescence incorporation *in vivo* and the solubilization of the fluorescent material by chitinase supported the view that the oligosaccharides were acting as β(1–6)glucan substitutes for a linkage to chitin and encouraged us to proceed to the next step. This was the use of digitonin-permeabilized cells as sources of chitin and enzymes, with again oligosaccharides as acceptors. Here, however, the system was much simplified, because the direct precursor of chitin, UDP-*N*-acetylglucosamine, was supplied externally and in its absence the extent of the reaction was dramatically decreased (Fig. 4, *G*, *H*, *J*, and *K*, and Fig. 5, *G* and *H*). It is interesting that the chitin synthase involved in the formation of polysaccharide here is Chs1p, not Chs3p, the physiological enzyme *in vivo* (Fig. 2*B*) (see also Ref. 14). This shows that we have set up here a truly artificial system. Because Chs1p is the enzyme accounting for most of the measurable chitin synthase activity (21), we believe that our old experiments on localization of the activity mainly dealt with this protein. We conclude that Chs1p is mostly attached to the plasma membrane, where it can catalyze a vectorial synthesis and extrusion of chitin through the membrane (8). Presumably, this is what occurs in permeabilized cells. To grab these nascent chitin chains and transfer them to β(1–6)glucan or oligosaccharides,

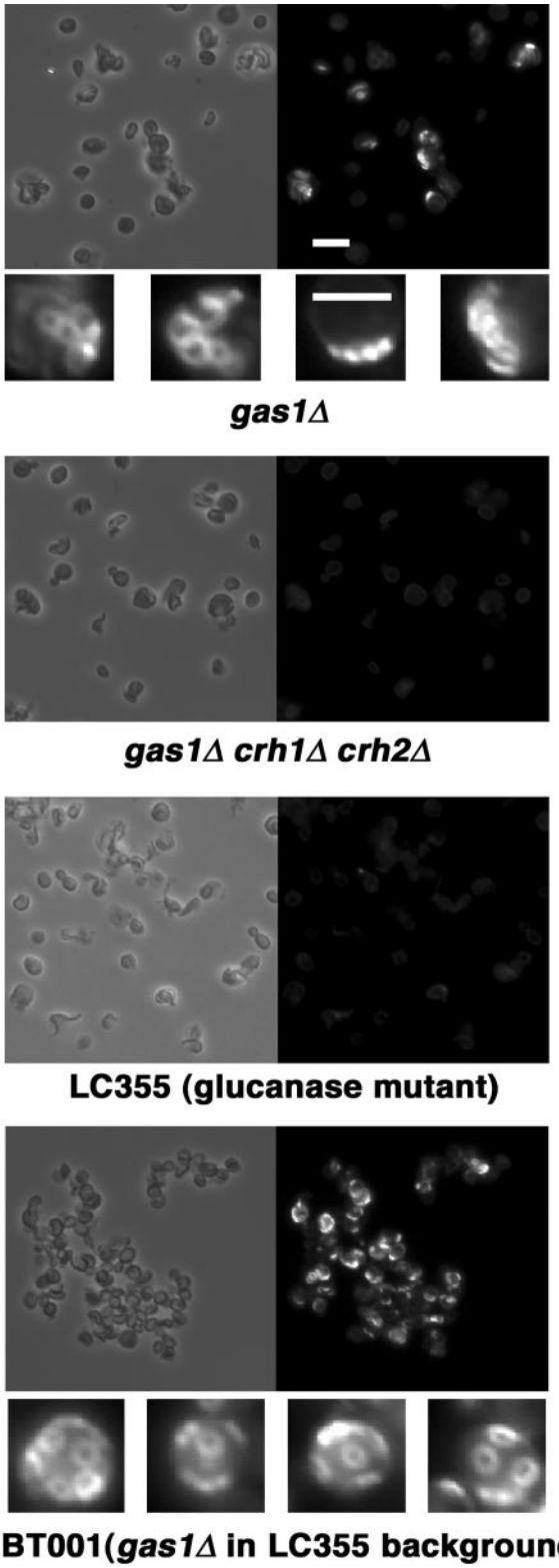

FIGURE 9. **Fluorescence microscopy of cell wall preparations from different strains after 1 h of incubation at 37 °C with SR-hexasaccharide.** LC355 is the strain with mutations in five β(1–3)glucanases; *gas1*Δ and *gas1*Δ *crh1*Δ *crh2*Δ are strains Y00897 and GR011, respectively, both in a BY4741 background, whereas NBT001 is similar to LC355 but with a *gas1* deletion (see Table 1). Cell walls were treated for fluorescence microscopy as described under "Experimental Procedures." The LC355 cells were grown at 38 °C, and those of the other strains were grown at 30 °C. The *four small panels below* the *gas1*Δ *picture* and *below* the *NBT001 picture* are magnified images of bright patches showing bud scar fluorescence. *Scale bar in upper panel*, 10 μm. *Scale bar in small panel*, 5 μm.

the Crh proteins must be placed nearby, either at the plasma membrane or at the cell wall. Although they have been detected only at the latter location (40), they must be attached to the plasma membrane through their glycosylphosphatidylinositol anchor at least transiently, before they are transferred to the wall. Thus, in permeabilized cells they may act at either location. All of this suggests that the local situation may be similar to that occurring *in vivo*, despite the use of a different chitin synthase. The free diffusion of the oligosaccharides, coupled to the even distribution of Chs1p on the membrane, explains the fairly uniform dispersion of fluorescence in the permeabilized cells. As in intact cells, here too the incorporation of fluorescence depends on the Crh proteins.

A very high incorporation of fluorescence was found in permeabilized cells of strain LC355, when they were previously grown at 38 °C. This high activity is probably because of several factors. One is that LC355 lacks several β(1–3)glucanases and does not degrade the oligosaccharides used as substrate. Second, at higher temperature the expression of Crh1p increases (15); the distribution of both Crh proteins becomes more diffuse (15); and *in vivo*, the proportion of chitin linked to β(1–6)glucan is higher (15). The migration of the Crh proteins from the bud scar to the cortex at 38 °C (15) may explain why little or no fluorescence was detected at the bud scar in the absence of UDP-GlcNAc (Fig. 7). Third, the effect of temperature seems to be higher in the genetic background of LC355, because the parent strain, W303, shows a similar, if somewhat less pronounced, behavior. The high fluorescence of the LC355 cells allowed us to follow quantitatively the course of the reaction, verifying at the same time that in this case too the fluorescent material was attached to chitin (Fig. 8). These results brought home the rather surprising result that less than 1% of the oligosaccharide was used in the reaction, showing that detection had been possible only thanks to the great sensitivity of the fluorescent label. The permeabilized cells of a *gas1*Δ mutant differed from those of wild type strains in that even in the absence of UDP-GlcNAc fluorescent patches could be seen (Fig. 5, *C*, *D*, *I*, and *J*). Thus, it seemed that two processes were taking place here, one which used the nascent chitin formed inside the cell and another that was able to utilize preexisting chitin, possibly in bud scars. In the hope that this second reaction might still function in a cell-free system, we disrupted either the permeabilized cells or intact cells and isolated cell walls. In both cases, the cell walls, when incubated with an SR-oligosaccharide, acquired fluorescence in patches, which could be seen in many cases to correspond to bud scars (Fig. 9). That endogenous chitin is a participant in this reaction is borne out by the solubilization of the fluorescent material by chitinase as well as by the inhibition of fluorescence incorporation by chitooligosaccharides (Fig. 10). Finally, also in the cell wall system the Crh proteins were required (Fig. 9). It is not clear why in a preparation of cell walls from a *gas1*Δ mutant endogenous chitin of bud scars can be transferred to oligosaccharides, whereas with the corresponding wild type this reaction cannot be detected. Perhaps this result is related to the much higher chitin content of the mutant cell wall (34) and/or to the greater length of the chitin chains (15). Both reactions, the one occurring at bud

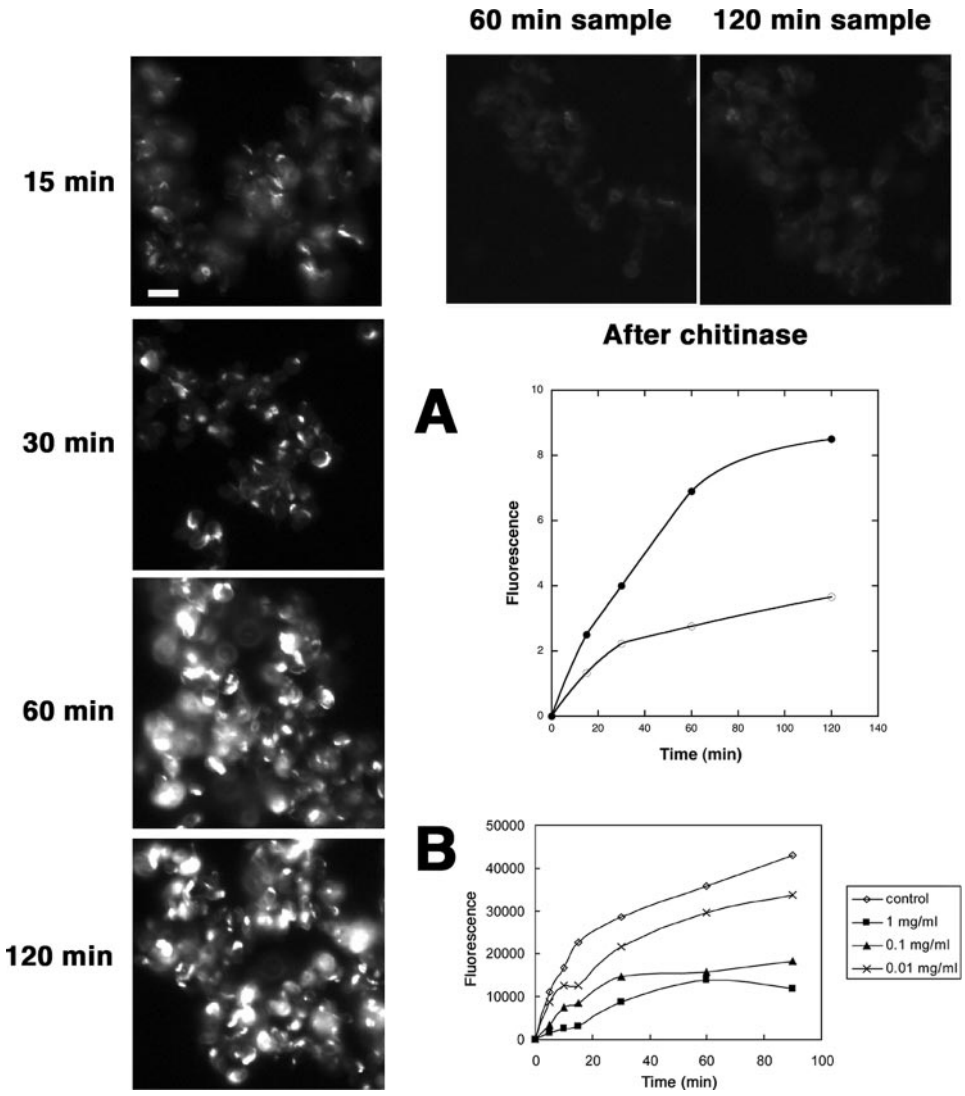

FIGURE 10. **Time course of fluorescence incorporation upon incubation of *gas1*Δ cell walls with SR-hexasaccharide.** *Left*, fluorescence of cell walls after different incubation times. Incubated cell walls were treated as outlined under "Experimental Procedures," before incubation with chitinase (*upper right*). *A*, fluorimetry of the chitinase supernatants from the cells shown *at left* (●) and from NBT001 cells in a similar experiment (○). *B*, effect of chitooligosaccharides on fluorescence incorporation in cell walls. See "Experimental Procedures" for the different technique used to measure fluorescence incorporation in this case. *A* and *B*, different arbitrary units were used. *Scale bar*, 10 μm.

scars with endogenous chitin and that taking place at the cell cortex with nascent chitin, depend on *CRH1* and *CRH2*, because their deletion abolished the fluorescence in both cases.

Unless there are still fragments of membrane attached to the bud scar region of the cell wall, the results suggest that the transglycosylases acting here are attached to the cell wall, as previously reported (40). Therefore, we have here an *in vitro* system, consisting of components exterior to the plasma membrane, that can generate new chitin-glucan links. The inability of a cell wall-free fraction to generate fluorescence, despite the presence of chitin synthase activity, suggests that the structural organization of the system components must be maintained for the production of the peripheral fluorescence observed in intact permeabilized cells. If here too the Crh proteins are linked to the cell wall, a close juxtaposition of membrane and wall may be required.

All these results, together with those of a previous study (15), support the notion that the Crh proteins act as transglycosylases, transferring chitin chains to an acceptor, either oligosaccharides or, physiologically, β(1–6)glucan. Despite all the progress made, we were unable to achieve a simple system in which the reaction could be shown with a purified protein and appropriate substrates. In an attempt to attain that goal, we expressed Crh2p in *Pichia pastoris* and isolated the recombinant protein (results not shown). To obtain a water-soluble protein, the engineered Crh2p lacked the last 29 amino acids at the carboxyl terminus, where the glycosylphosphatidylinositol anchor is attached, whereas six histidine residues were attached to the same end to facilitate purification. Although the isolation of the protein was successful, we were unable to demonstrate any catalytic activity in many different systems. Either nascent chitin, synthesized *in situ* with a soluble chitin synthase preparation, or soluble derivatives of chitin, such as carboxymethylchitin or glycolchitin, were used as potential donors and oligosaccharides or β(1–6)glucans were the acceptors. Either radioactivity or fluorescence was employed to tag the substrates, but no reaction could be detected. Also, no chitinase activity of the recombinant protein was found, as measured by viscosimetry with carboxymethylchitin as substrate. The lack of activity of the recombinant Crh2p in these reconstructed systems might be explained by the need of some other proteins for the reaction to proceed; however, the recombinant Crh2p was also unable to rescue a cell wall preparation from the *gas1*Δ *crh1*Δ *crh2*Δ mutant, which should contain any such protein(s). Thus, it seems that either the missing amino acids were needed for activity or that the protein must be tethered to a solid support, as it is *in vivo*, to function. Still, we cannot exclude that some other protein is required, in addition to Crh1p and Crh2p, for the transglycosylation, although at least Crh2p seems to be equipped completely for the reaction, with both a chitin-binding domain and a catalytic site. Many of the events that occur in the periplasmic space remain unexplained, but it is now clear that transglycosylation is at least one of the mechanisms by which cell wall assembly takes place. Transglycosylation has been known for many years, but we believe this

is the first time that it has been shown to play an essential role in the linkage of two different polysaccharides to each other.

Acknowledgments—We are greatly indebted to T. Moyer and D. Stephany for flow cytometry of permeabilized cells, to B. Bowers for an electron micrograph, and to C. R. Vázquez de Aldana and F. del Rey for strains. We thank J. Hanover for a critical reading of the manuscript and N. Dwyer and W. Coleman for useful discussions.

REFERENCES

1. Zlotnik, H., Fernández, M. P., Bowers, B., and Cabib, E. (1984) *J. Bacteriol.* **159,** 1018–1026
2. Cabib, E., Roh, D.-H., Schmidt, M., Crotti, L. B., and Varma, A. (2001) *J. Biol. Chem.* **276,** 19679–19682
3. Wiederhold, N. P., and Lewis, R. E. (2003) *Exp. Opin. Investig. Drugs* **12,** 1313–1333
4. Kollár, R., Petráková, E., Ashwell, G., Robbins, P. W., and Cabib, E. (1995) *J. Biol. Chem.* **270,** 1170–1178
5. Kollár, R., Reinhold, B. B., Petráková, E., Yeh, H. J. C., Ashwell, G., Drgonová, J., Kapteyn, J. C., Klis, F. M., and Cabib, E. (1997) *J. Biol. Chem.* **272,** 17762–17775
6. Kapteyn, J. C., Montijn, R. C., Vink, E., de la Cruz, J., Llobell, A., Shimoi, H., Lipke, P., and Klis, F. M. (1996) *Glycobiology* **6,** 337–345
7. Lesage, G., and Bussey, H. (2006) *Microbiol. Mol. Biol. Rev.* **70,** 317–343
8. Cabib, E., Bowers, B., and Roberts, R. L. (1983) *Proc. Natl. Acad. Sci. U. S. A.* **80,** 3318–3321
9. Shematek, E. M., Braatz, J. A., and Cabib, E. (1980) *J. Biol. Chem.* **255,** 888–894
10. Montijn, R. C., Vink, E., Müller, W. H., Verkleij, A. J., van den Ende, H., Henrissat, B., and Klis, F. M. (1999) *J. Bacteriol.* **181,** 7414–7420
11. Scheffers, D.-J., and Pinho, M. G. (2005) *Microbiol. Mol. Biol. Rev.* **69,** 585–607
12. Deits, T., Farrance, M., Kay, E. S., Medill, L., Turner, E. E., Weidman, P. J., and Shapiro, B. M. (1984) *J. Biol. Chem.* **259,** 13525–13533
13. Cabib, E., Bowers, B., Sburlati, A., and Silverman, S. J. (1988) *Microbiol. Sci.* **5,** 370–375
14. Cabib, E., and Durán, A. (2005) *J. Biol. Chem.* **280,** 9170–9179
15. Cabib, E., Blanco, N., Grau, C., Rodríguez-Peña, J. M., and Arroyo, J. (2007) *Mol. Microbiol.* **63,** 921–935
16. Rodríguez-Peña, J. M., Cid, V. J., Arroyo, J., and Nombela, C. (2000) *Mol. Cell. Biol.* **20,** 3245–3255
17. Gómez-Esquer, F., Rodríguez-Peña, J. M., Díaz, G., Rodríguez, E., Briza, P., Nombela, C., and Arroyo, J. (2004) *Microbiology* **150,** 3269–3280
18. Coutinho, P. M., and Henrissat, B. (1999) in *Recent Advances in Carbohydrate Bioengineering* (Gilbert, H. J., Davies, G., Henrissat, B., and Svensson, B., eds) pp. 3–12, Royal Society of Chemistry, Cambridge, UK
19. Boraston, A. B., Bolam, D. N., Gilbert, H. J., and Davies, G. J. (2004) *Biochem. J.* **382,** 921–935
20. Sikorski, R. S., and Hieter, P. (1989) *Genetics* **122,** 19–27
21. Crotti, L. B., Drgon, T., and Cabib, E. (2001) *Anal. Biochem.* **292,** 8–16
22. Wach, A. (1996) *Yeast* **12,** 259–265
23. Kosík, O., and Farkas, V. (2008) *Anal. Biochem.* **375,** 232–236
24. Park, J. T., and Johnson, M. J. (1949) *J. Biol. Chem.* **181,** 149–151
25. Roberts, R. L., and Cabib, E. (1982) *Anal. Biochem.* **127,** 402–412
26. Fernández, M. P., Correa, J. U., and Cabib, E. (1982) *J. Bacteriol.* **152,** 1255–1264
27. Magnelli, P., Cipollo, J. F., and Abeijón, C. (2002) *Anal. Biochem.* **301,** 136–150
28. Ait Mohand, F., and Farkas, V. (2006) *Carbohydr. Res.* **46,** 478–485
29. Scherrer, R., Louden, L., and Gerhardt, P. (1974) *J. Bacteriol.* **118,** 534–540
30. De Nobel, J. G., Klis, F. M., Munnik, T., Priem, J., and van den Ende, H. (1990) *Yeast* **6,** 483–490
31. Shaw, J. A., Mol, P. C., Bowers, B., Silverman, S. J., Valdivieso, M. H., Durán, A., and Cabib, E. (1991) *J. Cell Biol.* **114,** 111–123
32. Mouyna, I., Fontaine, T., Vai, M., Monod, M., Fonzi, W. A., Diaquin, M., Popolo, L., Hartland, L. P., and Latgé, J.-P. (2000) *J. Biol. Chem.* **275,** 14882–14889
33. Lagorce, A., Hauser, N. C., Labourdette, D., Rodríguez, C., Martin-Yken, H., Arroyo, J., Hoheisel, J. D., and François, J. (2003) *J. Biol. Chem.* **278,** 20345–20357
34. Popolo, L., and Vai, M. (1999) *Biochim. Biophys. Acta* **1426,** 385–400
35. Molano, J., Polacheck, I., Durán, A., and Cabib, E. (1979) *J. Biol. Chem.* **254,** 4901–4907
36. Correa, J. U., Elango, N., Polacheck, I., and Cabib, E. (1982) *J. Biol. Chem.* **257,** 1392–1397
37. Choi, W.-J., and Cabib, E. (1994) *Anal. Biochem.* **219,** 368–372
38. Baladrón, V., Ufano, S., Dueñas, E., Martín-Cuadrado, A. B., del Rey, F., and Vázquez de Aldana, C. R. (2002) *Eukaryot. Cell* **1,** 774–786
39. Voth, W. P., Olsen, A. E., Sbia, M., Freedman, K. H., and Stillman, D. J. (2005) *Eukaryot. Cell* **4,** 1018–1028
40. Yin, Q. Y., de Groot, P. W. J., de Jong, L., Klis, F. M., and De Koster, C. G. (2007) *FEMS Yeast Res.* **7,** 887–896

SUPPLEMENTAL FIGURES LEGENDS

FIGURE S1. **Effect of overexpression of Crh1p or Crh2p on incorporation of fluorescence in growing cells.** Conditions as in Fig. 2. *A*, wild type (FY001); *B*, FY001 transformed with a high-copy plasmid carrying *CRH1* (strain EPICRH1); *C*, FY001 transformed with a *CRH2* high copy plasmid (strain SECRH2). Scale bar, 10 μm.

FIGURE S2. **Fluorescence of cells grown in the presence of individual SR-linked oligosaccharides.** The strain is FY001 (wild type). *A*, disaccharide. *B*, trisaccharide. *C*, tetrasaccharide. *D*, pentasaccharide. *E*, hexasaccharide. *F*, heptasaccharide. To better show the difference between individual oligosaccharides, a shorter exposure than in Fig. 1 was used. *Scale bar*, 10 μm.

FIGURE S3**. Paper chromatography of SR-hexasaccharide before (*St*) or after overnight incubation with growing W303 cells (*wt*) or LC355 cells (*LC355*).** The faster moving bands in the *wt* lane are shorter oligosaccharides.

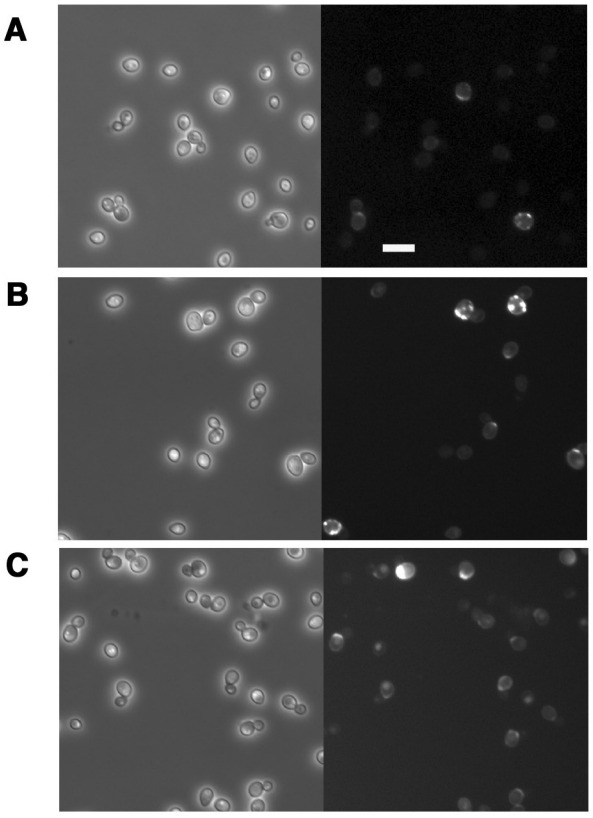

Fig. S1

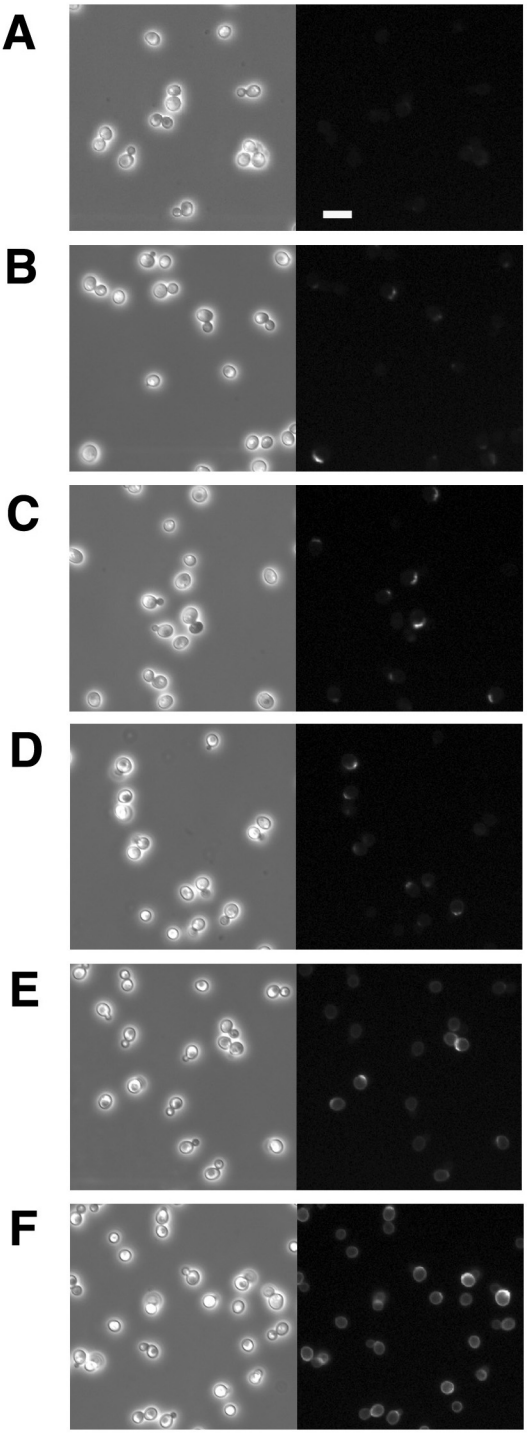

Fig. S2

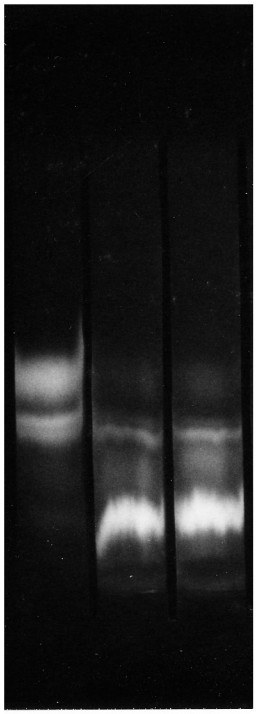

Fig. S3

CAPÍTULO 3

PROPIEDADES CATALÍTICAS DE LAS TRANSGLICOSILASAS Crh1 Y Crh2 *IN VIVO* E *IN VITRO*

RESUMEN DE LOS RESULTADOS DEL CAPÍTULO 3

En trabajos previos habíamos demostrado que las proteínas Crh1 y Crh2 actúan como transglicosilasas entre la quitina y el glucano *in vivo* (capítulo 1). Además, fuimos capaces de desarrollar un sistema en él que se reconstituyó la actividad transglicosilasa quitina-glucano de estas proteínas, utilizando tanto células permeabilizadas con digitonina como paredes celulares (capítulo 2). Con el objetivo de determinar las propiedades bioquímicas de la reacción, en este trabajo se ha desarrollado un sistema *in vitro* soluble de esta actividad transglicosilasa, utilizando las proteínas heterólogas Crh1 y Crh2 expresadas en *P. pastoris* y sustratos donadores y aceptores sintéticos solubles análogos a los componentes de la pared celular marcados con sulforodamina (SR). Los ensayos se realizaron en un tubo de ensayo que contenía las proteínas Crh1 y Crh2 junto al donador y al aceptor, en unas condiciones óptimas para la transglicosilación. El producto de la reacción de transglicosilación está compuesto por el respectivo sustrato aceptor y la porción correspondiente del sustrato donador unida al extremo no reducido del aceptor. El producto de la reacción de transglicosilación se separa del resto de los componentes de la reacción por absorción en un papel Whatman y el exceso de aceptor se elimina mediante lavados con etanol. Finalmente, se cuantifica mediante un lector ELISA el producto de la reacción de transglicosilación. De los diferentes donadores ensayados (carboximetil quitina (CM-quitina), glicol-quitina, β-1,3 glucano (laminarina), β-1,6 glucano (pustulán), una mezcla de β-1,3/β-1,6 glucano, Xiloglucano y α-manano), únicamente los derivados solubles de la quitina: CM-quitina, glicol-quitina y N-acetil-quito-oligosacáridos de tamaños superior a 5 unidades fueron donadores aptos para ambas enzimas. En relación a los aceptores y tal como se esperaba por los datos *in vivo*, estas proteínas fueron capaces de usar tanto los β-1,3 gluco-oligosacáridos como los β-1,6 gluco-oligosacáridos. Adicionalmente, los quito-oligosacáridos resultaron ser también reconocidos como aceptores de una forma incluso más eficiente que los β-1,3 quito-oligosacáridos y los β-1,6 quito-oligosacáridos. Este resultado se ve apoyado por las constantes de Michaelis-Menten obtenidas para cada proteína con cada tipo de aceptor, de modo que los quito-oligosacáridos se unen a la enzima más rápidamente que los β-1,3 gluco-oligosacáridos y los β-1,6 gluco-oligosacáridos, en este orden de prioridad. La reacción catalizada progresa linealmente en el tiempo en cuanto a cantidad de enzima presente en la reacción y formación de producto. Ambas proteínas presentan un máximo de actividad a pH ácidos y

a 37ºC. El tamaño mínimo del oligosacárido capaz de actuar como aceptor es de dos unidades. Ambas proteínas pierden el 50% de su actividad tras 15 minutos a 95ºC. El análisis por rayos infrarrojos, del producto generado tras la reacción de transglicosilación entre la CM-quitina como donador y la laminarina como aceptor, muestra un espectro de absorción característico de la CM-quitina. A su vez, observamos tanto *in vivo* como *in vitro* que los quito-oligosacáridos inhiben la reacción de transglicosilación entre la CM-quitina y los β-1,3 gluco-oligosacáridos. Los resultados de la gráfica de Dixon indican que esta inhibición es de naturaleza competitiva en relación al tipo de aceptor. Adicionalmente, ambas proteínas presentan una actividad quitinasa demostrada mediante ensayos de viscosimetría y ensayos fluorimétricos con carboximetil quitina rojo violeta brillante (CM-Q-RBV) y N-acetil-glucosamina metilumbeliferona (NAG-MU) como sustratos. La débil actividad quitinolítica se ve estimulada por la presencia en la reacción de quito-oligosacáridos y β-1,3 gluco-oligosacáridos. Con la finalidad de conocer sí estas enzimas actuaban como endoquitinasas o exoquitinasas, ensayamos diferentes sustratos que nos permitieron distinguir entre ambas actividades. Los resultados obtenidos muestran que ambas enzimas presentan una actividad endoquitinasa, aunque Crh2 también presenta cierta actividad exoquitinasa.

Con el objetivo de analizar el papel de Crh1 y Crh2 *in vivo* y a la vista de los resultados obtenidos *in vitro*, utilizamos los tres tipos de oligosacáridos fusionados a SR (β-1,3 gluco-oligosacáridos, β-1,6 gluco-oligosacáridos y quito-oligosacáridos) como aceptores sintéticos en ensayos de incorporación *in vivo* como se ha descrito en el capítulo 2. El análisis de la incorporación de los oligosacáridos en las paredes celulares de una cepa WT reveló que, coincidiendo con los datos previamente obtenidos en el capítulo 1 y 2 y los datos obtenidos *in vitro*, los gluco-oligosacáridos derivados de la laminarina y el pustulán se incorporan con un patrón similar (mayoritariamente en cicatrices y de manera puntual en pared lateral) y con una mayor eficiencia los β-1,3 gluco-oligosacáridos que los β-1,6 gluco-oligosacáridos. El hecho de que los β-1,6 gluco-oligosacáridos utilizados en estos experimentos se incorporaran en la pared de la célula y no lo hicieran en los ensayos realizados en el capítulo 2, es debido a que la mezcla de β-1,6 gluco-oligosacáridos utilizados en el presente estudio contiene una mayor proporción de gluco-oligosacáridos de cadena larga (grado de polimerización ≥5) que la mezcla previamente usada. Adicionalmente, de acuerdo con los resultados *in vitro*, los quito-oligosacáridos se incorporan con una gran eficiencia en las células y con un patrón de localización similar.

La comparación de la incorporación de fluorescencia de una cepa WT con los mutantes sencillos *crh1*Δ, *crh2*Δ y el doble mutante *crh1*Δ *crh2*Δ mostró que la incorporación de los β-1,6 gluco-oligosacáridos y los quito-oligosacáridos depende principalmente de Crh2, mientras que la incorporación de los β-1,3 gluco-oligosacáridos depende de ambas proteínas. La cepa *crh1*Δ *crh2*Δ no incorpora ninguno de los gluco-oligosacáridos fluorescentes ensayados, confirmando que toda la reacción de transglicosilación en la levadura depende de las proteínas Crh. A su vez, la sobreexpresión de *CRH1* y *CRH2* sobre un fondo *crh1*Δ *crh2*Δ permite la recuperación de la fluorescencia para cualquiera de los tres oligosacáridos.

ARTÍCULO 3

Catalytic properties and substrate specificity of Crh1 and Crh2 yeast cell wall transglycosylases in vivo and in vitro

Catalytic properties and substrate specificity of Crh1 and Crh2 yeast cell wall transglycosylases *in vivo* and *in vitro*

Authors:

Noelia Blanco[† §], Marian Mazáň* [§], Kristína Kováčová*, Zuzana Zemková*, Vladimír Farkaš* [‡], Javier Arroyo[† ‡]

§ These authors contributed equally to this work

***** *Institute of Chemistry, Center for Glycomics, Department of Glycobiology, Slovak Academy of Sciences, 84538 Bratislava, Slovakia.*

[†] *Departamento de Microbiología II, Facultad de Farmacía, Universidad Complutense de Madrid, IRYCIS, 28040 Madrid, Spain*

‡ Authors for correspondence: (jarroyo@farm.ucm.es); (chemvfar@savba.sk)

Author for communications with the Editorial Office:
Javier Arroyo. Departamento de Microbiología II, Fac. Farmacia, Pza. Ramón y Cajal s/n, UCM, Madrid, 28040 Spain. Tel: 34-91-3941746. Fax: 34-91-3941745. E-mail: jarroyo@farm.ucm.es

ABSTRACT

Mechanical properties of fungal cell walls are largely determined by composition and mutual cross-linking of their macromolecular components. Previous work showed that the Crh proteins are required for the cross-linking between chitin and glucan at the *Saccharomyces cerevisiae* cell wall. Here, the proteins encoded by *CRH1* and *CRH2* were heterologously expressed in *Pichia pastoris* and a sensitive fluorescent *in vitro* soluble assay was devised for determination of their transglycosylating activities. Both proteins act as chitin transglycosylases; they use soluble chitin derivatives, such as carboxymethyl-chitin, glycol-chitin and/or N-acetyl chitooligosaccharides of DP≥5 as the oligoglycosyl donors, and oligosaccharides derived from chitin, β-(1,3)-glucan (laminarin) and β-(1,6)-glucan (pustulan), fluorescently labeled with sulforhodamine or fluorescein isothiocyanate as acceptors. The minimal number of intact hexopyranose units required by Crh1 and/or Crh2 in the molecule of the acceptor oligosaccharide was two and the effectivity of the acceptor increased with the increasing length of its oligosaccharide chain. Both proteins exhibited a weak chitinolytic activity in different assays. In a viscometric assay with carboxymethyl-chitin as the substrate, the activity of Crh1 was markedly stimulated by N-acetyl chitooligosaccharides and, to a lesser extent, by laminarioligosaccharides. The pH optimum of both enzymes was 3.5 and the optimum temperature was 37 °C. The results obtained *in vitro* with different fluorescently labeled oligosaccharides as artificial chitin acceptors corroborated well with those observed *in vivo*.

INTRODUCTION

Fungal cells are surrounded by the cell wall, an essential structure that determines the cell shape, mediates cellular interactions, protects the cells from adverse effects of the environment and provides protection against internal turgor pressure that would cause bursting of the cell [1]. The yeast cell wall consists of three principal polysaccharides: β-(1-3)-glucan, the major structural component, β-(1-6)-glucan and chitin. Although chitin is a minor component representing 1-2 % of the cell wall dry weight, this polysaccharide is essential for cell survival. Additionally, mannoproteins (about 25-50 %) are present as an external layer of the cell wall [2, 3]. Individual polymer components of the cell wall are mutually linked by covalent bonds thus creating large macromolecular complexes. The backbone of these complexes is formed by β-(1,3)-glucan chains, branched at random by short chains of β-(1,6)-glucan extended by chitin linked by β-(1,4) glycosidic bonds at their non-reducing ends. In addition, glycosylphosphatidyl inositol (GPI)-anchored mannoproteins are linked to the complex via β-(1,6)-glucan side chains [3-5].

Despite its apparent rigidity, the cell wall structure needs to accommodate continuously to morphological changes during cell growth. Therefore, a balance between the biosynthesis of the wall constituents and their breakdown and reorganization is essential for both cell integrity and proper morphogenesis [6, 7]. The biosynthesis of the respective cell wall components takes place at different locations in the cell. The mannoproteins are synthesized in the endoplasmic reticulum, further glycosylated in the Golgi apparatus and transported by exocytosis to the cell wall, while the insoluble cell wall constituents chitin [8], β-(1,3)-glucan [9] and probably β-(1,6)-glucan [10, 11] are formed at the plasma membrane and extruded into the cell wall. Moreover, the synthesis of some of these polymers, like β-(1,3)-glucan and β-(1,6)-glucan seems to be coordinated [12].

The final stage of cell wall construction, the creation of a supramolecular structure through covalent cross-links between the individual components exported by the cells into the extracytoplasmic space, must therefore take place outside the plasma membrane, catalyzed by enzymes located in the cell wall. In analogy with the plant system [13], the most probable candidates for this function are the polysaccharide hydrolases/ transglycosylases capable of creating covalent bonds between individual polysaccharide molecules by transglycosylation. The transglycosylation mechanism consists in splitting a glycosidic bond in the polysaccharide molecule (called donor) and linking the formed fragment by its newly created reducing end to a hydroxyl group at the non-reducing end of other polysaccharide or oligosaccharide molecule (called acceptor) with the formation of a new glycosidic bond. The reaction mechanism is essentially a nucleophilic substitution S_{N2} involving double inversion of the anomeric bond, so that at the end, the anomeric character of the glycosidic bond remains retained [14]. The molecules of the acceptor can be of the same structural type as is the donor (in such case, the reaction is called homo-transglycosylation) or they can be of different type (hetero-transglycosylation). As there are no low-Mr energy carriers such as ATP in the cell wall, the new glycosidic bond must be formed at the expense of the energy released by breaking preexisting linkages [15]. Classic examples of plant cell wall-located transglycosylases are xyloglucan endotransglycosylase/ hydrolase (XET/XTH) cutting and transferring portions of xyloglucan molecules to other xyloglucan molecules or to oligosaccharide fragments derived from xyloglucan [16-19]. Other examples are the mixed-linkage beta-glucan: xyloglucan endotransglucosylase [19] or the mannan endotransglycosylase [20].

To date, several yeast proteins presumably involved in remodeling the cell wall have been characterized as transglycosylases. To this category belong the proteins of the Gas family *in vitro* acting as β-(1,3)-glucanosyl transferases [21-23] and their homologs

Phr1 and Phr2 from *Candida albicans* [24]; Bgl2 which removes laminaribiose units from non-reducing end of β-(1,3)-glucan and transfers them to non-reducing ends of other β-(1,3)-glucan molecules with formation of β-(1,6)-glycosidic linkage [25]; and the proteins of the Crh family that have been shown to be responsible for the linking chitin to β-glucans both *in vivo* and *in vitro* [26-28].

The three members of the Crh family, Crh1, Crh2 and Crr1 exhibit significant homologies with bacterial β-1,3/β-1,4 glucanases and xyloglucan endotransglycosylases/ hydrolases (XET/XTH) from plants [29] and they have been included into the family GH16 of glycohydrolases according to CAZY database [30]. Crr1 is involved in spore cell wall biogenesis [31] whereas Crh1 and Crh2 function in vegetative growth [29]. By using different methodologies for the analysis of polysaccharide crosslinks in the cell wall in wild-type and *crh* mutant strains, Cabib and coworkers [26, 28] found that all the chitin in a *crh1*Δ *crh2*Δ mutant is free, demonstrating that the formation of linkages between chitin and either β-(1-6)- or β-(1-3)-glucan *in vivo* depends on Crh1 and Crh2 activities. The linking reaction between chitin and glucan was explored recently *in vivo* and in isolated cell walls by using sulforhodamine (SR)-labeled laminarioligosaccharides as acceptor substitutes of β-(1,3)-glucan. *In vivo*, the incorporation of these acceptors was detected in bud scars and at a lower level in the lateral cell wall, being in both cases dependent on the *CRH* genes [27]. Furthermore, using digitonin-permeabilized cells or isolated cell walls as sources of chitin and enzymes, with SR-labeled β-(1,3)-glucan derived-oligosacharides as acceptors, it was possible to generate new chitin-glucan links *in vitro* [27]. With the permeabilized cells, the transfer largely depended on continued chitin synthesis suggesting that, in order to be attached to β-glucan core, the chains of chitin have to be in a nascent state, i. e. still not mutually associated by hydrogen bonds before they can be tethered to β-glucans by the Crh enzymes.

Despite all the progress demonstrating that both Crh1 and Crh2 act as transglycosylases both *in vivo* and *in vitro*, previous attempts of developing a simple cell- and cell wall-free *in vitro* system for assays of their activity failed. In the present work, we have devised a soluble fluorescent assay for determination of Crh1 and Crh2 transglycosylating activities *in vitro*. The assay uses soluble Na-carboxymethyl (CM) chitin as the glycosyl donor and (SR)-labeled laminari- or N-acetyl-chitooligosaccharides as acceptors. With the new assay, we have investigated the catalytic properties of recombinant Crh1 and Crh2 proteins. A perfect correlation of the obtained data with those from the *in vivo* experiments was found.

EXPERIMENTAL PROCEDURES

Strains and growth conditions

The *Saccharomyces cerevisiae* strains used in this study were: BY4741 (*MATa his3Δ1 leu2Δ0 met15Δ0 ura3Δ0*), GRA005 (*MATa his3Δ1 leu2Δ0 met15Δ0 ura3Δ0 crh1::hphMX4*), GRA006 (*MATa leu2Δ0 ura3Δ0 crh2::His3*), and GRA007 (*MATa leu2Δ0 ura3Δ0 crh2::His3 crh1::hphMX4*) [26]. Cells were grown at 24ºC or 30ºC in Synthetic complete (SC) medium (0.67% yeast nitrogen base, 2% glucose plus synthetic complete mixture).

Plasmids

The construction of plasmids pNBC13 (YEp352-*CRH2*-HA) and pNB10 (Yep352-*CRH1*-HA) has already been described [26]. The construction of the plasmid pHIL-CRH1MH,

used for the production of the recombinant tagged Crh1 protein was also previously described [32].

In order to create a fusion of the *CRH2* gene, lacking the putative GPI anchoring signal, plus a polyhistidine tag (6x) in the carboxyl terminal, we designed a PCR strategy using plasmid pJV40E [29] as template. CRH2-His was amplified using the primers: 5'-ACCGCTCGAGCTACATTTTGCAATGCAACTCAAG and 5'-ACGCGGATCCTCAATGATGATGATGATGATGGTCGACGGCTGTACTGCTGGAG GCGCTTC -3'). These primers allow amplification of a DNA fragment of 1248 bp encoding residues from A24 to S439 of Crh2. In addition to the *CRH2* specific sequences, the 5´oligonucleotide includes a *Xho*I restriction site whereas the 3´oligonucleotide includes a *Bam*HI restriction site, a stop codon and an in-frame 6 x His tag, respectively. The amplified DNA fragment was digested with *Xho*I and *Bam*HI and then cloned into the *P. pastoris* expression vector pHIL-S1 (Invitrogen, Barcelona, Spain) previously cleaved with the same enzymes. This plasmid (pHIL-CRH2-His) includes the *PHO1* secretion signal present in the vector, fused in-frame with the *CRH2* sequence from nucleotide 69 from the ATG to nucleotide 1317. The correct sequence of this construction was verified by DNA sequencing.

Production of recombinant Crh1 and Crh2 proteins

To express the recombinant proteins Crh1 and Crh2, the *P. pastoris*, *GS115* strain (Invitrogen) was transformed with the plasmids pHIL-CRH1-MHs and pHIL-CRH2-His, previously digested with *Bgl*II. Transformants were selected for Mut+ Muts phenotype, following manufacturer instructions. Production of recombinant proteins was carried out in methanol-containing medium according to manufacturer instructions. Briefly, cells were cultured in Buffered Glycerol-Complex (BMGY) medium at 30ºC for 2 days, then transferred to Buffered Methanol-complexed (BMMY) medium at 20ºC for 5 days, adding 1.25 % of methanol every 24 h to induce the expression of the protein. Supernatants were recovered by centrifugation at 5000 rpm (2300 x g) during 1 h and filtered through a 0.22 μm filter, followed by concentration to the desired volume using a Pellicon XL filter (Millipore, Madrid, Spain).The proteins were purified by affinity chromatography using Ni^{+2}-NTA agarose columns (Qiagen). Before binding, the column was equilibrated with Buffer B containing 20 mM Na_2HPO_4 and 500 mM NaCl, then the sample was allowed to soak into the column and incubated at 4 ºC during 1 h. After the column was washed with a 20 mM phosphate buffer pH 6, containing 0.5 M NaCl, proteins were eluted with 50 mM histidine solution. Finally, the eluted fraction was dialyzed against 2.5 mM histidine and stored at -80ºC. To determine the efficiency of the production, recombinant proteins were monitored by SDS-PAGE and Western blotting and quantified by Bradford analysis.

Substrates

CM-chitin, degree of substitution 0.16 - 0.2, was prepared from crab shell chitin (Sigma) using the procedure of [33]. Glycol-chitin (Gly-chitin) was prepared by acetylation of commercial glycol-chitosan (Sigma). Briefly, 100 mg of glycol-chitosan were dissolved in 12 ml of 10 % (v/v) acetic acid and 1.2 ml acetic anhydride was stepwise added under continuous stirring. After 4 h stirring at room temperature, the mixture was dialyzed against several changes of distilled water at 4 °C for 2 days and lyophilized. Oligosaccharides derived from chitin, from β-(1,3)-Glucan (laminarin), from β-(1,6)-glucan (pustulan) and from mixed-linkage β-(1,3)/β-(1,4)-glucan were in part prepared by limited hydrolysis of parent polysaccharides or they were from commercial sources (Megazyme, Seikagaku). The individual oligosaccharides were isolated from the respective hydrolysates by fractionation on Biogel P-6 column (1.8 x 110 cm) eluted with water or by

HPLC on TSK Gel Amide-80 column (21.5 i. d. x 300 mm, Tosoh) eluted with 70 % (v/v) acetonitrile. Tamarind seed xyloglucan was a gift from Dr. Mayumi Shirakawa (DSP Gokyo Food & Chemical Co. Ltd., Osaka, Japan). The yeast α-mannan was from the authors' laboratory resources. Fluorescent labeling of the oligosaccharides was accomplished by reacting the respective oligosaccharide glycamines with Lissamine rhodamine sulfonyl chloride (Acros Organics) or with fluorescein isothiocyanate, FITC (Sigma), according to a previously described protocol [34]. Glucanase-free chitinase from *Serratia marcescens* was a gift from Dr. Enrico Cabib (NIH, Bethesda, MD).

Crh1 and Crh2 assays

The standard incubation mixture contained 0.1 – 0.2% CM chitin, 20 – 40 μM SR-labeled oligosaccharides, 0.15-2.5 μg of the respective Crh protein and 50 mM citrate buffer, pH 3.5, in a total volume of 20 μl. The incubation was carried out at 37 °C for 10 to 60 min. The reaction was stopped by addition of 20 μl of 40 % (v/v) formic acid. Five-μl aliquots from the stopped mixture were spotted in quintuplicates onto a filter paper (Whatman 3MM) template, in size and shape corresponding to a standard 96-well microtitration plate. After drying, the paper was washed for 8-16 hours with 3-4 changes of 66 % (v/v) ethanol containing 5 % (v/v) formic acid. The washing removed unreacted label, whereas CM-chitin and the high-Mr products of its reaction with the SR-labeled acceptors remained attached to the paper. The paper was dried, placed between two glass plates and the fluorescence was measured in a Synergy HT-1 (Biotek) ELISA microplate reader equipped with a fluorescent detector and filters with excitation wavelength at 530 ±25 nm and emission wavelength at 575 ± 15 nm.

Product identification

Scaled-up incubation mixture (2 ml) contained 10 mg CM-chitin, 50 μM SR-laminaripentaose (L5-SR), 25 mM citrate buffer, pH 3.5, 2.5 μg Crh1 protein and 0.02 % NaN_3. The incubation was carried out at 37 °C for 16 h. Two volumes of ice-cold ethanol were added to precipitate the polysaccharide, and centrifuged. The sediment was washed several times with 66 % (v/v) ice-cold ethanol to separate the unreacted L5-SR until the supernatant was clear. The sediment containing CM-chitin-L5-SR hybrid product was dissolved in 1 ml 0.1 M citrate buffer, pH 6 and 10 μg of glucanase-free chitinase from *Serratia marcescens* were added and incubated at 37 °C for 1 h. Dilute solutions of the incubation mixture were then applied onto a preparative TLC plate with 0.5 mm thick Silicagel 60 layer (Merck) and ascending chromatography was run twice with intermittent drying using the solvent system n-butanol-ethanol-water (5:3:2, by vol.). The major fluorescent zones corresponding to hybrid products HP1 and HP2 were located under the UV light (Figure 4), scraped out from the TLC plate and eluted with 20 % (v/v) ethanol. The eluates were evaporated to dryness under reduced pressure and analyzed by Fourier Transform Infra-Red (FTIR) spectroscopy. The spectra were measured with Nicolet 6700 (Thermo Fisher Scientific, USA) spectrometer equipped with DTGS detector and Omnic 8.0 software. The spectral scans were collected in the middle region from 4,000 to 400 cm^{-1} at a resolution of 4 cm^{-1}. The number of scans was 128. For measurement in solid state, a Diamond Smart Orbit ATR accessory was applied.

Chitinolytic activity

For estimation of the weak chitinolytic activity of Crh proteins both viscosimetric and colorimetric assays were used. According to Staudinger's generalized viscosity law, the viscosity of dilute long chain polymer molecules is proportionally related to their molecular mass [35]. The viscosimetric method is especially suitable for measurements of

linear polysaccharide degradation by random-acting endohydrolases. For endochitinases, the activity can be estimated by reduction in viscosity of solutions of CM-chitin [36]. The measurements were performed in Cannon-Manning semi-micro viscometers in 1 ml reaction mixtures containing 0.25 % CM-chitin in 50 mM citrate buffer, pH 3.5 at 37 °C. After equilibrating the temperature and stabilizing the initial efflux time of the mixture, the reaction was initiated by addition of 10 µl enzyme solution containing 3 - 10 µg protein and efflux times were recorded in 10-15 min intervals. The relative viscosity was calculated according to formula $\eta_{rel}=(t_x/t_0) \times 100\%$, where t_0 is the efflux time of the reaction mixture at the beginning of the reaction and t_x is the efflux time after x min of the assay. Controls were run without enzyme.

To detect chitinase activity using soluble chitin polymer CM-chitin-Remazol Brillant Violet (CM-chitin-RBV) (Loewe Biochemica, Göttingen, Germany) as substrate, 100 µl of a 2 mg/ml CM-chitin-RBV suspension were incubated with 200 µl 0.1 M citrate buffer pH 3.6 and 20 µg of protein at 37ºC. After 1h of incubation, the reaction was stopped by the addition of 100 µl 0.5 M HCl pH 2.2 followed by cooling on ice for at least 10 min. After cooling, the samples were centrifuged for 1h at 21.000 x g at 4ºC to precipitate non-degraded substrate. The supernatants were transferred to a 96-well plate and absorbance at 550 nm was measured. A control sample without protein was used to determine the background fluorescence, which was subtracted from the experimental values of each reaction sample. Specific activities were expressed as $\Delta OD_{550}.min^{-1}.pmol^{-1}$.

Exochitinase and endochitinase activities were quantified using 4-Methylumbelliferyl (4-MU) chitooligosaccharide derivates. 4-MU 4-MU-N-acetyl-β-D-glucosamine, 4-MU-N-acetyl-β-D-N,N´-diacetylchitobiose and 4-MU-N-acetyl-β-D-N,N´,N´´-triacetylchitotriose (all from Sigma) were used as substrates to detect N-acetyl-β-glucosaminidase, chitobiosidase and endochitinase activities, respectively [37]. Reaction mixtures containinig 1 µl of 20 mg/ml of the respective 4-MU-derivate and 4 µg of protein in 0.1 M citrate buffer pH 3.6 in a final volume of 100 µl were incubated for 1 h at 37 ºC. The reactions were stopped with 200 µl of 400 mM sodium carbonate. Samples were centrifuged at maximum speed for 15 min. The released 4-methylumbelliferone in the supernantant was measured in a fluorescence reader (Bio-Tek FL600) using an excitation wavelength of 365 nm and an emission wavelength of 460 nm. Net values of each reaction were calculated by subtracting the fluorescence obtained in a parallel reaction using the corresponding heat inactivated protein. A standard curve for free 4-methylumbelliferone was used to determine the amount of the products formed. Enzyme activity was expressed as nmoles of released 4-methylumbelliferone (4-MU) per µg of protein.

Incorporation of fluorescent oligosaccharides in living yeast cells

Basically, the procedure previously described [27] was followed, although with some modifications to adjust conditions to smaller volumes. The labelling was carried out in final volume of 200 µl of culture in a vial adjusting the number of cells to have the culture in early stationary phase after overnight incubation at 30ºC. Either 5 µl of a 300 µM SR-oligosaccharide mixture (DP 2-7) or 5 µl of a 300 µM individual SR-oligosaccharide (DP4) were added to the cell culture for a final concentration of 7.5 µM. In some *in vivo* experiments, oligosaccharides labeled with fluorescein isothiocyanate (FITC) instead of SR were used. The culture was then incubated at 30ºC in the dark. After overnight growth, the cultures were centrifuged for 5 min at 1500 x g. Cells were then washed two times with 400 µl of 20% (v/v) ethanol and two times with 400 µl of water. Finally, the cells were resuspended in 25-40 µl of water for analysis by fluorescence microscopy, using a Nikon TE2000 fluorescence inverted microscope equipped with a CCD. Digital images were

acquired with an Orca C4742-95-12ER camera (Hamamatsu Photonics, Japan) and processed with the Hamamatsu HCImage Imaging systems software.

RESULTS

In vivo cell-wall labeling with fluorescent oligosaccharides

In previous work, we analyzed the crosslinking reaction between chitin and β-1,3 glucan *in vivo* by using SR-linked oligosaccharides derived from laminarin (β-1,3-glucan) as artificial chitin acceptors [27]. The labeled laminarioligosaccharides (SR-LamOS) were incorporated into bud scars, and at lower levels also into the lateral walls, suggesting that they were functioning as acceptors in place of β-glucan [27]. In agreement with our previous observations [27], the fluorescent β-1,3-linked glucose oligosaccharides were mainly detected as bright patches corresponding to bud scars (Figure 1A). The growth of cells in the presence of SR-β-1,6-linked glucose oligosaccharides resulted in a similar fluorescence localization pattern, suggesting that they were also functioning as acceptors of chitin (Figure 1A). The finding that SR-(β-1,6)-linked pustulooligosaccharides did incorporate into the living cells is in contrast with our previous observation [26] where they were inactive. The explanation of this apparent discrepancy is that the mixture of SR-PuOs used in the present study contained higer proportion of long-chain oligosaccharides (DP≥5) than the mixture used previously.

Since we had previously observed that N-acetyl chitooligosaccharides (ChitOS) were acting as effective inhibitors of β-1,3-linked oligosaccharide incorporation into the cell walls [27] we explored their ability to serve as acceptors as well. This assumption proved to be correct; SR-ChitOS were found to incorporate with high efficiency into the growing yeast cells with the same pattern of fluorescence localization as the one found for β-1,3-linked and β-1,6-linked glucose oligosaccharides (Figure 1A). Quantification of the fluorescence incorporated into the cells by analysis of the corresponding microscope images revealed different efficiencies for each type of the labeled-oligosaccharides: SR-ChitOS were incorporated with the highest efficiency, then the β-1,3-linked glucose oligosaccharides (SR-LamOS) and finally the β-1,6-linked oligosaccharides (SR-PustOS) (Figure 1B). These results were further confirmed by using FITC-labeled oligosaccharides (FITC-OS). The pattern of fluorescence localization for FITC-LamOS, FITC-PustOS and FITC-ChitoOS was idenditical to the one of cells labelled with SR-oligosaccharides (not shown). Moreover, quantification of fluorescence signals of cells labelled with the FITC-OS by flow cytometry confirmed the different efficiencies for each type of oligosaccharide (Figure S1).

To characterize further the involvement of Crh1 and Crh2 in the crosslinking of different acceptors to chitin in the cell wall, similar experiments were carried out with single *crh1*Δ and *crh2*Δ strains as well as with the double *crh1*Δ *crh2*Δ mutant strain. With the three types of oligosaccharides, there was almost no fluorescence incorporation in strains deleted in both *CRH1* and *CRH2* genes (Figure 2) indicating that there is no transglycosylation in the absence of both proteins. Comparison of the amount of fluorescence incorporated into the single mutants with respect to the WT strain revealed that for SR-β-1,6-linked oligosaccharides and SR-N-tetraacetyl chitotetraose, the crosslinking was mainly dependent on Crh2 and to a lesser extent on the Crh1 activity (Figure 2). However, for LamOS-SR, the fluorescence incorporation showed a small decrease in both *crh1*Δ and *crh2*Δ strains in respect to the WT strain (Figure 2). Apart from small differences, both mutants incorporated these oligosaccharides with a comparable

efficiency, suggesting that the transglycosylating activity depended in this case on both enzymes to a similar extent.

Setup of a fluorescent assay for Crh1/Crh2 mediated transglycosylation activity

To enable the study of the catalytic properties of the Crh proteins, we designed an *in vitro* assay of their transglycosylation activity. The natural donor, nascent chitin, was replaced by the soluble CM-chitin and as acceptors served the fluorescent SR-labeled oligosaccharides derived from β-(1,3)-glucan, β-(1,6)-glucan and from chitin. The products of transglycosylation were hybrid polymer molecules composed of the respective SR-labeled oligosaccharide acceptor and a portion of the donor polysaccharide attached to its nonreducing end (see below) and could be separated by adsorption on filter paper. The unused SR-labeled oligosaccharides were removed from the paper by washing in 66 % (v/v) ethanol. The application of 5 μl aliquots of the reaction mixture as discrete spots on the filter paper in a pattern corresponding exactly to the 96-well microtitration plate format allowed high-throughput determination of the fluorescence incorporated into the polymer with a fluorescent ELISA plate reader. When required, the absolute quantification of the products was done by employing a calibration curve constructed with known amounts of the respective labeled acceptor oligosaccharide.

Enzymatic properties and substrate specificity of Crh proteins *in vitro*

As potential oligosaccharyl donors, CM-chitin, glycol chitin (Gly-chitin), carboxymethyl cellulose (CMC), hydroxyethyl cellulose (HEC), β-(1,3)-glucan (laminarin), β-(1,6)-glucan (pustulan), barley mixed-linkage β-(1,3)/β-(1,6)-glucan, tamarind seed xyloglucan (TXG) and yeast α-mannan were tested in the *in vitro* assay using L5-SR as acceptor. From these, only the soluble chitin derivatives CM chitin, glycol chitin (Figure 3) and N-acetyl chitooligosaccharides of DP≥5 (Figure 7) proved to be able to serve as the oligosaccharyl donors with both enzymes. The donor efficiency of 0.25 % Gly-chitin was 22-25 % of that obtained with the same concentration of CM-chitin (Figure 3). The enzymatic character of the transglycosylation was confirmed by the fact that the rate of Crh1/Crh2-catalyzed incorporation of the labeled SR-oligosaccharides into the 66 % ethanol-insoluble fraction was directly proportional to the amount of enzyme present in the incubation mixture and that the reaction progressed linearly with time (not shown). Both Crh1 and Crh2 exhibited maximum activity at pH 3.5 and the optimum temperature was 37 °C (Figure S2). Divalent cations as well as 1 mM EDTA did not significantly influence the reaction. Both Crh1 and Crh2 lost about 50 % activity upon heating at 95 °C for 15 min (not shown).

The product obtained by Crh1-catalyzed reaction with CM-chitin as the donor and L5-SR as the acceptor was a high-Mr polysaccharide containing incorporated fluorescent label. The IR spectra of the principal fluorescent fragments HP1 and HP2 obtained after treating the product with purified glucanase-free *Serratia* chitinase (Figure 4) exhibited similar features as the spectrum of CM-chitin [37].The absorption band in the region 1410-1451 cm^{-1} is characteristic for symmetric vibrations of the carboxylate group while the absorption in the region of 1316-1326 cm^{-1} and 1540-1558 cm^{-1} can be assigned to vibrations ν(NH) of the amide group in N-acetyl glucosamine [38]. These data proved that compounds HP1 and HP2 are hybrid molecules consisting of the labeled acceptor oligosaccharide with fragments of CM-chitin covalently attached to it.

While the donor specificity of both enzymes was restricted to soluble chitin derivatives, both Crh1 and Crh2 exhibited considerable flexibility as concerns the nature of the acceptor. As expected on the basis of our previous findings *in vivo* demonstrating that both enzymes are responsible for the formation of the crosslinks between chitin and β-1,3 glucan as well as between chitin and β-1,6 glucan [26, 28], both enzymes were active with

SR-labeled oligosaccharides derived from laminarin and pustulan albeit with different efficiencies. Moreover, SR-oligosaccharides derived from chitin also served as acceptors in the *in vitro* reaction, in agreement with their incorporation into the cell wall of living yeast in a Crh1 and Crh2 dependent manner (Figures 1 and 2). From among the labeled tetrasaccharides, the most efficient acceptor was the SR-N-tetracetyl chitotetraose (CH4-SR), followed by β-(1,3)-linked L4-SR with both enzymes. In addition, Crh2 exhibited some activity also with β-(1,6)-linked P4-SR (Figure 5A). As previously observed *in vivo* [25], the individual native N-acetyl-chitooligosaccharides inhibited the transglycosylation between CM-chitin and LamOS-SR also *in vitro* whereby the extent of the inhibition was proportional to the concentration of the chitooligosaccharide. Dixon graph depicted in Figure 5B indicates that inhibition of the transferase reaction with N-triacetyl chitotriose (CH3) was of competitive nature in relation to the acceptor L5-SR.

The Michaelis constants (K_m) obtained with L4-SR and CH4-SR as the acceptors (Table I) show that with both enzymes, the chito- derivative binds to the enzyme more readily than the laminarioligosaccharide.

To identify the minimal length of oligosaccharides capable to act as the acceptors, relative rates of the transfer reactions were measured using individual LamOS-SR and ChitOS-SR of different length. Significant transfer rates were observed with oligosaccharides of DP 3 and larger, indicating that the minimal requirement for the acceptor were 2 intact hexopyranosyl units at the nonreducing end of the SR-oligosaccharide, applicable both for LamOS- and for ChitoOS-SR. In general, the acceptor efficiency of all types of labeled oligomers increased with their increasing oligosaccharide chain length throughout the whole range of DP's (2-7) of the respective oligosaccharide series (Figures 6A and 6B). It should be noted that a similar increase in transfer efficiency with oligosaccharide length was observed *in vivo* [26].

Besides CM-chitin and Gly-chitin, also the soluble fragments of chitin represented by N-acetyl chitooligosaccharides of DP≥5 served as glycosyl donors with both CH4-SR and L4-SR as the respective acceptors. The transferase reaction has led to a formation of a series of labeled products of different size indicating stepwise elongation of the acceptor molecule by transfer of sugar units from the oligosaccharide donor to the labeled acceptor. Interestingly, contrary to the reaction with Crh1, the transfer to L4-SR was rather slow with Crh2. Prolonged incubations yielded high-Mr fluorescent products remaining on the starting line during TLC (Figures 7A and 7B).

Chitinase activity of Crh1 and Crh2

The reaction mechanism of transglycosylases includes as an alternative glycosyl transfer from the glycosyl-enzyme intermediate to a molecule of water, i. e. hydrolysis, under conditions when the concentration of suitable acceptor is low [11]. To verify this possibility, we used different assays to determine the chitinolytic activity of Crh1 and Crh2. Both enzymes caused a slow reduction of the viscosity of CM-chitin solutions in a time-dependent manner. The rate of CM-chitin degradation by Crh1 was markedly stimulated by ChitOS and to a lesser extent also with LamOS (Figure 8). The extent of the stimulation depended on the concentration and increased with DP of the oligosaccharide. In contrast, we did not observe any appreciable effect of added oligosaccharides on the activity of Crh2 in the viscometric assay (not shown).

Chitin-depolymerizing activity of Crh1 and Crh2 was also measured by alternative fluorescent methods. Soluble chitin polymer CM-chitin-Remazol Brillant Violet (CM-chitin-RBV) was used as a substrate to detect chitinase activity of both proteins. Crh1, and even more Crh2 exibited chitinolytic activity against this substrate (Table II). To distinguish between exochitinase and endochitinase activities, 4-MU-N-acetyl-β-D-

glucosamine, 4-MU-N-acetyl-β-D-N,N´-diacetylchitobiose and 4-MU-N-acetyl-β-D-N,N´,N´´-triacetylchitotriose were used as substrates to detect N-acetyl-β-glucosaminidase, chitobiosidase and endochitinase activities, respectively [37]. The rates of hydrolysis of these compounds by Crh1 and Crh2 are shown in Table II. No N-Acetyl-β-D-glucosaminidase activity was detected for Crh1 whereas Crh2 exhibited a very low but measurable activity with the same substrate. Both enzymes produced 4-methylumbelliferone more readily from the 4-MU trisaccharide than from the disaccharide derivate (Table II) suggesting that they both function as endochitinases, although the prevailing modes of their action may be different (see discussion).

DISCUSSION

Cell wall remodeling is an essential process continuously taking place during fungal morphogenesis and growth. Since the firmness of the cell wall must not be compromised throughout the whole period of growth, it may be supposed that the restructuring is achieved by the coordinated action of cell wall synthesizing machinery and wall-located glycoside hydrolases that degrade the cell wall polysaccharides as well as of transglycosylases, which by linking together newly arriving polysaccharide molecules generate longer or branched polymers and facilitate their anchoring in the cell wall.

Our previous work demonstrated that both Crh1 and Crh2 are responsible for the attachment of chitin to β-(1,3)-glucan and to β-(1,6)-glucan at the yeast cell wall *in* vivo [26-28]. In accordance with this, all the chitin in a *crh1*Δ *crh2*Δ strain is free (i.e. not covalently bound to glucan) [28]. Moreover, earlier experiments also showed that (SR)-labeled β-(1,3)-oligosaccharides were abundantly incorporated in live cells at bud scars in a Crh1/Crh2 dependent manner, presumably functioning *in vivo* as artificial substrates for the transglycosylation reaction [27].

In this work, using soluble derivatives of chitin as the donors and (SR)-labeled oligosaccharides as the artificial acceptors, we were able to determine *in vitro* transglycosylase activities of recombinant proteins Crh1 and Crh2 expressed in *Pichia pastoris*. Experiments *in vitro* described herein confirmed some of the earlier *in vivo* observations [26-28] as concerns the nature of the donor and acceptor molecules. Both proteins use chitin derivatives (CM-chitin, Glycol-chitin and higher N-acetyl chitoligosaccharides) as glycosyl donors. Contrary to the strict donor specificity, the range of acceptors effective *in vivo* and *in vitro* included besides β-(1,3)-linked laminarioligosaccharides and β-(1,6)-linked glucooligosaccharides derived from pustulan also the (SR)-N-acetyl chitooligosaccharides. Comparison of the relative rates of transglycosylation indicates that, *in vitro*, N-acetyl-chitooligosaccharides are the preferred acceptor substrates for these enzymes followed by β-(1,3)-linked laminarioligosaccharides whereas the transfer to β-(1,6)-linked pustulooligosaccharides, although significant with Crh2, was clearly slower (Figure 5A). Supporting this, the values of Michaelis constants (K_m's), show that CH4-SR is interacting with the enzymes more readily than L4-SR (Table I). Interestingly, the results of the *in vitro* assays in respect to the preference of the different acceptors correlate well with the incorporation of the corresponding labeled-oligosaccharides *in vivo* (Figure 1).

The transglycosylation of CM-chitin to β-1,6-linked pustulooligosaccharides carried out by Crh1 *in vitro* was very inefficient. However, the analysis of the chitin crosslinked to β-1,6 glucan in a *crh1*Δ strain and in a *crh1*Δ *crh*2Δ mutant expressing Crh1 from a multicopy plasmid [26], together with the incorporation of SR-pustulooligosacharides into these cells overexpressing Crh1 (Blanco, N., Hurtado, R.,

Farkaš, V. and Arroyo, J., manuscript in preparation) provide evidences that *in vivo,* Crh1 is also able to react with β-1,6-linked oligoglucosides.

Such a broad substrate specificity of carbohydrate-active enzymes is quite unusual; nevertheless, there are few examples of promiscuous behavior of glycoside hydrolases. For example, for bacterial levansucrases belonging to the family 68 of glycoside hydrolases [30], a large variety of non-conventional fructosyl acceptors has been defined [39, 40]. Moreover, among the glycoside phosphorylases, sucrose phosphorylases (SP) also show acceptor promiscuity by transferring a glucosyl moiety to a wide variety of mono-, di- and trisaccharides [41]. Additionally, purified xyloglucan endotransglycosylase HvXET5 from barley, belonging equally as Crh proteins to the glycoside hydrolase family GH16, covalently link different donor polysaccharides tamarind xyloglucan (TXG), hydroxyethyl cellulose (HEC) and (1,3/1,4)-β-D-glucans with a range of acceptors, including oligo-xyloglucosides and cellodextrins, albeit with different efficiencies [42].

While the donor catalytic site of Crh1 and Crh2 is highly specific for chitin, the acceptor site must have a great plasticity in order to accept diverse β-linked oligosaccharides. The strict donor specificity for chitin derivatives suggests that the acetamide group at C2 in the N-acetyl glucosamine units is critical for the interaction with the donor site of the enzymes. We assume that it will be possible to explain the broad acceptor specificity of Crh1 and Crh2 only after their three-dimensional structure is available. For the time being, it is natural to ask what structural features have all these acceptors in common? Obviously, it is an unsubstituted β-linked hexopyranosyl unit at the non-reducing end of the acceptor oligosaccharide. This assumption is supported by the observation that SR-xyloglucooligosaccharides derived from xyloglucan, where the terminal nonreducing β-1,4-linked glucosyl unit is substituted at C-6 with α-xylose, as well as the α-(1,4)-linked SR-maltooligosaccharides were inactive as acceptors *in vitro* (not shown). The fact that the N-acetyl chitooligosaccharides are the most efficient acceptors confirms that the presence of an acetamide group at C-2 positions of the hexopyranosyl units of the substrate molecules potentiates the binding not only of the donor but also of the acceptor to the enzyme. In contrast, molecular kinks introduced in the acceptor substrate by β-1,6 linkages seem to cause a less favorable binding to the acceptor site of the enzymes.

A plausible mechanism for transglycosylase reactions catalyzed by Crh1 and Crh2 proteins involves the cleavage of the β-(1,4) linkages of the chitin molecule and subsequent linking of the fragment of the substrate through the newly formed reducing end onto the acceptor molecule which can be a saccharide or water. Therefore, it was not surprising to find that both proteins exhibited also a chitinase activity. The endochitinases cleave chitin chains randomly generating disperse molecular weight GlcNAc multimers whereas exochitinases hydrolyze chitin from the non-reducing end releasing monomeric (N-Acetyl-β-D-glucosaminidases) or dimeric (chitobiosidases) units of N-acetyl-glucosamine [43]. The stimulating effect of added N-acetyl chitooligosaccharides and laminarioligosaccharides on the rate of viscosity decrease of CM-chitin solutions catalyzed by Crh1 could be explained by their playing role of low-Mr glycosyl acceptors in the reaction. Transfer of cleaved polysaccharide fragments to low-Mr acceptors causes a reduction in the average molecular size of the polysaccharide and, consequently, the rate of viscosity reduction increases in their presence. It has been a characteristic of the so-called "true" transglycosylases that they exhibit only very low hydrolase activity but their action is accelerated in the presence of suitable oligoglycoside acceptors [44, 45]. Although both Crh1 and Crh2 used the endochitinase substrate 4-MU-N-acetyl-β-D-N,N´,N´´-triacetylchitotriose (MU-Ch3) more efficiently than 4-MU-N-acetyl-β-D-N,N´-diacetylchitobioside (MU-Ch2), the ratios of their activities with these two substrates were

different (Table II). While with Crh1, the ratio of activities MU-Ch3 vs. MU-Ch2 was 15, i.e. the endo- mechanism of transglycosylation clearly prevails, with Crh2 this ratio was 3.8 indicating that the enzyme possesses a substantial exo- activity. It can be imagined that Crh2 preferentially attacks the molecules of the donor substrate CM-chitin from their non-reducing end, transferring them to a suitable acceptor without resulting in an appreciable reduction in their size. This could explain why Crh2 has caused only negligible viscosity changes of CM-chitin solutions and why the added chito- and laminarioligosaccharides were without effect on the reaction rate. The different modes of action of both enzymes on chitin molecules are the probable reason why *in vivo*, the exogenous chitooligosaccharides, which caused morphological aberrations in a *cla4*Δ strain, provoked disappearance of chitin in a *cla4*Δ *crh2*Δ strain but not in *cla4*Δ *crh1*Δ strain [46].

The observed multiple specificities of Crh1 and Crh2 are tempting to speculate that *in vivo* they could act both as hetero-transglycosylases attaching nascent chains of chitin to β-(1,3)- and β-(1,6)-glucan as well as homo-transglycosylases mutually joining nascent chains of chitin. The hetero-transglycosylase activity of these proteins crosslinking chitin to β-(1,3)-glucan and to β-(1,6)-glucan, previously demonstrated *in vivo* [26-28], was corroborated here by the *in vitro* data. It should be noted that the possibility of Crh1 and Crh2 acting also as homo-transglycosylases *in vivo* linking together nascent chains of chitin among themselves is deduced from the findings *in vitro* and from experiments showing incorporation of SR-chitooligosacharides into cell walls of living cells, but is merely speculative since the formation of chitin-to-chitin linkages in the cell wall is difficult if not impossible to prove. Incorporation of SR-oligosaccharides in *crh1*Δ *crh2*Δ strains revealed that both proteins, Crh1 and Crh2, are required for the in vivo transglycosylation reaction at the mother-bud neck and bud scars, in accordance with the localization of both proteins in these sites [26, 29]. Moreover, experiments with the single *crh1*Δ and *crh2*Δ mutants suggested that Crh2 activity is more important, particularly for transglycosylation of chitin to β-1,6-linked oligosaccharides. These results corroborate well with previous chemical measurements of the chitin crosslinked to glucan *in vivo* showing that the amount of chitin attached to β-(1,3)-glucan is equally reduced in both *crh1*Δ and *crh2*Δ mutants and completely eliminated in a *crh1*Δ*crh2*Δ strain, whereas the amount of chitin bound to β-(1,6)-glucan is more reduced in a *crh2*Δ strain [28].

ACKNOWLEDGMENTS

We are indebted to Enrico Cabib for all his interest and support, for his bright and inspiring ideas and especially for the years of fruitful scientific collaboration, now ending due to his retirement. Critical reading of the manuscript by Ramón Hurtado and Enrico Cabib is acknowledged.

FUNDING

This work was financed by grant no. 2/0011/09 from the Agency for Science VEGA (Slovakia) to V. F. and grants BIO2010-22146 (MICCIN), GR58/08 (UCM) and S2010/BDM443 2414 (Comunidad de Madrid) to J. A. N.B. is the recipient of an FPI Ph.D. fellowship (BES-2008-003171) from MICINN. M. M. was the recipient of short term fellowship grant from FEBS.

REFERENCES

1 Orlean, P. (2012) Architecture and biosynthesis of the *Saccharomyces cerevisiae* cell wall. Genetics. **192**, 775-818

2 Klis, F. M., Boorsma, A. and De Groot, P. W. (2006) Cell wall construction in *Saccharomyces cerevisiae*. Yeast. **23**, 185-202

3 Lesage, G. and Bussey, H. (2006) Cell wall assembly in *Saccharomyces cerevisiae*. Microbiol. Mol. Biol. Rev. **70**, 317-343

4 Kollar, R., Petrakova, E., Ashwell, G., Robbins, P. W. and Cabib, E. (1995) Architecture of the yeast cell wall. The linkage between chitin and beta(1-->3)-glucan. J. Biol. Chem. **270**, 1170-1178

5 Kollar, R., Reinhold, B. B., Petrakova, E., Yeh, H. J., Ashwell, G., Drgonova, J., Kapteyn, J. C., Klis, F. M. and Cabib, E. (1997) Architecture of the yeast cell wall. Beta(1-->6)-glucan interconnects mannoprotein, beta(1-->)3-glucan, and chitin. J. Biol. Chem. **272**, 17762-17775

6 Bartinicki-García, S. and Lippman, E. (1972) The bursting tendency of hyphal tips of fungi: presumptive evidence for a delicate balance between wall synthesis and wall lysis in apical growth. J. Gen. Microbiol. **73**, 487-500

7 Levin, D. E. (2011) Regulation of cell wall biogenesis in *Saccharomyces cerevisiae*: the cell wall integrity signaling pathway. Genetics. **189**, 1145-1175

8 Cabib, E., Bowers, B. and Roberts, R. L. (1983) Vectorial synthesis of a polysaccharide by isolated plasma membranes. Proc. Natl. Acad. Sci.U.S.A. **80**, 3318-3321

9 Wloka, C. and Bi, E. (2012) Mechanisms of cytokinesis in budding yeast. Cytoskeleton. **26**, 21046

10 Montijn, R. C., Vink, E., Muller, W. H., Verkleij, A. J., Van Den Ende, H., Henrissat, B. and Klis, F. M. (1999) Localization of synthesis of beta1,6-glucan in *Saccharomyces cerevisiae*. J. Bacteriol. **181**, 7414-7420

11 Vink, E., Rodriguez-Suarez, R. J., Gerard-Vincent, M., Ribas, J. C., de Nobel, H., van den Ende, H., Duran, A., Klis, F. M. and Bussey, H. (2004) An in vitro assay for (1 --> 6)-beta-D-glucan synthesis in *Saccharomyces cerevisiae*. Yeast. **21**, 1121-1131

12 Aimanianda, V., Clavaud, C., Simenel, C., Fontaine, T., Delepierre, M. and Latge, J. P. (2009) Cell wall beta-(1,6)-glucan of S*accharomyces cerevisiae*: structural characterization and in situ synthesis. J. Biol. Chem. **284**, 13401-13412

13 Fry, S. C. (2004) Primary cell wall metabolism: tracking the careers of wall polimers in living plant cells. New Phytologist. **161**, 647-675

14 Sinnott, M. (1990) Catalytic mechanism of enzymatic glycosyl transfer. Chem. Rev. **90**, 1171-1202

15 Cabib, E., Bowers, B., Sburlati, A. and Silverman, S. J. (1988) Fungal cell wall synthesis: the construction of a biological structure. Microbiol. Sci. **5**, 370-375.

16 Fry, S. C., Smith, R. C., Renwick, K. F., Martin, D. J., Hodge, S. K. and Matthews, K. J. (1992) Xyloglucan endotransglycosylase, a new wall-loosening enzyme activity from plants. Biochem. J. **282**, 821-828

17 Nishitani, K. and Tominaga, R. (1992) Endo-xyloglucan transferase, a novel class of glycosyltransferase that catalyzes transfer of a segment of xyloglucan molecule to another xyloglucan molecule. J. Biol. Chem. **267**, 21058-21064

18 Farkaš, V., Sulova, Z., Stratilova, E., Hanna, R. and Maclachlan, G. (1992) Cleavage of xyloglucan by nasturtium seed xyloglucanase and transglycosylation to xyloglucan subunit oligosaccharides. Arch. Biochem. Biophys. **298**, 365-370

19 Fry, S. C., Mohler, K. E., Nesselrode, B. H. and Frankova, L. (2008) Mixed-linkage beta-glucan: xyloglucan endotransglucosylase, a novel wall-remodelling enzyme from Equisetum (horsetails) and charophytic algae. Plant J. **55**, 240-252
20 Schroder, R., Atkinson, R. G. and Redgwell, R. J. (2009) Re-interpreting the role of endo-beta-mannanases as mannan endotransglycosylase/hydrolases in the plant cell wall. Ann. Bot. **104**, 197-204
21 Mouyna, I., Fontaine, T., Vai, M., Monod, M., Fonzi, W. A., Diaquin, M., Popolo, L., Hartland, R. P. and Latge, J. P. (2000) Glycosylphosphatidylinositol-anchored glucanosyltransferases play an active role in the biosynthesis of the fungal cell wall. J. Biol. Chem. **275**, 14882-14889
22 Ragni, E., Fontaine, T., Gissi, C., Latge, J. P. and Popolo, L. (2007) The Gas family of proteins of *Saccharomyces cerevisiae*: characterization and evolutionary analysis. Yeast. **24**, 297-308
23 Mazáň, M., Ragni, E., Popolo, L. and Farkaš, V. (2011) Catalytic properties of the Gas family beta-(1,3)-glucanosyltransferases active in fungal cell-wall biogenesis as determined by a novel fluorescent assay. Biochem. J. **438**, 275-282
24 Calderón, J., Zavrel, M., Ragni, E., Fonzi, W. A., Rupp, S. and Popolo, L. (2010) *PHR1*, a pH-regulated gene of Candida albicans encoding a glucan-remodelling enzyme, is required for adhesion and invasion. Microbiology. **156**, 2484-249425
25 Goldman, R. C., Sullivan, P. A., Zakula, D. and Capobianco, J. O. (1995) Kinetics of beta-1,3 glucan interaction at the donor and acceptor sites of the fungal glucosyltransferase encoded by the *BGL2* gene. Eur. J. Biochem. **227**, 372-378
26 Cabib, E., Blanco, N., Grau, C., Rodriguez-Peña, J. M. and Arroyo, J. (2007) Crh1p and Crh2p are required for the cross-linking of chitin to beta(1-6)glucan in the Saccharomyces cerevisiae cell wall. Mol. Microbiol. **63**, 921-935
27 Cabib, E., Farkaš, V., Kosik, O., Blanco, N., Arroyo, J. and McPhie, P. (2008) Assembly of the yeast cell wall. Crh1p and Crh2p act as transglycosylases in vivo and in vitro. J. Biol. Chem. **283**, 29859-29872
28 Cabib, E. (2009) Two novel techniques for determination of polysaccharide cross-links show that Crh1p and Crh2p attach chitin to both beta(1-6)- and beta(1-3)glucan in the *Saccharomyces cerevisiae* cell wall. Eukaryot.Cell. **8**, 1626-1636
29 Rodriguez-Peña, J. M., Cid, V. J., Arroyo, J. and Nombela, C. (2000) A novel family of cell wall-related proteins regulated differently during the yeast life cycle. Mol. Cell. Biol. **20**, 3245-3255
30 Cantarel, B. L., Coutinho, P. M., Rancurel, C., Bernard, T., Lombard, V. and Henrissat, B. (2009) The Carbohydrate-Active EnZymes database (CAZy): an expert resource for Glycogenomics. Nucl. Acids Res. **37**, D233-238
31 Gomez-Esquer, F., Rodriguez-Peña, J. M., Diaz, G., Rodriguez, E., Briza, P., Nombela, C. and Arroyo, J. (2004) *CRR1*, a gene encoding a putative transglycosidase, is required for proper spore wall assembly in *Saccharomyces cerevisiae*. Microbiology. **150**, 3269-3280
32 Arroyo, J., Sarfati, J., Baixench, M. T., Ragni, E., Guillen, M., Rodriguez-Pena, J. M., Popolo, L. and Latge, J. P. (2007) The GPI-anchored Gas and Crh families are fungal antigens. Yeast. **24**, 289-296
33 Trujillo, R. (1968) Preparation of carboxymethylchitin. Carbohydr. Res. **7**, 483-485
34 Kosik, O. and Farkaš, V. (2008) One-pot fluorescent labeling of xyloglucan oligosaccharides with sulforhodamine. Anal. Biochem. **375**, 232-236
35 Staudinger, H. (1933) Viscosity investigations for the examination of constitution of natural products of high molecular weight and of rubber and cellulose. Trans.Faraday Soc. **29**, 18-32

36 Ohtakara, A. (1988) Chitosanase from *Streptomyces griseus*. Methods Enzymol. **161**, 505-510
37 Tronsmo, A. and Harman, G. E. (1993) Detection and quantification of N-acetyl-beta-D-glucosaminidase, chitobiosidase, and endochitinase in solutions and on gels. Anal. Biochem. **208**, 74-79.
38 Sandula, J., Kogan, G., Kacuráková, M. and Machová, E. (1999) Microbial (1→3)-β-D-glucans, their preparation, physico-chemical characterization and immunomodulatory activity. Carbohydr. Polym. **38**, 247-253
39 Seibel, J., Moraru, R., Gotze, S., Buchholz, K., Na'amnieh, S., Pawlowski, A. and Hecht, H. J. (2006) Synthesis of sucrose analogues and the mechanism of action of *Bacillus subtilis* fructosyltransferase (levansucrase). Carbohydr. Res. **341**, 2335-2349.
40 Beine, R., Moraru, R., Nimtz, M., Na'amnieh, S., Pawlowski, A., Buchholz, K. and Seibel, J. (2008) Synthesis of novel fructooligosaccharides by substrate and enzyme engineering. J. Biotechnol. **138**, 33-41
41 Aerts, D., Verhaeghe, T. F., Roman, B. I., Stevens, C. V., Desmet, T. and Soetaert, W. (2011) Transglucosylation potential of six sucrose phosphorylases toward different classes of acceptors. Carbohydr. Res. **346**, 1860-1867
42 Hrmova, M., Farkaš, V., Lahnstein, J. and Fincher, G. B. (2007) A Barley xyloglucan xyloglucosyl transferase covalently links xyloglucan, cellulosic substrates, and (1,3;1,4)-beta-D-glucans. J. Biol. Chem. **282**, 12951-12962
43 Cohen-Kupiec, R. and Chet, I. (1998) The molecular biology of chitin digestion. Curr. Opin. Biotechnol. **9**, 270-277
44 Saladie, M., Rose, J. K., Cosgrove, D. J. and Catala, C. (2006) Characterization of a new xyloglucan endotransglucosylase/hydrolase (XTH) from ripening tomato fruit and implications for the diverse modes of enzymic action. Plant J. **47**, 282-295
45 Piens, K., Faure, R., Sundqvist, G., Baumann, M. J., Saura-Valls, M., Teeri, T. T., Cottaz, S., Planas, A., Driguez, H. and Brumer, H. (2008) Mechanism-based labeling defines the free energy change for formation of the covalent glycosyl-enzyme intermediate in a xyloglucan endo-transglycosylase. J Biol Chem. **283**, 21864-21872
46 Blanco, N., Reidy, M., Arroyo, J. and Cabib, E. (2012) Cross-links in the cell wall of budding yeast control morphogenesis at the mother-bud neck. J. Cell Sci.**125**, 5781-5789

Table I: Kinetic parameters of Crh1 and Crh2 with L4-SR and CH4-SR as the respective acceptors. The average values from three independent measurements are given.

Enzyme	Acceptor	K_m (µM)	V_{max} ($pmol.s^{-1}.ml^{-1}$)	k_{cat} ($s^{-1}. 10^{-3}$)	k_{cat}/K_m ($s^{-1}. \mu M^{-1}.10^{-3}$)
Crh1	**L4-SR**	61.0	1.880	26.642	0.426
	CH4-SR	27.9	0.366	5.105	0.182
Crh2	**L4-SR**	65.1	0.926	1.038	0.016
	CH4-SR	8.5	0.161	0.282	0.034

Table II. Chitinolyitic activities of Crh1 and Crh2

Protein	CM-Chitin-RBV ($\Delta OD550.pmol^{-1}.min^{-1}$)	4MU-(GlucNAc)	4MU-$(GlucNAc)_2$	4MU-$(GlucNAc)_3$
		(nmole MU'. μg^{-1})		
Crh1	17.76 ± 3.2	0.0002 ± 0.0001	0.0194 ± 0.0009	0.2896 ± 0.0108
Crh2	38.53 ± 6.9	0.0080 ± 0.0004	0.0224 ± 0.0014	0.0842 ± 0.0055

Chitinase activities were measured with carboxymethyl-chitin-Remazol Brillant Violet (CM-chitin-RBV) and three different 4-Methylumberlliferyl (4-MU) derivates as described in materials and Methods. For CM-chitin-RBV the specific activities were expressed as $\Delta A550\ min^{-1}$ per pmole of protein. For 4-MU derivates an enzyme unit was defined as nmole of 4-methylumbelliferone released per microgram protein per hour. Standard deviations are given from at least three independent experiments.

Figure Legends:

Figure 1. Incorporation of different oligosaccharides in the wild-type strain. BY4741 cells were labelled with: SR- β,1-3 oligosaccharides (DP 2-7), SR-β-(1-6) oligosaccharides (DP 2-7) or SR-Chitotetraose (DP-4) and analyzed by fluorescence microscopy. A) Lower panels show images of the cells in the rodhamine fluorescence chanel whereas upper panels show the same cells observed under Nomarski. All images were obtained with the same exposition. B) Oligosaccharide incorporation in the bud scars was quantified in the microscopy images by using HCimage Imaging software and shown in bar histograms. The signals, expressed as arbitrary fluorescence units (F.U.), correspond to the average of three independent experiments. More than $2x10^3$ cells were always analyzed in each experiment.

Figure 2. Incorporation of different oligosaccharides in *crh*Δ mutant strains. WT, *crh1*Δ, *crh2*Δ and *crh1*Δ *crh2*Δ cells were labelled overnight with: SR- β,1-3 oligosaccharides (DP 2-7) (Panel A); SR-β, 1-6 oligosaccharides (DP 2-7) (Panel B) and SR-Chitotetraose (DP-4) (Panel C) and incorporation was followed by fluorescence microscopy. Lower panels show images in the rodhamine fluorescence chanel whereas upper panels show the same cells observed under Nomarski. For each oligosaccharide, the same exposure was used for WT and mutants. Oligosaccharide incorporation in the bud scars was quantified by using HCimage Imaging software and shown in bar histograms. The signals, expressed as arbitrary fluorescence units, correspond to the media of three independent experiments. More than $2x10^3$ cells were always analyzed in each experiment.

Figure 3. Donor specificity. The efficiency of selected soluble polysaccharides to serve as oligoglycosyl donors in the reactions catalyzed by Crh1 and Crh2. Standard 20 µl reaction mixtures contained 1 $mg.ml^{-1}$ of the respective polysaccharide, 0.15 µg Crh1 or 2.5 µg of Crh2 and 30 µM L5-SR as the acceptor. FU correspond to relative fluorescence units.

Figure 4. Analysis of the hybrid polysaccharide product formed from CM-chitin and L5-SR by Crh1p-catalyzed transglycosylation reaction. A) The transglycosylation product was hydrolyzed with purified Serratia chitinase and after the indicated time intervals, the incubation mixture was resolved by TLC. S, standard L5-SR; HP1, HP2, hydrolysis products. B) The hydrolysis products HP1 and HP2 were isolated by preparative TLC and their Fourier Transform Infra-Red Spectroscopy (FTIR) spectra were recorded. Note the presence of absorption bands at 1547-1556 cm-1 and 1392-1404 cm-1 characteristic for chitin and absent in the spectrum of L5-SR.

Figure 5. Acceptor efficiency of different types of oligosaccharides. A) Comparison of the rates of transglycosylation catalyzed by Crh1 and Crh2 using equimolar concentrations (25 µM) of the respective SR-labeled tetrasaccharide and CM-chitin as a donor. The reactions were carried out under standard conditions; B) Dixon graph illustrating the inhibitory effect of N-triacetyl chitotriose (CH3) on the transglycosylation reaction between CM-chitin and L4-SR catalyzed by Crh1. Standard incubation mixtures contained 1 $mg.ml^{-1}$ CM-chitin, indicated concentrations of L4-SR and 0.15 µg Crh1 in a total volume of 20 µl.

Figure 6. Effect of the sugar chain length of the acceptor SR-oligosaccharide on transglycosylation activity of Crh1 and Crh2. The standard 20 µl reaction mixtures contained 0.25 % CM-chitin as the donor and 66-70 µM SR-laminarioligosacharides (A) or 40-43 µM ChitoOS-SR (B) of different DP as acceptors.

Figure 7. Native N-acetyl chitooligosaccharides can serve as glycosyl donors in Crh1 and Crh2-mediated tranglycosylation. Reaction mixtures contained 30 μM SR-labeled N-tetraacetyl chitotetraose Ch4-SR (A) or 30 μM SR-labeled laminariteraose L4-SR (B) as the respective acceptors and 1 mg ml^{-1} of individual N-acetyl chitooligosaccharides (GlcNAc)n of different lenghts (DP 2 to 6) as the respective donors, 0.15 μg Crh1 or 2.5 μg Crh2 respectively in 20 μl of 25 mM citrate buffer, pH 3.5. The incubations were carried out at 37 °C for 16 h. Aliquots of the reaction mixtures were resolved by TLC on silicagel in the solvent system 2-propanol-water-25% ammonia (7:2:1, by vol.) run twice with intermittent drying. Photographed under the UV light.

Figure 8. Stimulatory effect of chitooligosaccharides and laminarioligosaccharides on the rate of viscosity reduction of CM-chitin catalyzed by Crh1. One-ml reaction mixtures contained 50 mM citrate buffer, pH 3.5, 0.25% CM-chitin, indicated concentrations of added oligosaccharides and 3 μg of Crh1 protein. Control incubation was performed without oligosaccharides added. The assay was carried out at 37 °C. N-tetraacetyl chitotetraose (CH4) and laminaritetraose (L4) were used as the representatives of the respective types of oligosaccharides.

Supplementary Figure Legends:

Figure S1. Quantification of fluorescence signals of cells labelled with the FITC-OS by flow cytometry. BY4741 cells were labelled with: FITC- β,1-3 oligosaccharides (DP 2-7), FITC-β-(1-6) oligosaccharides (DP 2-7) or FITC-Chitotetraose (DP-4) and analyzed by flow cytometry. Control corresponds to the background fluorescence of non-labeled cells.

Figure S2. pH- and temperature optima of Crh1 and Crh2. Standard 20 μl incubation mixtures contained 0.5 mg. ml^{-1} CM-chitin, 0.1 M of the appropriate citrate buffer, 30 μM L5-SR and 0.15 or 2.5 μg of Crh1 and Crh2 respectively. The incubations were carried out for 1h.

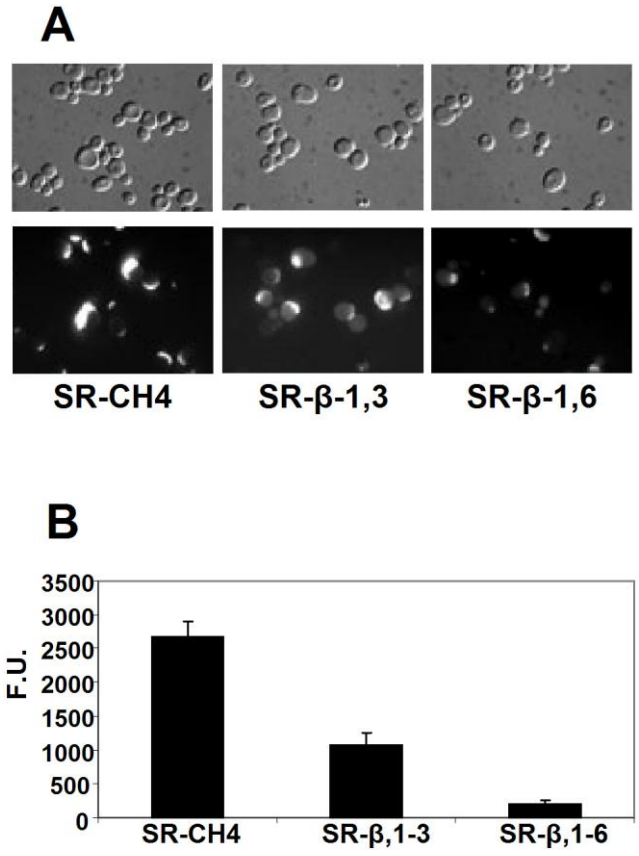
A
SR-CH4
SR-β-1,3
SR-β-1,6
B
F.U.
3500
3000
2500
2000
1500
1000
500
0
SR-CH4
SR-β,1-3
SR-β,1-6

Figure 1

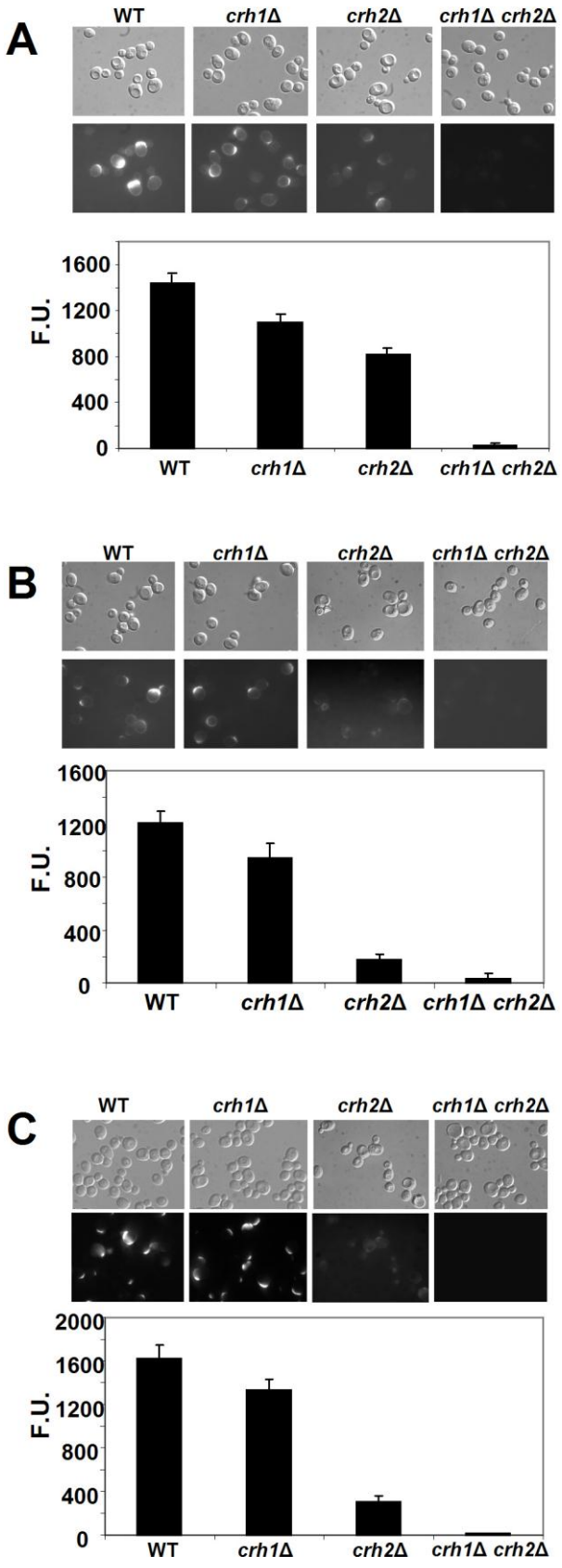
A
WT
crh1Δ
crh2Δ
crh1Δ crh2Δ
F.U.
1600
1200
800
400
0
WT
crh1Δ
crh2Δ
crh1Δ crh2Δ
B
WT
crh1Δ
crh2Δ
crh1Δ crh2Δ
F.U.
1600
1200
800
400
0
WT
crh1Δ
crh2Δ
crh1Δ crh2Δ
C
WT
crh1Δ
crh2Δ
crh1Δ crh2Δ
F.U.
2000
1600
1200
800
400
0
WT
crh1Δ
crh2Δ
crh1Δ crh2Δ

Figure 2

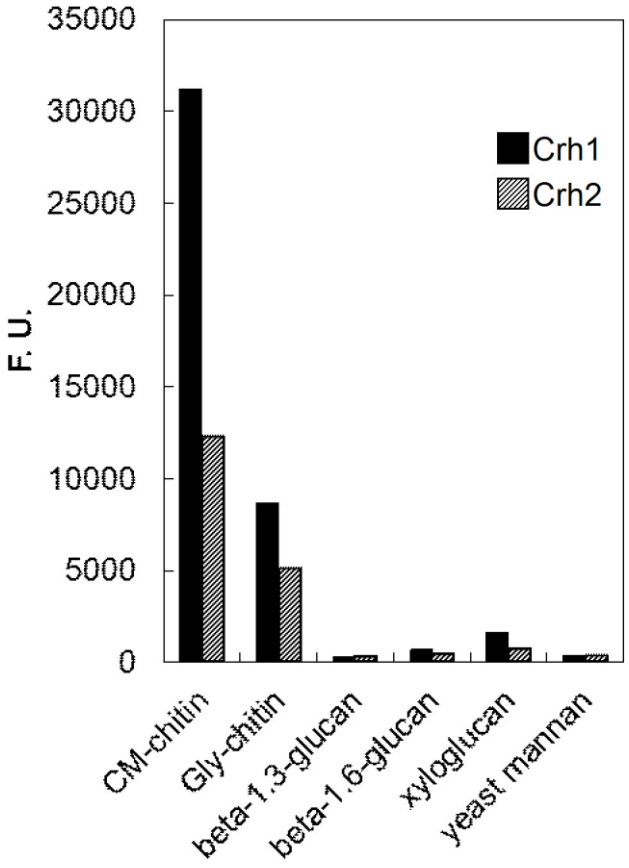
35000
30000
25000
20000
15000
10000
5000
0
F. U.
Crh1
Crh2
CM-chitin
Gly-chitin
beta-1,3-glucan
beta-1,6-glucan
xyloglucan
yeast mannan

Figure 3

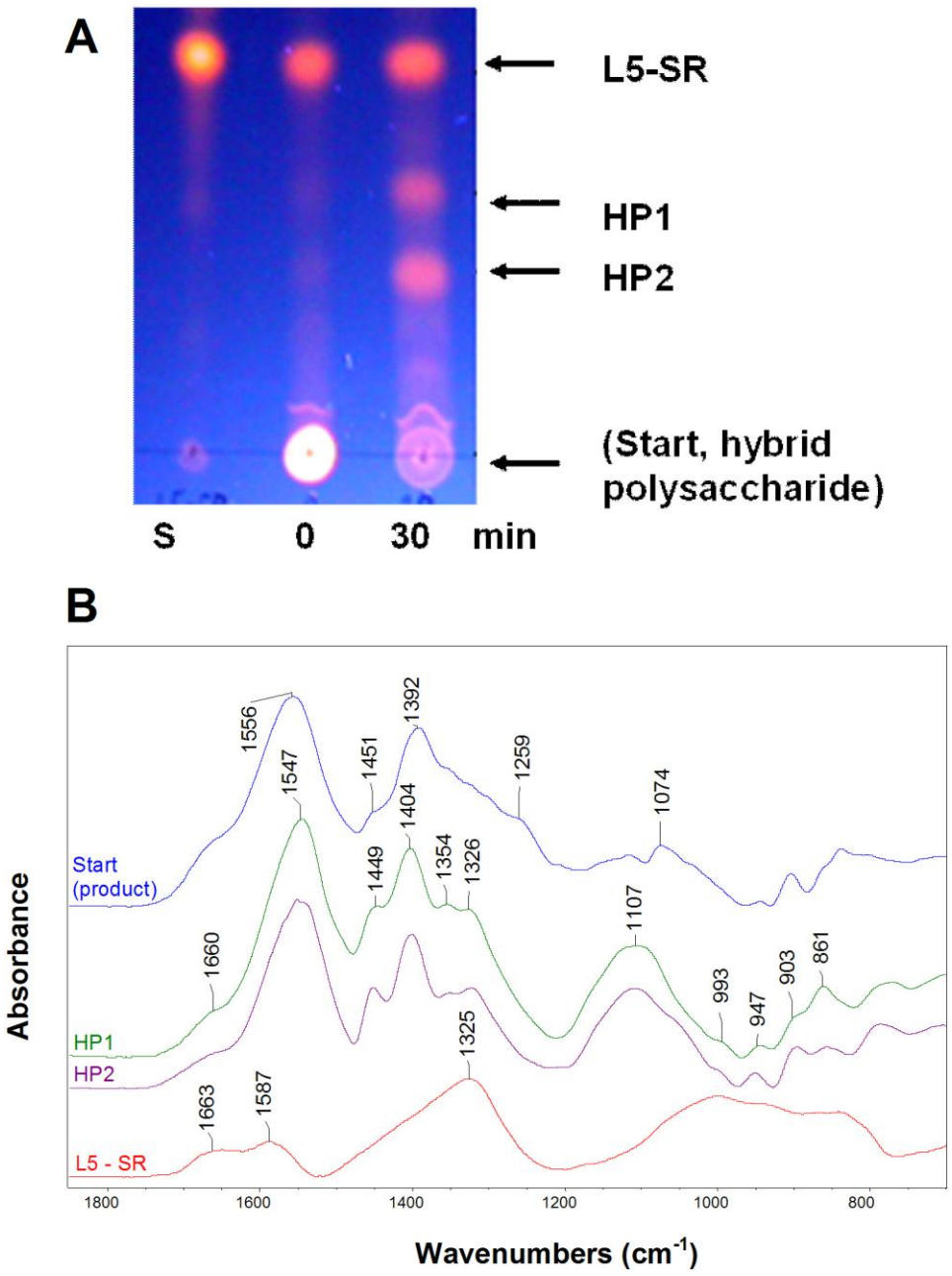
A
L5-SR
HP1
HP2
(Start, hybrid polysaccharide)
S
0
30
min
B
Absorbance
Start (product)
HP1
HP2
L5 - SR
1556
1547
1451
1392
1259
1074
1404
1449
1354
1326
1107
1660
993
947
903
861
1325
1663
1587
1800
1600
1400
1200
1000
800
Wavenumbers (cm-1)

Figure 4

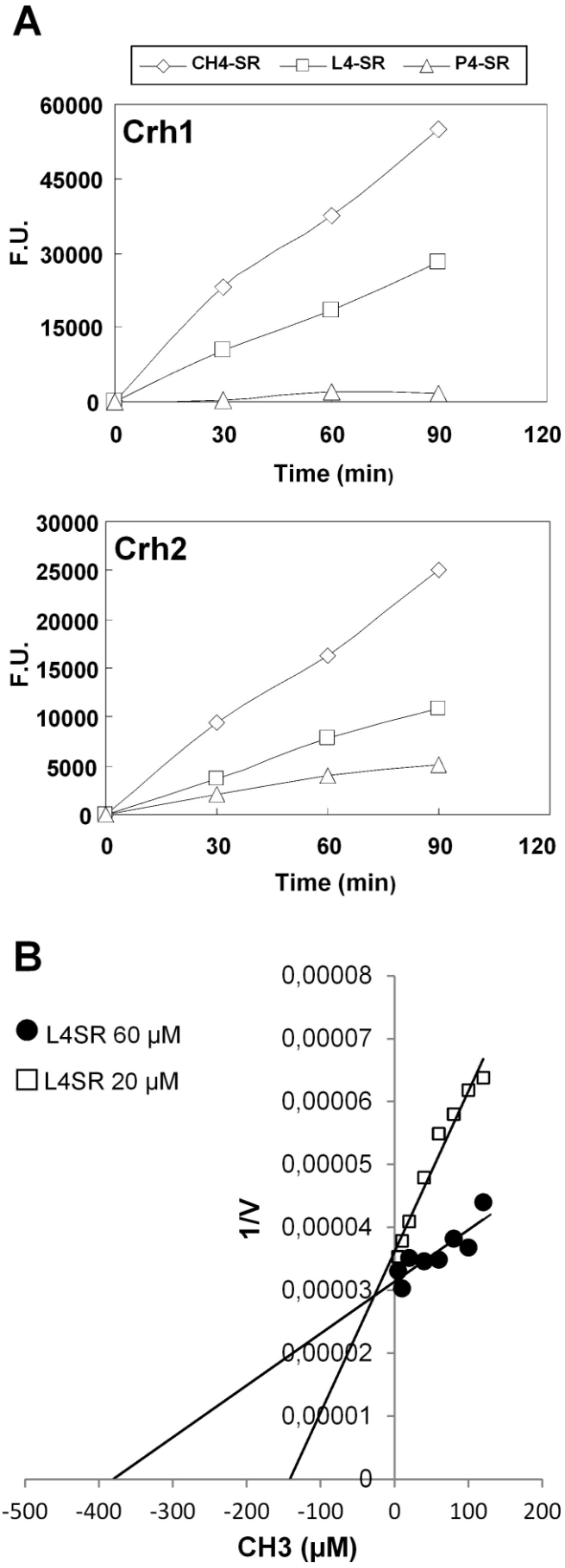
A
CH4-SR
L4-SR
P4-SR
Crh1
F.U.
60000
45000
30000
15000
0
0
30
60
90
120
Time (min)
Crh2
F.U.
30000
25000
20000
15000
10000
5000
0
0
30
60
90
120
Time (min)
B
L4SR 60 µM
L4SR 20 µM
1/V
0,00008
0,00007
0,00006
0,00005
0,00004
0,00003
0,00002
0,00001
0
-500
-400
-300
-200
-100
0
100
200
CH3 (µM)

Figure 5

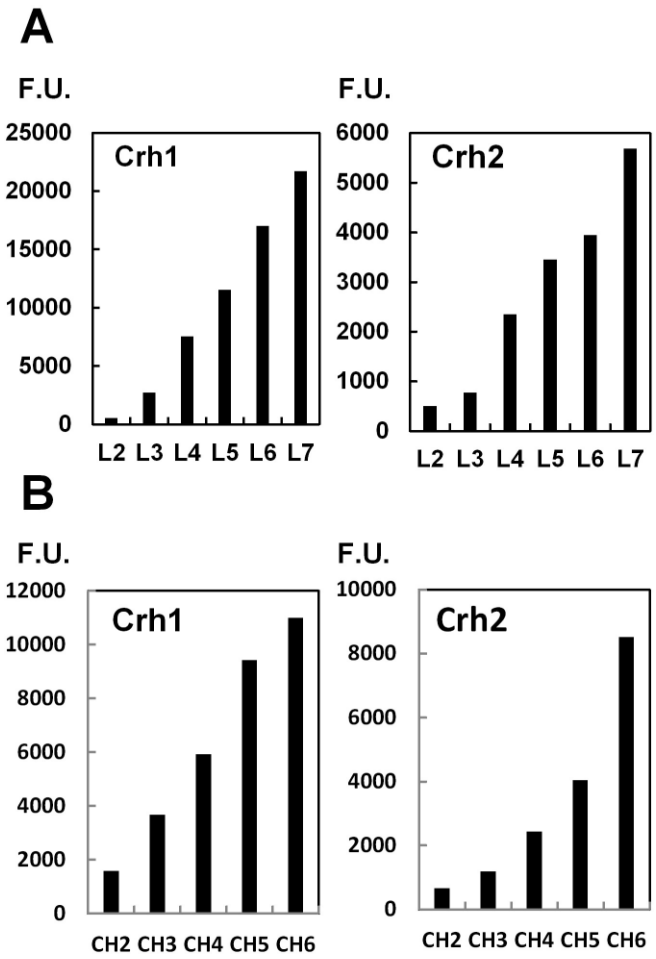
A
F.U.
25000
20000
15000
10000
5000
0
Crh1
L2 L3 L4 L5 L6 L7
F.U.
6000
5000
4000
3000
2000
1000
0
Crh2
L2 L3 L4 L5 L6 L7
B
F.U.
12000
10000
8000
6000
4000
2000
0
Crh1
CH2 CH3 CH4 CH5 CH6
F.U.
10000
8000
6000
4000
2000
0
Crh2
CH2 CH3 CH4 CH5 CH6

Figure 6

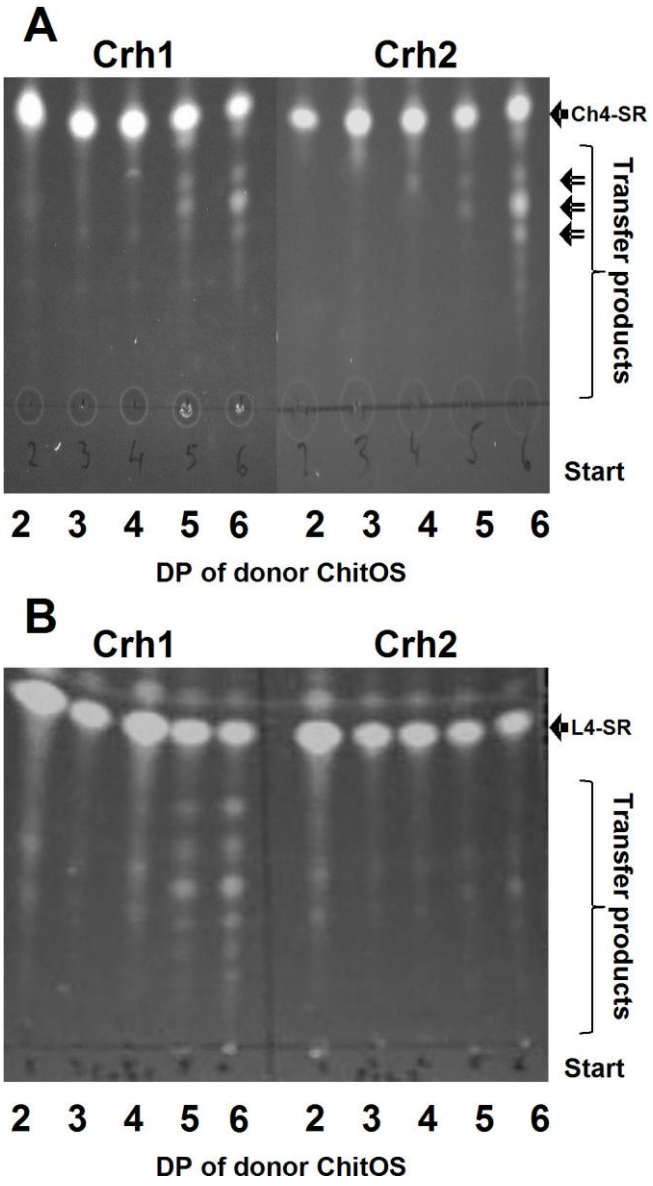
A
Crh1
Crh2
Ch4-SR
Transfer products
Start
2 3 4 5 6 2 3 4 5 6
DP of donor ChitOS
B
Crh1
Crh2
L4-SR
Transfer products
Start
2 3 4 5 6 2 3 4 5 6
DP of donor ChitOS

Figure 7

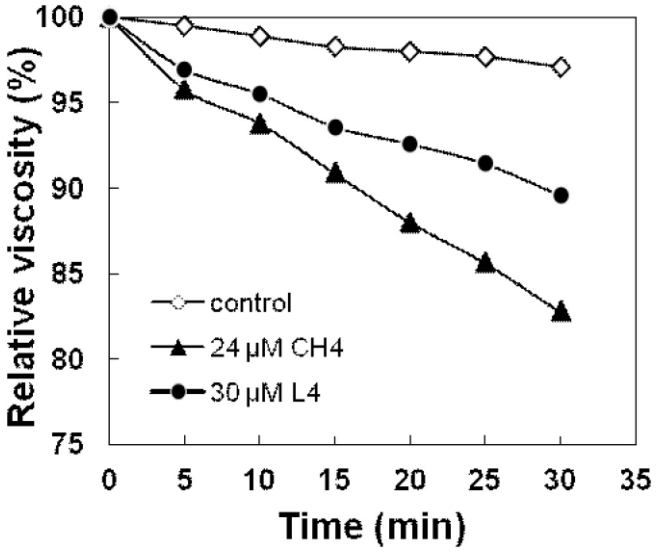
Relative viscosity (%)
100
95
90
85
80
75
0
5
10
15
20
25
30
35
Time (min)
control
24 μM CH4
30 μM L4

Figure 8

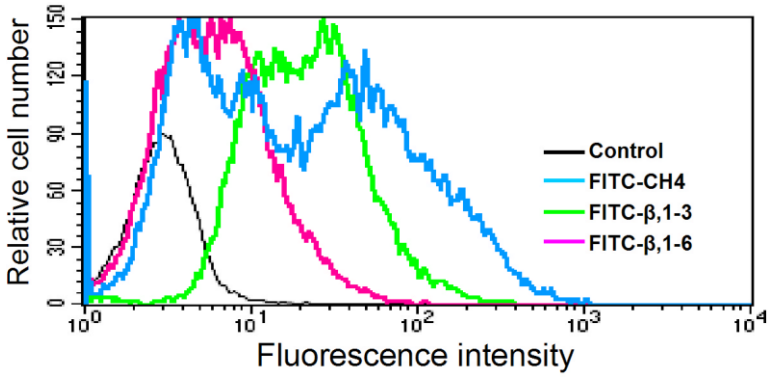

Figure S1

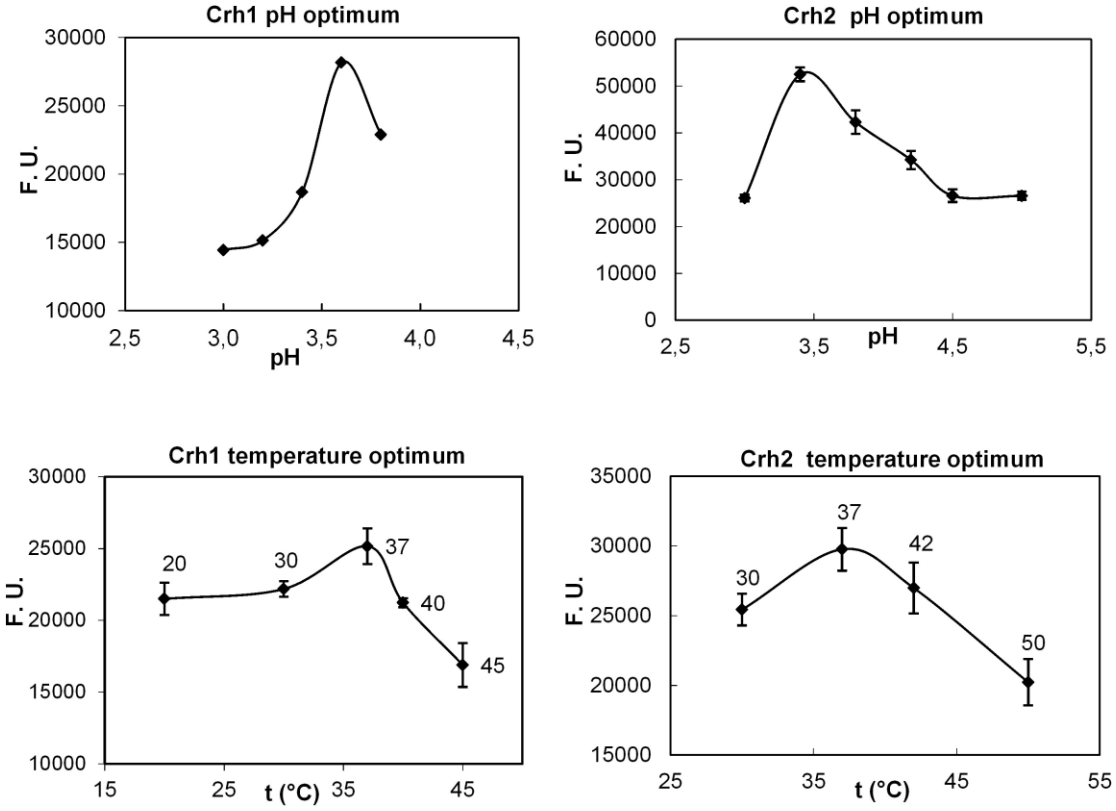

Figure S2

CAPÍTULO 4

ESTUDIO ESTRUCTURA-FUNCIÓN DE LA ACTIVIDAD TRANSGLICOSILASA DE Crh1 Y Crh2

RESUMEN DE LOS RESULTADOS DEL CAPÍTULO 4

En trabajos previos habíamos demostrado que las proteínas Crh1 y Crh2 son responsables del enlace covalente entre la quitina el β-1,3 glucano y el β-1,6 glucano, tanto *in vivo* como *in vitro*. Este enlace lo realizan mediante una reacción de transglicosilación de naturaleza enzimática. Teniendo en cuenta que estas proteínas conservan totalmente el dominio catalítico de las enzimas de la familia GH16, es muy probablemente que lleven a cabo la clásica reacción de sustitución nucleófila SN_2 típica de otras hidrolasas clasificadas dentro de esta familia (Sinnott, 1990), como las liquenasas (Planas, 2000) o las xiloglucan-xiloglucosiltransferasas (Vaaje-Kolstad et al., 2010). Estas glicosilhidrolasa actúan a través de un mecanismo de doble desplazamiento que da lugar a la retención de la configuración del carbono anomérico del azúcar que sufre la catálisis. Así, en la secuencia de Crh1 y Crh2 podemos identificar el dominio catalítico altamente conservado perteneciente a la familia 16 de glicosilhidrolasas (GH16) según la base de datos CAZY (*carbohydrate active enzymes database*). Adicionalmente, Crh2 presenta en su secuencia un dominio de unión a carbohidratos clasificado en la familia 18 (CBM18) según la base de datos anteriormente citada. Con el objetivo de entender mejor el mecanismo catalítico que llevan a cabo estas proteínas hemos diseñado un estudio estructura-función de los diferentes dominios presentes en estas proteínas. Para ello, hemos diseñado un modelo de la estructura tridimensional de la proteína Crh1 basado en la estructura de la β-1,3-1,4 glucanasa de *bacillus macerans*. De él inferimos que el núcleo de la proteína Crh1 está formado por dos láminas β antiparalelas apiladas en forma de sándwich. La región de unión al carbohidrato viene definida por un canal expuesto hacia el exterior en la cara cóncava de la proteína formado por residuos ácidos y residuos aromáticos. La verificación de este modelo ha sido posible gracias a la cuantificación de la actividad transglicosilasa *in vivo* realizada mediante la incorporación de oligosacáridos fusionados a sulforodamina a las paredes celulares descrito en los anteriores capítulos. Inicialmente, evaluamos los aminoácidos catalíticos resultantes del alineamiento múltiple de las proteínas Crh de *S. cerevisiae* con sus ortólogos en *C. albicans*, *A. fumigatus*, *B. licheniformis* (β-1,3-1,4-glucanasa), *A. thaliana* (xiloglucan-endotransglicosilasa) y la liquenasa de *B. macerans* usada para el modelo tridimensional de Crh1. Los resultados obtenidos muestran que los ácidos glutámicos E134 y E138 serían el respectivo ácido/base y nucleófilo teóricos del centro activo de Crh1 y los residuos E166 y E170 lo serían para Crh2. Adicionalmente, los ácidos

aspárticos D136 de Crh1 y D168 de Crh2 también están altamente conservados y parecen estar implicados en la catálisis. Para el estudio de estos residuos procedimos a generar versiones mutagenizadas de cada proteína en dichos aminoácidos. Las versiones mutagenizadas y la versión silvestre de las proteínas fueron expresadas en un mutante *crh1*Δ *crh2*Δ y se procedió a la cuantificación de la actividad transglicosilasa *in vivo* usando como aceptores β-1,3 gluco-oligosacáridos, β-1,6 gluco-oligosacáridos y quito-oligosacáridos. Los resultados obtenidos muestran que los residuos E134, D136 y E138 de Crh1, así como sus homólogos de Crh2 E166, D168 y E170 son esenciales para la actividad transglicosilasa *in vivo*. En paralelo, se hizo estudios fenotípicos de la sensibilidad de las cepas transformadas con las diferentes versiones mutagenizadas de las proteínas al compuesto RC. Los resultados obtenidos coinciden con los datos de actividad transglicosilasa *in vivo*, es decir, estas cepas presentan una sensibilidad al compuesto RC similar a la que presenta el mutante *crh1*Δ *crh2*Δ como consecuencia de la pérdida de la actividad transglicosilasa de las proteínas Crh1 y Crh2, apoyando la importancia de estos residuos para la actividad transglicosilasa. En base al modelo obtenido para Crh1, otros aminoácidos que estarían implicados en el posicionamiento del azúcar en el centro activo son la Tyr 160 (Y160), el Trp 233 (W233) y la Phe 152 (F152). Como controles examinamos la Tyr 103 (Y103) y la Met 105 (M105) que se encuentran cercanas al centro activo pero que no estarían implicadas en la actividad transglicosilasa de la proteína. Como se ha descrito anteriormente, se procedió a generar mutaciones puntuales de estos residuos. Las diferentes versiones mutagenizadas de la proteína Crh1, así como la versión nativa de la misma, se expresaron en un mutante *crh1*Δ *crh2*Δ, en el cuál no existe actividad transglicosilasa. A continuación, se cuantificó la incorporación tanto de los β-1,3 gluco-oligosacáridos y los β-1,6 gluco-oligosacáridos como de los quito-oligosacáridos en células *in vivo* mediante el método descrito en el capítulo 3. Los resultados obtenidos muestran que las mutaciones Y160A, W233A y F152A reducen drásticamente la actividad transglicosilasa y son incapaces de revertir el fenotipo de sensibilidad al RC de la versión silvestre de la proteína. El conjunto de los datos avalan el modelo tridimensional propuesto para Crh1.

Adicionalmente, estudiamos los residuos aminoacídicos presentes en el CBM de la proteína Crh2, mediante la generación de mutaciones dirigidas de los aminoácidos conservados dentro del domino de unión a carbohidratos de la familia 18 presentes en los ortólogos de Crh2 en hongos, bacterias y plantas. Al, igual que en los casos anteriores las

diferentes versiones mutagenizadas junto con la versión silvestre de la proteína se expresaron en un mutante *crh1*Δ *crh2*Δ y se procedió a la cuantificación de la incorporación de los tres oligosacáridos a las paredes celulares *in vivo*. Los resultados obtenidos muestran que las cisteínas, altamente consevadas, en las posiciones 33, 39 y 40 de este dominio son esenciales para la estabilidad y el plegamiento de la proteína Crh2. Además, las mutaciones en los residuos Pro 38 (P38), Ser 41 (S41), Tyr 43 (Y43), Gly 44 (G44), Gly 47 (G47), Tyr 51 (Y51) y Phe 62 (F62) de este dominio disminuyen considerablemente la actividad transglicosilasa de Crh2, mientras que el residuo glicina 49 (G49) es esencial para esta actividad. A su vez, las mutaciones en los aminoácidos Phe 26 y Pro 34 no afectan a la actividad transglicosilasa de la proteína. Los resultados obtenidos de la participación de cada aminoácido en la actividad transglicosilas, están en concordancia con su capacidad para revertir el fenotipo de sensibilidad al compuesto RC.

ARTÍCULO 4

Structural and functional analysis of yeast Crh1 and Crh2 transglycosilases

Structural and functional analysis of yeast Crh1 and Crh2 transglycosylases

Noelia Blanco[†], Ramón Hurtado[§], A. Belén Sanz[†], Jose Manuel Rodríguez-Peña[†], Vladimír Farkaš*, César Nombela and Javier Arroyo[† ‡]

[†] *Departamento de Microbiología II, Facultad de Farmacia, Universidad Complutense de Madrid, IRYCIS, 28040 Madrid, Spain.*

***** *Institute of Chemistry, Center for Glycomics, Department of Glycobiology, Slovak Academy of Sciences, 84538 Bratislava, Slovakia.*

§Instituto de Biocomputación y Física de Sistemas Complejos (BIFI), Universidad de Zaragoza, 50018 Zaragoza, Spain.

‡ Authors for correspondence: (jarroyo@farm.ucm.es)

Author for communications with the Editorial Office:
Javier Arroyo. Departamento de Microbiología II, Fac. Farmacia, Pza. Ramón y Cajal s/n, UCM, Madrid, 28040 Spain. Tel: 34-91-3941746. Fax: 34-91-3941745. E-mail: jarroyo@farm.ucm.es

INTRODUCTION

The fungal cell wall determines cell shape, protects cells against bursting caused by internal turgor pressure and against mechanical stress, being therefore an essential structure for cell survival [1, 2]. The cell wall of *Saccharomyces cerevisiae* is made up of four elements, β-1,3 glucan, β-1,6 glucan, mannoproteins and chitin, that are interconnected between them to form a mesh network (See references [3] and [4] for recent comprehensive reviews of yeast cell wall structure). β-1,3 glucan, the most abundant component of the yeast cell wall, serve as a backbone to which the other cell wall components are convalently linked. The non-reducing end of β-1,3 glucan chains, branched through β-1,6 linkages, is attached to the reducing end of β-1,6 glucan by an uncharacterized link and to the reducing end of chitin by a β-1,4 linkage [5, 6]. Cell wall mannoproteins (CWPs) can be linked to the β-1,3 glucan via alkali-labile bonds [7] and to β-1,6 glucan through a processed glicosylphosphatidylinositol (GPI) motif [8, 9]. The β-1,6 glucan bear side -branching β-1,3 Glc at which the reducing end of chitin seems to be attached via β-1,2 or β-1,4 linkages [10].

Cell wall remodelling is necessary for growth. This remodelling includes breakage of preformed crosslinks and incorporation of new synthesized material into the cell wall by formation of new crosslinks between the different components. CWPs are synthesized in the ER and delivered by the secretory pathway to the periplasmic space [3, 4]. Chitin and glucans are synthetized at the cell membrane and extruded into the periplasmic space [11-13] where the cross-linking reactions must occur. The first component to be incorporated is the β-1,3 glucan, followed by β-1,6 glucan and mannoproteins [14]. Chitin is the last component to reach the cell wall as deduced from the fact that this polysaccharide is incorporated into the lateral cell walls only after septation [15]. Part of this chitin is free but the rest is attached to β-1,3 glucan or β-1,6 glucan. By using a novel strategy for the analysis of chitin-glucan crosslinks, Cabib and Duran [16] demonstrated that chitin at the neck in early budding cells is mostly attached to β-1,3 glucan whereas chitin dispersed in the lateral cell walls is mainly attached to β-1,6 glucan.

Covalent crosslinking between chitin and glucans in would be created by transglycosilation [17]. More than ten years ago, we proposed that GPI Crh1 and Crh2 proteins, belonging to the Crh family of proteins (for Congo Red Hypersensitive), could be good candidates to acts as transglycosylases in the formation of chitin-glucan linkages in yeast [18]. The *S. cerevisiae* Crh family is composed of three proteins encoded by the

genes *CRH1*, *CRH2* and *CRR1*. While Crh1 and Crh2 have a role under vegetative growth [18], Crr1 is involved in the spore wall biogenesis [19]. That suggestion was based on a higher ratio of the alkali-soluble to the alkali-insoluble glucan fraction of a *crh1Δcrh2Δ* mutant respect to a wild type strain and on the localization of these proteins which matches that of chitin [18]. Later on, this turned out to be the case. By using the strategy mentioned above for analysis of chitin-glucan crosslinks [16] and others developed later [20], it was demonstrated that there is no chitin covalently bound to β-1,3 glucan or β-1,6 glucan in a *crh1Δ crh2Δ* strain [20, 21]. Therefore, Crh1 and Crh2 are responsible for the linkages between chitin and either β-1,3 glucan or β-1,6 glucan in yeast. The linking reaction was further studied *in vivo* by using fluorescent sulforhodamine-linked laminari- and pustulo-oligosacharides as artifcial acceptors. These oligosacharides were incorporated to yeast growing cells at bud scars and at a lower level in the lateral cell walls in a Crh dependent manner[22, 23], further demonstrating that the Crh proteins act as transglycosilases in vivo. Moreover, we have recently developed a soluble fluorescent assay for determination of Crh1 and Crh2 transglycosylating activities in vitro. Both proteins, Crh1 and Crh2, use soluble chitin derivatives, such as carboxymethyl-chitin, glycol-chitin and/or N-acetyl chitooligosaccharides of DP≥5 as oligoglycosyl donors, and oligosaccharides derived from β-(1,3)-glucan (laminarin), β-(1,6)-glucan (pustulan) and chitin, fluorescently labeled with sulforhodamine or fluorescein isothiocyanate as acceptors [23].

Proteins of the Crh familyy have been included in the glycoside hydrolase family 16 (GH16) of the Carbohydrate Active Enzymes database (CAZy) [24]. This family includes a number of bacterial, fungal and plant enzymes with unrelated functions but sharing sequence and structure similarities [25]. They contain a highly conserved catalytic domain (DE(I/L)DXE) and a jellyroll β-sandwich structure. Probably, the best characterized proteins within this family are the bacterial 1-3, 1-4-β-glucanases or lichenases, which hydrolyse linear β-glucans containing β-1,3 and β-1,4 linkages with a cleavage specificity for β-1,4 glycosidic bonds on 3-0-substituted glucopyranosyl residues [26, 27]. A number of *Bacillus* species secrete these lichenases [27]. Plant xyloglucan endotransglycosylases (XETs) are also included in the GH16 family. These enzymes catalyze endo-type hydrolysis of xyloglucan molecules and linking of the a newly generated reducing end to another xyloglucan molecule [28, 29], a process required for plant cell wall expansion and elongation [30]. Other unrelated enzyme activities of family 16 glycosyl hydrolases are the β-1,3 glucanases, active on β-1,3 glucans (laminarins and curdlans) [31], agarases, κ-carrageenases and endo-β-galactosidases [25]. In addition to the

conserved catalytic site of the GH16 gycosyl hydrolases, Crh1 and Crh2 show several structural features such as a secretory signal peptide at the N-terminus, a family 18 chitin binding domain (CBM18) which is devoid in Crh1, a Ser-Thr-rich region and a GPI attachment signal, which is necessary for their anchoring to the plasma membrane [32].

The catalytic mechanism for enzymes of family 16 of glycosyl hydrolases was first deduced by ^{1}H-NMR monitoring for the endo-1,3-1,4-β-D-glucan -glucanohydrolase from *Bacillus licheniformis* [33]. These enzymes are retaining glycoside hydrolases operating via a double diasplacement mechanism that leads to the retention of the configuration at the anomeric carbon of the sugar ring undergoing catalysis [34]. The catalytic residues of *Bacillus* 1,3-1,4-β-glucanases have been identified by mutational analysis, affinity labelling and X-ray crystallography, and thereafter the assignment extended to other enzymes included in the family 16 glycosyl hidrolases based on sequence similarities [27].

To get new insights into the catalytic mechanisms developed by the Crh1 and Crh2 transglycosylases, we have generated here an structural model of Crh1 based on the structure of the *Bacillus* H (A16-M) 1,3-1,4-β-D-Glucanase [35, 36] and investigated the importance of individual residues within the functional domains of these proteins for their catalytic activity. To achieve this goal, wild-type and site-directed mutant versions of Crh1 or Crh2 were expressed in a *crh1*Δ *crh2*Δ yeast strain, devoted of any Crh activity and the their transglycosylation activities further studied in vivo by analysis of the incorporation of fluorescent sulforhodamine-linked laminari-, chito- and pustulo-oligosacharides acceptors to the chitin at the cell wall.

EXPERIMENTAL PROCEDURES

Strains and growth conditions

The *Saccharomyces cerevisiae* strain used in this study was GRA007 (*MATa leu2Δ0 ura3Δ0 crh2::His3 crh1::hphMX4*) [21]. Cells were grown at 30ºC in Synthetic complete (SC) medium (0.17% yeast nitrogen base, 0.5% ammonium sulphate, 2% glucose) or minimal medium (2% glucose, 0,7% yeast nitrogen base) plus amino acids requirements in the case of strains bearing plasmids. Routinely, cells were grown overnight in liquid media at 220 rpm and to an optical density of 0.8-1 (A_{600}), then the culture refreshed to 0.2 (A_{600}) in YPD, grown at 30ºC for three-four additional hours to yield cells at logarithmic phase and processed depending on the experimental approach.

Plasmids and Site-directed mutagenesis

The QuikChange II Site-Directed Mutagenesis Kit (Agilent Technologies, Strategene, La Jolla, CA) was used to create single point mutations in the pNBc13 (*CRH2*-HA) and pNBc15(*CRH1*-HA) plasmids [37]. Primers design and PCR conditions were carried out as described in the manufacturer's instructions. A list of the site-directed mutant constructs created with the primer pairs used in each case is included in Table S1. The presence of the desired mutation in the resulting mutated plasmids was always verified by DNA sequencing. Plasmids pNBc13, pNBc15 and the corresponding mutant versions were transformed in a *crh1Δ crh2Δ* strain by the lithium acetate protocol [38].

Preparation of yeast extracts and immunoblotting procedures

The procedures used for immunoblot analyses, including cell collection and lysis, collection of proteins, fractionation by SDS-PAGE, and transfer to nitrocellulose membranes, have been described previously [39]. For inmmunoblotting, membranes were blocked for 1 h with Odyssey blocking buffer and incubated overnight with the primary antibody in the same buffer but containing 0.1% Tween 20. Immunodetection of HA-tagged proteins, actin and His-tagged proteins was carried out using the anti-HA monoclonal antibody 16B12 (Covance, Emeryville,CA), the mouse anti-actin monoclonal antibody C4 (ICN Biomedical, Aurora, OH) and the monoclonal anti-polyHistidine Clone HIS-1 (Sigma-Aldrich, St. Louis,MO), respectively. Membranes were washed and incubated for 1 hour with the secondary antibody, IgG IRdye ® 680 anti-mouse antibody (LI-COR Biosciences, Germany). Finally, membranes were scanned, after washing, with the Odyssey Infrared Imaging System (Lycor, Fisher Scientific).

Modeling of *Sc*Crh1

Crh1 was modelled using the program Modeller [40] and PDB 1UOA or 2AYH [35, 36], corresponding to the hybrid *Paenibacillus macerans* lichenase (*Pm*lichenase) H(A16-M), as the templates. H (A16-M) is derived from the 1,3-1,4-β-glucanase from *Bacillus macerans* in which the 16 N-terminal residues have been replaced by the respective residues of the enzyme from *Bacillus amyloliquefaciens*. Initially PDBs 1AJK, 1BYH, 1CPN, 1GBG, 1UOA and 2AYH were selected based on their sequence identity to *Sc*Crh1. Among these proteins, PDBs 1U0A or 2AYH were selected due to their high sequence identity of 27% with *Sc*Crh1 and crystallographic high resolution (1.64 and 1.6 Å,

respectively). The modeled sequence of *Sc*Crh1 contained amino acids from Ala55 to Thr255. The three-dimensional structure was visualized and analyzed with COOT and PyMOL.

For Crh2, the modeling failed due to a combination of two reasons: a poor sequence identity with potential templates; and a CBM only present in this enzyme, unlike Crh1, that structurally has not been solved and for which not structural homologues are known.

Incorporation of fluorescent oligosaccharides in living yeast cells

The labelling assays were carried out as previously described [22, 23, 41]. Either SR-β-1,3 or SR-β-1,6 oligosaccharide mixtures (DP 2-7) or individual SR-chito-oligosaccharides (DP4) were added to the cell culture for a final concentration of 7.5 µM. The labelling was carried out at 30ºC, overnight in the dark, in a final volume of 200 µl of cell culture adjusting the number of cells to have the culture in early stationary phase after the overnight incubation. After labelling, cultures were centrifuged, the pellet then washed two times with 20% (v/v) ethanol, two times with water and finally resuspended in water. Labelled cells were then analysed by fluorescence microscopy, using a Nikon TE2000 fluorescence inverted microscope equipped with a CCD. Digital images were acquired with an Orca C4742-95-12ER camera (Hamamatsu Photonics, Japan) and processed with the Hamamatsu HCImage Imaging systems software. Fluorescence intensity was quantified using the HCI imaging tools. Data were collected by analysis of approximately 2000 cells from at least three independent experiments and subjected to a non-parametric *t-test* analysis using GraphPad prism software. Data were considered significant if $P < 0.05$.

Immunodetection and fluorescence microscopy

For immunodetection of Crh1-HA and Crh2-HA, 3 ml of cells were collected, washed twice with PBS and suspended in 10% formaldehyde for permeabilization. After 60 min at room temperature, cells were washed again twice with PBS and incubated with goat serum diluted 1:1000 (Sigma-Aldrich, St. Louis, MO) for 30 min at room temperature. After additional washing with PBS, cells were incubated overnight at 4°C with the anti-HA monoclonal antibody 16B12 (Covance, Emeryville,CA), washed three times with PBS and incubated with the Alexa Fluor ® 488 goat anti-mouse IgG (Invitrogen) for 45 min at room temperature. Finally, cells were analyzed by fluorescence microscopy using a Nikon TE2000 fluorescence inverted microscope equipped with a CCD.

Phenotypic analysis

Sensitivity of the different strains to Congo Red was determined basically as previously described [39]. Yeast cells were grown at 24ºC in YPD or SD-Ura (for cells bearing plasmids). 5 µl of log-phase cultures (approximately $15x10^3$ cells) plus five 1:5 serial dilutions were spotted onto YPD solid media containing different concentrations of Congo Red. Growth was monitored on the plates after incubation over 2 days at 30ºC.

Production of recombinant Crh1 and Crh2 proteins

Production and purification of the recombinant proteins Crh1 and Crh2 in the *P. pastoris, GS115* strain (Invitrogen) transformed with the plasmids pHIL-CRH1-MHs and pHIL-CRH2-His[23, 42] was carried out as previously described [23]. Briefly, cells were cultured in Buffered Glycerol-Complex (BMGY) medium at 30ºC for 2 days, then transferred to Buffered Methanol-complexed (BMMY) medium at 20ºC for 5 days, adding 1.25 % of methanol every 24 h to induce the expression of the protein. Supernatants were recovered by centrifugation, filtered through a 0.22 µm filter, followed by concentration to the desired volume using a Pellicon XL filter (Millipore, Madrid, Spain).The proteins were purified by affinity chromatography using Ni^{+2}-NTA agarose columns (Qiagen). To determine the efficiency of the production, recombinant proteins were monitored by SDS-PAGE and Western blotting and quantified by using **a** NanoDrop 2000C spectrophotometer microvolume sample retention system (Thermo Scientific).

Chitin-binding assays

200 µl of chitin beads (New England, Biolabs, UK) were covered with BSA (Bovine Serum Albumin) in 200µl of citrate buffer 0.1M pH 3,5 at 37ºC. After 90 min, beads were washed twice with 0.1M citrate buffer pH 3,5 and incubated with 5 µg of the purified recombinant protein in a final volume of 200µl of 0.1M citrate buffer pH 3,5. After incubation at 37ºC for 2,5 hours, the slurries were centrifugated at 12.000 rpm for 5 min and washed five times with the same buffer and three times with the same buffer plus 1M NaCl. Then, beads were resuspended in 200µl 1X Laemmli buffer and incubated at 99ºC for 10 min. Samples were centrifuged at 12.000 rpm and the supernatant subjected to 10% SDS-PAGE electrophoresis. Finally, immunoblotting was carried out as described above.

RESULTS

We have previously set up an *in vivo* assay to measure the transglycosylase activity mediated by Crh proteins using fluorescent sulforhodamine laminari-, pustulan or chito-oligosaccharides [22, 23] as artificial chitin acceptors *in vivo*. Fluorescence was detected mainly in bud scars and at a lower level in the lateral cell wall, being dependent on the Crh proteins, as deduced from the fact that there is almost no fluorescence detected in a *crh1*Δ *crh2*Δ strain [22, 23]. The activity of Crh2 seems to be more relevant *in vivo* as deduced from the quantification of the fluorescence incorporated in single *crh1*Δ and *crh2*Δ mutants [23] as well as from the analysis of the chitin covalently linked to glucan in these strains [20, 21]. However, both proteins show a redundant activity and therefore overexpression of either *CRH1* or *CRH2* from a multicopy plasmid (plasmids pNBC15 and pNBC13) in a mutant strain *crh1*Δ *crh2*Δ, devoted of the transglycosylase glucan-chitin activity, results in the recovery of this activity measured as incorporation of the fluorescent sulforhodamine laminari- (Figure 1A), pustulan (Figure 1B) or chito-oligosaccharides (Figure 1C) into the bud scars of exponentially growing cells. On the basis of these results, we would be able to explore the functional relevance of individual residues of both Crh1 and Crh2 by expression of wild-type and site-directed mutated versions of *CRH1* and *CRH2* in a *crh1*Δ *crh2*Δ strain, and analysis of the transglycosylase activity *in vivo*. With the aim of checking the levels of the expressed proteins by immunoblotting procedures and proper localization, by immunofluoresescence assays, HA-tagged versions of *CRH1* and *CRH2* constructions (Table S1) were designed.

A Crh1 model shows the typical β-jelly folding and serves as a template to infer residues involved in catalysis and binding to carbohydrates

To gain information on how Chr1 and Crh2 perform carbohydrate binding and catalysis, we tried to generate models of these proteins based on the three-dimensional structure of proteins belonging to family 16 of glycosyl hydrolases (GH16) already characterized by X-ray crytallography . A model of Crh1, based on the structure of the *Bacillus* H (A16-M) 1,3-1,4-β-D-Glucanase [35, 36](see experimental procedures for details), was generated. For Crh2, the modeling failed due to a combination of two reasons: a poor sequence identity with potential templates; and a carbohydrate binding domain (CBM18) only present in this enzyme.

The model of Crh1 (Figure 2, panel B) shows the typical β-jelly roll arrengment which is common in GH16 family [30, 36, 43]. The core of the protein is formed by two antiparallel β sheets stacked in a sandwich-like manner. A deep channel cross the concave face which contains a number of aromatic residues on its walls and acidic residues at the bottom, defining the carbohydrate binding cleft. A closer inspection of the model with a tetrasaccharide, obtained from a superimposition of Crh1 with *Pm*lichenase in complex with β-1,4-tetrasaccharide [36], shows the donor and the acceptor sites of Crh1 with Glu134 and Glu138 as the nucleophile and acid/base respectively on a single strand that is offset of the center of the sheet (Fig. 2, panel B). To validate this model we have further performed site-directed mutagenesis in residues involved in catalysis and carbohydrate binding. Firstly we evaluated Glu134, Asp136 and Glu138 as potential catalytic residues based on the alignment of *Sc*Crh1 with *Pm*lichenase (Figure 2A). The consensus pattern and the logo sequence for the family 16 (GH16) of glycosyl hydrolases at the Prosite database is shown in Figure 3A (left panel). Multiple alignment of the sequences of the hypothetical catalytic domain of Crh1 and Crh2 from *Saccharomyces cerevisiae* and those from their fungal orthologs in *Candida albicans* and *Aspergillus fumigatus*,1,3-1,4-β-D glucanases from bacteria and xyloglucan endotransglycosidases from plants (Figure 3A) show two glutamic residues (E134 and E138 in Crh1), two aspartic acids residues (D133 and 136 in Crh1) and one glycine (G141 in Crh1), shown in bold in Figure 3A, conserved in all of them. Residues E134 and E138 should correspond to the general acid-base and nucleophile residues of the *Bacillus licheniformis* endo-β-1,3-1,4 glucanase enzyme, respectively [44, 45]. Glu134, Asp136 and Glu138 amino acids of Crh1 were mutated to the corresponding Gln and Asn (Crh1-E134Q, Crh1-E138Q and Crh1-D136N). Quantification of the fluorescence incorporated into bud scars of *crh1*Δ *crh2*Δ cells expressing wild-type or mutated versions of Crh1 grown in the presence of β-1,3-glucooligosaccarides-SR, β-1,6-glucooligosaccarides-SR or Chitoligosacharides-SR showed that these residues are essential in the incorporation of the different SR-oligosaccharides into the chitin molecule acting as the donor at the cell wall (Figure 3B, left panel). Moreover, contrary to the pNBC15 construction (Crh1-HA) none of the mutant constructs were able to revert the sensitive phenotype to Congo red of a *crh1*Δ *crh2*Δ strain (Figure 3C), further proving the importance of those residues in the transglycosilase activity *in vivo*.

In agreement with the similarity and redundancy between Crh1 and Crh2, mutagenesis of the corresponding Crh2 residues within the catalytic site, namely E166Q,

E10Q and D168N9, also resulted in the complete lack of Crh2 function (Figure 3 B and C). Based on the Crh1 model (Figure 2), other residues of this protein that might be involved in binding to carbohydrates were Phe152, Tyr160 and Trp219. F152A, Y160A and W219A mutated versions of *CRH1* were created to evaluate their role in binding whereas Y103A and M105A were generated as positive controls since. The transglycosylase activity of Crh1 and its mutant variants was evaluated *in vivo* in *crh1*Δ *crh2*Δ cells transformed with the plasmid pNBC15 (CRH1-HA) or the corresponding mutated versions. As expected, both Y103A and M105A did not show significant changes in activity compared to the WT enzyme confirming the quality of the model. In contrast, the activity of Y160A was significantly reduced respect to the wild type whereas this effect was more pronounced for the F152A mutation and particularly for W219A in which the incorporation of the different SR-oligosaccharides was almost lack. It is important to note that all these mutant versions as well those of Crh1 and Crh2 described above were produced at levels similar to those of the wild type protein (Figure S1) and localized properly (Figure S2). Therefore, these results confirm the importance of F152, Y160 and particularly W219 in binding to sugars.

Analysis of the carbohydrate-binding module (CBM18) of Crh2

Carbohydrate-binding modules (CBMs) are present in many carbohydrate-active enzymes, having a functional role to increase their catalytic efficiency [46, 47]. Thus, proteins containing a chitin-binding domains have been found in many organisms, being classified into several CBM families in the CAZy database (families 1,2, 12, 14, 18, 19 and 33) [25]. Interestingly, a CBM18 is included at the N-terminus of the mature Crh2 protein, which is not present in Crh1. In agreement with the glucan-chitin transglycosilase activity of Crh1 and Crh2 [21-23], both proteins but not GST, used as negative control, were able to bind to chitin *in vitro* in a pull down assay, apparently with similar efficiencies (Figure 4). On the basis of the specific presence of the CBM18 domain in Crh2, we were prompted to study the function of this domain *in vivo*. The CBM18 of Crh2 extends from residue 22 to residue 63 and corresponds to chitin-binding domain type-1, a common structural motif of 30 to 43 residues present in most of chitin-binding proteins [48]. The consensus pattern and the logo sequence defined at Prosite database for this motif is shown in Figure 6A together with a multiple sequence alignment of several proteins that contains this pattern, including Crh2, several fungal Crh2 orthologs, hevein, wheat germ agglutinins and plant endochitinases. The structure of this domain is organized around a conserved four-disulfide core [48, 49]. To verify the importance of some of the conserved cysteine residues in the

folding of the CBM of Crh2, cysteins at 33, 39 and 40 were replaced by serine. As shown in Figure S1, no Crh2 was detected in total extracts from *crh1*Δ*crh2*Δ strain expressing any of the mutated proteins, suggesting that these Cys are involved in essential disulfide bonds for protein folding and stability.

To further studying the functional role of individual residues of the CBM, transglycosylase activity of Crh2 was measured by incorporation of SR- β-1,3-glucooligosaccarides, SR-β-1,6-glucooligosaccarides-SR or SR-Chitoligosacharides-SR in *crh1*Δ *crh2*Δ cells transformed with the plasmid pNBC13 (CRH2-HA) or the corresponding pNBC13 expressing different site-directed mutated versions of *CRH2*. The residues analyzed included Pro34, Ser41, Gly44, Gly47 and Tyr51, all of them highly conserved in the pattern (Figure 6A), Pro38 and Gly49 which are present in all Crh2 fungal orthologs, and additional aromatic residues including, Phe26, Tyr43, Tyr60 and Phe62, because aromatic side chains are strongly associated to carbohydrate binding [46]. In all cases the corresponding aminoacid was mutated to Ala. All Crh2 versions were expressed to levels similar to those of the wild type (Figure S1) and localized properly (Figure S2). Quantification of the fluorescece associated to the bud scars revealed that the levels of transglycosylase activity of mutants F26A and P34A, F26 being included in the chitin-binding domain but outside of the consensus pattern, were similar to those of Crh2 (Figure 6B), whereas in the case of Y60A the activity slightly decreased. However, a significant reduction of enzymatic activity (around 50%-60%) with respect to the wild-type protein was found for mutants P38A, S41A, Y43A, G44A, G47A, Y51A and F62A. This activity was even severely impaired in mutant G49A. Moreover, as inferred from results shown in Figure 6C, the levels of transglycosilase activity for each mutant perfectly correlated with the phenotype of Congo Red sensitivity of *crh1*Δ *crh2*Δ cells expressing wild-type or mutated versions of Crh2, further demonstrating the importance of the above mentioned residues within the CBM of Crh2 for its activity.

DISCUSSION

Conserved fungal proteins belonging to the *S. cerevisiae* Crh family [18] have been included in the family 16 of gycosyl hydrolases [25]. We have previously demonstrated that both Crh1 and Crh2 are responsible *in vivo* for the cross-links between chitin and glucan at the yeast cell wall [20, 21]. Moreover, these cross-links are essential for the control of morphogenesis at the mother-bud neck [50]. The Crh proteins act as

transglycosylases. *In vivo*, they incorporate β-1,3-linked, β-1,6-linked and chito-oligosaccahrides into the cell wall as chitin acceptors [22, 23]. *In vitro*, soluble recombinant Crh1 and Crh2 proteins also act as chitin transglycosylases using soluble chitin derivates as glycosyl donors and oligosaccahrides derived from β-1,3-glucan, β-1,6-glucan and chitin as acceptors [23].

In contrast to the functional knowledge gained in the last few years, there is a lack of structural information about the Crh proteins. In the absence of crystallographic studies and taking into account that the three-dimensional structure of several 1,3-1,4-β-glucanases from *Bacillus*, free or complexed with a β-glucan oligosaccharide, has been already solved [35, 36, 43], we have inferred a model for the structure of Crh1. Site-directed mutagenesis of both *CRH1* and *CRH2*, together with the functional analysis of the transglycosylase activity of the respective proteins, allowed us not only to validate this model but also, together with our previously knowledge on *in vivo* and *in vitro* activities to suggest a catalytic mechanism for Crh1 and Crh2.

The catalytic machinery of bacterial endo-1,3-1,4-β-glucanases of the family 16 is highly conserved and involves an active center with two acidic catalytic residues acting as the nucleophile (Glu134 in *Bacillius licheniformis*) and general acid/base (Glu138 in *Bacillius licheniformis*) residues respectively, and a third acidic residue (Glu136 in *Bacillius licheniformis*) which forms a tight hydrogen bond with the nucleophile, therefore acting as an auxiliary residue important for catalysis [27, 36, 44, 51]. The three-active site acidic residues are conserved with similar conformations in the family GH16 structures [30]. Both enzymes, Crh1 and Crh2, conserve the structure of this catalytic site. The catalytic residues of Crh1 and probably Crh2 should be anchored in one β-strand with the nucleophile (E134 in Crh1 and E166 in Crh2), the general acid/base residue (E138 in Crh1 and E170 in Crh2) and the auxiliary Glu at 136 (Crh1) or 168 (Crh2) being essential for their transglycosylase activities.

Therefore, a plausible mechanism for reactions catalyzed by Crh1 and Crh2 proteins could include the cleavage of the β-(1,4) linkages of the chitin backbone and subsequently transfer the fragment of the original substrate through the newly formed reducing end onto the acceptor that could be either β-1,3 glucan, β-1,6 glucan or chitin. In agreement, we have previously shown that both Crh1 and Crh2 exhibit a weak chitinolytic activity, that in the case of Crh1 is markedly stimulated by N-acetyl chitooligosaccharides and laminari-oligosaccharides [23]. Based on the data presented here and in the context of the catalytic mechanisms proposed for enzymes of the family 16 [27, 30, 34], it is tempting

to speculate that both proteins would act as retaining gycosyl hydrolases probably operating via a double displacement mechanism, following the classical SN2 reaction observed for other transglycosylases and in particular for hydrolases of the family 16, that results in the retention of the configuration of the anomeric carbon. In the glycosylation step, the side chain carboxylate of residue at E138 (Crh1) or E170 (Crh2) should act as a nucleophile that attacks the anomeric carbon of the sugar ring in a reaction assisted by the simultaneous proton transfer to the glycosidic oxygen from the general acid residue at E134 (Crh1) or E166 (Crh2). In the deglycosylation step, Glu134 (Crh1) or Glu166 (Crh2) should function as a general base to activate the incoming nucleophile, an alcohol in this case, which hydrolyze the glycosyl-enzyme intermediate. In agreement with an important role for Asp136 of Crh1 (Asp 168 in Crh2) in the catalysis, Asp136 of the *Bacillus licheniformis* enzyme was also found to be important, possibly modulating the pKa of the general acid [27]. Based on the role of the corresponding residue Asp107 of the hybrid 1,3-1,4-β-D-glucanase H(A16-M), residues Asp136 and Asp168 of Crh1 and Crh2 respectively, could have a role not only stabilizing the nucleophile but also contributing to carbohydrate binding [36].

Further validation of our Crh1 model came out from results with the Y103A and M105A mutants showing a trsnglycosylase activity similar to that of the wild type Crh1. In the model, both residues, Y103 and M105, are anchored in one of the β strands of the β-jellyroll-type structure, but with their side-chains pointing outside of the sugar binding cleft. Additionally to the residues within the catalytic site commented above, the Crh1 model suggested the participation of residues Phe152, Tyr160 and Tyr219 in sugar binding. This turned out to be the case since transglicosylase activity of Crh1 is significantly reduced in mutants F152A and Y160 and severely impaired in mutant W219A. Side-chains of Tyr219 should be oriented towards the donor site of Crh1, whereas Phe152 and Tyr160 should interact with the substrate at the acceptor site (Figure 2). Active clefts of sugar binding enzymes are often lined with several aromatic residues that can establish van der Waals interactions with potential polysaccharide substrates [30]. The structure of the *Bacillus* 1,3-1,4-β-D-glucanase in complex to β-glucan tetrasaccharide shows that the substrate binding cleft includes residues acting as hydrogen donors or acceptors to form hydrogen bonds to the glycosyl units in different subsites (-IV to-I) but additionally aminocids with aromatic-side chains that should promote binding and positioning of the polysaccharide substrate [36]. Interestingly, the aromatic ring of Trp184

of lichenases, which is equivalent to position Trp 219 of Crh1, is positioned perpendicular to the glucosyl ring in subsite -I, forming a hydrogen bond to Glc-I O^6 [36].

As commented above, both Crh1 and Crh2 are redundant proteins required for the crosslinking between chitin and glucan at the cell wall [20, 21]. Therefore, the lack of chitin covalently bound to β-1,3 and β-1,6 glucan or the absence of transglycosylase activity measured *in vivo* by incorporation of fluorescent-labeled chitin acceptors requires the simultaneous deletion of *CRH1* and *CRH2* [20, 22]. In spite of their redundant function, analysis of the above mentioned activities in single *crh1*Δ and *crh2*Δ strains suggest that the activity of Crh2 is more important *in vivo* [21, 23], at least under normal growth conditions. This could be explained, at least in part, by differences in gene expression between *CRH1* and *CRH2* [18] and consequently in the levels of Crh1 and Crh2 [18, 21] and by their different modes of action to process chitin molecules *in vitro* [23]. Additionally, Crh2, but not Crh1, includes a Carbohydrate-binding module (CBM18) at the N-terminus of the mature protein. Therefore it was interesting to test if this domain, like other CBMs present in many carbohydrate-active enzymes [46, 47], could have a functional role to increase substrate affinity and enhance catalytic efficiency of Crh2. We have shown here that cysteins at 33, 39 and 40 within this domain are probably involved in disulfide bonds and therefore essential for protein folding and stability.

A significant reduction in the trasnglycosylase activity of Crh2 was found when several residues of the CBM were individually mutated in *CRH2*, indicating that this domain is required for increasing the catalytic efficiency of the protein. Aromatic side chains within CBMs are strongly associated to carboydrate binding [46]. In agreement, mutations at Tyr43, Tyr51, Phe62 and to a lesser extent Tyr60 reduce the transglycosylase activity of Crh2 *in vivo.* Moreover, mutagenesis of residues Pro38, Ser41, Gly44, Gly47 and particularly Gly49 within consensus pattern of the chitin binding domain also affects the catalytic activity, further indicating the importance of the CBM for the transglycosylase activity of Crh2. The chitin-binding domain of Crh2 must be structurally related to other similar domains present in proteins belonging to the family 18 of CBMs like WGA or hevein. Information about hevein and its binding features to diferent ligands have been inferred from X-ray crystallography and NMR studies [52-54]. Thus, several residues involved in the recognition of chitooligosaccahrides have been identified. Aromatic residues Trp21, Trp23 and Tyr30 of hevein stabilize the complex by CH-π interactions and van der Waals contacts. In agreement, Tyr51 and Tyr43 of Crh2, corresponding to hevein Tyr30 and Trp21, respectively are important for its transglycosylase activity. Additionally

the hydroxyl groups of Ser19 and Tyr30 of hevein are involved in hydrogen bonding with the acetamide carbonyl group and the hydroxyl group at position 3 of a GlcNAc residue [54] and mutagenesis of the corresponding residues in Crh2 (Ser41 and Tyr51) also affects the catalytic activity. Other residues of Crh2 like Gly44 and Gly47, involved in the transglycosylase activity, are also conserved in hevein (Gly 22 and Gly 25).

Although only the crystallization and characterization of the corresponding three-dimensional structures of Crh1 and Crh2 will uncover precisely those residues interacting with the donor and acceptor molecules as well as the molecular reasons for the broad acceptor substrate specificity of these enzymes, the data presented here shed light into the catalytic mechanisms mediated by the transglycosylases Crh1 and Crh2, the first transglycosylases involved in the cross-linking between polymers at the fungal cell wall.

Acknowledgments

We are indebted to Enrico Cabib for his support and critical reading of the manuscript.

Funding

This work was supported by grants BIO2010-22146 (MICINN, Spain), GR58/08 (Ref. 920640/UCM), S2010/BDM-2414 (Comunidad de Madrid) and 06-RNP-132 (ESF) to J.A, grant no. 2/0011/09 from the Agency for Science VEGA (Slovakia) to V. F. N.B. is the recipient of an FPI Ph.D. fellowship (BES-2008-003171) from MICINN.

Figure Legends:

Figure 1. Overexpression of *CRH1* or *CRH2* in *crh1*Δ *crh2*Δ cells reverts the defect of this mutant to incorporate different SR-oligosaccharides into the cell wall. *crh1*Δ *crh2*Δ cells and the same mutant transformed with pNBC15 (CRH1-HA) or pNBC13 (CRH2-HA) were labelled overnight with: SR- β-1,3 oligosacharides (DP 2-7) (panel A), SR-β-1,6 oligosacharides (DP 2-7) (Panel B) or SR-Chitotetraose (Panel C) and analyzed by fluorescence microscopy. Oligosaccharide incorporation in the bud scars was quantified in the images by using HCimage Imaging software and shown in bar histograms. The signals, expressed as arbitrary fluorescence units, correspond to the media of three independent experiments. Data are means ± SD. Statistical analysis was done with a two-tailed, unpaired, Student's *t* test ($P < 0.05$). Compared to the *crh1Δcrh2Δ* strains, ***$P < 0.0001$.

Figure 2. Overall structure of ScCrh1 model. A) Multiple alignment of ScCrh1, ScCrh2 and PmLichenase. The signal peptide, the CBM of ScCrh2 and Ser/Thr rich domain are shown in green, magenta and blue colours, respectively. Mutations described in this manuscript are illustrated in yellow. B) Schematic ribbon diagram of Crh1 model showing a β-jelly roll arrengment which is common in GH16 famliy. By comparison with bacterial

1,3-1,4-β-D-glucanase crystal structures, the catalytic machinery is shown in blue sticks while potential residues involved in sugar binding are shown in black. Residues Y103 and M105, with their side-chains pointing outside of the sugar binding cleft and used as controls are also shown. A tetrasaccharide based on a superimposition of ScCrh1 with Pmlichenase (*Bacillus* H (A16-M) 1,3-1,4-β-D-Glucanase in complex with β-1,4-tetrasaccharide [35, 36] is shown as green sticks to indicate the donor and acceptor sites of ScCrh1. C) Surface representation of the active site. Mutated residues of the catalytic machinery are shown in pink and other mutated residues are shown in yellow.

Figure 3. Residues within the catalytic site of Crh1 and Crh2 are essential for the transglycosylase activity of these proteins *in vivo*. A) Consensus pattern and sequence logo of the glycosyl hydrolases family 16 catalytic domain generated by the Prosite database is shown in the left panel. The overall height of each stack indicates the sequence conservation at that position (measured in bits), whereas the height of symbols within the stack reflects the relative frequency of the corresponding amino acid at that position. Multiple sequence alignment of the conserved catalytic domain Crh proteins from *S. cerevisiae* and their orthologs in *C.albicans, A. fumigatus*, *B. licheniformis* (1-3-1-4 β-glucanase) and *A. thaliana* (xyloglucan endotransdglycosidase) is shown in the right panel. The sequences were aligned using ClustalW. Conserved residues are underlined and dotted, while identical residues are indicated in bold and labelled with asterisks. B) Transglicosylase activity measured by incorporation of SR- β-1,3 oligosacharides (DP 2-7), SR-β-1,6 oligosacharides (DP 2-7) or SR-Chitotetraose into a *crh1Δcrh2Δ* strain transformed with plasmids pNB15 (*CRH1*), pNBC13 (*CRH2*) and plasmids expressing the indicated site-directed mutant versions of *CRH1* or *CRH2*, respectively. Oligosaccharide incorporation in the bud scars was quantified and shown in bar histograms. The signals, expressed as arbitrary fluorescence units, correspond to the media of three independent experiments. Data are means ± SD. Statistical analysis was done with a two-tailed, unpaired, Student's *t* test ($P < 0.05$). Compared to the *crh1Δcrh2Δ* strains expressing wild-type *CRH1* or *CRH2*, ***$P < 0.0001$. C) Sensitivity to Congo Red (CR) of the same yeast strains. Strains were exponentially grown and 1/5 dilution series were spotted into YPD plates containing 100 μg/ml of Congo Red.

Figure 4. Residues M105, W219 and Y160 of Crh1 are important for the transglycsylase activity. A) Transglicosylase activity measured by incorporation of SR- β-1,3 oligosacharides (DP 2-7), SR-β-1,6 oligosacharides (DP 2-7) or SR-Chitotetraose into a *crh1Δcrh2Δ* strain transformed with plasmids pNB15 (*CRH1*), and plasmids expressing the indicated site-directed mutant versions of *CRH1* or *CRH2*. Oligosaccharide incorporation in the bud scars was quantified and shown in bar histograms. The signals, expressed as arbitrary fluorescence units, correspond to the media of three independent experiments. Data are means ± SD. Statistical analysis was done with a two-tailed, unpaired, Student's *t* test ($P < 0.05$). Compared to the *crh1Δcrh2Δ* strain expressing wild-type *CRH1*, ***$P < 0.0001$, **$P < 0.003$. B) Sensitivity to Congo Red (CR) of the same strains indicated above. Strains were exponentially grown and 1/5 dilution series were spotted into YPD plates containing 100 μg/ml of Congo Red.

Figure 5. Crh1 and Crh2 bind to Chitin. Crh1 and Crh2 proteins were incubated with chitin beads in citrate buffer 0,1 M pH 3,5 at 37ºC for 90 min. After incubation, the beads were washed repeatedly (see experimental procedures for details). The material bound to the beads was separated by 10% SDS-PAGE and immunoblotted with the anti-HA

monoclonal antibody 16B12. As a controls, native GST protein and Crh1-HA and Crh2-HA heat-inactivate proteins were included.

Figure 6. Characterization of residues within the carbohydrate-binding module (CBM18) of Crh2 in the transglycosilase activity of this protein *in vivo.* A) Consensus pattern and sequence logo of the family 18 CBM, generated by Prosite is shown in the left panel. Multiple sequence alignment of the CBM of Crh2 (*Saccharomyces cerevisiae*), Utr2 (*Aspergillus fumigatus*), Utr2 (*Candida albicans*), Crh2 (*Yarrowia lipolytica*), FoxB (*Fusarium oxysporum*), C5P1l7 (*Coccidioides posadasii*), E6QY05 (*Cryptococcus gattii*,), Hevb6x5 (*Hevea brasiliensis*), ChiB (*Arabidopsis thaliana*) and Agi1 (*Triticum aestivum*) is shown in the right panel. The sequences were aligned using ClustalW. Conserved residues are underlined and dotted, while identical residues are indicated in bold and labelled with asterisks. B) Transglicosylase activity of *crh1Δcrh2Δ* strains transformed with pNBC13 (CRH2-HA) or plasmids expressing the indicated site-directed mutant versions of *CRH2*. Oligosaccharide incorporation in the bud scars was quantified and shown in bar histograms. The signals, expressed as arbitrary fluorescence units, correspond to the media of three independent experiments. Data are means ± SD. Statistical analysis was done with a two-tailed, unpaired, Student's *t* test ($P < 0.05$). Compared to the *crh1Δcrh2Δ* strain expressing wild-type *CRH2*, ***$P < 0.0001$, **$P < 0.003$**.** C) Sensitivity to Congo Red (CR) of the same yeast strains. Strains were exponentially grown and 1/5 dilution series were spotted into YPD plates containing 300 μg/ml of Congo Red.

Supplementary Figure 1. Quantification of Crh1-HA and Crh2-HA protein levels in the different mutants. Total protein extracts from exponential cultures of a *crh1Δcrh2Δ* strain transformed with the Yep352 empty vector or Yep352 harbouring *CRH1, CRH2 or the corresponding CRH* mutant gene versions were subjected to 10% SDS-PAGE and immunoblotted using the anti-HA monoclonal antibody 16B12. Protein loading was monitorized using an anti-actin mAb

Supplementary Figure 2. Localization of Crh1-HA and Crh2-HA in the different site-directed mutant strains. Crh1-HA and Crh2-HA was immunodetected as detailed in Experimental Procedures in *crh1*Δ *crh2*Δ cells transformed with pNBC15 plasmid (Yep352-*CRH1*-HA) and the indicated *CRH1* site-directed mutants (Panel A) or pNBC13 (Yep352-CRH2-HA) and the corresponding *CRH2* site-directed mutants (Panel B).

REFERENCES

1 Cid, V. J., Duran, A., del Rey, F., Snyder, M. P., Nombela, C. and Sanchez, M. (1995) Molecular basis of cell integrity and morphogenesis in Saccharomyces cerevisiae. Microbiol.Rev. **59**, 345-386

2 Levin, D. E. (2011) Regulation of cell wall biogenesis in Saccharomyces cerevisiae: the cell wall integrity signaling pathway. Genetics. **189**, 1145-1175

3 Lesage, G. and Bussey, H. (2006) Cell wall assembly in Saccharomyces cerevisiae. Microbiol.Mol.Biol.Rev. **70**, 317-343

4 Orlean, P. (2012) Architecture and biosynthesis of the Saccharomyces cerevisiae cell wall. Genetics. **192**, 775-818. doi: 710.1534/genetics.1112.144485.

5 Kollar, R., Petrakova, E., Ashwell, G., Robbins, P. W. and Cabib, E. (1995) Architecture of the yeast cell wall. The linkage between chitin and beta(1-->3)-glucan. The Journal of biological chemistry. **270**, 1170-1178

6 Kollar, R., Reinhold, B. B., Petrakova, E., Yeh, H. J., Ashwell, G., Drgonova, J., Kapteyn, J. C., Klis, F. M. and Cabib, E. (1997) Architecture of the yeast cell wall. Beta(1-->6)-glucan interconnects mannoprotein, beta(1-->)3-glucan, and chitin. The Journal of biological chemistry. **272**, 17762-17775

7 Kapteyn, J. C., Van Egmond, P., Sievi, E., Van Den Ende, H., Makarow, M. and Klis, F. M. (1999) The contribution of the O-glycosylated protein Pir2p/Hsp150 to the construction of the yeast cell wall in wild-type cells and beta 1,6-glucan-deficient mutants. Molecular microbiology. **31**, 1835-1844

8 Kapteyn, J. C., Van Den Ende, H. and Klis, F. M. (1999) The contribution of cell wall proteins to the organization of the yeast cell wall. Biochim Biophys Acta. **1426**, 373-383

9 Klis, F. M., Mol, P., Hellingwerf, K. and Brul, S. (2002) Dynamics of cell wall structure in Saccharomyces cerevisiae. FEMS Microbiol Rev. **26**, 239-256

10 Kollar, R., Reinhold, B. B., Petrakova, E., Yeh, H. J., Ashwell, G., Drgonova, J., Kapteyn, J. C., Klis, F. M. and Cabib, E. (1997) Architecture of the yeast cell wall. Beta(1-->6)-glucan interconnects mannoprotein, beta(1-->)3-glucan, and chitin. J.Biol.Chem. **272**, 17762-17775

11 Cabib, E., Bowers, B. and Roberts, R. L. (1983) Vectorial synthesis of a polysaccharide by isolated plasma membranes. Proc.Natl.Acad.Sci.U.S.A. **80**, 3318-3321

12 Shematek, E. M., Braatz, J. A. and Cabib, E. (1980) Biosynthesis of the yeast cell wall. I. Preparation and properties of beta-(1 leads to 3)glucan synthetase. J Biol Chem. **255**, 888-894

13 Montijn, R. C., Vink, E., Muller, W. H., Verkleij, A. J., Van Den Ende, H., Henrissat, B. and Klis, F. M. (1999) Localization of synthesis of beta1,6-glucan in Saccharomyces cerevisiae. J Bacteriol. **181**, 7414-7420.

14 Roh, D. H., Bowers, B., Riezman, H. and Cabib, E. (2002) Rho1p mutations specific for regulation of beta(1-->3)glucan synthesis and the order of assembly of the yeast cell wall. Mol.Microbiol. **44**, 1167-1183

15 Shaw, J. A., Mol, P. C., Bowers, B., Silverman, S. J., Valdivieso, M. H., Duran, A. and Cabib, E. (1991) The function of chitin synthases 2 and 3 in the Saccharomyces cerevisiae cell cycle. J.Cell Biol. **114**, 111-123

16 Cabib, E. and Duran, A. (2005) Synthase III-dependent chitin is bound to different acceptors depending on location on the cell wall of budding yeast. J.Biol.Chem. **280**, 9170-9179

17 Cabib, E., Bowers, B., Sburlati, A. and Silverman, S. J. (1988) Fungal cell wall synthesis: the construction of a biological structure. Microbiol Sci. **5**, 370-375.

18 Rodriguez-Pena, J. M., Cid, V. J., Arroyo, J. and Nombela, C. (2000) A novel family of cell wall-related proteins regulated differently during the yeast life cycle. Mol.Cell Biol. **20**, 3245-3255

19 Gomez-Esquer, F., Rodriguez-Pena, J. M., Diaz, G., Rodriguez, E., Briza, P., Nombela, C. and Arroyo, J. (2004) CRR1, a gene encoding a putative transglycosidase, is required for proper spore wall assembly in Saccharomyces cerevisiae. Microbiology. **150**, 3269-3280

20 Cabib, E. (2009) Two novel techniques for determination of polysaccharide cross-links show that Crh1p and Crh2p attach chitin to both beta(1-6)- and beta(1-3)glucan in the Saccharomyces cerevisiae cell wall. Eukaryot.Cell. **8**, 1626-1636

21 Cabib, E., Blanco, N., Grau, C., Rodriguez-Pena, J. M. and Arroyo, J. (2007) Crh1p and Crh2p are required for the cross-linking of chitin to beta(1-6)glucan in the Saccharomyces cerevisiae cell wall. Mol.Microbiol. **63**, 921-935

22 Cabib, E., Farkas, V., Kosik, O., Blanco, N., Arroyo, J. and McPhie, P. (2008) Assembly of the yeast cell wall. Crh1p and Crh2p act as transglycosylases in vivo and in vitro. J.Biol.Chem. **283**, 29859-29872
23 Mazáň, M., Blanco, N., Kováčová, K., Zemková, Z., Farkaš, V and Arroyo, J. (2013) Catalytic properties and substrate specificity of Crh1 and Crh2 yeast cell wall transglycosylases in vivo and in vitro Biochem J. **Submitted**
24 Henrissat, B., Callebaut, I., Fabrega, S., Lehn, P., Mornon, J. P. and Davies, G. (1995) Conserved catalytic machinery and the prediction of a common fold for several families of glycosyl hydrolases. Proceedings of the National Academy of Sciences of the United States of America. **92**, 7090-7094
25 Cantarel, B. L., Coutinho, P. M., Rancurel, C., Bernard, T., Lombard, V. and Henrissat, B. (2009) The Carbohydrate-Active EnZymes database (CAZy): an expert resource for Glycogenomics. Nucleic Acids Res. **37**, D233-238. doi: 210.1093/nar/gkn1663. Epub 2008 Oct 1095.
26 Tabernero, C., Coll, P. M., Fernandez-Abalos, J. M., Perez, P. and Santamaria, R. I. (1994) Cloning and DNA sequencing of bgaA, a gene encoding an endo-beta-1,3-1,4-glucanase, from an alkalophilic Bacillus strain (N137). Applied and environmental microbiology. **60**, 1213-1220
27 Planas, A. (2000) Bacterial 1,3-1,4-beta-glucanases: structure, function and protein engineering. Biochim Biophys Acta. **1543**, 361-382.
28 Fry, S. C., Smith, R. C., Renwick, K. F., Martin, D. J., Hodge, S. K. and Matthews, K. J. (1992) Xyloglucan endotransglycosylase, a new wall-loosening enzyme activity from plants. Biochem J. **282**, 821-828.
29 Rose, J. K., Braam, J., Fry, S. C. and Nishitani, K. (2002) The XTH family of enzymes involved in xyloglucan endotransglucosylation and endohydrolysis: current perspectives and a new unifying nomenclature. Plant Cell Physiol. **43**, 1421-1435.
30 Johansson, P., Brumer, H., 3rd, Baumann, M. J., Kallas, A. M., Henriksson, H., Denman, S. E., Teeri, T. T. and Jones, T. A. (2004) Crystal structures of a poplar xyloglucan endotransglycosylase reveal details of transglycosylation acceptor binding. Plant Cell. **16**, 874-886. Epub 2004 Mar 2012.
31 Gueguen, Y., Voorhorst, W. G., van der Oost, J. and de Vos, W. M. (1997) Molecular and biochemical characterization of an endo-beta-1,3- glucanase of the hyperthermophilic archaeon Pyrococcus furiosus. J Biol Chem. **272**, 31258-31264.
32 Hamada, K., Fukuchi, S., Arisawa, M., Baba, M. and Kitada, K. (1998) Screening for glycosylphosphatidylinositol (GPI)-dependent cell wall proteins in Saccharomyces cerevisiae. Mol Gen Genet. **258**, 53-59
33 Malet, C., Jimenez-Barbero, J., Bernabe, M., Brosa, C. and Planas, A. (1993) Stereochemical course and structure of the products of the enzymic action of endo-1,3-1,4-beta-D-glucan 4-glucanohydrolase from Bacillus licheniformis. The Biochemical journal. **296 (Pt 3)**, 753-758
34 Sinnott, M. (1990) Catalytic mechanim of enzymatic glycosyl transfer Chemival Reviews. **90**, 1171-1202
35 Hahn, M., Keitel, T. and Heinemann, U. (1995) Crystal and molecular structure at 0.16-nm resolution of the hybrid Bacillus endo-1,3-1,4-beta-D-glucan 4-glucanohydrolase H(A16-M). Eur J Biochem. **232**, 849-858.
36 Gaiser, O. J., Piotukh, K., Ponnuswamy, M. N., Planas, A., Borriss, R. and Heinemann, U. (2006) Structural basis for the substrate specificity of a Bacillus 1,3-1,4-beta-glucanase. J Mol Biol. **357**, 1211-1225. Epub 2006 Jan 1225.

37 Cabib, E., Blanco, N., Grau, C., Rodriguez-Pena, J. M. and Arroyo, J. (2007) Crh1p and Crh2p are required for the cross-linking of chitin to beta(1-6)glucan in the Saccharomyces cerevisiae cell wall. Molecular microbiology. **63**, 921-935
38 Gietz, R. D. and Woods, R. A. (2002) Transformation of yeast by lithium acetate/single-stranded carrier DNA/polyethylene glycol method. Methods in enzymology. **350**, 87-96
39 Bermejo, C., Rodriguez, E., Garcia, R., Rodriguez-Pena, J. M., Rodriguez de la Concepcion, M. L., Rivas, C., Arias, P., Nombela, C., Posas, F. and Arroyo, J. (2008) The sequential activation of the yeast HOG and SLT2 pathways is required for cell survival to cell wall stress. Mol.Biol.Cell. **19**, 1113-1124
40 Eswar, N., Webb, B., Marti-Renom, M. A., Madhusudhan, M. S., Eramian, D., Shen, M. Y., Pieper, U. and Sali, A. (2006) Comparative protein structure modeling using Modeller. Curr Protoc Bioinformatics. **Chapter**, Unit 5.6. doi: 10.1002/0471250953.bi0471250506s0471250915.
41 Mazan M, B. N., Zemková Z, Arroyo J* and Vladimír Farkaš*. (2012) Catalytic properties and substrate specificity of Crh1 and Crh2 yeast cell wall transglycosylases in vivo and in vitro.
42 Arroyo, J., Sarfati, J., Baixench, M. T., Ragni, E., Guillen, M., Rodriguez-Pena, J. M., Popolo, L. and Latge, J. P. (2007) The GPI-anchored Gas and Crh families are fungal antigens. Yeast (Chichester, England). **24**, 289-296
43 Keitel, T., Simon, O., Borriss, R. and Heinemann, U. (1993) Molecular and active-site structure of a Bacillus 1,3-1,4-beta-glucanase. Proc Natl Acad Sci U S A. **90**, 5287-5291.
44 Juncosa, M., Pons, J., Dot, T., Querol, E. and Planas, A. (1994) Identification of active site carboxylic residues in Bacillus licheniformis 1,3-1,4-beta-D-glucan 4-glucanohydrolase by site-directed mutagenesis. J Biol Chem. **269**, 14530-14535.
45 Viladot, J. L., de Ramon, E., Durany, O. and Planas, A. (1998) Probing the mechanism of Bacillus 1,3-1,4-beta-D-glucan 4-glucanohydrolases by chemical rescue of inactive mutants at catalytically essential residues. Biochemistry. **37**, 11332-11342.
46 Boraston, A. B., Bolam, D. N., Gilbert, H. J. and Davies, G. J. (2004) Carbohydrate-binding modules: fine-tuning polysaccharide recognition. Biochem J. **382**, 769-781.
47 Hashimoto, H. (2006) Recent structural studies of carbohydrate-binding modules. Cell Mol Life Sci. **63**, 2954-2967.
48 Wright, H. T., Sandrasegaram, G. and Wright, C. S. (1991) Evolution of a family of N-acetylglucosamine binding proteins containing the disulfide-rich domain of wheat germ agglutinin. J Mol Evol. **33**, 283-294.
49 Drenth, J., Low, B. W., Richardson, J. S. and Wright, C. S. (1980) The toxin-agglutinin fold. A new group of small protein structures organized around a four-disulfide core. J Biol Chem. **255**, 2652-2655.
50 Blanco, N., Reidy, M., Arroyo, J. and Cabib, E. (2012) Cross-links in the cell wall of budding yeast control morphogenesis at the mother-bud neck. J Cell Sci. **125**, 5781-5789
51 Hahn, M., Pons, J., Planas, A., Querol, E. and Heinemann, U. (1995) Crystal structure of Bacillus licheniformis 1,3-1,4-beta-D-glucan 4-glucanohydrolase at 1.8 A resolution. FEBS Lett. **374**, 221-224.
52 Reyes-Lopez, C. A., Hernandez-Santoyo, A., Pedraza-Escalona, M., Mendoza, G., Hernandez-Arana, A. and Rodriguez-Romero, A. (2004) Insights into a conformational epitope of Hev b 6.02 (hevein). Biochem Biophys Res Commun. **314**, 123-130.

53 Asensio, J. L., Canada, F. J., Bruix, M., Gonzalez, C., Khiar, N., Rodriguez-Romero, A. and Jimenez-Barbero, J. (1998) NMR investigations of protein-carbohydrate interactions: refined three-dimensional structure of the complex between hevein and methyl beta-chitobioside. Glycobiology. **8**, 569-577.
54 Hernandez-Gay, J. J., Arda, A., Eller, S., Mezzato, S., Leeflang, B. R., Unverzagt, C., Canada, F. J. and Jimenez-Barbero, J. (2010) Insights into the dynamics and molecular recognition features of glycopeptides by protein receptors: the 3D solution structure of hevein bound to the trisaccharide core of N-glycoproteins. Chemistry. **16**, 10715-10726. doi: 10710.11002/chem.201000939.

Figure 1

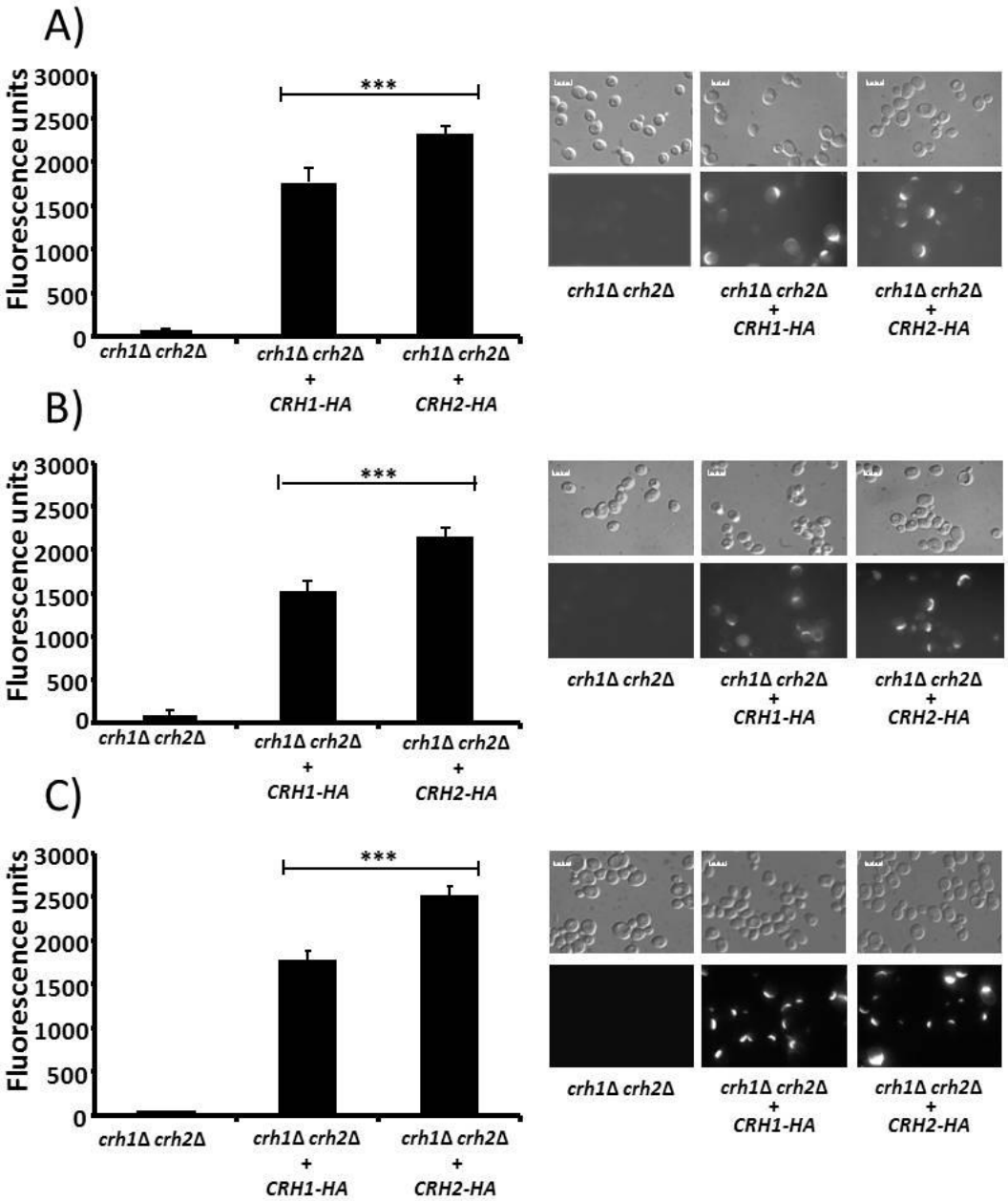
A)
Fluorescence units
3000
2500
2000
1500
1000
500
0
***
crh1Δ crh2Δ
crh1Δ crh2Δ + CRH1-HA
crh1Δ crh2Δ + CRH2-HA
B)
Fluorescence units
3000
2500
2000
1500
1000
500
0
***
crh1Δ crh2Δ
crh1Δ crh2Δ + CRH1-HA
crh1Δ crh2Δ + CRH2-HA
C)
Fluorescence units
3000
2500
2000
1500
1000
500
0
***
crh1Δ crh2Δ
crh1Δ crh2Δ + CRH1-HA
crh1Δ crh2Δ + CRH2-HA

Figure 2

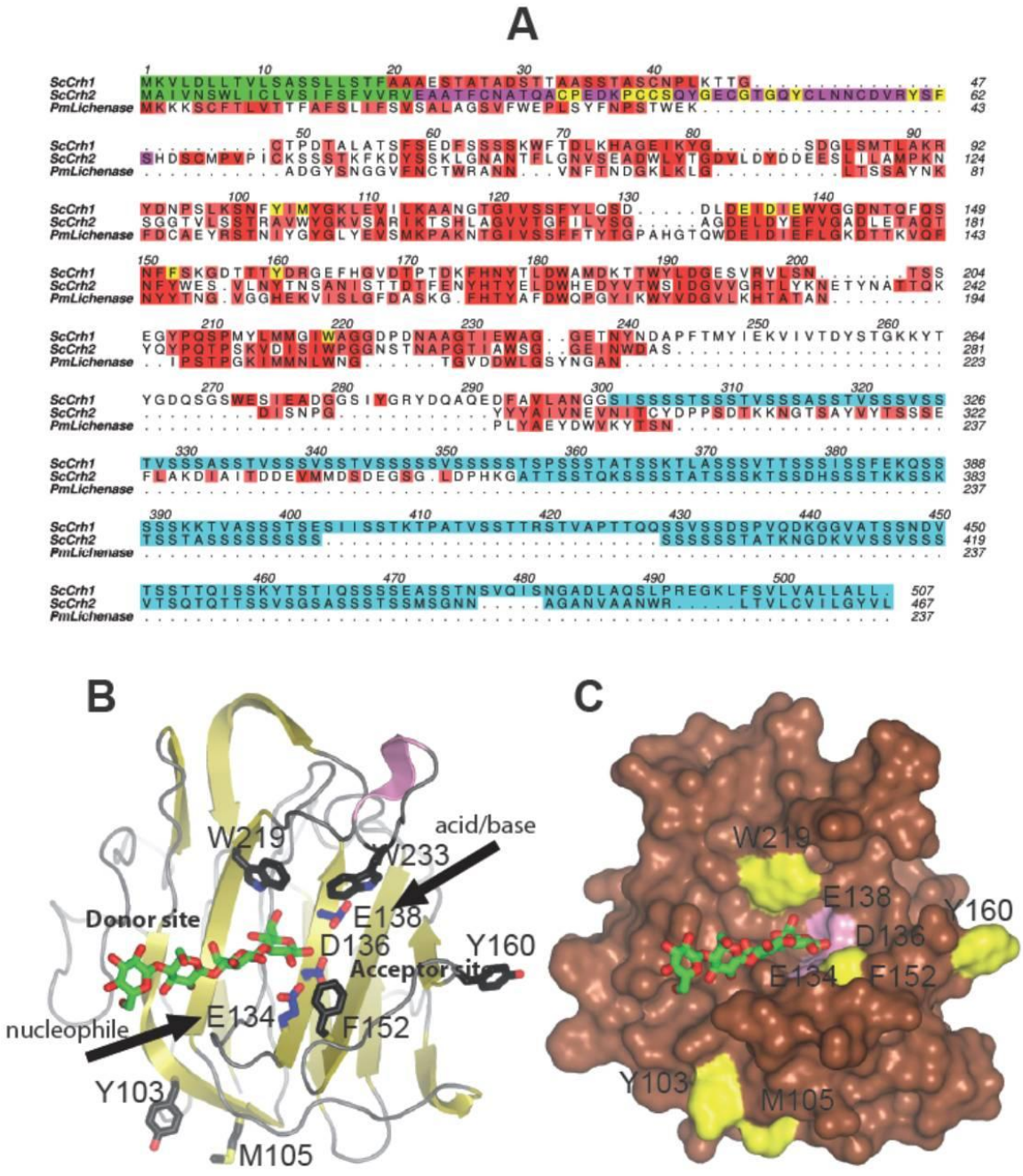
A
ScCrh1
ScCrh2
PmLichenase
B
W219
W233
acid/base
E138
Donor site
D136
Y160
Acceptor site
nucleophile
E134
F152
Y103
M105
C
W219
E138
Y160
D136
E134
F152
Y103
M105

Figure 3

A)

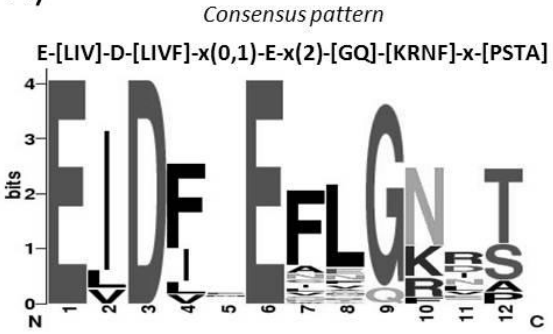

		.. **.* *. *
S. cerevisiae	Crh1 (129-141)	SDDLDEIDIEWVG
S. cerevisiae	Crh2 (160-173)	SGAGDELDYEFVG
C.albicans	Crh11 (114-126)	SDDLDEIDIEMFG
C.albicans	Utr2 (163-175)	SDVQDEIDYEFVG
A. fumigatus	Crf1 (114-126)	SDDLDEVDWEVLG
A. fumigatus	AFU6A (104-116)	SDDLDEIDWECTG
B. licheniformis	Bg1 (129-141)	GTPWDEIDIEFLG
A. thaliana	Xth2 (100-113)	GTTWDEIDFEFLG

B)

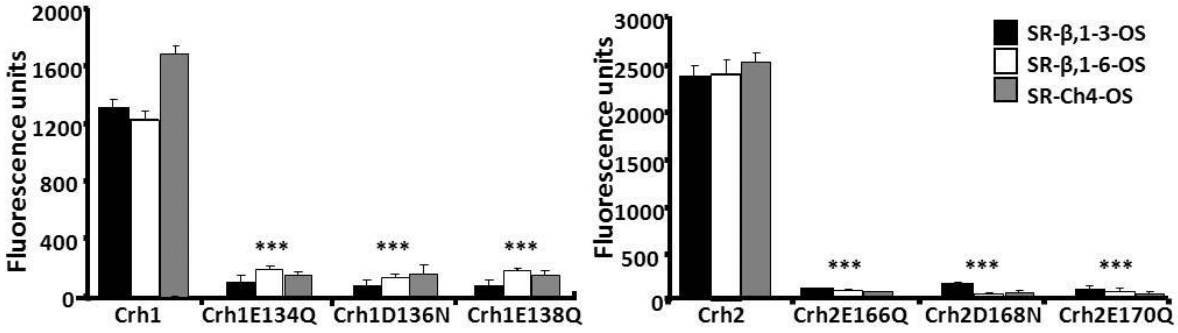

C)

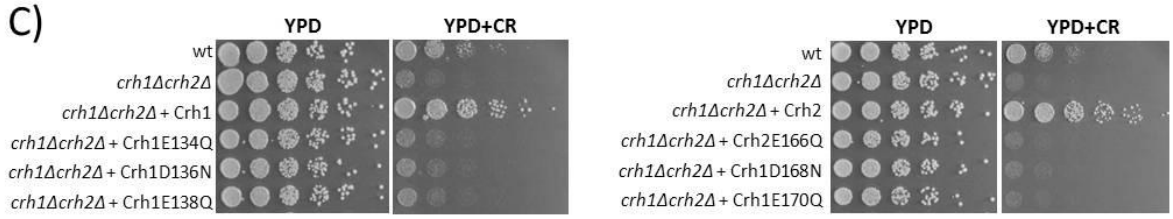

Figure 4

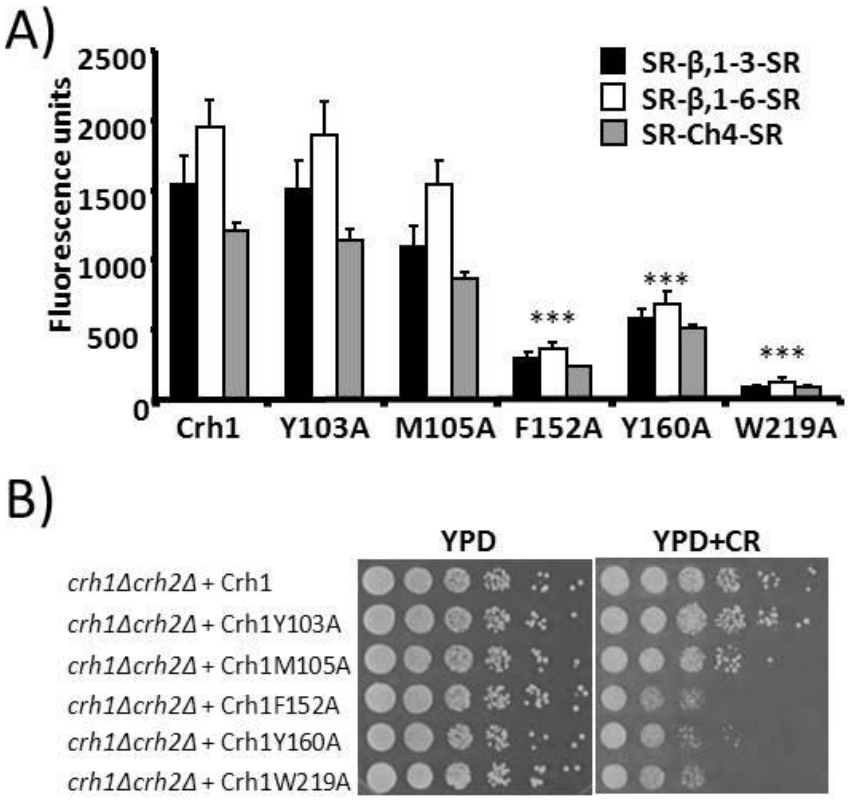
A)
2500
2000
1500
1000
500
0
Fluorescence units
SR-β,1-3-SR
SR-β,1-6-SR
SR-Ch4-SR
***
***
***
Crh1
Y103A
M105A
F152A
Y160A
W219A
B)
YPD
YPD+CR
crh1Δcrh2Δ + Crh1
crh1Δcrh2Δ + Crh1Y103A
crh1Δcrh2Δ + Crh1M105A
crh1Δcrh2Δ + Crh1F152A
crh1Δcrh2Δ + Crh1Y160A
crh1Δcrh2Δ + Crh1W219A

Figure 5

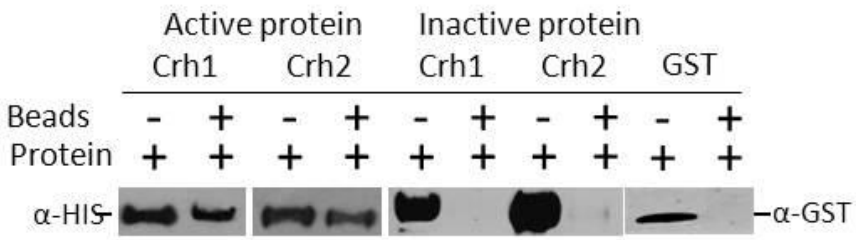
Active protein
Inactive protein
Crh1
Crh2
Crh1
Crh2
GST
Beads
Protein
α-HIS
α-GST

Figure 6

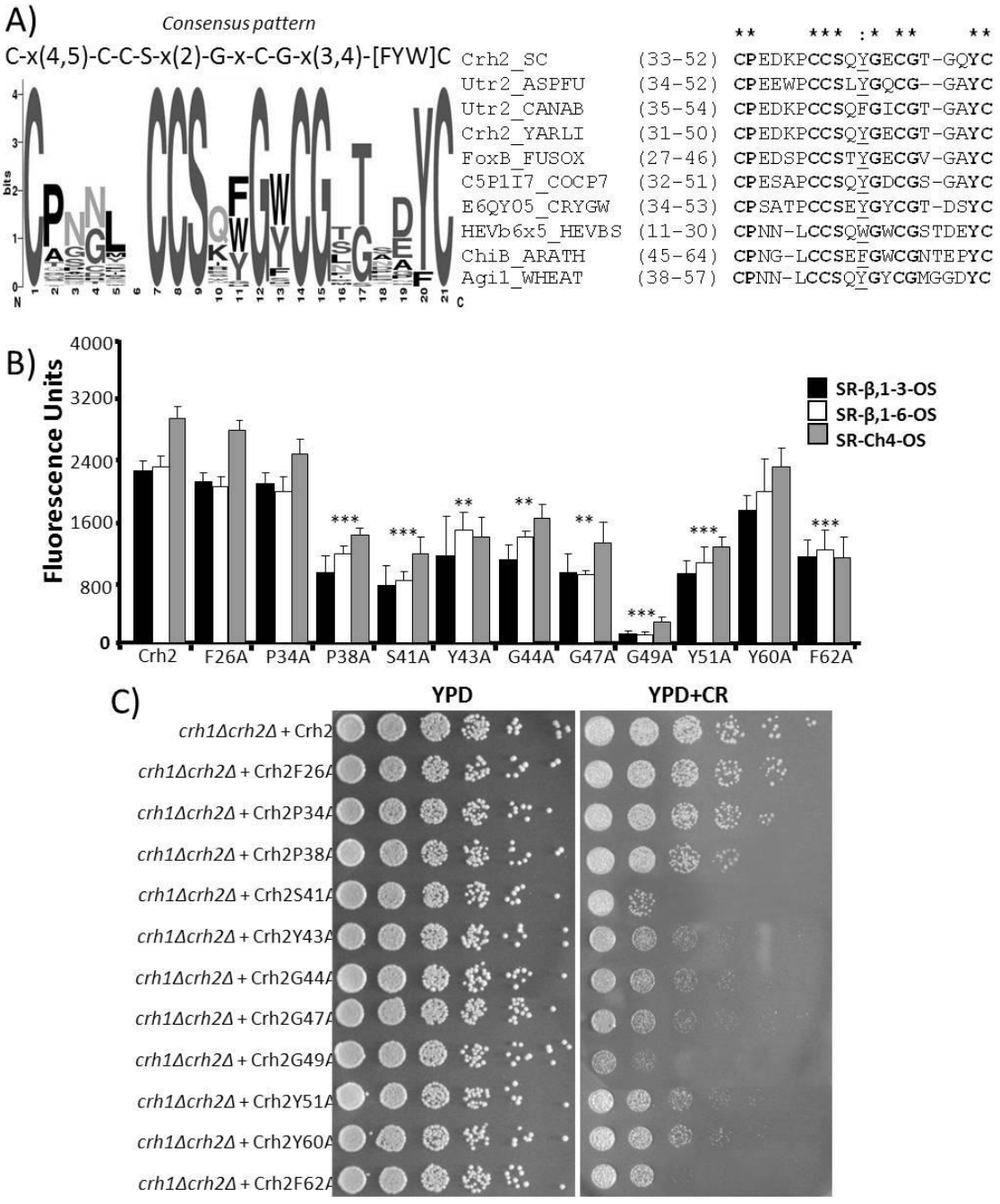
A)
Consensus pattern
C-x(4,5)-C-C-S-x(2)-G-x-C-G-x(3,4)-[FYW]C
bits
N
C
** *** :* ** **
Crh2_SC (33-52) CPEDKPCCSQYGECGT-GQYC
Utr2_ASPFU (34-52) CPEEWPCCSLYGQCG--GAYC
Utr2_CANAB (35-54) CPEDKPCCSQFGICGT-GAYC
Crh2_YARLI (31-50) CPEDKPCCSQYGECGT-GAYC
FoxB_FUSOX (27-46) CPEDSPCCSTYGECGV-GAYC
C5P1I7_COCP7 (32-51) CPESAPCCSQYGDCGS-GAYC
E6QY05_CRYGW (34-53) CPSATPCCSEYGYCGT-DSYC
HEVb6x5_HEVBS (11-30) CPNN-LCCSQWGWCGSTDEYC
ChiB_ARATH (45-64) CPNG-LCCSEFGWCGNTEPYC
Agi1_WHEAT (38-57) CPNN-LCCSQYGYCGMGGDYC
B)
Fluorescence Units
4000
3200
2400
1600
800
0
SR-β,1-3-OS
SR-β,1-6-OS
SR-Ch4-OS
Crh2
F26A
P34A
P38A
S41A
Y43A
G44A
G47A
G49A
Y51A
Y60A
F62A
C)
YPD
YPD+CR
crh1Δcrh2Δ + Crh2
crh1Δcrh2Δ + Crh2F26A
crh1Δcrh2Δ + Crh2P34A
crh1Δcrh2Δ + Crh2P38A
crh1Δcrh2Δ + Crh2S41A
crh1Δcrh2Δ + Crh2Y43A
crh1Δcrh2Δ + Crh2G44A
crh1Δcrh2Δ + Crh2G47A
crh1Δcrh2Δ + Crh2G49A
crh1Δcrh2Δ + Crh2Y51A
crh1Δcrh2Δ + Crh2Y60A
crh1Δcrh2Δ + Crh2F62A

Figure S1

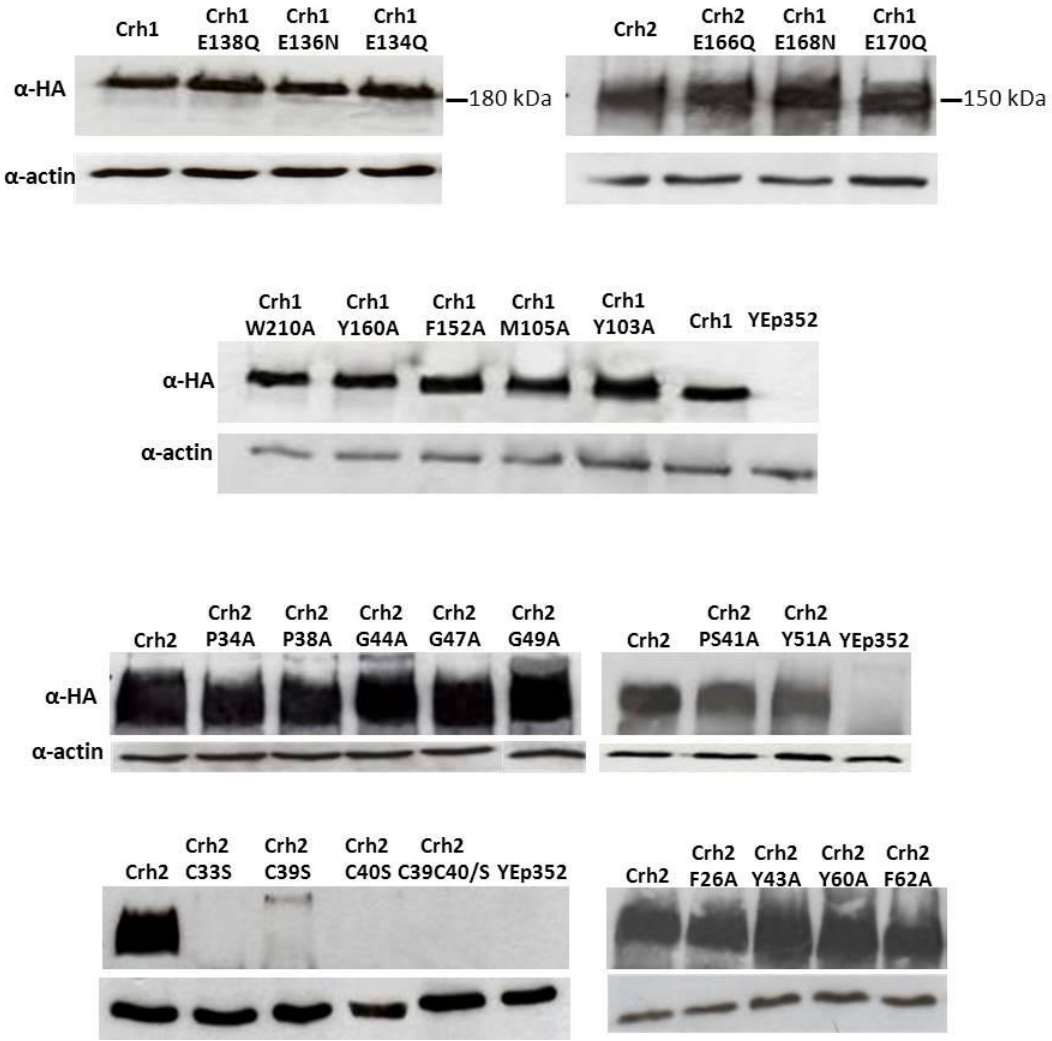
Crh1
Crh1 E138Q
Crh1 E136N
Crh1 E134Q
α-HA
α-actin
180 kDa
Crh2
Crh2 E166Q
Crh1 E168N
Crh1 E170Q
150 kDa
Crh1 W210A
Crh1 Y160A
Crh1 F152A
Crh1 M105A
Crh1 Y103A
Crh1
YEp352
Crh2
Crh2 P34A
Crh2 P38A
Crh2 G44A
Crh2 G47A
Crh2 G49A
Crh2 PS41A
Crh2 Y51A
Crh2 C33S
Crh2 C39S
Crh2 C40S
Crh2 C39C40/S
Crh2 F26A
Crh2 Y43A
Crh2 Y60A
Crh2 F62A

Figure S2

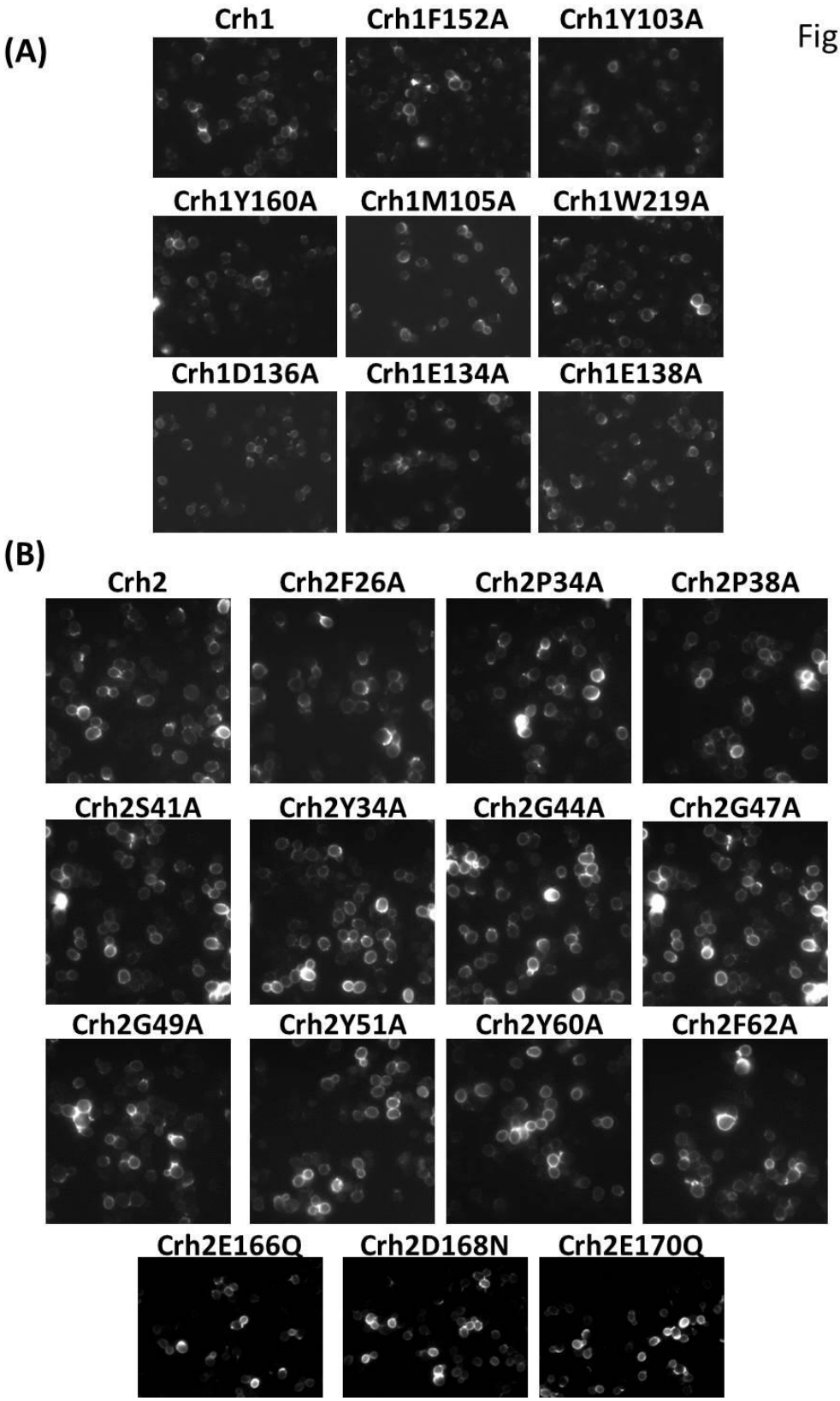
(A)
Crh1
Crh1F152A
Crh1Y103A
Crh1Y160A
Crh1M105A
Crh1W219A
Crh1D136A
Crh1E134A
Crh1E138A
(B)
Crh2
Crh2F26A
Crh2P34A
Crh2P38A
Crh2S41A
Crh2Y34A
Crh2G44A
Crh2G47A
Crh2G49A
Crh2Y51A
Crh2Y60A
Crh2F62A
Crh2E166Q
Crh2D168N
Crh2E170Q

Table S1. Plasmids generated in this study with the description of the oligonucleotides used in each case for the generation of all *CRH1* and *CRH2* site-directed mutants.

PLASMID[a]	PRIMERS[b]	SEQUENCE (5'----3')[c]
pNB23 (Yep352-*CRH2*E166Q-HA)	Crh2_E166Q_F	CCGGCGCAGGTGAT**CAA**CTTGATTACGAATTCG
	Crh2_E166Q_R	CGAATTCGTAATCAAG**TTG**ATCACCTGCGCCGG
pNB24 (Yep352-*CRH2*D168N-HA)	Crh2_D168N_F	GCAGGTGATGAACTT**AAT**TACGAATTCGTCGG
	Crh2_D168N_R	CCGACGAATTCGTA**ATT**AAGTTCATCACCTGC
pNB25 (Yep352-*CRH2*E170Q-HA)	Crh2_E170Q_F	GATGAACTTGATTAC**CAA**TTCGTCGGTGCTG
	Crh2_E170Q_R	CAGCACCGACGAA**TTG**GTAATCAAGTTCATC
pNB31 (Yep352-*CRH2*C33S-HA)	Crh2_C33A_F	GCAATGCAACTCAAGCA**TCT**CCCGAAGATAAAC
	Crh2_C33A_R	GTTTATCTTCGGG**AGA**TGCTTGAGTTGCATTGC
pNB33 (Yep352-*CRH2*C39S-HA)	Crh2_C39A_F	CCGAAGATAAACCA**TCT**TGCTCACAATATGG
	Crh2_C39A_R	CCATATTGTGAGCA**AGA**TGGTTTATCTTCGG
pNB35 (Yep352-*CRH2*C40S-HA)	Crh2_C40A_F	CCGAAGATAAACCATGT**TCC**TCACAATATGG
	Crh2_C40A_R	CCATATTGTGA**GGA**ACATGGTTTATCTTCGG
pNB57 (Yep352-*CRH2*F26A-HA)	Crh2_F26A_F	GAGGCCGCTACA**GCT**TGCAATGCAACTC
	Crh2_F26A_R	GAGTTGCATTGCA**AGC**TGTAGCGGCCTC
pNB37 (Yep352-*CRH2*P34A-HA)	Crh2_P34A_F	GCAACTCAAGCATGT**GCC**GAAGATAAACC
	Crh2_P34A_R	GGTTTATCTTC**GGC**ACATGCTTGAGTTGC
PNB38 (Yep352-*CRH2*P38A-HA)	Crh2_P38A_F	CCCGAAGATAAA**GCA**TGTTGCTCACAATAT
	Crh2_P38A_R	ATATTGTGAGCAACA**TGC**TTTATCTTCGGG
pNB42 (Yep352 + *CRH2*S41A-HA)	Crh2_S41A_F	GATAAACCATGTTGC**GCA**CAATATGGTGAATG
	Crh2_S41A_R	CATTCACCATATTG**TGC**GCAACATGGTTTATC
pNB58 (Yep352-*CRH2*Y43A-HA)	Crh2_Y43A_F	CCATGTTGCTCACAA**GCT**GGTGAATGTGG
	Crh2_Y43A_R	CCACATTCACC**AGC**TTGTGAGCAACATGG
pNB39 (Yep352-*CRH2*G44A-HA)	Crh2_G44A_F	GTTGCTCACAATAT**GCT**GAATGTGGTACTG
	Crh2_G44A_R	CAGTACCACATTC**AGC**ATATTGTGAGCAAC
pNB40 (Yep352-*CRH2*G47A-HA)	Crh2_G47A_F	CAATATGGTGAATGT**GCT**ACTGGTCAATATT
	Crh2_G47A_R	AATATTGACCAGT**AGC**ACATTCACCATATTG
pNB44 (Yep352-*CRH2*G49A-HA)	Crh2_G49A_F	GTGAATGTGGTACT**GCT**CAATATTGTCTGA
	Crh2_G49A_R	TCAGACAATATTG**AGC**AGTACCACATTCAC
pNB43 (Yep352 + *CRH2*Y51A-HA)	Crh2_Y51A_F	GGTACTGGTCAA**GCT**TGTCTGAACAACTGTG
	Crh2_Y51A_R	CACAGTTGTTCAGACA**AGC**TTGACCAGTACC
pNB59 (Yep352-CRH2Y60A-HA)	Crh2_Y60A_F	CTGTGATGTAAGA**GCT**TCGTTTAGTCATG
	Crh2_Y60A_R	CATGACTAAACGA**AGC**TCTTACATCACAG
pNB60 (Yep352-*CRH2*Y62A-HA)	Crh2_F62A_F	GATGTAAGATATTCG**GCT**AGTCATGATTCATG
	Crh2_F62A_R	CATGAATCATGACT**AGC**CGAATATCTTACATC
pNB48 (Yep352-*CRH1*E134Q-HA)	Crh1_E134Q_F	GTGAGATTTGGAT**CAA**ATTGATATTGAATGGG
	Crh1_E134Q_R	CCCATTCAATATCAAT**TTG**ATCCAAATCTCAC
pNB49 (Yep352-*CRH1*D136N-HA)	Crh1_D136N_F	GATTTGGATGAAATT**AAT**ATTGAATGGGTGGG
	Crh1_D136N_R	CCCACCCATTCAAT**ATT**AATTTCATCCAAATC
pNB50 (Yep352-*CRH1*E138Q-HA)	Crh1_E138Q_F	GATGAAATTGATATT**CAA**TGGGTGGGTGGTGAC
	Crh1_E138Q_R	GTCACCACCCACCCA**TTG**AATATCAATTTCATC
pNB55 (Yep352-*CRH1*M105A-HA)	Crh1_M105A_F	GAAGTCTAACTTTTATATC**GCG**TATGGAAGT
	Crh1_M105A_R	ACTTCCATA**CGC**GATATAAAAGTTAGACTTC
pNB54 (Yep352-*CRH1*Y103A-HA)	Crh1_Y103A_F	GAAGTCTAACTTT**GCT**ATCATGTATGGTAA
	Crh1_Y103A_R	TTACCATACATGAT**AGC**AAAGTTAGACTTC
pNB56 (Yep352-*CRH1*F152A-HA)	Crh1_F152A_F	CAGTTCCAATCTAACTTC**GCT**TCTAAAGGTG
	Crh1_F152_R	CACCTTTAGA**AGC**GAAGTTAGATTGGAACTG

pNB51 (Yep352-*CRH1*Y160A-HA)	Crh1_Y160A_F	GTGATACCACAACA**GCC**GACAGAGGCGAATTTC
	Crh1_Y160A_R	GAAATTCGCCTCTGTC**GGC**TGTTGTGGTATCAC
pNB52 (Yep352-*CRH1*W219A-HA)	Crh1_W219A_F	CTAATGATGGGTATC**GCG**GCCGGTGGTGACCC
	Crh1_W219A_R	GGGTCACCACCGGC**CGC**GATACCCATCATTAG

[a] Name and description of the plasmid.
[b] The suffixes F (for forward) and R (for reverse) at the end of the primer names refer to the sense and antisense strands, respectively.
[c] The nucleotides subjected to mutagenesis are shown in bold type.

CAPÍTULO 5

PARTICIPACIÓN DEL COMPLEJO QUITINA-β-1,3 GLUCANO EN LA MORFOGÉNESIS DE *Saccharomyces cerevisiae*

RESUMEN DE LOS RESULTADOS DEL CAPÍTULO 5

Durante el crecimiento celular, la pared celular se ve sometida a cambios de tamaño. Sin embargo, el cuello es la única zona que no cambia de tamaño durante la gemación. La regulación del tamaño del cuello viene dada por dos mecanismos simultáneos: la correcta organización del collar de septinas y la localización adecuada del anillo de quitina sintetizado por Chs3. Datos previos (Schmidt et al., 2003) sugerían que el papel del anillo de quitina en mantener el tamaño del cuello, vendría dado por la competitividad de la quitina con el β-1,6 glucano por unirse al extremo no reducido del β-1,3 glucano, evitando la ramificación del mismo y por consiguiente el crecimiento de la pared celular en dicha zona. De acuerdo con esta hipótesis, la mayoría de la quitina presente en el cuello está unida al β-1,3 glucano, mientras que la quitina localizada en la pared lateral lo está al β-1,6 glucano (Cabib and Duran, 2005). Adicionalmente, la unión de la quitina al β-1,3 glucano en el cuello evitaría su remodelación, a su vez necesaria para el crecimiento celular. Este trabajo ha consistido en validar esta premisa. Para ello desarrollamos un nuevo método bioquímico de extracción suave que permite aislar el β-1,3 glucano en su estado más nativo a partir de paredes celulares. Para ello, inicialmente se crecieron las células en presencia de ^{14}C-glucosa. Las paredes celulares purificadas se sometieron a una digestión con β-1,6 glucanasa, generando una fracción soluble formada por β-1,6 glucano y manoproteínas y otra fracción insoluble formada por β-1,3 glucano, quitina libre, quitina unida al β-1,3 glucano y quitina procedente de la unión con β-1,6 glucano. La verificación del contenido de la fracción insoluble se hizo mediante su tratamiento con quitinasa y β-1,3 glucanasa que permitió la solubilización total de la misma. La fracción insoluble se sometió a un tratamiento suave en álcali que generó dos fracciones (soluble/insoluble en álcali) que posteriormente fueron carboximetiladas y fraccionadas en cromatografía de exclusión para su análisis. Los resultados mostraron que existen dos poblaciones de β-1,3 glucano diferentes. Un glucano de alto peso molecular procedente de la fracción álcali insoluble y otro de tamaño más pequeño y aspecto polidisperso procedente de la fracción álcali soluble. El análisis de las paredes celulares del mutante *gas1*Δ, donde la mayoría del β-1,3 glucano está sin ramificar, confirmó que el glucano polidisperso corresponde con glucano en estado inmaduro que se puede remodelar, mientras que el glucano de alto peso molecular es glucano maduro. Una vez determinadas las dos poblaciones de glucano, quisimos determinar cuál de las dos estaba unida a la quitina. Para ello, las paredes

celulares digeridas con β-1,6 glucanasa fueron sometidas a un tratamiento con álcali a altas Tª para distinguir el β-1,3 glucano libre del unido a la quitina debido a que el complejo quitina-glucano es resistente a este tratamiento. Sorprendentemente, cuando las paredes celulares del mutante *crh1*Δ *crh2*Δ, que no tienen quitina unida a glucano, fueron analizadas de esta forma apareció una fracción insoluble que evidenciaba la presencia de quitina unida a β-1,3 glucano. Sobre la base de nuestros resultados previos y de resultados publicados por el Dr. Cabib (Cabib, 2009), que demostraban que las proteínas Crh son responsables de la unión de la quitina tanto al β-1,3 glucano como al β-1,6 glucano, esto sólo se podía explicar sí en este caso, ambos componentes permanecieran unidos de manera no covalente. Para diferenciar la unión covalente y no covalentes entre el β-1,3 glucano y la quitina en la fracción insoluble en álcali a altas Tª, se carboximetilaron dichas fracciones de modo que si ambas cadenas no estuvieran covalentemente unidas al introducir un grupo acético se repelerían entre sí. El análisis de estas fracciones en las cepas WT y *crh1*Δ *crh2*Δ tras su carboximetilación, posterior separación en una columna de afinidad con WGA y análisis final mediante fraccionamiento en columnas de Sephacryl S-500, reveló que la fracción de glucano de mayor peso molecular es la que contiene quitina unida covalentemente, mientras que la fracción polidispersa de glucano no está unida a quitina, validando nuestra hipótesis de partida.

ARTÍCULO 5

Presence of a large beta(1-3)glucan linked to chitin at the Saccharomyces cerevisiae mother-bud neck suggests involvement in localized growth control

EC
Journals.ASM.org

Presence of a Large β(1-3)Glucan Linked to Chitin at the *Saccharomyces cerevisiae* Mother-Bud Neck Suggests Involvement in Localized Growth Control

Enrico Cabib,[a] Noelia Blanco,[b] and Javier Arroyo[b]

Laboratory of Biochemistry and Genetics, NIDDK, National Institutes of Health, Department of Health and Human Services, Bethesda, Maryland, USA,[a] and Departamento de Microbiología II, Facultad de Farmacia, Universidad Complutense de Madrid, Madrid, Spain[b]

Previous results suggested that the chitin ring present at the yeast mother-bud neck, which is linked specifically to the nonreducing ends of β(1-3)glucan, may help to suppress cell wall growth at the neck by competing with β(1-6)glucan and thereby with mannoproteins for their attachment to the same sites. Here we explored whether the linkage of chitin to β(1-3)glucan may also prevent the remodeling of this polysaccharide that would be necessary for cell wall growth. By a novel mild procedure, β(1-3)glucan was isolated from cell walls, solubilized by carboxymethylation, and fractionated by size exclusion chromatography, giving rise to a very high-molecular-weight peak and to highly polydisperse material. The latter material, soluble in alkali, may correspond to glucan being remodeled, whereas the large-size fraction would be the final cross-linked structural product. In fact, the β(1-3)glucan of buds, where growth occurs, is solubilized by alkali. A *gas1* mutant with an expected defect in glucan elongation showed a large increase in the polydisperse fraction. By a procedure involving sodium hydroxide treatment, carboxymethylation, fractionation by affinity chromatography on wheat germ agglutinin-agarose, and fractionation by size chromatography on Sephacryl columns, it was shown that the β(1-3)glucan attached to chitin consists mostly of high-molecular-weight material. Therefore, it appears that linkage to chitin results in a polysaccharide that cannot be further remodeled and does not contribute to growth at the neck. In the course of these experiments, the new finding was made that part of the chitin forms a noncovalent complex with β(1-3)glucan.

The cell wall imparts shape to the fungal cell. For many years, we have used the cell wall of *Saccharomyces cerevisiae* and its specialized component, the septum, as models of morphogenesis (5). The yeast cell wall consists of three polysaccharides, β(1-3)glucan, the major structural component, β(1-6)glucan, and chitin, a minor component that is, however, essential for cell survival. In addition, mannoproteins are present as an external layer of the cell wall. All of these constituents are linked together to form a tight network capable of preventing osmotic or mechanical injuries to the cell (Fig. 1; for reviews, see references 11 and 15). During the cell cycle, the cell wall must undergo a constant process of synthesis and remodeling to accompany cell growth. However, after early budding, one area of the cell wall that does not change is the neck at the mother-bud interface. In yeast, this is a crucial region, because it is the site where cytokinesis and septation take place (16, 26). We previously showed that control of growth at the neck is exerted, in a redundant fashion, by the septin and the chitin ring present at that location (27). A defect in either one of the rings, such as in a *chs3*Δ mutant, which lacks the chitin ring (28), or in a *cla*Δ mutant, where the septin ring is poorly organized, leads to only minor morphological abnormalities. However, when both rings are faulty, control of growth is lost, the neck widens, and cytokinesis does not take place (27). It is probable that the septin ring acts through its barrier function (6), impeding access to the neck of membrane proteins necessary for cell wall synthesis. As for the chitin ring, we suggested that it may work by interfering with wall assembly (27). By the action of the Crh1p and Crh2p transferases (2, 3), cell wall chitin is attached to both β(1-6)glucan, at a branch point, and β(1-3)glucan, at the nonreducing ends (Fig. 1 and references12 and 13). These nonreducing ends of β(1-3)glucan are those to which β(1-6)glucan is linked (Fig. 1). It seemed possible that at the neck, where most of the chitin and of Crh2p (23, 24) is localized, chitin could compete with β(1-6)glucan and prevent its attachment to those sites. As a consequence, mannoproteins, which attach to β(1-6)glucan, would also be unable to join the cell wall structure (27). One prediction of this hypothesis is that most of the chitin at the neck would be specifically linked to β(1-3)glucan. By applying new techniques to the analysis of chitin linkages formed during different segments of the cell cycle, we found that, indeed, almost all of the bound chitin at the neck is attached to β(1-3)glucan, whereas β(1-6)glucan is the chitin acceptor in lateral walls (4). However, to restrict formation of the cell wall at the neck, it would also be necessary to prevent remodeling and growth of β(1-3)glucan itself. Could the attachment of chitin to the glucan also accomplish this function? This is the question that we tried to answer in the present work, by comparing the size distribution of the chitin-free β(1-3)glucan, which is dispersed all over the cell, with that of the chitin-linked β(1-3)glucan, which is present only at the neck.

Received 27 December 2011 **Accepted** 15 February 2012
Published ahead of print 24 February 2012
Address correspondence to Enrico Cabib, enricoc@bdg10.niddk.nih.gov.
Supplemental material for this article may be found at http://ec.asm.org/.

doi:10.1128/EC.05328-11

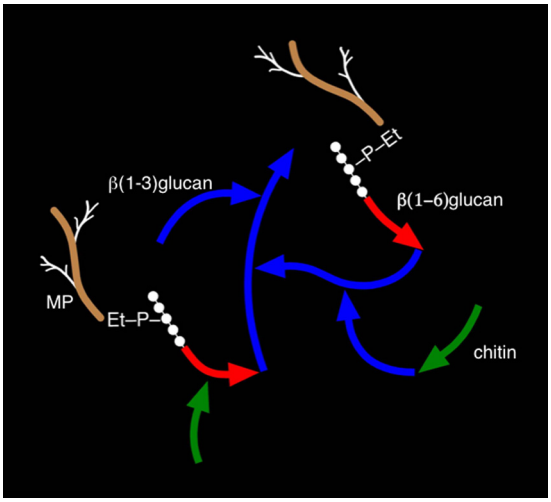

FIG 1 Schematic representation of the cell wall structure of *Saccharomyces cerevisiae* (13). The arrowheads indicate the reducing ends of the different polysaccharides. MP is mannoprotein, where the amino acid chain is brown and the branched mannosyl chains are white. The connection between mannoprotein and β(1-6)glucan consists of the remnant of a glycosylphosphatidylinositol anchor, where Et stands for ethanolamine, P stands for phosphate, and the five white dots represent mannose residues (13). Chitin is attached to β(1-6)glucan through a β(1-3)-linked glucose branch, which is not shown here. Part of the chitin that is free is not shown.

MATERIALS AND METHODS

Strains and growth conditions. The strains used in this study are listed in Table 1. Cells were grown at 30°C in YEPD (2% peptone, 1% yeast extract, 2% glucose), except where indicated otherwise.

For the construction of the *crh1*Δ *crh2*Δ double mutant (strain NBT014 [Table 1]) in the YPH499 background, the *CRH2* open reading frame (ORF) was deleted from YPH499 using the His3MX6 module as previously described (23). Correct ORF replacement was verified by PCR using primers 5′-GCCCAGATGCGAAGTTAAG-3′ and 5′-CGTCGGAG GAGATATTTATTA-3′. In the resulting strain, the *CRH1* ORF was replaced by using a hygromycin B resistance marker (hpHMX4 module). The BsgI insert from plasmid pCG01 was employed as an interruption cassette in this case as previously described (3). Correct ORF replacement was verified by PCR with primers 5′-GCCCAGATGCGAAGTTAAG-3′ and 5′-AGCTGAAATGCGAGGATTG-3′.

Preparation of [^{14}C]CM–β(1-3)glucan and [^{14}C]CM-chitin. [^{14}C]CM–β(1-3)glucan (CM stands for carboxymethyl) was prepared as already described (2). For the preparation of [^{14}C]CM-chitin, strain FY001 was grown and labeled with [^{14}C]glucosamine as previously reported (4), except that the growth temperature was 38°C rather than 30°C, to increase the incorporation into chitin (3). Cell walls were prepared and treated with sodium hydroxide as described previously (4, 8) and divided into six aliquots, each containing about 800,000 cpm. Each aliquot, in a total volume of 375 μl, was incubated for 3 h at 37°C with 0.05 M sodium acetate, pH 5, and 22 μl (~0.6 mg of protein) of recombinant β(1-6)glucanase (1). After incubation, 18 μl of 1 M phosphate at pH 6.3, 15 μl of 0.2 M sodium hydroxide, and 17 μl of Zymolyase 100T (Associates of Cape Cod) at 10 mg/ml were added and incubation was continued for 3 h at 37°C to hydrolyze the β(1-3)glucan. Tubes were centrifuged for 10 min at 18,000 × *g* in a refrigerated centrifuge, and pellets were carboxymethylated as previously reported (4). For each aliquot, the final product contained 600,000 to 700,000 cpm. The carboxymethylated mixtures were pooled and concentrated by centrifugation in an Amicon Centricon with a molecular weight cutoff of 3,000 to a final volume of 1 ml.

Preparation of carboxymethylated cell walls. From YPH499 cells (1.2 g, wet weight), cell walls were prepared, treated with sodium hydroxide, and carboxymethylated as previously outlined (4), using volumes of reagents 9 times larger than those described (4). Because of the scaled-up procedure, the mixture was in a 14-ml polypropylene tube and mixing had to be done by either shaking the tube by hand or using a glass rod, rather than in the BeadBeater. The final drying was done by adding ether, centrifuging the mixture, and allowing the ether to evaporate under a hood. The dried pellet was suspended in 3 ml of water. After centrifugation, another 2 ml of water was added to dissolve the remaining pellet. Both fractions were dialyzed against water overnight and then mixed in the original proportions. The resulting solution was clear.

Preparation of CM-curdlan. Carboxymethylation of curdlan was carried out with 0.5 g of the commercial product (Carbomer, San Diego, CA) as described above for yeast cell walls. The final product was dialyzed overnight against water. The solution, 37.5 ml, was extremely viscous and formed a gel after storage at 4°C. It could be liquefied by heating in a boiling water bath for 10 min, and 5-fold dilution with water gave rise to a low-viscosity solution. In the undiluted preparation, the final concentration was 45 mM glucose equivalents, as measured with anthrone (30), using glucose as the standard. The yield of the operation was about 55%.

Chitinase purification. Chitinase from *Serratia marcescens* was purified by adsorption-digestion on chitin as previously described (22) and dialyzed against 0.05 M phosphate, pH 6.3. To eliminate traces of β(1-3)glucanase, affinity adsorption on curdlan, an insoluble β(1-3)glucan, was carried out. Curdlan gel was prepared from a 2% suspension of the polysaccharide as described previously (2), except that the buffer was 0.05 M 2-(*N*-morpholino)ethanesulfonic acid, pH 6. To gel from 0.3 ml of a curdlan suspension, 250 μl of dialyzed chitinase was added; this was followed by shaking of the tube in a Mini-BeadBeater (Biospec Products, Bartlesville, OK) for 20 s, rotation at room temperature for 30 min, and centrifugation. The supernatants from two batches were pooled and treated in the same way with curdlan gel from 0.3 ml of a 2% suspension. The final supernatant was the purified chitinase. In this operation, the chitinase was diluted about 40%.

Isolation of bulk β(1-3)glucan. A schematic diagram of the β(1-3)glucan isolation procedure used is shown in Fig. 2A. All centrifugations were for 5 min at 16,000 × *g*. Yeast cells were labeled during logarithmic growth with [^{14}C]glucose as previously described for the preparation of ^{14}C-labeled β(1-3)glucan (2). To cells from a 20-ml culture (2) in 50 mM Tris chloride, pH 7.5, in a total volume of 1 ml in a 2-ml Mini-BeadBeater tube, 2 g of glass beads (0.5-mm diameter) was added. To break the cells, the tube was shaken in a Mini-BeadBeater for 8 periods of 30 s, with 1-min periods of cooling in ice in between. Washing of the cell walls was done as already described (8). To 200 μl of a cell wall suspension containing 1.3 ×

TABLE 1 Strains used in this study

Strain	Genotype	Source or reference
YPH499	*MAT***a** *ura3-52 lys2-801 ade2-101 trp1-Δ63 his3-Δ200 leu2-Δ1*	29
NBTO14	*MAT***a** *ura3-52 lys2-801 ade2-101 trp1-Δ63 his3-Δ200 leu2-Δ1 crh1*::*HygrB crh2*::*HIS3*	This work
ECY46-4-1B	*MAT***a** *ura3-52 lys2-801 ade2-101 trp1-Δ63 his3-Δ200 leu2-Δ1 chs3*::*LEU2*	7
BY4741	*MAT***a** *ura3Δ0 his3Δ1 leu2Δ0 met15Δ0*	EUROSCARF
YHR307W	*MAT***a** *ura3Δ0 his3Δ1 leu2Δ0 met15Δ0 gas1*::*KanMX4*	EUROSCARF
FY001	*MATα his3Δ200 ura3-52 leu2Δ1 trp1Δ63*	3

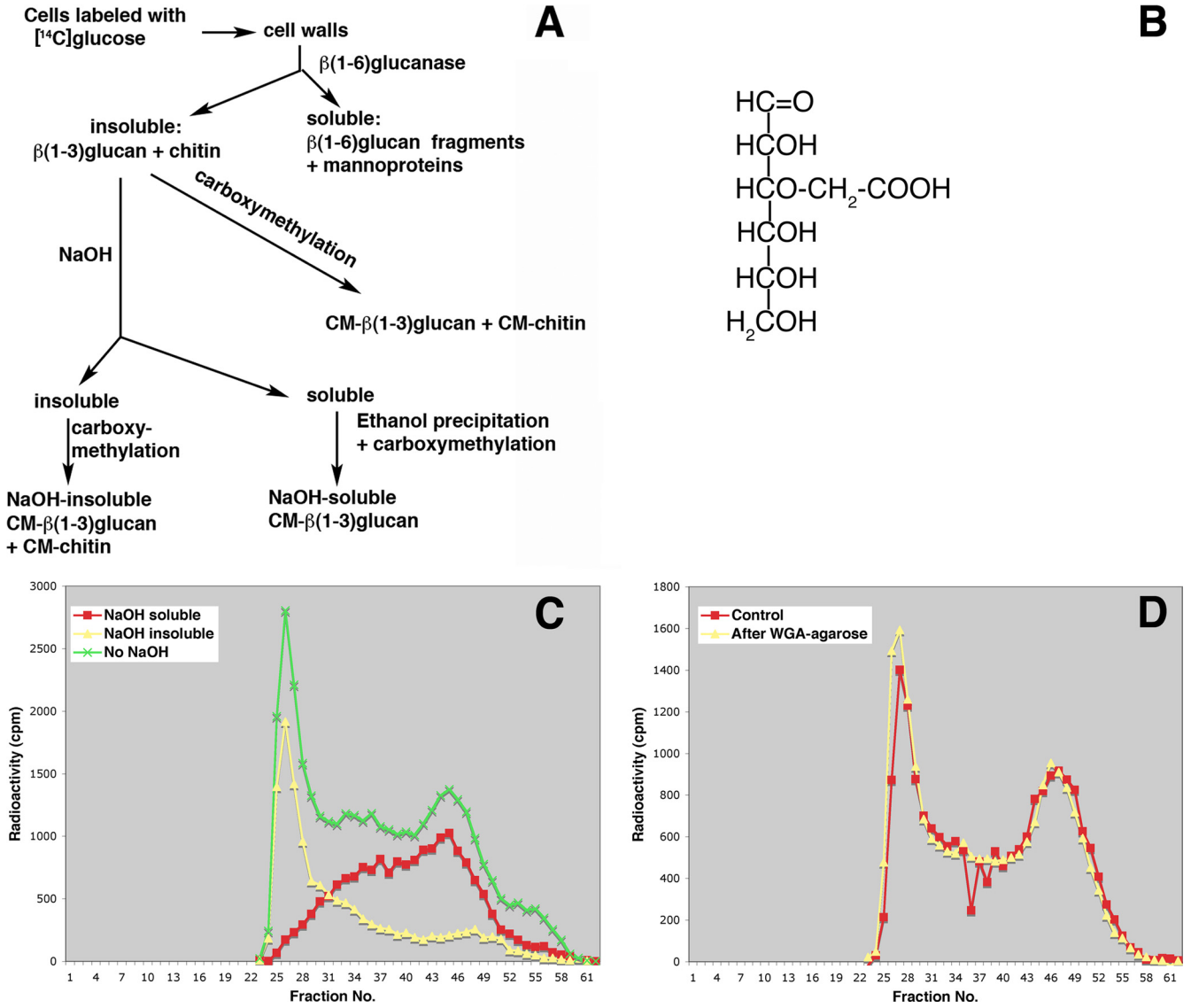

FIG 2 Isolation and fractionation of β(1-3)glucan. (A) Scheme for isolation of β(1-3)glucan from yeast cell walls. All carboxymethylated (CM) fractions are soluble in water. (B) Chemical linkage of acetic acid to hexose in a carboxymethylated sugar. The open structure of the sugar is shown for simplicity. Monochloroacetic acid is the reactant, and an ether linkage is formed as shown. The acetic acid residue may be attached to any of the free hydroxyl groups in a polysaccharide and will be negatively charged at neutral pH. (C) Chromatography of total (no NaOH), alkali-soluble, and alkali-insoluble β(1-3)glucan on Sephacryl S-500. Here as in subsequent columns, fractions of 1 ml were collected. The void volume of the column is at fractions 24 to 26. For glucose, the position of the peak maximum was at fraction 57, as determined with [^{14}C]glucose as the standard. (D) Chromatography of total β(1-3)glucan on Sephacryl S-500 before and after filtration through WGA-agarose.

10^6 to 1.6×10^6 cpm, 11.6 μl of 1 M sodium acetate, pH 5, and 20 μl of recombinant β(1-6)glucanase (1) were added. The mixture, in a screw-cap microcentrifuge tube, was incubated overnight at 37°C on a rotator and then centrifuged. The supernatant was saved, and the pellet was washed with 200 μl of water, which was added to the first supernatant. The pellet was suspended in 200 μl of water, 50 μl of 5 M sodium hydroxide was added, and the tube was vortexed for 1 min before centrifugation. The supernatant was saved. The pellet (P1) was washed with 200 μl of water, which was added to the supernatant. To this combined supernatant, 2 volumes of ethanol were added. The tube was stored at 4°C overnight and then centrifuged in a refrigerated microcentrifuge. The resulting pellet (P2) was saved.

In a parallel experiment, cell walls were incubated with β(1-6)glucanase as described above and centrifuged but the pellet (P3) was not treated further. Radioactivity was monitored in all supernatants and pellets. The three pellets, P1, P2, and P3, were transferred to 2-ml BeadBeater tubes with three 0.1-ml portions of 60% sodium hydroxide–0.2% sodium dodecyl sulfate, and carboxymethylation was carried out as previously described (4). As already mentioned (4), extraction of the carboxymethylated material with water gave rise to two fractions, the first of which had a high salt concentration. This fraction was usually desalted by centrifugation in an Amicon Ultra device with a molecular weight cutoff of 10,000 before being mixing with the second fraction.

Chromatography on Sephacryl S-500. Chromatography of the pooled fractions on a Sephacryl S-500 column (1 by 76 cm) was carried out with the same buffer (50 mM Tris chloride, pH 7.5, containing 150 mM sodium chloride and 0.02% sodium azide) and conditions previously described for Sephacryl S-300 (4). The void volume could not be mea-

sured in the Sephacryl S-500 column with dextran blue because dextran blue was in the included volume of the column. By comparison with a Sephacryl S-400 column of the same size, it was judged to be 25 to 26 ml (fractions 25 and 26). We were also able to measure the void volume directly by using colloidal gold particles 60 nm in diameter (nanoComposix, San Diego, CA). The colloidal gold can be detected by its absorbance at 534 nm. The void volume measured in this way was at fraction 24, similar to the calculated value.

Preparation of cell walls for observation by microscope. Cell walls were prepared as described in the section on the isolation of bulk β(1-3)glucan, except that the cell mixture with glass beads was in a 12-ml polycarbonate tube, rather than in a Mini-BeadBeater tube. The tube was vortexed for 6 periods of 1 min, with 1-min periods of cooling in ice in between. Washing of cell walls, incubation with β(1-6)glucanase, and treatment with sodium hydroxide at room temperature were carried out as in the above-mentioned section.

Isolation of chitin-linked β(1-3)glucan. Cells were labeled with [^{14}C]glucose, and cell walls were prepared and treated with β(1-6)glucanase as described above. The β(1-6)glucanase-resistant pellet was suspended in 200 μl of water, and 50 μl of 5 M sodium hydroxide was added. The mixture was placed in a dry bath at 80°C for 1 h; this was followed by centrifugation and suspension of the pellet in 250 μl of 1 M sodium hydroxide. The tube was heated again at 80°C for 1 h and centrifuged. The pellet was washed with 200 μl of water, subjected to carboxymethylation, and desalted as outlined above. To the desalted material, 5 M NaCl and 1 M Tris-HCl, pH 7.5, were added to make the final concentration of NaCl 1 M and that of Tris 0.1 M in a total volume of 1 ml.

Wheat germ agglutinin (WGA)-agarose (Vector Laboratories, Burlingame, CA) columns of 0.88 ml were set up in tubes 0.7 cm in diameter. The columns were washed with 2 ml of 1 M NaCl–0.1 M Tris-HCl, pH 7.5. The above-described carboxymethylated mixture (100,000 cpm) was applied to a column, allowed to percolate, and reapplied. This operation was repeated once more to ensure maximum adsorption of the chitin-bound material. A 1-ml washing with 1 M NaCl–0.1 M Tris-HCl, pH 7.5, was pooled with the column filtrate to yield fraction 1 (total percolate). The column was successively washed with 1 ml of the NaCl-Tris solution (fraction 2) and 1 ml of water (fraction 3). The chitin-containing material was eluted with three 1-ml portions (fractions 4 to 6) of 0.1 M sodium hydroxide. Addition to the sodium hydroxide of CM-curdlan, to a final concentration of 9 mM glucose equivalents, somewhat increased the yield of radioactivity in these fractions. Most of the radioactivity applied to the column was found in fractions 1, 4, and 5, and very little was found in the other fractions, which were discarded.

Fraction 1 was desalted and concentrated to 0.4 ml by centrifugation in an Amicon Ultra device with a molecular weight cutoff of 10,000. To the desalted fraction, 40 μl of Tris-HCl, pH 7.5, and 13 μl of 5 M NaCl were added. The mixture was fractionated on Sephacryl S-500 as outlined above.

Fractions 4 and 5 were pooled and neutralized with hydrochloric acid. The following additions were made: 100 μl of 1 M Tris-HCl, pH 7.5; 62 μl of 5 M NaCl; 100 μl of carboxymethylated cell walls; and 200 μl of 0.5% CM-chitin. The last two items were added as carriers because of the very small amount of radioactive material in these fractions. The mixture was subjected to chromatography on Sephacryl S-500.

For treatment of the WGA-agarose fractions with β(1-3)glucanase, the pH of either desalted fraction 1 or pooled fractions 4 and 5 was adjusted to 7.5 and 40 μl of chitinase-free Zymolyase (2) was added. Mixtures were incubated for 3 h at 37°C and then fractionated on Sephacryl S-500 after the additions mentioned above.

For chitinase digestion, the pH of fraction 1 or fractions 4 and 5 was adjusted to 6.3 and 20 μl of curdlan-purified chitinase was added. Incubation was overnight at 37°C. To the digested mixtures, additions were made as described above, followed by chromatography on Sephacryl S-500.

TABLE 2 Isolation of β(1-3)glucan by β(1-6)glucanase and sodium hydroxide treatment of cell walls[a]

Strain	β(1-6)glucanase supernatant[b]	NaOH-soluble fraction[c]
YPH499 (wild type)	53.2 ± 3.3 (33)	55.6 ± 3.8 (10)
ECY46-4-1B (*chs3*Δ)	47.1 ± 4.6 (9)	79.8 ± 2.6 (5)
NBT014 (*crh1*Δ *crh2*Δ)	46.8 ± 3 (18)	67.9 ± 5 (4)
BY4741 (wild type)	59.3 (1)	58 (1)
YHR307W (*gas1*Δ)	48.4 ± 5 (3)	52.8 ± 1.7 (3)

[a] Cells were labeled with [^{14}C]glucose as described in Materials and Methods.
[b] Mean percentage of cell wall radioactivity in β(1-6)glucanase supernatant ± standard deviation. Values in parentheses indicate how many independent determinations were carried out in each case.
[c] Mean percentage of the radioactivity of the β(1-6)glucanase-insoluble fraction in the 1 M NaOH supernatant ± standard deviation. Values in parentheses indicate how many independent determinations were carried out.

RESULTS

Two populations in bulk β(1-3)glucan. In the past, β(1-3)glucan was prepared by extraction of intact yeast cells with sodium hydroxide and acetic acid at high temperatures (18). Treatment of cell walls with hot alkali results in the extraction of part of β(1-3)- and β(1-6)glucan and of proteins, which are degraded in the procedure. The β(1-3)glucan may also be partly degraded, but the portion bound to chitin remains insoluble (19). We wished to use mild conditions conducive to the formation of a product as similar as possible to the native polysaccharide. To this end, we first labeled wild-type cells (strain YPH499) *in vivo* with [^{14}C]glucose to tag all of the cell wall components. Cell walls were then isolated and digested with recombinant β(1-6)glucanase (Fig. 2A and Materials and Methods). Hydrolysis of β(1-6)glucan by the endoglucanase also liberated the mannoproteins, which are water soluble (see Fig. 1). About half of the radioactivity was found in the supernatant after centrifugation (Table 2), in line with previously published results (17). The insoluble fraction consists mostly of β(1-3)glucan, with a small amount of chitin, some of it previously linked to β(1-6)glucan, some free, and some bound to β(1-3)glucan. Accordingly, sequential treatment of this material with chitinase and β(1-3)glucanase (Zymolyase) solubilized all of the radioactivity. To make the insoluble residue accessible to fractionation, it was carboxymethylated (Fig. 2B), a procedure that results in the attachment of acetic acid residues to the polysaccharide. The negative charges thus introduced counteract the attraction between carbohydrate chains due to hydrogen bonds, and both β(1-3)glucan and chitin become soluble in water (4). The solubilized material was fractionated on a Sephacryl S-500 size exclusion column. The elution profile showed a sharp peak at the void volume position, followed by radioactivity extending through most of the column included volume (Fig. 2C, green line). When a portion of the fraction that remains insoluble after β(1-6)glucanase digestion was briefly treated with 1 M NaOH at room temperature, more than half of the radioactivity was solubilized (Table 2). The solubilized polysaccharide was precipitated with ethanol. Both this material and the fraction that remained insoluble in alkali were carboxymethylated (Fig. 2A) and fractionated on Sephacryl S-500 (Fig. 2C). Here it can be seen that the alkali-insoluble fraction (yellow curve) contained mostly high-molecular-weight material, whereas the soluble polysaccharide (red curve) was highly polydisperse. The range of molecular weights in the alkali-insoluble material cannot be assessed because most of it emerges from the

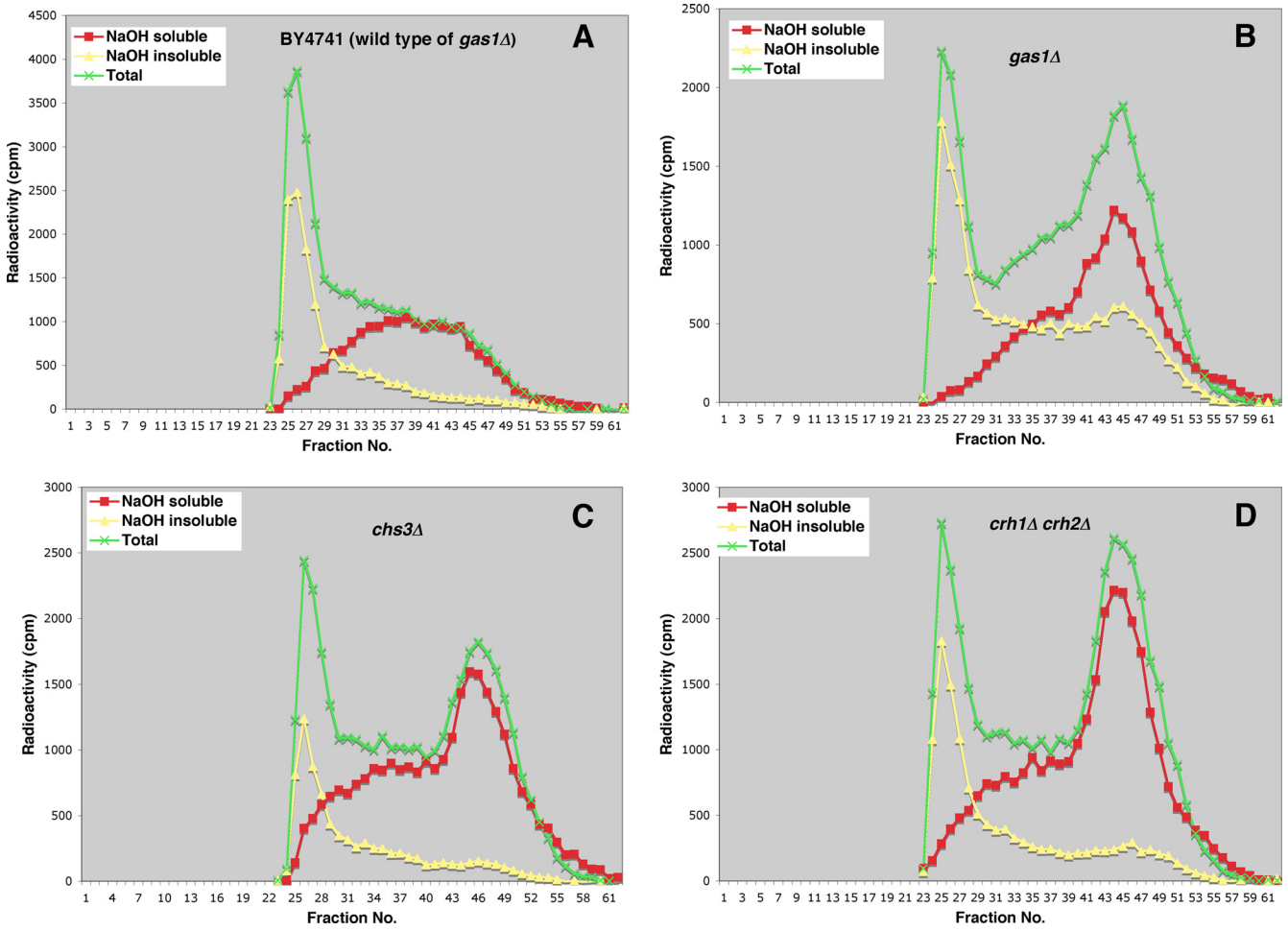

FIG 3 Chromatography of total, NaOH-soluble, and NaOH-insoluble fractions of different strains on Sephacryl S-500. (A) Strain BY4741 (wild type of the *gas1*Δ mutant). (B) Strain YHR307W (*gas1*Δ). (C) Strain ECY46-4-1B (*chs3*Δ). (D) Strain NBT014 (*crh1*Δ *crh2*Δ). The two latter mutations are in the YPH499 background. In all cases, the procedure was as that used for Fig. 2A.

column at the void volume. As mentioned above, the β(1-6)glucanase-resistant fraction contains, in addition to β(1-3)glucan, free and β(1-3)glucan-bound chitin, whose presence could conceivably affect the elution pattern. We assumed that this effect would be negligible, in view of the small amount of chitin present in the cell wall, and this turned out to be the case, as shown below.

The results of these experiments are consistent with the presence in yeast cell walls of two β(1-3)glucan populations, one of extremely high molecular weight and the other one showing a broad range of smaller sizes.

Cell wall mutants show an abnormal size distribution of β(1-3)glucan. To validate our procedure, we applied it to mutants known or presumed to be affected in cell wall structure. One of them was a *gas1* mutant. Gas1p, a protein identified about 27 years ago, has been found to exhibit a transglucosidase activity *in vitro*, transferring glucose chains from a β(1-3)-linked glucose oligosaccharide to another (20). On that basis, it has been speculated that the enzyme functions in the elongation of β(1-3)glucan, but no *in vivo* evidence that this is the case has been published. We performed the experiment shown in Fig. 2C with a *gas1* deletion mutant and with the corresponding wild-type strain, BY4741. The results obtained with the wild type (Fig. 3A) were very similar to those obtained with strain YPH499, but those obtained with the mutant were quite different, showing a sharp shift toward the lower molecular weights in both the NaOH-soluble and insoluble fractions (Fig. 3B). Because the shift occurred in both fractions, the percentage of NaOH-soluble material changed little from that of the wild type (Table 2). These results indicate that Gas1p participates somehow in the polymerization of β(1-3)glucan *in vivo*.

Another mutant we tested was a *chs3*Δ mutant strain, in the same genetic background as YPH499. This strain lacks the chitin attached to both β(1-3) and β(1-6)glucan (28). Rather surprisingly, here too there was some shift toward the smaller sizes of β(1-3)glucan, although it occurred only with the alkali-soluble fraction (Fig. 3C). A very similar pattern (Fig. 3D) was found with a *crh1*Δ *crh2*Δ mutant strain, which has a normal level of chitin (23) but in which the chitin is not bound to either β(1-3) or β(1-6)glucan (2, 3). In contrast to the *gas1* mutant, in both the *chs3* and *crh1 crh2* mutant strains, all of the increase in smaller-size β(1-3)glucan occurred in the NaOH-soluble fraction (Fig. 3C and D; Table 2), which points to a different mechanism. We will return to these results in the Discussion.

Morphological assessment of the effect of sodium hydroxide. A question raised was whether the solubilization of part of the

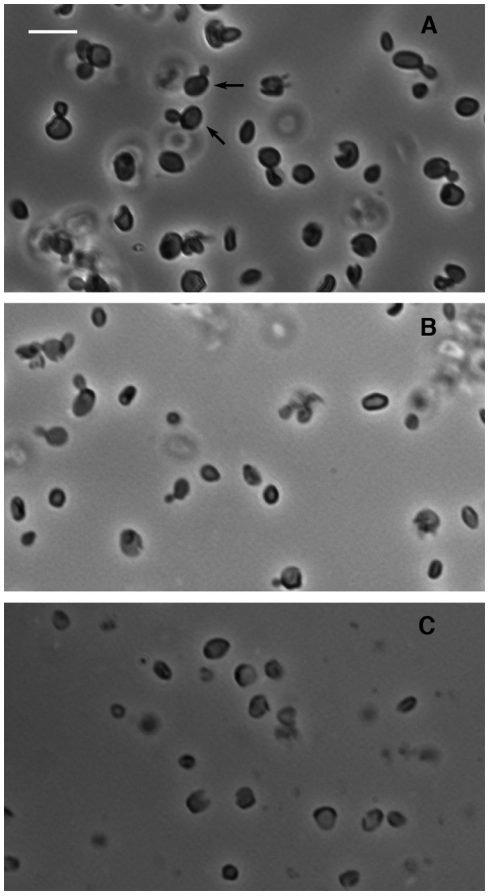

FIG 4 Cell walls before and after different treatments. (A) Untreated cell walls. Note that bud cell walls are in several cases attached to mother walls (arrows). (B) Cell walls after incubation with β(1-6)glucanase. (C) Cell walls after further treatment with 1 M sodium hydroxide at room temperature. No bud cell walls are visible here. Scale bar represents 10 μm.

β(1-3)glucan by sodium hydroxide could be somehow visualized by observation of untreated and treated cell walls. The cell walls prepared with the BeadBeater were unsuitable for this purpose because their shredding had gone too far. However, walls prepared by vortexing with glass beads (see Materials and Methods) better maintained the original cell shape and in many cases (26%, $n = 414$) showed attached walls of the buds (Fig. 4A). After treatment with β(1-6)glucanase, the walls were less dark but the general morphology did not change and the percentage of joined mother-bud cell walls was 23.4% ($n = 393$; Fig. 4B). However, when those cell walls were briefly treated with 1 M sodium hydroxide at room temperature, practically all of the bud cell walls disappeared, with only 0.6% ($n = 314$) remaining (Fig. 4C). Thus, these results strongly suggest that it is mainly the β(1-3)glucan of daughter cells, the ones that are growing, that is solubilized by alkali.

Both the wild type and a *crh1*Δ *crh2*Δ mutant contain β(1-3)glucan apparently bound to chitin. Having established the size distribution pattern of the bulk β(1-3)glucan, we turned to that portion of the polysaccharide that is bound to chitin. Previous results indicated that the chitin-glucan complex is resistant to alkali at relatively high temperatures (19). Therefore, in an attempt to solubilize as much of the free β(1-3)glucan as possible, the β(1-6)glucanase-resistant fraction was incubated with 1 M NaOH at 80°C for 1 h and the treatment was repeated. As shown in Table 3, about 30% of the radioactivity remained insoluble. This fraction was incubated overnight with chitinase, which solubilized some radioactivity, and the insoluble residue was treated with 1 M NaOH at room temperature, in the same way as was done for bulk glucan. This treatment solubilized about two-thirds of the radioactivity (Table 3), which should represent part or all of the glucan previously bound to chitin. Surprisingly, a *crh1*Δ *crh2*Δ mutant strain, which should have no glucan bound to chitin, also yielded soluble material, although only about half of the amount of the wild type (Table 3). Since the lack of β(1-3)- or β(1-6)glucan covalently linked to chitin in such a mutant was previously shown by three different methods (2), we reasoned that perhaps part of the chitin was forming a noncovalent complex with β(1-3)glucan in both the wild-type and mutant strains. Support for this notion came from previous experiments in which we found that finely divided chitin, obtained by adding water to a chitin solution in *N*,*N*′dimethylacetamide–6% LiCl, efficiently adsorbed CM–β(1-3)glucan, showing an affinity between the two molecules (results not shown). The challenge was to distinguish between a covalent and a noncovalent complex of the polysaccharides.

High-molecular-weight β(1-3)glucan and chitin bind to each other covalently and noncovalently. If our hypothesis were correct, the components of the alkali-insoluble residue should include free chitin, a covalent and a noncovalent chitin–β(1-3)glucan complex, and possibly some high-molecular-weight β(1-3)glucan (Fig. 5A, left). The *crh1*Δ *crh2*Δ mutant should have the same components, except for the covalent complex. Obviously, it would not be possible to analyze this mixture as long as all of the components are insoluble. Therefore, the first step should be solubilization, which can be attained by carboxymethylation of the material. This would also partially simplify the mixture, since the noncovalent complex should give rise to free CM-chitin and CM–β(1-3)glucan. These should not bind to each other because the negative charges introduced by the carboxymethylation would induce repulsion between the polysaccharide chains. Thus, the components of the solubilized mixture should be CM-chitin, CM-glucan, and the covalent CM–chitin–β(1-3)glucan in the wild type (Fig. 5A, right) and only the first two in the *crh1*Δ *crh2*Δ mutant. It seemed that a first step in the separation of these components could be adsorption-elution on WGA-agarose because WGA specifically binds compounds with β(1-4)*N*-acetylglucosamine linkages, such as those of chitin. Thus, CM-chitin, free or in a complex, should be adsorbed, but β(1-3)glucan should not. However, we found that a large percentage of [^{14}C]CM–β(1-

TABLE 3 Fractionation of β(1-6)glucanase-insoluble material by treatment with sodium hydroxide at 80°C, followed by incubation with chitinase and new treatment with sodium hydroxide at room temperature[a]

Fraction	Wild type[b]	*crh1*Δ *crh2*Δ mutant
NaOH (80°C) insoluble	29.5 ± 3.2	23.1 ± 3.1
NaOH (room temp) soluble after chitinase	20.7 ± 0.8	10.6 ± 3

[a] Cells were labeled with [^{14}C]glucose as described in Materials and Methods.
[b] Values represent the radioactivity in each fraction as a percentage of the β(1-6)glucanase-insoluble radioactivity. The data in the first row are averages of five experiments, and those in the second row are averages of two experiments.

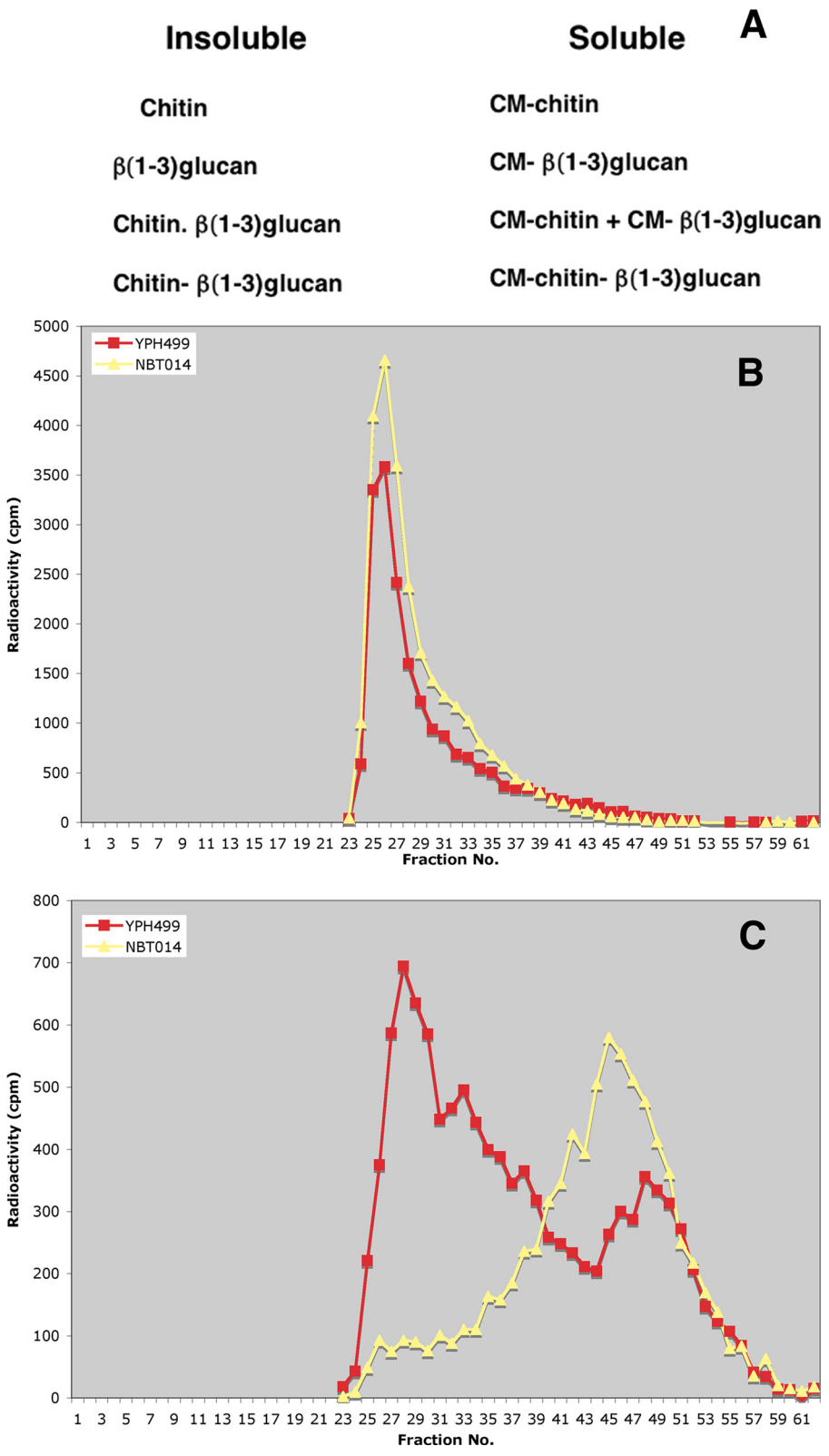

FIG 5 Isolation of the covalent chitin–β(1-3)glucan complex. (A) Left, components of the sodium hydroxide-insoluble fractions. The covalent complex of chitin and β(1-3)glucan is symbolized by a hyphen between the two, whereas the noncovalent complex has a dot. Right, components of the fraction solubilized by carboxymethylation. Note that the number of components decreased from 4 to 3 after carboxymethylation. The carboxymethylated mixtures from the wild type and the *crh1*Δ *crh2*Δ mutant were applied to WGA-agarose columns (B) Sephacryl S-500 chromatography of material not retained by WGA-agarose for YPH499 (wild type) and NBT014 (*crh1*Δ *crh2*Δ). This represents free CM–β(1-3)glucan (C) fractionation of 0.1 NaOH eluates of WGA-agarose columns on Sephacryl S-500. For the wild type, the first peak contains the CM–chitin–β(1-3)glucan covalent complex, while the second peak corresponds to free chitin. Only the free chitin peak is present in the mutant fraction. See text and Materials and Methods for details.

TABLE 4 Fractionation of carboxymethylated, NaOH-insoluble fraction on WGA-agarose[a]

Fraction	Wild type[b]	*crh1*Δ *crh2*Δ mutant
Column percolate	54.8 ± 3.1	74 ± 0.55
0.1 M NaOH eluate	26.6 ± 3	20.7 ± 1.5
Total recovery	81.4	94.7

[a] Cells were labeled with [^{14}C]glucose as described in Materials and Methods.
[b] Data represent percentages of the radioactivity applied to the columns and are the averages of three experiments ± the standard deviations.

3)glucan from yeast was adsorbed by WGA-agarose. In view of the specificity of WGA, it seemed probable that this adsorption was unspecific and due to the negative charges introduced by carboxymethylation. A high ionic strength should abolish that kind of binding. Accordingly, when a [^{14}C]CM–β(1-3)glucan solution containing 1 M sodium chloride was applied to WGA-agarose, 90% of the radioactivity was recovered in the filtrate. Under the same conditions, 100% of a sample of [^{14}C]CM-chitin from yeast was adsorbed. There still remained the problem of eluting the chitin-containing material from the column. Several procedures, such as high concentrations of *N*-acetylglucosamine or of unlabeled CM-chitin, did not work at all. Finally, it was found that 0.1 M sodium hydroxide eluted 85 to 95% of the adsorbed [^{14}C]CM-chitin.

With this knowledge, β(1-6)glucanase-resistant fractions of both the wild-type and *crh1*Δ *crh2*Δ mutant strains were treated with alkali at 80°C and solubilized by carboxymethylation. After the sodium chloride concentration was adjusted to 1 M, they were applied to WGA-agarose columns. The percolates were expected to consist of free β(1-3)glucan. The columns were then washed with 0.1 M sodium hydroxide to elute any CM-chitin and CM–chitin–β(1-3)glucan present. The amount of radioactivity not retained by the column was always higher for the mutant than for the wild type (Table 4), and so was the total recovery. In the case of the wild type, some radioactivity was tenaciously retained by the WGA-agarose. When, after the elution, the WGA-agarose was suspended and transferred to a scintillation vial, very little, if any, radioactivity was found in the mutant column. The wild-type column had a much larger amount, which brought the total recovery to a value similar to that for the *crh1*Δ *crh2*Δ mutant when added to the other fractions. We assume that this tightly bound material is high-molecular-weight CM–chitin–β(1-3)glucan.

Both the column percolates and the material eluted with alkali were fractionated on Sephacryl S-500 columns (Fig. 5B and C). The profiles of the percolates were very similar for both strains and showed single peaks of very high molecular weight (Fig. 5B). Those of the alkali-eluted material, however, were sharply different: the wild type gave rise to two peaks, the first of which was somewhat jagged (Fig. 5 C); the *crh1*Δ *crh2*Δ mutant yielded a single peak that emerged a little earlier than the second peak of the wild type (Fig. 5 C). The position of the second wild-type peak is the same as for CM-chitin from yeast (see Fig. 7A). The single peak of the mutant is also believed to be CM-chitin, because in this strain the free chitin is significantly larger than that of the wild type, presumably because none of it is transferred to β(1-3)glucan or β(1-6)glucan (2). Therefore, the first peak of the wild type should be the CM–chitin–β(1-3)glucan covalent complex, in agreement with its higher molecular weight. This material is lacking in the *crh1*Δ *crh2*Δ mutant, as expected.

Further characterization of WGA-agarose fractions by enzymatic treatments. To verify the chemical nature of the WGA-agarose fractions, both percolates and NaOH eluates were treated with either β(1-3)glucanase or chitinase before Sephacryl chromatography. Incubation of a CM–β(1-3)glucan sample with chitinase-free Zymolyase (2), followed by fractionation on Sephacryl S-500, resulted in a large displacement of the peak toward the lower-molecular-weight area (see Fig. S1 in the supplemental material). Total hydrolysis of β(1-3)glucan by this enzyme should result in an oligosaccharide of 5 glucose units (10). In the Sephacryl S-500 column, it would probably run about the same as glucose, whose maximum is found in fractions 56 and 57. The digested peak emerges somewhat earlier (see Fig. S1), indicating that the breakdown of the polysaccharide is not complete, most probably because of the presence of acetate groups that hinder the action of the enzyme. Incubation of the WGA-agarose percolates with Zymolyase gave a similar result (Fig. 6A and B), confirming that these fractions consist of CM–β(1-3)glucan. In the alkali-eluted fraction of the wild type, the first peak was shifted in the same way (Fig. 6C), as expected if it contained CM–β(1-3)glucan. Because of the superimposition of the digested material with the position of CM-chitin, no information can be furnished by this experiment about the position of the glucan-bound chitin or of the second peak. Finally, the alkali-eluted material from the *crh1*Δ *crh2*Δ mutant strain was somewhat displaced, although not as much as for the percolates, by glucanase digestion (Fig. 6D). This result was unexpected and may indicate the presence of some β(1-3)glucan in this fraction.

When chitinase was used on the WGA-agarose percolates, a surprising result was obtained because the peaks, which should not contain chitin, were significantly shifted to the right (see Fig. S2 in supplemental material). Although when the chitinase was first prepared we found no β(1-3)glucanase activity in it with laminarin as the substrate (22), this result indicated the possibility of a small amount of contamination with such an activity. To eliminate the putative glucanase, we treated the chitinase preparation with curdlan gel. Curdlan is a β(1-3)glucan from bacteria that is very insoluble in water and forms a gel at 56°C. It seemed probable that the gel could adsorb the glucanase, for which it is a substrate. After curdlan treatment, CM-chitin was still degraded by the chitinase to the same extent as before (Fig. 7A), with limitations similar to those previously observed for β(1-3)glucanase acting on β(1-3)glucan. However, the purified chitinase only slightly modified the profiles of the percolates (Fig. 7B and C). The small effect may be due to remaining traces of β(1-3)glucanase activity. No effect of the purified chitinase on the first peak of the wild-type alkaline eluate was observed, whereas the second peak was shifted, confirming that it consists of CM-chitin (Fig. 7 D). Although the shift is small, it is comparable to that obtained with CM-chitin (Fig. 7A). The lack of displacement of the first peak may be explained by the relatively small amount and low molecular weight of the chitin bound to β(1-3)glucan. In the case of the *crh1*Δ *crh2*Δ mutant, chitinase caused a pronounced shift, supporting the notion that this peak corresponds to CM-chitin (Fig. 7E).

The results of treatments with β(1-3)glucanase and chitinase are in general agreement with the notion that the material not adsorbed by the WGA-agarose columns is CM–β(1-3)glucan, whereas that absorbed and later eluted consists of a covalent CM–chitin–β(1-3)glucan complex plus free chitin for the wild type and

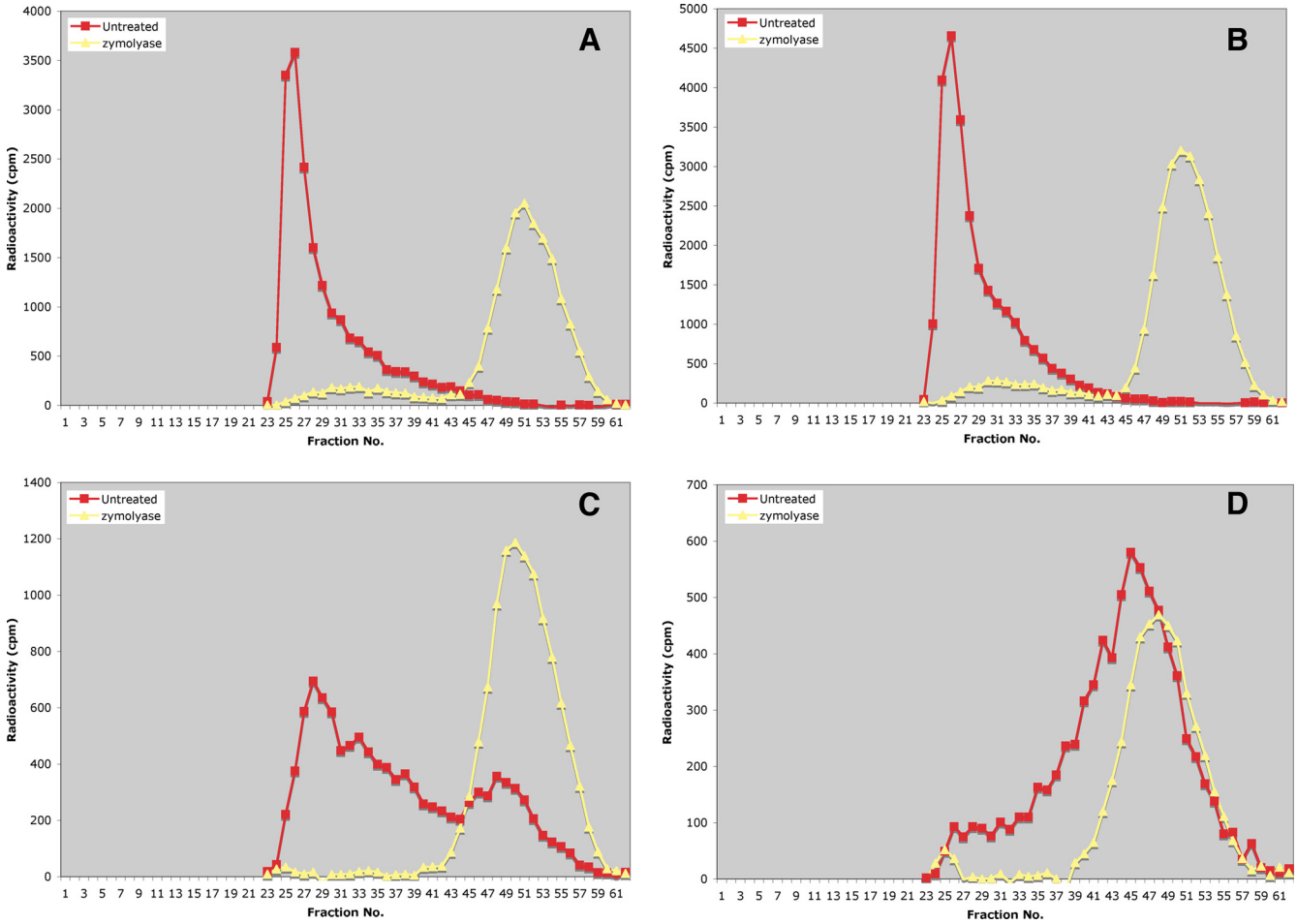

FIG 6 Chromatography of WGA-agarose fractions on Sephacryl S-500 after treatment with Zymolyase [β(1-3)glucanase]. (A) Percolates of strain YPH499 (wild type). (B) Percolates of NBT014 (*crh1*Δ *crh2*Δ). (C) NaOH fractions of the wild type. (D) NaOH fractions of the *crh1*Δ *crh2*Δ mutant.

only the latter for the *crh1*Δ *crh2*Δ mutant. Thus, the results are in agreement with those predicted in Fig. 5A.

The WGA-agarose procedure provided an opportunity to verify whether the presence of chitin affected the elution pattern of the bulk β(1-3)glucan (as in Fig. 2C, green curve). To this end, a preparation of carboxymethylated total β(1-3)glucan was split in two. One portion was left untreated, and the other was filtered through a WGA-agarose column to remove both free and bound chitin. Fractionation of both samples on Sephacryl S-500 yielded the same elution pattern (Fig. 2D), showing that the effect of chitin on those chromatographic results is negligible.

Labeling with [^{14}C]glucosamine confirms the presence of covalently linked β(1-3)glucan and chitin only in the wild type. Because of uncertainty about some results, such as the slight effect of even purified chitinase on WGA-agarose percolates or the shift observed in the NaOH-eluted fraction of the *crh1*Δ *crh2*Δ mutant strain after glucanase treatment, we felt the need for independent verification of the experimental evidence. To this end, cells were labeled with [^{14}C]glucosamine rather than with [^{14}C]glucose. As we showed previously, under these conditions, chitin is labeled specifically and no radioactivity is found in the glucans (4). Labeled cells were processed as before, and the carboxymethylated, NaOH-insoluble fraction was applied to a WGA-agarose column. Here one would expect no radioactivity in the percolate, if it indeed consists of CM–β(1-3)glucan. This was the case for the *crh1*Δ *crh2*Δ mutant, but in the wild type, some radioactivity, about 10 to 15% of the total, was not retained by the column. We do not know the nature of this material, which could be glucan with a very small amount of chitin. The alkali eluates, when fractionated on Sephacryl S-500, showed patterns similar to those in which [^{14}C]glucose was the label (compare Fig. 8A and B with Fig. 5C). This result confirms that the first wild-type peak contains chitin in addition to β(1-3)glucan, whereas the second wild-type peak and the only peak of the mutant consist of chitin only.

Although the results are in general agreement with the previous data, in Fig. 8A, the amount of chitin bound to β(1-3)glucan seems a very small percentage of the total chitin. However, when one adds to it the fraction of radioactivity present in the WGA-agarose percolate and that remaining tightly bound to the same column, the final result is 43% of the total (average of two determinations), which is comparable to the ~40% that was found with a different methodology for the same strain (4).

DISCUSSION

The data presented here offer the first glimpse of the size distribution of β(1-3)glucan, the main structural component of the yeast

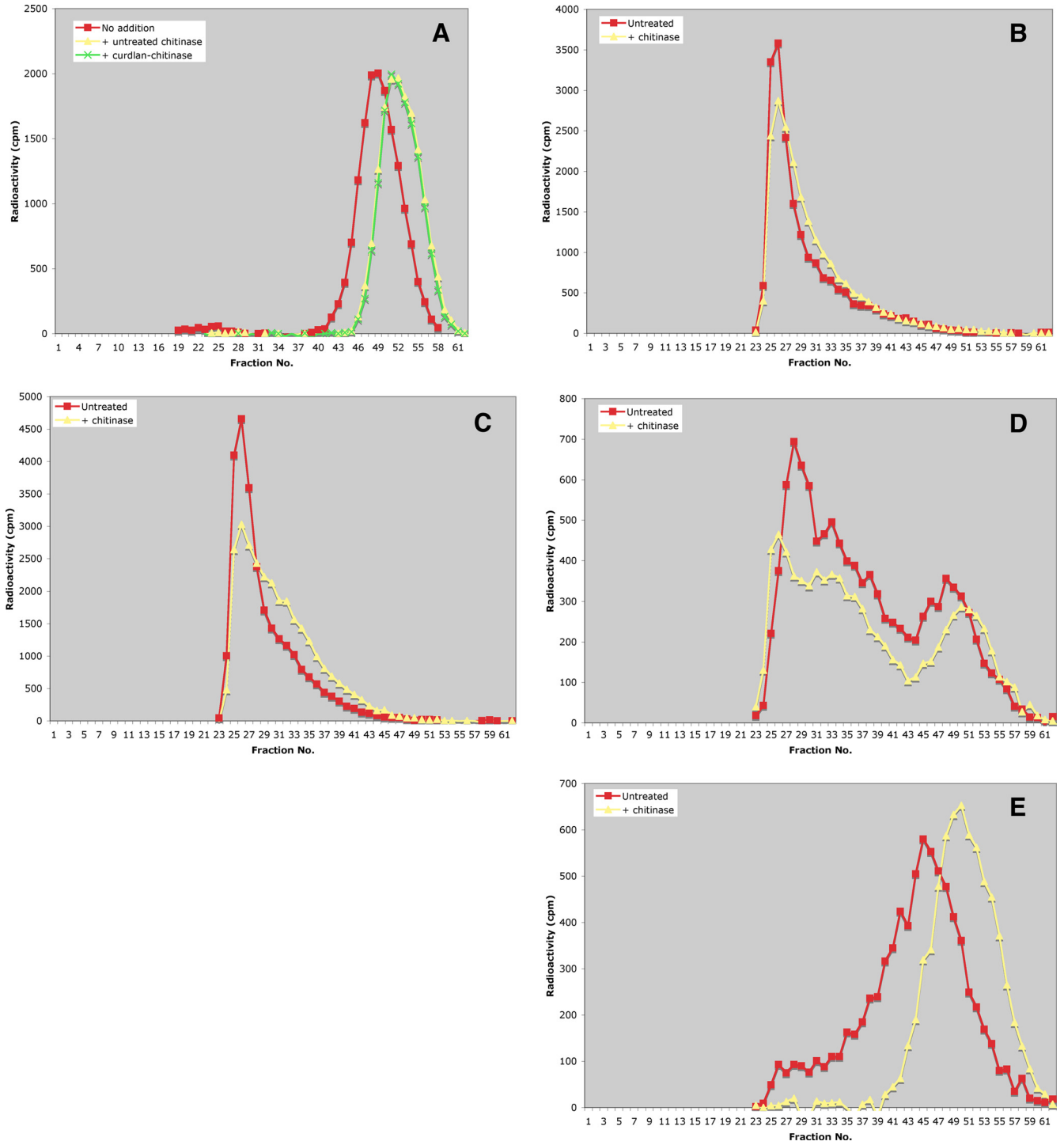

FIG 7 Chromatography of WGA-agarose fractions on Sephacryl S-500 after treatment with chitinase. (A) Chromatography of [^{14}C]CM-chitin before and after treatment with untreated or curdlan-treated chitinase. (B) Percolates of the wild type. (C) Percolates of the *crh1*Δ *crh2*Δ mutant. (D) NaOH fractions of the wild type. (E) NaOH fractions of the *crh1*Δ *crh2*Δ mutant.

cell wall. Because of the mild conditions used in the isolation of the polysaccharide and its solubilization, it seems probable that the results of fractionation on a Sephacryl column are a fairly faithful reflection of the *in vivo* distribution of β(1-3)glucan. Sodium hydroxide at room temperature solubilizes roughly half of the glucan. In size chromatography, the soluble fraction shows a greatly polydisperse distribution, whereas the insoluble portion, emerging at the void volume, consists of very high-molecular-weight material. According to the manufacturer, the limit for inclusion of a carbohydrate polymer in Sephacryl S-500 is a molecular weight of 2×10^7. A molecule of that size would contain more than 120,000 glucose units. According to a determination of β(1-3)glu-

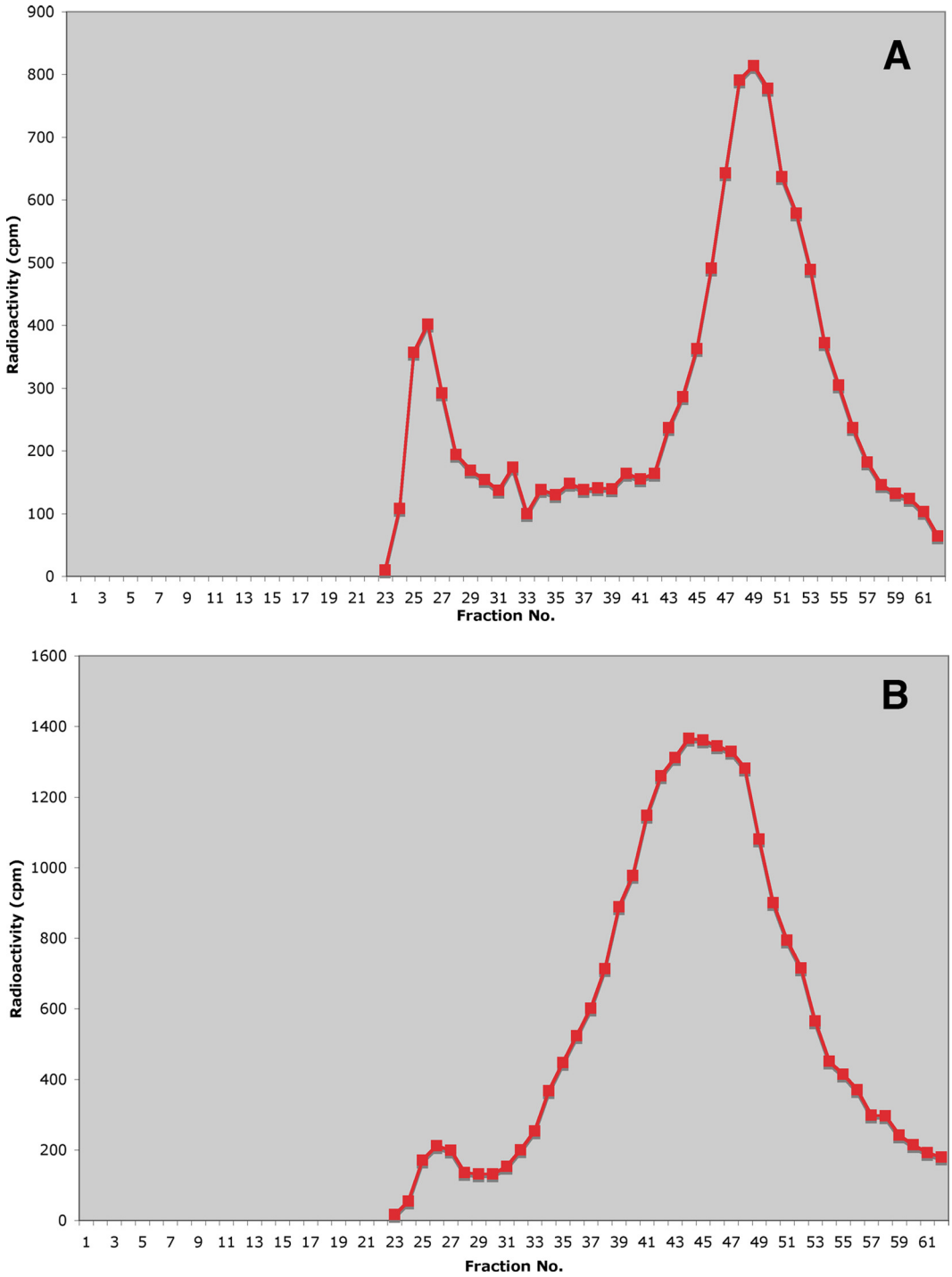

FIG 8 Chromatography on Sephacryl S-500 of WGA-agarose fractions from cells labeled with [^{14}C]glucosamine. (A) NaOH fraction of the wild type. (B) NaOH fraction of the *crh1*Δ *crh2*Δ mutant. The positions of peaks in these graphs should be compared to those in Fig. 5C.

can chain length by methylation, there would be about 1,500 glucose units per chain (18). The explanation for the much greater size that we found most probably is that the chains are cross-linked through the β(1-6) linkages that were also found in the polysaccharide (18), as depicted in Fig. 1. The cross-links would allow β(1-3)glucan to form an almost continuous network over the surface of the cell. Such a network was detected by electron microscopy (14). Because of its very high molecular weight, the alkali-insoluble fraction probably represents the structural network. Although the cell wall must at all times present a strong and continuous frame to counteract the internal turgor pressure and prevent lysis of the cell, it is also a dynamic structure that needs to be constantly remodeled to accompany cell growth. This remodeling may consist of breakage of some bonds and addition of new

material and would be expected to give rise to polysaccharide chains of many different sizes. We propose that the highly polydisperse alkali-soluble fraction represents the material that is going through remodeling. This notion receives some support from the results obtained with the *gas1* mutant. Because of its *in vitro* transglycosylase activity, Gas1p has been proposed to participate in the elongation of β(1-3)glucan (20). However, no *in vivo* data were available to corroborate this idea. An increase in the ratio of alkali-soluble to insoluble total glucan was reported in a *gas1* mutant, but it was attributed to a decrease in alkali-insoluble β(1-6)glucan (21). Our results (Fig. 3) clearly show that a *gas1* deletion mutant manifests a large increase in the polydisperse fraction of β(1-3)glucan, which is observed in both the alkali-soluble and alkali-insoluble fractions. This result is consistent with a role for Gas1p in the size increase of the polysaccharide, although elucidation of the mechanism by which this protein acts *in vivo* will require further work. The large perturbation in the presumably cross-linked β(1-3)glucan observed in a *gas1* mutant (Fig. 3B) is consistent with a function of Gas1p in the cross-linking process, as previously suggested (20). While this is a rather speculative concept, what is fairly clear is that the reduction in the high-molecular-weight glucan found here in the mutant weakens the cell wall. The somewhat larger and rounder aspect of *gas1* mutant cells is consistent with a defect in cell wall maturation. Furthermore, *gas1* mutants have a greatly increased content of cell wall chitin (9), which probably helps to stabilize the cell wall, because elimination of that chitin by a *chs3* mutation results in *gas1 chs3* mutant cells that grow very poorly (21). These findings support our argument that the high-molecular-weight β(1-3)glucan is the structural component of the polysaccharide. Further backing for this concept came from observation in the microscope of cell walls before or after different treatments (Fig. 4). About one-fourth of the mother cell walls were attached to bud cell walls. This morphology survived β(1-6)glucanase digestion, but the bud cell walls disappeared upon mild sodium hydroxide treatment. Since the bud is where growth and cell wall remodeling occur, this result strongly supports our proposal that the alkali-soluble fraction represents material undergoing remodeling.

A rather surprising result was the increase in polydisperse β(1-3)glucan, albeit smaller than that in a *gas1* mutant strain, found both in a *chs3* mutant, which lacks chitin both in lateral walls and at the neck, and in a *crh1 crh2* mutant, which has the chitin but all in a free form (2). An increase in total glucan soluble in hot alkali in the *crh1 crh2* mutant was reported earlier (23). The fact that both the *chs3*Δ and *crh1*Δ *crh2*Δ mutants yield very similar size distributions of β(1-3)glucan implies that it is the attachment of chitin to the polysaccharide, rather than its mere presence, that causes the difference from the wild type. In lateral walls, chitin appears in the daughter cell after septation and during the residual growth before new budding (28). The defect found in the *chs3*Δ and *crh1*Δ *crh2*Δ mutants suggests that this chitin, mostly bound to β(1-6)glucan (4), may have some role in the arrest of growth at the end of the cell cycle, although the mechanism of such an action is still unknown.

Once the size distribution of the bulk β(1-3)glucan was established, it was possible to address the main subject of this work, i.e., the structure of the polysaccharide linked to chitin in the neck region, which, as we previously determined, is almost all β(1-3)glucan (4). Initially, isolation of this fraction of β(1-3)glucan was attempted by digestion of cell walls with β(1-6)glucanase, followed by alkali treatment, incubation with chitinase, and a new brief exposure to sodium hydroxide. This procedure led to the unexpected result that a *crh1*Δ *crh2*Δ mutant, in which all chitin had been found to be free, apparently had some chitin bound to β(1-3)glucan. An answer to this conundrum was found after solubilizing by carboxymethylation the material resistant to β(1-6)glucanase and alkali and subjecting it to fractionation on WGA-agarose columns, followed by chromatography on Sephacryl S-500. The results are consistent with the presence, in both the wild type and the *crh1*Δ *crh2*Δ mutant, of a tight, alkali-resistant, noncovalent complex of β(1-3)glucan and chitin. Because of the possible presence in the analyzed mixture of some free β(1-3)glucan of high molecular weight, it is not possible to calculate how much glucan is bound to chitin in this manner. A minimal amount is 10% of the total, the fraction solubilized by alkali after chitinase treatment in the *crh1*Δ *crh2*Δ mutant (Table 3). The localization of this complex is unknown, and it may well be in the lateral cell wall. The glucan in the noncovalent complex is part of the percolate of the WGA-agarose columns, which is all of high molecular weight (Fig. 5B); therefore, it appears to belong to the final structural product. Is the noncovalent chitin–β(1-3)glucan complex present *in vivo*, or could it be an extraction artifact? Although the mild conditions used here suggest that the complex was already present in the cell, it is conceivable that stripping away the β(1-6)glucan and mannoproteins somehow brought chitin and β(1-3)glucan together. This is, however, rather unlikely, because β(1-6)glucan and attached proteins are in the external layer of the cell wall, while chitin and β(1-3)glucan are believed to populate an inner layer (11).

In contrast to the physical complex of chitin and β(1-3)glucan, the covalent one is found only in the wild type (Fig. 5C). That this material contains both glucan and chitin was shown both by the enzymatic treatments and by labeling of the cells with [^{14}C]glucosamine rather than [^{14}C]glucose (Fig. 6 to 8). Our calculations indicate that about 7% of the total β(1-3)glucan is covalently linked to chitin, in consonance with its presence only at the mother-bud neck, a small portion of the cell wall. Most of the complex is of high molecular weight, supporting the notion that the β(1-3)glucan linked to chitin at the neck is not being metabolized, in agreement with our hypothesis. The recent report that localization of Gas1p at the mother-bud neck requires Crh1p and Crh2p (25), together with our previous finding that Crh2p is concentrated at the same location (23), suggests that these enzymes cooperate in the maturation of the cell wall at the neck: Gas1p could act in glucan cross-linking and the transferases in blocking further remodeling of the polysaccharide by adding chitin chains to it. However, we are not implying that the cell wall at the mother-bud neck consists only of the chitin–β(1-3)glucan complex. In fact, electron micrographs show at the neck, as in the remainder of the cell surface, an external darker and hairy-cell-like wall layer that has been generally associated with the presence of mannoproteins (see, for instance, Fig. 2 of reference 28). Most probably, the cell wall at the neck in the early phase of budding has the same composition as the remainder, but as the chitin ring and the septin ring are formed, they redundantly block further synthesis by the mechanisms discussed in the introduction. One may ask why there should be two overlapping programs, one based on the chitin ring and the other on the septin ring, for the control of growth at the neck. The answer may be that the structural preservation at the neck, the future site of cytokinesis, is so important that a dou-

ble protection mechanism conferred an evolutionary advantage under conditions encountered in the wild.

One prediction of our hypothesis, as formulated in the introduction, is that free chitin, not covalently linked to glucan, such as in a *crh1*Δ *crh2*Δ mutant, would not be effective in preventing growth at the neck when septins are defective. In another study (N. Blanco, M. Reidy, J. Arroyo, and E. Cabib, unpublished data), we addressed this question and verified that the predicted outcome was correct.

In conclusion, we have shown that the cell wall β(1-3)glucan consists of a very high-molecular-weight fraction and another smaller fraction that varies in size. The latter material is dramatically increased in a *gas1* mutant believed to have problems in β(1-3)glucan polymerization and a weaker wall. Therefore, we assume that the large-size material is the final structural polysaccharide, whereas the polydisperse fraction represents the portion undergoing remodeling during cell wall growth. The β(1-3)glucan attached to chitin at the mother-bud neck is mostly of high molecular weight, supporting the idea that the linkage between the two polysaccharides contributes to maintenance of the cell wall in a quiescent state at the neck. Finally, a noncovalent complex of β(1-3)glucan and chitin has been identified for the first time.

Aside from these findings, the novel techniques developed in this work may well be useful in future studies of the mechanism of cell wall growth and its control.

ACKNOWLEDGMENTS

We thank V. Farkas for a sample of carboxymethylchitin.

This study was supported by a National Institutes of Health grant (Intramural Research Program, NIDDK). J.A. and N.B. were supported by projects BIO2010-22146 (Ministerio de Ciencia e Innovacion [MICINN], Spain) and GR58/08 (reference no. 920640; Universidad Complutense de Madrid) and the European Science Foundation Research Networking Programme (06-RNP-132). N.B. is the recipient of an FPI Ph.D. fellowship (BES-2008-003171) from MICINN.

REFERENCES

1. **Bom IJ, et al.** 1998. A new tool for studying the molecular architecture of the fungal cell wall: one step purification of recombinant *Trichoderma* β-(1-6)-glucanase expressed in *Pichia pastoris*. Biochim. Biophys. Acta **1425**:419–424.
2. **Cabib E.** 2009. Two novel techniques for determination of polysaccharide cross-links show that Crh1p and Crh2p attach chitin to both β(1-6)- and β(1-3)glucan in the *Saccharomyces cerevisiae* cell wall. Eukaryot. Cell **8**:1626–1636.
3. **Cabib E, Blanco N, Grau C, Rodríguez-Peña JM, Arroyo J.** 2007. Crh1p and Crh2p are required for the cross-linking of chitin to β(1-6)glucan in the *Saccharomyces cerevisiae* cell wall. Mol. Microbiol. **63**:921–935.
4. **Cabib E, Durán A.** 2005. Synthase III-dependent chitin is bound to different acceptors depending on location on the cell wall of budding yeast. J. Biol. Chem. **280**:9170–9179.
5. **Cabib E, Roh D-H, Schmidt M, Crotti LB, Varma A.** 2001. The yeast cell wall and septum as paradigms of cell growth and morphogenesis. J. Biol. Chem. **276**:19679–19682.
6. **Caudron F, Barral Y.** 2009. Septins and the lateral compartmentation of eukaryotic membranes. Dev. Cell **16**:493–506.
7. **Crotti LB, Drgon T, Cabib E.** 2001. Yeast cell permeabilization by osmotic shock allows determination of enzymatic activities *in situ*. Anal. Biochem. **292**:8–16.
8. **Drgonová J, Drgon T, Roh D-H, Cabib E.** 1999. The GTP-binding protein Rho1p is required for cell cycle progression and polarization of the yeast cell. J. Cell Biol. **146**:373–387.
9. **Kapteyn JC, et al.** 1997. Altered extent of cross-linking of β1,6-glucosylated mannoproteins to chitin in *Saccharomyces cerevisiae* mutants with reduced cell wall β1,3-glucan content. J. Bacteriol. **179**:6279–6284.
10. **Kitamura K, Kaneko T, Yamamoto Y.** 1974. Lysis of viable yeast cells by enzymes of *Arthrobacter luteus*. II. Purification and properties of an enzyme, Zymolyase, which lyses viable yeast cells. J. Gen. Appl. Microbiol. **20**:323–344.
11. **Klis FM, Boorsma A, De Groot PWJ.** 2006. Cell wall construction in *Saccharomyces cerevisiae*. Yeast **23**:185–202.
12. **Kollár R, Petráková E, Ashwell G, Robbins PW, Cabib E.** 1995. Architecture of the yeast cell wall. The linkage between chitin and β(1→3)-glucan. J. Biol. Chem. **270**:1170–1178.
13. **Kollár R, et al.** 1997. Architecture of the yeast cell wall. β(1→6)-Glucan interconnects mannoprotein, β(1→3)-glucan, and chitin. J. Biol. Chem. **272**:17762–17775.
14. **Kopecká M, Phaff HG, Fleet GH.** 1974. Demonstration of a fibrillar component in the cell wall of the yeast *Saccharomyces cerevisiae* and its chemical nature. J. Cell Biol. **62**:66–76.
15. **Lesage G, Bussey H.** 2006. Cell wall assembly in *Saccharomyces cerevisiae*. Microbiol. Mol. Biol. Rev. **70**:317–343.
16. **Lippincott J, Li R.** 1998. Sequential assembly of myosin II, an IQGAP-like protein, and filamentous actin to a ring structure involved in budding yeast cytokinesis. J. Cell Biol. **140**:355–366.
17. **Magnelli P, Cipollo JF, Abeijón C.** 2002. A refined method for the determination of *Saccharomyces cerevisiae* cell wall composition and β-1,6-glucan fine structure. Anal. Biochem. **301**:136–150.
18. **Manners DJ, Masson AJ, Patterson JC.** 1973. The structure of a β-(1→3)-D-glucan from yeast cell walls. Biochem. J. **135**:19–30.
19. **Mol PC, Wessels JGH.** 1987. Linkages between glucosaminoglycan and glucan determine alkali-insolubility of the glucan in walls of *Saccharomyces cerevisiae*. FEMS Microbiol. Lett. **41**:95–99.
20. **Mouyna I, et al.** 2000. Glycosylphosphatidylinositol-anchored glucanosyltransferases play an active role in the biosynthesis of the fungal cell wall. J. Biol. Chem. **275**:14882–14889.
21. **Popolo L, Gilardelli D, Bonfante P, Vai M.** 1997. Increase in chitin as an essential response to defects in assembly of cell wall polymers in the *ggp1*Δ mutant of *Saccharomyces cerevisiae*. J. Bacteriol. **179**:463–469.
22. **Roberts RL, Cabib E.** 1982. *Serratia marcescens* chitinase: one-step purification and use for the determination of chitin. Anal. Biochem. **127**:402–412.
23. **Rodríguez-Peña JM, Cid VJ, Arroyo J, Nombela C.** 2000. A novel family of cell wall-related proteins regulated differentially during the yeast life cycle. Mol. Cell. Biol. **20**:3245–3255.
24. **Rodríguez-Peña JM, Rodríguez C, Alvarez A, Nombela C, Arroyo J.** 2002. Mechanisms for targeting of the *Saccharomyces cerevisiae* GPI-anchored cell wall protein Crh2p to polarized growth sites. J. Cell Sci. **115**:2549–2558.
25. **Rolli E, et al.** 2009. Immobilization of the glycosylphosphatidylinositol-anchored Gas1 protein into the chitin ring and septum is required for proper morphogenesis in yeast. Mol. Biol. Cell **20**:4856–4870.
26. **Schmidt M, Bowers B, Varma A, Roh D-H, Cabib E.** 2002. In budding yeast, contraction of the actomyosin ring and formation of the primary septum at cytokinesis depend on each other. J. Cell Sci. **115**:293–302.
27. **Schmidt M, Varma A, Drgon T, Bowers B, Cabib E.** 2003. Septins, under Cla4p regulation, and the chitin ring are required for neck integrity in budding yeast. Mol. Biol. Cell **14**:2128–2141.
28. **Shaw JA, et al.** 1991. The function of chitin synthases 2 and 3 in the *Saccharomyces cerevisiae* cell cycle. J. Cell Biol. **114**:111–123.
29. **Sikorski R, Hieter P.** 1989. A system of shuttle vectors and host strains designed for efficient manipulation of DNA in *Saccharomyces cerevisiae*. Genetics **122**:19–28.
30. **Trevelyan WE, Harrison JS.** 1952. Studies on yeast metabolism 1. Fractionation and microdetermination of cell carbohydrates. Biochem. J. **50**:298–303.

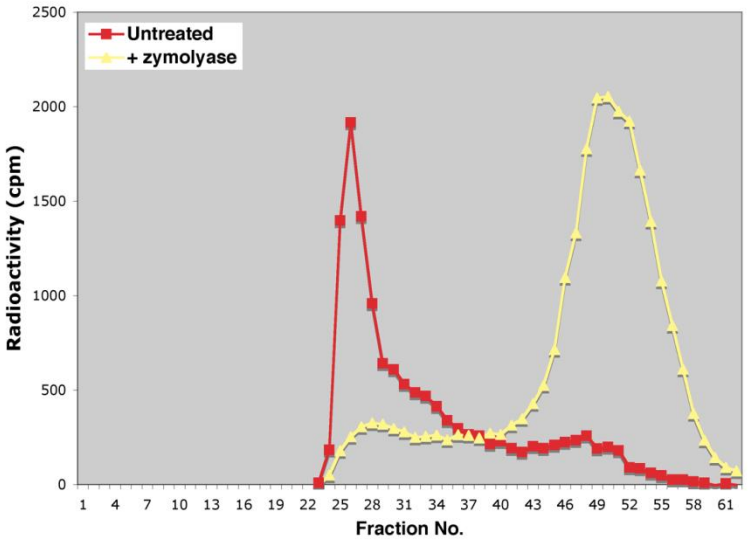

Suppl. FIG. 1. Chromatography of [^{14}C]β(1-3)glucan on Sephacryl S-500 before or after treatment with zymolyase.

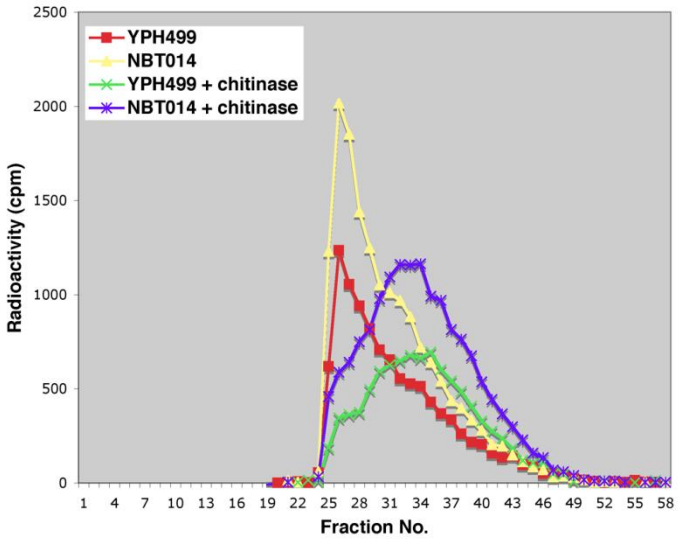

Suppl. FIG. 2. Chromatography on Sephacryl S-500 of WGA-agarose percolates of YPH499 (wild type) or NBT014 (*crh1Δ crh2Δ*) before or after digestion with untreated chitinase.

CAPÍTULO 6

IMPLICACIÓN DEL ENLACE ENTRE LA QUITINA Y EL GLUCANO EN EL CONTROL DE LA MORFOGÉNESIS DEL CUELLO DURANTE LA DIVISIÓN DE *Saccharomyces cerevisiae*

RESUMEN DE LOS RESULTADOS DEL CAPÍTULO 6

En *S. cerevisiae*, el anillo de quitina en mutantes *cla4*Δ es esencial para mantener el tamaño del cuello constante durante el crecimiento cuando el anillo de septinas está comprometido, sugiriendo que dicho anillo y las septinas están colaborando en el control de la morfogénesis (Schmidt et al., 2003). ¿Cuál es el papel funcional del anillo de quitina en este proceso? Previamente habíamos descrito (capítulo 5) que la unión de la quitina al β-1,3 glucano, principal componente estructural de la pared celular, interfiere con el metabolismo de este polisacárido. De este modo el β-1,3 glucano unido a la quitina, que predominantemente se localiza en el cuello, impediría el crecimiento en esta zona. Dado que la quitina en el cuello está en dos fracciones, una covalentemente unida y otra no covalentemente unida al β-1,3 glucano, se comprobó si la mera presencia de la quitina en el cuello era capaz de controlar el crecimiento del cuello o necesitaba estar covalentemente unida al glucano. Para ello se delecionaron los genes *CRH1* y *CRH2*, responsables de la unión entre la quitina y el glucano en la levadura, en un fondo *cla4*Δ que no tiene afectado el contenido de quitina. El triple mutante es viable, pero presenta una baja tasa de crecimiento, una alta sensibilidad a Tª y una morfología aberrante con cuellos ensanchados y yemas extremadamente alargadas. Las células forman rápidamente agregados y sedimentan. Este fenotipo es similar al que presenta la cepa *cla4*Δ *chs3*Δ a pesar de que esta cepa si contiene quitina en sus paredes. A pesar de los daños morfológicos, la división celular no parece verse afectada según los datos de la tinción con DAPI. Además, los defectos morfológicos del triple mutante fueron complementados mediante la transformación de plásmidos que contienen *CLA4*, *CRH1* o *CRH2*, mientras que la expresión de variantes no activas de *CRH1* y *CRH2* no complementaron el fenotipo. Los dobles mutantes *cla4*Δ *crh1*Δ y *cla4*Δ *crh2*Δ muestran un fenotipo intermedio con respecto al triple mutante en cuanto a morfología aberrante y engrosamiento del cuello, siendo la deleción de *CRH2* la que más empeora el fenotipo de la cepa *cla4*Δ. El análisis de la pared celular del triple mutante por microscopía electrónica reveló la presencia de cuellos ensanchados y septos anormales con localizaciones aberrantes propias de mutantes con defectos en división celular. Además, las septinas y en concreto Cdc10, están completamente desorganizadas en esta cepa con respecto al mutante *cla4*Δ y a la cepa WT. Adicionalmente, se obtuvieron mutantes combinados de los genes *CRH1*, *CRH2*, *CHS3* y *CLA4*. La formación de agregados y la sensibilidad a RC fueron analizadas en todos los

mutantes generados: *crh1*Δ *chs3*Δ, *crh2*Δ *chs3*Δ, *crh1*Δ *crh2*Δ *chs3*Δ *y crh1*Δ *crh2*Δ *chs3*Δ *cla4*Δ. Los resultados confirmaban que la deleción de *CRH1* y/o *CRH2* no afectaba al fenotipo de agregación y resistencia a RC del mutante c*hs3*Δ. El cuádruple mutante *crh1*Δ *crh2*Δ *chs3*Δ *cla4*Δ no agrava los defectos morfológicos de la cepa *crh1*Δ *crh2*Δ *cla4*Δ confirmando que es el enlace quitina-glucano y no la quitina *per se* quien regula el grosor del cuello. Para evaluar el defecto en morfogénesis que provoca la eliminación del enlace quitina-glucano se procedió a medir el diámetro de los cuellos de las diferentes cepas. Los resultados mostraron unas diferencias estadísticamente significativas entre el tamaño del cuello del triple mutante con respecto a su cepa WT, *cla4*Δ y *chs3*Δ *cla4*Δ. Adicionalmente, analizamos si el fenotipo de hiperpolarización/elongación de la yema en el triple mutante estaba relacionado con el ensanchamiento del cuello. El punto de control morfogenético que regula el crecimiento polarizado se realiza mediante la acción de la quinasa Swe1. La deleción de *SWE1* en el triple mutante dio lugar a una disminución en el tamaño de las yemas, no así en el diámetro de los cuellos que permanecían engrosados, de modo que el ensanchamiento del cuello es un proceso morfogenético independiente del crecimiento hiperpolarizado. A su vez, comprobamos que el ensanchamiento del cuello ocurre en la etapa de crecimiento de la yema. Por tanto, la pérdida de los enlaces entre la quitina y el β-1,3 glucano en el anillo de quitina en el cuello entre la célula madre y la hija claramente dan lugar al engrosamiento del mismo. Estos resultados fueron confirmados mediante la inhibición de las proteínas Crh *in vivo* en presencia de quito-oligosacáridos (tri-acetil-quitotriosa). Así, cuando células *cla4*Δ *crh1*Δ fueron crecidas en presencia de tri-acetil-quitotriosa, se observó la aparición de aberraciones morfológicas, ensanchamiento del cuello y yemas alargadas similares a las que crea la deleción de los genes *CRH*.

ARTÍCULO 6

Cross-links in the cell wall of budding yeast control morphogenesis at the mother-bud neck

Crosslinks in the cell wall of budding yeast control morphogenesis at the mother–bud neck

Noelia Blanco[1], Michael Reidy[2], Javier Arroyo[1,*] and Enrico Cabib[2,*]

[1]Departamento de Microbiología II, Facultad de Farmacia, Universidad Complutense de Madrid, 28040 Madrid, Spain
[2]Laboratory of Biochemistry and Genetics, NIDDK, National Institutes of Health, Department of Health and Human Services, Bethesda, MD 20892, USA
*Authors for correspondence (jarroyo@farm.ucm.es; enricoc@bdg10.niddk.nih.gov)

Accepted 17 September 2012
Journal of Cell Science 125, 5781–5789

doi: 10.1242/jcs.110460

Summary

Previous work has shown that, in *cla4Δ* cells of budding yeast, where septin ring organization is compromised, the chitin ring at the mother–daughter neck becomes essential for prevention of neck widening and for cytokinesis. Here, we show that it is not the chitin ring *per se*, but its linkage to β(1-3)glucan that is required for control of neck growth. When in a *cla4Δ* background, *crh1Δ crh2Δ* mutants, in which the chitin ring is not connected to β(1-3)glucan, grew very slowly and showed wide and growing necks, elongated buds and swollen cells with large vacuoles. A similar behavior was elicited by inhibition of the Crh proteins. This aberrant morphology matched that of *cla4Δ chs3Δ* cells, which have no chitin at the neck. Thus, this is a clear case in which a specific chemical bond between two substances, chitin and glucan, is essential for the control of morphogenesis. This defines a new paradigm, in which chemistry regulates growth.

Key words: Morphogenesis, Yeast, Cell wall, Chitin, Glucan

Introduction

Morphogenesis is an essential process during development in all organisms. It must be under strict control to produce precise shapes and reproduce them indefinitely. Despite its importance, little is known about its regulation at the molecular level. For many years, we have studied the structure and synthesis of the yeast cell wall, which determines cell shape, and of a specialized portion of the wall, the septum, and used them as models for morphogenesis (Cabib et al., 2001). We have especially focused on the synthesis and function of chitin, a minor component of the cell wall that is essential for cell survival. A chitin ring is formed at bud emergence at the neck between mother and daughter cell. Synthesis of this chitin is catalyzed by chitin synthase 3 (Chs3). At cytokinesis, chitin synthesis starts again, in the form of a primary septum that advances centripetally to close the channel between mother and daughter cell, in synchrony with the contraction of an actomyosin ring (Lippincott and Li, 1998; Schmidt et al., 2002). Here, the polysaccharide synthesis is catalyzed by chitin synthase 2 (Chs2). After the primary septum is completed and secondary septa begin to be formed, chitin is also laid down in the cell wall of the daughter cell, under Chs3 control (Shaw et al., 1991).

It should be noted that during the cell cycle the diameter of the mother–bud neck, where the chitin ring and the primary septum arise, remains the same throughout. Therefore, some mechanism must limit growth to the bud and block it at the boundary between mother and daughter cell. The importance of this growth control is obvious, because in *Saccharomyces cerevisiae*, in contrast with fission yeast or animal cells, the site for cytokinesis is created and partially organized when and where the bud emerges. For the tightly orchestrated process of cytokinesis to take place smoothly, it would seem imperative to maintain a strict control on the topography of that site.

The function of Chs2 and the primary septum are clear, but that of the chitin ring was not, especially because it could be abolished by mutation of the *CHS3* gene (Shaw et al., 1991) without affecting budding or cell survival. In the past, we ran a genetic screen for mutants synthetically lethal with *chs3* (Schmidt et al., 2003). Two genes emerging from this screen were *CLA4*, a protein kinase, and *CDC11*, a septin gene. Cla4 shares some essential function with Ste20, but has also some functions of its own, one of which is its participation in the assembly of the septin ring, a structure required for cytokinesis (Longtine and Bi, 2003; Versele and Thorner, 2004). In *cla4* mutants, the septin ring is still formed, but it is often partially defective (Cvrcková et al., 1995; Schmidt et al., 2003).

When *cla4Δ* unbudded cells were allowed to bud in the presence of nikkomycin Z, an inhibitor of Chs3, the chitin ring did not form and elongated buds with very wide necks were generated, followed by growth arrest and lysis (Schmidt et al., 2003). A similar course of events took place in cells containing the *cdc11* mutation isolated in the same screen (Schmidt et al., 2003). These results show that the chitin ring becomes essential for maintenance of the neck structure when the septin ring is compromised and suggests that septins and chitin ring share a redundant function in the control of growth at the neck. Thus the chitin and the septin ring would control growth at the neck by different mechanisms.

The septin ring is made out of proteins and is positioned internally to the plasma membrane, therefore it is unlikely that it would act in a mechanical fashion. However, it has been found in several cases to act as a barrier to the movement of proteins in the plasma membrane (Caudron and Barral, 2009; Orlando et al., 2011). This seems a probable way in which it would act here, preventing proteins needed for cell wall synthesis from reaching the neck.

Journal of Cell Science

Although the existence of the chitin ring had been known since the early 1970s (Hayashibe and Katohda, 1973; Cabib and Bowers, 1975), this was the first time that a function could be assigned to it. How could the effect of the ring be explained? One possibility was that it was working in a mechanical fashion, by making the wall more rigid at the neck. However, in *chs3* mutants (Shaw et al., 1991) or in wild-type cells treated with Nikkomycin Z, which lack the chitin ring, no widening of the neck is observed. Therefore, the cell wall appears to be able to maintain the shape of the neck in the absence of the chitin ring, so long as the septin ring is normal. Thus, we were lead to seek a different interpretation, based on the cell wall structure that we previously elucidated (Kollár et al., 1997). In this structure, chitin is partially attached to the nonreducing end of β(1-3)glucan and partially to a β(1-3)-linked glucose side chain of β(1-6)glucan, whereas β(1-6)glucan, to which the mannoproteins are linked, is also bound to nonreducing ends of β(1-3)glucan. We reasoned that at the neck, where the concentration of chitin is high, it might be mostly linked to β(1-3)glucan. Thus, it would compete with the attachment to the same sites of β(1-6)glucan, which is linked to the cell wall after β(1-3)glucan is synthesized (Roh et al., 2002a). As a consequence, mannoprotein also could not become a part of the cell wall (Schmidt et al., 2003). The linkage of chitin to end residues of β(1-3)glucan might also interfere with the metabolism of this polysaccharide, the main structural component of the cell wall. Thus, synthesis of the cell wall at the neck would eventually be stopped. As previously discussed (Cabib et al., 2012), the growth control systems would be switched on after a cell wall of normal composition was laid down at the neck.

In so far as the chitin ring is concerned, this hypothesis makes three predictions. First, that in the neck region chitin should be mostly attached to β(1-3)glucan, whereas it might be preponderantly bound to β(1-6)glucan in lateral walls. Second, that the structure of β(1-3)glucan at the neck should be somehow different from that of lateral walls, to reflect a less active metabolism. Third, that the mere presence of chitin would not block growth at the neck, unless the chitin is glucan-bound.

To verify the first prediction, we devised new procedures for the quantitative analysis of chitin crosslinks with other polysaccharides (Cabib and Durán, 2005). By applying this methodology to a mutant blocked at cytokinesis at a nonpermissive temperature, we found that the linkage of chitin to β(1-3)glucan was preponderant at the neck, whereas that to β(1-6)glucan predominated in lateral walls (Cabib and Durán, 2005), in accordance with expectations.

For the second prediction, methodologies for the isolation and fractionation of both free β(1-3)glucan and β(1-3)glucan attached to chitin were devised. The results showed that the bulk β(1-3)glucan consisted of two fractions, one soluble in alkali and highly polydisperse, the other insoluble and of very large molecular weight (Cabib et al., 2012). The large-size crosslinked polysaccharide was identified as part of the cell wall structural network, whereas the polydisperse material corresponded to the fraction being remodeled during cell growth (Cabib et al., 2012). The β(1-3)glucan attached to chitin, which is restricted to the neck, only consisted of high molecular weight material, supporting the idea that the cell wall at the neck is quiescent (Cabib et al., 2012).

Although these results were in agreement with our expectations, stronger evidence was needed to prove our third and crucial prediction, the subject of the present study; that is, that it is the binding of chitin to glucan, rather than its mere presence, that controls growth at the neck. To obtain this evidence, it was necessary first to uncover the mechanism by which the crosslinks between the polysaccharides are generated. Because this process takes place in the periplasmic space, where no ATP or other energy source is available, it was earlier suggested that the crosslinking would occur by transglycosylation, a neutral reaction in terms of free energy change (Cabib et al., 1988). This turned out to be the case. We showed that Crh1 and Crh2 act as transglycosylases to transfer chitin chains to β(1-6)glucan (Cabib et al., 2007) and also to β(1-3)glucan (Cabib, 2009). Armed with this knowledge, we could test the third prediction of our proposal, by deleting *CRH1* and *CRH2* in a *cla4Δ* mutant, thus eliminating chitin–glucan linkages without presumably affecting chitin content. As will be shown below, the results confirmed our hypothesis.

Results

Similar morphologies in *cla4Δ chs3Δ* and *cla4Δ crh1Δ crh2Δ* cells

Despite the synthetic lethality between *chs3* and *cla4* mutants observed in a genetic screen, we were able to isolate a *cla4Δ chs3Δ* strain (YMS90, see supplementary material Table S3) (Schmidt et al., 2003) in a YPH499 background. In an attempt to understand the reason why this double mutant survived, we mated it to a wild type with the same genetic background as YPH499 but the opposite mating type, and carried out tetrad analysis of the diploid. When mutations in two genes segregate, one would expect an equal number of spores with each one of the mutations, with no mutations and with both mutations. As shown in supplementary material Table S1, the recovery of the double mutant was one order of magnitude less than that of the single mutants or wild type. This might indicate that survival of the double mutant is the result of multiple factors, such as suppressor mutations arising during the generation of the double mutant strain. Another, more likely possibility, is that survival was initially resulting from the different genetic backgrounds of YPH499 and ECY101, the strain with which the genetic screen was carried out (Schmidt et al., 2003), but germination of double mutant spores is severely impaired. This would not be surprising, in view of the many defects of the double mutant. This strain grew very slowly and exhibited a conspicuously aberrant morphology, with extremely elongated buds, wide necks and bloated cells with large vacuoles (Fig. 1B, compare with Fig. 1A). Because of the lack of Chs3, the only chitin in these cells is that of the primary septum and little staining is visible with Calcofluor White (CFW) (Fig. 1B). To obtain a strain that would still have all the chitin but would be unable to link it to glucans, we deleted *CRH1* and *CRH2* in a *cla4Δ* mutant. The resulting triple mutant, NBT017, was viable, but showed slow growth and temperature sensitivity that was suppressed by addition of sorbitol to the growth medium (supplementary material Fig. S1A). Cells formed clumps that sedimented rapidly (supplementary material Fig. S1B). The appearance of the triple mutant was strikingly similar to that of the *cla4Δ chs3Δ* cells (Fig. 1G), despite the presence of chitin at bud necks and cell walls, as shown by Calcofluor White staining (Fig. 1G). In fact, the chitin content of this strain was 3.5 times that of wild type (Table 1). The large increase in chitin could be ascribed to the hyperpolarized growth of the mutant (Schmidt et al., 2008). This type of growth also results in weaker cell walls (Schmidt

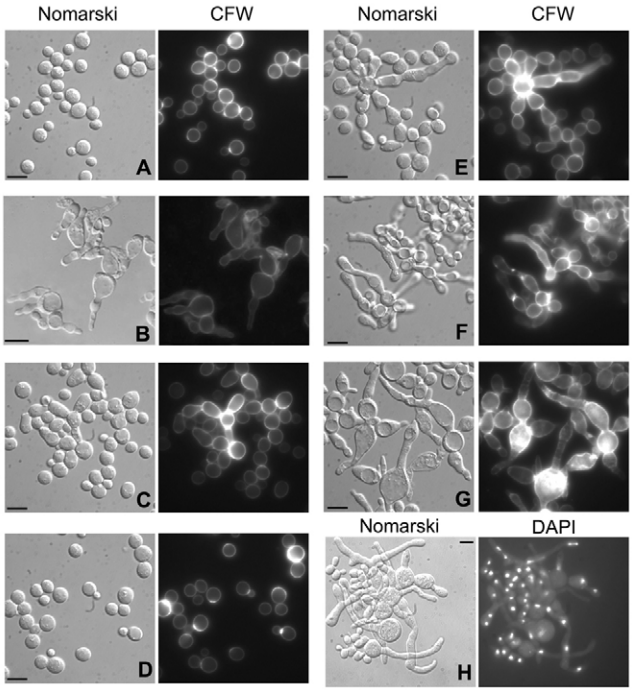

Fig. 1. Double or triple mutants of *CLA4* and the *CRH* genes show aberrant morphology similar to that of *cla4Δ chs3Δ* cells. Morphology of different strains and chitin staining with Calcofluor White (CFW) after growth in YEPD at 25℃. (**A**) Wild type (YPH499); (**B**) *cla4Δ chs3Δ* (YMS90); (**C**) *cla4Δ* (YMS134); (**D**) *crh1Δ crh2Δ* (NBT014); (**E**) *cla4Δ crh1Δ* (NBT011); (**F**) *cla4Δ crh2Δ* (NBT015); and (**G**) *cla4Δ crh1Δ crh2Δ* (NBT017). The exposure for the Calcofluor frames of C and E–G was shorter than for the other frames to compensate for a high fluorescence that would have masked the distribution of chitin. In **H**, staining of nuclei with DAPI is shown. Scale bars: 10 μm.

et al., 2008), which explains the extensive lysis we observed at 37℃ and the protection by sorbitol mentioned above.

Despite the morphological abnormalities of the triple mutant, some roundish, apparently normal cells were observed (Fig. 1G). The number of these cells increased when the strain was grown in minimal medium. To investigate the possible presence of two different populations, round cells, unbudded or with very tiny buds, were isolated by sucrose gradient centrifugation (Fig. 2A; see Materials and Methods) and incubated with YEPD in the presence of hydroxyurea, to limit growth to one generation. These cells gave rise to mostly elongated daughter cells (Fig. 2B,C). In an experiment in which the round cells were incubated at different temperatures, 60% of 218 cells yielded elongated buds at 25℃ and 75% of 223 cells at 30℃. These results show that the round cells and elongated cells belong to the same population.

Single deletions of *CRH1* or *CRH2* in a *cla4Δ* background (Fig. 1E,F) led to cells with an intermediate morphology between

Table 1. Chitin content of different strains

Strain	Chitin (% of cell dry weight)
YPH 499 (wild type)	0.83
YMS 134 (*cla4Δ*)	1.3
NBT017 (*cla4Δ crh1Δ crh2Δ*)	2.95

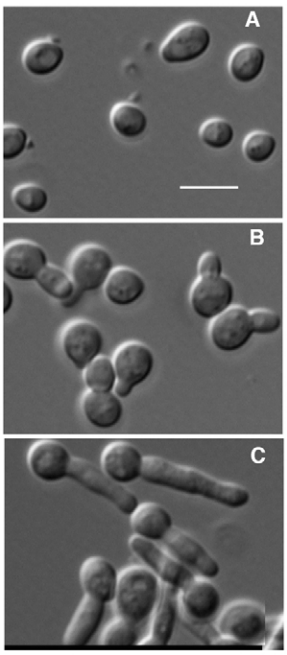

Fig. 2. Round cells of NBT017 (*cla4Δ crh1Δ crh2Δ*) give rise to elongated cells. Round cells were isolated after growth in YEPD-supplemented minimal medium (see Materials and Methods) and transferred to hydroxyurea-containing YEPD. Pictures were taken at 0 time (**A**), after 3.5 hours (**B**) and after 5.5 hours (**C**). Scale bar: 10 μm.

that of *cla4Δ*, which does show some elongated buds (Fig. 1C) and that of the triple mutant (Fig. 1G). Crh2 function seemed to be more important than that of Crh1, because *cla4Δ crh2Δ* cells were considerably more abnormal than *cla4Δ crh1Δ* cells (Fig. 1E,F). This result might be related to the preferential localization of Crh2 at the mother–bud neck (Rodríguez-Peña et al., 2000). The morphological defects of the triple mutant were completely corrected by transformation with a plasmid carrying *CLA4* and partially by plasmids with *CRH1* or *CRH2* (Fig. 3), giving rise to morphologies similar to those of the corresponding double mutants (compare Fig. 3 with Fig. 1). By contrast, plasmids harboring mutations of *CRH1* or *CRH2* in the putative glutamyl proton donor (Carbohydrate-Active Enzyme Database, www.cazy.org) did not complement the defect (Fig. 3), showing that the transglycosylase activity of the Crh proteins is required for correct morphogenesis.

Despite the anomalous morphology, nuclear division seemed to take place efficiently in the triple mutant, as judged from 4′,6-diamidino-2-phenylindole (DAPI) staining (Fig. 1H). The same cannot be said for septin organization and localization. Septin defects have been noted in *cla4* mutants (Cvrcková et al., 1995; Schmidt et al., 2003; supplementary material Fig. S2), but those in the triple mutant *cla4Δ crh1Δ crh2Δ* are more extensive (supplementary material Fig. S2), especially with reference to localization, because septins are often observed in places distant from the mother–bud neck. Because of the importance of septins for cell division (Longtine and Bi, 2003), it was not surprising that often septa were abnormal, as visualized by electron microscopy (Fig. 4I). As in the case of septin mutants (Slater et al., 1985; Roh et al., 2002b), we found instances in which septa were being formed adjacent to a lateral cell wall (Fig. 4J). Wide

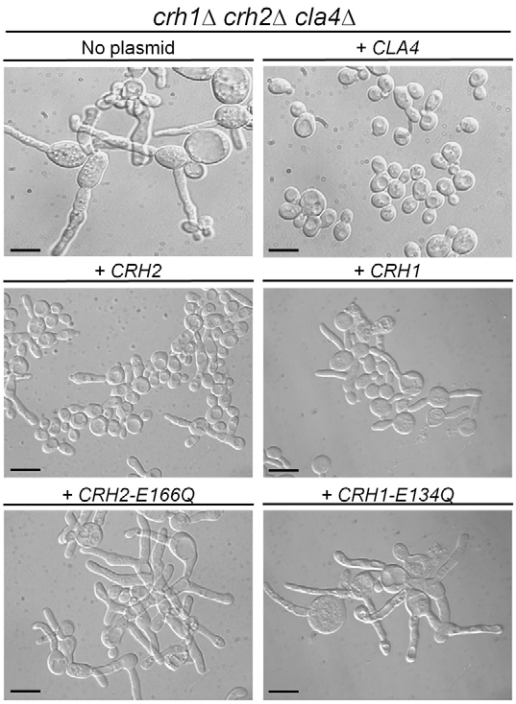

Fig. 3. Mutants in the putative active site of Crh1p and Crh2p do not complement the defects of the *cla4Δ crh1Δ crh2Δ* strain. Complementation of NBT017 (*cla4Δ crh1Δ crh2Δ*) defects with different plasmids. *CLA4* stands for pMS17 (pRS200-*CLA4*), *CRH2* for pNBc13 (YEp352-*CRH2-HA*), *CRH1* for pNBc15 (YEp352-*CRH1-HA*), *CRH2-E166Q* for pNB23 (pNBc13-$CRH2^{E166Q}$) and *CRH1-E134Q* for pNB48 (pNBc15-$CRH1^{E134Q}$). Note in the two bottom frames that a plasmid with a Crh protein mutated in the presumed active site does not complement the defect of the triple mutant. Scale bars: 10 μm.

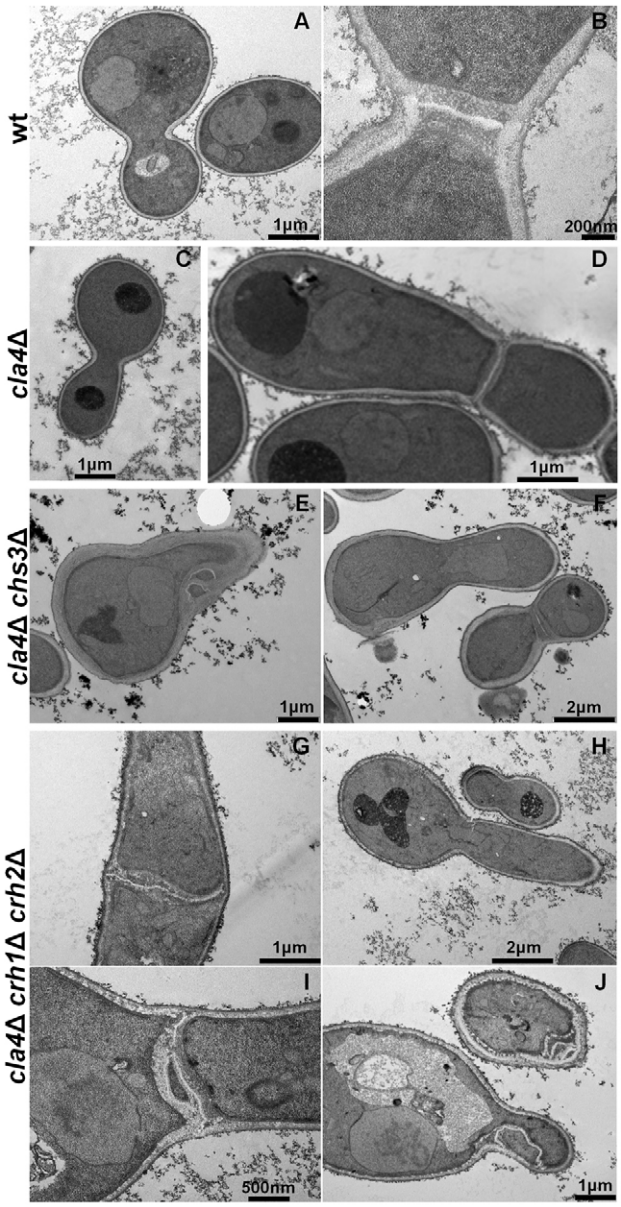

Fig. 4. Electron microscopy of cells of different strains. (**A**) Emerging bud and (**B**) complete septum of the wild-type strain YPH499. (**C**) Emerging bud and (**D**) complete septum of the *cla4Δ* strain YMS134. For examples of abnormal septa in a *cla4Δ* strain (see Schmidt et al., 2003). (**E**) Ectopic septum and (**F**) emerging bud and normal septum in the *cla4Δ chs3Δ* strain YMS90. Ectopic septa were rare in this strain. (**G**) Normal-like but wide septum, (**H**) emerging bud, (**I**) abnormal septum and (**J**) ectopic septa of the *cla4Δ crh1Δ crh2Δ* strain NBT017. Note that emerging buds are wider in YMS90 and NBT017 than in YPH499 or YMS134.

necks could be observed in the *cla4Δ chs3Δ* and the *cla4Δ crh1Δ crh2Δ* mutants (Fig. 4F,H).

Some of the strains described above contain mutations either in the *CRH* genes or in the *CHS3* gene, but none of them has mutations in both. For a more complete genetic analysis, the phenotype of a *crh1Δ crh2Δ chs3Δ* strain was compared to those of wild type and of *crh1Δ crh2Δ* and *chs3Δ* mutants. Two properties were examined: one, the morphology of the cells and clumped growth as consequence of the *chs3* mutation (Shaw et al., 1991); the other, the sensitivity of the different strains to Congo Red (Rodríguez-Peña et al., 2000). Only the two strains containing the *CHS3* deletion gave rise to clumps during growth (supplementary material Fig. S2). Wild type was sensitive and a *crh1Δ crh2Δ* strain hypersensitive to Congo Red, as previously observed (Rodríguez-Peña et al., 2000). The *chs3Δ* mutant was resistant to Congo Red, as expected and the triple mutant showed the same behavior (supplementary material Fig. S3). Thus, in both cases the introduction of mutations in the *CRH* genes did not affect the phenotype of a *chs3Δ* strain. This was expected, because the chitin made through Chs3 is the substrate for the Crh proteins, therefore in the absence of that chitin the presence or absence of Crh1 and/or Crh2 does not make a difference.

We were also able to obtain a quadruple mutant, *cla4Δ crh1Δ crh2Δ chs3Δ*. Again, the phenotype of this strain is the same as that of *cla4Δ crh1Δ crh2Δ* or *cla4Δ chs3Δ* (supplementary material Fig. S3), comfirming that Crh1 and Crh2 are not operative in the absence of Chs3.

Neck widening is independent from hyperpolarized growth and occurs during bud development

The first effect observed in *cla4Δ* cells incubated with nikkomycin Z was widening of the mother cell-bud neck (Schmidt et al., 2003). Events at the neck give rise to further

abnormal morphology, because washing out Nikkomycin Z at the small bud size did not prevent bud elongation (Schmidt et al., 2003). The bud elongation observed in the triple mutant probably results from the neck widening, which leads to disorganization of the septin ring and subsequent activation of the morphogenesis checkpoint (Lew, 2003). Here, the protein kinase Swe1 becomes activated and inactivates, by phosphorylation, the master kinase of the cell cycle, Cdc28, leading to arrest of the cycle and persistent apical growth. To suppress that growth, we deleted *SWE1* in the triple mutant. As expected, the length of the buds decreased dramatically (Fig. 5), although not completely; however, the necks remained wide (see also below). This result clearly shows that neck widening is independent from polarized growth.

Because of the effect of sorbitol on the growth of the triple mutant (supplementary material Fig. S1), it was of interest to determine its influence upon the morphology of the different strains. The appearance of wild-type (YPH499) and *cla4Δ* (YMS134) cells was not perturbed by growth in the presence of 0.8 M sorbitol, except for some general shrinkage. However, with the *cla4Δ crh1Δ crh2Δ* mutant (NBT017), a decrease in elongated buds and a concomitant increase in roundish cells was detected (Fig. 5). A similar effect could be observed in the *cla4Δ chs3Δ* mutant (YMS90) (Fig. 5). In the *cla4Δ crh1Δ crh2Δ swe1Δ* strain (ECY108), which already had shorter buds, little change was seen in the presence of sorbitol (Fig. 5).

Because of the crucial importance of events at the neck, we measured neck diameter in the different strains (see Materials and Methods for the procedure). There was a small increase in diameter going from wild type to a *cla4Δ* mutant (Fig. 6), which was however significant, according to a *t*-test, with a $P<0.001$. The necks of the triple mutant were much wider, in fact even wider than those of the *cla4Δ chs3Δ* strain (Fig. 6), whereas those of the triple mutant deleted for *SWE1* showed only a small decrease relative to NBT017. Interestingly, although growth in the presence of sorbitol led in general to a small decrease in neck width, the ratio between the values of the different mutants and those of *cla4Δ* remained about the same, indicating that the effect of sorbitol is not specific (Fig. 6).

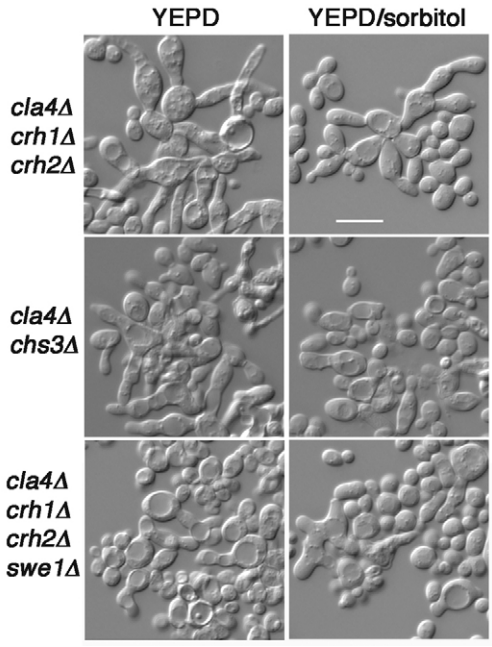

Fig. 5. *SWE1* deletion and addition of sorbitol to the medium reduce bud elongation. *cla4Δ crh1Δ crh2Δ* is NBT017, *cla4Δ chs3Δ* is YMS90 and *cla4Δ crh1Δ crh2Δ swe1Δ* is ECY108. Cells were grown at 25℃ in YEPD or YEPD containing 0.8 M sorbitol. Scale bar: 10 μm.

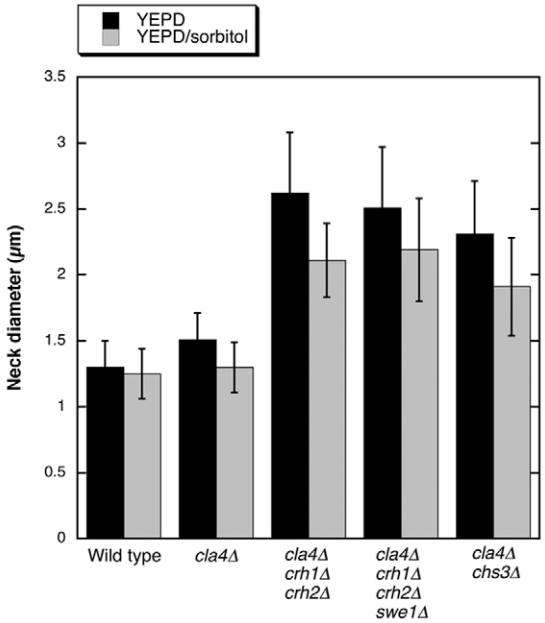

Fig. 6. Mother–bud neck diameters are enlarged in cells with defects in both septins and chitin–glucan crosslinks. The strains used were YPH499 (wild type), YMS134 (*cla4Δ*), NBT017 (*cla4Δ crh1Δ crh2Δ*), ECY108 (*cla4Δ crh1Δ crh2Δ swe1Δ*) and YMS90 (*cla4Δ chs3Δ*). The number of cells measured, from left to right in the figure, was 120, 108, 166, 134, 133, 95, 103, 105, 185 and 135. Standard deviation is shown. For technical details of the measurements, see Materials and Methods. Cells were grown in YEPD at 25℃, with the addition of 0.8 M sorbitol where indicated.

A question that came up is whether the neck in the triple mutant is already wide at the beginning of bud emergence or if it widens during bud development. To answer this question, we used the experiment of Fig. 2. Neck diameters were measured at the small bud stage (Fig. 2B) and again after the buds had completely developed (Fig. 2C). At the first stage, the value was 2.2±0.23 μm (s.d.; 102 cells), at the final stage 2.68±0.35 μm (110 cells). The difference was highly significant with $P<<0.001$ by the *t*-test. Given that one can measure neck diameters only when a bud, albeit small, is fully formed, the measured difference is a minimal value.

In summary, lack of linkages between the chitin ring and β(1-3)glucan at the mother–bud neck lead to neck growth and consequent widening.

Inhibition of the Crh proteins in a *cla4Δ* mutant causes morphological aberrations

In the experiments described above, linkage of chitin to β(1-3)glucan was abolished by deletion of *CHS3* or of *CRH1* and *CRH2*, whereas in earlier work it was done by inhibition of Chs3 with Nikkomycin Z (Schmidt et al., 2003). It is not known how the deletants suppress lethality in the presence of the *cla4*

mutation, and in that sense an inhibition experiment would be more straightforward. Thus, it seemed desirable to test the effect of a Crh inhibitor on a *cla4Δ* strain. We previously found that chitin oligosaccharides inhibited the transfer of chitin to sulforhodamine-labeled β(1-3)-linked glucose oligosaccharides, presumably by interfering with Crh1 and Crh2 activity (Cabib et al., 2008). Indeed, when a *cla4Δ* strain was grown in the presence of triacetylchitotriose, pronounced morphological aberrations were observed. However, staining with Calcofluor White showed loss of fluorescence at the neck, suggesting that it was the loss of chitin, rather than of its linkage to β(1-3)glucan, that caused those changes. Further work with the use of different mutants indicated that the chitin loss was associated with the presence or Crh1 in the cell. We used therefore a *cla4Δ crh1Δ* strain, which does not appear to lose chitin, as detected with Calcofluor White, in the presence of moderate concentrations of triacetylchitotriose (Fig. 7A–D). When chitin was labeled *in vivo* with ^{14}C-glucosamine (Cabib and Durán, 2005) and the distribution of chitin was determined, a pronounced decrease in the percentage of chitin bound to β(1-3)glucan was detected in the presence or triacetylchitotriose (supplementary material Table S2). Upon incubation of single cells of this strain with the oligosaccharide, pronounced neck widening and bud elongation were observed (Fig. 7E,F; Table 2). The differences in neck diameter, although significant, are reduced by the fact that the strain is already abnormal because of the *crh1* mutation. These results show that inhibition of the Crh proteins has similar effects to the deletion of the corresponding genes.

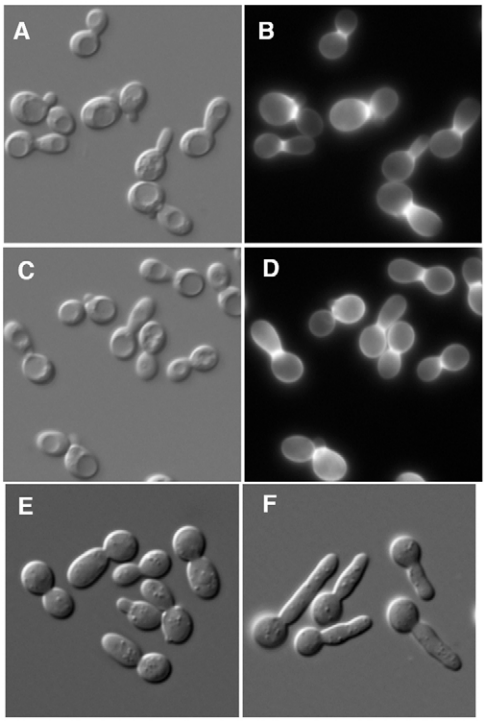

Fig. 7. Incubation of NBT012 (*cla4Δ crh1Δ*) with triacetylchitotriose leads to bud elongation. All pictures were taken with Nomarski optics, except for (B) and (D), which show chitin fluorescence after staining with Calcofluor White. Unbudded cells were isolated by sucrose gradient centrifugation and incubated at 25℃ in YEPD supplemented with 0.1 M hydroxyurea for 3 hours (**A–D**) or, in a separate experiment, for 4 hours (**E,F**). In A, B and E, there were no additions; in C, D and F, 2 mM chitooligosaccharide was added. As shown in B and D, the addition of oligosaccharide had little effect on chitin staining, but caused bud elongation (E,F). Addition of 4 mM oligosaccharide caused a similar effect, but with greater elongation (supplementary material Table S2).

Discussion

Our results clearly show that loss of Crh1 and Crh2 function in a strain partially defective in septin ring organization leads to dramatic morphological changes (Fig. 1). Deletion of *CRH1* and *CRH2* in a wild-type background has no effect in the morphology (Fig. 1D) and that of *CLA4* causes only minor defects (Fig. 1C). The morphological aberrations observed in deletion mutants of the Crh proteins are caused by a loss of the chitin transferase activity in those strains, because mutations in the putative active site lead to the same outcome (Fig. 3). The aspect of the *crh1Δ crh2Δ cla4Δ* cells is practically undistinguishable from that of a *chs3Δ cla4Δ* mutant, which completely lacks the chitin ring (Fig. 1B,G). Given that the triple mutant has plenty of chitin (Table 1) and also shows chitin rings (Fig. 1G), it must be concluded that the mere presence of a chitin ring is not sufficient for the control of morphogenesis. It is necessary that the chitin be attached to glucan, in agreement with our hypothesis. The primary defect in the triple mutant is clearly located at the mother–bud neck. Not only is the neck of the mutant much wider than that of wild type, but it also remains so when the bud elongation is largely eliminated by deletion of *SWE1* (Figs 5, 6). In addition to deletion of *SWE1*, another factor that partially limits bud elongation is the presence of an osmotic protector, sorbitol, in the growth medium (Fig. 5). The mechanism of this effect is not clear. However, it is important to note that necks remain wide in the presence of sorbitol (Fig. 6). This supports our interpretation that crosslinks interfere with growth, and is evidence against one suggesting that they mechanically increase the rigidity of the cell wall. If this were the case, sorbitol should prevent neck widening by neutralizing the turgor pressure of the cell.

The neck diameter in the *crh1Δ crh2Δ cla4Δ* and in the *chs3Δ cla4Δ* strains, although large, is smaller than those observed in a *cla4Δ* mutant after exposure to Nikkomycin Z (Schmidt et al., 2003) and so is the increase in diameter during budding. In our view, the explanation for this difference is that in the Nikkomycin experiment there was no time for the emergence of mechanisms to circumvent the damage, and in fact the cells died (Schmidt et al., 2003). However, the mutants survived by the activation of some suppressor, and they presumably could do so by limiting growth at the neck to some degree. This remedy was only partial and had stochastic effects, as shown by the variability in morphology during growth of the mutants, and in particular by

Table 2. Effect of triacetylchitotriose on bud length and neck diameter of NBT012 (*cla4Δ crh1Δ*)

	Ratio length:width[a,b]	Neck diameter (μm)[b]
Control	1.67±0.79 (113 cells)	1.75±0.19 (116 cells)
2 mM oligosaccharide	2.25±1.07 (117 cells)	1.94±0.18 (103 cells)
4 mM oligosaccharide	2.6±1.3 (124 cells)	2.05±0.19 (99 cells)

Results are ±s.d.

[a]The ratio is a measure of bud elongation. The length was measured from the neck to the bud tip.

[b]All differences between control and incubation with oligosaccharide are significant at $P<0.001$ by Student's *t*-test.

the presence of round cells, which however, gave rise to elongated cells after budding (Fig. 5). We could avoid the genetic or regulatory changes by growing the cells in the presence of a chitin oligosaccharide, which inhibits Crh1 and Crh2 and caused neck widening and bud elongation (Fig. 7). In this case, we had to use a *cla4Δ crh1Δ* strain, because of the finding that triacetylchitotriose elicits a strong chitinase activity in Crh1. This effect also occurs, albeit at a reduced level, with Crh2 (M. Mazán, N.B., Z. Zemková, J.A. and V. Farkas, unpublished data); therefore, it was necessary to use the oligosaccharide at a moderate concentration, with less dramatic effects than those shown by Nikkomycin Z.

From our earlier results (Schmidt et al., 2003) and those of the present study, it is clear that the chitin ring and the septin ring have a redundant function in the control of neck growth. The two rings apparently work independently and certainly by different mechanisms. The need to maintain the integrity of the neck region, where cytokinesis takes place, for cell survival, might have led to development of two parallel systems for its control, during evolution. Although the two rings seem to act independently, there is a relationship between them: Chs3, the synthase responsible for the formation of the chitin ring, is linked to the septin ring through Chs4, Bni4 and Glc7 (De Marini et al., 1997; Kozubowski et al., 2003). Thus, formation of the septin ring ensures correct localization of the chitin ring. This function appears to be maintained in *cla4Δ* mutants, which have normal chitin rings.

With our previous results and those presented here, all three predictions of our hypothesis for growth control at the mother–bud neck have been verified: (1) the chitin ring at the neck is specifically attached to β(1-3)glucan (Cabib and Durán, 2005); (2) the β(1-3)glucan linked to chitin has the properties expected from a component of a quiescent cell wall (Cabib et al., 2012); (3) from the findings of the present study it can be concluded with certainty that the linkage of chitin to β(1-3)glucan and not just the presence of the chitin ring, is necessary for the control of growth at the mother–daughter neck. This conclusion would be valid even if the chitin ring had some mechanical stabilizing function at the neck. Thus, here is a straightforward case in which a chemical linkage between two molecules has an essential role in the control of morphogenesis. It would not be surprising if nature had used this device in other systems.

Materials and Methods

Strains and growth

The strains used are listed in supplementary material Table S3. Cells were grown in YEPD (2% glucose, 2% peptone, 1% yeast extract) or in minimal medium (2% glucose, 0.7% yeast nitrogen base) plus requirements, unless indicated otherwise. Synthetic complete (SC) medium (Rose et al., 1990) was used in some cases.

Strain construction

To obtain the single *crh2Δ* and double *cla4Δ crh2Δ* mutants, the *CRH2* ORF was deleted in YPH499 or YMS134 as previously described (Cabib et al., 2012). To obtain the single *crh1Δ* and double *cla4Δ crh1Δ* mutants, the *CRH1* ORF was replaced in YPH499, YMS134 or YMS306 strains as already outlined (Cabib et al., 2012). Finally, to generate the triple mutant *cla4Δ crh1Δ crh2Δ*, the *CRH2* ORF was replaced in the double mutant *cla4Δ crh1Δ*, by using the His3MX6 module (Rodríguez-Peña et al., 2000). Correct replacement was verified using the same primers described previously.

To obtain the *chs3Δ*, *chs3Δ crh1Δ crh2Δ* and *crh1Δ crh2Δ cla4Δ chs3Δ* mutants in the YPH499 background, the *CHS3* ORF was replaced in wt, *crh1Δ crh2Δ* and *crh1Δ crh2Δ cla4Δ* strains, respectively, by the geneticin resistant marker (KanMX4 module), using the Short Flanking Homology PCR technique (Rodríguez Peña et al., 1998) and the following primers: 5′-GGTCCTGTTTAGACTATCCGCAGGAAAGAAATTAGAATGCGTACGCTGCAGGTCGAC-3′ and 5′-CATACTGTCTATGCAACGAAGGAGTCACTTTCCTCCTTCCGATCGATGAATTCGAGCTCG-3′. Correct ORF replacement was verified by PCR using the following primer pairs: 5′-GCACGTACTACGTAGCCAC-3′ and 5′-CCGTGCGGCCATCAAAATG-3′; 5′-ACGGCCACATCAAATACCC-3′ and 5′-GCCCAGATGCGAAGTTAAG-3′.

The *swe1::KanMX4* deletion cassette was amplified by PCR as previously described (Schmidt et al., 2003) and the PCR product was used to transform NBT017, yielding strain ECY108. Strain YMS90, containing both a *CHS3* and a *CLA4* deletion, was obtained by transforming strain ECY46-4-1B (*chs3::LEU2*; Crotti et al., 2001) with a *cla4::URA3* deletion cassette described by Schmidt and colleagues (Schmidt et al. 2003).

Plasmid construction

Plasmids pNB23 and pNB48 were obtained from plasmids pNBc13 and pNBc15, respectively (Cabib et al., 2007). Both plasmids were used as templates for PCR site-directed mutagenesis using the QuikChange Site-Directed Mutagenesis Kit (Agilent Technologies, Stratagene, La Jolla, CA). To obtain plasmid pNB23, primers 5′-CCGGCGCAGGTGATCAACTTGATTACGAATTCG-3′ and 5′-CGAATTCGTAATCAAGTTGATCACCTGCGCCGG-3′ were used to bring about the change E166Q in the *CRH2* gene. To construct plasmid pNB48, primers 5′-GTGAGATTTGGATCAAATTGATATTGAATGGG-3′ and 5′-CCCATTCAATATCAATTTGATCCAAATCTCAC-3′ were used to effect the change E134Q in the *CRH1* gene. Primer design and PCR conditions were as suggested by the manufacturer. The presence of the designed mutation as well as the absence of additional mutations within the construction were verified by DNA sequencing. Plasmids used in this study are listed in supplemental material Table S4.

Phenotypic analysis

Yeast cells were grown overnight in YEPD liquid media at 24℃ to mid-log phase. The cultures were then diluted in YEPD to 3×10^6 cells ml^{-1} and incubated at 24℃ for an additional 3 hours. Five µl (~15×10^3 cells) plus five 1:5 serial dilutions were spotted on YEPD solid media and YEPD plus 0.5 M Sorbitol. Growth was monitored on the plates after 2 days at 24℃ and 37℃, respectively.

Microscopic analysis

Yeast cells were grown at 24℃ overnight in YEPD, SC-URA (for cells bearing the plasmids pLA10, pNBc13, pNB23, pNBc15 or pNB48) or SC-LEU (for cells bearing the pMS17 plasmid). The cultures were then diluted in YEPD to 3×10^6 cells ml^{-1} and maintained at 24℃ or 37℃ for an additional 3 hours. After this time, cells were collected, washed with PBS and analyzed before and after staining with Calcofluor White, DAPI or propidium iodide.

For Calcofluor White staining, cells were stained with Fluorescent brightener 28 (Sigma-Aldrich, St Louis, MO, final concentration: 50 mg ml^{-1} in PBS) for 10 minutes. Cells were washed twice with PBS and suspended in a suitable volume of the same buffer. For staining of nuclear DNA, cells were fixed in 70% ethanol for 15 minutes, then washed twice with PBS and incubated with DAPI (final concentration 50 ng ml^{-1}) for 5 minutes. Cells were then washed twice with PBS and resuspended in this buffer. For analysis of cell lysis, yeasts were stained with propidium iodide (0.05 mg ml^{-1}), as previously described (de la Fuente et al., 1992).

Nonstained cells were visualized by DIC. Stained yeast cells were analyzed by fluorescence microscopy and DIC, using a Nikon TE2000 fluorescence inverted microscope equipped with CCD (Melville, NY). Digital images were acquired with an Orca C4742-95-12ER camera (Hamamatsu Photonics, Japan) and processed with the Imaging Aquacosmos or Hamamatsu HCImage Imaging systems software. Alternatively, images were obtained with a Zeiss Axioskop microscope equipped with a Retiga Exi camera and analyzed with iVision software.

For *CDC10-GFP* localization, yeast cells transformed with pLA10 (Cid et al., 1998), were grown as explained above, washed twice with PBS and visualized with the same fluorescence microscope.

Genetic analysis

YMS90 was mated to YPH499-B followed by sporulation and tetrad dissection as described (Rose et al., 1990). For spore germination, plates were incubated at 25℃. Segregants were identified by nutritional requirements and morphology.

Electron microscopy

For transmission electron microscopy, samples were prepared as previously described (Gómez-Esquer et al., 2004). Basically, cells were grown overnight at 28℃ to mid-log phase in YEPD liquid media. The culture was diluted to 3×10^6 cells ml^{-1} in YEPD and incubated at 28℃ for an additional few hours until a concentration of 2×10^7 cells ml^{-1} was reached. Then, 1 ml of cell suspension was collected and washed with PBS. Cells were fixed with 500 µl of fixative solution (0.05 M sodium cacodylate buffer, pH 7.2, 2% paraformaldehyde, 1.5% glutaraldehyde) at 4℃ overnight. The cells were subsequently washed three times with PBS, treated with 1% (w/v) potassium permanganate for 90 minutes at room temperature and washed again with PBS three times. After washing, cells were dehydrated through an ethanol gradient (30, 40, 50, 60, 70, 80, 90 and 100%, v/v; 10 minutes each) and embedded in Epon 812 resin (Electron Microscopy Sciences) following the manufacturer's

instructions. The solid product was cut into ultrathin slices, stained with uranyl acetate and examined with a Zeiss EM902 electron microscope.

Single-cell experiments

For the budding of round cells of strain NBT017 (*crh1Δ crh2Δ cla4Δ*, Fig. 2) the strain was grown at 25℃ in minimal medium to which 10% YEPD was added. Under these conditions, the occurrence of single round cells was relatively high and the doubling time was 3–3.5 hours, whereas in minimal medium growth was extremely slow and in YEPD few round cells were found. Single round cells were isolated by centrifugation in sucrose gradients as previously reported (Drgonová et al., 1999) and incubated at 25℃ or 30℃ in YEPD, in the presence of 100 mM hydroxyurea. At different times, digital images of cells were acquired and measurements were made.

In the experiments in which triacetylchitotriose was used to inhibit the Crh proteins (Fig. 7), NBT012 (*cla4Δ crh1Δ*) was grown in YEPD at 25° and unbudded cells were isolated as outlined above. The unbudded cells were incubated at 25℃ in YEPD containing different concentrations of the chitooligosaccharide and 100 mM hydroxyurea, and the morphology was observed and recorded at different times.

Chitin distribution in the absence and presence of triacetylchitotriose

Chitin was labeled *in vivo* with ^{14}C-glucosamine as described (Cabib and Durán, 2005) either with no addition (control) or in the presence of 2 mM triacetylchitotriose. Cell walls were prepared, treated with alkali and solubilized by carboxymethylation before or after treatment with β(1-6)glucanase, as previously outlined (Cabib and Durán, 2005). Chitin distribution was determined with the curdlan method (Cabib, 2009).

Measurement of mother–bud neck diameter

The measurement of neck diameter was done on phase contrast photographs obtained with a Zeiss Axioskop microscope and a Retiga Exi digital camera, with the measuring tool of the iVision software. Because of the aberrant morphology of some of the strains used, it was often difficult to identify newly emerged buds. To facilitate their recognition, we stained the cells with fluorescein-conjugated Concanavalin A (Tkacz et al., 1971) and let them grow for about one generation. The new buds are easily distinguished from older cells, because their surface is not fluorescent.

Congo Red sensitivity

To determine the sensitivity of the different strains to Congo Red, cells were grown overnight in YEPD media at 30℃ to mid-log phase. Cultures were diluted in YEPD to 3×10^6 cells ml^{-1} and 5 µl plus five 1:5 serial dilutions were spotted on YEPD solid media and YEPD plus Congo Red. Growth was monitored on the plates after 2 days at 30℃.

Chitin determination

Chitin was measured in cell walls as previously described (Cabib and Sburlati, 1988). Results were referred to cell dry weight.

Acknowledgements

We are greatly indebted to D. Masison for help with tetrad dissection and to R. Wickner for useful discussions. We thank J. M. Rodríguez-Peña and V. J. Cid for a critical reading of the manuscript and A. Fernández for help in the electron microscopy experiments.

Funding

This study was supported by the National Institutes of Health (Intramural Research Program, NIDDK), the Ministerio de Educación y Ciencia (BIO2010-22146), Comunidad de Madrid (S2010/BDM 2414) and the Programme for UCM Research Groups (920640). Deposited in PMC for release after 12 months.

Supplementary material available online at
http://jcs.biologists.org/lookup/suppl/doi:10.1242/jcs.110460/-/DC1

References

Cabib, E. (2009). Two novel techniques for determination of polysaccharide cross-links show that Crh1p and Crh2p attach chitin to both β(1-6)- and β(1-3)glucan in the *Saccharomyces cerevisiae* cell wall. *Eukaryot. Cell* **8**, 1626-1636.

Cabib, E. and Bowers, B. (1975). Timing and function of chitin synthesis in yeast. *J. Bacteriol.* **124**, 1586-1593.

Cabib, E. and Durán, A. (2005). Synthase III-dependent chitin is bound to different acceptors depending on location on the cell wall of budding yeast. *J. Biol. Chem.* **280**, 9170-9179.

Cabib, E. and Sburlati, A. (1988). Enzymatic determination of chitin. *Methods Enzymol.* **161**, 457-459.

Cabib, E., Bowers, B., Sburlati, A. and Silverman, S. J. (1988). Fungal cell wall synthesis: the construction of a biological structure. *Microbiol. Sci.* **5**, 370-375.

Cabib, E., Roh, D.-H., Schmidt, M., Crotti, L. B. and Varma, A. (2001). The yeast cell wall and septum as paradigms of cell growth and morphogenesis. *J. Biol. Chem.* **276**, 19679-19682.

Cabib, E., Blanco, N., Grau, C., Rodríguez-Peña, J. M. and Arroyo, J. (2007). Crh1p and Crh2p are required for the cross-linking of chitin to β(1-6)glucan in the *Saccharomyces cerevisiae* cell wall. *Mol. Microbiol.* **63**, 921-935.

Cabib, E., Farkas, V., Kosík, O., Blanco, N., Arroyo, J. and McPhie, P. (2008). Assembly of the yeast cell wall. Crh1p and Crh2p act as transglycosylases in vivo and in vitro. *J. Biol. Chem.* **283**, 29859-29872.

Cabib, E., Blanco, N. and Arroyo, J. (2012). Presence of a large β(1-3)glucan linked to chitin at the Saccharomyces cerevisiae mother-bud neck suggests involvement in localized growth control. *Eukaryotic Cell* **11**, 388-400.

Caudron, F. and Barral, Y. (2009). Septins and the lateral compartmentalization of eukaryotic membranes. *Dev. Cell* **16**, 493-506.

Cid, V. J., Adamíková, L., Cenamor, R., Molina, M., Sánchez, M. and Nombela, C. (1998). Cell integrity and morphogenesis in a budding yeast septin mutant. *Microbiology* **144**, 3463-3474.

Crotti, L. B., Drgon, T. and Cabib, E. (2001). Yeast cell permeabilization by osmotic shock allows determination of enzymatic activities *in situ. Anal. Biochem.* **292**, 8-16.

Cvrcková, F., De Virgilio, C., Manser, E., Pringle, J. R. and Nasmyth, K. (1995). Ste20-like protein kinases are required for normal localization of cell growth and for cytokinesis in budding yeast. *Genes Dev.* **9**, 1817-1830.

de la Fuente, J. M., Alvarez, A., Nombela, C. and Sánchez, M. (1992). Flow cytometric analysis of *Saccharomyces cerevisiae* autolytic mutants and protoplasts. *Yeast* **8**, 39-45.

DeMarini, D. J., Adams, A. E. M., Fares, H., De Virgilio, C., Valle, G., Chuang, J. S. and Pringle, J. R. (1997). A septin-based hierarchy of proteins required for localized deposition of chitin in the *Saccharomyces cerevisiae* cell wall. *J. Cell Biol.* **139**, 75-93.

Drgonová, J., Drgon, T., Roh, D.-H. and Cabib, E. (1999). The GTP-binding protein Rho1p is required for cell cycle progression and polarization of the yeast cell. *J. Cell Biol.* **146**, 373-387.

Gómez-Esquer, F., Rodríguez-Peña, J. M., Díaz, G., Rodríguez, E., Briza, P., Nombela, C. and Arroyo, J. (2004). *CRR1*, a gene encoding a putative transglycosidase, is required for proper spore wall assembly in *Saccharomyces cerevisiae*. *Microbiology* **150**, 3269-3280.

Hayashibe, M. and Katohda, S. (1973). Initiation of budding and chitin-ring. *J. Gen. Appl. Microbiol.* **101**, 295-301.

Kollár, R., Reinhold, B. B., Petráková, E., Yeh, H. J. C., Ashwell, G., Drgonová, J., Kapteyn, J. C., Klis, F. M. and Cabib, E. (1997). Architecture of the yeast cell wall. β(1—>6)-glucan interconnects mannoprotein, β(1—>3)-glucan, and chitin. *J. Biol. Chem.* **272**, 17762-17775.

Kozubowski, L., Panek, H., Rosenthal, A., Bloecher, A., DeMarini, D. J. and Tatchell, K. (2003). A Bni4-Glc7 phosphatase complex that recruits chitin synthase to the site of bud emergence. *Mol. Biol. Cell* **14**, 26-39.

Lew, D. J. (2003). The morphogenesis checkpoint: how yeast cells watch their figures. *Curr. Opin. Cell Biol.* **15**, 648-653.

Lippincott, J. and Li, R. (1998). Sequential assembly of myosin II, an IQGAP-like protein, and filamentous actin to a ring structure involved in budding yeast cytokinesis. *J. Cell Biol.* **140**, 355-366.

Longtine, M. S. and Bi, E. (2003). Regulation of septin organization and function in yeast. *Trends Cell Biol.* **13**, 403-409.

Orlando, K., Sun, X., Zhang, J., Lu, T., Yokomizo, L., Wang, P. and Guo, W. (2011). Exo-endocytic trafficking and the septin-based diffusion barrier are required for the maintenance of Cdc42p polarization during budding yeast asymmetric growth. *Mol. Biol. Cell* **22**, 624-633.

Rodriguez-Peña, J. M., Cid, V. J., Sánchez, M., Molina, M., Arroyo, J. and Nombela, C. (1998). The deletion of six ORFs of unknown function from *Saccharomyces cerevisiae* chromosome VII reveals two essential genes: *YGR195w* and *YGR198w*. *Yeast* **14**, 853-860.

Rodríguez-Peña, J. M., Cid, V. J., Arroyo, J. and Nombela, C. (2000). A novel family of cell wall-related proteins regulated differently during the yeast life cycle. *Mol. Cell. Biol.* **20**, 3245-3255.

Roh, D.-H., Bowers, B., Riezman, H. and Cabib, E. (2002a). Rho1p mutations specific for regulation of β(1—>3)glucan synthesis and the order of assembly of the yeast cell wall. *Mol. Microbiol.* **44**, 1167-1183.

Roh, D.-H., Bowers, B., Schmidt, M. and Cabib, E. (2002b). The septation apparatus, an autonomous system in budding yeast. *Mol. Biol. Cell* **13**, 2747-2759.

Rose, M. D., Winston, F. and Hieter, P. (1990). Methods in yeast genetics. *A Laboratory Course Manual*. Cold Spring Harbor, NY: Cold Spring Harbor Press.

Schmidt, M., Bowers, B., Varma, A., Roh, D.-H. and Cabib, E. (2002). In budding yeast, contraction of the actomyosin ring and formation of the primary septum at cytokinesis depend on each other. *J. Cell Sci.* **115**, 293-302.

Schmidt, M., Varma, A., Drgon, T., Bowers, B. and Cabib, E. (2003). Septins, under Cla4p regulation, and the chitin ring are required for neck integrity in budding yeast. *Mol. Biol. Cell* **14**, 2128-2141.

Schmidt, M., Drgon, T., Bowers, B. and Cabib, E. (2008). Hyperpolarized growth of *Saccharomyces cerevisiae cak1*^{P212S} and *cla4* mutants weakens cell walls and renders cells dependent on chitin synthase 3. *FEMS Yeast Res.* **8**, 362-373.

Shaw, J. A., Mol, P. C., Bowers, B., Silverman, S. J., Valdivieso, M. H., Durán, A. and Cabib, E. (1991). The function of chitin synthases 2 and 3 in the Saccharomyces cerevisiae cell cycle. *J. Cell Biol.* **114**, 111-123.

Sikorski, R. S. and Hieter, P. (1989). A system of shuttle vectors and yeast host strains designed for efficient manipulation of DNA in Saccharomyces cerevisiae. *Genetics* **122**, 19-27.

Slater, M. L., Bowers, B. and Cabib, E. (1985). Formation of septum-like structures at locations remote from the budding sites in cytokinesis-defective mutants of Saccharomyces cerevisiae. *J. Bacteriol.* **162**, 763-767.

Tkacz, J. S., Cybulska, E. B. and Lampen, J. O. (1971). Specific staining of wall mannan in yeast cells with fluorescein-conjugated concanavalin A. *J. Bacteriol.* **105**, 1-5.

Versele, M. and Thorner, J. (2004). Septin collar formation in budding yeast requires GTP binding and direct phosphorylation by the PAK, Cla4. *J. Cell Biol.* **164**, 701-715.

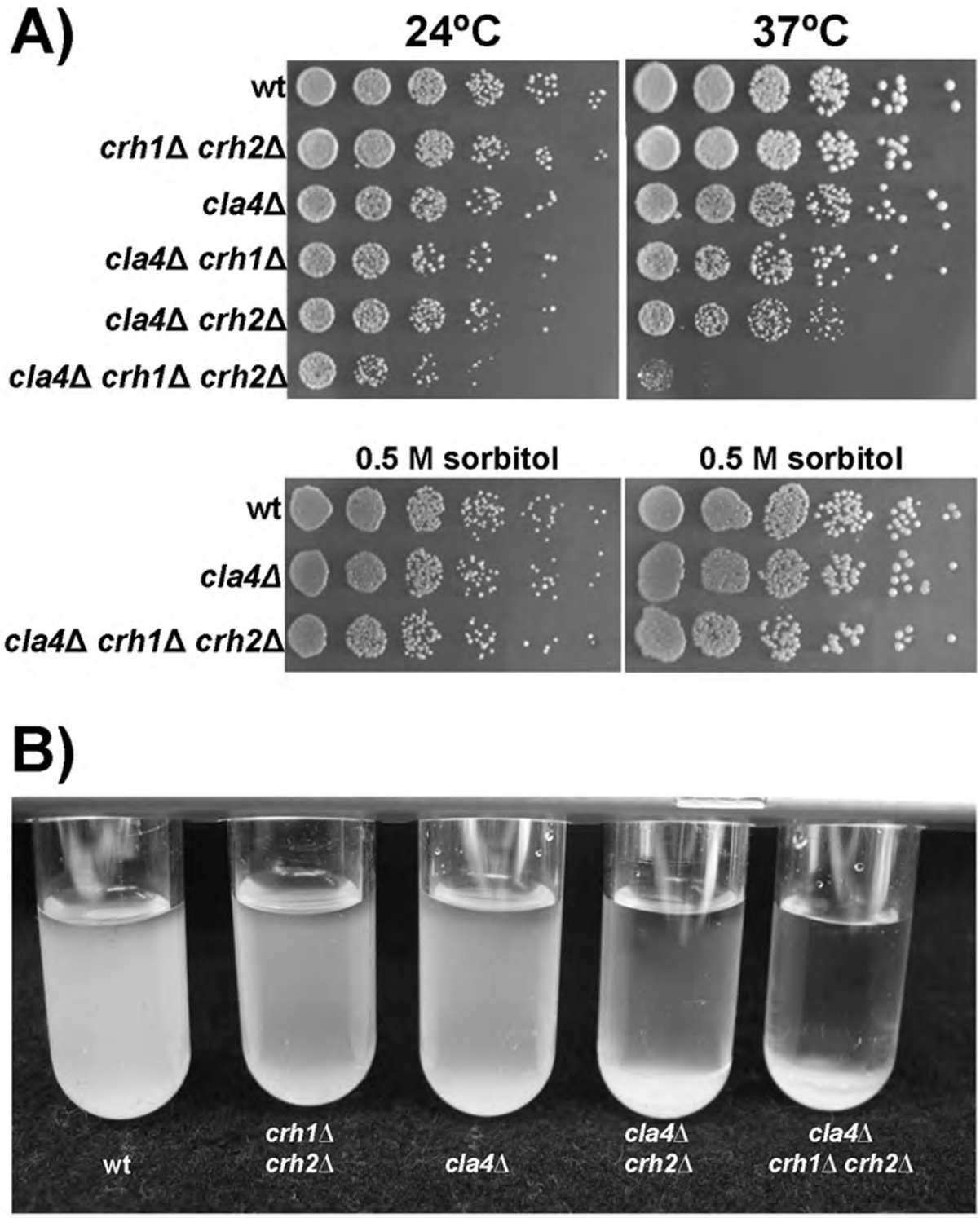

Fig. S1 **Effect of sorbitol on temperature sensitivity of mutants and clumping in mutants.** (A) Strains with both *CLA4* and *CRH* defects show temperature sensitivity that is corrected by 0.5 M sorbitol. The medium was YEPD with the addition of sorbitol where indicated. (B) The triple mutant *cla4Δ crh1Δ crh2Δ* and the double mutant *cla4Δ crh2Δ* form large clumps that sediment rapidly. Sedimentation time was 10 min.

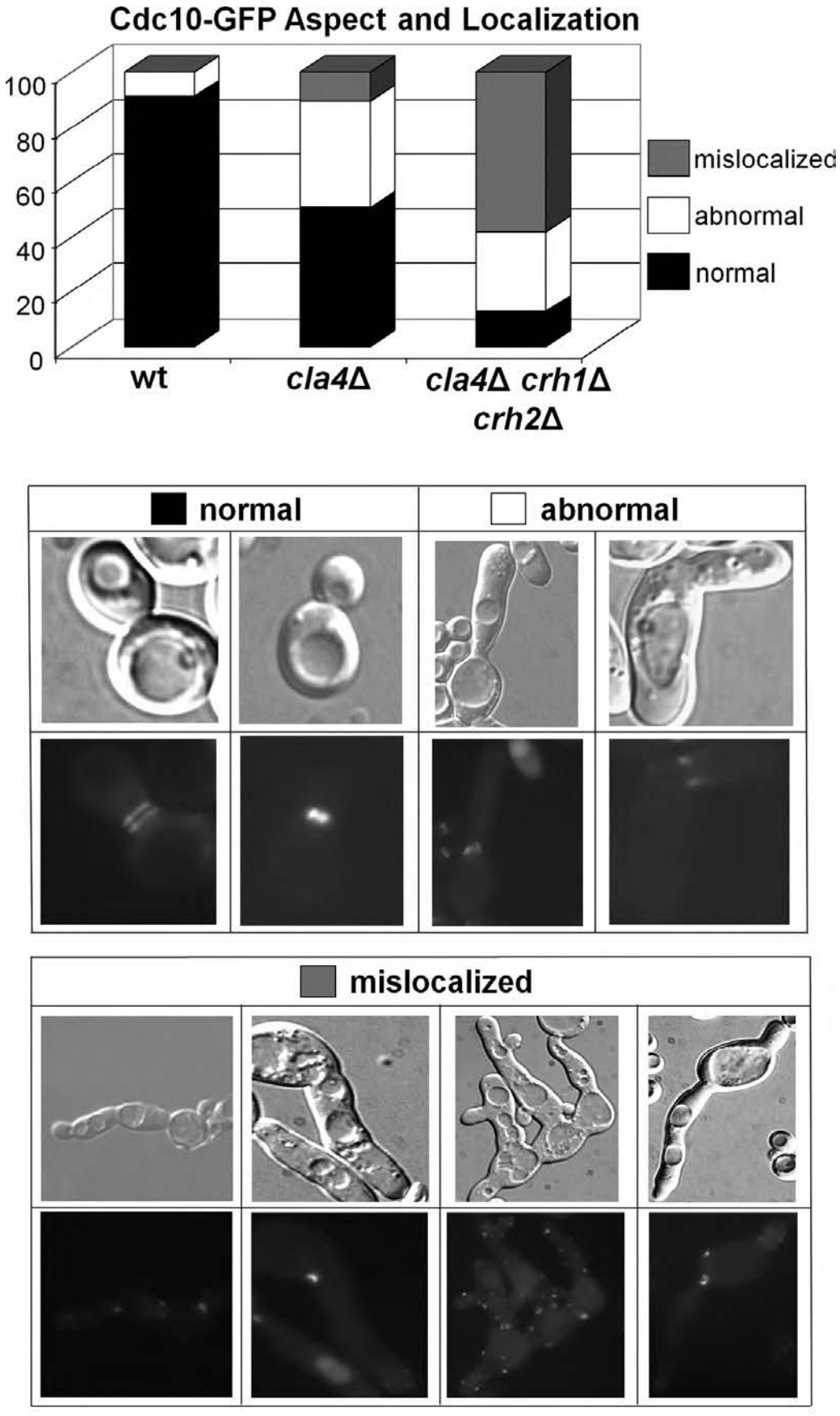

Fig. S2. **Septin mislocalization in the triple mutant *cla4Δ crh1Δ crh2Δ* compared to other strains**. Examples of each septin configuration are shown. Normal examples are from YPH499, abnormal from YMS134 and mislocalized from NBT017. wt, YPH499; *cla4*, YMS134; *cla4 crh1 crh2*, NBT017.

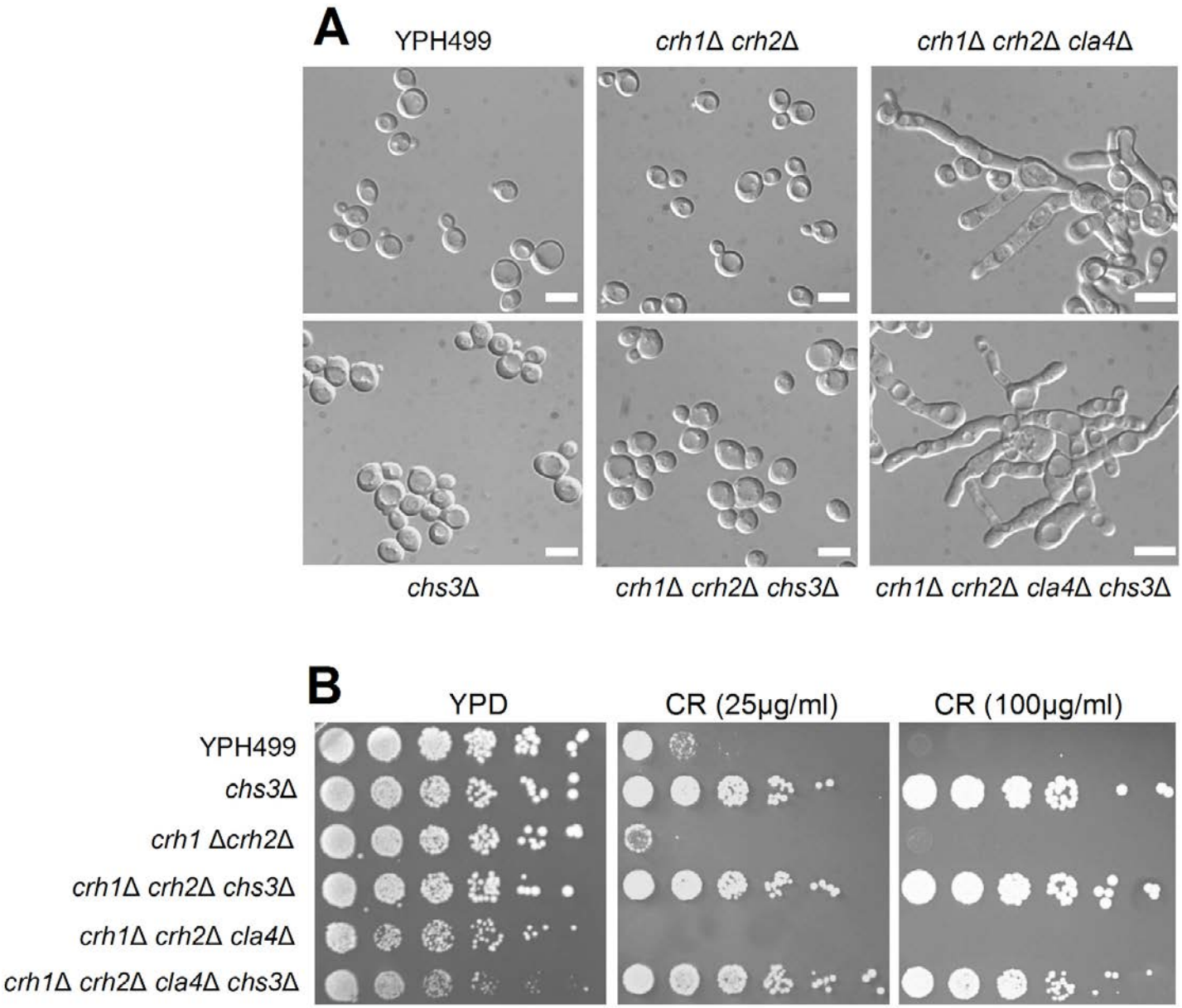

Fig. S3. **The phenotype of *chs3Δ* cells is not affected by *crh1* and *crh2* mutations**. Strains are wild type, YPH499; *chs3Δ*, NBT025; *crh1Δ crh2Δ*, NBT014; *crh1Δ crh2Δ cla4Δ*, NBT017; *crh1Δ crh2Δ chs3Δ*, NBT026; *crh1Δ crh2Δ chs3Δ cla4Δ*, NBT027. **A**, cells containing the *chs3* deletion give rise to clumps. **B**, cells containing the *chs3* deletion are resistant to Congo Red (CR).

Table S1. Segregation of genotypes in a cross between YMS90 (*chs3Δ cla4*) and YPH499-B[a]

Genotype	Germinated spores
CHS3 CLA4	89
CHS3 cla4::URA3	68
chs3::LEU2 CLA4	75
chs3::LEU2 cla4::URA3	8

[a]A total of 85 tetrads were dissected.

Table S2. Chitin distribution in a *cla4Δ crh1Δ* strain in the presence of triacetylchitotriose

	Percent of total chitin			
	Free	Bound	Bound to β(1-6)glucan	Bound to β(1-3)glucan
Control	44.8	55.2	12.8	42.4
2mM triacetylchitotriose	62.5	37.4	10.8	26.6

Table 3. Strains used in this study.

Strain	Genotype	Source
YPH499	*MAT***a** *ura3-52 lys2-801 ade2-101 trp1-Δ63 his3-Δ200 leu2-Δ1*	Sikorski and Hieter (1989)
YPH499-B	*MATα ura3-52 lys2-801 ade2-101 trp1-Δ63 his3-Δ200 leu2-Δ1*	Crotti et al. (2001)
YMS90	*MAT***a** *ura3-52 lys2-801 ade2-101 trp1-Δ63 his3-Δ200 leu2-Δ1 chs3::LEU2 cla4::URA3*	Schmidt et al. (2003)
YMS134	*MAT***a** *ura3-52 lys2-801 ade2-101 trp1-Δ63 his3-Δ200 leu2-Δ1 cla4::LEU2*	Schmidt et al. (2003)
YMS306	*MAT*a *ura3-52 lys2-801 ade2-101 trp1-Δ63 his3-Δ200 leu2-Δ1 cla4::TRP1*	Schmidt et al. (2003)
NBT010	*MAT***a** *ura3-52 lys2-801 ade2-101 trp1-Δ63 his3-Δ200 leu2-Δ1 crh1::hphMX4*	This work
NBT011	*MAT***a** *ura3-52 lys2-801 ade2-101 trp1-Δ63 his3-Δ200 leu2-Δ1 cla4::LEU2 crh1::hphMX4*	This work
NBT012	*MAT*a *ura3-52 lys2-801 ade2-101 trp1-Δ63 his3-Δ200 leu2-Δ1 cla4::TRP1 crh1::hphMX4*	This work
NBT013	*MAT***a** *ura3-52 lys2-801 ade2-101 trp1-Δ63 his3-Δ200 leu2-Δ1 crh2::HIS3*	This work
NBT014	*MAT***a** *ura3-52 lys2-801 ade2-101 trp1-Δ63 his3-Δ200 leu2-Δ1 crh1::hphMX4 crh2::HIS3*	Cabib et al. (2012)
NBT015	*MAT***a** *ura3-52 lys2-801 ade2-101 trp1-Δ63 his3-Δ200 leu2-Δ1 cla4::LEU2 crh2::HIS3*	This work
NBT017	*MAT***a** *ura3-52 lys2-801 ade2-101 trp1-Δ63 his3-Δ200 leu2-Δ1 cla4::LEU2 crh1::hphMX4 crh2::HIS3*	This work
NBT025	*MAT***a** *ura3-52 lys2-801 ade2-101 trp1-Δ63 his3-Δ200 leu2-Δ1 chs3::KanMX4*	This work

NBT026	*MAT***a** *ura3-52 lys2-801 ade2-101 trp1-Δ63 his3-Δ200 leu2-Δ1 chs3::KanMX4 crh1::hphMX4 crh2::HIS3*	This work
NBT027	*MAT***a** *ura3-52 lys2-801 ade2-101 trp1-Δ63 his3-Δ200 leu2-Δ1 chs3::KanMX4 crh1::hphMX4 crh2::HIS3 cla4::LEU2*	This work
ECY108	*MAT***a** *ura3-52 lys2-801 ade2-101 trp1-Δ63 his3-Δ200 leu2-Δ1 cla4::LEU2 crh1::hphMX4 crh2::HIS3 swe1::kanMX4*	This work This work
ECY46-4-1B	*MAT***a** *ura3-52 lys2-801 ade2-101 trp1-Δ63 his3-Δ200 leu2-Δ1 chs3::LEU2*	Crotti et al., 2001

Table 4. Plasmids used in this study

Plasmid	Description	Source
pLA10	pGFP-C-FUS-CDC10	Cid et al. (1998)
pNB23	YEp352-CRH2-HA-E166Q	This work
pNB48	YEp352-CRH1-HA-E134Q	This work
pNBc13	YEp352-CRH2-HA	Cabib et al. (2007)
pNBc15	YEp352-CRH1-HA	Cabib et al. (2007)
pMS17	pRS200-CLA4	Schmidt et al. (2003)

DISCUSIÓN GENERAL

Al mismo tiempo que la pared celular ofrece protección frente al estrés osmótico, debe acompañar a la célula en su crecimiento, lo que supone una continua remodelación de la misma. El crecimiento celular conlleva la reorganización de la pared celular mediante la ruptura de los enlaces de los polisacáridos existentes, la introducción de los nuevos polisacáridos y la formación de nuevos complejos. Debido a que los polímeros están accesibles en el espacio intracelular, es muy probable que la reacción de entrecruzamiento ocurra en esta zona. Sin embargo, para solventar la escasez de fuente de energía libre (ATP) en el espacio periplasmático, hace años el grupo del Dr. E. Cabib propuso que la energía necesaria para la formación de los nuevos enlaces procedería de la ruptura de los enlaces existentes, en una reacción de transglicosilación (Cabib et al., 1988).

A pesar del gran avance en el conocimiento sobre las actividades biosintéticas y la estructura de los componentes de la pared celular, la información disponible sobre las actividades remodeladoras y de entrecruzamiento entre los componentes de la pared celular era escasa o inexistente respectivamente. Hasta el desarrollo de este trabajo, se conocía la participación de la familia Gas en remodelación *in vitro* (Carotti et al., 2004; Mazan et al., 2012), pero no existía ninguna demostración *in vivo* e *in vitro* sobre las actividades ensambladoras entre los diferentes componentes de la pared celular. Teniendo en cuenta los resultados previos de nuestro laboratorio, en los cuales la fracción de glucano álcali soluble en el mutante *crh1*Δ *crh2*Δ es al menos el doble que en la cepa WT y que la localización de estas proteínas, en los sitios de crecimiento polarizado (área de gemación, cuello, septo, cicatriz) y en menor proporción en pared lateral (Rodriguez-Pena et al., 2000),coincide con los depósitos de quitina, hacían de las proteínas Crh1 y Crh2 unas buenas candidatas para actuar como transglicosilasas.

El objetivo general de este trabajo ha sido la caracterización del papel de las proteínas Crh1 y Crh2 en la biogénesis de la pared celular de *S. cerevisiae*. Gracias al desarrollo de técnicas y aproximaciones experimentales específicas e innovadoras hemos descubierto que estas enzimas son las responsables del enlace entre la quitina y el β-1,3 glucano y la quitina y el β-1,6 glucano de la pared celular. Hemos caracterizado las propiedades bioquímicas de la reacción enzimática que llevan a cabo estas proteínas *in vivo* e *in vitro*. Con el objetivo de profundizar en el mecanismo de acción de estas proteínas en el ensamblaje de los componentes de la pared celular, hemos llevado a cabo un estudio estructura-función de los diferentes dominios implicados en la catálisis. Los

resultados obtenidos han proporcionado información relevante y detallada sobre el papel catalítico de determinados aminoácidos en la reacción de transglicosilación llevada a cabo por estas proteínas. Adicionalmente, hemos estudiado la relevancia del enlace entre el glucano y la quitina en la morfogénesis de la levadura. Los resultados obtenidos de estudios fenotípicos realizados sobre mutantes que presentan un defecto en morfogénesis (septinas, *cla4*Δ, *chs3*Δ,…etc.), junto a la ausencia del enlace entre la quitina y el glucano (*crh1*Δ *crh2*Δ), han revelado un papel en regulación de la morfogénesis celular hasta ahora desconocido, llevado a cabo a nivel molecular por el enlace químico entre la quitina y el glucano. Este control lo realizaría mediante la restricción del crecimiento en la zona del cuello, ya que la quitina unida al β-1,3 glucano, evita la remodelación del mismo mediante su unión al β-1,6 glucano y a las manoproteínas. Esta premisa se encuentra avalada por la presencia mayoritaria de quitina unida a β-1,3 glucano en esta zona, frente a quitina unida al β-1,6 glucano en la pared lateral (Cabib and Duran, 2005) y por la existencia de dos poblaciones de β-1,3 glucano: una sin remodelar y polidispersa, y otra remodelada y de alto peso molecular unida a la quitina.

1. Crh1 y Crh2 SON LAS RESPONSABLES DEL ENSAMBLAJE DEL GLUCANO Y LA QUITINA EN LA PARED CELULAR DE LA LEVADURA

A pesar del gran avance en el conocimiento de la estructura de la pared celular en estos últimos 20 años, se desconocía la naturaleza y el mecanismo de las enzimas encargadas del entrecruzamiento entre los componentes de la pared celular. El abordaje de este objetivo suponía el reto de salvar la insolubilidad en agua de los complejos existentes en la pared celular, para posteriormente separarlos y cuantificarlos. La introducción de cargas negativas procedentes del ácido acético contrarresta la atracción entre sí de las cadenas de carbohidratos y permite la solubilización en agua del mismo. Este procedimiento conocido como carboximetilación, aplicado sobre las paredes celulares, permitió la solubilización de los complejos formados por la quitina y el glucano (Cabib and Duran, 2005). Así, los complejos definidos fueron: quitina libre preferentemente localizada en el septo, quitina (de cadena corta o larga) unida al β-1,3 glucano que se localiza preferentemente en el cuello y quitina unida al β-1,6 glucano presente mayoritariamente en

la pared lateral. La digestión previa a la carboximetilación con β-1,3 o β-1,6 glucanasa de células crecidas previamente en presencia de ^{14}C-glucosamina y su posterior fraccionamiento, permitió la cuantificación del porcentaje de cada fracción presente en la pared celular de una cepa WT (Cabib and Duran, 2005).

El estudio mediante carboximetilación y fraccionamiento de las paredes celulares de las cepas *crh1*Δ, *crh2*Δ y *crh1*Δ *crh2*Δ reveló una disminución de la fracción correspondiente a quitina unida a β-1,6 glucano en *crh1*Δ, mucho mayor en *crh2*Δ y ausente en *crh1*Δ *crh2*Δ. Este resultado manifiesta cuantitativamente que *in vivo* Crh2 tiene un papel más relevante en la formación de este enlace que Crh1. Descartada la posibilidad de que estuvieran implicadas en la ramificación del β-1,6 glucano, los resultados obtenidos en este trabajo demuestran que las proteínas Crh1 y Crh2 son las responsables de la unión entre la quitina y el β-1,6 glucano. Como dato destacable, está el hecho de que la fracción de quitina libre se incrementa conforme se deleciona cada gen por separado. Este resultado es de gran relevancia en relación a la biogénesis de la pared celular fúngica, pues es la primera vez que se describen las proteínas implicadas en el entrecruzamiento entre la quitina y el glucano *in vivo*. Adicionalmente, observamos una disminución de la fracción de quitina de cadena corta unida al β-1,3 glucano en las tres cepas con respecto a la cepa WT. Sin embargo, la quitina de cadena larga unida al β-1,3 glucano permanecía constante, de modo que en las paredes celulares del mutante *crh1*Δ *crh2*Δ existía quitina unida al β-1,3 glucano. A pesar de que la sobrexpresión de Crh1 y Crh2 sobre *crh1*Δ *crh2*Δ aumentaba la fracción de quitina de cadena corta unida al β-1,3 glucano, los demás resultados sugerían que estas proteínas no eran las únicas responsables de este enlace. El hecho de que la deleción de *CRH1* y *CRH2* impidiera la unión de la quitina al β-1,6 glucano *in vivo*, pero no afectara el enlace quitina-β-1,3 glucano nos resultó en cierto modo sorprendente. El desarrollo posterior de un método de medida de la actividad transglicosilasa *in vivo* utilizando gluco-oligosacáridos marcados con SR (ver capítulo 2 y discusión posterior) como aceptores artificiales de la reacción en células en crecimiento, reveló que los β-1,3 gluco-oligosacáridos se incorporaban a las paredes celulares de forma Crh1 y Crh2 dependiente. Este resultado pudiera parecer sorprendente en base a los resultados discutidos arriba sobre el papel de las proteínas Crh en la formación del enlace quitina-β-16 glucano, pero no en el enlace quitina-β-1,3 glucano. Sin embargo, esto podía explicarse teniendo en cuenta que la unión del β-1,6 glucano a la quitina en la pared celular no es directa, sino a través de una ramificación compuesta por

varios residuos glúcidos unidos mediante enlaces β-1,3. No obstante, estos resultados nos hicieron reconsiderar en cierto modo la aproximación experimental previa.

Así, en un trabajo el Dr. E. Cabib desarrolla dos nuevos métodos bioquímicos, el método curdlan y el método quitosán, para la cuantificación de los complejos quitina-glucano presentes en la pared celular (Cabib, 2009). El método curdlan se basa en la afinidad del polisacárido curdlan por las cadenas carboximetiladas del β-glucano. Este polisacárido forma un gel cuando es calentado a 56ºC. La aplicación de las paredes celulares carboximetiladas sobre una columna de gel curdlan permite la absorción específica de las cadenas de β-glucano y la elución de la quitina libre. El pretratamiento de las paredes celulares con β-1,6 glucanasa antes de su carboximetilación y su posterior aplicación en la columna de gel curdlan, permite cuantificar el porcentaje de quitina unida al β-16 glucano liberada con el tratamiento, tras sustraer el porcentaje de quitina libre procedente de las paredes celulares sin tratar. El segundo método consiste en la deacetilación *in vivo* de la quitina mediante el tratamiento de las paredes celulares con hidróxido sódico a altas temperaturas durante treinta minutos para la generación de quitosán, que es un análogo de la quitina soluble en ácido acético. De esta manera se puede medir la quitina libre presente en las paredes de la cepa WT. Sí, subsecuentemente a la cuantificación de la quitina libre, se trata las paredes con β-1,6 glucanasa y se vuelve a generar quitosán mediante el tratamiento previamente descrito, se obtiene el porcentaje de quitina unida al β-1,6 glucano. La aplicación de estos dos métodos sobre las paredes celulares procedentes de una cepa WT arrojó porcentajes similares, a los que obtuvimos con el método de carboximetilación-fraccionamiento descrito en el capítulo 1, para los diferentes complejos en lo que se encuentra la quitina en la pared celular. Sin embargo, el análisis de las paredes celulares de la cepa *crh1*Δ *crh2*Δ mediante estos dos métodos demostró que toda la quitina se encuentra en estado libre. El reanálisis del método de carboximetilación-fraccionamiento anteriormente usado, reveló la presencia de una contaminación de quitinasa en la preparación de β-1,3 glucanasa usada (Zimoliasa), que nos llevó a unos resultados erróneos sobre la fracción β-1,3 glucano-quitina en la cepa *crh1*Δ *crh2*Δ. Una vez solventada esta contaminación, los resultados del análisis de las paredes celulares procedentes de los mutantes *crh1*Δ, *crh2*Δ y *crh1*Δ *crh2*Δ por los tres métodos coinciden (Cabib, 2009). De nuevo, se observó que la fracción de quitina unida al β-1,6 glucano dependía mayoritariamente de la presencia de Crh2 en la pared celular, como previamente habíamos observado. Sin embargo, en los mutantes individuales los

niveles del complejo quitina-β-1,3 glucano apenas presentan diferencias con respecto a la cepa WT, de modo que la ausencia de una proteína se ve compensada por la presencia de la otra. Dicho de otro modo, ambas proteínas están participando en la formación de este complejo. Adicionalmente y como ya habíamos visto, la fracción de quitina libre aumenta conforme se delecionan los genes *CRH*. Estos resultados, sumados a que en las paredes celulares del mutante *crh1*Δ *crh2*Δ toda la quitina aparentemente se encuentra en estado libre, es decir no covalentemente unida al glucano, permiten concluir que Crh1 y Crh2 no solo son responsables de la unión de la quitina al β-1,6 glucano, sino también del componente estructural mayoritario de la pared celular, el β-1,3 glucano. El descubrimiento de las proteínas implicadas en la biogénesis de los complejos de la pared celular supone un avance importante hacia el completo entendimiento de esta estructura.

Como discutiremos más adelante, en las paredes del mutante *crh1*Δ *crh2*Δ hay quitina unida a glucano mediante enlaces no covalentes, esta unión debe solventar de alguna manera el déficit de una organización adecuada entre los componentes de la pared celular de esta cepa, evitando la aparición de fenotipos aberrantes al menos en condiciones normales. Sin embargo, cuando la célula presenta defectos en la biosíntesis de la pared celular o se somete a un estrés, el papel de las proteínas Crh en el ensamblaje de los componentes se vuelve esencial para la supervivencia celular. Así, mutantes combinados de los genes *CRH* con los genes *FKS1* y *GAS1* que participan en la biogénesis de la pared, tienen activado el mecanismo compensatorio y un mayor acúmulo de quitina unida a manoproteínas mediante β-1,6 glucano en sus paredes celulares (Kapteyn et al., 1997), presentan un aumento de los defectos morfológicos presente en los mutantes sencillos: lisis, crecimiento, viabilidad y sensibilidad al RC. Interesantemente, destacamos el hecho de que el triple mutante *crh1*Δ *crh2*Δ *fks1*Δ muestre una sensibilidad al RC similar a la cepa delecionada en la MAP quinasa de la ruta de integridad s*lt2*Δ, apoyando la importancia de la formación de un complejo covalente entre los componentes de la pared celular en supervivencia celular cuando la célula presenta la estructura del β-1,3 glucano dañada o ausente.

Con el objetivo de conservar la integridad y funcionalidad, cuando se produce un daño o alteración sobre la pared celular, la célula desarrolla un complejo mecanismo de respuesta, fundamentalmente dependiente de la ruta CWI, para conseguir remodelar la pared celular y compensar los daños existentes. Este proceso denominado mecanismo

compensatorio (Popolo et al., 2001) conlleva el incremento en la síntesis de β-1,3 glucano, un aumento del contenido de quitina mediado por Chs3 (Carotti et al., 2002) y un incremento de la expresión e incorporación de proteínas de pared. Con el objetivo de estudiar el papel funcional de las proteínas Crh sobre la pared celular bajo un estrés mediado por la ruta CWI, sometimos a las células a un estrés transitorio establecido por un cambio de Tª durante su crecimiento (38ºC). Los resultados muestran un incremento de quitina en las paredes laterales (tinción con CFW) que se refleja en un aumento claro de la fracción de quitina unida al β-1,6 glucano, dependiente de las proteínas Crh y de la MAP quinasa de la ruta de integridad Slt2. Estos resultados apoyan la relevancia del complejo quitina-β-1,6 glucano para la supervivencia celular en condiciones de estrés sobre la pared celular.

Cabe destacar, que sí bien el aumento de la fracción de quitina unida al β-1,6 glucano en condiciones de estrés térmico depende tanto de Crh1 como de Crh2, la transcripción y los niveles proteicos de Crh1 se incrementan tras el choque térmico, mientras que los niveles de RNAm y proteína de Crh2 no se ven modificados. Esta respuesta diferencial coinciden con datos publicados previamente en nuestro laboratorio en los cuales la transcripción de *CRH1,* no así la de *CRH2*, se incrementa ante diferentes daños en la pared celular (Garcia et al., 2004). A su vez, los niveles de proteína de Crh1 están regulados de manera ciclo dependiente, mientras que los niveles de Crh2 permanecen constante durante todo el ciclo celular (Rodriguez-Pena et al., 2000). Existen más casos en levaduras en los cuales dos proteínas homólogas en función presentan un patrón de regulación transcripcional diferente, por ejemplo Fks1 y Fks2. Aunque tras el choque térmico no se produce un aumento de los niveles de Crh2, si se produce un cambio de localización, pasando de hallarse preferentemente en sitios de crecimiento polarizado (24ºC) a localizarse uniformemente por la pared lateral en estas condiciones (38ºC). Así, Crh1 también presenta este patrón de localización tras el estrés transitorio. Estos resultados tienen todo su sentido funcional, ya que en condiciones de estrés térmico se aumenta la síntesis de quitina en toda la pared lateral y existe una relocalización de Chs3 en membrana plasmática (Valdivia and Schekman, 2003). Este aumento de quitina requiere de un aumento de su capacidad de transglicosilación al glucano para lograr su unión covalente y esto requiere de la actividad transglicosilasa de las proteínas Crh. De hecho, como muestran los resultados del capítulo 2, la fluorescencia tanto en cicatriz como en pared lateral procedente de la incorporación de los gluco-oligosacáridos en el mutante *gas1*Δ,

que presenta el nivel de quitina aumentado con respecto a la cepa silvestre, se encuentra aumentada en un 93% con respecto a la cepa WT, es decir, la actividad transglicosilasa en estas células ha aumentado y como consecuencia se ha producido un incremento en la incorporación del gluco-oligosacárido a la pared celular, que a su vez coincide con los sitios donde la quitina ha sido sintetizada por Chs3.

Una vez conocidas las enzimas responsables del ensamblaje de los componentes de la pared celular, cabe preguntarse: ¿Qué tipo de reacción enzimática están catalizando estas proteínas?, ¿Cómo ocurre este ensamblaje?, ¿Cuáles son las propiedades bioquímicas de la reacción? Nosotros proponemos un modelo donde la quitina naciente (donador) es directamente transferida al glucano, sin modificación del aceptor y sin la necesidad de un aporte extra de energía, ya que ocurrirá mediante una reacción de transglicosilación, que explicaría que a pesar de la escasa disposición de energía presente en el espacio periplasmático se pueda llevar a cabo el ensamblaje de los componentes. Así, la hidrólisis del donador aporta la energía necesaria para su enlace con el aceptor. De este modo, las proteínas Crh ancladas transitoriamente en la membrana mediante su anclaje GPI y localizadas principalmente en los sitios de crecimiento polarizado, coincidiendo con los depósitos de quitina, realizarían la transglicosilación de la quitina al aceptor, antes de que las cadenas de quitina se unan entre sí a través de puentes de hidrogeno y formen fibras insolubles en agua. Apoyando esta hipótesis está el hecho de que aparentemente las proteínas Crh son capaces de transferir las cadenas de quitina de diferentes tamaños, como se ha visto en el primer capítulo de este trabajo y posteriormente verificado en los diferentes trabajos realizados en esta tesis e individualmente por el Dr.Cabib (Cabib, 2009). Así, la quitina derivada tanto de la unión al β-1,3 glucano o β-1,6 glucano es de similar tamaño y más pequeña que la quitina libre, siendo la quitina libre de mayor tamaño y complejidad, de acuerdo con la visualización microscópica de la quitina en fibrillas debido a la fuerte atracción de las cadenas entre sí para solventar su hidrofobicidad (Muzzarelli et al., 1979).

2. PROPIEDADES BIOQUÍMICAS DE LA REACCIÓN ENZIMÁTICA CATALIZADA POR Crh1 Y Crh2

2.1. DESARROLLO DE UN SISTEMA DE TRANSGLICOSIDACIÓN *IN VIVO*

El estudio *in vitro* de una reacción enzimática requiere que los sustratos (donador y aceptor) sean solubles en algún tipo de solvente. Dada la insolubilidad en agua de la quitina y con el objetivo de demostrar que ambas proteínas, Crh1 y Crh2 llevan a cabo la transglicosilación de la quitina al glucano, se desarrollaron sistemas *in vivo* e *in vitro* para medir esta actividad. Para el desarrollo del modelo *in vivo* se utilizaron oligosacáridos sintéticos marcados con el fluoróforo sulforodamina como aceptores sintéticos y como donador la quitina presente en la pared de la célula. Gracias a que la pared celular es permeable a moléculas de pequeño tamaño, oligosacáridos entre 2 y 8 unidades pueden penetrar en el espacio periplasmático e interaccionar con la quitina naciente. Como consecuencia de la reacción de transglicosilación, el oligosacárido pasaría a formar parte del producto que se incorporaría a la pared celular, donde se visualizaría la emisión de fluorescencia. El uso de oligosacáridos artificiales como sustratos en estudios enzimáticos ya había sido previamente descrito en plantas (Mohand and Farkas, 2006). La estabilidad en la fluorescencia, tanto del aceptor como del producto fue crucial para la detección y localización de la reacción. Así, células silvestres crecidas en presencia de los β-1,3 gluco-oligosacáridos y los β-1,6 gluco-oligosacáridos mostraron un patrón de fluorescencia localizado preferentemente en las cicatrices y también en la pared lateral de la cepa, aunque de forma minoritaria. Cabe mencionar que la incorporación de los β-1,6 gluco-oligosacáridos es mucho menos eficiente que la incorporación de los oligosacáridos derivados de β-1,3 glucano. De hecho en los primeros estudios no se observó dicha incorporación (capítulo 2). La utilización de una mezcla de β-1,6 gluco-oligosacáridos con un mayor grado de polimerización permitió su detección. ¿Por qué en estas localizaciones? En la cicatriz existen tres fuentes a las que se pueden unir los gluco-oligosacáridos: quitina libre procedente del anillo de quitina (aunque la del anillo de quitina está preferentemente unida al β-1,3 glucano, un tercio está libre), quitina procedente del septo primario (mayoritariamente libre) y quitina libre procedente de la síntesis *de novo*. La detección de

fluorescencia en la pared lateral era esperable dado que ahí es donde se localiza preferentemente el complejo quitina-β-1,6 glucano, al igual que era esperable una menor incorporación de los gluco-oligosacáridos en la pared lateral que en la cicatriz, al menos en condiciones de crecimiento estándar, debido a que el complejo quitina-glucano presente en la pared lateral solo representa el 16% del total de la quitina presente en la pared celular. Ambas localizaciones tienen su sentido biológico, ya que como se ha comentado antes, situaciones de estrés sobre la pared celular o defectos en la estructura de la misma (*gas1*Δ y *fks1*Δ) que provocan un aumento en la síntesis de quitina, producen un aumento claro de la fluorescencia en ambas localizaciones, que es a su vez dependiente de Crh1 y Crh2, dado que las cepas *gas1*Δ *crh1*Δ *crh2*Δ o *fks1*Δ *crh1*Δ *crh2*Δ muestran una ausencia total de fluorescencia tanto en cicatriz como en pared lateral.

El hecho de que los quito-oligosacáridos resultaran ser efectivos inhibidores de la incorporación de los β-1,3 gluco-oligosacáridos nos hizo explorar la posibilidad de que los quito-oligosacáridos fluorescentes se incorporaran también a las paredes celulares. Pudimos comprobar no solo que se incorporaban, sino que lo hacían con extraordinaria eficiencia y un patrón de localización similar al de los β-1,3- y β-1,6 gluco-oligosacáridos. Estos resultados *in vivo*, están completamente de acuerdo con los resultados de los ensayos *in vitro*, discutidos más adelante, en los que los quito-oligosacáridos funcionan también con extraordinaria eficiencia como aceptores de la reacción de transglicosilación. Como se discute posteriormente, estos datos serían compatibles con la función de las proteínas Crh en la formación de enlaces quitina-glucano.

La incorporación de los tres tipos de oligosacáridos en la pared celular (β-1,3-, β-1,6 gluco-oligosacáridos y quito-oligosacáridos), medida como detección de fluorescencia, depende de Crh1 y Crh2, dado que la deleción conjunta de los genes provoca la desaparición de toda la fluorescencia, mientras que la sobreexpresión de las proteínas desde de un plásmido multicopia en el mutante *crh1*Δ *crh2*Δ genera un incremento en los niveles de fluorescencia, como consecuencia de la incorporación de los oligosacáridos, similares a los de la cepa WT. A su vez, el patrón de localización de ambas proteínas concuerda con la detección de fluorescencia en la cicatriz y en la pared lateral, ya que en situaciones basales estas proteínas se ubican mayoritariamente en los sitios de crecimiento polarizado y de manera puntual en la pared lateral. La solubilización de la fluorescencia mediante el uso de quitinasa, nos permitió asegurar que los oligosacáridos estaban

uniéndose a la quitina. Otro aspecto digno de comentar es que no se detecta parches de fluorescencia en todas las células crecidas en presencia del oligosacárido marcado porque preferentemente se incorpora a las cicatrices y no todas las células del cultivo tienen cicatrices.

La puesta a punto de estos ensayos de actividad transglicosilasa *in vivo* (capítulo 2) nos permitían, utilizando los mutantes individuales y dobles de los genes *CRH1* y *CRH2*, estudiar el papel individual de cada proteína en la reacción *in vivo*. Por ello, se realizaron ensayos de incorporación *in vivo* con oligosacáridos marcados derivados de: laminarina (β-1,3 glucano), pustulán (β-1,6 glucano) y quito-oligosacáridos en los mutantes sencillos *crh1*Δ y *crh2*Δ y en el doble mutante *crh1*Δ *crh2*Δ (capítulo 3). Coincidiendo con los resultados descritos en el capítulo 1 respecto al análisis de las diferentes fracciones de quitina en estos mutantes, la incorporación de los β-1,3 gluco-oligosacáridos a la pared celular depende de ambas proteínas, ya que los mutantes sencillos muestran pequeñas diferencias de fluorescencia con respecto a la cepa silvestre y el doble mutante *crh1*Δ *crh2*Δ no presenta fluorescencia ninguna. Sin embargo, de nuevo y coincidiendo con los datos obtenidos en los experimentos del fraccionamiento de las paredes celulares, observamos que la incorporación del β-1,6 glucano depende preferentemente de Crh2, ya que su ausencia provoca una drástica disminución de la fluorescencia con respecto a la cepa silvestre, mientras que en la cepa *crh1*Δ los niveles de fluorescencia apenas varían. No obstante, la ausencia total de fluorescencia para este gluco-oligosacárido en la cepa *crh1*Δ *crh2*Δ y la recuperación de la fluorescencia en estas células expresando un plásmido multicopia de *CRH1*, suministran datos inequívocos en cuanto a la participación de Crh1 en la transglicosilación entre la quitina y el β-1,6 glucano *in vivo*, como era de esperar en base a los resultados de los experimentos de análisis de las distintas fracciones de quitina en las paredes celulares de los mutantes (capítulo 1).

Aunque ambas proteínas poseen capacidad para realizar la transglicosilación entre el β-1,3 glucano o el β-1,6 glucano y la quitina, el predominio funcional de una proteína sobre la otra podría explicarse al menos en parte en base a su localización. De este modo, aunque ambas proteínas se localizan en pared lateral y sitios de crecimiento polarizado (sitio de gemación, septo, cuello y cicatriz), Crh1, aunque se localiza también en la pared lateral, mayoritariamente lo hace en los sitios de crecimiento polarizado, mientras que Crh2 se localiza por igual en ambas posiciones. De este modo, el hecho de que la

localización del complejo quitina-β-1,6 glucano sea mayoritariamente en la pared lateral, estaría de acuerdo con un papel más relevante de Crh2 con respecto a Crh1 en este enlace en situaciones basales. Por otro lado, el complejo quitina-β-1,3 glucano se localiza preferentemente en los sitios de crecimiento polarizado donde también colocalizan ambas proteínas coincidiendo con la participación de ambas proteínas en este enlace.

Los experimentos que acabamos de discutir con células intactas muestran la posibilidad de utilizar oligosacáridos fluorescentes como aceptores de quitina en un sistema que mimetiza la transglicosilación quitina-glucano *in vivo*. Adicionalmente, se desarrolló un sistema *in vitro* con células permeabilizadas con digitonina e incubadas a 30ºC como fuente de enzimas y quitina, en presencia de UDP-NAG y oligosacáridos marcados con sulforodamina como aceptores (capítulo 2). En este sistema se produce también la incorporación de la fluorescencia a las paredes celulares y por tanto la reacción de transglicosilación de manera Crh dependiente. La transglicosilación es mayoritariamente dependiente de la presencia del precursor de la síntesis de quitina UDP-NAG, lo que confirma que la reacción enzimática tiene lugar preferiblemente sobre la quitina naciente. A diferencia de lo que ocurre *in vivo*, aquí la síntesis de quitina se lleva a cabo por Chs1 y no por Chs3. Estos resultados soportan el modelo, ya discutido anteriormente, en el que las proteínas Crh, ancladas en la membrana a través de su anclaje GPI, de manera probablemente transitoria antes de su localización final en la pared celular, transferirían la quitina naciente al glucano. En células *gas1*Δ permeabilizadas, incluso en ausencia de UDP-NAG se observa la aparición de parches fluorescentes que se corresponden con cicatrices. Estos datos sugieren la existencia de dos procesos de transglicosilación. Uno de ellos requeriría quitina naciente sintetizada en ese momento y otro, que utilizaría quitina pre-sintetizada, posiblemente en las cicatrices. De hecho, este segundo mecanismo funciona incluso en un sistema *in vitro* en presencia de paredes celulares en lugar de células permeabilizadas.

2.2.DETERMINACIÓN DE LAS PROPIEDADES BIOQUÍMICAS DE LA REACCIÓN DE TRANSGLICOSILACIÓN *IN VITRO*

A pesar del gran avance hacia un sistema de ensayo *in vitro*, demostrando que los oligosacáridos marcados funcionan como aceptores en lugar del glucano *in vivo*,

carecíamos hasta entonces de un sistema puro *in vitro* para chequear la veracidad de la hipótesis de partida: las proteínas Crh realizan el ensamblaje de los componentes mediante transglicosilación, es decir sin necesidad de una fuente de energía externa. Por ello, el desarrollo de un donador soluble en agua, la mejora de la capacidad funcional de los aceptores y el establecimiento de las condiciones adecuadas para el ensayo, fueron cruciales para la detección de la actividad transglicosilasa de Crh1 y Crh2 *in vitro*. Los resultados obtenidos muestran que las proteínas heterólogas Crh1 y Crh2, expresadas en *P. pastoris*, realizan la unión de la quitina a los diferentes aceptores mediante una reacción de transglicosilación, ya que estas proteínas en presencia del donador y aceptor sin una fuente de energía externa forman un producto estable.

En cuanto a la naturaleza de la molécula donadora, ambas proteínas mostraron preferencia por derivados solubles de la quitina procedentes de CM-quitina, glicol-quitina y N-acetil-quito-oligosacáridos. En contraste con la homogeneidad del donador, ambas proteínas son capaces de usar β-1,3 gluco-oligosacáridos, β-1,6 gluco-oligosacáridos y quito-oligosacáridos como aceptores. Mientras, el hecho de que los glucanos actuaran como aceptores de la reacción era esperable en función de los resultados que mostraban la ausencia de quitina unida al β-1,6 glucano y β-1,3 glucano en un mutante *crh1*Δ *crh2*Δ, el hallazgo de que los quito-oligosacáridos actuaban como aceptores, tanto en el ensayo *in vivo* como *in vitro*, se reveló sorprendente, no solo por la elevada plasticidad que requería el sitio aceptor, sino por su preferencia frente a los β-1,3 gluco-oligosacáridos y los β-1,6 gluco-oligosacáridos como muestran los parámetros cinéticos de las reacciones enzimáticas catalizadas por ambas proteínas. Así, los quito-oligosacáridos junto a los β-1,3 gluco-oligosacáridos son incorporados o catalizados de manera preferente frente a los β-1,6 gluco-oligosacáridos. Las actividades transglicosilasas quitina-β-1,3 glucano y quitina-β-1,6 glucano detectadas *in vitro* y en los ensayos de incorporación de los oligosacáridos marcados en células *in vivo*, estarían de acuerdo con el modelo previamente propuesto de heterotransglicosilación en base a nuestros resultados de fraccionamiento de paredes celulares y determinación de las diferentes fracciones de quitina en los mutantes de los genes *CRH*. Tanto los datos *in vitro* como la incorporación de los oligosacáridos *in vivo*, apuntan a una posible participación adicional de las proteínas Crh como homotransglicosilasas en la formación de enlaces quitina-quitina, si bien hasta la fecha no se ha demostrado la existencia de esta actividad *in vivo*. Esta enorme promiscuidad respecto a la naturaleza del aceptor es inusual en enzimas de unión a carbohidratos. Sin

embargo, se han descrito comportamientos similares en otras enzimas pertenecientes a la misma familia de transglicosilasas (GH16) que las proteínas Crh. Así, la xyloglucan endotransglicosilasa HvXET5, cataliza la unión de diferentes donadores como T-xiloglucano, hidroxi-etil celulosa y (1,3/1,4)-β-D-glucanos con un amplio rango de aceptores como oligoxiloglucósidos y celodextrinas con diferentes eficiencias (Hrmova et al., 2007).

El sitio donador del centro activo de Crh1 y Crh2 debe, por tanto, acomodar quitina con bastante especificidad, lo que sugiere que el grupo acetamido en C2 de la N-acetil-glucosamina es crítico para su interacción con este sitio. Por el contario, el sitio aceptor debe tener una amplia plasticidad. Aunque no será posible explicar de forma fehaciente el amplio rango de especificidad del sitio aceptor hasta que no contemos con la resolución de la estructura tridimensional de estas proteínas conjugadas a diferentes polisacáridos, podríamos hacer cierta especulación sobre la base de una comparación química y estructural de los diferentes aceptores. Así, una estructura común a todos ellos es la presencia de una hexopiranosa no sustituida y unida por enlaces β en el extremo no reducido del oligosacárido, dado que los xilo-gluco-oligosacáridos y los α-(1,4) maltooligosacáridos no funcionan como aceptores de la reacción. El hecho de que los quito-oligosacáridos sean los aceptores incorporados con mayor eficiencia, confirma que el grupo acetamido en C2 en estos sustratos potencia la unión no solo del donador sino también del aceptor.

2.3.ESTUDIOS ESTRUCTURA-FUNCIÓN DE LAS PROTEÍNAS Crh

En ausencia de estudios estructurales y con la ayuda de la estructura tridimensional resuelta de varias β-1,3-1,4 glucanasas de *Bacillus* libres o en complejo junto a oligosacáridos (Gaiser et al., 2006; Hahn et al., 1995), hemos inferido un modelo para la estructura de Crh1 (capítulo 4). Los resultados procedentes de mutaciones dirigidas sobre aminoácidos presentes en el centro catalítico de Crh1 y Crh2 han permitido validar el modelo propuesto, que junto con los datos procedentes de los estudios *in vivo* e *in vitro* nos han permitido proponer un posible mecanismo catalítico para Crh1 y Crh2. Este mecanismo incluiría la ruptura de enlaces β-1,4 de la molécula de quitina y la trasferencia

posterior del fragmento procedente del sustrato original a través del nuevo extremo reductor generado al extremo no reductor del aceptor, que podría ser quitina, β-1,3 glucano o β-1,6 glucano. Teniendo en cuenta que estas enzimas conservan totalmente el dominio catalítico de las enzimas de la familia GH16, es muy probable que lleven a cabo la clásica reacción de sustitución nucleófila S_{N_2} típica de otras hidrolasas de esta familia (Sinnott, 1990) como las liquenasas (Planas, 2000) o las xiloglucan xiloglucosil transferasas (Vaaje-Kolstad et al., 2010). Estas glicosilhidrolasas actúan a través de un mecanismo de doble desplazamiento que da lugar a la retención de la configuración del carbono anomérico del azúcar que sufre la catálisis (figura 10). En un primer paso (glicosilación) el grupo carboxilo del aminoácido que actúa como nucleófilo desplaza el aglicón asistido por la transferencia simultánea de un protón desde el grupo carboxilo del residuo ácido/base, con la consiguiente formación de un intermediario glicosil-enzima. En un segundo paso (desglicosilación), el residuo ácido/base activa al nucleófilo entrante (una molécula de agua en el caso de hidrólisis o un grupo alcohol en el caso de una transglicosilación), dando lugar a la hidrólisis del glicosil-enzima (figura 10).

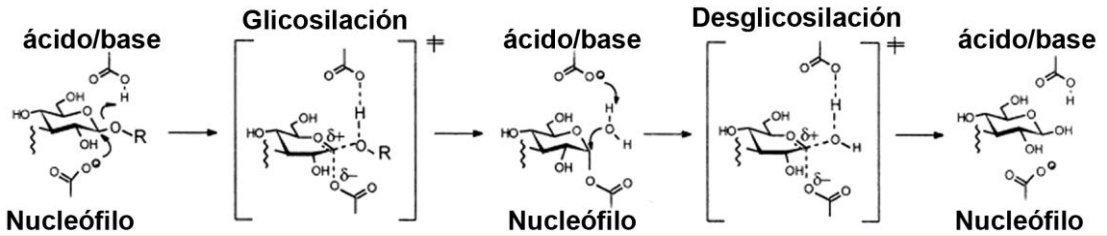

Figura 10. Mecanismo catalítico de las glicosidasas. Imagen adaptada de Planas A. (2000). En la imagen se muestra el mecanismo clásico de doble sustitución nucleófila S_{N_2}, en el cual el nucleófilo atacante reemplaza a un sustituyente (grupo saliente) mediante un primer paso de glicosilación sobre un átomo saturado del sustrato donador. A continuación, ocurre una segunda sustitución nucleófila realizada por el nucleófilo entrante mediante una reacción de desglicosilación.

De acuerdo con el mecanismo catalítico de la familia 16 glicosilhidrolasas se distinguen dos residuos ácidos que actúan como nucleófilo atacante (E134 en Crh1 y E166 en Crh2) y ácido/base general (E138 en Crh1 y E170 en Crh2). Adicionalmente, existe un tercer aminoácido, ácido aspártico (D136 en Crh1 y D168 en Crh2), que forma puentes de hidrógeno con el nucleófilo y por tanto es importante para la catálisis (Johansson et al., 2004). Mutaciones puntuales en cada uno de los tres residuos de ambas proteínas reducen drásticamente la actividad transglicosilasa *in vivo* y son incapaces de revertir el fenotipo de sensibilidad al RC como lo hace la versión silvestre de la proteína. Estos datos están apoyando el mecanismo catalítico propuesto de modo que, durante el paso de glicosilación

el residuo E138 (Crh1) o E170 (Crh2) actuaría como nucleófilo atacante sobre el carbono anomérico del azúcar, en una reacción asistida por el residuo ácido E134 (Crh1) o E166 (Crh2). En el paso de desglicosilación, esta vez el residuo E134 (Crh1) o E166 (Crh2) funcionaría como base general activando al nucleófilo entrante que hidroliza el intermediario glicosil-enzima. Con respecto al papel del Asp136 de Crh1 y Asp138 de Crh2 en la actividad catalítica, existen evidencias en cuanto a su papel como modulador del Pka del residuo ácido/base general garantizando su estabilidad (Planas, 2000), así como un posible papel en la unión del carbohidrato (Gaiser et al., 2006).

De acuerdo con este mecanismo, tanto Crh1 como Crh2 muestran cierta actividad quitinasa (capítulo4). Por otro lado, tanto la presencia de quito-oligosacáridos como de laminarioligosacáridos estimulan dicha actividad, lo que apoya el mecanismo de transglicosilación. En esta situación, estos oligosacáridos actuarían como aceptores de pequeño tamaño en la reacción acelerando el procesamiento de la molécula donadora (quitina). Situaciones similares han sido descritas para diversas transglicosilasas (Piens et al., 2008; Saladie et al., 2006). Sin embargo, cabe destacar que la estimulación de la actividad quitinolítica se produce en presencia de Crh1 pero no de Crh2. Las endoquitinasas cortan cadenas de quitina aleatoriamente generando multímeros de NAG de diferentes tamaños, mientras que las exoquitinasas hidrolizan quitina por el extremo no reductor liberando monómeros (N-acetil-β-D-glucosaminidasas) o dímeros (quito-biosidasas) de NAG. Tanto Crh1 como Crh2 son capaces de degradar el sustrato 4-MU-N-acetyl-β-D-N,N´,N´´-tri-acetil-quitotriosa (MU-NAG_3) específico para endoquitinasas, más eficientemente que el 4-MU-N-acetyl-β-D-N,N´-di-acetil-quitobiosidosa (MU-NAG_2) (sustrato para actividad quitobiosidasa). Sin embargo, lo hacen con distinta eficiencia. Estos resultados sugieren que para Crh1 el mecanismo de endo-transglicosilación prevalece, mientras que en el caso de Crh2, esta enzima posee también una sustancial actividad exoquitinasa.

Las similitudes y las diferencias en cuanto a la capacidad endoquitinasa de cada proteína sugieren diferencias en sus mecanismos de acción. La disponibilidad de realizar la reacción de transglicosilación con un rango abierto para el tamaño del donador permite probablemente a la célula responder de una manera más eficiente frente a las necesidades del entorno. De este modo, Crh2 como proteína con un papel prioritario *in vivo* frente a Crh1 en la transglicosilación, llevaría a cabo perfectamente la reacción de

transglicosilación de pequeñas unidades de quitina naciente (una, dos o tres moléculas de NAG) al glucano, mientras que Crh1 transglicosilaría cadenas de quitina de mayor tamaño. Esto tendría un sentido funcional dado que Crh1 se induce en condiciones de estrés y en estas condiciones se produce un incremento en la síntesis de quitina. Esta dualidad de comportamientos de cada proteína en diferentes situaciones sería compatible, con el hecho de que ambas proteínas son redundantes, de modo que la ausencia de una en parte se compensa por la presencia de la otra. De ahí que en ausencia de Crh2, Crh1 pudiera seguir realizando la transglicosilación entre el glucano y la quitina.

Adicionalmente, estudiamos el papel de otros residuos aromáticos inferidos del modelo tridimensional de Crh1, en cuanto a su participación en la unión del carbohidrato al centro activo (capítulo 4). La participación de los residuos aromáticos en la formación de fuerzas de Van der Waals entre la proteína y los sustratos ha sido previamente demostrado (Johansson et al., 2004). Así, mutaciones en los residuos Tyr103 y Met105, que estarían localizados en una de las dos láminas β antiparalelas del centro activo, pero orientados hacia el exterior del surco de unión al carbohidrato, no afectan a la actividad transglicosilasa *in vivo* de la proteína. Sin embargo, las mutaciones en los residuos Phe152, Tyr160 y Trp219 generan una drástica disminución de la actividad transglicosilasa *in vivo*. Los residuos Phe152 y Tyr160 quedarían orientados hacia sitio aceptor, sugiriendo un posible papel en la unión al aceptor, mientras que el anillo aromático del aminoácido Trp218 queda orientado hacia el sitio donador. Estudios cristalográficos de la β-D-1,3-1,4 glucanasa de *Bacillus* en complejo con tetrasacáridos muestran que en el surco de unión al carbohidrato existen aminoácidos aromáticos que están promoviendo la unión y el posicionamiento del azúcar en el centro activo (Gaiser et al., 2006). Interesantemente, el anillo aromático del aa Trp184 que equivale al Trp219 de Crh1 está formando un puente de hidrógeno con el azúcar del tretasacárido (Gaiser et al., 2006).

Como se ha comentado anteriormente, Crh1 y Crh2 son proteínas redundantes en cuanto al entrecruzamiento entre la quitina y el glucano de la pared celular. A pesar de la función redundante, Crh2 es más importante *in vivo* que Crh1. Esto se podría explicar en base a las diferencias de expresión durante el ciclo celular (Rodriguez-Pena et al., 2000) o mediante sus diferencias de procesar la quitina *in vitro*. Adicionalmente, Crh2 presenta un dominio de unión a carbohidratos (CBM) no incluido en la secuencia de Crh1, por lo que era interesante el estudio funcional de este dominio en relación a la actividad

transglicosilasa de las proteínas Crh (capítulo 4). Los resultados obtenidos mediante estudios de mutaciones dirigidas de residuos conservados en el dominio CBM de Crh2 que están conservados en sus ortólogos en hongos, plantas y bacterias muestran que las cisteínas de las posiciones 33, 39 y 40 son fundamentales para el plegamiento y estabilidad de la proteína Crh2. Adicionalmente, mutaciones en los residuos aromáticos Tyr43, Tyr51, Phe62 y en menor medida Tyr60 reducen la actividad transglicosilasa *in vivo* de Crh2. Estos datos están en concordancia con la función de los aa aromáticos del CBM en la unión del carbohidrato al centro activo (Boraston et al., 2004). Además, mutaciones en las posiciones conservadas dentro del dominio CBM, Pro38, Ser41, Gly44, Gly47 y particularmente Gly49 afectan a la actividad catalítica de la proteína, apoyando la importancia del dominio en la actividad transglicosilasa de Crh2. La resolución de la estructura tridimensional de la heveina, sola y en complejo con los ligandos, ha ayudado a esclarecer el papel de los aminoácidos del CBM en la reacción catalítica (Hernandez-Gay et al., 2010; Reyes-Lopez et al., 2004). Así, los aa Trp21 y Tyr30 de la heveina, que corresponden con los aa Tyr43 y Tyr51 de Crh2, están formando interacciones de tipo Van der Waals con el aceptor (quito-oligosacáridos). El grupo hidroxilo de la Ser19 y Tyr30 de la heveina están implicados en la formación de puentes de hidrógeno con los residuos NAG. Estos dos residuos corresponden con los aa Ser41 y Tyr51 de Crh2, cuya mutación hemos observado reduce la capacidad transglicosilasa *in vivo* de Crh2. Aunque solamente la cristalización y caracterización de la estructura de las proteínas Crh descubrirá exactamente los residuos que están interaccionando con el aceptor y el donador dentro del centro catalítico, este estudio funcional de la estructura de las proteínas Crh ha esclarecido algunos detalles sobre las posibles interacciones entre los aminoácidos del centro catalítico de las proteínas Crh y los carbohidratos.

3. IMPLICACIÓN DEL ENLACE QUITINA-GLUCANO EN LA REGULACIÓN DE LA MORFOGÉNESIS

La pared celular ha sido usada durante muchos años como modelo para la morfogénesis. La pared celular de la levadura se ve sometida a un continuo proceso de síntesis y remodelación para acompañar a su crecimiento, sin embargo existe una estructura especializada que no cambia de tamaño a lo largo del ciclo celular, el cuello entre la célula madre y la hija, donde se formará el septo de división. Durante el proceso de

división celular, el diámetro del cuello debe permanecer constante para evitar defectos morfológicos, existiendo una estricta regulación durante todo el proceso de gemación. Inicialmente, se observó que los defectos en la división celular que presenta el alelo mutante *cdc42*^{V44A} dependen de la existencia de un evento previo a la transición G2/M que era el responsable de la activación del *checkpoint* morfogenético G2/M. Así, se determinó que la organización y el correcto ensamblaje del anillo de septinas dependían de Cdc42 y Cla4 y ambos sucesos eran necesarios para el progreso del *checkpoint* morfogenético G2/M (Richman et al., 1999). Estudios posteriores mostraron que la deslocalización del anillo de septinas no era suficiente para explicar los defectos en el grosor del cuello y en citoquinesis que presenta el doble mutante *ste20*Δ *cla4*Δ, sugiriendo que debía existir otro mecanismo alternativo implicado en el control del ensanchamiento del cuello (Holly and Blumer, 1999). Finalmente, nuevos estudios dilucidaron que cuando la organización de anillo de septinas está comprometida, es el anillo de quitina depositado en la base de la yema durante la emergencia de la misma, el encargado de mantener el tamaño del cuello constante y permitir el avance en la citoquinesis (Schmidt et al., 2003). Estos resultados sugerían que el anillo de quitina y el anillo de septinas jugaban un papel redundante en la prevención del crecimiento del cuello. De modo que un fallo simultáneo en ambas estructura conllevaría la lisis celular. Respecto al anillo de septinas, éste podría estar actuando a través de su conocida función como barrera (Barral et al., 2000; Caudron and Barral, 2009), permitiendo el acceso de las proteínas requeridas para la síntesis de la membrana y la pared celular a la membrana plasmática en el cuello, así como restringiendo el acceso de las proteínas necesarias para la remodelación de la pared celular en el área del cuello.

¿Cómo participa el anillo de quitina en la prevención del crecimiento del cuello? Aunque la existencia del anillo de quitina se conoce desde 1973 (Hayashibe, 1973), existen pocas evidencias acerca de su función. Al ser una estructura rica en quitina, una posible función podría ser meramente mecánica aportando rigidez al cuello. Sin embargo, células *chs3*Δ, que no poseen anillo de quitina, no muestran engrosamiento del cuello y pueden vivir bajo condiciones de laboratorio normales. Sobre la base del conocimiento actual de la estructura y la síntesis de la pared celular, parecía razonable pensar que en el cuello, donde existe una gran concentración de quitina, este polisacárido podría ocupar la mayoría de los extremos no reducidos del β-1,3 glucano al que está normalmente unido y por tanto competir con el β-1,6 glucano que se une a los mismos sitios (figura 11). Esto impediría la

unión posterior de las manoproteínas, incluidas aquellas que están implicadas en la biogénesis de la pared celular y por tanto interferiría con la remodelación de esta estructura, lo que impediría la expansión de la pared celular en el cuello (figura 11). A su vez, la prevención de la remodelación del β-1,3 glucano y su crecimiento también serían necesarios para evitar el crecimiento de la pared celular. La unión de la quitina al β-1,3 glucano debería obstaculizar su maduración. La veracidad de esta hipótesis conlleva el cumplimento de varias premisas:

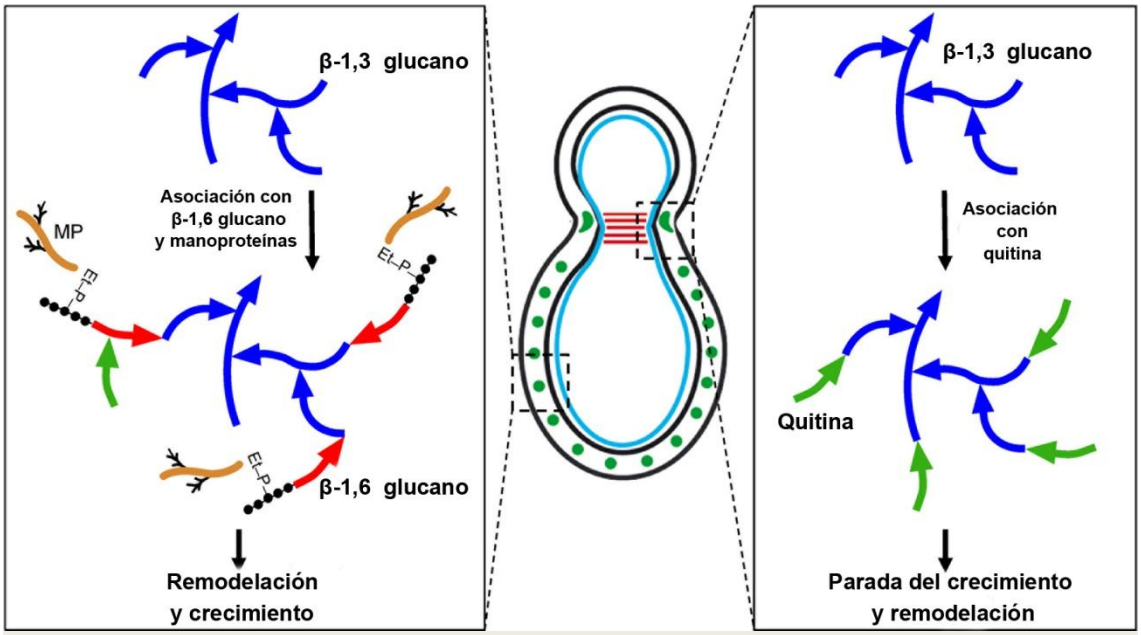

Figura 11. Modelo del control del crecimiento durante la morfogénesis. Imagen adaptada de Cabib and Arroyo (2013). Durante la gemación, existen dos zonas que presentan una estructura de la pared celular diferente. Mientras que en el cuello, la asociación covalente de la quitina al extremo no reducido del β-1,3 glucano, evita la remodelación del mismo y el crecimiento del cuello; en la pared lateral, donde la quitina no es tan abundante como en el cuello, el β-1,3 glucano se asocia tanto con la quitina como con el β-1,6 glucano y a su vez con las manoproteínas. De este modo la pared celular continúa expandiéndose y creciendo.

- La primera implicaría que la quitina unida al β-1,3 glucano preferentemente estuviera localizada en el cuello, mientras que la quitina unida al β-1,6 glucano se localizará dispersa por la pared lateral, como efectivamente se demostró en trabajos previos realizados por los doctores E. Cabib y A. Durán (Cabib and Duran, 2005).
- La segunda implicaría que la estructura del β-1,3 glucano presente en el cuello fuera diferente del resto de la pared celular.
- Por último, que el enlace entre la quitina y el glucano sea el responsable de mantener el grosor del cuello constante, de modo que la mera presencia de la

quitina y el glucano en el septo no sea suficiente para mantener el grosor de la zona, a no ser que exista una unión covalente entre ambos.

Trabajos realizados en esta tesis han permitido corroborar las dos últimas premisas. En primer lugar comprobamos la distribución de tamaño del β-1,3 glucano libre (no unido a quitina) con el del β-1,3 glucano unido a quitina, que está presente en el cuello (capítulo 5). A pesar de que el β-1,3 glucano es el componente estructural mayoritario de la pared celular, poco se ha estudiado su estructura a nivel bioquímico. La veracidad de la hipótesis de partida sugiere la existencia de dos poblaciones de β-1,3 glucano: una correspondiente a glucano maduro y otra correspondiente a glucano sin remodelar. El análisis de la red de β-1,3 glucano se consiguió gracias a la disponibilidad de β-1,6 glucanasa recombinante y la solubilización de las paredes celulares por carboximetilación. Las paredes celulares digeridas con β-1,6 glucanasa procedentes de células marcadas con ^{14}C-glucosa, en las cuales solo queda β-1,3 glucano y quitina, son sometidas a tratamientos suaves en álcali que permiten la obtención del glucano lo más parecido a su estado nativo en la pared celular. A continuación, las fracciones obtenidas (solubles e insolubles) se analizan por carboximetilación y fraccionamiento por cromatografía. Los resultados obtenidos muestran la existencia de dos poblaciones de glucano: una de alto peso molecular que eluye en el volumen muerto de la columna y corresponde con la fracción insoluble tras el tratamiento con hidróxido sódico y otro pico de aspecto polidisperso y de menor tamaño correspondiente con la fracción soluble a álcali. La alteración de los perfiles de elución por la presencia de quitina libre la descartamos debido a la pequeña cantidad existente en la pared celular y su pequeño tamaño. El gran tamaño de la primera población (>2x10^7 M.W.) encaja con el tamaño que adquiere la asociación de varias cadena de β-1,3 glucano mediante enlaces β-1,6 (Manners et al., 1973a). A su vez, la asociación de varias cadenas de β-1,3 glucano encajaría con la estructura observada mediante microscopía electrónica para la capa interna de la pared celular, de modo que esta capa está formada por una extensa red de β-1,3 glucano de aspecto fibrilar y comportamiento estático (Kopecka et al., 1974). El análisis de las paredes celulares de las cepas *gas1*Δ, *chs3*Δ y *crh1*Δ *crh2*Δ implicadas en la ramificación de las cadenas de β-1,3 glucano, síntesis de quitina y entrecruzamiento entre la quitina y el glucano, respectivamente mostraron variación de ambas poblaciones. Así, la cepa *gas1*Δ muestra un descenso en el tamaño de ambas fracciones con respecto a la cepa WT. Este resultado está en concordancia con el papel de elongación de las cadenas de β-1,3 glucano de la proteína Gas1. Sin embargo, en las cepas

*chs3*Δ y *crh1*Δ *crh2*Δ es la fracción polidispersa la única que se ve incrementada en cantidad y disminuida en tamaño con respecto a la cepa WT. Este resultado sugería que es la unión de la quitina al polisacárido más que su mera presencia en la pared celular la causa de esta diferencia con la cepa WT y que la fracción de alto peso molecular correspondería con glucano maduro, mientras que la segunda población de aspecto polidisperso y menor tamaño correspondería con glucano que será remodelado durante el crecimiento celular.

Con el objetivo de saber cuál de estas dos poblaciones estaba unida a la quitina, desarrollamos un esquema de fraccionamiento que permitiera diferenciar los componentes existentes en las fracciones: quitina libre, β-1,3 glucano libre y quitina unida covalentemente al β-1,3 glucano. Para ello introducimos un paso de absorción en una columna de WGA (*wheat germ agglutinin*) que une específicamente β-1,4-NAG. El análisis de las paredes celulares procedentes de la cepa WT y del mutante *crh1*Δ *crh2*Δ reveló que la quitina unida covalentemente al β-1,3 glucano eluía en la fracción de alto peso molecular al igual que lo hace el β-1,3 glucano maduro que constituye la red interna. Un resultado novedoso fue el hallazgo por primera vez de glucano unido a quitina no covalentemente en las paredes de la cepa *crh1*Δ *crh2*Δ. Este complejo no covalente entre ambos componentes no está presente en la cepa silvestre. Los resultados revelan que en una cepa WT aproximadamente un 7% del total del β-1,3 glucano está unido covalentemente a la quitina, hecho esperable ya que la superficie del cuello representa un pequeño porcentaje con respecto al total de la pared celular. La mayor parte de este porcentaje corresponde con glucano de alto peso molecular, en consonancia con la hipótesis que la unión de la quitina al glucano evitaría su remodelación.

La tercera premisa a cumplir en nuestra hipótesis es que la quitina libre, no unida al glucano covalentemente, como la presente en las paredes celulares del mutante *crh1*Δ *crh2*Δ no sería suficiente para evitar el crecimiento en el cuello cuando las septinas están desorganizadas. Esta tercera premisa implica un estudio a nivel molecular de los mecanismos de control de la morfogénesis. Para verificar la tercera premisa necesitábamos una cepa en la que la síntesis de quitina no estuviera alterada, el anillo de septinas se encontrara defectuoso y no existiera ningún enlace entre la quitina y el glucano. Estas tres condiciones se encuentran presentes en la cepa *crh1*Δ *crh2*Δ *cla4*Δ (capítulo 6). Al analizar las características morfológicas de esta cepa, observamos los mismos defectos morfológicos que la cepa *chs3*Δ *cla4*Δ: cuellos anchos, yemas alargadas, septos anormales

y lisis celular; si bien el tamaño del cuello y los niveles de quitina son superiores en el triple mutante. El engrosamiento del cuello permanece a pesar de la deleción de la quinasa responsable del *checkpoint* morfogenético Swe1, no así el tamaño de la yema que se ve reducido. De modo que parece que el aumento del tamaño del cuello es un defecto morfológico específico de la ausencia de unión entre los componentes en dicha zona, mientras que el tamaño de la yema es una consecuencia secundaria asociada a la activación del *checkpoint* morfogenético. Por lo tanto, estos datos sugieren que el enlace entre la quitina y el glucano es el responsable del engrosamiento del cuello. Adicionalmente, se analizó el efecto osmótico protector del sorbitol en la morfología de las diferentes cepas. Al medir el diámetro del cuello tras el tratamiento con sorbitol observamos que se produce un descenso en todas las cepas, incluidas la cepa WT, mientras que los ratios entre los diferentes mutantes continúan invariables. Este resultado descarta que el anillo de quitina medie un mecanismo meramente mecánico de reforzamiento del cuello, ya que si el ensanchamiento del cuello fuera debido a la debilidad de la pared celular, el sorbitol remediaría este fenotipo y esto no ocurre. Finalmente, con el objetivo de verificar que la inhibición de las proteínas Crh tenía un efecto similar a la deleción de sus genes, se usaron pequeños quito-oligosacáridos, que como ya habíamos visto anteriormente inhiben la incorporación de los gluco-oligosacáridos a la célula *in vivo*, presumiblemente mediante la interferencia con la actividad de Crh1 y Crh2. El uso de tri-acetil-quitotriosa permitió revalidar los resultados anteriormente descritos. El conjunto de todos los resultados permite concluir que, dado que los defectos morfológicos de la pérdida del control del crecimiento en el cuello se observan tanto en mutantes *cla4*Δ carentes del anillo de quitina, como en mutantes *cla4*Δ que poseen el anillo de quitina pero han perdido los enlaces entre la quitina y el β-1,3 glucano, es el enlace entre la quitina y el β-1,3 glucano en el cuello necesario para el control de la morfogénesis en el cuello durante la división celular.

Como ya se ha comentado, el anillo de quitina y el anillo de septinas tienen una función solapante en el control del crecimiento del cuello. Por ello, una cuestión importante que cabe preguntarse es el ¿Por qué de dos programas solapados? Uno basado en el anillo de quitina y otro en el anillo de septinas, para el control del crecimiento en el cuello. Una respuesta puede ser la importancia de conservar esta zona ya que es el futuro sitio de septación y citoquinesis, de manera que se garantice una reproducción fiel y consecutiva en el tiempo. Así, este doble mecanismo de protección le conferiría una ventaja evolutiva con respecto a las demás especies. Es importante destacar que en *S.*

cerevisiae a diferencia de otros hongos, el proceso de reproducción completo ocurre siempre en el mismo sitio, por ello es lógico que exista un control exhaustivo, ya que como hemos visto el fallo de los dos mecanismos puede tener consecuencias desastrosas para la supervivencia celular. Aunque los dos anillos, el de quitina y el de septinas, actuarían aparentemente mediante mecanismos diferentes, existen evidencias claras de la interacción funcional entre ambos. Existe una coordinación entre la localización del anillo de septinas y la formación del anillo de quitina mediante las proteínas Bni4 y Chs4. Así, Bni4 se acumula en el sitio de emergencia antes de la formación de la yema y se une directamente al anillo de septinas. A su vez, Chs4 se moviliza al sitio de gemación justo antes de la formación de la yema y requiere a Bni4 para acumularse en el cuello en fases tempranas del ciclo. La localización de Chs4 condiciona la localización de Chs3. De este modo, Chs3 responsable de la síntesis del anillo de quitina, estaría interaccionando indirectamente con las septinas mediante su unión con Chs4 y Bni4 (DeMarini et al., 1997; Kozubowski et al., 2003; Ono et al., 2000). Como mecanismo adicional de comunicación estaría el complejo Bni4-Glc7, que además su participación en la organización de las septinas, es necesario para el depósito de quitina en las etapas tempranas del ciclo (Kozubowski et al., 2003). Adicionalmente a la función del anillo de septinas en el cuello actuando como andamio, así como barrera física para prevenir la difusión de proteínas de membrana entre la célula madre y la hija durante el crecimiento y la división celular, se ha sugerido que las septinas podían actuar también como "corrales" en los que se secuestrarían a nivel de cuello proteínas requeridas para la citoquinesis y la septación (Dobbelaere and Barral, 2004; Oh and Bi, 2011). Datos recientes de la estructura tridimensional de la red de filamentos de actina obtenidos mediante tomografía muestran una organización ortogonal de filamentos en disposición axial y circunferencial (Bertin et al., 2012) que estaría de acuerdo con esta función. Se podría especular sobre un mecanismo por el cual las levaduras, mediante la acción de las septinas, restringiría el acceso de proteínas implicadas en la remodelación de la pared celular, como las proteínas Crh, al área del cuello para crear aquellos enlaces químicos, como los enlaces quitina-glucano, necesarios para controlar la morfogénesis de esta estructura. A su vez, el anillo de quitina participaría en la prevención del engrosamiento del cuello a dos niveles: (I) la localización de Chs3 en el cuello depende de su interacción con Chs4, Bni4 y con el anillo de septinas. Al existir un anillo de septinas defectuoso, se produciría una incorrecta localización de Chs3 que conlleva a que el anillo de quitina en la base de la yema no se deposite correctamente y el grosor del cuello no quede regulado; (II) el anillo de quitina colaboraría con el collar de septinas en su papel de

barrera física, limitando el movimiento libre de las proteínas por la membrana desde la célula madre a la célula hija.

En resumen, la morfología del mutante triple *cla4*Δ *crh1*Δ *crh2*Δ, junto con la localización de los enlaces quitina-β-1,3 glucano y quitina-β-1,6 glucano en la pared celular y los datos de caracterización del tamaño del β-1,3 glucano libre y unido a la quitina, soportan la idea de que en el cuello, la unión de la quitina al glucano bloquea el metabolismo de este último y por tanto el crecimiento de la pared celular en esta localización (figura 11). En la pared lateral, las manoproteínas unidas al β-1,6 glucano, incluidas aquellas necesarias para la biogénesis de la pared celular, permitirían la remodelación de la pared celular y el crecimiento. Sin embargo, la quitina unida al β-1,3 glucano en el cuello, competiría con la unión del β-1,6 glucano y por tanto de las manoproteínas. De esta forma se bloquearía la remodelación de la pared celular y el crecimiento en el cuello (figura 11).

CONCLUSIONES

1) Las proteínas Crh1 y Crh2 son responsables de la formación de los enlaces quitina-glucano de la pared celular de *Saccharomyces cerevisiae*. Las dos proteínas son funcionalmente redundantes, si bien la actividad de Crh2 tiene un papel más relevante en la formación de estos enlaces.

2) En situaciones de estrés, por aumento de temperatura, se produce un aumento de la fracción de quitina unida al β-1,6 glucano, que depende tanto de Crh1como de Crh2. En estas condiciones se induce la expresión de Crh1 y se produce una redistribución de ambas proteínas en la pared lateral.

3) La deleción simultanea de *CRH1* y *CRH2* agrava de forma importante los fenotipos de los mutantes *fks1*Δ y *gas1*Δ, indicando un papel esencial del enlace quitina-glucano para la supervivencia celular en situaciones en las que la integridad de la pared celular está comprometida.

4) Utilizando oligosacáridos fluorescentes derivados de β-1,3 glucano como aceptores, se han desarrollado diversos sistemas de transglicosilación en células vivas, células permeabilizadas y paredes celulares aisladas. En todos los casos se produce la formación de los enlaces quitina-glucano mediante la transglicosilación de la molécula donadora (quitina naciente o pre-existente) al aceptor (β-1,3 glucano o β-1,6 glucano) de forma Crh dependiente.

5) Se ha desarrollado un sistema soluble *in vitro* de transglicosilación quitina-glucano, utilizando proteínas Crh1 y Crh2 recombinantes. Ambas proteínas desarrollan reacciones de transglicosilación utilizando derivados de quitina como donadores y β-1,3 gluco-oligosacáridos, β-1,6 gluco-oligosacáridos y quito-oligosacáridos como aceptores. Esta reacción es inhibida de manera competitiva en presencia de N-acetil-quitotriosa.

6) Los datos de la actividad transglicosilasa *in vitro* se correlacionan perfectamente con la incorporación de los diversos oligosacáridos marcados con sulforodamina *in vivo*. Estos experimentos *in vivo* han permitido confirmar la redundancia funcional de Crh1 y Crh2 y la mayor relevancia de Crh2 respecto a la incorporación de los diferentes aceptores a la pared celular.

7) Se ha generado y validado mediante mutagénesis dirigida y ensayos de actividad transglicosilasa *in vivo* un modelo estructural de Crh1, basado en la estructura tridimensional conocida de una β-D-1,3-1,4 glucanasa de *Bacillus macerans*. Los residuos Glu134 (ácido/base), Asp136 y Glu138 (nucleófilo) del teórico centro activo de Crh1 y sus homólogos en Crh2, son esenciales para la catálisis. Otros residuos, probablemente implicados en la unión de azúcares, como W219, F152 y Y160 también son importantes para la actividad transglicosilasa de Crh1.

8) Crh2 presenta un dominio de unión a carbohidratos (CBM) de la familia 18. Mutaciones en los residuos P38, S41, Y43, G44, G47, Y51, F62 y especialmente G49 de este dominio disminuyen considerablemente la actividad transglicosilasa de Crh2. Además los residuos C33, C39 y C40 de este dominio son esenciales para la estabilidad de la proteína.

9) Proponemos un modelo de catálisis para Crh1 y Crh2 que incluiría un mecanismo de doble desplazamiento similar al de otras glicosilhidrolasas de la familia 16 (GH16) con la rotura de enlaces β-1,4 de la molécula de quitina y la trasferencia posterior del fragmento a través del nuevo extremo reductor generado al extremo no reductor del aceptor, β-1,3 glucano o β-1,6 glucano.

10) En el cuello entre la célula madre y la hija, la unión de la quitina al glucano bloquea el metabolismo de este último y por tanto el crecimiento de la pared celular en esta localización.

11) Los defectos morfológicos de pérdida de control del crecimiento en el cuello de las levaduras durante su división se observan tanto en mutantes *cla4*Δ *chs3*Δ, carentes de anillo de quitina, como en mutante *cla4*Δ *crh1*Δ *crh2*Δ, que poseen anillo de quitina pero han perdido los enlaces quitina-glucano. Por tanto, el enlace quitina-glucano es esencial para el control de la morfogénesis en el cuello.

BIBLIOGRAFÍA

Adamo, J.E., J.J. Moskow, A.S. Gladfelter, D. Viterbo, D.J. Lew, and P.J. Brennwald. 2001. Yeast Cdc42 functions at a late step in exocytosis, specifically during polarized growth of the emerging bud. *The Journal of cell biology*. 155:581-592.

Adams, A.E., D.I. Johnson, R.M. Longnecker, B.F. Sloat, and J.R. Pringle. 1990. CDC42 and CDC43, two additional genes involved in budding and the establishment of cell polarity in the yeast *Saccharomyces cerevisiae*. *The Journal of cell biology*. 111:131-142.

Adams, A.E., and J.R. Pringle. 1984. Relationship of actin and tubulin distribution to bud growth in wild-type and morphogenetic-mutant *Saccharomyces cerevisiae*. *The Journal of cell biology*. 98:934-945.

Aimanianda, V., C. Clavaud, C. Simenel, T. Fontaine, M. Delepierre, and J.P. Latge. 2009. Cell wall beta-(1,6)-glucan of *Saccharomyces cerevisiae*: structural characterization and in situ synthesis. *The Journal of biological chemistry*. 284:13401-13412.

Amberg, D.C. 1998. Three-dimensional imaging of the yeast actin cytoskeleton through the budding cell cycle. *Molecular biology of the cell*. 9:3259-3262.

Amberg, D.C., J.E. Zahner, J.W. Mulholland, J.R. Pringle, and D. Botstein. 1997. Aip3p/Bud6p, a yeast actin-interacting protein that is involved in morphogenesis and the selection of bipolar budding sites. *Molecular biology of the cell*. 8:729-753.

Appeltauer, U., and T. Achstetter. 1989. Hormone-induced expression of the *CHS1* gene from *Saccharomyces cerevisiae. European journal of biochemistry / FEBS*. 181:243-247.

Arroyo, J., M. Garcia-Gonzalez, M.I. Garcia-Saez, M. Sanchez, and C. Nombela. 1997. DNA sequence analysis of a 23,002 bp DNA fragment of the right arm of *Saccharomyces cerevisiae* chromosome VII. *Yeast (Chichester, England)*. 13:357-363.

Arroyo, J., J. Sarfati, M.T. Baixench, E. Ragni, M. Guillen, J.M. Rodriguez-Pena, L. Popolo, and J.P. Latge. 2007. The GPI-anchored Gas and Crh families are fungal antigens. *Yeast (Chichester, England)*. 24:289-296.

Bacon, J.S., V.C. Farmer, D. Jones, and I.F. Taylor. 1969. The glucan components of the cell wall of baker's yeast (*Saccharomyces cerevisiae*) considered in relation to its ultrastructure. *The Biochemical journal*. 114:557-567.

Baladron, V., S. Ufano, E. Duenas, A.B. Martin-Cuadrado, F. del Rey, and C.R. Vazquez de Aldana. 2002. Eng1p, an endo-1,3-beta-glucanase localized at the daughter side of the septum, is involved in cell separation in *Saccharomyces cerevisiae*. *Eukaryotic cell*. 1:774-786.

Balasubramanian, M.K., E. Bi, and M. Glotzer. 2004. Comparative analysis of cytokinesis in budding yeast, fission yeast and animal cells. *Curr Biol*. 14:R806-818.

Ballou, C. 1976. Structure and biosynthesis of the mannan component of the yeast cell envelope. *Adv Microb Physiol*. 14:93-158.

Ballou, C.E. 1990. Isolation, characterization, and properties of *Saccharomyces cerevisiae* mnn mutants with nonconditional protein glycosylation defects. *Methods in enzymology*. 185:440-470.

Barr, F.A., and U. Gruneberg. 2007. Cytokinesis: placing and making the final cut. *Cell*. 131:847-860.

Barral, Y., V. Mermall, M.S. Mooseker, and M. Snyder. 2000. Compartmentalization of the cell cortex by septins is required for maintenance of cell polarity in yeast. *Molecular cell*. 5:841-851.

Barral, Y., M. Parra, S. Bidlingmaier, and M. Snyder. 1999. Nim1-related kinases coordinate cell cycle progression with the organization of the peripheral cytoskeleton in yeast. *Genes & development*. 13:176-187.

Bartnicki-Garcia, S. 1968. Cell wall chemistry, morphogenesis, and taxonomy of fungi. *Annual review of microbiology*. 22:87-108.

Beauvais, A., M. Monod, J.P. Debeaupuis, M. Diaquin, H. Kobayashi, and J.P. Latge. 1997. Biochemical and antigenic characterization of a new dipeptidyl-peptidase isolated from *Aspergillus fumigatus*. *The Journal of biological chemistry*. 272:6238-6244.

Bender, A., and J.R. Pringle. 1991. Use of a screen for synthetic lethal and multicopy suppressee mutants to identify two new genes involved in morphogenesis in *Saccharomyces cerevisiae*. *Molecular and cellular biology*. 11:1295-1305.

Benton, B.K., A. Tinkelenberg, I. Gonzalez, and F.R. Cross. 1997. Cla4p, a *Saccharomyces cerevisiae* Cdc42p-activated kinase involved in cytokinesis, is activated at mitosis. *Molecular and cellular biology*. 17:5067-5076.

Benton, B.K., A.H. Tinkelenberg, D. Jean, S.D. Plump, and F.R. Cross. 1993. Genetic analysis of Cln/Cdc28 regulation of cell morphogenesis in budding yeast. *The EMBO journal*. 12:5267-5275.

Bertin, A., M.A. McMurray, J. Pierson, L. Thai, K.L. McDonald, E.A. Zehr, G. Garcia, 3rd, P. Peters, J. Thorner, and E. Nogales. 2012. Three-dimensional ultrastructure of the septin filament network in *Saccharomyces cerevisiae*. *Molecular biology of the cell*. 23:423-432.

Bertin, A., M.A. McMurray, L. Thai, G. Garcia, 3rd, V. Votin, P. Grob, T. Allyn, J. Thorner, and E. Nogales. 2010. Phosphatidylinositol-4,5-bisphosphate promotes budding yeast septin filament assembly and organization. *J Mol Biol*. 404:711-731.

Bi, E. 2001. Cytokinesis in budding yeast: the relationship between actomyosin ring function and septum formation. *Cell Struct Funct*. 26:529-537.

Bi, E., P. Maddox, D.J. Lew, E.D. Salmon, J.N. McMillan, E. Yeh, and J.R. Pringle. 1998. Involvement of an actomyosin contractile ring in *Saccharomyces cerevisiae* cytokinesis. *The Journal of cell biology*. 142:1301-1312.

Bi, E., and H.O. Park. 2012. Cell polarization and cytokinesis in budding yeast. *Genetics*. 191:347-387.

Bloecher, A., and K. Tatchell. 2000. Dynamic localization of protein phosphatase type 1 in the mitotic cell cycle of *Saccharomyces cerevisiae*. *The Journal of cell biology*. 149:125-140.

Boone, C., S.S. Sommer, A. Hensel, and H. Bussey. 1990. Yeast *KRE* genes provide evidence for a pathway of cell wall beta-glucan assembly. *The Journal of cell biology*. 110:1833-1843.

Boorsma, A., H. de Nobel, B. ter Riet, B. Bargmann, S. Brul, K.J. Hellingwerf, and F.M. Klis. 2004. Characterization of the transcriptional response to cell wall stress in *Saccharomyces cerevisiae*. *Yeast (Chichester, England)*. 21:413-427.

Boraston, A.B., D.N. Bolam, H.J. Gilbert, and G.J. Davies. 2004. Carbohydrate-binding modules: fine-tuning polysaccharide recognition. *The Biochemical journal*. 382:769-781.

Bowen, A.R., J.L. Chen-Wu, M. Momany, R. Young, P.J. Szaniszlo, and P.W. Robbins. 1992. Classification of fungal chitin synthases. *Proceedings of the National Academy of Sciences of the United States of America*. 89:519-523.

Boyce, K.J., and A. Andrianopoulos. 2011. Ste20-related kinases: effectors of signaling and morphogenesis in fungi. *Trends in microbiology*. 19:400-410.

Bretscher, A., B. Drees, E. Harsay, D. Schott, and T. Wang. 1994. What are the basic functions of microfilaments? Insights from studies in budding yeast. *The Journal of cell biology*. 126:821-825.

Brown, J.L., and H. Bussey. 1993. The yeast *KRE9* gene encodes an O glycoprotein involved in cell surface beta-glucan assembly. *Molecular and cellular biology*. 13:6346-6356.

Brown, J.L., Z. Kossaczka, B. Jiang, and H. Bussey. 1993. A mutational analysis of killer toxin resistance in *Saccharomyces cerevisiae* identifies new genes involved in cell wall (1-->6)-beta-glucan synthesis. *Genetics*. 133:837-849.

Bryan, B.A., G.S. Knapp, L.M. Bowen, and M. Polymenis. 2004. The UV response in *Saccharomyces cerevisiae* involves the mitogen-activated protein kinase Slt2p. *Curr Microbiol*. 49:32-34.

Buehrer, B.M., and B. Errede. 1997. Coordination of the mating and cell integrity mitogen-activated protein kinase pathways in *Saccharomyces cerevisiae*. *Molecular and cellular biology*. 17:6517-6525.

Bulawa, C.E. 1992. *CSD2*, *CSD3*, and *CSD4*, genes required for chitin synthesis in *Saccharomyces cerevisiae*: the *CSD2* gene product is related to chitin synthases and to developmentally regulated proteins in Rhizobium species and Xenopus laevis. *Molecular and cellular biology*. 12:1764-1776.

Bulawa, C.E. 1993. Genetics and molecular biology of chitin synthesis in fungi. *Annual review of microbiology*. 47:505-534.

Bulawa, C.E., and B.C. Osmond. 1990. Chitin synthase I and chitin synthase II are not required for chitin synthesis in vivo in *Saccharomyces cerevisiae*. *Proceedings of the National Academy of Sciences of the United States of America*. 87:7424-7428.

Bulawa, C.E., M. Slater, E. Cabib, J. Au-Young, A. Sburlati, W.L. Adair, Jr., and P.W. Robbins. 1986. The *S. cerevisiae* structural gene for chitin synthase is not required for chitin synthesis in vivo. *Cell*. 46:213-225.

Bulik, D.A., M. Olczak, H.A. Lucero, B.C. Osmond, P.W. Robbins, and C.A. Specht. 2003. Chitin synthesis in *Saccharomyces cerevisiae* in response to supplementation of growth medium with glucosamine and cell wall stress. *Eukaryotic cell*. 2:886-900.

Burda, P., and M. Aebi. 1999. The dolichol pathway of N-linked glycosylation. *Biochimica et biophysica acta*. 1426:239-257.

Cabib, E. 1987. The synthesis and degradation of chitin. *Advances in enzymology and related areas of molecular biology*. 59:59-101.

Cabib, E. 2000. On the zymogenic character of chitin synthase 3. *Microbiology (Reading, England)*. 146 (Pt 8):1760-1761.

Cabib, E. 2004. The septation apparatus, a chitin-requiring machine in budding yeast. *Archives of biochemistry and biophysics*. 426:201-207.

Cabib, E. 2009. Two novel techniques for determination of polysaccharide cross-links show that Crh1p and Crh2p attach chitin to both beta(1-6)- and beta(1-3)glucan in the *Saccharomyces cerevisiae* cell wall. *Eukaryotic cell*. 8:1626-1636.

Cabib, E., and B. Bowers. 1971. Chitin and yeast budding. Localization of chitin in yeast bud scars. *The Journal of biological chemistry*. 246:152-159.

Cabib, E., and B. Bowers. 1975. Timing and function of chitin synthesis in yeast. *Journal of bacteriology*. 124:1586-1593.

Cabib, E., B. Bowers, and R.L. Roberts. 1983. Vectorial synthesis of a polysaccharide by isolated plasma membranes. *Proceedings of the National Academy of Sciences of the United States of America*. 80:3318-3321.

Cabib, E., B. Bowers, A. Sburlati, and S.J. Silverman. 1988. Fungal cell wall synthesis: the construction of a biological structure. *Microbiological sciences*. 5:370-375.

Cabib, E., T. Drgon, J. Drgonova, R.A. Ford, and R. Kollar. 1997. The yeast cell wall, a dynamic structure engaged in growth and morphogenesis. *Biochemical Society transactions*. 25:200-204.

Cabib, E., J. Drgonova, and T. Drgon. 1998. Role of small G proteins in yeast cell polarization and wall biosynthesis. *Annual review of biochemistry*. 67:307-333.

Cabib, E., and A. Duran. 2005. Synthase III-dependent chitin is bound to different acceptors depending on location on the cell wall of budding yeast. *The Journal of biological chemistry*. 280:9170-9179.

Cabib, E., and V. Farkas. 1971. The control of morphogenesis: an enzymatic mechanism for the initiation of septum formation in yeast. *Proceedings of the National Academy of Sciences of the United States of America*. 68:2052-2056.

Cabib, E., and M.S. Kang. 1987. Fungal 1,3-beta-glucan synthase. *Methods in enzymology*. 138:637-642.

Cabib, E., M.S. Kang, and J. Au-Young. 1987. Chitin synthase from *Saccharomyces cerevisiae*. *Methods in enzymology*. 138:643-649.

Cabib, E., and F.A. Keller. 1971. Chitin and yeast budding. Allosteric inhibition of chitin synthetase by a heat-stable protein from yeast. *The Journal of biological chemistry*. 246:167-173.

Cabib, E., P.C. Mol, J.A. Shaw, and W.J. Choi. 1993. Biosynthesis of cell wall and septum during yeast growth. *Archives of medical research*. 24:301-303.

Cabib, E., R. Roberts, and B. Bowers. 1982. Synthesis of the yeast cell wall and its regulation. *Annual review of biochemistry*. 51:763-793.

Cabib, E., D.H. Roh, M. Schmidt, L.B. Crotti, and A. Varma. 2001. The yeast cell wall and septum as paradigms of cell growth and morphogenesis. *The Journal of biological chemistry*. 276:19679-19682.

Cabib, E., A. Sburlati, B. Bowers, and S.J. Silverman. 1989. Chitin synthase 1, an auxiliary enzyme for chitin synthesis in *Saccharomyces cerevisiae*. *The Journal of cell biology*. 108:1665-1672.

Cabib, E., and M. Schmidt. 2003. Chitin synthase III activity, but not the chitin ring, is required for remedial septa formation in budding yeast. *FEMS microbiology letters*. 224:299-305.

Cabib, E., S.J. Silverman, and J.A. Shaw. 1992. Chitinase and chitin synthase 1: counterbalancing activities in cell separation of *Saccharomyces cerevisiae*. *Journal of general microbiology*. 138:97-102.

Cabib, E., and R. Ulane. 1973. Chitin synthetase activating factor from yeast, a protease. *Biochemical and biophysical research communications*. 50:186-191.

Cabib, E., R. Ulane, and B. Bowers. 1973. Yeast chitin synthetase. Separation of the zymogen from its activating factor and recovery of the latter in the vacuole fraction. *The Journal of biological chemistry*. 248:1451-1458.

Campbell, P., and J. Braam. 1998. Co- and/or post-translational modifications are critical for *TCH4* XET activity. *Plant J*. 15:553-561.

Cappellaro, C., C. Baldermann, R. Rachel, and W. Tanner. 1994. Mating type-specific cell-cell recognition of *Saccharomyces cerevisiae*: cell wall attachment and active sites of a- and alpha-agglutinin. *The EMBO journal*. 13:4737-4744.

Cappellaro, C., V. Mrsa, and W. Tanner. 1998. New potential cell wall glucanases of *Saccharomyces cerevisiae* and their involvement in mating. *Journal of bacteriology*. 180:5030-5037.

Carlstrom, D. 1957. The crystal structure of alpha-chitin (poly-N-acetyl-D-glucosamine). *J Biophys Biochem Cytol*. 3:669-683.

Caro, L.H., H. Tettelin, J.H. Vossen, A.F. Ram, H. van den Ende, and F.M. Klis. 1997. In silicio identification of glycosyl-phosphatidylinositol-anchored plasma-membrane and cell wall proteins of *Saccharomyces cerevisiae*. *Yeast (Chichester, England)*. 13:1477-1489.

Carotti, C., L. Ferrario, C. Roncero, M.H. Valdivieso, A. Duran, and L. Popolo. 2002. Maintenance of cell integrity in the gas1 mutant of *Saccharomyces cerevisiae* requires the Chs3p-targeting and activation pathway and involves an unusual Chs3p localization. *Yeast (Chichester, England)*. 19:1113-1124.

Carotti, C., E. Ragni, O. Palomares, T. Fontaine, G. Tedeschi, R. Rodriguez, J.P. Latge, M. Vai, and L. Popolo. 2004. Characterization of recombinant forms of the yeast Gas1 protein and identification of residues essential for glucanosyltransferase activity and folding. *European journal of biochemistry / FEBS*. 271:3635-3645.

Casamayor, A., and M. Snyder. 2003. Molecular dissection of a yeast septin: distinct domains are required for septin interaction, localization, and function. *Molecular and cellular biology*. 23:2762-2777.

Catlett, N.L., and L.S. Weisman. 1998. The terminal tail region of a yeast myosin-V mediates its attachment to vacuole membranes and sites of polarized growth. *Proceedings of the National Academy of Sciences of the United States of America*. 95:14799-14804.

Caudron, F., and Y. Barral. 2009. Septins and the lateral compartmentalization of eukaryotic membranes. *Dev Cell*. 16:493-506.

Caviston, J.P., M. Longtine, J.R. Pringle, and E. Bi. 2003. The role of Cdc42p GTPase-activating proteins in assembly of the septin ring in yeast. *Molecular biology of the cell*. 14:4051-4066.

Cid, V.J., L. Adamikova, R. Cenamor, M. Molina, M. Sanchez, and C. Nombela. 1998a. Cell integrity and morphogenesis in a budding yeast septin mutant. *Microbiology (Reading, England)*. 144 (Pt 12):3463-3474.

Cid, V.J., L. Adamikova, M. Sanchez, M. Molina, and C. Nombela. 2001a. Cell cycle control of septin ring dynamics in the budding yeast. *Microbiology (Reading, England)*. 147:1437-1450.

Cid, V.J., R. Cenamor, M. Sanchez, and C. Nombela. 1998b. A mutation in the Rho1-GAP-encoding gene *BEM2* of *Saccharomyces cerevisiae* affects morphogenesis and cell wall functionality. *Microbiology (Reading, England)*. 144 (Pt 1):25-36.

Cid, V.J., A. Duran, F. del Rey, M.P. Snyder, C. Nombela, and M. Sanchez. 1995. Molecular basis of cell integrity and morphogenesis in *Saccharomyces cerevisiae*. *Microbiological reviews*. 59:345-386.

Cid, V.J., J. Jimenez, M. Molina, M. Sanchez, C. Nombela, and J.W. Thorner. 2002. Orchestrating the cell cycle in yeast: sequential localization of key mitotic regulators at the spindle pole and the bud neck. *Microbiology (Reading, England)*. 148:2647-2659.

Cid, V.J., M.J. Shulewitz, K.L. McDonald, and J. Thorner. 2001b. Dynamic localization of the Swe1 regulator Hsl7 during the *Saccharomyces cerevisiae* cell cycle. *Molecular biology of the cell*. 12:1645-1669.

Colman-Lerner, A., T.E. Chin, and R. Brent. 2001. Yeast Cbk1 and Mob2 activate daughter-specific genetic programs to induce asymmetric cell fates. *Cell*. 107:739-750.

Correa, J., C.R. Vazquez de Aldana, P. San Segundo, and F. del Rey. 1992. Genetic mapping of 1,3-beta-glucanase-encoding genes in *Saccharomyces cerevisiae*. *Current genetics*. 22:283-288.

Correa, J.U., N. Elango, I. Polacheck, and E. Cabib. 1982. Endochitinase, a mannan-associated enzyme from *Saccharomyces cerevisiae*. *The Journal of biological chemistry*. 257:1392-1397.

Cos, T., R.A. Ford, J.A. Trilla, A. Duran, E. Cabib, and C. Roncero. 1998. Molecular analysis of Chs3p participation in chitin synthase III activity. *European journal of biochemistry / FEBS*. 256:419-426.

Cvrckova, F., C. De Virgilio, E. Manser, J.R. Pringle, and K. Nasmyth. 1995. Ste20-like protein kinases are required for normal localization of cell growth and for cytokinesis in budding yeast. *Genes & development*. 9:1817-1830.

Cvrckova, F., and K. Nasmyth. 1993. Yeast G1 cyclins *CLN1* and *CLN2* and a GAP-like protein have a role in bud formation. *The EMBO journal*. 12:5277-5286.

Chant, J. 1996. Generation of cell polarity in yeast. *Current opinion in cell biology*. 8:557-565.

Chant, J. 1999. Cell polarity in yeast. *Annual review of cell and developmental biology*. 15:365-391.

Chant, J., K. Corrado, J.R. Pringle, and I. Herskowitz. 1991. Yeast *BUD5*, encoding a putative GDP-GTP exchange factor, is necessary for bud site selection and interacts with bud formation gene *BEM1*. *Cell*. 65:1213-1224.

Chant, J., and I. Herskowitz. 1991. Genetic control of bud site selection in yeast by a set of gene products that constitute a morphogenetic pathway. *Cell*. 65:1203-1212.

Chant, J., M. Mischke, E. Mitchell, I. Herskowitz, and J.R. Pringle. 1995. Role of Bud3p in producing the axial budding pattern of yeast. *The Journal of cell biology*. 129:767-778.

Chant, J., and J.R. Pringle. 1991. Budding and cell polarity in *Saccharomyces cerevisiae*. *Curr Opin Genet Dev*. 1:342-350.

Chant, J., and J.R. Pringle. 1995. Patterns of bud-site selection in the yeast *Saccharomyces cerevisiae*. *The Journal of cell biology*. 129:751-765.

Chant, J., and L. Stowers. 1995. GTPase cascades choreographing cellular behavior: movement, morphogenesis, and more. *Cell*. 81:1-4.

Chenevert, J., K. Corrado, A. Bender, J. Pringle, and I. Herskowitz. 1992. A yeast gene (*BEM1*) necessary for cell polarization whose product contains two SH3 domains. *Nature*. 356:77-79.

Choi, W.J., and E. Cabib. 1994. The use of divalent cations and pH for the determination of specific yeast chitin synthetases. *Analytical biochemistry*. 219:368-372.

Choi, W.J., B. Santos, A. Duran, and E. Cabib. 1994a. Are yeast chitin synthases regulated at the transcriptional or the posttranslational level? *Molecular and cellular biology*. 14:7685-7694.

Choi, W.J., A. Sburlati, and E. Cabib. 1994b. Chitin synthase 3 from yeast has zymogenic properties that depend on both the *CAL1* and the *CAL3* genes. *Proceedings of the National Academy of Sciences of the United States of America*. 91:4727-4730.

Chuang, J.S., and R.W. Schekman. 1996. Differential trafficking and timed localization of two chitin synthase proteins, Chs2p and Chs3p. *The Journal of cell biology*. 135:597-610.

Dallies, N., J. Francois, and V. Paquet. 1998. A new method for quantitative determination of polysaccharides in the yeast cell wall. Application to the cell wall defective mutants of *Saccharomyces cerevisiae*. *Yeast (Chichester, England)*. 14:1297-1306.

Davenport, K.R., M. Sohaskey, Y. Kamada, D.E. Levin, and M.C. Gustin. 1995. A second osmosensing signal transduction pathway in yeast. Hypotonic shock activates the *PKC1* protein kinase-regulated cell integrity pathway. *The Journal of biological chemistry*. 270:30157-30161.

Davis, C.R., T.J. Richman, S.B. Deliduka, J.O. Blaisdell, C.C. Collins, and D.I. Johnson. 1998. Analysis of the mechanisms of action of the *Saccharomyces cerevisiae* dominant lethal *cdc42G12V* and dominant negative *cdc42D118A* mutations. *The Journal of biological chemistry*. 273:849-858.

de Groot, P.W., A.D. de Boer, J. Cunningham, H.L. Dekker, L. de Jong, K.J. Hellingwerf, C. de Koster, and F.M. Klis. 2004. Proteomic analysis of *Candida albicans* cell walls reveals covalently bound carbohydrate-active enzymes and adhesins. *Eukaryotic cell*. 3:955-965.

De Groot, P.W., K.J. Hellingwerf, and F.M. Klis. 2003. Genome-wide identification of fungal GPI proteins. *Yeast (Chichester, England)*. 20:781-796.

De Groot, P.W., A.F. Ram, and F.M. Klis. 2005. Features and functions of covalently linked proteins in fungal cell walls. *Fungal Genet Biol*. 42:657-675.

de Nobel, H., C. Ruiz, H. Martin, W. Morris, S. Brul, M. Molina, and F.M. Klis. 2000. Cell wall perturbation in yeast results in dual phosphorylation of the Slt2/Mpk1 MAP kinase and in an Slt2-mediated increase in *FKS2*-lacZ expression, glucanase resistance and thermotolerance. *Microbiology (Reading, England)*. 146 (Pt 9):2121-2132.

de Nobel, J.G., F.M. Klis, J. Priem, T. Munnik, and H. van den Ende. 1990. The glucanase-soluble mannoproteins limit cell wall porosity in *Saccharomyces cerevisiae*. *Yeast (Chichester, England)*. 6:491-499.

DeMarini, D.J., A.E. Adams, H. Fares, C. De Virgilio, G. Valle, J.S. Chuang, and J.R. Pringle. 1997. A septin-based hierarchy of proteins required for localized deposition of chitin in the *Saccharomyces cerevisiae* cell wall. *The Journal of cell biology*. 139:75-93.

DeMay, B.S., R.A. Meseroll, P. Occhipinti, and A.S. Gladfelter. 2009. Regulation of distinct septin rings in a single cell by Elm1p and Gin4p kinases. *Molecular biology of the cell*. 20:2311-2326.

Dijkgraaf, G.J., M. Abe, Y. Ohya, and H. Bussey. 2002. Mutations in Fks1p affect the cell wall content of beta-1,3- and beta-1,6-glucan in Saccharomyces cerevisiae. *Yeast (Chichester, England)*. 19:671-690.

Dijkgraaf, G.J., J.L. Brown, and H. Bussey. 1996. The *KNH1* gene of *Saccharomyces cerevisiae* is a functional homolog of *KRE9*. *Yeast (Chichester, England)*. 12:683-692.

Dobbelaere, J., and Y. Barral. 2004. Spatial coordination of cytokinetic events by compartmentalization of the cell cortex. *Science (New York, N.Y.* 305:393-396.

Douglas, C.M. 2001. Fungal beta(1,3)-D-glucan synthesis. *Med Mycol*. 39 Suppl 1:55-66.

Douglas, C.M., F. Foor, J.A. Marrinan, N. Morin, J.B. Nielsen, A.M. Dahl, P. Mazur, W. Baginsky, W. Li, M. el-Sherbeini, and et al. 1994. The *Saccharomyces cerevisiae FKS1* (*ETG1*) gene encodes an integral membrane protein which is a subunit of 1,3-beta-D-glucan synthase. *Proceedings of the National Academy of Sciences of the United States of America*. 91:12907-12911.

Douglas, L.M., F.J. Alvarez, C. McCreary, and J.B. Konopka. 2005. Septin function in yeast model systems and pathogenic fungi. *Eukaryotic cell*. 4:1503-1512.

Drgonova, J., T. Drgon, K. Tanaka, R. Kollar, G.C. Chen, R.A. Ford, C.S. Chan, Y. Takai, and E. Cabib. 1996. Rho1p, a yeast protein at the interface between cell polarization and morphogenesis. *Science (New York, N.Y.* 272:277-279.

Duran, A., B. Bowers, and E. Cabib. 1975. Chitin synthetase zymogen is attached to the yeast plasma membrane. *Proceedings of the National Academy of Sciences of the United States of America*. 72:3952-3955.

Duran, A., and E. Cabib. 1978. Solubilization and partial purification of yeast chitin synthetase. Confirmation of the zymogenic nature of the enzyme. *The Journal of biological chemistry*. 253:4419-4425.

Duran, A., and C. Nombela. 2004. Fungal cell wall biogenesis: building a dynamic interface with the environment. *Microbiology (Reading, England)*. 150:3099-3103.

Eby, J.J., S.P. Holly, F. van Drogen, A.V. Grishin, M. Peter, D.G. Drubin, and K.J. Blumer. 1998. Actin cytoskeleton organization regulated by the PAK family of protein kinases. *Curr Biol*. 8:967-970.

Ecker, M., R. Deutzmann, L. Lehle, V. Mrsa, and W. Tanner. 2006. Pir proteins of *Saccharomyces cerevisiae* are attached to beta-1,3-glucan by a new protein-carbohydrate linkage. *The Journal of biological chemistry*. 281:11523-11529.

Elango, N., J.U. Correa, and E. Cabib. 1982. Secretory character of yeast chitinase. *The Journal of biological chemistry*. 257:1398-1400.

Elorza, M.V., A. Murgui, H. Rico, F. Miragall, and R. Sentandreu. 1987. Formation of a new cell wall by protoplasts of *Candida albicans*: effect of papulacandin B, tunicamycin and Nikkomycin. *Journal of general microbiology*. 133:2315-2325.

Elorza, M.V., H. Rico, and R. Sentandreu. 1983. Calcofluor white alters the assembly of chitin fibrils in *Saccharomyces cerevisiae* and *Candida albicans* cells. *Journal of general microbiology*. 129:1577-1582.

Evangelista, M., K. Blundell, M.S. Longtine, C.J. Chow, N. Adames, J.R. Pringle, M. Peter, and C. Boone. 1997. Bni1p, a yeast formin linking cdc42p and the actin cytoskeleton during polarized morphogenesis. *Science (New York, N.Y.* 276:118-122.

Evangelista, M., D. Pruyne, D.C. Amberg, C. Boone, and A. Bretscher. 2002. Formins direct Arp2/3-independent actin filament assembly to polarize cell growth in yeast. *Nature cell biology*. 4:260-269.

Fang, X., J. Luo, R. Nishihama, C. Wloka, C. Dravis, M. Travaglia, M. Iwase, E.A. Vallen, and E. Bi. 2010. Biphasic targeting and cleavage furrow ingression directed by the tail of a myosin II. *The Journal of cell biology*. 191:1333-1350.

Farkas, V. 1990. Fungal Cell Wall: Their structure, Biosinthesis and Biotechnological Aspects *Acta Biotechnology*. 10:225-238.

Farkas, V. 2003. Structure and biosynthesis of fungal cell walls: methodological approaches. *Folia microbiologica*. 48:469-478.

Farkas, V., J. Kovarik, A. Kosinova, and S. Bauer. 1974. Autoradiographic study of mannan incorporation into the growing cell walls of *Saccharomyces cerevisiae*. *Journal of bacteriology*. 117:265-269.

Field, C., R. Li, and K. Oegema. 1999. Cytokinesis in eukaryotes: a mechanistic comparison. *Current opinion in cell biology*. 11:68-80.

Field, C.M., and D. Kellogg. 1999. Septins: cytoskeletal polymers or signalling GTPases? *Trends in cell biology*. 9:387-394.

Finger, F.P., T.E. Hughes, and P. Novick. 1998. Sec3p is a spatial landmark for polarized secretion in budding yeast. *Cell*. 92:559-571.

Finger, F.P., and P. Novick. 1998. Spatial regulation of exocytosis: lessons from yeast. *The Journal of cell biology*. 142:609-612.

Fleet, G.H. 1985. Composition and structure of yeast cell walls. *Current topics in medical mycology*. 1:24-56.

Fleet, G.H. 1991. Cell Walls. *Rose and J.S. Harrison (ed.), The yeast*. 4.

Ford, R.A., J.A. Shaw, and E. Cabib. 1996. Yeast chitin synthases 1 and 2 consist of a non-homologous and dispensable N-terminal region and of a homologous moiety essential for function. *Mol Gen Genet*. 252:420-428.

Frazier, J.A., M.L. Wong, M.S. Longtine, J.R. Pringle, M. Mann, T.J. Mitchison, and C. Field. 1998. Polymerization of purified yeast septins: evidence that organized filament arrays may not be required for septin function. *The Journal of cell biology*. 143:737-749.

Fujimura-Kamada, K., T. Hirai, and K. Tanaka. 2012. Essential role of the NH2-terminal region of Cdc24 guanine nucleotide exchange factor in its initial polarized localization in *Saccharomyces cerevisiae*. *Eukaryotic cell*. 11:2-15.

Gaiser, O.J., K. Piotukh, M.N. Ponnuswamy, A. Planas, R. Borriss, and U. Heinemann. 2006. Structural basis for the substrate specificity of a *Bacillus* 1,3-1,4-beta-glucanase. *J Mol Biol*. 357:1211-1225.

Garcia-Rodriguez, L.J., J.A. Trilla, C. Castro, M.H. Valdivieso, A. Duran, and C. Roncero. 2000. Characterization of the chitin biosynthesis process as a compensatory mechanism in the fks1 mutant of *Saccharomyces cerevisiae*. *FEBS letters*. 478:84-88.

Garcia, R., C. Bermejo, C. Grau, R. Perez, J.M. Rodriguez-Pena, J. Francois, C. Nombela, and J. Arroyo. 2004. The global transcriptional response to transient cell wall damage in *Saccharomyces cerevisiae* and its regulation by the cell integrity signaling pathway. *The Journal of biological chemistry*. 279:15183-15195.

Garcia, R., J.M. Rodriguez-Pena, C. Bermejo, C. Nombela, and J. Arroyo. 2009. The high osmotic response and cell wall integrity pathways cooperate to regulate transcriptional responses to zymolyase-induced cell wall stress in *Saccharomyces cerevisiae*. *The Journal of biological chemistry*. 284:10901-10911.

Gemmill, T.R., and R.B. Trimble. 1999. Overview of N- and O-linked oligosaccharide structures found in various yeast species. *Biochimica et biophysica acta*. 1426:227-237.

Giaever, G., A.M. Chu, L. Ni, C. Connelly, L. Riles, S. Veronneau, S. Dow, A. Lucau-Danila, K. Anderson, B. Andre, A.P. Arkin, A. Astromoff, M. El-Bakkoury, R. Bangham, R. Benito, S. Brachat, S. Campanaro, M. Curtiss, K. Davis, A. Deutschbauer, K.D. Entian, P. Flaherty, F. Foury, D.J. Garfinkel, M. Gerstein, D. Gotte, U. Guldener, J.H. Hegemann, S. Hempel, Z. Herman, D.F. Jaramillo, D.E. Kelly, S.L. Kelly, P. Kotter, D. LaBonte, D.C. Lamb, N. Lan, H. Liang, H. Liao, L. Liu, C. Luo, M. Lussier, R. Mao, P. Menard, S.L. Ooi, J.L. Revuelta, C.J. Roberts, M. Rose, P. Ross-Macdonald, B. Scherens, G. Schimmack, B. Shafer, D.D. Shoemaker, S. Sookhai-Mahadeo, R.K. Storms, J.N. Strathern, G. Valle, M. Voet, G. Volckaert, C.Y. Wang, T.R. Ward, J. Wilhelmy, E.A. Winzeler, Y. Yang, G. Yen, E. Youngman, K. Yu, H. Bussey, J.D. Boeke, M. Snyder, P. Philippsen, R.W. Davis, and M. Johnston. 2002. Functional profiling of the *Saccharomyces cerevisiae* genome. *Nature*. 418:387-391.

Gladfelter, A.S. 2010. Guides to the final frontier of the cytoskeleton: septins in filamentous fungi. *Current opinion in microbiology*. 13:720-726.

Gladfelter, A.S., I. Bose, T.R. Zyla, E.S. Bardes, and D.J. Lew. 2002. Septin ring assembly involves cycles of GTP loading and hydrolysis by Cdc42p. *The Journal of cell biology*. 156:315-326.

Gladfelter, A.S., L. Kozubowski, T.R. Zyla, and D.J. Lew. 2005. Interplay between septin organization, cell cycle and cell shape in yeast. *Journal of cell science*. 118:1617-1628.

Gladfelter, A.S., J.J. Moskow, T.R. Zyla, and D.J. Lew. 2001. Isolation and characterization of effector-loop mutants of *CDC42* in yeast. *Molecular biology of the cell*. 12:1239-1255.

Gladfelter, A.S., T.R. Zyla, and D.J. Lew. 2004. Genetic interactions among regulators of septin organization. *Eukaryotic cell*. 3:847-854.

Goldman, R.C., P.A. Sullivan, D. Zakula, and J.O. Capobianco. 1995. Kinetics of beta-1,3 glucan interaction at the donor and acceptor sites of the fungal glucosyltransferase encoded by the *BGL2* gene. *European journal of biochemistry / FEBS*. 227:372-378.

Gomez-Esquer, F., J.M. Rodriguez-Pena, G. Diaz, E. Rodriguez, P. Briza, C. Nombela, and J. Arroyo. 2004. *CRR1*, a gene encoding a putative transglycosidase, is required for proper spore wall assembly in *Saccharomyces cerevisiae*. *Microbiology (Reading, England)*. 150:3269-3280.

Gomez, A., J. Perez, A. Reyes, A. Duran, and C. Roncero. 2009. Slt2 and Rim101 contribute independently to the correct assembly of the chitin ring at the budding yeast neck in *Saccharomyces cerevisiae*. *Eukaryotic cell*. 8:1449-1459.

Grabinska, K.A., P. Magnelli, and P.W. Robbins. 2007. Prenylation of *Saccharomyces cerevisiae* Chs4p Affects Chitin Synthase III activity and chitin chain length. *Eukaryotic cell*. 6:328-336.

Hahn, M., T. Keitel, and U. Heinemann. 1995. Crystal and molecular structure at 0.16-nm resolution of the hybrid *Bacillus* endo-1,3-1,4-beta-D-glucan 4-glucanohydrolase H(A16-M). *European journal of biochemistry / FEBS*. 232:849-858.

Hamada, K., S. Fukuchi, M. Arisawa, M. Baba, and K. Kitada. 1998. Screening for glycosylphosphatidylinositol (GPI)-dependent cell wall proteins in *Saccharomyces cerevisiae*. *Mol Gen Genet*. 258:53-59.

Harkins, H.A., N. Page, L.R. Schenkman, C. De Virgilio, S. Shaw, H. Bussey, and J.R. Pringle. 2001. Bud8p and Bud9p, proteins that may mark the sites for bipolar budding in yeast. *Molecular biology of the cell*. 12:2497-2518.

Harrison, J.C., E.S. Bardes, Y. Ohya, and D.J. Lew. 2001. A role for the Pkc1p/Mpk1p kinase cascade in the morphogenesis checkpoint. *Nature cell biology*. 3:417-420.

Hartland, R.P., C.A. Vermeulen, F.M. Klis, J.H. Sietsma, and J.G. Wessels. 1994. The linkage of (1-3)-beta-glucan to chitin during cell wall assembly in *Saccharomyces cerevisiae*. *Yeast (Chichester, England)*. 10:1591-1599.

Hartwell, L.H., J. Culotti, J.R. Pringle, and B.J. Reid. 1974. Genetic control of the cell division cycle in yeast. *Science (New York, N.Y.* 183:46-51.

Hayashibe, M., and Katohda, S. 1973. Initiation of budding and chitin-ring. *The Journal of General and Applied Microbiology*. 19:23-39.

Hector, R.F., and D.E. Bierer. 2011. New beta-glucan inhibitors as antifungal drugs. *Expert Opin Ther Pat*. 21:1597-1610.

Heinrich, M., T. Kohler, and H.U. Mosch. 2007. Role of Cdc42-Cla4 interaction in the pheromone response of *Saccharomyces cerevisiae*. *Eukaryotic cell*. 6:317-327.

Henrissat, B., I. Callebaut, S. Fabrega, P. Lehn, J.P. Mornon, and G. Davies. 1995. Conserved catalytic machinery and the prediction of a common fold for several families of glycosyl hydrolases. *Proceedings of the National Academy of Sciences of the United States of America*. 92:7090-7094.

Hernandez-Gay, J.J., A. Arda, S. Eller, S. Mezzato, B.R. Leeflang, C. Unverzagt, F.J. Canada, and J. Jimenez-Barbero. 2010. Insights into the dynamics and molecular recognition features of glycopeptides by protein receptors: the 3D solution structure of hevein bound to the trisaccharide core of N-glycoproteins. *Chemistry*. 16:10715-10726.

Herrero, A.B., P. Magnelli, M.K. Mansour, S.M. Levitz, H. Bussey, and C. Abeijon. 2004. *KRE5* gene null mutant strains of *Candida albicans* are avirulent and have altered

cell wall composition and hypha formation properties. *Eukaryotic cell*. 3:1423-1432.

Hill, K.L., N.L. Catlett, and L.S. Weisman. 1996. Actin and myosin function in directed vacuole movement during cell division in *Saccharomyces cerevisiae*. *The Journal of cell biology*. 135:1535-1549.

Hofken, T., and E. Schiebel. 2002. A role for cell polarity proteins in mitotic exit. *The EMBO journal*. 21:4851-4862.

Hofken, T., and E. Schiebel. 2004. Novel regulation of mitotic exit by the Cdc42 effectors Gic1 and Gic2. *The Journal of cell biology*. 164:219-231.

Hofmann, C., M. Shepelev, and J. Chernoff. 2004. The genetics of Pak. *Journal of cell science*. 117:4343-4354.

Holt, L.J., B.B. Tuch, J. Villen, A.D. Johnson, S.P. Gygi, and D.O. Morgan. 2009. Global analysis of Cdk1 substrate phosphorylation sites provides insights into evolution. *Science (New York, N.Y.* 325:1682-1686.

Holly, S.P., and K.J. Blumer. 1999. PAK-family kinases regulate cell and actin polarization throughout the cell cycle of *Saccharomyces cerevisiae*. *The Journal of cell biology*. 147:845-856.

Horisberger, M., and M. Vonlanthen. 1977. Location of mannan and chitin on thin sections of budding yeasts with gold markers. *Archives of microbiology*. 115:1-7.

Howell, A.S., and D.J. Lew. 2012. Morphogenesis and the cell cycle. *Genetics*. 190:51-77.

Hrmova, M., V. Farkas, J. Lahnstein, and G.B. Fincher. 2007. A Barley xyloglucan xyloglucosyl transferase covalently links xyloglucan, cellulosic substrates, and (1,3;1,4)-beta-D-glucans. *The Journal of biological chemistry*. 282:12951-12962.

Hurtado-Guerrero, R., A.W. Schuttelkopf, I. Mouyna, A.F. Ibrahim, S. Shepherd, T. Fontaine, J.P. Latge, and D.M. van Aalten. 2009. Molecular mechanisms of yeast cell wall glucan remodeling. *The Journal of biological chemistry*. 284:8461-8469.

Hutchins, K., and H. Bussey. 1983. Cell wall receptor for yeast killer toxin: involvement of (1 leads to 6)-beta-D-glucan. *Journal of bacteriology*. 154:161-169.

Hwang, J.S., D.H. Seo, and J.Y. Kim. 2006. Soluble forms of YlCrh1p and YlCrh2p, cell wall proteins of *Yarrowia lipolytica*, have beta-1,3-glycosidase activity. *Yeast (Chichester, England)*. 23:803-812.

Igual, J.C., A.L. Johnson, and L.H. Johnston. 1996. Coordinated regulation of gene expression by the cell cycle transcription factor Swi4 and the protein kinase C MAP kinase pathway for yeast cell integrity. *The EMBO journal*. 15:5001-5013.

Imamura, H., K. Tanaka, T. Hihara, M. Umikawa, T. Kamei, K. Takahashi, T. Sasaki, and Y. Takai. 1997. Bni1p and Bnr1p: downstream targets of the Rho family small G-proteins which interact with profilin and regulate actin cytoskeleton in *Saccharomyces cerevisiae*. *The EMBO journal*. 16:2745-2755.

Imhof, I., I. Flury, C. Vionnet, C. Roubaty, D. Egger, and A. Conzelmann. 2004. Glycosylphosphatidylinositol (GPI) proteins of *Saccharomyces cerevisiae* contain ethanolamine phosphate groups on the alpha1,4-linked mannose of the GPI anchor. *The Journal of biological chemistry*. 279:19614-19627.

Inoue, S.B., H. Qadota, M. Arisawa, T. Watanabe, and Y. Ohya. 1999. Prenylation of Rho1p is required for activation of yeast 1, 3-beta-glucan synthase. *The Journal of biological chemistry*. 274:38119-38124.

Inoue, S.B., N. Takewaki, T. Takasuka, T. Mio, M. Adachi, Y. Fujii, C. Miyamoto, M. Arisawa, Y. Furuichi, and T. Watanabe. 1995. Characterization and gene cloning of 1,3-beta-D-glucan synthase from *Saccharomyces cerevisiae*. *European journal of biochemistry / FEBS*. 231:845-854.

Jiang, B., J. Sheraton, A.F. Ram, G.J. Dijkgraaf, F.M. Klis, and H. Bussey. 1996. *CWH41* encodes a novel endoplasmic reticulum membrane N-glycoprotein involved in beta 1,6-glucan assembly. *Journal of bacteriology*. 178:1162-1171.

Jimenez, C., C. Sacristan, M.I. Roncero, and C. Roncero. 2010. Amino acid divergence between the CHS domain contributes to the different intracellular behaviour of Family II fungal chitin synthases in *Saccharomyces cerevisiae*. *Fungal Genet Biol*. 47:1034-1043.

Jimenez, J., V.J. Cid, R. Cenamor, M. Yuste, G. Molero, C. Nombela, and M. Sanchez. 1998. Morphogenesis beyond cytokinetic arrest in *Saccharomyces cerevisiae*. *The Journal of cell biology*. 143:1617-1634.

Johansson, P., H. Brumer, 3rd, M.J. Baumann, A.M. Kallas, H. Henriksson, S.E. Denman, T.T. Teeri, and T.A. Jones. 2004. Crystal structures of a poplar xyloglucan endotransglycosylase reveal details of transglycosylation acceptor binding. *Plant Cell*. 16:874-886.

Jung, U.S., and D.E. Levin. 1999. Genome-wide analysis of gene expression regulated by the yeast cell wall integrity signalling pathway. *Molecular microbiology*. 34:1049-1057.

Kadota, J., T. Yamamoto, S. Yoshiuchi, E. Bi, and K. Tanaka. 2004. Septin ring assembly requires concerted action of polarisome components, a PAK kinase Cla4p, and the actin cytoskeleton in *Saccharomyces cerevisiae*. *Molecular biology of the cell*. 15:5329-5345.

Kalebina, T.S., V. Farkas, D.K. Laurinavichiute, P.M. Gorlovoy, G.V. Fominov, P. Bartek, and I.S. Kulaev. 2003. Deletion of *BGL2* results in an increased chitin level in the cell wall of *Saccharomyces cerevisiae*. *Antonie van Leeuwenhoek*. 84:179-184.

Kalebina, T.S., D.K. Laurinavichyute, A.B. Shevelev, G.V. Fominov, E.I. Levitin, O.V. Alekseeva, S. Chzhan, N.V. Pan'kova, V.N. Ksenzenko, V.M. Stepanov, and I.S. Kulaev. 1998. Purification and characterization of P33 protein of *Candida utilis* homologous to bgl2p of *Saccharomyces cerevisiae*; comparative analysis of the role of these proteins in molecular organization of the yeast cell walls. *Biochemistry (Mosc)*. 63:1419-1423.

Kalebina, T.S., T.A. Plotnikova, A.A. Gorkovskii, I.O. Selyakh, O.V. Galzitskaya, E.E. Bezsonov, G. Gellissen, and I.S. Kulaev. 2008. Amyloid-like properties of *Saccharomyces cerevisiae* cell wall glucantransferase Bgl2p: prediction and experimental evidences. *Prion*. 2:91-96.

Kalebina, T.S., T.A. Plotnikova, E.V. Karpova, and I.S. Kulaev. 2006. [A new phenotypic manifestation of deletion of the *BGL2* gene encoding glucanotransferase of the *Saccharomyces cerevisiae* cell wall]. *Mikrobiologiia*. 75:717-719.

Kamei, T., K. Tanaka, T. Hihara, M. Umikawa, H. Imamura, M. Kikyo, K. Ozaki, and Y. Takai. 1998. Interaction of Bnr1p with a novel Src homology 3 domain-containing Hof1p. Implication in cytokinesis in *Saccharomyces cerevisiae*. *The Journal of biological chemistry*. 273:28341-28345.

Kang, M.S., and E. Cabib. 1986. Regulation of fungal cell wall growth: a guanine nucleotide-binding, proteinaceous component required for activity of (1----3)-beta-D-glucan synthase. *Proceedings of the National Academy of Sciences of the United States of America*. 83:5808-5812.

Kang, M.S., N. Elango, E. Mattia, J. Au-Young, P.W. Robbins, and E. Cabib. 1984. Isolation of chitin synthetase from *Saccharomyces cerevisiae*. Purification of an enzyme by entrapment in the reaction product. *The Journal of biological chemistry*. 259:14966-14972.

Kapteyn, J.C., R.C. Montijn, E. Vink, J. de la Cruz, A. Llobell, J.E. Douwes, H. Shimoi, P.N. Lipke, and F.M. Klis. 1996. Retention of *Saccharomyces cerevisiae* cell wall proteins through a phosphodiester-linked beta-1,3-/beta-1,6-glucan heteropolymer. *Glycobiology*. 6:337-345.

Kapteyn, J.C., A.F. Ram, E.M. Groos, R. Kollar, R.C. Montijn, H. Van Den Ende, A. Llobell, E. Cabib, and F.M. Klis. 1997. Altered extent of cross-linking of beta1,6-glucosylated mannoproteins to chitin in *Saccharomyces cerevisiae* mutants with reduced cell wall beta1,3-glucan content. *Journal of bacteriology*. 179:6279-6284.

Kapteyn, J.C., B. ter Riet, E. Vink, S. Blad, H. De Nobel, H. Van Den Ende, and F.M. Klis. 2001. Low external pH induces HOG1-dependent changes in the organization of the *Saccharomyces cerevisiae* cell wall. *Molecular microbiology*. 39:469-479.

Kapteyn, J.C., H. Van Den Ende, and F.M. Klis. 1999a. The contribution of cell wall proteins to the organization of the yeast cell wall. *Biochimica et biophysica acta*. 1426:373-383.

Kapteyn, J.C., P. Van Egmond, E. Sievi, H. Van Den Ende, M. Makarow, and F.M. Klis. 1999b. The contribution of the O-glycosylated protein Pir2p/Hsp150 to the construction of the yeast cell wall in wild-type cells and beta 1,6-glucan-deficient mutants. *Molecular microbiology*. 31:1835-1844.

Keller, F.A., and E. Cabib. 1971. Chitin and yeast budding. Properties of chitin synthetase from *Saccharomyces carlsbergensis*. *The Journal of biological chemistry*. 246:160-166.

Kim, H.B., B.K. Haarer, and J.R. Pringle. 1991. Cellular morphogenesis in the *Saccharomyces cerevisiae* cell cycle: localization of the *CDC3* gene product and the timing of events at the budding site. *The Journal of cell biology*. 112:535-544.

Klebl, F., and W. Tanner. 1989. Molecular cloning of a cell wall exo-beta-1,3-glucanase from *Saccharomyces cerevisiae*. *Journal of bacteriology*. 171:6259-6264.

Klis, F.M. 1994. Review: cell wall assembly in yeast. *Yeast (Chichester, England)*. 10:851-869.

Klis, F.M., A. Boorsma, and P.W. De Groot. 2006. Cell wall construction in *Saccharomyces cerevisiae*. *Yeast (Chichester, England)*. 23:185-202.

Klis, F.M., S. Brul, and P.W. De Groot. 2010. Covalently linked wall proteins in ascomycetous fungi. *Yeast (Chichester, England)*. 27:489-493.

Klis, F.M., L.H. Caro, J.H. Vossen, J.C. Kapteyn, A.F. Ram, R.C. Montijn, M.A. Van Berkel, and H. Van den Ende. 1997. Identification and characterization of a major building block in the cell wall of *Saccharomyces cerevisiae*. *Biochemical Society transactions*. 25:856-860.

Klis, F.M., P. Mol, K. Hellingwerf, and S. Brul. 2002. Dynamics of cell wall structure in *Saccharomyces cerevisiae*. *FEMS microbiology reviews*. 26:239-256.

Koch, G., K. Tanaka, T. Masuda, W. Yamochi, H. Nonaka, and Y. Takai. 1997. Association of the Rho family small GTP-binding proteins with Rho GDP dissociation inhibitor (Rho GDI) in *Saccharomyces cerevisiae*. *Oncogene*. 15:417-422.

Kohno, H., K. Tanaka, A. Mino, M. Umikawa, H. Imamura, T. Fujiwara, Y. Fujita, K. Hotta, H. Qadota, T. Watanabe, Y. Ohya, and Y. Takai. 1996. Bni1p implicated in cytoskeletal control is a putative target of Rho1p small GTP binding protein in *Saccharomyces cerevisiae*. *The EMBO journal*. 15:6060-6068.

Kollar, R., E. Petrakova, G. Ashwell, P.W. Robbins, and E. Cabib. 1995. Architecture of the yeast cell wall. The linkage between chitin and beta(1-->3)-glucan. *The Journal of biological chemistry*. 270:1170-1178.

Kollar, R., B.B. Reinhold, E. Petrakova, H.J. Yeh, G. Ashwell, J. Drgonova, J.C. Kapteyn, F.M. Klis, and E. Cabib. 1997. Architecture of the yeast cell wall. Beta(1-->6)-glucan interconnects mannoprotein, beta(1-->)3-glucan, and chitin. *The Journal of biological chemistry*. 272:17762-17775.

Kopecka, M., and D.R. Kreger. 1986. Assembly of microfibrils in vivo and in vitro from (1----3)-beta-D-glucan synthesized by protoplasts of *Saccharomyces cerevisiae*. *Archives of microbiology*. 143:387-395.

Kopecka, M., H.J. Phaff, and G.H. Fleet. 1974. Demonstration of a fibrillar component in the cell wall of the yeast *Saccharomyces cerevisiae* and its chemical nature. *The Journal of cell biology*. 62:66-76.

Korinek, W.S., E. Bi, J.A. Epp, L. Wang, J. Ho, and J. Chant. 2000. Cyk3, a novel SH3-domain protein, affects cytokinesis in yeast. *Curr Biol*. 10:947-950.

Kota, J., and P.O. Ljungdahl. 2005. Specialized membrane-localized chaperones prevent aggregation of polytopic proteins in the ER. *The Journal of cell biology*. 168:79-88.

Kozminski, K.G., L. Beven, E. Angerman, A.H. Tong, C. Boone, and H.O. Park. 2003. Interaction between a Ras and a Rho GTPase couples selection of a growth site to the development of cell polarity in yeast. *Molecular biology of the cell*. 14:4958-4970.

Kozubowski, L., J.R. Larson, and K. Tatchell. 2005. Role of the septin ring in the asymmetric localization of proteins at the mother-bud neck in *Saccharomyces cerevisiae*. *Molecular biology of the cell*. 16:3455-3466.

Kozubowski, L., H. Panek, A. Rosenthal, A. Bloecher, D.J. DeMarini, and K. Tatchell. 2003. A Bni4-Glc7 phosphatase complex that recruits chitin synthase to the site of bud emergence. *Molecular biology of the cell*. 14:26-39.

Kozubowski, L., K. Saito, J.M. Johnson, A.S. Howell, T.R. Zyla, and D.J. Lew. 2008. Symmetry-breaking polarization driven by a Cdc42p GEF-PAK complex. *Curr Biol*. 18:1719-1726.

Krainer, E., R.E. Stark, F. Naider, K. Alagramam, and J.M. Becker. 1994. Direct observation of cell wall glucans in whole cells of *Saccharomyces cerevisiae* by magic-angle spinning 13C-NMR. *Biopolymers*. 34:1627-1635.

Kuranda, M.J., and P.W. Robbins. 1991. Chitinase is required for cell separation during growth of *Saccharomyces cerevisiae*. *The Journal of biological chemistry*. 266:19758-19767.

Kurischko, C., G. Weiss, M. Ottey, and F.C. Luca. 2005. A role for the *Saccharomyces cerevisiae* regulation of Ace2 and polarized morphogenesis signaling network in cell integrity. *Genetics*. 171:443-455.

Lagorce, A., N.C. Hauser, D. Labourdette, C. Rodriguez, H. Martin-Yken, J. Arroyo, J.D. Hoheisel, and J. Francois. 2003. Genome-wide analysis of the response to cell wall mutations in the yeast *Saccharomyces cerevisiae*. *The Journal of biological chemistry*. 278:20345-20357.

Larriba, G., E. Andaluz, R. Cueva, and R.D. Basco. 1995. Molecular biology of yeast exoglucanases. *FEMS microbiology letters*. 125:121-126.

Latge, J.P. 2010. Tasting the fungal cell wall. *Cellular microbiology*. 12:863-872.

Leberer, E., D. Dignard, D. Harcus, D.Y. Thomas, and M. Whiteway. 1992. The protein kinase homologue Ste20p is required to link the yeast pheromone response G-protein beta gamma subunits to downstream signalling components. *The EMBO journal*. 11:4815-4824.

Lesage, G., and H. Bussey. 2006. Cell wall assembly in *Saccharomyces cerevisiae*. *Microbiol Mol Biol Rev*. 70:317-343.

Lesage, G., A.M. Sdicu, P. Menard, J. Shapiro, S. Hussein, and H. Bussey. 2004. Analysis of beta-1,3-glucan assembly in *Saccharomyces cerevisiae* using a synthetic interaction network and altered sensitivity to caspofungin. *Genetics*. 167:35-49.

Levin, D.E. 2005. Cell wall integrity signaling in *Saccharomyces cerevisiae*. *Microbiol Mol Biol Rev*. 69:262-291.

Levin, D.E. 2011. Regulation of cell wall biogenesis in *Saccharomyces cerevisiae*: the cell wall integrity signaling pathway. *Genetics*. 189:1145-1175.

Levinson, J.N., S. Shahinian, A.M. Sdicu, D.C. Tessier, and H. Bussey. 2002. Functional, comparative and cell biological analysis of *Saccharomyces cerevisiae* Kre5p. *Yeast (Chichester, England)*. 19:1243-1259.

Lew, D.J. 2003. The morphogenesis checkpoint: how yeast cells watch their figures. *Current opinion in cell biology*. 15:648-653.

Lew, D.J., and S.I. Reed. 1995a. Cell cycle control of morphogenesis in budding yeast. *Curr Opin Genet Dev*. 5:17-23.

Lew, D.J., and S.I. Reed. 1995b. A cell cycle checkpoint monitors cell morphogenesis in budding yeast. *The Journal of cell biology*. 129:739-749.

Li, R., and R. Wedlich-Soldner. 2009. Bem1 complexes and the complexity of yeast cell polarization. *Curr Biol*. 19:R194-195; author reply R195.

Lillie, S.H., and S.S. Brown. 1994. Immunofluorescence localization of the unconventional myosin, Myo2p, and the putative kinesin-related protein, Smy1p, to the same regions of polarized growth in *Saccharomyces cerevisiae*. *The Journal of cell biology*. 125:825-842.

Lin, M., K. Grillitsch, G. Daum, U. Just, and T. Hofken. 2009a. Modulation of sterol homeostasis by the Cdc42p effectors Cla4p and Ste20p in the yeast *Saccharomyces cerevisiae*. *The FEBS journal*. 276:7253-7264.

Lin, M., H. Unden, N. Jacquier, R. Schneiter, U. Just, and T. Hofken. 2009b. The Cdc42 effectors Ste20, Cla4, and Skm1 down-regulate the expression of genes involved in sterol uptake by a mitogen-activated protein kinase-independent pathway. *Molecular biology of the cell*. 20:4826-4837.

Lipke, P.N., and R. Ovalle. 1998. Cell wall architecture in yeast: new structure and new challenges. *Journal of bacteriology*. 180:3735-3740.

Lippincott, J., and R. Li. 1998a. Dual function of Cyk2, a cdc15/PSTPIP family protein, in regulating actomyosin ring dynamics and septin distribution. *The Journal of cell biology*. 143:1947-1960.

Lippincott, J., and R. Li. 1998b. Sequential assembly of myosin II, an IQGAP-like protein, and filamentous actin to a ring structure involved in budding yeast cytokinesis. *The Journal of cell biology*. 140:355-366.

Lippincott, J., and R. Li. 2000. Involvement of PCH family proteins in cytokinesis and actin distribution. *Microscopy research and technique*. 49:168-172.

Lippincott, J., K.B. Shannon, W. Shou, R.J. Deshaies, and R. Li. 2001. The Tem1 small GTPase controls actomyosin and septin dynamics during cytokinesis. *Journal of cell science*. 114:1379-1386.

Longtine, M.S., D.J. DeMarini, M.L. Valencik, O.S. Al-Awar, H. Fares, C. De Virgilio, and J.R. Pringle. 1996. The septins: roles in cytokinesis and other processes. *Current opinion in cell biology*. 8:106-119.

Longtine, M.S., H. Fares, and J.R. Pringle. 1998. Role of the yeast Gin4p protein kinase in septin assembly and the relationship between septin assembly and septin function. *The Journal of cell biology*. 143:719-736.

Longtine, M.S., C.L. Theesfeld, J.N. McMillan, E. Weaver, J.R. Pringle, and D.J. Lew. 2000. Septin-dependent assembly of a cell cycle-regulatory module in *Saccharomyces cerevisiae*. *Molecular and cellular biology*. 20:4049-4061.

Lu, C.F., R.C. Montijn, J.L. Brown, F. Klis, J. Kurjan, H. Bussey, and P.N. Lipke. 1995. Glycosyl phosphatidylinositol-dependent cross-linking of alpha-agglutinin and beta 1,6-glucan in the *Saccharomyces cerevisiae* cell wall. *The Journal of cell biology*. 128:333-340.

Lussier, M., A.M. Sdicu, and H. Bussey. 1999. The KTR and MNN1 mannosyltransferase families of *Saccharomyces cerevisiae*. *Biochimica et biophysica acta*. 1426:323-334.

Lussier, M., A.M. White, J. Sheraton, T. di Paolo, J. Treadwell, S.B. Southard, C.I. Horenstein, J. Chen-Weiner, A.F. Ram, J.C. Kapteyn, T.W. Roemer, D.H. Vo, D.C. Bondoc, J. Hall, W.W. Zhong, A.M. Sdicu, J. Davies, F.M. Klis, P.W. Robbins, and H. Bussey. 1997. Large scale identification of genes involved in cell surface biosynthesis and architecture in *Saccharomyces cerevisiae*. *Genetics*. 147:435-450.

Magnelli, P., J.F. Cipollo, and C. Abeijon. 2002. A refined method for the determination of *Saccharomyces cerevisiae* cell wall composition and beta-1,6-glucan fine structure. *Analytical biochemistry*. 301:136-150.

Manners, D.J., A.J. Masson, and J.C. Patterson. 1973a. The structure of a beta-(1 leads to 3)-D-glucan from yeast cell walls. *The Biochemical journal*. 135:19-30.

Manners, D.J., A.J. Masson, J.C. Patterson, H. Bjorndal, and B. Lindberg. 1973b. The structure of a beta-(1--6)-D-glucan from yeast cell walls. *The Biochemical journal*. 135:31-36.

Marco, E., R. Wedlich-Soldner, R. Li, S.J. Altschuler, and L.F. Wu. 2007. Endocytosis optimizes the dynamic localization of membrane proteins that regulate cortical polarity. *Cell*. 129:411-422.

Martin-Cuadrado, A.B., E. Duenas, M. Sipiczki, C.R. Vazquez de Aldana, and F. del Rey. 2003. The endo-beta-1,3-glucanase eng1p is required for dissolution of the primary septum during cell separation in *Schizosaccharomyces pombe*. *Journal of cell science*. 116:1689-1698.

Martin-Cuadrado, A.B., T. Fontaine, P.F. Esteban, J.E. del Dedo, M. de Medina-Redondo, F. del Rey, J.P. Latge, and C.R. de Aldana. 2008. Characterization of the endo-beta-1,3-glucanase activity of *S. cerevisiae* Eng2 and other members of the GH81 family. *Fungal Genet Biol*. 45:542-553.

Martin, H., A. Mendoza, J.M. Rodriguez-Pachon, M. Molina, and C. Nombela. 1997. Characterization of *SKM1*, a *Saccharomyces cerevisiae* gene encoding a novel Ste20/PAK-like protein kinase. *Molecular microbiology*. 23:431-444.

Martinez-Rucobo, F.W., L. Eckhardt-Strelau, and A.C. Terwisscha van Scheltinga. 2009. Yeast chitin synthase 2 activity is modulated by proteolysis and phosphorylation. *The Biochemical journal*. 417:547-554.

Mazan, M., E. Ragni, L. Popolo, and V. Farkas. 2012. Catalytic properties of the Gas family beta-(1,3)-glucanosyltransferases active in fungal cell-wall biogenesis as determined by a novel fluorescent assay. *The Biochemical journal*. 438:275-282.

Mazanka, E., and E.L. Weiss. 2010. Sequential counteracting kinases restrict an asymmetric gene expression program to early G1. *Molecular biology of the cell*. 21:2809-2820.

Mazur, P., and W. Baginsky. 1996. In vitro activity of 1,3-beta-D-glucan synthase requires the GTP-binding protein Rho1. *The Journal of biological chemistry*. 271:14604-14609.

Mazur, P., N. Morin, W. Baginsky, M. el-Sherbeini, J.A. Clemas, J.B. Nielsen, and F. Foor. 1995. Differential expression and function of two homologous subunits of yeast 1,3-beta-D-glucan synthase. *Molecular and cellular biology*. 15:5671-5681.

McCusker, D., C. Denison, S. Anderson, T.A. Egelhofer, J.R. Yates, 3rd, S.P. Gygi, and D.R. Kellogg. 2007. Cdk1 coordinates cell-surface growth with the cell cycle. *Nature cell biology*. 9:506-515.

McMillan, J.N., M.S. Longtine, R.A. Sia, C.L. Theesfeld, E.S. Bardes, J.R. Pringle, and D.J. Lew. 1999a. The morphogenesis checkpoint in *Saccharomyces cerevisiae*: cell cycle control of Swe1p degradation by Hsl1p and Hsl7p. *Molecular and cellular biology*. 19:6929-6939.

McMillan, J.N., R.A. Sia, E.S. Bardes, and D.J. Lew. 1999b. Phosphorylation-independent inhibition of Cdc28p by the tyrosine kinase Swe1p in the morphogenesis checkpoint. *Molecular and cellular biology*. 19:5981-5990.

McMurray, M.A., and T. Jeremy. 2008. Biochemical Properties and Supramolecular Architecture of Septin Hetero-Oligomers and Septin Filaments. *in The Septins*

McMurray, M.A., and J. Thorner. 2008. Septin stability and recycling during dynamic structural transitions in cell division and development. *Curr Biol*. 18:1203-1208.

McMurray, M.A., and J. Thorner. 2009a. Reuse, replace, recycle. Specificity in subunit inheritance and assembly of higher-order septin structures during mitotic and meiotic division in budding yeast. *Cell Cycle*. 8:195-203.

McMurray, M.A., and J. Thorner. 2009b. Septins: molecular partitioning and the generation of cellular asymmetry. *Cell Div*. 4:18.

Meaden, P., K. Hill, J. Wagner, D. Slipetz, S.S. Sommer, and H. Bussey. 1990. The yeast *KRE5* gene encodes a probable endoplasmic reticulum protein required for (1----6)-beta-D-glucan synthesis and normal cell growth. *Molecular and cellular biology*. 10:3013-3019.

Meitinger, F., M.E. Boehm, A. Hofmann, B. Hub, H. Zentgraf, W.D. Lehmann, and G. Pereira. 2011. Phosphorylation-dependent regulation of the F-BAR protein Hof1 during cytokinesis. *Genes & development*. 25:875-888.

Meitinger, F., S. Palani, and G. Pereira. 2012. The power of MEN in cytokinesis. *Cell Cycle*. 11:219-228.

Meitinger, F., B. Petrova, I.M. Lombardi, D.T. Bertazzi, B. Hub, H. Zentgraf, and G. Pereira. 2010. Targeted localization of Inn1, Cyk3 and Chs2 by the mitotic-exit network regulates cytokinesis in budding yeast. *Journal of cell science*. 123:1851-1861.

Minke, R., and J. Blackwell. 1978. The structure of alpha-chitin. *J Mol Biol*. 120:167-181.

Mitchison, T.J., and C.M. Field. 2002. Cytoskeleton: what does GTP do for septins? *Curr Biol*. 12:R788-790.

Mohand, F.A., and V. Farkas. 2006. Screening for hetero-transglycosylating activities in extracts from nasturtium (Tropaeolum majus). *Carbohydrate research*. 341:577-581.

Mol, P.C., H.M. Park, J.T. Mullins, and E. Cabib. 1994. A GTP-binding protein regulates the activity of (1-->3)-beta-glucan synthase, an enzyme directly involved in yeast cell wall morphogenesis. *The Journal of biological chemistry*. 269:31267-31274.

Mol, P.C.a.W., J.G.H. 1987. Linkages between glucosaminoglycan and glucan determine alkali-insolubility of the glucan in walls of *Sccharomyces cerevisiae*. *FEMS Microbiol* 41:95-99.

Molano, J., B. Bowers, and E. Cabib. 1980. Distribution of chitin in the yeast cell wall. An ultrastructural and chemical study. *The Journal of cell biology*. 85:199-212.

Molina, M., C. Gil, J. Pla, J. Arroyo, and C. Nombela. 2000. Protein localisation approaches for understanding yeast cell wall biogenesis. *Microscopy research and technique*. 51:601-612.

Montijn, R.C., E. Vink, W.H. Muller, A.J. Verkleij, H. Van Den Ende, B. Henrissat, and F.M. Klis. 1999. Localization of synthesis of beta1,6-glucan in *Saccharomyces cerevisiae*. *Journal of bacteriology*. 181:7414-7420.

Moseley, J.B., and B.L. Goode. 2006. The yeast actin cytoskeleton: from cellular function to biochemical mechanism. *Microbiol Mol Biol Rev*. 70:605-645.

Mouyna, I., M. Monod, T. Fontaine, B. Henrissat, B. Lechenne, and J.P. Latge. 2000. Identification of the catalytic residues of the first family of beta(1-3)glucanosyltransferases identified in fungi. *The Biochemical journal*. 347 Pt 3:741-747.

Mrsa, V., M. Ecker, S. Strahl-Bolsinger, M. Nimtz, L. Lehle, and W. Tanner. 1999. Deletion of new covalently linked cell wall glycoproteins alters the electrophoretic mobility of phosphorylated wall components of *Saccharomyces cerevisiae*. *Journal of bacteriology*. 181:3076-3086.

Mrsa, V., F. Klebl, and W. Tanner. 1993. Purification and characterization of the *Saccharomyces cerevisiae BGL2* gene product, a cell wall endo-beta-1,3-glucanase. *Journal of bacteriology*. 175:2102-2106.

Mrsa, V., T. Seidl, M. Gentzsch, and W. Tanner. 1997. Specific labelling of cell wall proteins by biotinylation. Identification of four covalently linked O-mannosylated proteins of *Saccharomyces cerevisiae*. *Yeast (Chichester, England)*. 13:1145-1154.

Mrsa, V., and W. Tanner. 1999. Role of NaOH-extractable cell wall proteins Ccw5p, Ccw6p, Ccw7p and Ccw8p (members of the Pir protein family) in stability of the *Saccharomyces cerevisiae* cell wall. *Yeast (Chichester, England)*. 15:813-820.

Munchow, S., C. Sauter, and R.P. Jansen. 1999. Association of the class V myosin Myo4p with a localised messenger RNA in budding yeast depends on She proteins. *Journal of cell science*. 112 (Pt 10):1511-1518.

Muthukumar, G., S.H. Suhng, P.T. Magee, R.D. Jewell, and D.A. Primerano. 1993. The *Saccharomyces cerevisiae SPR1* gene encodes a sporulation-specific exo-1,3-beta-glucanase which contributes to ascospore thermoresistance. *Journal of bacteriology*. 175:386-394.

Muzzarelli, R.A., F. Tanfani, G. Scarpini, and M.G. Muzzarelli. 1979. ESR characterization of chitins and chitosans. *Biochemical and biophysical research communications*. 89:706-712.

Nagahashi, S., M. Lussier, and H. Bussey. 1998. Isolation of Candida glabrata homologs of the *Saccharomyces cerevisiae KRE9* and *KNH1* genes and their involvement in cell wall beta-1,6-glucan synthesis. *Journal of bacteriology*. 180:5020-5029.

Nagahashi, S., M. Sudoh, N. Ono, R. Sawada, E. Yamaguchi, Y. Uchida, T. Mio, M. Takagi, M. Arisawa, and H. Yamada-Okabe. 1995. Characterization of chitin synthase 2 of *Saccharomyces cerevisiae*. Implication of two highly conserved domains as possible catalytic sites. *The Journal of biological chemistry*. 270:13961-13967.

Nagaraj, S., A. Rajendran, C.E. Jackson, and M.S. Longtine. 2008. Role of nucleotide binding in septin-septin interactions and septin localization in *Saccharomyces cerevisiae*. *Molecular and cellular biology*. 28:5120-5137.

Nakanishi-Shindo, Y., K. Nakayama, A. Tanaka, Y. Toda, and Y. Jigami. 1993. Structure of the N-linked oligosaccharides that show the complete loss of alpha-1,6-polymannose outer chain from och1, och1 mnn1, and och1 mnn1 alg3 mutants of *Saccharomyces cerevisiae*. *The Journal of biological chemistry*. 268:26338-26345.

Nakayama, K., T. Nagasu, Y. Shimma, J. Kuromitsu, and Y. Jigami. 1992. *OCH1* encodes a novel membrane bound mannosyltransferase: outer chain elongation of asparagine-linked oligosaccharides. *The EMBO journal*. 11:2511-2519.

Nebreda, A.R., C.R. Vazquez, T.G. Villa, J.R. Villanueva, and F. del Rey. 1987. Heterogeneous glycosylation of the *EXG1* gene product accounts for the two extracellular exo-beta-glucanases of *Saccharomyces cerevisiae*. *FEBS letters*. 220:27-30.

Nebreda, A.R., T.G. Villa, J.R. Villanueva, and F. del Rey. 1986. Cloning of genes related to exo-beta-glucanase production in *Saccharomyces cerevisiae*: characterization of an exo-beta-glucanase structural gene. *Gene*. 47:245-259.

Nelson, B., C. Kurischko, J. Horecka, M. Mody, P. Nair, L. Pratt, A. Zougman, L.D. McBroom, T.R. Hughes, C. Boone, and F.C. Luca. 2003. RAM: a conserved signaling network that regulates Ace2p transcriptional activity and polarized morphogenesis. *Molecular biology of the cell*. 14:3782-3803.

Nern, A., and R.A. Arkowitz. 1999. A Cdc24p-Far1p-Gbetagamma protein complex required for yeast orientation during mating. *The Journal of cell biology*. 144:1187-1202.

Nguyen, T.H., G.H. Fleet, and P.L. Rogers. 1998. Composition of the cell walls of several yeast species. *Applied microbiology and biotechnology*. 50:206-212.

Nierman, W.C., A. Pain, M.J. Anderson, J.R. Wortman, H.S. Kim, J. Arroyo, M. Berriman, K. Abe, D.B. Archer, C. Bermejo, J. Bennett, P. Bowyer, D. Chen, M. Collins, R. Coulsen, R. Davies, P.S. Dyer, M. Farman, N. Fedorova, T.V. Feldblyum, R. Fischer, N. Fosker, A. Fraser, J.L. Garcia, M.J. Garcia, A. Goble, G.H. Goldman, K. Gomi, S. Griffith-Jones, R. Gwilliam, B. Haas, H. Haas, D. Harris, H. Horiuchi, J. Huang, S. Humphray, J. Jimenez, N. Keller, H. Khouri, K. Kitamoto, T. Kobayashi, S. Konzack, R. Kulkarni, T. Kumagai, A. Lafon, J.P. Latge, W. Li, A. Lord, C. Lu, W.H. Majoros, G.S. May, B.L. Miller, Y. Mohamoud, M. Molina, M. Monod, I. Mouyna, S. Mulligan, L. Murphy, S. O'Neil, I. Paulsen, M.A. Penalva, M. Pertea, C. Price, B.L. Pritchard, M.A. Quail, E. Rabbinowitsch, N. Rawlins, M.A. Rajandream, U. Reichard, H. Renauld, G.D. Robson, S. Rodriguez de Cordoba, J.M. Rodriguez-Pena, C.M. Ronning, S. Rutter, S.L. Salzberg, M. Sanchez, J.C. Sanchez-Ferrero, D. Saunders, K. Seeger, R. Squares, S. Squares, M. Takeuchi, F. Tekaia, G. Turner, C.R. Vazquez de Aldana, J. Weidman, O. White, J. Woodward, J.H. Yu, C. Fraser, J.E. Galagan, K. Asai, M. Machida, N. Hall, B. Barrell, and D.W. Denning. 2005. Genomic sequence of the pathogenic and allergenic filamentous fungus *Aspergillus fumigatus*. *Nature*. 438:1151-1156.

Nishihama, R., J.H. Schreiter, M. Onishi, E.A. Vallen, J. Hanna, K. Moravcevic, M.F. Lippincott, H. Han, M.A. Lemmon, J.R. Pringle, and E. Bi. 2009. Role of Inn1 and its interactions with Hof1 and Cyk3 in promoting cleavage furrow and septum formation in S. cerevisiae. *The Journal of cell biology*. 185:995-1012.

Nombela, C., M. Molina, R. Cenamor, and M. Sanchez. 1988. Yeast beta-glucanases: a complex system of secreted enzymes. *Microbiological sciences*. 5:328-332.

Nuoffer, C., A. Horvath, and H. Riezman. 1993. Analysis of the sequence requirements for glycosylphosphatidylinositol anchoring of *Saccharomyces cerevisiae* Gas1 protein. *The Journal of biological chemistry*. 268:10558-10563.

Oh, Y., and E. Bi. 2011. Septin structure and function in yeast and beyond. *Trends in cell biology*. 21:141-148.

Oh, Y., K.J. Chang, P. Orlean, C. Wloka, R. Deshaies, and E. Bi. 2012. Mitotic exit kinase Dbf2 directly phosphorylates chitin synthase Chs2 to regulate cytokinesis in budding yeast. *Molecular biology of the cell*.

Okada, H., M. Abe, M. Asakawa-Minemura, A. Hirata, H. Qadota, K. Morishita, S. Ohnuki, S. Nogami, and Y. Ohya. 2010. Multiple functional domains of the yeast l,3-beta-glucan synthase subunit Fks1p revealed by quantitative phenotypic analysis of temperature-sensitive mutants. *Genetics*. 184:1013-1024.

Ono, N., T. Yabe, M. Sudoh, T. Nakajima, T. Yamada-Okabe, M. Arisawa, and H. Yamada-Okabe. 2000. The yeast Chs4 protein stimulates the trypsin-sensitive activity of chitin synthase 3 through an apparent protein-protein interaction. *Microbiology (Reading, England)*. 146 (Pt 2):385-391.

Orlean, P. 1987. Two chitin synthases in *Saccharomyces cerevisiae*. *The Journal of biological chemistry*. 262:5732-5739.

Orlean, P. 1997. Biogenesis of yeast cell wall and surface components. *In J.R. Pringle, J.R. Broach and E.W. Jones (ed)*:229-362.

Orlean, P. 2012. Architecture and Biosynthesis of the *Saccharomyces cerevisiae* Cell Wall. *Genetics*. 192:775-818.

Osmond, B.C., C.A. Specht, and P.W. Robbins. 1999. Chitin synthase III: synthetic lethal mutants and "stress related" chitin synthesis that bypasses the *CSD3/CHS6* localization pathway. *Proceedings of the National Academy of Sciences of the United States of America*. 96:11206-11210.

Osumi, M. 1998. The ultrastructure of yeast: cell wall structure and formation. *Micron*. 29:207-233.

Page, N., M. Gerard-Vincent, P. Menard, M. Beaulieu, M. Azuma, G.J. Dijkgraaf, H. Li, J. Marcoux, T. Nguyen, T. Dowse, A.M. Sdicu, and H. Bussey. 2003. A *Saccharomyces cerevisiae* genome-wide mutant screen for altered sensitivity to K1 killer toxin. *Genetics*. 163:875-894.

Pammer, M., P. Briza, A. Ellinger, T. Schuster, R. Stucka, H. Feldmann, and M. Breitenbach. 1992. *DIT101* (*CSD2, CAL1*), a cell cycle-regulated yeast gene required for synthesis of chitin in cell walls and chitosan in spore walls. *Yeast (Chichester, England)*. 8:1089-1099.

Pardini, G., P.W. De Groot, A.T. Coste, M. Karababa, F.M. Klis, C.G. de Koster, and D. Sanglard. 2006. The CRH family coding for cell wall glycosylphosphatidylinositol proteins with a predicted transglycosidase domain affects cell wall organization and virulence of *Candida albicans*. *The Journal of biological chemistry*. 281:40399-40411.

Park, H.O., and E. Bi. 2007. Central roles of small GTPases in the development of cell polarity in yeast and beyond. *Microbiol Mol Biol Rev*. 71:48-96.

Park, H.O., J. Chant, and I. Herskowitz. 1993. BUD2 encodes a GTPase-activating protein for Bud1/Rsr1 necessary for proper bud-site selection in yeast. *Nature*. 365:269-274.

Park, H.O., A. Sanson, and I. Herskowitz. 1999. Localization of Bud2p, a GTPase-activating protein necessary for programming cell polarity in yeast to the presumptive bud site. *Genes & development*. 13:1912-1917.

Pashkova, N., N.L. Catlett, J.L. Novak, G. Wu, R. Lu, R.E. Cohen, and L.S. Weisman. 2005. Myosin V attachment to cargo requires the tight association of two functional subdomains. *The Journal of cell biology*. 168:359-364.

Peter, M., A.M. Neiman, H.O. Park, M. van Lohuizen, and I. Herskowitz. 1996. Functional analysis of the interaction between the small GTP binding protein Cdc42 and the Ste20 protein kinase in yeast. *The EMBO journal*. 15:7046-7059.

Piens, K., R. Faure, G. Sundqvist, M.J. Baumann, M. Saura-Valls, T.T. Teeri, S. Cottaz, A. Planas, H. Driguez, and H. Brumer. 2008. Mechanism-based labeling defines the free energy change for formation of the covalent glycosyl-enzyme intermediate in a

xyloglucan endo-transglycosylase. *The Journal of biological chemistry*. 283:21864-21872.

Pitarch, A., A. Jimenez, C. Nombela, and C. Gil. 2006. Decoding serological response to Candida cell wall immunome into novel diagnostic, prognostic, and therapeutic candidates for systemic candidiasis by proteomic and bioinformatic analyses. *Mol Cell Proteomics*. 5:79-96.

Pittet, M., and A. Conzelmann. 2007. Biosynthesis and function of GPI proteins in the yeast *Saccharomyces cerevisiae*. *Biochimica et biophysica acta*. 1771:405-420.

Planas, A. 2000. Bacterial 1,3-1,4-beta-glucanases: structure, function and protein engineering. *Biochimica et biophysica acta*. 1543:361-382.

Popolo, L., P. Cavadini, M. Vai, and L. Alberghina. 1993a. Transcript accumulation of the *GGP1* gene, encoding a yeast GPI-anchored glycoprotein, is inhibited during arrest in the G1 phase and during sporulation. *Current genetics*. 24:382-387.

Popolo, L., D. Gilardelli, P. Bonfante, and M. Vai. 1997. Increase in chitin as an essential response to defects in assembly of cell wall polymers in the ggp1delta mutant of *Saccharomyces cerevisiae*. *Journal of bacteriology*. 179:463-469.

Popolo, L., T. Gualtieri, and E. Ragni. 2001. The yeast cell-wall salvage pathway. *Med Mycol*. 39 Suppl 1:111-121.

Popolo, L., E. Ragni, C. Carotti, O. Palomares, R. Aardema, J.W. Back, H.L. Dekker, L.J. de Koning, L. de Jong, and C.G. de Koster. 2008. Disulfide bond structure and domain organization of yeast beta(1,3)-glucanosyltransferases involved in cell wall biogenesis. *The Journal of biological chemistry*. 283:18553-18565.

Popolo, L., and M. Vai. 1999. The Gas1 glycoprotein, a putative wall polymer cross-linker. *Biochimica et biophysica acta*. 1426:385-400.

Popolo, L., M. Vai, E. Gatti, S. Porello, P. Bonfante, R. Balestrini, and L. Alberghina. 1993b. Physiological analysis of mutants indicates involvement of the *Saccharomyces cerevisiae* GPI-anchored protein gp115 in morphogenesis and cell separation. *Journal of bacteriology*. 175:1879-1885.

Pringle, J.R., E. Bi, H.A. Harkins, J.E. Zahner, C. De Virgilio, J. Chant, K. Corrado, and H. Fares. 1995. Establishment of cell polarity in yeast. *Cold Spring Harb Symp Quant Biol*. 60:729-744.

Pruyne, D., and A. Bretscher. 2000a. Polarization of cell growth in yeast. *Journal of cell science*. 113 (Pt 4):571-585.

Pruyne, D., and A. Bretscher. 2000b. Polarization of cell growth in yeast. I. Establishment and maintenance of polarity states. *Journal of cell science*. 113 (Pt 3):365-375.

Pruyne, D., L. Gao, E. Bi, and A. Bretscher. 2004a. Stable and dynamic axes of polarity use distinct formin isoforms in budding yeast. *Molecular biology of the cell*. 15:4971-4989.

Pruyne, D., A. Legesse-Miller, L. Gao, Y. Dong, and A. Bretscher. 2004b. Mechanisms of polarized growth and organelle segregation in yeast. *Annual review of cell and developmental biology*. 20:559-591.

Qadota, H., C.P. Python, S.B. Inoue, M. Arisawa, Y. Anraku, Y. Zheng, T. Watanabe, D.E. Levin, and Y. Ohya. 1996. Identification of yeast Rho1p GTPase as a regulatory subunit of 1,3-beta-glucan synthase. *Science (New York, N.Y.* 272:279-281.

Ragni, E., A. Coluccio, E. Rolli, J.M. Rodriguez-Pena, G. Colasante, J. Arroyo, A.M. Neiman, and L. Popolo. 2007a. *GAS2* and *GAS4*, a pair of developmentally regulated genes required for spore wall assembly in *Saccharomyces cerevisiae*. *Eukaryotic cell*. 6:302-316.

Ragni, E., T. Fontaine, C. Gissi, J.P. Latge, and L. Popolo. 2007b. The Gas family of proteins of *Saccharomyces cerevisiae*: characterization and evolutionary analysis. *Yeast (Chichester, England)*. 24:297-308.

Ram, A.F., S.S. Brekelmans, L.J. Oehlen, and F.M. Klis. 1995. Identification of two cell cycle regulated genes affecting the beta 1,3-glucan content of cell walls in *Saccharomyces cerevisiae*. *FEBS letters*. 358:165-170.

Ram, A.F., J.C. Kapteyn, R.C. Montijn, L.H. Caro, J.E. Douwes, W. Baginsky, P. Mazur, H. van den Ende, and F.M. Klis. 1998. Loss of the plasma membrane-bound protein Gas1p in *Saccharomyces cerevisiae* results in the release of beta1,3-glucan into the medium and induces a compensation mechanism to ensure cell wall integrity. *Journal of bacteriology*. 180:1418-1424.

Ram, A.F., and F.M. Klis. 2006. Identification of fungal cell wall mutants using susceptibility assays based on Calcofluor white and Congo red. *Nature protocols*. 1:2253-2256.

Ram, A.F., A. Wolters, R. Ten Hoopen, and F.M. Klis. 1994. A new approach for isolating cell wall mutants in *Saccharomyces cerevisiae* by screening for hypersensitivity to calcofluor white. *Yeast (Chichester, England)*. 10:1019-1030.

Reyes-Lopez, C.A., A. Hernandez-Santoyo, M. Pedraza-Escalona, G. Mendoza, A. Hernandez-Arana, and A. Rodriguez-Romero. 2004. Insights into a conformational epitope of Hev b 6.02 (hevein). *Biochemical and biophysical research communications*. 314:123-130.

Richman, T.J., M.M. Sawyer, and D.I. Johnson. 1999. The Cdc42p GTPase is involved in a G2/M morphogenetic checkpoint regulating the apical-isotropic switch and nuclear division in yeast. *The Journal of biological chemistry*. 274:16861-16870.

Roberts, R.L., B. Bowers, M.L. Slater, and E. Cabib. 1983. Chitin synthesis and localization in cell division cycle mutants of *Saccharomyces cerevisiae*. *Molecular and cellular biology*. 3:922-930.

Rodriguez-Escudero, I., F.M. Roelants, J. Thorner, C. Nombela, M. Molina, and V.J. Cid. 2005. Reconstitution of the mammalian PI3K/PTEN/Akt pathway in yeast. *The Biochemical journal*. 390:613-623.

Rodriguez-Pena, J.M., V.J. Cid, J. Arroyo, and C. Nombela. 2000. A novel family of cell wall-related proteins regulated differently during the yeast life cycle. *Molecular and cellular biology*. 20:3245-3255.

Rodriguez-Pena, J.M., V.J. Cid, M. Sanchez, M. Molina, J. Arroyo, and C. Nombela. 1998. The deletion of six ORFs of unknown function from *Saccharomyces cerevisiae* chromosome VII reveals two essential genes: *YGR195w* and *YGR198*w. *Yeast (Chichester, England)*. 14:853-860.

Rodriguez-Pena, J.M., R. Garcia, C. Nombela, and J. Arroyo. 2010. The high-osmolarity glycerol (HOG) and cell wall integrity (CWI) signalling pathways interplay: a yeast dialogue between MAPK routes. *Yeast (Chichester, England)*. 27:495-502.

Rodriguez-Pena, J.M., C. Rodriguez, A. Alvarez, C. Nombela, and J. Arroyo. 2002. Mechanisms for targeting of the *Saccharomyces cerevisiae* GPI-anchored cell wall protein Crh2p to polarised growth sites. *Journal of cell science*. 115:2549-2558.

Roemer, T., and H. Bussey. 1991. Yeast beta-glucan synthesis: *KRE6* encodes a predicted type II membrane protein required for glucan synthesis in vivo and for glucan synthase activity in vitro. *Proceedings of the National Academy of Sciences of the United States of America*. 88:11295-11299.

Roemer, T., and H. Bussey. 1995. Yeast Kre1p is a cell surface O-glycoprotein. *Mol Gen Genet*. 249:209-216.

Roemer, T., S. Delaney, and H. Bussey. 1993. *SKN1* and *KRE6* define a pair of functional homologs encoding putative membrane proteins involved in beta-glucan synthesis. *Molecular and cellular biology*. 13:4039-4048.

Roemer, T., K. Madden, J. Chang, and M. Snyder. 1996a. Selection of axial growth sites in yeast requires Axl2p, a novel plasma membrane glycoprotein. *Genes & development*. 10:777-793.

Roemer, T., G. Paravicini, M.A. Payton, and H. Bussey. 1994. Characterization of the yeast (1-->6)-beta-glucan biosynthetic components, Kre6p and Skn1p, and genetic interactions between the PKC1 pathway and extracellular matrix assembly. *The Journal of cell biology*. 127:567-579.

Roemer, T., L. Vallier, Y.J. Sheu, and M. Snyder. 1998. The Spa2-related protein, Sph1p, is important for polarized growth in yeast. *Journal of cell science*. 111 (Pt 4):479-494.

Roemer, T., L.G. Vallier, and M. Snyder. 1996b. Selection of polarized growth sites in yeast. *Trends in cell biology*. 6:434-441.

Roh, D.H., B. Bowers, H. Riezman, and E. Cabib. 2002a. Rho1p mutations specific for regulation of beta(1-->3)glucan synthesis and the order of assembly of the yeast cell wall. *Molecular microbiology*. 44:1167-1183.

Roh, D.H., B. Bowers, M. Schmidt, and E. Cabib. 2002b. The septation apparatus, an autonomous system in budding yeast. *Molecular biology of the cell*. 13:2747-2759.

Rolli, E., E. Ragni, M. de Medina-Redondo, J. Arroyo, C.R. de Aldana, and L. Popolo. 2011. Expression, stability, and replacement of glucan-remodeling enzymes during developmental transitions in *Saccharomyces cerevisiae*. *Molecular biology of the cell*. 22:1585-1598.

Rolli, E., E. Ragni, J.M. Rodriguez-Pena, J. Arroyo, and L. Popolo. 2010. *GAS3*, a developmentally regulated gene, encodes a highly mannosylated and inactive protein of the Gas family of *Saccharomyces cerevisiae*. *Yeast (Chichester, England)*. 27:597-610.

Romero, P.A., G.J. Dijkgraaf, S. Shahinian, A. Herscovics, and H. Bussey. 1997a. The yeast *CWH41* gene encodes glucosidase I. *Glycobiology*. 7:997-1004.

Romero, P.A., M. Lussier, A.M. Sdicu, H. Bussey, and A. Herscovics. 1997b. Ktr1p is an alpha-1,2-mannosyltransferase of *Saccharomyces cerevisiae*. Comparison of the enzymic properties of soluble recombinant Ktr1p and Kre2p/Mnt1p produced in Pichia pastoris. *The Biochemical journal*. 321 (Pt 2):289-295.

Romero, P.A., M. Lussier, S. Veronneau, A.M. Sdicu, A. Herscovics, and H. Bussey. 1999. Mnt2p and Mnt3p of *Saccharomyces cerevisiae* are members of the Mnn1p family of alpha-1,3-mannosyltransferases responsible for adding the terminal mannose residues of O-linked oligosaccharides. *Glycobiology*. 9:1045-1051.

Roncero, C., and A. Duran. 1985. Effect of Calcofluor white and Congo red on fungal cell wall morphogenesis: in vivo activation of chitin polymerization. *Journal of bacteriology*. 163:1180-1185.

Roncero, C., and Y. Sanchez. 2010. Cell separation and the maintenance of cell integrity during cytokinesis in yeast: the assembly of a septum. *Yeast (Chichester, England)*. 27:521-530.

Roncero, C., M.H. Valdivieso, J.C. Ribas, and A. Duran. 1988a. Effect of calcofluor white on chitin synthases from *Saccharomyces cerevisiae*. *Journal of bacteriology*. 170:1945-1949.

Roncero, C., M.H. Valdivieso, J.C. Ribas, and A. Duran. 1988b. Isolation and characterization of *Saccharomyces cerevisiae* mutants resistant to Calcofluor white. *Journal of bacteriology*. 170:1950-1954.

Roumanie, O., H. Wu, J.N. Molk, G. Rossi, K. Bloom, and P. Brennwald. 2005. Rho GTPase regulation of exocytosis in yeast is independent of GTP hydrolysis and polarization of the exocyst complex. *The Journal of cell biology*. 170:583-594.

Ruiz-Herrera, J. 1991. Biosynthesis of beta-glucans in fungi. *Antonie van Leeuwenhoek*. 60:72-81.

Ruiz-Herrera, J., J.M. Gonzalez-Prieto, and R. Ruiz-Medrano. 2002. Evolution and phylogenetic relationships of chitin synthases from yeasts and fungi. *FEMS yeast research*. 1:247-256.

Ruiz-Herrera, J., and A.D. Martinez-Espinoza. 1999. Chitin biosynthesis and structural organization in vivo. *Exs*. 87:39-53.

Sacristan, C., A. Reyes, and C. Roncero. 2012. Neck compartmentalization as the molecular basis for the different endocytic behaviour of Chs3 during budding or hyperpolarized growth in yeast cells. *Molecular microbiology*. 83:1124-1135.

Sacher, M., J. Barrowman, D. Schieltz, J.R. Yates, 3rd, and S. Ferro-Novick. 2000. Identification and characterization of five new subunits of TRAPP. *Eur J Cell Biol*. 79:71-80.

Sakchaisri, K., S. Asano, L.R. Yu, M.J. Shulewitz, C.J. Park, J.E. Park, Y.W. Cho, T.D. Veenstra, J. Thorner, and K.S. Lee. 2004. Coupling morphogenesis to mitotic entry. *Proceedings of the National Academy of Sciences of the United States of America*. 101:4124-4129.

Saladie, M., J.K. Rose, D.J. Cosgrove, and C. Catala. 2006. Characterization of a new xyloglucan endotransglucosylase/hydrolase (XTH) from ripening tomato fruit and implications for the diverse modes of enzymic action. *Plant J*. 47:282-295.

San Segundo, P., J. Correa, C.R. Vazquez de Aldana, and F. del Rey. 1993. *SSG1*, a gene encoding a sporulation-specific 1,3-beta-glucanase in *Saccharomyces cerevisiae*. *Journal of bacteriology*. 175:3823-3837.

Sanchez-Diaz, A., V. Marchesi, S. Murray, R. Jones, G. Pereira, R. Edmondson, T. Allen, and K. Labib. 2008. Inn1 couples contraction of the actomyosin ring to membrane ingression during cytokinesis in budding yeast. *Nature cell biology*. 10:395-406.

Sanders, S.L., and C.M. Field. 1994. Cell division. Septins in common? *Curr Biol*. 4:907-910.

Santos, B., A. Duran, and M.H. Valdivieso. 1997. *CHS5*, a gene involved in chitin synthesis and mating in *Saccharomyces cerevisiae*. *Molecular and cellular biology*. 17:2485-2496.

Santos, B., and M. Snyder. 1997. Targeting of chitin synthase 3 to polarized growth sites in yeast requires Chs5p and Myo2p. *The Journal of cell biology*. 136:95-110.

Sanz, M., F. Castrejon, A. Duran, and C. Roncero. 2004. *Saccharomyces cerevisiae* Bni4p directs the formation of the chitin ring and also participates in the correct assembly of the septum structure. *Microbiology (Reading, England)*. 150:3229-3241.

Sarthy, A.V., T. McGonigal, M. Coen, D.J. Frost, J.A. Meulbroek, and R.C. Goldman. 1997. Phenotype in *Candida albicans* of a disruption of the *BGL2* gene encoding a 1,3-beta-glucosyltransferase. *Microbiology (Reading, England)*. 143 (Pt 2):367-376.

Sburlati, A., and E. Cabib. 1986. Chitin synthetase 2, a presumptive participant in septum formation in *Saccharomyces cerevisiae*. *The Journal of biological chemistry*. 261:15147-15152.

Schmidt, M., B. Bowers, A. Varma, D.H. Roh, and E. Cabib. 2002. In budding yeast, contraction of the actomyosin ring and formation of the primary septum at cytokinesis depend on each other. *Journal of cell science*. 115:293-302.

Schmidt, M., A. Varma, T. Drgon, B. Bowers, and E. Cabib. 2003. Septins, under Cla4p regulation, and the chitin ring are required for neck integrity in budding yeast. *Molecular biology of the cell*. 14:2128-2141.

Schott, D., J. Ho, D. Pruyne, and A. Bretscher. 1999. The COOH-terminal domain of Myo2p, a yeast myosin V, has a direct role in secretory vesicle targeting. *The Journal of cell biology*. 147:791-808.

Sekiya-Kawasaki, M., M. Abe, A. Saka, D. Watanabe, K. Kono, M. Minemura-Asakawa, S. Ishihara, T. Watanabe, and Y. Ohya. 2002. Dissection of upstream regulatory components of the Rho1p effector, 1,3-beta-glucan synthase, in *Saccharomyces cerevisiae*. *Genetics*. 162:663-676.

Selvaggini, S., C.A. Munro, S. Paschoud, D. Sanglard, and N.A. Gow. 2004. Independent regulation of chitin synthase and chitinase activity in *Candida albicans* and *Saccharomyces cerevisiae*. *Microbiology (Reading, England)*. 150:921-928.

Seshan, A., and A. Amon. 2005. Ras and the Rho effector Cla4 collaborate to target and anchor Lte1 at the bud cortex. *Cell Cycle*. 4:940-946.

Shahinian, S., and H. Bussey. 2000. beta-1,6-Glucan synthesis in *Saccharomyces cerevisiae*. *Molecular microbiology*. 35:477-489.

Shahinian, S., G.J. Dijkgraaf, A.M. Sdicu, D.Y. Thomas, C.A. Jakob, M. Aebi, and H. Bussey. 1998. Involvement of protein N-glycosyl chain glucosylation and processing in the biosynthesis of cell wall beta-1,6-glucan of *Saccharomyces cerevisiae*. *Genetics*. 149:843-856.

Shannon, K.B. 2012. IQGAP Family Members in Yeast, Dictyostelium, and Mammalian Cells. *Int J Cell Biol*. 2012:894817.

Shaw, J.A., P.C. Mol, B. Bowers, S.J. Silverman, M.H. Valdivieso, A. Duran, and E. Cabib. 1991. The function of chitin synthases 2 and 3 in the *Saccharomyces cerevisiae* cell cycle. *The Journal of cell biology*. 114:111-123.

Sheu, Y.J., Y. Barral, and M. Snyder. 2000. Polarized growth controls cell shape and bipolar bud site selection in *Saccharomyces cerevisiae*. *Molecular and cellular biology*. 20:5235-5247.

Sheu, Y.J., B. Santos, N. Fortin, C. Costigan, and M. Snyder. 1998. Spa2p interacts with cell polarity proteins and signaling components involved in yeast cell morphogenesis. *Molecular and cellular biology*. 18:4053-4069.

Shulewitz, M.J., C.J. Inouye, and J. Thorner. 1999. Hsl7 localizes to a septin ring and serves as an adapter in a regulatory pathway that relieves tyrosine phosphorylation of Cdc28 protein kinase in *Saccharomyces cerevisiae*. *Molecular and cellular biology*. 19:7123-7137.

Silverman, S.J. 1989. Similar and different domains of chitin synthases 1 and 2 of S. cerevisiae: two isozymes with distinct functions. *Yeast (Chichester, England)*. 5:459-467.

Silverman, S.J., A. Sburlati, M.L. Slater, and E. Cabib. 1988. Chitin synthase 2 is essential for septum formation and cell division in *Saccharomyces cerevisiae*. *Proceedings of the National Academy of Sciences of the United States of America*. 85:4735-4739.

Simon, V.R., S.L. Karmon, and L.A. Pon. 1997. Mitochondrial inheritance: cell cycle and actin cable dependence of polarized mitochondrial movements in *Saccharomyces cerevisiae*. *Cell Motil Cytoskeleton*. 37:199-210.

Sinnott, M. 1990. Catalytic mechanism of enzymatic glycosyl transfer. *Chem Rev*. 90:1171-1202.

Slaughter, B.D., A. Das, J.W. Schwartz, B. Rubinstein, and R. Li. 2009. Dual modes of cdc42 recycling fine-tune polarized morphogenesis. *Dev Cell*. 17:823-835.

Sloat, B.F., A. Adams, and J.R. Pringle. 1981. Roles of the *CDC24* gene product in cellular morphogenesis during the *Saccharomyces cerevisiae* cell cycle. *The Journal of cell biology*. 89:395-405.

Spellman, P.T., G. Sherlock, M.Q. Zhang, V.R. Iyer, K. Anders, M.B. Eisen, P.O. Brown, D. Botstein, and B. Futcher. 1998. Comprehensive identification of cell cycle-regulated genes of the yeast *Saccharomyces cerevisiae* by microarray hybridization. *Molecular biology of the cell*. 9:3273-3297.

Spiliotis, E.T., and A.S. Gladfelter. 2012. Spatial guidance of cell asymmetry: septin GTPases show the way. *Traffic*. 13:195-203.

Stevenson, B.J., B. Ferguson, C. De Virgilio, E. Bi, J.R. Pringle, G. Ammerer, and G.F. Sprague, Jr. 1995. Mutation of *RGA1*, which encodes a putative GTPase-activating protein for the polarity-establishment protein Cdc42p, activates the pheromone-response pathway in the yeast *Saccharomyces cerevisiae*. *Genes & development*. 9:2949-2963.

Strahl-Bolsinger, S., M. Gentzsch, and W. Tanner. 1999. Protein O-mannosylation. *Biochimica et biophysica acta*. 1426:297-307.

Sucher, A.J., E.B. Chahine, and H.E. Balcer. 2009. Echinocandins: the newest class of antifungals. *Ann Pharmacother*. 43:1647-1657.

Tabernero, C., P.M. Coll, J.M. Fernandez-Abalos, P. Perez, and R.I. Santamaria. 1994. Cloning and DNA sequencing of bgaA, a gene encoding an endo-beta-1,3-1,4-glucanase, from an alkalophilic *Bacillus* strain (N137). *Applied and environmental microbiology*. 60:1213-1220.

Takizawa, P.A., A. Sil, J.R. Swedlow, I. Herskowitz, and R.D. Vale. 1997. Actin-dependent localization of an RNA encoding a cell-fate determinant in yeast. *Nature*. 389:90-93.

Tang, C.S., and S.I. Reed. 2002. Phosphorylation of the septin cdc3 in g1 by the cdc28 kinase is essential for efficient septin ring disassembly. *Cell Cycle*. 1:42-49.

Teh, E.M., C.C. Chai, and F.M. Yeong. 2009. Retention of Chs2p in the ER requires N-terminal CDK1-phosphorylation sites. *Cell Cycle*. 8:2964-2974.

Theesfeld, C.L., J.E. Irazoqui, K. Bloom, and D.J. Lew. 1999. The role of actin in spindle orientation changes during the *Saccharomyces cerevisiae* cell cycle. *The Journal of cell biology*. 146:1019-1032.

Tiedje, C., I. Sakwa, U. Just, and T. Hofken. 2008. The Rho GDI Rdi1 regulates Rho GTPases by distinct mechanisms. *Molecular biology of the cell*. 19:2885-2896.

Tjandra, H., J. Compton, and D. Kellogg. 1998. Control of mitotic events by the Cdc42 GTPase, the Clb2 cyclin and a member of the PAK kinase family. *Curr Biol*. 8:991-1000.

Toh-e, A., S. Yasunaga, H. Nisogi, K. Tanaka, T. Oguchi, and Y. Matsui. 1993. Three yeast genes, *PIR1*, *PIR2* and *PIR3*, containing internal tandem repeats, are related to each other, and *PIR1* and *PIR2* are required for tolerance to heat shock. *Yeast (Chichester, England)*. 9:481-494.

Tolliday, N., M. Pitcher, and R. Li. 2003. Direct evidence for a critical role of myosin II in budding yeast cytokinesis and the evolvability of new cytokinetic mechanisms in the absence of myosin II. *Molecular biology of the cell*. 14:798-809.

Tolliday, N., L. VerPlank, and R. Li. 2002. Rho1 directs formin-mediated actin ring assembly during budding yeast cytokinesis. *Curr Biol*. 12:1864-1870.

Tomishige, N., Y. Noda, H. Adachi, H. Shimoi, A. Takatsuki, and K. Yoda. 2003. Mutations that are synthetically lethal with a gas1Delta allele cause defects in the cell wall of *Saccharomyces cerevisiae*. *Mol Genet Genomics*. 269:562-573.

Trautwein, M., C. Schindler, R. Gauss, J. Dengjel, E. Hartmann, and A. Spang. 2006. Arf1p, Chs5p and the ChAPs are required for export of specialized cargo from the Golgi. *The EMBO journal*. 25:943-954.

Trilla, J.A., T. Cos, A. Duran, and C. Roncero. 1997. Characterization of *CHS4* (*CAL2*), a gene of *Saccharomyces cerevisiae* involved in chitin biosynthesis and allelic to *SKT5* and *CSD4*. *Yeast (Chichester, England)*. 13:795-807.

Trilla, J.A., A. Duran, and C. Roncero. 1999. Chs7p, a new protein involved in the control of protein export from the endoplasmic reticulum that is specifically engaged in the regulation of chitin synthesis in *Saccharomyces cerevisiae*. *The Journal of cell biology*. 145:1153-1163.

Tully, G.H., R. Nishihama, J.R. Pringle, and D.O. Morgan. 2009. The anaphase-promoting complex promotes actomyosin-ring disassembly during cytokinesis in yeast. *Molecular biology of the cell*. 20:1201-1212.

Ufano, S., M.E. Pablo, A. Calzada, F. del Rey, and C.R. Vazquez de Aldana. 2004. Swm1p subunit of the APC/cyclosome is required for activation of the daughter-specific gene expression program mediated by Ace2p during growth at high temperature in *Saccharomyces cerevisiae*. *Journal of cell science*. 117:545-557.

Utsugi, T., M. Minemura, A. Hirata, M. Abe, D. Watanabe, and Y. Ohya. 2002. Movement of yeast 1,3-beta-glucan synthase is essential for uniform cell wall synthesis. *Genes Cells*. 7:1-9.

Vaaje-Kolstad, G., V. Farkas, M. Hrmova, and G.B. Fincher. 2010. Xyloglucan xyloglucosyl transferases from barley (Hordeum vulgare L.) bind oligomeric and polymeric xyloglucan molecules in their acceptor binding sites. *Biochimica et biophysica acta*. 1800:674-684.

Valdivia, R.H., and R. Schekman. 2003. The yeasts Rho1p and Pkc1p regulate the transport of chitin synthase III (Chs3p) from internal stores to the plasma membrane. *Proceedings of the National Academy of Sciences of the United States of America*. 100:10287-10292.

Valdivieso, M.H., P.C. Mol, J.A. Shaw, E. Cabib, and A. Duran. 1991. *CAL1*, a gene required for activity of chitin synthase 3 in *Saccharomyces cerevisiae*. *The Journal of cell biology*. 114:101-109.

van Drogen, F., and M. Peter. 2002. Spa2p functions as a scaffold-like protein to recruit the Mpk1p MAP kinase module to sites of polarized growth. *Curr Biol*. 12:1698-1703.

Vazquez de Aldana, C.R., J. Correa, P. San Segundo, A. Bueno, A.R. Nebreda, E. Mendez, and F. del Rey. 1991. Nucleotide sequence of the exo-1,3-beta-glucanase-encoding gene, *EXG1*, of the yeast *Saccharomyces cerevisiae*. *Gene*. 97:173-182.

VerPlank, L., and R. Li. 2005. Cell cycle-regulated trafficking of Chs2 controls actomyosin ring stability during cytokinesis. *Molecular biology of the cell*. 16:2529-2543.

Versele, M., and J. Thorner. 2004. Septin collar formation in budding yeast requires GTP binding and direct phosphorylation by the PAK, Cla4. *The Journal of cell biology*. 164:701-715.

Versele, M., and J. Thorner. 2005. Some assembly required: yeast septins provide the instruction manual. *Trends in cell biology*. 15:414-424.

Vilella, F., E. Herrero, J. Torres, and M.A. de la Torre-Ruiz. 2005. Pkc1 and the upstream elements of the cell integrity pathway in *Saccharomyces cerevisiae*, Rom2 and Mtl1, are required for cellular responses to oxidative stress. *The Journal of biological chemistry*. 280:9149-9159.

Vink, E., R.J. Rodriguez-Suarez, M. Gerard-Vincent, J.C. Ribas, H. de Nobel, H. van den Ende, A. Duran, F.M. Klis, and H. Bussey. 2004. An in vitro assay for (1 --> 6)-beta-D-glucan synthesis in *Saccharomyces cerevisiae*. *Yeast (Chichester, England)*. 21:1121-1131.

Vojtek, A.B., and J.A. Cooper. 1995. Rho family members: activators of MAP kinase cascades. *Cell*. 82:527-529.

Walther, A., and J. Wendland. 2003. Septation and cytokinesis in fungi. *Fungal Genet Biol*. 40:187-196.

Watanabe, D., M. Abe, and Y. Ohya. 2001. Yeast Lrg1p acts as a specialized RhoGAP regulating 1,3-beta-glucan synthesis. *Yeast (Chichester, England)*. 18:943-951.

Weirich, C.S., J.P. Erzberger, and Y. Barral. 2008. The septin family of GTPases: architecture and dynamics. *Nat Rev Mol Cell Biol*. 9:478-489.

Weiss, E.L., A.C. Bishop, K.M. Shokat, and D.G. Drubin. 2000. Chemical genetic analysis of the budding-yeast p21-activated kinase Cla4p. *Nature cell biology*. 2:677-685.

Weiss, E.L., C. Kurischko, C. Zhang, K. Shokat, D.G. Drubin, and F.C. Luca. 2002. The *Saccharomyces cerevisiae* Mob2p-Cbk1p kinase complex promotes polarized growth and acts with the mitotic exit network to facilitate daughter cell-specific localization of Ace2p transcription factor. *The Journal of cell biology*. 158:885-900.

Wloka, C., and E. Bi. 2012. Mechanisms of cytokinesis in budding yeast. *Cytoskeleton (Hoboken)*.

Wu, C., S.F. Lee, E. Furmaniak-Kazmierczak, G.P. Cote, D.Y. Thomas, and E. Leberer. 1996. Activation of myosin-I by members of the Ste20p protein kinase family. *The Journal of biological chemistry*. 271:31787-31790.

Wu, C., V. Lytvyn, D.Y. Thomas, and E. Leberer. 1997. The phosphorylation site for Ste20p-like protein kinases is essential for the function of myosin-I in yeast. *The Journal of biological chemistry*. 272:30623-30626.

Yeong, F.M. 2005. Severing all ties between mother and daughter: cell separation in budding yeast. *Molecular microbiology*. 55:1325-1331.

Yin, Q.Y., P.W. de Groot, H.L. Dekker, L. de Jong, F.M. Klis, and C.G. de Koster. 2005. Comprehensive proteomic analysis of *Saccharomyces cerevisiae* cell walls: identification of proteins covalently attached via glycosylphosphatidylinositol remnants or mild alkali-sensitive linkages. *The Journal of biological chemistry*. 280:20894-20901.

Zhang, G., R. Kashimshetty, K.E. Ng, H.B. Tan, and F.M. Yeong. 2006. Exit from mitosis triggers Chs2p transport from the endoplasmic reticulum to mother-daughter neck via the secretory pathway in budding yeast. *The Journal of cell biology*. 174:207-220.

Zhao, C., U.S. Jung, P. Garrett-Engele, T. Roe, M.S. Cyert, and D.E. Levin. 1998. Temperature-induced expression of yeast *FKS2* is under the dual control of protein kinase C and calcineurin. *Molecular and cellular biology*. 18:1013-1022.

Zheng, Y., A. Bender, and R.A. Cerione. 1995. Interactions among proteins involved in bud-site selection and bud-site assembly in *Saccharomyces cerevisiae*. *The Journal of biological chemistry*. 270:626-630.

Ziman, M., J.S. Chuang, and R.W. Schekman. 1996. Chs1p and Chs3p, two proteins involved in chitin synthesis, populate a compartment of the *Saccharomyces cerevisiae* endocytic pathway. *Molecular biology of the cell*. 7:1909-1919.

Ziman, M., J.S. Chuang, M. Tsung, S. Hamamoto, and R. Schekman. 1998. Chs6p-dependent anterograde transport of Chs3p from the chitosome to the plasma

membrane in *Saccharomyces cerevisiae*. *Molecular biology of the cell*. 9:1565-1576.

Ziman, M., J.M. O'Brien, L.A. Ouellette, W.R. Church, and D.I. Johnson. 1991. Mutational analysis of *CDC42*Sc, a *Saccharomyces cerevisiae* gene that encodes a putative GTP-binding protein involved in the control of cell polarity. *Molecular and cellular biology*. 11:3537-3544.

Zlotnik, H., M.P. Fernandez, B. Bowers, and E. Cabib. 1984. *Saccharomyces cerevisiae* mannoproteins form an external cell wall layer that determines wall porosity. *Journal of bacteriology*. 159:1018-1026.